Development of New, Physiologically Useful Nitroxyl (HNO) Donors

by

Daryl Austin Guthrie

A dissertation submitted to Johns Hopkins University in conformity with the requirements for the degree of Doctor of Philosophy

Baltimore, Maryland

May, 2014

Abstract

Heart failure, defined as the inability of the heart to pump enough blood to supply the metabolic demands of the body, affects more than 23 million people worldwide with total annual costs in 2013 of $32 billion in the US alone. In *in vitro* and *in vivo* models of failing hearts, HNO has been shown to improve both vasorelaxation and myocardial contractility via unique mechanisms leading to enhanced intracellular Ca^{2+} cycling. Due to its inherent reactivity as a biologically relevant reactive intermediate, HNO must be generated *in situ* through the use of donor compounds, but very few physiologically useful HNO donors exist. HNO, an "aldehyde mimetic", was used as a reagent to synthesize a variety of HNO donors in what can be considered an *N*-selective HNO-aldol reaction in up to quantitative yields with bimolecular rate constants reaching 8×10^5 $M^{-1}s^{-1}$. The hydroxylamino–X (HAX) general class of HNO donors, where X is based on Meldrum's acid (HAMA), barbituric acid (HABA), or pyrazolone (HAPY), is capable of releasing HNO quantitatively under nonenzymatic, physiological conditions, with the rate and amount of HNO released being dependent mainly on the nature of the carbon-based leaving group. Experimental and computational investigations suggest that the HNO release rate correlates with HAX and X–H pK_a.

Advisor: Professor John P. Toscano

Readers: Professor Gary H. Posner

Professor Thomas Lectka

Acknowledgments

Foremost, I would like to express my sincere gratitude to my advisor, Professor John P. Toscano, for the continuous support of my PhD study and research. His patience, motivation, enthusiasm, and immense knowledge have been collectively a guiding light throughout the course of my PhD candidacy (and beyond). I could not have imagined having a better advisor and mentor. We gratefully acknowledge the National Science Foundation, Cardioxyl Pharmaceuticals, and the Martin and Mary Kilpatrick Fellowship for generous support of this research.

I would also like to thank Professor Gary H. Posner and Professor Thomas Lectka for serving on my thesis committee all of these years. Thank you for your encouragement, insightful comments, but above all, for being very fine organic chemists.

I thank my fellow labmates and HNO advocates: Dr. Anthony Evans, Dr. Art Sutton, Dr. Meredith Cline, Dr. Gizem Keceli, Tyler Chavez, Christopher Bianco, Hyunah Cho, and Saghar Nourian, for the stimulating discussions, for the sleepless nights we were working together before deadlines, and for all the fun we have had in the last five years.

My sincere thanks go to my "undergraduate army": Nam Kim (JHU '11), Matthew Morris (JHU '12), Anthony Ho (JHU '13), Anthony Collins (JHU '13), and Cyrus Takahashi (JHU '14), for inspiring me to be a better chemist, mentor, and friend.

Most of all, thank you Violeta, my wife, George, my son, Charlie and Ginger, my parents, and Chris and Erin, my brother and sister, for loving me, for standing by me, and for always doing right by me. I love you all very much!

Table of Contents

Abstract ii

Acknowledgments iii

Table of Contents v

List of Figures ix

List of Schemes xi

List of Tables xiv

Chapter 1. Introduction 1

1.1 Chemistry of Nitroxyl (HNO) 1

1.1.1 Nitroxyl (HNO) and Related Nitrogen Oxides 1

1.1.2 HNO Reactivity and Fundamental Chemical Properties 4

1.2 Previously Reported Classes of HNO Donors 7

1.2.1 Angeli's Salt (AS) 8

1.2.2 Piloty's Acid (PA) and its Derivatives 9

1.2.3 Primary Amine-Based Diazeniumdiolates (IPA/NO) 10

1.2.4 Acyloxy Nitroso Compounds (AcON) 12

1.2.5 Precursors to Acyl Nitroso Compounds (AcN) 13

1.2.6 Cyanamide 14

1.3 Introduction to This Work 16

1.4 References 18

Chapter 2. Development of *N*-Sustituted Hydroxylamines as Efficient Nitroxyl (HNO) Donors 24

2.1 Abstract 24

2.2 Introduction 25

2.3 Results and Discussion 27

2.4 Conclusion 35

2.5 Experimental 36

2.5.1 Methods and Materials 36

2.5.2 Nitrous Oxide (N_2O) Quantification by Gas Chromatographic (GC) Headspace Analysis 37

2.5.3 ^{1}H NMR Kinetic Experiment with Barbiturate Donor 4a 38

2.5.4 Decomposition Kinetics by UV-vis Spectroscopy 39

2.5.5 Experimental Procedures 42

2.6 References 51

2.7 Supporting Information 54

2.7.1 X-Ray Crystallography Data 58

2.7.2 ^{1}H and ^{13}C NMR Spectra 62

Chapter 3. The "Catch-and-Release" of Nitroxyl (HNO) with Pyrazolones 92

3.1 Abstract 92

3.2 Introduction 93

3.3 Results and Discussion 97

3.3.1 Early Studies 97

3.3.2 Synthesis 98

3.3.3 Kinetic Evaluation 102

3.3.4 DFT Calculations 105

3.3.5 HNO Release from the Expanded HAPY Class 106
3.4 Conclusion 115
3.5 Experimental 116
3.5.1 Materials and Methods 116
3.5.2 Incubation Procedure of HAPY Donors at pH 7.4, 37 °C with TXPTS 117
3.5.3 Experimental Procedures 118
3.6 References 128
3.7 Supporting Information 132
3.7.1 X-Ray Crystallography Data 132
3.7.2 Density Functional Theory (DFT) Calculations 134
3.7.3 ^{1}H and ^{13}C NMR Spectra 217
Chapter 4. Curtailing the Hydroxylaminobarbituric Acid–Hydantoin Rearrangement to Favor Nitroxyl (HNO) Generation 253
4.1 Abstract 253
4.2 Introduction 254
4.3 Results and Discussion 258
4.3.1 Synthesis 258
4.3.2 HNO Release from the Expanded HABA Class 259
4.3.3 Rearrangement Studies 264
4.3.4 Barbiturates as HNO Donors 269
4.4 Conclusion 271
4.5 Experimental 272

4.5.1 Methods and Materials 272

4.5.2 Incubation Procedure of HABA Donors at pH 7.4, 37 °C with TXPTS 273

4.5.3 Experimental Procedures 274

4.6 References 279

4.7 Supporting Information 282

4.7.1 X-Ray Crystallography Data 282

4.7.2 Density Functional Theory (DFT) Calculations 284

4.7.3 ^{1}H and ^{13}C NMR Spectra 296

Chapter 5. The HNO-Aldol Screening Assay Using ^{1}H NMR Spectroscopy 306

Curriculum Vita 317

List of Figures

Figure 1-1. The biologically relevant properties and reactivities of HNO 7

Figure 1-2. Previously reported classes of HNO donors 8

Figure 2-1. Previously reported classes of HNO donors 25

Figure 2-2. ^{1}H NMR analysis of the decomposition of **4a** to **4b** and **6a** to **6b** in 10% D_2O, PBS, pH 7.4 at room temperature 30

Figure 2-3. Plot of the concentration of **4b**, **4b-H$^+$** and **6b**, **6b-H$^+$** as a function of pH 31

Figure 2-4. UV-vis analysis of the decomposition of **4a** and **6a** 32

Figure 2-5. ^{1}H NMR spectra of the decomposition of Meldrum's acid donor **1a** in PBS, pH 7.4 54

Figure 2-6. ^{1}H NMR spectra of the decomposition of Meldrum's acid donor **2a** in PBS, pH 7.4 55

Figure 2-7. ^{1}H NMR spectra of the decomposition of Meldrum's acid donor **3a** in PBS, pH 7.4 56

Figure 2-8. UV-vis spectral and kinetic data for the decomposition of barbituric acid donor **4a** and pyrazolone donor **6a** in pH 4 buffer at room temperature 57

Figure 2-9. UV-vis spectra at low and high pH for byproducts of decomposition from barbituric acid donor **4a** and pyrazolone donor **6a** 57

Figure 3-1. Previous examples from the HAMA, HABA, and HAPY classes of HNO donors 95

Figure 3-2. The *N*-selective HNO-aldol reaction between PY-2 and Angeli's salt-

derived HNO 99

Figure 3-3. Competition for HABA-1-derived HNO at pH 7.4, 37 °C: PY-2 vs. TXPTS 104

Figure 3-4. Incubation of HAPY-2 at pH 7.4, 37 °C after 48 h as a function of $[TXPTS]_0$ 108

Figure 3-5. Timecourse for the disappearance of HAPY-2 and appearance of PY-2 and TXPTS aza-ylide with added TXPTS 109

Figure 3-6. Plot of UV-vis determined decomposition rates as a function of pH at 25 °C for HAPY-5, HAPY-10, HAPY-11, and HAPY-12 113

Figure 3-7. UV-vis determined pK_a of HAPY-6 132

Figure 4-1. Decomposition of HABA donors of HNO 261

Figure 4-2. UV-vis analysis of HABA-3 – HABA-6 263

Figure 4-3. Hydantoin formation from HABA-2 vs. compound **2** 265

Figure 4-4. B3LYP/6-31G* calculations and stepwise scheme of the rearrangement of HABA-2 and HABA-3 involving a tetrahedral intermediate 268

Figure 5-1. Decomposition rates for the HAX general class of HNO donors as a function pK_a of X–H, the byproduct of HNO release 307

List of Schemes

Scheme 1-1. Possible biosynthetic pathways to HNO 3

Scheme 1-2. HNO reactivity with HNO 4

Scheme 1-3. HNO vs. NO reactivity with thiols 5

Scheme 1-4. Secondary amine-based diazeniumdiolates as versatile NO donors ... 9

Scheme 1-5. Angeli's salt decomposition pathways to HNO and NO 9

Scheme 1-6. Piloty's acid decomposition pathways to HNO and NO 10

Scheme 1-7. IPA/NO decomposition pathways to HNO and NO 11

Scheme 1-8. IPA/NO-AcOM and IPA/NO-aspirin decomposition pathway to HNO 12

Scheme 1-9. Direct and HNO-mediated reactions of acyloxy nitroso compounds . 13

Scheme 1-10. Generation of acyl nitroso compounds 14

Scheme 1-11. Cyanamide oxidative decomposition pathways to HNO 15

Scheme 1-12. Hydrolysis pathway to HNO via acyl nitroso intermediate 16

Scheme 1-13. General strategies for HNO release 16

Scheme 2-1. General strategy for HNO release 26

Scheme 2-2. Potential HNO release pathways from Meldrum's acid derivatives **1a** and **2a** and barbituric acid derivatives **3a** and **4a** 27

Scheme 2-3. Synthesis of Meldrum's acid derivative **1a** 27

Scheme 2-4. Major reaction pathway for barbiturate **3a** 29

Scheme 2-5. HNO release from pyrazolone derivative **6a** 33

Scheme 2-6. Synthesis of Meldrum's acid donors **1a** and **2a** 40

Scheme 2-7. Synthesis of barbituric acid donors **3a** and **4a** 41

Scheme 2-8. Synthesis of pyrazolone donor **6a** 42

Scheme 3-1. General HNO release from HAPY class 96

Scheme 3-2. Possible synthetic strategies: traditional vs. umpolung 100

Scheme 3-3. Competitive HNO trapping experiment at pH 7.4, 37 °C 102

Scheme 3-4. Possible reactions involving HNO with pyrazolones 105

Scheme 3-5. Proposed mechanism of HNO release 114

Scheme 3-6. Synthesis of 4-acetyl-1,3-dimethyl-pyrazolone (**1**) 118

Scheme 3-7. Synthesis of 3-(2-chlorophenyl)-4-formyl-1-methyl-pyrazolone (**2**) 119

Scheme 3-8. Synthesis of 4-(acetyl-*O*-methoxyoxime)-1,3-dimethyl-pyrazolone (PY-3) 120

Scheme 3-9. Synthesis of 4-(acetyl-*O*-methoxyoxime)-3-methyl-pyrazolone (PY-5) 120

Scheme 3-10. Synthesis of 4-methyl-*N*-(4-chlorophenyl)-3-methyl-pyrazolone (PY-7) 121

Scheme 3-11. Synthesis of 4-methyl-*N*-(2-chlorophenyl)-3-methyl-pyrazolone (PY-8) 122

Scheme 3-12. Synthesis of 4-methyl-*N*-methyl-3-(2-chlorophenyl)-pyrazolone (PY-12) 122

Scheme 3-13. Synthesis of HAPY donors via the HNO-aldol procedure 123

Scheme 4-1. General strategy for HNO release 255

Scheme 4-2. Previous examples of the HABA class of potential HNO donors 256

Scheme 4-3. Decomposition of amino- and hydroxylamino-barbituric acids …… 264

Scheme 4-4. Mechanism of HNO release in pH 7.4 phosphate buffer at 37 °C …... 270

Scheme 4-5. Synthesis of HABA donors via the HNO-aldol procedure ……... 274

Scheme 4-6. Synthesis of the model compound, **2** ……... 277

Scheme 5-1. The HNO-aldol screening assay using ^{1}H NMR spectroscopy ……... 310

List of Tables

Table 1-1. Nitroxyl (HNO) and related nitrogen oxides 2

Table 2-1. Decomposition of HNO donors 28

Table 3-1. HNO-aldol reaction of pyrazolones 101

Table 3-2. Gibbs free energy differences in reactions I, II, and III 106

Table 3-3. Incubation of HAPY-1 – HAPY-12 in pH 7.4 phosphate buffer at 37 °C under argon with added TXPTS 111

Table 3-4. B3LYP/6-31G* optimized geometries, energies, and entropy corrections for nitroxyl (HNO) 134

Table 3-5. B3LYP/6-31G* calculated IR frequencies (cm^{-1}, uncorrected) and intensities for nitroxyl (HNO) 134

Table 3-6. B3LYP/6-31G* optimized geometries, energies, and entropy corrections for water (H_2O) 134

Table 3-7. B3LYP/6-31G* calculated IR frequencies (cm^{-1}, uncorrected) and intensities for water (H_2O) 135

Table 3-8. B3LYP/6-31G* optimized geometries, energies, and entropy corrections for hydronium (H_3O^+) 135

Table 3-9. B3LYP/6-31G* calculated IR frequencies (cm^{-1}, uncorrected) and intensities for hydronium (H_3O^+) 135

Table 3-10. B3LYP/6-31G* optimized geometries, energies, and entropy corrections for enol of PY-1 135

Table 3-11. B3LYP/6-31G* calculated IR frequencies (cm^{-1}, uncorrected) and

intensities for enol of PY-1 136

Table 3-12. B3LYP/6-31G* optimized geometries, energies, and entropy corrections for PY-1_{anion} 137

Table 3-13. B3LYP/6-31G* calculated IR frequencies (cm^{-1}, uncorrected) and intensities for PY-1_{anion} 138

Table 3-14. B3LYP/6-31G* optimized geometries, energies, and entropy corrections for HAPY-1 139

Table 3-15. B3LYP/6-31G* calculated IR frequencies (cm^{-1}, uncorrected) and intensities for HAPY-1 140

Table 3-16. B3LYP/6-31G* optimized geometries, energies, and entropy corrections for HAPY-1_{anion} 141

Table 3-17. B3LYP/6-31G* calculated IR frequencies (cm^{-1}, uncorrected) and intensities for HAPY-1_{anion} 142

Table 3-18. B3LYP/6-31G* optimized geometries, energies, and entropy corrections for enol of PY-2 143

Table 3-19. B3LYP/6-31G* calculated IR frequencies (cm^{-1}, uncorrected) and intensities for enol of PY-2 144

Table 3-20. B3LYP/6-31G* optimized geometries, energies, and entropy corrections for PY-2_{anion} 145

Table 3-21. B3LYP/6-31G* calculated IR frequencies (cm^{-1}, uncorrected) and intensities for PY-2_{anion} 146

Table 3-22. B3LYP/6-31G* optimized geometries, energies, and entropy corrections for HAPY-2 147

Table 3-23. B3LYP/6-31G* calculated IR frequencies (cm^{-1}, uncorrected) and intensities for HAPY-2 148

Table 3-24. B3LYP/6-31G* optimized geometries, energies, and entropy corrections for HAPY-2_{anion} 148

Table 3-25. B3LYP/6-31G* calculated IR frequencies (cm^{-1}, uncorrected) and intensities for HAPY-2_{anion} 149

Table 3-26. B3LYP/6-31G* optimized geometries, energies, and entropy corrections for enol of PY-3 150

Table 3-27. B3LYP/6-31G* calculated IR frequencies (cm^{-1}, uncorrected) and intensities for enol of PY-3 151

Table 3-28. B3LYP/6-31G* optimized geometries, energies, and entropy corrections for PY-3_{anion} 152

Table 3-29. B3LYP/6-31G* calculated IR frequencies (cm^{-1}, uncorrected) and intensities for PY-3_{anion} 153

Table 3-30. B3LYP/6-31G* optimized geometries, energies, and entropy corrections for HAPY-3 153

Table 3-31. B3LYP/6-31G* calculated IR frequencies (cm^{-1}, uncorrected) and intensities for HAPY-3 154

Table 3-32. B3LYP/6-31G* optimized geometries, energies, and entropy corrections for HAPY-3_{anion} 155

Table 3-33. B3LYP/6-31G* calculated IR frequencies (cm^{-1}, uncorrected) and intensities for HAPY-3_{anion} 156

Table 3-34. B3LYP/6-31G* optimized geometries, energies, and entropy corrections for enol of PY-4 157

Table 3-35. B3LYP/6-31G* calculated IR frequencies (cm^{-1}, uncorrected) and intensities for enol of PY-4 158

Table 3-36. B3LYP/6-31G* optimized geometries, energies, and entropy corrections for PY-4_{anion} 158

Table 3-37. B3LYP/6-31G* calculated IR frequencies (cm^{-1}, uncorrected) and intensities for PY-4_{anion} 159

Table 3-38. B3LYP/6-31G* optimized geometries, energies, and entropy corrections for HAPY-4 160

Table 3-39. B3LYP/6-31G* calculated IR frequencies (cm^{-1}, uncorrected) and intensities for HAPY-4 160

Table 3-40. B3LYP/6-31G* optimized geometries, energies, and entropy corrections for HAPY-4_{anion} 161

Table 3-41. B3LYP/6-31G* calculated IR frequencies (cm^{-1}, uncorrected) and intensities for HAPY-4_{anion} 162

Table 3-42. B3LYP/6-31G* optimized geometries, energies, and entropy corrections for enol of PY-5 163

Table 3-43. B3LYP/6-31G* calculated IR frequencies (cm^{-1}, uncorrected) and intensities for enol of PY-5 164

Table 3-44. B3LYP/6-31G* optimized geometries, energies, and entropy corrections for PY-5_{anion} 164

Table 3-45. B3LYP/6-31G* calculated IR frequencies (cm^{-1}, uncorrected) and intensities for PY-5_{anion} 165

Table 3-46. B3LYP/6-31G* optimized geometries, energies, and entropy corrections for HAPY-5 166

Table 3-47. B3LYP/6-31G* calculated IR frequencies (cm^{-1}, uncorrected) and intensities for HAPY-5 167

Table 3-48. B3LYP/6-31G* optimized geometries, energies, and entropy corrections for HAPY-5_{anion} 168

Table 3-49. B3LYP/6-31G* calculated IR frequencies (cm^{-1}, uncorrected) and intensities for HAPY-5_{anion} 169

Table 3-50. B3LYP/6-31G* optimized geometries, energies, and entropy corrections for enol of PY-6 169

Table 3-51. B3LYP/6-31G* calculated IR frequencies (cm^{-1}, uncorrected) and intensities for enol of PY-6 170

Table 3-52. B3LYP/6-31G* optimized geometries, energies, and entropy corrections for PY-6_{anion} 171

Table 3-53. B3LYP/6-31G* calculated IR frequencies (cm^{-1}, uncorrected) and intensities for PY-6_{anion} 171

Table 3-54. B3LYP/6-31G* optimized geometries, energies, and entropy corrections for HAPY-6 172

Table 3-55. B3LYP/6-31G* calculated IR frequencies (cm^{-1}, uncorrected) and intensities for HAPY-6 173

Table 3-56. B3LYP/6-31G* optimized geometries, energies, and entropy corrections for HAPY-6_{anion} 173

Table 3-57. B3LYP/6-31G* calculated IR frequencies (cm^{-1}, uncorrected) and intensities for HAPY-6_{anion} 174

Table 3-58. B3LYP/6-31G* optimized geometries, energies, and entropy corrections for enol of PY-7 174

Table 3-59. B3LYP/6-31G* calculated IR frequencies (cm^{-1}, uncorrected) and intensities for enol of PY-7 175

Table 3-60. B3LYP/6-31G* optimized geometries, energies, and entropy corrections for PY-7_{anion} 176

Table 3-61. B3LYP/6-31G* calculated IR frequencies (cm^{-1}, uncorrected) and intensities for PY-7_{anion} 177

Table 3-62. B3LYP/6-31G* optimized geometries, energies, and entropy corrections for HAPY-7 178

Table 3-63. B3LYP/6-31G* calculated IR frequencies (cm^{-1}, uncorrected) and intensities for HAPY-7 179

Table 3-64. B3LYP/6-31G* optimized geometries, energies, and entropy corrections for HAPY-7_{anion} 179

Table 3-65. B3LYP/6-31G* calculated IR frequencies (cm^{-1}, uncorrected) and intensities for HAPY-7_{anion} 180

Table 3-66. B3LYP/6-31G* optimized geometries, energies, and entropy corrections for enol of PY-8 181

Table 3-67. B3LYP/6-31G* calculated IR frequencies (cm^{-1}, uncorrected) and intensities for enol of PY-8 182

Table 3-68. B3LYP/6-31G* optimized geometries, energies, and entropy corrections for PY-8_{anion} 183

Table 3-69. B3LYP/6-31G* calculated IR frequencies (cm^{-1}, uncorrected) and intensities for PY-8_{anion} 184

Table 3-70. B3LYP/6-31G* optimized geometries, energies, and entropy corrections for HAPY-8 184

Table 3-71. B3LYP/6-31G* calculated IR frequencies (cm^{-1}, uncorrected) and intensities for HAPY-8 185

Table 3-72. B3LYP/6-31G* optimized geometries, energies, and entropy corrections for HAPY-8_{anion} 186

Table 3-73. B3LYP/6-31G* calculated IR frequencies (cm^{-1}, uncorrected) and intensities for HAPY-8_{anion} 187

Table 3-74. B3LYP/6-31G* optimized geometries, energies, and entropy corrections for enol of PY-9 188

Table 3-75. B3LYP/6-31G* calculated IR frequencies (cm^{-1}, uncorrected) and intensities for enol of PY-9 189

Table 3-76. B3LYP/6-31G* optimized geometries, energies, and entropy corrections for PY-9_{anion} 190

Table 3-77. B3LYP/6-31G* calculated IR frequencies (cm^{-1}, uncorrected) and intensities for PY-9_{anion} 191

Table 3-78. B3LYP/6-31G* optimized geometries, energies, and entropy corrections for HAPY-9 191

Table 3-79. B3LYP/6-31G* calculated IR frequencies (cm^{-1}, uncorrected) and intensities for HAPY-9 192

Table 3-80. B3LYP/6-31G* optimized geometries, energies, and entropy corrections for HAPY-9_{anion} 193

Table 3-81. B3LYP/6-31G* calculated IR frequencies (cm^{-1}, uncorrected) and intensities for HAPY-9_{anion} 194

Table 3-82. B3LYP/6-31G* optimized geometries, energies, and entropy corrections for enol of PY-10 195

Table 3-83. B3LYP/6-31G* calculated IR frequencies (cm^{-1}, uncorrected) and intensities for enol of PY-10 196

Table 3-84. B3LYP/6-31G* optimized geometries, energies, and entropy corrections for PY-10_{anion} 197

Table 3-85. B3LYP/6-31G* calculated IR frequencies (cm^{-1}, uncorrected) and intensities for PY-10_{anion} 198

Table 3-86. B3LYP/6-31G* optimized geometries, energies, and entropy corrections for HAPY-10 199

Table 3-87. B3LYP/6-31G* calculated IR frequencies (cm^{-1}, uncorrected) and intensities for HAPY-10 200

Table 3-88. B3LYP/6-31G* optimized geometries, energies, and entropy corrections for HAPY-10_{anion} 201

Table 3-89. B3LYP/6-31G* calculated IR frequencies (cm^{-1}, uncorrected) and intensities for HAPY-10_{anion} 202

Table 3-90. B3LYP/6-31G* optimized geometries, energies, and entropy corrections for enol of PY-11 203

Table 3-91. B3LYP/6-31G* calculated IR frequencies (cm^{-1}, uncorrected) and intensities for enol of PY-11 204

Table 3-92. B3LYP/6-31G* optimized geometries, energies, and entropy corrections for PY-11_{anion} 204

Table 3-93. B3LYP/6-31G* calculated IR frequencies (cm^{-1}, uncorrected) and intensities for PY-11_{anion} 205

Table 3-94. B3LYP/6-31G* optimized geometries, energies, and entropy corrections for HAPY-11 206

Table 3-95. B3LYP/6-31G* calculated IR frequencies (cm^{-1}, uncorrected) and intensities for HAPY-11 207

Table 3-96. B3LYP/6-31G* optimized geometries, energies, and entropy corrections for HAPY-11_{anion} 208

Table 3-97. B3LYP/6-31G* calculated IR frequencies (cm^{-1}, uncorrected) and intensities for HAPY-11_{anion} 209

Table 3-98. B3LYP/6-31G* optimized geometries, energies, and entropy corrections for enol of PY-12 209

Table 3-99. B3LYP/6-31G* calculated IR frequencies (cm^{-1}, uncorrected) and intensities for enol of PY-12 210

Table 3-100. B3LYP/6-31G* optimized geometries, energies, and entropy corrections for PY-12_{anion} 211

Table 3-101. B3LYP/6-31G* calculated IR frequencies (cm^{-1}, uncorrected) and intensities for PY-12_{anion} 212

Table 3-102. B3LYP/6-31G* optimized geometries, energies, and entropy corrections for HAPY-12 213

Table 3-103. B3LYP/6-31G* calculated IR frequencies (cm^{-1}, uncorrected) and intensities for HAPY-12 214

Table 3-104. B3LYP/6-31G* optimized geometries, energies, and entropy corrections for HAPY-12_{anion} 215

Table 3-105. B3LYP/6-31G* calculated IR frequencies (cm^{-1}, uncorrected) and intensities for HAPY-12_{anion} 216

Table 4-1. HNO-aldol reaction of barbituric acids 259

Table 4-2. Incubation of HABA-3 – HABA-6 in pH 7.4 phosphate buffer at 37 °C under argon with added TXPTS 260

Table 4-3. B3LYP/6-31G* optimized geometries, energies, and entropy corrections for HABA-2 284

Table 4-4. B3LYP/6-31G* calculated IR frequencies (cm^{-1}, uncorrected) and intensities for HABA-2 285

Table 4-5. B3LYP/6-31G* optimized geometries, energies, and entropy corrections for tetrahedral intermediate from HABA-2 286

Table 4-6. B3LYP/6-31G* calculated IR frequencies (cm^{-1}, uncorrected) and intensities for tetrahedral intermediate from HABA-2 287

Table 4-7. B3LYP/6-31G* optimized geometries, energies, and entropy corrections for hydantoin from HABA-2 287

Table 4-8. B3LYP/6-31G* calculated IR frequencies (cm^{-1}, uncorrected) and intensities for hydantoin from HABA-2 288

Table 4-9. B3LYP/6-31G* optimized geometries, energies, and entropy corrections for HABA-3 289

Table 4-10. B3LYP/6-31G* calculated IR frequencies (cm^{-1}, uncorrected) and intensities for HABA-3 290

Table 4-11. B3LYP/6-31G* optimized geometries, energies, and entropy corrections for tetrahedral intermediate from HABA-3 291

Table 4-12. B3LYP/6-31G* calculated IR frequencies (cm^{-1}, uncorrected) and intensities for tetrahedral intermediate from HABA-3 292

Table 4-13. B3LYP/6-31G* optimized geometries, energies, and entropy corrections for hydantoin from HABA-3 293

Table 4-14. B3LYP/6-31G* calculated IR frequencies (cm^{-1}, uncorrected) and intensities for hydantoin from HABA-3 294

Table 5-1. The HNO-aldol screening assay using ^{1}H NMR spectroscopy: results 310

Chapter 1.
Introduction

▪ 1.1 Chemistry of Nitroxyl (HNO)

1.1.1 Nitroxyl (HNO) and Related Nitrogen Oxides

Endogenous nitric oxide (NO) generation in mammalian systems was discovered more than 25 years ago.[1-3] As a result of this significant finding, a fundamentally new paradigm in mammalian cell signaling emerged. That is, a specific biological function could be highly regulated through the use of small, freely diffusible, and reactive molecules. NO, a diatomic radical known previously only as a noxious environmental pollutant, is now known for its capability of regulating, among other things, smooth muscle relaxation and platelet adhesion/aggregation. For their discoveries concerning NO as a signaling molecule in the cardiovascular system, Robert F. Furchgott, Louis J. Ignarro, and Ferid Murad were awarded the Nobel Prize in Medicine in 1998.[4]

In certain aerobic, biological environments, NO can react to form other oxidized species, specifically nitrogen dioxide (NO_2), peroxynitrite ($ONOO^-$), and nitrite (NO_2^-), which are all regarded as important biological effectors, cellular toxins, and/or cellular signaling agents.[5] As the biological fate of NO is thought to be primarily oxidative, research has been focused more on nitrogen oxide species with higher oxidation states. Thus, the one-electron reduced, protonated redox partner to NO, nitroxyl (HNO), has received significantly less attention.

As it turns out, HNO chemistry is significantly more complicated when compared to the chemistry of other nitrogen oxides. At neutral pH in the absence of chemical traps, HNO efficiently dimerizes (k = 8 × 10^6 $M^{-1}s^{-1}$) to hyponitrous acid (HON=NOH), which subsequently dehydrates to nitrous oxide (N_2O).[6] Thus, unlike all other commonly studied nitrogen oxides shown in Table 1-1, HNO cannot be used directly; donor molecules are required for the generation of HNO *in situ*.

Table 1-1. Nitroxyl (HNO) and Related Nitrogen Oxides

Compound	Structure	Oxidation State	Endogenous?
nitrate	NO_3^-	+5	Yes
nitrogen dioxide	NO_2	+4	Yes
nitrite	NO_2^-	+3	Yes
nitric oxide	NO	+2	Yes
nitroxyl	**HNO**	**+1**	***Maybe***
nitrogen	N_2	0	Yes
hydroxylamine	NH_2OH	-1	Yes
ammonia	NH_3	-3	Yes

Much of the recent interest in HNO has been catalyzed by research suggesting that it may be a novel therapeutic of heart failure.[7-11] The discovery of endogenous HNO generation in mammalian systems has yet to be unequivocally demonstrated. Given its inherent reactivity, one of the most important issues in the field is developing a specific and sensitive detector or trap for HNO *in vivo* in order to fully understand the biology of HNO. Such a discovery would imply that regulation pathways for this biologically relevant reactive intermediate might already exist, relieving many toxicology issues regarding HNO as a potential heart failure therapeutic. Indeed, there are several possible biosynthetic pathways to HNO (Scheme 1-1).[12]

Scheme 1-1. Possible Biosynthetic Pathways to HNO[a]

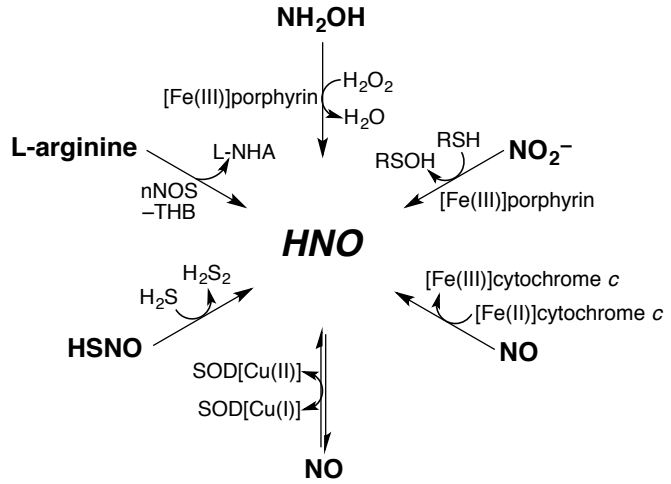

[a]L-NHA = *N*-hydroxy-L-arginine; nNOS = neuronal nitric oxide synthase; SOD = superoxide dismutase; THB = tetrahydrobiopterin. Adapted from Wrobel, A. T.; Johnstone, T. C.; Liang, A. D.; Lippard, S. J.; Rivera-Fuentes, P. *J. Am. Chem. Soc.* **2014**, *136*, 467–4705.

NO is generated from a family of enzymes known as the nitric oxide synthases (NOS), which convert arginine to citrulline and NO in the presence of the cofactor tetrahydrobiopterin (THB).[13,14] Isolated neuronal NOS produces HNO instead of NO in the absence of THB.[14] Other possible redox pathways include the oxidation of hydroxylamine (NH_2OH),[15] the reduction of NO_2^-,[16] or the reduction of NO[17] with heme-containing proteins. In addition, NO and HNO has been demonstrated to interconvert in the presence of superoxide dismutase (SOD).[18] Lastly, nitrosothiols, such as the smallest derivative, HSNO, can serve as HNO donors upon disulfide formation with an additional thiol.[19] Taken together, these results are promising indicators that the endogenous generation of HNO is highly likely, thus providing motivation to those in the field pursuing improved methods for the detection of HNO *in vivo*.

1.1.2 HNO Reactivity and Fundamental Chemical Properties

HNO is a triatomic molecule, yet its structural simplicity belies the complexity of some of its fundamental chemical properties. As described above and shown in Scheme 1-2, dimerization and subsequent N_2O formation precludes straightforward experimentation on HNO.

Scheme 1-2. HNO Reactivity with HNO

Controversy surrounding the pK_a of HNO led to some of the original dismissiveness of HNO as a biologically relevant species. Since the pK_a of HNO was originally reported to be ca. 4.7 based on pulse radiolysis experiments, the nitroxyl anion (NO^-) was expected to dominate at physiological pH.[20] Ellison and co-workers demonstrated that NO^- is bound by only ca. 0.6 kcal/mol relative to electron detachment suggesting that it should be readily oxidized to NO under physiological conditions.[21] However, the biological properties of NO and HNO appear to be different.[7-11, 22-27] For example, Paolocci, Kass, and co-workers at the JHU School of Medicine reported increased level of cGMP, which leads to enhanced relaxation, following administration of the NO donor, diethylamine diazeniumdiolate (DEA/NO). Yet, administration of the HNO donor, Angeli's salt (AS), does not provide increased levels of cGMP.[7,8] Rather, in models of heart failure, defined as the inability of the heart to pump enough blood to supply the metabolic demands of the body, AS-derived HNO has been shown to improve both vasorelaxation and

myocardial contractility via unique mechanisms leading to enhanced intracellular Ca^{2+} cycling.[28]

In addition, the reactivity of HNO with thiols is distinct from that of NO with thiols.[29,30] One of the hallmarks of HNO biological chemistry is the highly thiophilic property of HNO, forming sulfinamides or disulfides depending on the concentration of thiol (Scheme 1-3a), whereas NO requires dioxygen (O_2) for reactivity with thiols, the end products of which are nitrosothiols (Scheme 1-3b).

Scheme 1-3. HNO Versus NO Reactivity with Thiols

(a)

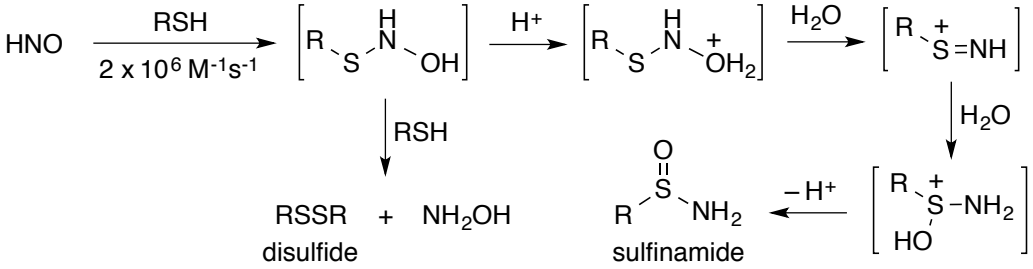

(b)

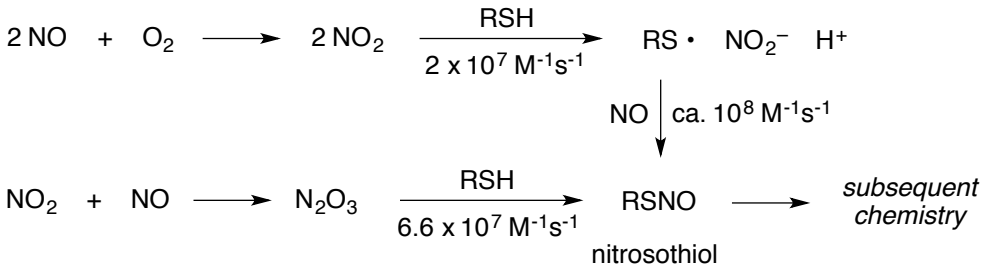

Due to these reports of HNO reactivity at physiological pH, the validity of the pK_a value was called into question. At the time of the original pK_a measurement, the spin states of the HNO/NO^- system were ignored. NO^- is isoelectronic with O_2 and, like O_2, has a triplet ground state.[31] Thus, simple protonation of $^3NO^-$ is formally spin forbidden[32] and uncertainties regarding the pK_a of HNO[6,31] have only recently

been clarified; a value of approximately 11.4 has been obtained by several methods, confirming that HNO is the physiologically relevant protonation state.[6,33,34]

HNO is capable of serving as either an oxidant, as demonstrated by its propensity to react with thiols, or as a reductant. For example, HNO reduces metals including iron (Fe),[35-38] copper (Cu),[39,40] and manganese (Mn)[41,42] via reductive nitrosylation. Also, the H–NO bond strength is only ca. 50 kcal mol^{-1}, indicating that H-atom abstraction by other radical species is facile and, concurrently, generates another established antioxidant, NO.[43]

HNO is isoelectronic with formaldehyde; hence one can envision HNO as an "aldehyde mimetic." Nagasawa and co-workers were among the first to study the biology of HNO as an effective inhibitor of mitochondrial aldehyde dehydrogenase,[44] an enzyme with an active cite cysteine residue responsible for the oxidation of acetaldehyde to acetic acid. Inhibition of aldehyde dehydrogenase results in acetaldehydemia, a condition with general "hangover"-like symptoms such as facial flushing, light-headedness, palpitations, and nausea. Cyanamide (H_2NCN), an alcohol deterrent used clinically in Europe, Canada, and Japan, has been shown to generate HNO following metabolic activation.[44-46] These reports were the first to indicate the pharmacological utility of HNO. A summary of the biologically relevant properties and reactivities of HNO is shown in Figure 1-1.

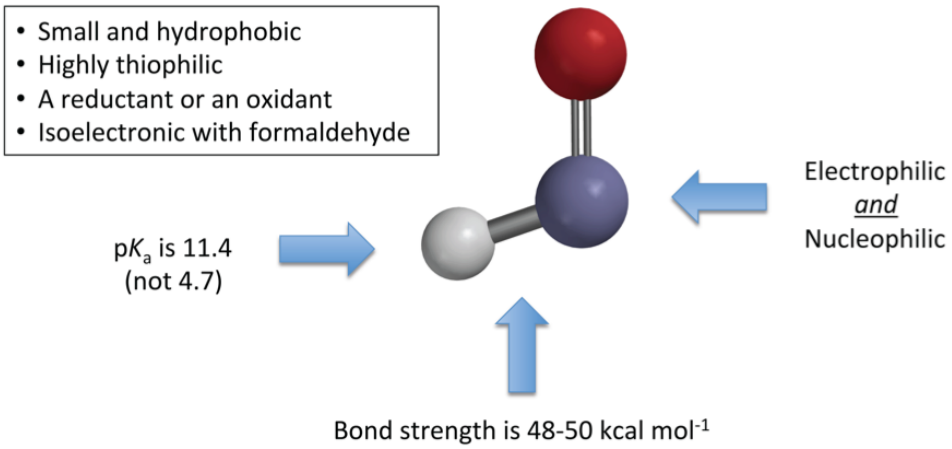

Figure 1-1. The biologically relevant properties and reactivities of HNO.

▪ 1.2 Previously Reported Classes of HNO Donors

Given its inherent activity, HNO cannot be used directly; donor molecules are required for the generation of HNO *in situ*. The most commonly used HNO donor is Angeli's salt (AS), a compound that has been known since 1896.[47] That same year, another HNO donor, Piloty's acid (PA), was also reported.[48] In the intervening 115 years, very few other classes of HNO donors suitable for use under physiological conditions have been developed.[49,50] These include primary amine-based diazeniumdiolates such as IPA/NO,[51-52] acyloxy nitroso compounds (AcON),[53-54] and precursors to the acyl nitroso compounds (AcN),[55-56] which themselves are unstable. Indeed, several recent reviews of HNO chemistry and biology have made pleas for new donors: (1) "As this field grows, there will certainly be a call for the development of new and novel HNO donors."[57] (2) "Sensitive, specific detection methods and a larger variety of HNO donors than Angeli's salt and Piloty's acid, which were first synthesized in the late 1800's, will be required to advance this

promising area of biomedical research."[58] (3) "The design and development of novel HNO donors with distinct properties (e.g., different half-lives and/or release kinetics, cellular permeability and so on) is paramount to further our understanding of the biological activity and therapeutic utility of HNO."[22]

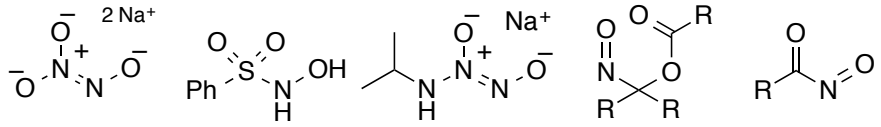

Figure 1-2. Previously reported classes of HNO donors.

1.2.1 Angeli's Salt (AS)

The availability of NO donors such as secondary amine-based diazeniumdiolates (e.g., DEA/NO, Scheme 1-4) was invaluable to the elucidation of the biological properties and endogenous production of NO.[59-62] Angeli's salt (AS), an oxygen-based diazeniumdiolate, releases HNO under physiological conditions and becomes an NO donor under acidic conditions (pH < 4) as shown in Scheme 1-5.[63-64] Due to the relatively short half-life of AS ($t_{1/2}$ = 2.5 min), only the acute biological properties of HNO may be examined. Unfortunately, AS is not amenable to chemical modification without sacrificing the capacity to release HNO.

Scheme 1-4. Secondary Amine-Based Diazeniumdiolates as Versatile NO Donors

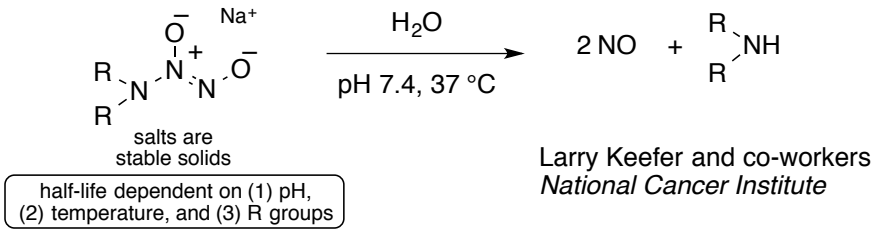

DEA/NO (R = Et) is a commonly used NO donor

Scheme 1-5. Angeli's Salt Decomposition Pathways to HNO and NO

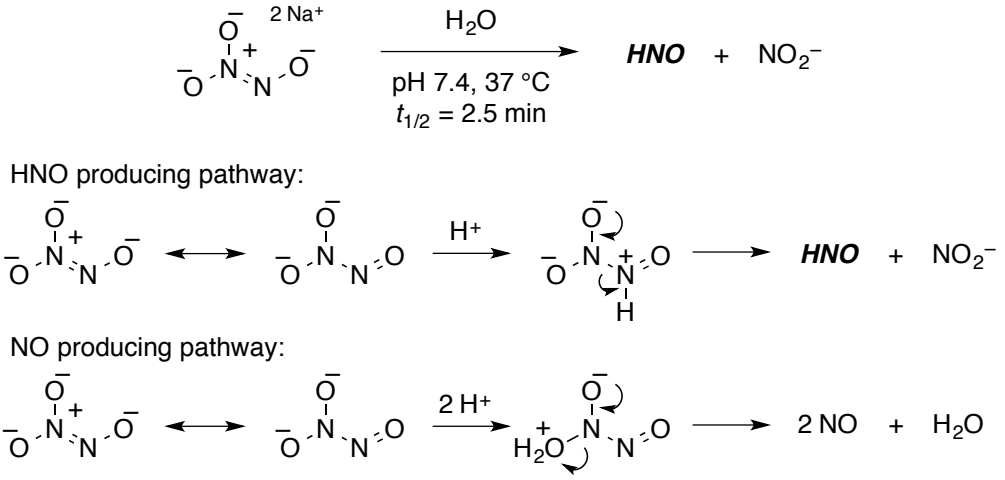

1.2.2 Piloty's Acid (PA) and its Derivatives

Piloty's acid (PA) is an *N*-substituted hydroxylamine derivative equipped with a sulfinate leaving group and releases HNO under alkaline conditions (Scheme 1-6a).[65] However, at neutral pH, PA itself is quite stable ($t_{1/2}$ > 1 h), and under physiological conditions is oxidized, presumably to the corresponding nitroxide, and becomes an NO donor (Scheme 1-6b).[66] In order to favor deprotonation and HNO formation, vs. oxidation, electron-withdrawing groups were attached to the phenyl ring such that the pK_a of the *N*-hydroxysulfonamide precursor was decreased along

with an increased stability of the sulfinate leaving group.[67] The Toscano Lab has generated a wide variety of PA derivatives, most notably 2-bromo-Piloty's acid (2-BrPA), which decomposes with a half-life ($t_{1/2}$ = 2.4 min) and quantitative HNO production at pH 7.4, 37 °C, comparable to AS making it a viable alternative for the study of HNO (Scheme 1-6c).

Scheme 1-6. Piloty's Acid Decomposition Pathways to HNO and NO

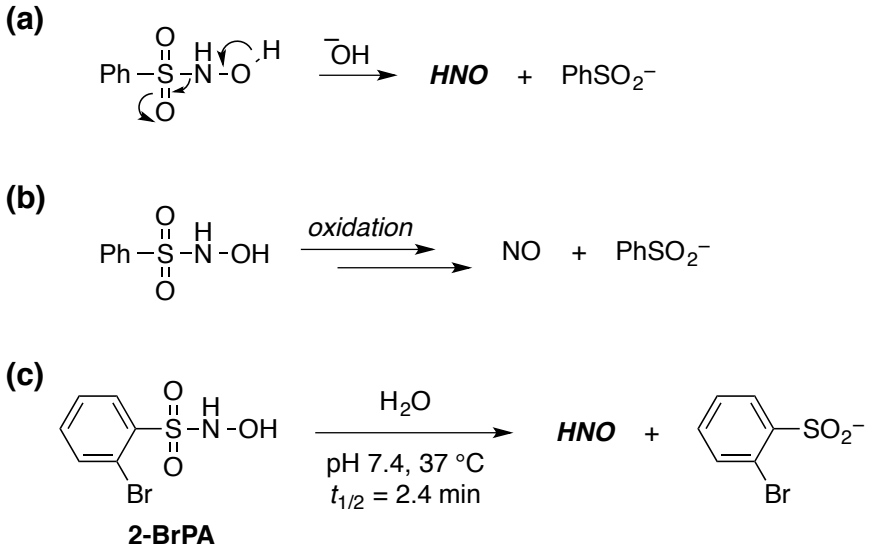

1.2.3 Primary Amine-Based Diazeniumdiolates (IPA/NO)

Primary amine-based diazeniumdiolates may be useful as HNO donors in complement to the existing series of secondary amine-based derivatives, however the comparison in versatility is proving to be no match.[51,52] So far, the only reported example in its salt form is the isopropyl amine derivative IPA/NO, as these compounds are prone to explosive degradation and must be stored in small batches at -78 °C under inert atmosphere with a large headspace in the storage vial. Even so,

IPA/NO efficiently produces ca. equimolar amounts of HNO and NO at neutral pH along with a nitrosamine and isopropylamine, respectively (Scheme 1-7a). The HNO formation pathway requires tautomerization of a labile proton, which explains the thermal instability of these structures. Furthermore, the nitrosamine byproduct, known for its toxicity as an alkylating agent, further decomposes into N_2 and either isopropylene gas or an alkylated nucleophile (Scheme 1-7b).

Scheme 1-7. IPA/NO Decomposition Pathways to HNO and NO

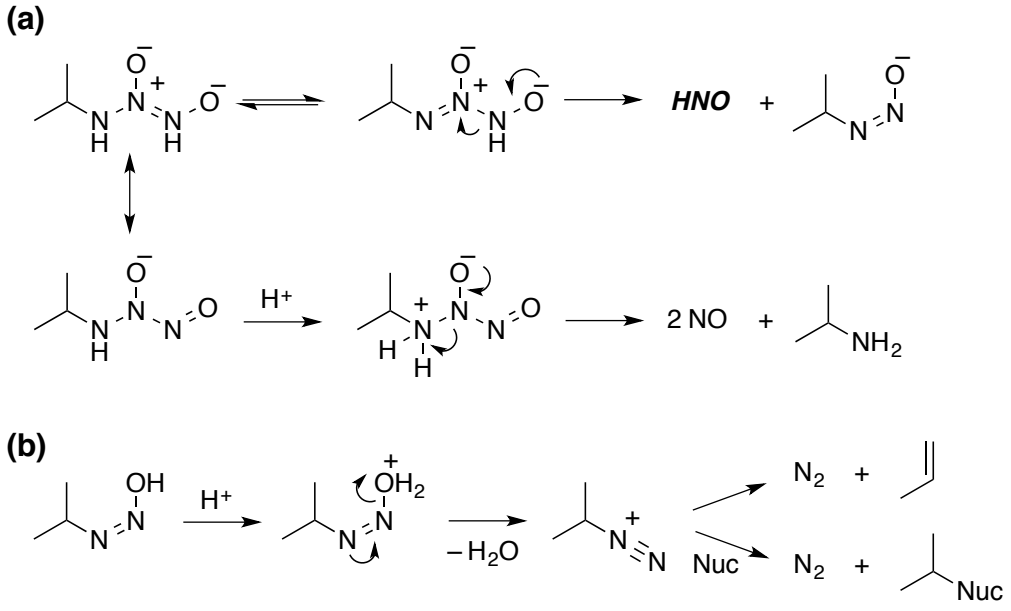

The *O*[2]-protected variants of IPA/NO, on the other hand, provide solid-state stability to this class of compounds. Unexpectedly, dual mechanisms of HNO generation by IPA/NO-AcOM (*i*PrHN-N(O)=NO–CH_2OAc) and IPA/NO-aspirin can occur in the absence of esterases (Scheme 1-8).[68-69]

Scheme 1-8. IPA/NO-AcOM and IPA/NO-aspirin Decomposition Pathway to HNO

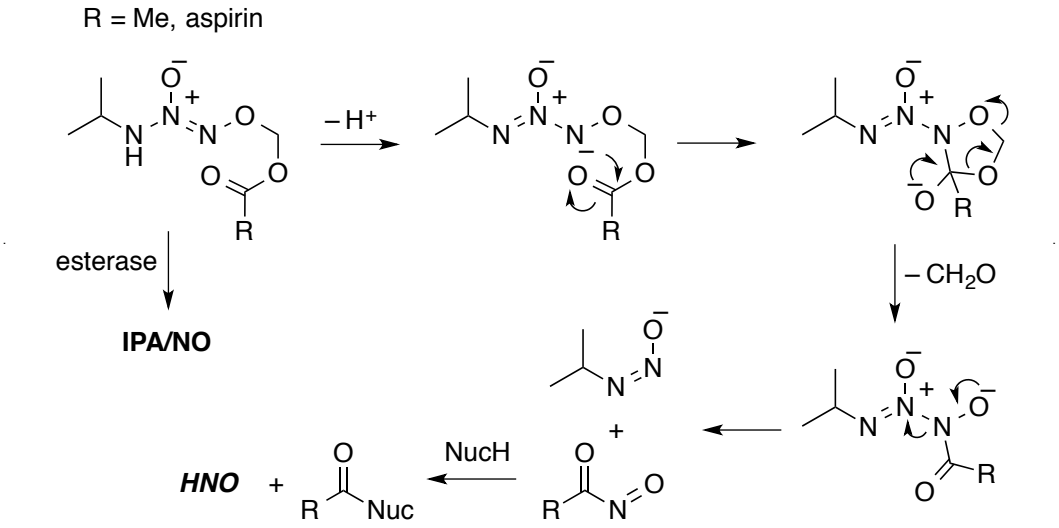

1.2.4 Acyloxy Nitroso Compounds (AcON)

Acyloxy nitroso compounds (AcON) exist as blue monomeric *C*-nitroso compounds and are prepared from the oxidation of oximes in the presence of carboxylic acids.[53,54] Hydrolysis of these compounds releases HNO at rates dependent on the structure of the acyl group (Scheme 1-9a). However, the overall chemistry of this class of HNO donors is more complicated than was originally anticipated. For example, direct and HNO-mediated reactions of acyloxy nitroso compounds have been demonstrated with thiol-containing proteins (Scheme 1-9b).[70,71] Interestingly, some of the same thiol modifications are observed as with HNO.

Scheme 1-9. Direct and HNO-Mediated Reactions of Acyloxy Nitroso Compounds[70]

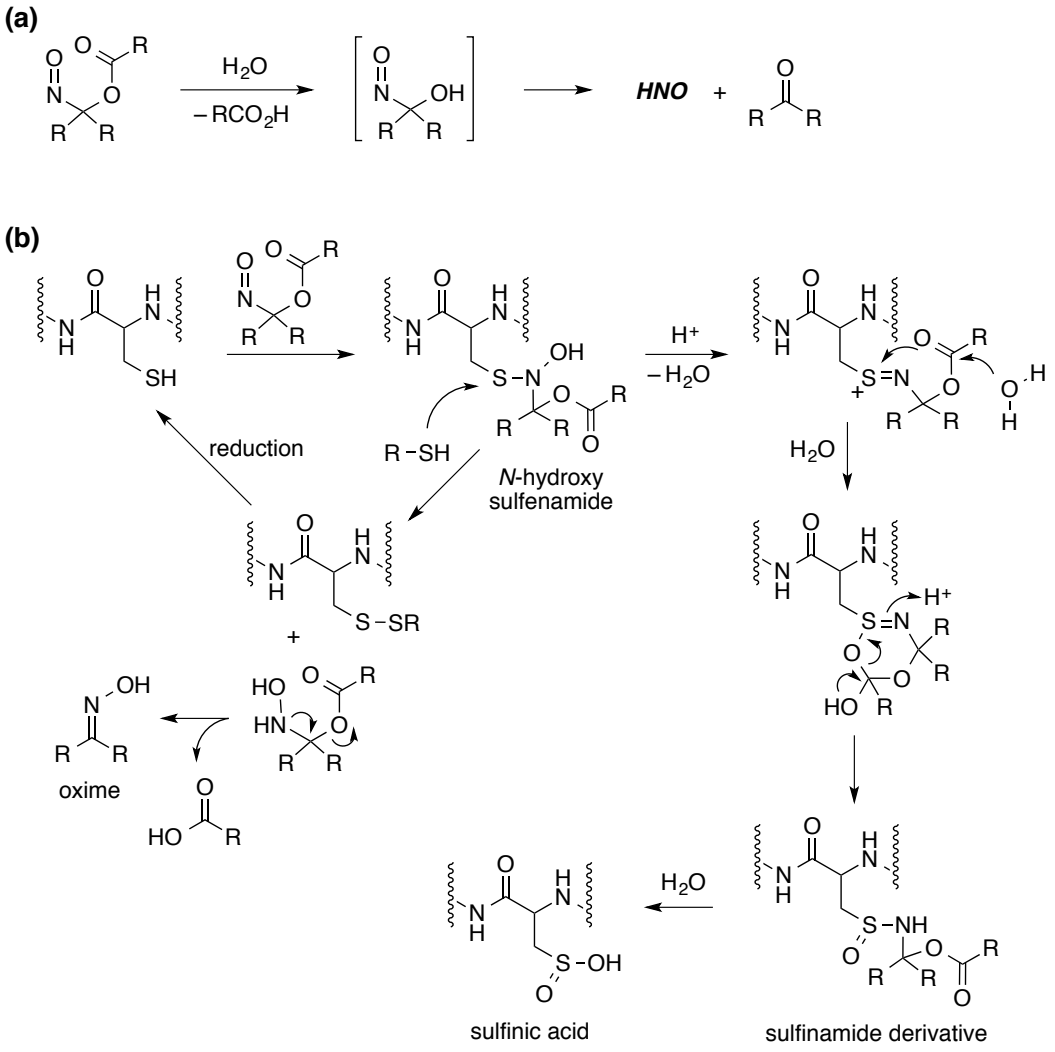

1.2.5 Precursors to Acyl Nitroso Compounds (AcN)

Acyl nitroso compounds are transient electrophiles that react with nucleophiles to yield HNO, and are the most common organic precursors to HNO.[49,72-75] These species are generated by a variety of chemical processes, including the reaction of tertiary amine *N*-oxide with nitrile oxides,[76-78] the dehydrogenation of hydroxamic acids,[73-75,78,79] the hydrolysis of *N*,*O*-*bis*-acylated

hydroxylamine derivatives,[81,82] the thermal fragmentation of Diels-Alder adducts,[73-75,79,83-87] the rearrangement of nitrocarbenes,[88,89] and the photo- or thermal-induced fragmentation of 1,2,4-oxadiazole-4-oxide derivatives.[90,91] The Toscano Lab has generated a wide variety of both thermal and photochemical precursors to AcN compounds, applying time-resolved IR studies for the direct spectroscopic observation of these reactive intermediates (Scheme 1-10).[56]

Scheme 1-10. Generation of Acyl Nitroso Compounds

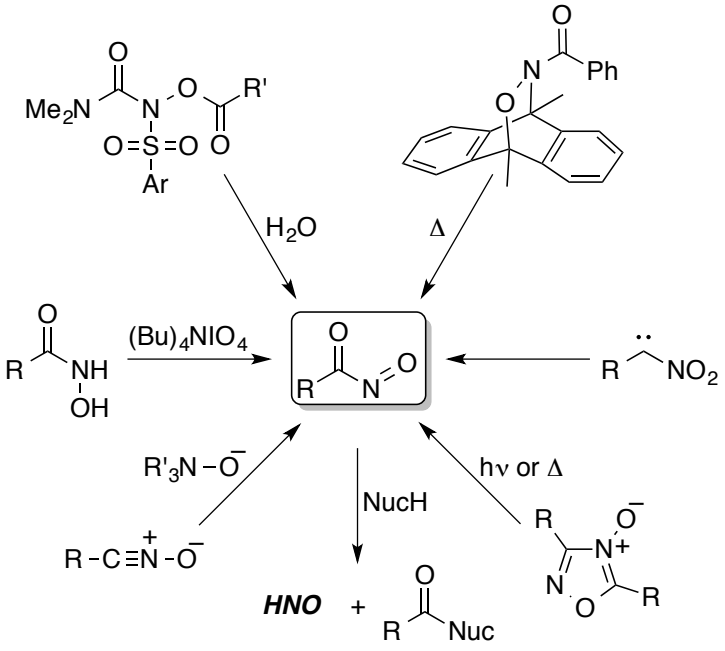

1.2.6 Cyanamide

N-Hydroxycyanamide (HOHN–CN) is an *N*-substituted hydroxylamine with a carbon-based leaving group (cyanide) and a proposed intermediate in the oxidative bioactivation of cyanamide (H_2NCN), an alcohol deterrent used clinically in Europe, Canada, and Japan.[42-44] Cyanamide has been shown to generate HNO, which is a potent inhibitor of aldehyde dehydrogenase, following metabolic activation.

However, *N*-hydroxycyanamide is unstable and has not yet been isolated to confirm its reactivity. In addition, evidence exists that it can be further oxidatively metabolized to a nitrosyl cyanide intermediate (O=NCN) that can also generate HNO following hydrolysis of the nitrile group to form an acyl nitroso compound (Scheme 1-11).[44] An *N*,*O*-dibenzoyl derivative of *N*-hydroxycyanamide has been reported, but this precursor releases HNO not via *N*-hydroxycyanamide, but presumably via an acyl nitroso intermediate, and only following treatment with esterase or base (Scheme 1-12).[81]

Scheme 1-11. Cyanamide Oxidative Decomposition Pathways to HNO

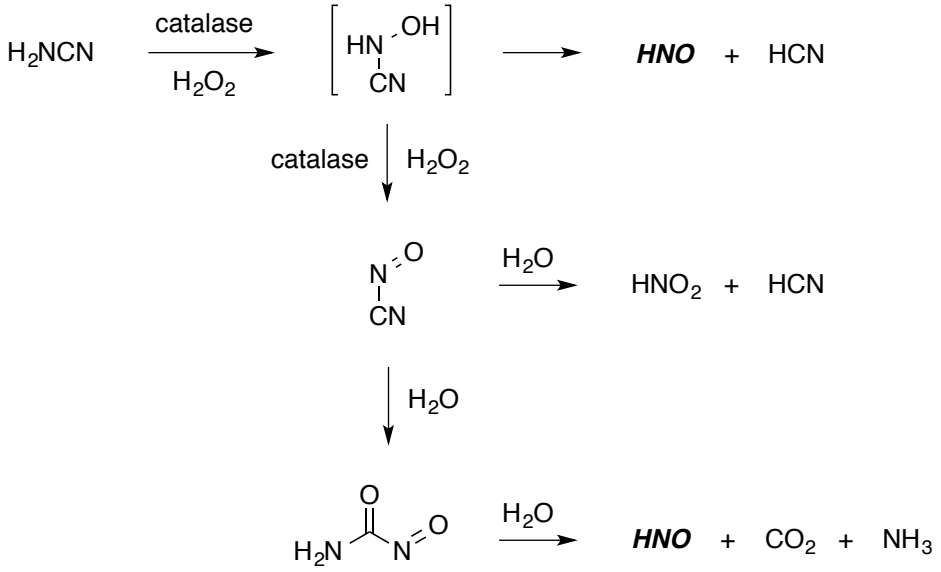

Scheme 1-12. Hydrolysis Pathway to HNO via Acyl Nitroso Intermediate

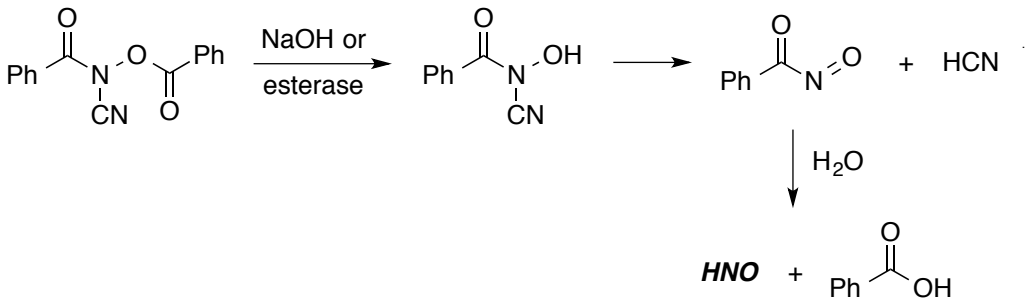

▪ 1.3 Introduction to This Work

The two general strategies we have used to generate HNO at physiological pH and temperature are the dissociation of *N*-substituted hydroxylamines where X is a good leaving group and the generation and hydrolysis of AcN compounds (Scheme 1-13). Piloty's acid and its derivatives, with sulfinate leaving groups, are classic examples of the former strategy.

Scheme 1-13. General Strategies for HNO Release

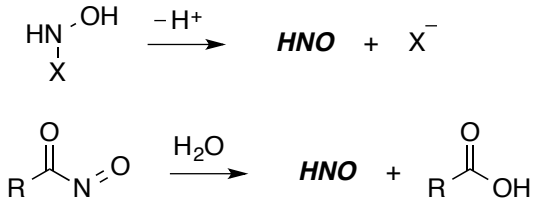

As organic chemists studying in this field, there is a desire to "add carbon" to HNO such that we may continue to call ourselves organic chemists. Therefore, we have synthesized and examined alternative carbon-based leaving groups suitable for HNO generation at neutral pH without enzymatic activation. Importantly, these derivatives avoid the release of toxic cyanide. With a pK_a of 9.4, HCN is a weak acid.

Fortunately, much stronger carbon-based acids exist that we propose could be suitable leaving groups. Chapter 2 introduces three new classes of HNO donors based on Meldrum's acid, barbituric acid, and pyrazolone scaffolds. Chapter 3 deals with the expansion of the pyrazolone scaffold, while Chapter 4 expands on the barbituric acid scaffold, which includes overcoming alternative, non-HNO formation pathways. Lastly, Chapter 5 discusses the application of an assay developed to identify, among other things, potential HNO donors.

▪ 1.4 References

(1) Furchgott, R. F. Studies on relaxation of rabbit aorta by sodium nitrite: The basis for the proposal that the acid-activatable inhibitory factor from retractor penis is inorganic nitrite and the endothelium-derived relaxing factor is nitric oxide. In Vasodilation: Vascular Smooth Muscle, Peptides, Autonomic Nerves and Endothelium; VanHoutte, P. M., Ed.; Raven Press: New York, 1988; pp 401–414.

(2) Ignarro, L. J.; Buga, G. M.; Wood, K. S.; Byrns, R. E.; Chaudhuri, G. *Proc. Natl. Acad. Sci. U.S.A*. **1987**, *84*, 9265**–**9269.

(3) Palmer, R. M. J.; Ferrige, A. G.; Moncada, S. *Nature* **1987**, *327*, 524–526.

(4) "Physiology or Medicine for 1998 - Press Release". Nobelprize.org. Nobel Media AB 2013. Web. 21 May 2014.
<http://www.nobelprize.org/nobel_prizes/medicine/laureates/1998/press.html>

(5) Miranda, K. M.; Espey, M. G.; Jourd'heuil, D.; Grisham, M. B.; Fukuto, J. M.; Feelisch, M.; Wink, D. A. The chemical biology of nitric oxide. In Nitric Oxide Biology and Pathobiology; Ignarro, L. J., Ed.; Academic Press: San Diego, 2000; Chapter 3, pp 41–55.

(6) Shafirovich, V.; Lymar, S. V. *Proc. Natl. Acad. Sci. U.S.A.* **2002**, *99*, 7340−7345.

(7) Paolocci, N.; Saavedra, W. F.; Miranda, K. M.; Martignani, C.; Isoda, T.; Hare, J. M.; Espey, M. G.; Fukuto, J. M.; Feelisch, M.; Wink, D. A.; Kass, D. A. *Proc. Natl. Acad. Sci. U.S.A.* **2001**, *98*, 10463−10468.

(8) Paolocci, N.; Katori, T.; Champion, H. C. St.; John, M. E.; Miranda, K. M.; Fukuto, J. M.; Wink, D. A.; Kass, D. A. *Proc. Natl. Acad. Sci. U.S.A*. **2003**, *100*, 5537−5542.

(9) Paolocci, N.; Jackson, M. I.; Lopez, B. E.; Miranda, K.; Tocchetti, C. G.; Wink, D. A.; Hobbs, A. J.; Fukuto, J. M. *Pharmacol. Ther*. **2007**, *113*, 442−458.

(10) Tocchetti, C. G.; Wang, W.; Froehlich, J. P.; Huke, S.; Aon, M. A.; Wilson, G. M.; Di Benedetto, G.; O'Rourke, B.; Gao, W. D.; Wink, D. A.; Toscano, J. P.; Zaccolo, M.; Bers, D. M.; Valdivia, H. H.; Cheng, H.; Kass, D. A.; Paolocci, N. *Circ. Res.* **2007**, *100*, 96–104.

(11) Froehlich, J. P.; Mahaney, J. E.; Keceli, G.; Pavlos, C. M.; Goldstein, R.; Redwood, A. J.; Sumbilla, C.; Lee, D. I.; Tocchetti, C. G.; Kass, D. A.; Paolocci, N.; Toscano, J. P. *Biochemistry* **2008**, *47*, 13150−13152.

(12) Wrobel, A. T.; Johnstone, T. C.; Liang, A. D.; Lippard, S. J.; Rivera-Fuentes, P. *J. Am. Chem. Soc.* **2014**, *136*, 4697–4705.

(13) Sakai, N.; Kaufman, S.; Milstien, S. *Mol. Pharmacol*. **1993**, *43*, 6–10.

(14) Adak, S.; Wang, Q.; Stuehr, D. J. *J. Biol. Chem*. **2000**, *275*, 33554–33561.

(15) Choe, C.-u.; Lewerenz, J.; Fischer, G.; Uliasz, T. F.; Espey, M. G.; Hummel, F. C.; King, S. B.; Schwedhelm, E.; Böger, R. H.; Gerloff, C.; Hewett, S. J.; Magnus, T.; Donzelli, S. *J. Neurochem*. **2009**, *110*, 1766–1773.

(16) Miljkovic, J. L.; Kenkel, I.; Ivanović-Burmazović, I.; Filipovic, M. R. *Angew. Chem., Int. Ed*. **2013**, *52*, 12061–12064.

(17) Sharpe, M. A.; Cooper, C. E. *Biochem. J*. **1998**, *332*, 9–19.

(18) Murphy, M. E.; Sies, H. *Proc. Natl. Acad. Sci. U.S.A*. **1991**, *88*, 10860–10864.

(19) Filipovic, M. R.; Miljkovic, J. L.; Nauser, T.; Royzen, M.; Klos, K.; Shubina, T.; Koppenol, W. H.; Lippard, S. J.; Ivanović-Burmazović, I. *J. Am. Chem. Soc*. **2012**, *134*, 12016**–**12027.

(20) Gratzel, M.; Taniguchi, S.; Henglein, A. *Ber. Bunsen-Ges. Phys. Chem*. **1970**, *74*, 1003–1010.

(21) Ellis, Jr., H. B.; Ellison, G. B. *J. Chem. Phys.* **1983**, *78*, 6541–6558.

(22) Miranda, K. *Coord. Chem. Rev*. **2005**, *249*, 433–455.

(23) Fukuto, J. M.; Bartberger, M. D.; Dutton, A. S.; Paolocci, N.; Wink, D. A.; Houk, K. N. *Chem. Res. Toxicol*. **2005**, *18*, 790–801.

(24) Irvine, J. C.; Ritchie, R. H.; Favaloro, J. L.; Andrews, K. L.; Widdop, R. E.; Kemp-Harper, B. K. *Trends Pharmacol. Sci*. **2008**, *29*, 601–608.

(25) Fukuto, J. M.; Bianco, C. L.; Chavez, T. A. *Free Radical Biol. Med*. **2009**, *47*, 1318–1324.

(26) Flores-Santana, W.; Salmon, D. J.; Donzelli, S.; Switzer, C. H.; Basudhar, D.; Ridnour, L.; Cheng, R.; Glynn, S. A.; Paolocci, N.; Fukuto, J. M.; Miranda, K. M.; Wink, D. A. *Antioxid. Redox Signaling* **2011**, *14*, 1659–1674.

(27) Kemp-Harper, B. K. *Antioxid. Redox Signaling* **2011**, *14*, 1609–1613.

(28) Tocchetti, C. G.; Stanley, B. A.; Murray, C. I.; Sivakumaran, V.; Donzelli, S.; Mancardi, D.; Pagliaro, P.; Gao, W. D.; van Eyk, J.; Kass, D. A.; Wink, D. A.; Paolocci, N. *Antioxid. Redox Signaling* **2011**, *14*, 1687–1698.

(29) Doyle, M. P.; Mahapatro, S. N.; Broene, R. D.; Guy, J. K. *J. Am. Chem. Soc.* **1988**, *110*, 593–599.

(30) Wong, P. S. Y.; Hyun, J.; Fukuto, J. M.; Shirota, F. N.; DeMaster, E. G.; Shoeman, D. W.; Nagasawa, H. T. *Biochemistry* **1998**, *37*, 5362–5371.

(31) Bartberger, M. D.; Fukuto, J. M.; Houk, K. N. *Proc. Natl. Acad. Sci. U.S.A.* **2001**, *98*, 2194–2198.

(32) Janaway, G. A.; Brauman, J. I. *J. Phys. Chem. A* **2000**, *104*, 1795–1798.

(33) Bartberger, M. D.; Liu, W.; Ford, E.; Miranda, K. M.; Switzer, C.; Fukuto, J. M.; Farmer, P. J.; Wink, D. A.; Houk, K. N. *Proc. Natl. Acad. Sci. U.S.A.* **2002**, *99*, 10958–10963.

(34) Shafirovich, V.; Lymar, S. V. *J. Am. Chem. Soc.* **2003**, *125*, 6547–6552.

(35) Bazylinski, D. A.; Hollocher, T. C. *J. Am. Chem. Soc.* **1985**, *107*, 7982–6.

(36) Farmer, P. J.; Sulc, F. *J. Inorg. Biochem.* **2005**, 99, 166–184.

(37) Sulc, F.; Immoos, C. E.; Pervitsky, D.; Farmer, P. J. *J. Am. Chem. Soc.* **2004**, *126*, 1096–1101.

(38) Immoos, C. E.; Sulc, F.; Farmer, P. J.; Czarnecki, K.; Bocian, D. F.; Levina, A.; Aitken, J. B.; Armstrong, R. S.; Lay, P. A. *J. Am. Chem. Soc.* **2005**, *127*, 814–815.

(39) Murphy, M. E.; Sies, H. *Proc. Natl. Acad. Sci. U.S.A.* **1991**, *88*, 10860–4.

(40) Liochev, S. I.; Fridovich, I. *J. Biol. Chem.* **2001**, *276*, 35253–35257.

(41) Marti, M. A.; Bari, S. E.; Estrin, D. A.; Doctorovich, F. *J. Am. Chem. Soc.* **2005**, *127*, 4680–4684.

(42) Dobmeier, K. P.; Riccio, D. A.; Schoenfisch, M. H. *Anal. Chem.* **2008**, *80*, 1247–1254.

(43) Dixon, R. N. *J. Chem. Phys.* **1996,** *104*, 6905–6906.

(44) DeMaster, E. G.; Redfern, B.; Nagasawa, H. T. *Biochem. Pharmacol*. **1998**, *55*, 2007–2015.

(45) Nagasawa, H. T.; DeMaster, E. G.; Redfern, B.; Shirota, F. N.; Goon, D. J. W. *J. Med. Chem*. **1990**, *33*, 3120–3122.

(46) Shirota, F. N.; Goon, D. J. W.; DeMaster, E. G.; Nagasawa, H. T. *Biochem. Pharmacol*. **1996**, *52*, 141–147.

(47) Angeli, A. *Gazz. Chim. Ital.* **1896**, *26*, 17–25.

(48) Piloty, O. *Ber. Dtsch. Chem. Ges.* **1896**, *29*, 1559–1567.

(49) Miranda, K. M.; Nagasawa, H. T.; Toscano, J. P. *Curr. Top. Med. Chem.* **2005**, *5*, 649–664.

(50) DuMond, J. F.; King, S. B. *Antioxid. Redox Signaling* **2011**, *14*, 1637–1648.

(51) Miranda, K. M.; Katori, T.; Torres de Holding, C. L.; Thomas, L.; Ridnour, L. A.; McLendon, W. J.; Cologna, S. M.; Dutton, A. S.; Champion, H. C.; Mancardi, D.; Tocchetti, C. G.; Saavedra, J. E.; Keefer, L. K.; Houk, K. N.; Fukuto, J. M.; Kass, D. A.; Paolocci, N.; Wink, D. A. *J. Med. Chem.* **2005**, *48*, 8220–8228.

(52) Salmon, D. J.; Torres de Holding, C. L.; Thomas, L.; Peterson, K. V.; Goodman, G. P.; Saavedra, J. E.; Srinivasan, A.; Davies, K. M.; Keefer, L. K.; Miranda, K. M. *Inorg. Chem.* **2011**, *50*, 3262–3270.

(53) Sha, X.; Isbell, T. S.; Patel, R. P.; Day, C. S.; King, S. B. *J. Am. Chem. Soc.* **2006**, *128*, 9687–9692.

(54) Shoman, M. E.; DuMond, J. F.; Isbell, T. S.; Crawford, J. H.; Brandon, A.; Honovar, J.; Vitturi, D. A.; White, C. R.; Patel, R. P.; King, S. B. *J. Med. Chem.* **2011**, *54*, 1059–1070.

(55) Corrie, J. E. T.; Kirby, G. W.; Mackinnon, J. W. M. *J. Chem. Soc., Perkin Trans. 1* **1985**, 883–886.

(56) Cohen, A. D.; Zeng, B.-B.; King, S. B.; Toscano, J. P. *J. Am. Chem. Soc.* **2003**, *125*, 1444–1445.

(57) Fukuto, J. M.; Bartberger, M. D.; Dutton, A. S.; Paolocci, N.; Wink, D. A.; Houk, K. N. *Chem. Res. Toxicol.* **2005**, *18*, 790–801.

(58) Miranda, K. M. *Coord. Chem. Rev.* **2005**, *249*, 433–455.

(59) Hrabie, J. A.; Keefer, L. K. *Chem. Rev*. **2002**, *102*, 1135–1154.

(60) Thomas, D. D.; Miranda, K. M.; Espey, M. G.; Citrin, D.; Jourd'Heuil, D.; Paolocci, N.; Hewett, S. J.; Colton, C. A.; Grisham, M. B.; Feelisch, M.; Wink, D. A. *Methods Enzymol*. **2002**, *359*, 84–105.

(61) Keefer, L. K. *Annu. Rev. Pharmacol. Toxicol*. **2003**, *43*, 585–607.

(62) Feelisch, M.; Stamler, J. S. Donors of Nitrogen Oxides. In Methods in Nitric Oxide Research; Feelisch, M., Stamler, J. S., Eds.; John Wiley & Sons: New York, 1996; pp 71–115.

(63) Bonner, F. T.; Ravid, B. *Inorg. Chem*. **1975**, *14*, 558–563.

(64) Hughes, M. N.; Wimbledon, P. E. *J. Chem. Soc., Dalton Trans*. **1976**, *8*, 703–707.

(65) Bonner, F.T.; Ko, Y. *Inorg. Chem*. **1992**, *31*, 2514–2519.

(66) Zamora, R.; Grzesiok, A.; Weber, H.; Feelisch, M. *Biochem. J.* **1995**, *312*, 333–339.

(67) Toscano, J. P.; Brookfield, F. A.; Cohen, A. D.; Courtney, S. M.; Frost, L. M.; Kalish, V. J. "*N*-Hydroxysulfonamide Derivatives as Physiologically Useful Nitroxyl Donors" U.S. Patent 8,030,356, **2011**.

(68) Andrei, D.; Salmon, D. J.; Donzelli, S.; Wahab, A.; Klose, J. R.; Citro, M. L.; Saavedra, J. E.; Wink, D. A.; Miranda, K. M.; Keefer, L. K. *J. Am. Chem. Soc.* **2010**, *132*, 16526–16532.

(69) Basudhar, D.; Bharadwaj, G.; Cheng, R. Y.; Jain, S.; Shi, S.; Heinecke, J. L.; Holland, R. J.; Ridnour, L. A.; Caceres, V. M.; Spadari-Bratfisch, R. C.; Paolocci, N.; Velázquez-Martínez, C. A.; Wink, D. A.; Miranda, K. M. *J. Med. Chem*. **2013**, *56*, 7804–7820.

(70) Mitroka, S.; Shoman, M. E.; DuMond, J. F.; Bellavia, L.; Aly, O. M.; Abdel-Aziz, M.; Kim-Shapiro, D. B.; King, S. B. *J. Med. Chem*. **2013**, *56*, 6583–6592.

(71) Shoman, M. E.; DuMond, J. F.; Isbell, T. S.; Crawford, J. H.; Brandon, A.; Honovar, J.; Vitturi, D. A.; White, C. R.; Patel, R. P.; King, S. B. *J. Med. Chem*. **2011**, *54*, 1059–1070.

(72) King, S. B.; Nagasawa, H. T. *Methods Enzymol*. **1999**, *301*, 211–220.

(73) Atkinson, R. N.; Storey, B. M.; King, S. B. *Tetrahedron Lett*. **1996**, *37*, 9287–9290.

(74) Kirby, G. W.; Sweeny, J. G. *J. Chem. Soc. Perkin Trans. 1* **1981**, 3250–3254.

(75) Corrie, J. E. T.; Kirby, G. W.; Mackinnon, J. W. M. *J. Chem. Soc. Perkin Trans. 1* **1985**, 883–886.

(76) Quadrelli, P.; Invernizzi, A. G.; Caramella, P. *Tetrahedron Lett*. **1996**, *37*, 1909–1912.

(77) Quadrelli, P.; Mella, M.; Caramella, P. *Tetrahedron Lett*. **1998**, *39*, 3233–3236.

(78) Quadrelli, P.; Mella, M.; Invernizzi, A. G.; Caramella, P. *Tetrahedron* **1999**, *55*, 10497–10510.

(79) Kirby, G. W. *Chem. Soc. Rev*. **1977**, *6*, 1–24.

(80) Kirby, G. W.; Sweeny, J. G. *Chem. Commun*. **1973**, 704–705.

(81) Nagasawa, H. T.; Lee, M. J.; Kwon, C. H.; Shirota, F. N.; DeMaster, E. G. *Alcohol* **1992**, *9*, 349–353.

(82) Sutton, A. D.; Williamson, M.; Weismiller, H.; Toscano, J. P. *Org. Lett*. **2012**, *14*, 472–475.

(83) Keck, G. E.; Webb, R. R.; Yates, J. B. *Tetrahedron Lett*. **1981**, *37*, 4007–4016.

(84) Ensley, H. E.; Mahadevan, S. *Tetrahedron Lett*. **1989**, *30*, 3255–3258.

(85) Xu, Y. P.; Alavanja, M. M.; Johnson, V. L.; Yasaki, G.; King, S. B. *Tetrahedron Lett*. **2000**, *41*, 4265–4269.

(86) Zeng, B. B.; King, S. B. *Synthesis* **2002**, 2335–2337.

(87) Zeng, B. B.; Huang, J. M.; Wright, M. W.; King, S. B. *Bioorg. Med. Chem. Lett*. **2004**, *14*, 5565–5568.

(88) O'Bannon, P. E.; Dailey, W. P. *Tetrahedron Lett*. **1988**, *29*, 987–990.

(89) O'Bannon, P. E.; Dailey, W. P. *Tetrahedron Lett*. **1988**, *29*, 5719–5722.

(90) Quadrelli, P.; Mella, M.; Caramella, P. *Tetrahedron Lett*. **1999**, *40*, 797–800.

(91) Quadrelli, P.; Campari, G.; Mella, M.; Caramella, P. *Tetrahedron Lett*. **2000**, *41*, 2019–2022.

Chapter 2.

Development of *N*-Substituted Hydroxylamines as Efficient Nitroxyl (HNO) Donors

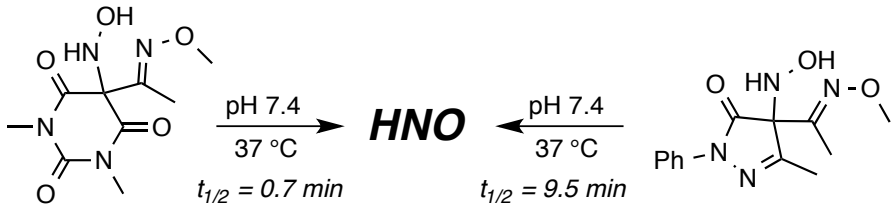

▪ 2.1 Abstract

Due to its inherent reactivity, nitroxyl (HNO) must be generated *in situ* through the use of donor compounds, but very few physiologically useful HNO donors exist. Novel *N*-substituted hydroxylamines with carbon-based leaving groups have been synthesized, and their structures confirmed by X-ray crystallography. These compounds generate HNO under nonenzymatic, physiological conditions, with the rate and amount of HNO released being dependent mainly on the nature of the leaving group. A barbituric acid and a pyrazolone derivative have been developed as efficient HNO donors with half-lives at pH 7.4, 37 °C of 0.7 and 9.5 min, respectively.

▪ 2.2 Introduction

Nitroxyl (HNO) has been shown to have biological activity distinct from that of its redox cousin, nitric oxide (NO), and related nitrogen oxides.[1–11] Much of the recent interest in HNO has been catalyzed by research suggesting that it may be a novel therapeutic for the treatment of heart failure.[1–5] At neutral pH in the absence of chemical traps, HNO efficiently dimerizes (k = 8 × 10^6 $M^{-1}s^{-1}$) to hyponitrous acid (HON=NOH), which subsequently dehydrates to nitrous oxide (N_2O).[12] Given this inherent reactivity, HNO cannot be used directly; donor molecules are required for the generation of HNO *in situ*.

The most commonly used HNO donor is Angeli's salt (**AS**) (Figure 2-1), a compound that has been known since 1896.[13] That same year, another HNO donor, Piloty's acid (**PA**), was also reported.[14] In the intervening 115 years, very few other classes of HNO donors suitable for use under physiological conditions have been developed.[15,16] These include primary amine-based diazeniumdiolates such as **IPA/NO**,[17,18] acyloxy nitroso compounds (**AcON**),[19,20] and precursors to the acyl nitroso compounds (**AcN**),[21–23] which themselves are unstable. Indeed, several recent reviews of HNO chemistry and biology have made pleas for new donors.[6–8]

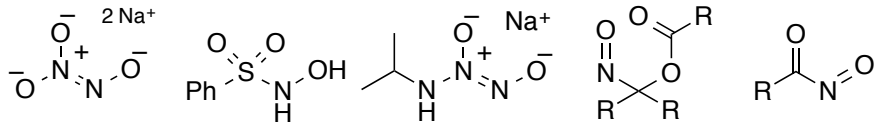

Figure 2-1. Previously reported classes of HNO donors.

Herein, we are pleased to report a new class of HNO donors based on the general strategy shown in Scheme 2-1 for *N*-substituted hydroxylamines where X is

a good leaving group. Piloty's acid and its derivatives,[24] with sulfinate leaving groups, are classic examples of this strategy. We have employed good carbon-based leaving groups such that HNO is released along with a stable carbanion at neutral pH.

Scheme 2-1. General Strategy for HNO Release

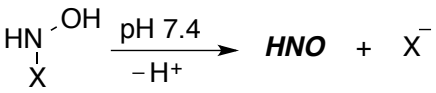

N-Hydroxycyanamide (HOHN–CN) is an *N*-substituted hydroxylamine with a carbon-based leaving group (cyanide) and a proposed intermediate in the oxidative bioactivation of cyanamide (H_2NCN), an alcohol deterrent used clinically in Europe, Canada, and Japan.[25–27] Cyanamide has been shown to generate HNO, which is a potent inhibitor of aldehyde dehydrogenase, following metabolic activation. However, *N*-hydroxycyanamide is unstable and has not yet been isolated to confirm its reactivity. In addition, evidence exists that it can be further oxidatively metabolized to a nitrosyl cyanide intermediate (O=NCN) that can also generate HNO following hydrolysis of the nitrile group to form an acyl nitroso compound.[26] An *N*,*O*-dibenzoyl derivative of *N*-hydroxycyanamide has been reported, but this precursor releases HNO not via *N*-hydroxycyanamide, but presumably via an acyl nitroso intermediate, and only following treatment with esterase or base.[28]

We have synthesized and examined alternative *N*-substituted hydroxylamines with carbon-based leaving groups suitable for HNO generation at neutral pH without enzymatic activation. In addition, these derivatives importantly avoid the release of toxic cyanide.

▪ 2.3 Results and Discussion

We first considered Meldrum's acid derivative **1a**, which was expected to generate HNO as shown in Scheme 2-2a. This precursor was easily synthesized without the need for chromatographic purification by formation of the corresponding bromide followed by reaction with *N*,*O*-*bis*(*tert*-butoxycarbonyl) hydroxylamine and subsequent acid deprotection, as shown in Scheme 2-3. The other precursors reported here were synthesized analogously, and all structures were confirmed by X-ray crystallography. (See Experimental and Supporting Information for experimental details concerning the synthesis and characterization of all precursors.)

Scheme 2-2. Potential HNO Release Pathways from (a) Meldrum's Acid Derivatives 1a and 2a and (b) Barbituric Acid Derivatives 3a and 4a

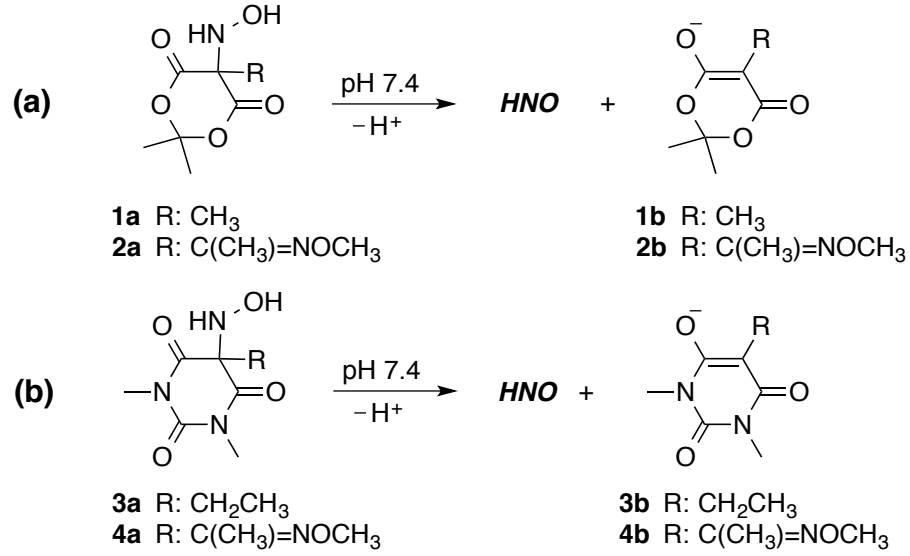

Scheme 2-3. Synthesis of Meldrum's Acid Derivative 1a

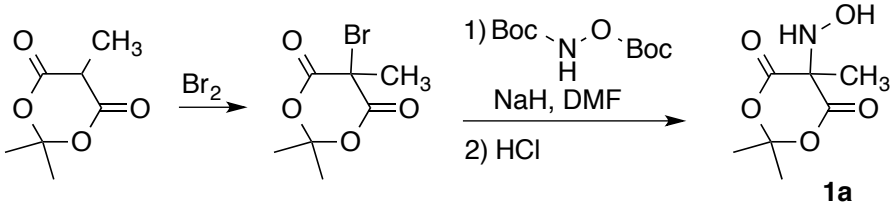

Compound **1a** was examined for HNO generation by gas chromatographic (GC) headspace analysis to quantify the amount of its dimerization product, N_2O, formed following decomposition in pH 7.4 phosphate buffered saline (PBS) at 37 °C. (See Experimental for details.) Unfortunately, only trace amounts of N_2O are observed (Table 2-1). Meldrum's acid (pK_a = 4.8)[29] is completely ionized at pH 7.4, and its 5,5-dimethyl derivative has a hydrolysis half-life of about 12 h under physiological conditions.[30] Nonetheless, the major product observed for **1a** by ^{1}H NMR spectroscopy is acetone (Supporting Information), indicative of a dominant ring-opening reaction pathway.

Table 2-1. Decomposition of HNO Donors

donor	% HNO[a]	% carbanion[b]	$t_{1/2}$ (min)[c]
1a	2	4[d]	*f*
2a	25	34[d]	0.9
3a	2	6[e]	*f*
4a	110	>95	0.7
6a	110	>95	9.5

[a]Donor compounds (0.1 mM) were incubated at 37 °C in PBS, pH 7.4. HNO yields are reported relative to the standard HNO donor, Angeli's salt, as determined by N_2O headspace analysis (SEM ± 5%; $n \geq 3$). N_2O production was completely quenched with added glutathione (0.2 mM). [b]Yields of carbanions **1b**–**4b**, **6b** were determined by ^{1}H NMR spectroscopy. [c]Determined from UV-vis kinetic experiments. [d]Relative to the major byproduct, acetone. [e]Relative to rearrangement byproduct **5**. [f]Not determined.

We next examined Meldrum's acid derivative **2a**, equipped with an electron-deficient *O*-methyloxime moiety. Relative to **1a**, an enhanced HNO yield is observed (Table 2-1), attributed to **2b** being a better leaving group. However, acetone is still the major product, indicating that the non-HNO producing ring-opening reaction pathway remains competitive with the desired pathway. Evidently, a more robust ring system that disfavors alternative decomposition pathways is necessary.

To explore the impact of a different ring system, we evaluated barbituric acid derivatives **3a** and **4a** (Scheme 2-2b). Barbiturate **3a** unexpectedly produced very little HNO (Table 2-1). Following a large-scale decomposition, the major organic byproduct was isolated and identified by X-ray crystallography, revealing that barbiturate **3a** primarily undergoes an intramolecular rearrangement to compound **5** in pH 7.4 buffer solutions (Scheme 2-4).

Scheme 2-4. Major Reaction Pathway for Barbiturate 3a

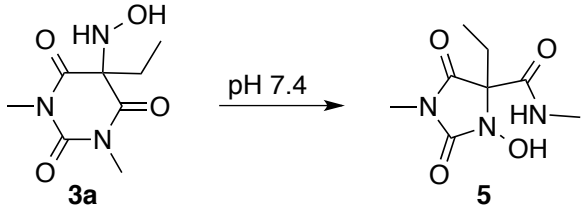

3a **5**

Given the positive impact that an electron-deficient *O*-methyloxime group had on HNO production from Meldrum's acid derivatives above, we analyzed an analogous substitution on the barbituric acid ring system. Satisfyingly, exchanging the ethyl group in **3a** with an *O*-methyloxime in barbiturate **4a** strongly favors the generation of HNO, as reflected by the high yield of N_2O observed following decomposition (Table 2-1). HNO was confirmed as the source of N_2O for this and the other precursors examined by quenching with glutathione, a known efficient trap for HNO.[31,32]

The decomposition of **4a** was monitored by ^{1}H NMR spectroscopy in PBS (pH 7.4, room temperature), and the only detectable organic byproduct was the expected carbanion **4b** (Figure 2-2a). With an estimated pK_a of ca. 4 (Figure 2-3a), the byproduct is completely ionized at neutral pH. Influenced by the *O*-methyloxime group, this pK_a is slightly lower than that of *N*,*N*-dimethyl barbituric acid (pK_a =

4.7).[33] Although the pharmacology of **4b** has not yet been evaluated, barbituric acids and their C5-substituted derivatives in general have an expansive history in medicinal chemistry including hypnotic, sedative, antiepileptic, and immunomodulation applications.[34]

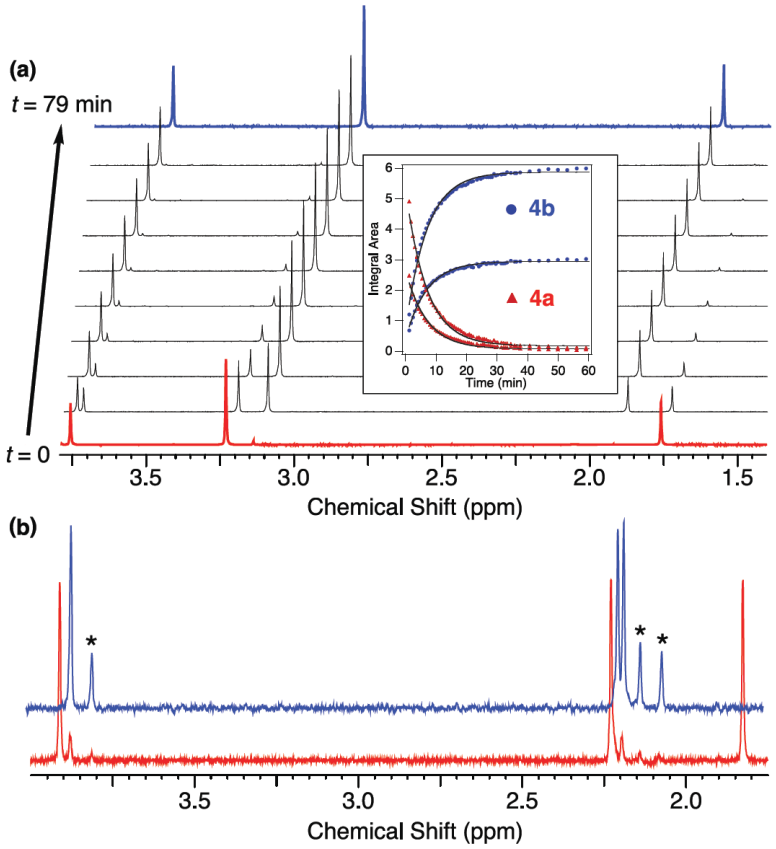

Figure 2-2. ^{1}H NMR analysis of the decomposition of (a) **4a** to **4b** and (b) **6a** to **6b** in 10% D_2O, PBS, pH 7.4 at room temperature. In each case, the red spectrum was collected at the start of the experiment, and the blue spectrum after complete decomposition. In the insert of (a), the kinetics of decomposition are shown. The red triangles represent the N-*CH*$_3$'s (6H) and the oxime C-*CH*$_3$ (3H) of **4a**, and the blue circles represent the N-*CH*$_3$'s (6H) and the oxime C-*CH*$_3$ (3H) of carbanion **4b**. The solid curves are calculated best fits to a single exponential function (k = 2.4 × 10^{-3} s^{-1} for each fit). In (b), the asterisks (*) indicate signals due to the minor *anti*-**6b** isomer.

The kinetics of decomposition from **4a** to **4b** was easily monitored by UV-vis spectroscopy given the distinctive absorbance of anion **4b** (λ_{max} = 261 nm) (Figure

2-4a). Analysis of the decomposition rate as a function of pH reveals a sharp increase near pH 8 (Figure 2-4b). Barbiturate **4a** has a half-life of ca. 1 min at pH 7.4 and 37 °C (Figure 2-4a) but is relatively stable at pH 4.0 and room temperature, with a half-life of approximately 12 h under these conditions (Supporting Information).

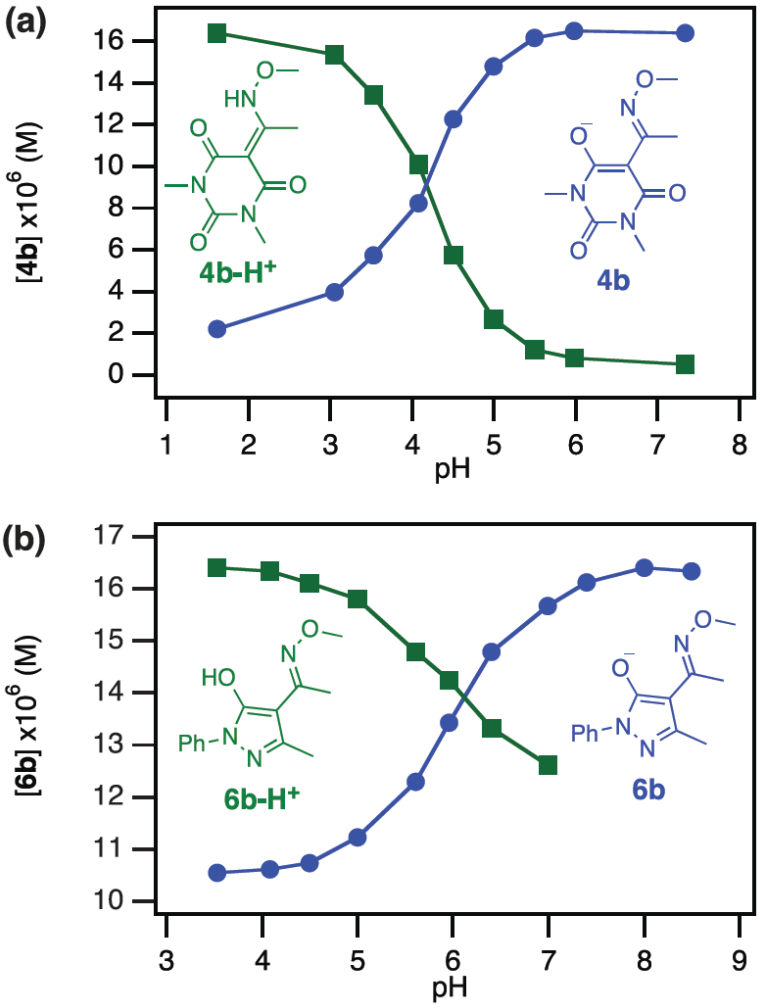

Figure 2-3. Plot of the concentration of (a) **4b**, **4b-H**$^+$, and (b) **6b**, **6b-H**$^+$ as a function of pH. In (a), the green squares represent **4b-H**$^+$ (λ_{max} = 298 nm), and blue circles represent carbanion **4b** (λ_{max} = 261 nm). In (b), the green squares represent **6b-H**$^+$ (λ_{max} = 270 nm), where the last three data points were omitted due to spectral overlap, and the blue circles represent carbanion **6b** (λ_{max} = 253 nm). See Supporting Information for representative UV-vis spectra of **4b** and **6b** at high and low pH.

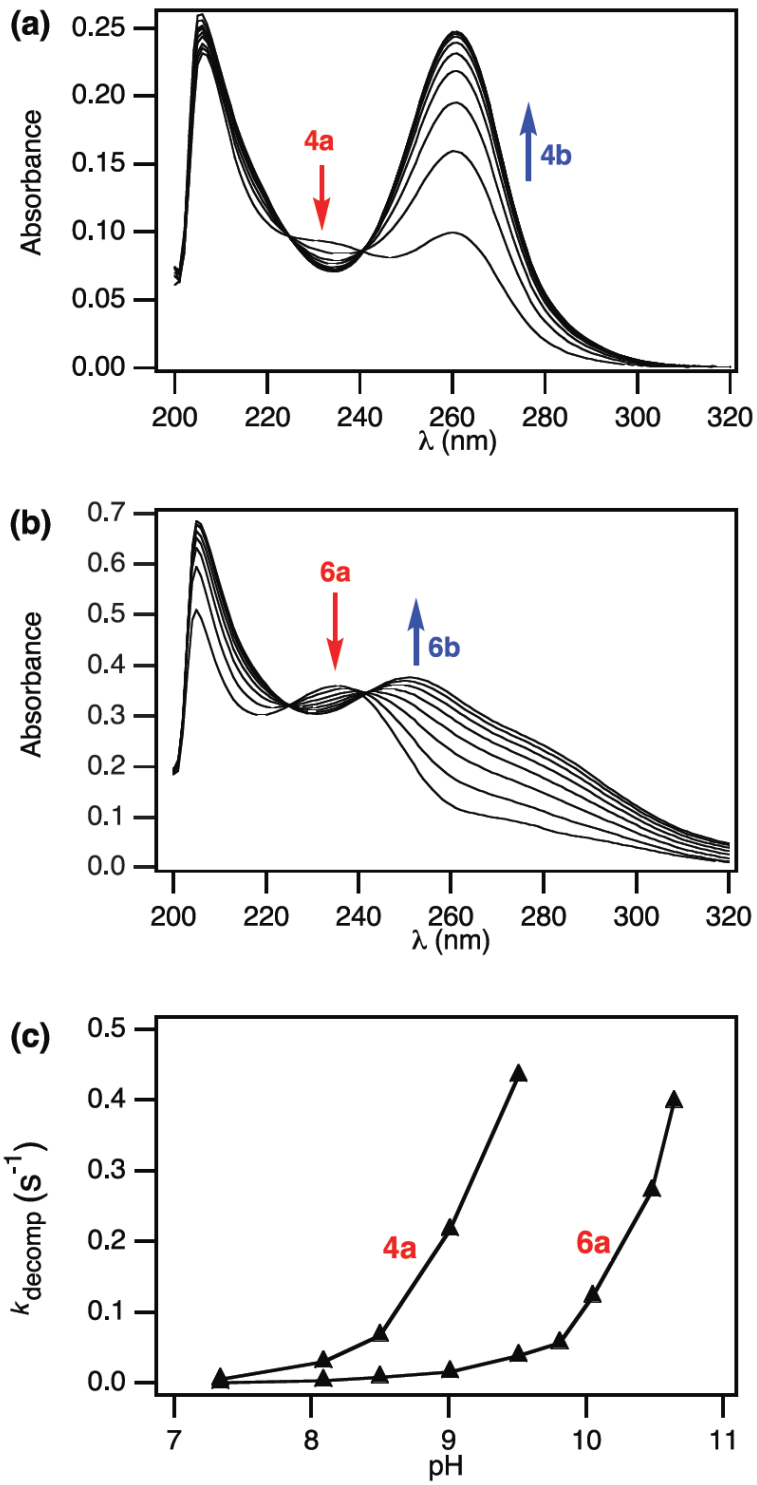

Figure 2-4. UV-vis analysis of the decomposition of (a) **4a** (time between traces = 30 s) and (b) **6a** (time between traces = 240 s) at 37 °C in PBS, pH 7.4. (c) Plot of UV-vis determined decomposition rate as a function of pH at 25 °C for **4a** (monitored at 261 nm) and **6a** (monitored at 253 nm).

To demonstrate the generality of this approach for HNO generation, we have also examined another *N*-substituted hydroxylamine with a suitable carbon-based leaving group. Like barbiturates **3a** and **4a**, pyrazolone **6a** (synthesized analogously to compounds **1a**–**4a**) also takes advantage of the formation of an aromatic byproduct (**6b**) (Scheme 2-5) and efficiently produces HNO with a half-life of ca. 10 min at pH 7.4, 37 °C (Table 2-1). Another potentially practical benefit enjoyed by precursor **6a** is that byproduct **6b**, formed along with HNO, is a 4-substituted derivative of edaravone (Scheme 2-5), a potent antioxidant already in clinical use for the treatment of stroke and cardiovascular disease.[35,36] Moreover, a variety of 4-substituted edaravone analogues have also shown strong antioxidant activity.[37]

Scheme 2-5. HNO Release from Pyrazolone Derivative 6a

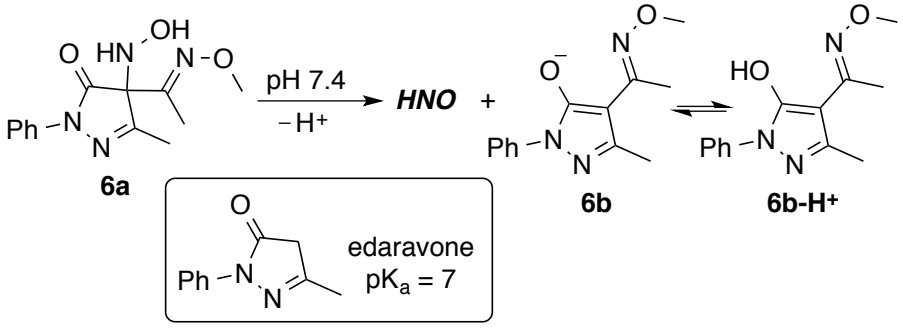

The decomposition of **6a** was analyzed similarly to that of **4a** by ^{1}H NMR spectroscopy in PBS (pH 7.4, room temperature) (Figure 2-2b). The only organic byproducts observed by this analysis are the syn (major) and anti (minor) isomers of **6b** (Scheme 2-5), and the relative abundance of these isomers is unchanged at high and low pH. Donors **6a**, **2a**, and **4a** are observed to be all syn by NMR analysis and X-ray crystallography.

The pK_a of **6b**/**6b-H$^+$** is estimated to be ca. 6 (Figure 2-3b), shifted below that of edaravone (pK_a = 7) by *O*-methyloxime substitution, indicating that nearly all of

this byproduct is ionized at pH 7.4. As was the case for precursor **4a**, the decomposition rate of pyrazolone **6a** is highly pH dependent, here with a sharp increase near pH 10 (Figure 2-4c); **6a** is much more stable at pH 4.0, with a half-life of about 25 h at room temperature (Supporting Information).

▪ 2.4 Conclusion

The data presented on compounds **1a**–**4a** and **6a** suggest that the ability of these *N*-substituted hydroxylamines to generate HNO is based mainly on the nature of the leaving group. To produce HNO efficiently, the driving force for the formation of a stabilized carbanion must overcome other non-HNO producing reaction pathways. Barbiturate **4a** and pyrazolone **6a**, easily synthesized without the need for chromatographic purification, have been developed as effective HNO donors with half-lives at pH 7.4, 37 °C of 0.7 and 9.5 min, respectively. These compounds represent new examples of the general strategy for HNO production from *N*-substituted hydroxylamines with good leaving groups. Future work will involve the further development of this strategy with other suitable carbon-based leaving groups.

▪ 2.5 Experimental

2.5.1 Methods and Materials

All starting materials were of reagent grade and used without further purification. 5-Bromo-5-methyl-Meldrum's acid[38] was obtained through bromination of 5-methyl-Meldrum's acid (sodium bicarbonate, bromine, water). 5-Acetyl-Meldrum's acid[39] was obtained through acylation of Meldrum's acid (acetic acid, *N*,*N*-dicyclohexylcarbodiimide, 4-dimethylaminopyridine, dichloromethane). 5-Acetyl *N*,*N*-dimethylbarbituric acid[39,40] was obtained through acylation of *N*,*N*-dimethylbarbituric acid (acetyl chloride, pyridine, dichloromethane). 5-Ethyl barbituric acid[41] was obtained through reduction of 5-acetyl-Meldrum's acid (sodium cyanoborohydride, acetic acid). 4-Acetyl-*N*-phenyl-5-methyl-pyrazolone[42] was obtained through acylation of *N*-phenyl-5-methyl-pyrazolone (acetyl chloride, calcium oxide, dioxane). *N*,*O-bis*(*tert*-butoxycarbonyl)-hydroxylamine[43] was obtained through *N*,*O* diBoc protection of hydroxylamine hydrochloride (di-*tert*-butyl dicarbonate, triethylamine, petroleum ether, *tert*-butyl methyl ether, water). NMR spectra were obtained on a Bruker Avance 400 MHz FT-NMR spectrometer. All chemical shifts are reported in parts per million (ppm) relative to residual $CHCl_3$ (7.26 ppm for ^{1}H, 77.23 ppm for ^{13}C), residual DMSO (2.50 ppm for ^{1}H, 39.52 for ^{13}C), or residual H_2O (4.8 ppm for ^{1}H). High-resolution mass spectra were obtained on a VG Analytical VG70SE magnetic sector mass spectrometer operating in fast atom bombardment (FAB) mode. Gas chromatography (GC) headspace analysis was performed on a Varian CP-3800 instrument equipped with ECD detection and a RestekShinCarbon ST 80/100 molecular sieve packed column. Ultraviolet-visible

(UV-vis) absorption spectra were obtained using a Hewlett Packard 8453 diode array spectrometer. Phosphate-buffered saline (PBS) solutions (0.1 M) were prepared with 140 mM NaCl and 3 mM KCl, with 100 mM diethylenetriaminepentaacetic acid (DTPA), adjusted to pH 7.4. Buffered solutions (0.1 M) for UV-vis experiments were prepared from HCl/NaCl (pH 1.7), AcOH/AcONa (pH 3.0, 3.5, 4.0, 4.5, 5.0, 5.5), or $NaPO_3H_2/Na_2PO_3H$ (pH 6.0, 6.5, 7.0, 8.0, 9.0, 9.5, 9.8, 10.0, 10.5, 10.6).

2.5.2 Nitrous Oxide (N_2O) Quantification by Gas Chromatographic Headspace Analysis

Gas chromatography was performed on a Varian CP-3800 instrument equipped with a 1041 manual injector, electron capture detector, and a 25m 5Å molecular sieve capillary column. Grade 5.0 nitrogen was used as both the carrier (8 mL/min) and the make-up (22 mL/min) gas. The injector oven and the detector oven were kept at 200 °C and 300 °C, respectively. All nitrous oxide analyses were performed with the column oven held constant at 150 °C. All gas injections were made using a 100 μL gastight syringe with a sample-lock. Samples were prepared in 15 mL amber headspace vials with volumes pre-measured for sample uniformity (actual vial volume ranges from 15.19 – 15.20 mL). Vials were charged with 5 mL of PBS buffer containing DTPA, purged with argon, and sealed with a rubber septum. The vials were equilibrated for at least 10 minutes at 37 °C in a dry block heater. A 10 mM stock solution of Angeli's salt (AS) was prepared in 10 mM sodium hydroxide, and HNO donors **1a** – **4a**, **6a** (10 mM) were prepared in acetonitrile or

methanol and used immediately after preparation. From these stock solutions, 50 μL was introduced into individual thermally-equilibrated headspace vials using a gastight syringe, yielding final substrate concentrations of 0.1 mM. Substrates were then incubated long enough to ensure complete decomposition and equilibration of N_2O with the headspace. The headspace (60 μL) was then sampled and injected five successive times using a gastight syringe with a sample lock. This was repeated for n≥3 vials per donor. The N_2O yield was averaged and reported relative to the standard, Angeli's salt. For chemical trapping of HNO, glutathione (100 μL of 10 mM in PBS) was added prior to HNO donor addition to give a final glutathione concentration of 0.2 mM, and headspace sampling for N_2O was analogously performed as stated above.

2.5.3 ^{1}H NMR Kinetic Experiment with Barbituate Donor 4a

A 20 mM aqueous solution of **4a** (2.6 mg, 0.1 mL D_2O, 0.4 mL DI H_2O) was freshly prepared, and an initial ^{1}H NMR spectrum using a 1 s presaturation pulse to suppress the H_2O signal was obtained. The sample was removed from the magnet and thin-walled Teflon tubing (18-guage) was extended through the NMR cap into the NMR tube to just above the HNO donor solution. The Teflon tube was fitted on a syringe with needle containing 2.4 mL 0.5 M PBS, pH 7.4, which accounts for the empty space in the tube plus the deliverable 0.5 mL of buffer solution. The sample was carefully returned to the magnet and shimmed to address any changes in the homogeneity of the field. A canned pulse sequence (Bruker sequence lc2pr) was used to acquire a solvent suppressed spectrum every 37 s for ca. 80 minutes; the

experiment was started prior to the initiation of the reaction. At the end of the first spectral acquisition, the reaction was started by syringing the buffer solution into the HNO donor solution, and the resultant solution was mixed three times by drawing and dispensing ca. 0.5 mL. At the conclusion of mixing, the excess solution was cleared from the tube leaving ca. 0.5 mL of the reaction in the NMR tube; this coincided with the end of the second spectral acquisition. At the end of the experiment, the ser file was split (using the au program splitser) in 128 individual free induction decays (FID's) for post-acquisition processing and analysis. The data were processed with the academic version of ACDLabs NMRprocessor software: each FID was Fourier transformed, phased, baseline corrected, and integral areas measured for each of the peaks in the spectrum. The most downfield reactant and product peak were integrated as one signal and served as the internal standard for the calculated integration areas for the other signals. Integral areas were plotted as a function of time and fit to a single exponential function to obtain the rates.

2.5.4 Decomposition Kinetics by UV-vis Spectroscopy

Stock solutions of HNO donor (1 mM) were prepared in acetonitrile immediately prior to use. To a quartz cuvette was added 3 mL of PBS buffer at the appropriate pH. The cuvette was then placed in a heated cell block, which was held at 25 °C or 37 °C by a circulating water bath. The buffer was allowed to thermally equilibrate until a constant baseline was achieved, after which 50 μL of HNO donor stock solution was added, the cuvette solution briefly mixed, and the kinetic run started. Complete spectra at 37 °C in pH 7.4 buffer were obtained every 30 s for the

conversion of **4a** to **4b** and 240 s for the conversion of **6a** to **6b**. In addition, complete spectra at 25 °C in pH 7.4, 8.1, 8.5, 9.0, and 9.5 buffers were obtained every 0.5 s for the conversion of **4a** to **4b**, and complete spectra at 25 °C in pH 7.4, 8.1, 8.5, 9.0, 9.5, 9.8, 10.0, 10.5, and 10.6 buffers were obtained every 0.5 s for the conversion of **6a** to **6b**. The stability at pH 4, room temperature of **4a** and **6a** was obtained by the intermittent collection of complete spectra from pH 4 solutions of each donor, which were prepared as stated above. Kinetic traces were derived from the spectra by plotting the absorbance at a given wavelength versus time and fit to a single exponential function to obtain the rates.

Scheme 2-6. Synthesis of Meldrum's Acid Donors 1a and 2a

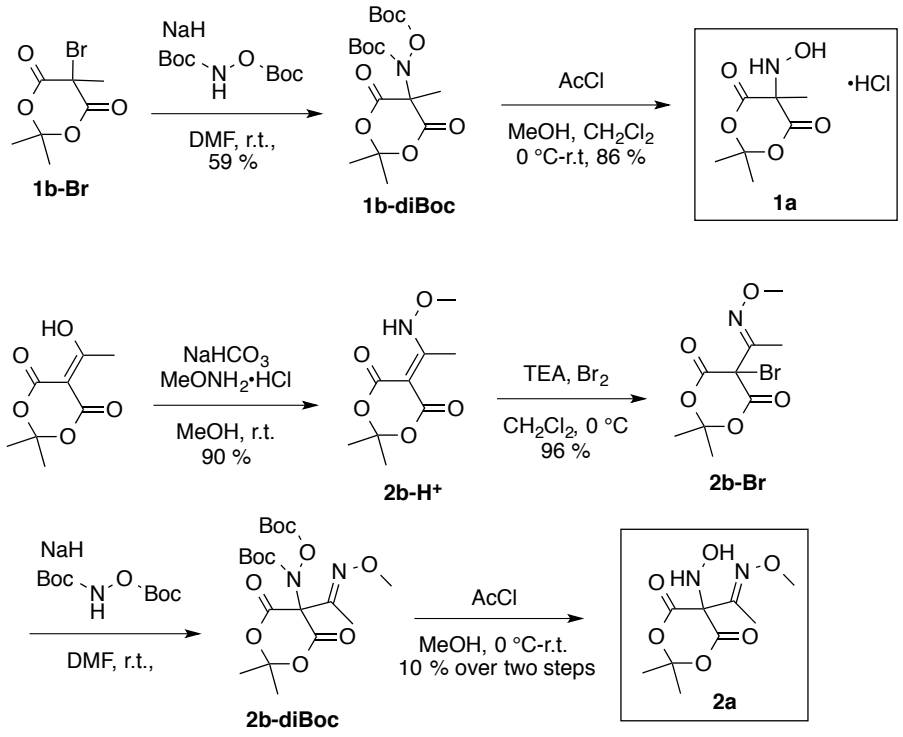

Scheme 2-7. Synthesis of Barbituric Acid Donors 3a and 4a

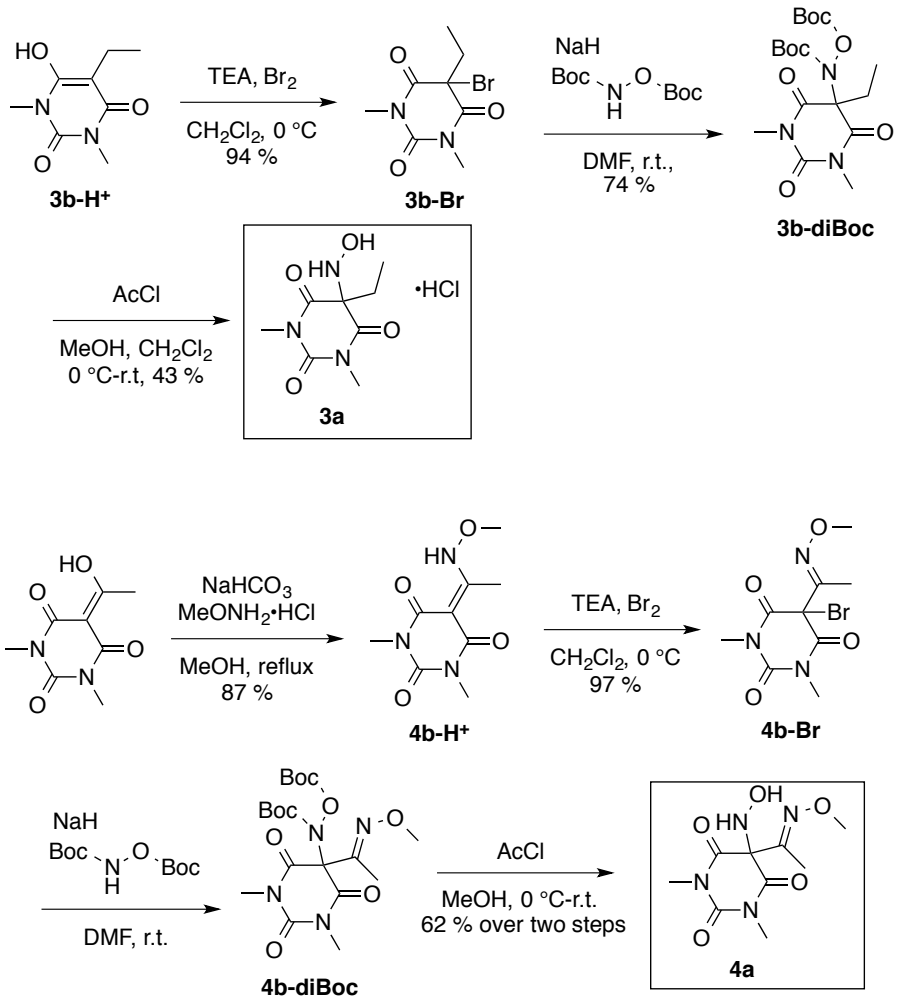

Scheme 2-8. Synthesis of Pyrazolone Donor 6a

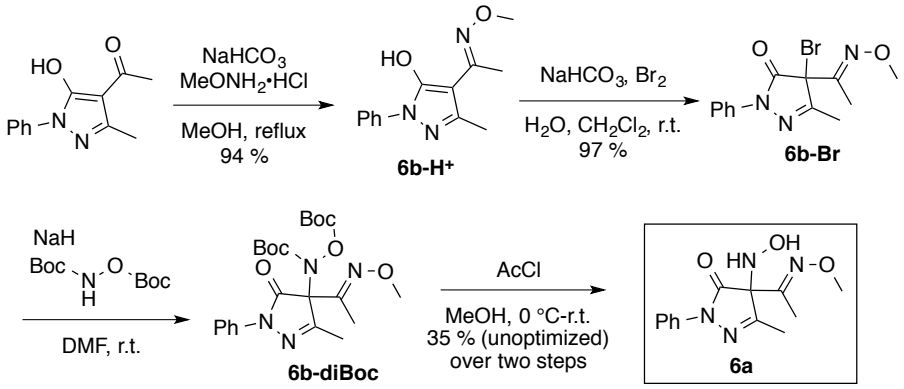

2.5.5 Experimental Procedures

5-(*N*-(*N*,*O*-*bis*(*tert*-butoxycarbonyl))-hydroxylamine)-5-methyl-Meldrum's acid (1b-diBoc). To a solution of *N*,*O*-*bis*(*tert*-butoxycarbonyl)-hydroxylamine (1.81 g, 7.75 mmol) in dimethylformamide (25 mL) at room temperature was added sodium hydride, 60% (0.340 g, 8.52 mmol), and the reaction stirred for one hour. To this solution was added **1b-Br** (1.84 g, 7.75 mmol), and the reaction proceeded at room temperature for an additional 17 hours. The reaction was diluted with ether (50 mL) and washed with ammonium chloride (x2), water, and brine. The solvent was removed via rotary evaporation, which gave the title compound as an oil that aerated and solidified *in vacuo*. Recrystallization from dichloromethane and hexanes gave the title compound as a white solid (1.79 g, 59%). ^{1}H NMR (400 MHz, $CDCl_3$) δ: 1.90 (s, 3H), 1.83 (s, 3H), 1.80 (s, 3H). ^{13}C NMR (100 MHz, $CDCl_3$) δ: 167.04, 163.92, 154.77, 151.91, 107.49, 85.51, 84.88, 64.80, 28.78, 28.00, 27.59, 21.84.

5-(*N*-hydroxylamine)-5-methyl-Meldrum's acid hydrochloride monohydrate (1a). To a solution of **1b-diBoc** (0.190 g, 0.488 mmol) in dichloromethane (10 mL) and methanol (0.99 mL) at 0 °C was added acetyl chloride (1.7 mL, 24 mmol) over two minutes. The reaction was allowed warm to room temperature in the ice bath, and continued to stir overnight. The white precipitate was filtered and characterized as the title compound (0.094 g, 86%). Recrystallization from methanol and dichloromethane gave X-ray quality crystals. ^{1}H NMR (400 MHz, d_6-DMSO) δ: 10.32 (s, 1H), 8.40 (br. s, 3H), 1.73 (s, 3H), 1.71 (s, 3H), 1.44 (s, 3H). ^{13}C NMR (100 MHz, d_6-DMSO) δ: 168.99, 105.57, 66.14, 28.88, 28.33, 20.96.

5-(acetyl-*O*-methoxyoxime)-Meldrum's acid (2b-H$^+$). To a solution of 5-acetyl-Meldrum's acid (1.644 g, 8.831 mmol) in methanol (50 mL) at room temperature was added *O*-methoxyhydroxylamine hydrochloride (0.738 g, 8.84 mmol) and sodium bicarbonate (0.743 g, 8.84 mmol), and the reaction continued at room temperature for 24 hours. The reaction was concentrated *in vacuo*, redissolved in dichloromethane, filtered, and concentrated *in vacuo* to give the title compound as a light yellow solid (1.714 g, 90%). ^{1}H NMR (400 MHz, $CDCl_3$) δ: 13.11 (s, 1H), 3.88 (s, 3H), 2.71 (s, 3H), 1.69 (6H). ^{13}C NMR (100 MHz, $CDCl_3$) δ: 169.77, 166.95, 162.58, 103.12, 80.79, 64.68, 26.46, 14.86. HR-MS (FAB): found m/z = 216.08696 (MH^+); calc. for $C_9H_{13}NO_5$: 216.08720.

5-(acetyl-*O*-methoxyoxime)-5-bromo-Meldrum's acid (2b-Br). To a solution of **4b-H$^+$** (0.681 g, 2.87 mmol) and triethylamine (0.40 mL, 2.87 mmol) in dichloromethane (20 mL) at 0 °C was added a solution of bromine (0.15 mL, 2.87

mmol) in dichloromethane (2 mL). The reaction was stirred for five minutes then extracted with water and brine, dried over magnesium sulfate, and concentrated *in vacuo* to give the title compound as an orange solid (0.810 g, 96%). ^{1}H NMR (400 MHz, $CDCl_3$) δ: 3.94 (s, 3H), 2.19 (s, 3H), 1.85 (s, 3H), 1.78 (s, 3H). ^{13}C NMR (100 MHz, $CDCl_3$) δ: 161.53, 151.23, 107.27, 63.19, 55.82, 28.74, 28.38, 12.71. HR-MS (FAB): found m/z = 295.99537 (MH^+); calc. for $C_9H_{12}BrNO_5$: 295.99566.

5-(acetyl-*O*-methoxyoxime)-5-(*N*-(*N*,*O*-*bis*(*tert*-butoxycarbonyl))-hydroxylamine)-Meldrum's acid (2b-diBoc). To a solution of *N*,*O*-*bis*(*tert*-butoxycarbonyl)-hydroxylamine (0.642 g, 2.75 mmol) in dimethylformamide (20 mL) at room temperature was added sodium hydride, 60% (0.121 g, 3.03 mmol), and the reaction stirred for one hour. To this solution was added **2b-Br** (0.810 g, 2.75 mmol), and the reaction proceeded at room temperature for an additional 24 hours. The reaction was diluted with ether (50 mL) and washed with ammonium chloride (x2), water, and brine then concentrated *in vacuo* to give crude **2b-diBoc** ~30-40% pure by ^{1}H NMR, which was used without further purification. ^{1}H NMR (400 MHz, $CDCl_3$) δ: 3.94 (s, 3H), 1.99 (br. s., 3H), 1.82 (br. s., 3H), 1.73 (s, 3H), 1.51 (s, 9H), 1.48 (s, 9H).

5-(*N*-hydroxylamine)-5-(acetyl-*O*-methoxyoxime)-Meldrum's acid (2a). To a solution of **2b-diBoc** from the previous reaction in methanol (20 mL) at 0 °C was added acetyl chloride (4 mL) over three minutes. The reaction was allowed warm to room temperature in the ice bath, and continued to stir overnight. The reaction was concentrated *in vacuo*, redissolved in dichloromethane, filtered, and the filtrate was concentrated *in vacuo*. Recrystallization from dichloromethane and

hexanes gave the title compound as pale orange needles (0.68 g, 10% over two steps). ^{1}H NMR (400 MHz, d_6-DMSO) δ: 8.38 (d, 1H, J = 2.3 Hz), 6.94 (d, 1H, J = 2.4 Hz), 3.81 (s, 3H), 1.91 (s, 3H), 1.74 (s, 3H), 1.71 (s, 3H). ^{13}C NMR (100 MHz, d_6-DMSO) δ: 163.88, 150.39, 107.08, 74.46, 62.97, 29.78, 27.97, 11.32. HR-MS (FAB): found m/z = 247.09360 (MH^+); calc. for $C_9H_{14}N_2O_6$: 247.09301.

5-bromo-5-ethyl-*N*,*N*-dimethylbarbituric acid (3b-Br). To a solution of **3b-H$^+$** (1.06 g, 5.74 mmol) and triethylamine (0.81 mL, 5.74 mmol) in dichloromethane (50 mL) at 0 °C was added a solution of bromine (0.30 mL, 5.74 mmol) in dichloromethane (2 mL). The reaction was stirred for five minutes then extracted with water and brine, dried over magnesium sulfate, and concentrated *in vacuo* to give the title compound as a white solid (1.42 g, 94%). ^{1}H NMR (400 MHz, $CDCl_3$) δ: 3.38 (s, 6H), 2.61 (q, 2H), 0.85 (t, 3H). ^{13}C NMR (100 MHz, $CDCl_3$) δ: 166.07, 150.09, 49.93, 30.30, 29.66, 10.70. HR-MS (FAB): found m/z = 265.00118 (MH^+); calc. for $C_8H_{11}BrN_2O_3$: 265.00108.

5-(*N*-(*N*,*O*-*bis*(*tert*-butoxycarbonyl))-hydroxylamine)-5-ethyl-*N*,*N*-dimethylbarbituric acid (3b-diBoc). To a solution of *N*,*O*-*bis*(*tert*-butoxycarbonyl)-hydroxylamine (1.26 g, 5.41 mmol) in dimethylformamide (50 mL) at room temperature was added sodium hydride, 60% (0.238 g, 5.95 mmol), and the reaction stirred for one hour. To this solution was added **3b-Br** (1.42 g, 5.41 mmol), and the reaction proceeded at room temperature for an additional 20 hours. The reaction was diluted with ether (50 mL) and washed with ammonium chloride (x2), water, and brine. The solvent was removed via rotary evaporation, which gave the title compound as an oil that aerated and solidified *in vacuo*. Recrystallization from

dichloromethane and hexanes gave the title compound as a white solid (1.67 g, 74%). ^{1}H NMR (400 MHz, $CDCl_3$) δ: 3.35 (s, 3H), 3.33 (s, 3H), 2.17 (m, 2H), 1.54 (s, 9H), 1.41 (br.s., 9H), 0.89 (t, 3H). ^{13}C NMR (100 MHz, $CDCl_3$) δ: 169.60, 166.47, 151.81, 150.74, 85.20, 84.40, 70.70, 29.41, 29.03, 28.82, 27.99, 27.94, 27.61, 27.57, 7.88. HR-MS (FAB): found m/z = 416.20253 (MH^+); calc. for $C_{18}H_{29}N_3O_8$: 416.20329.

5-(*N*-hydroxylamine)-5-ethyl-*N*,*N*-dimethylbarbituric acid hydrochloride (3a). To a solution of **3b-diBoc** (0.415 g, 1 mmol) in dichloromethane (20 mL) and methanol (2.0 mL) at 0 °C was added acetyl chloride (3.5 mL, 50 mmol) over three minutes. The reaction was allowed warm to room temperature in the ice bath, and continued to stir overnight. The white precipitate was filtered and characterized as the title compound (0.109 g, 43%). Recrystallization from methanol and dichloromethane gave X-ray quality crystals. ^{1}H NMR (400 MHz, d_6-DMSO) δ: 10. 27 (s, 1H), 7.24 (t, 1H, J = 50.8 Hz), 3.21 (s, 6H), 1.78 (q, 2H, J = 7.4 Hz), 0.72 (t, 3H, J = 7.7 Hz). Rearrangement to **5** precluded the collection of ^{13}C NMR. HR-MS (FAB): found m/z = 216.09879 (MH^+); calc. for $C_8H_{13}N_3O_4$: 216.09843.

5-(acetyl-*O*-methoxyoxime)-*N*,*N*-dimethylbarbituric acid (4b-H$^+$). To a suspension of 5-acetyl-*N*,*N*-dimethylbarbituric acid (15.43 g, 77.8 mmol) in methanol (125 mL) was added *O*-methoxyhydroxylamine hydrochloride (6.50 g, 77.8 mmol) and sodium bicarbonate (6.54 g, 77.8 mmol). The reaction was heated to reflux for one hour then allowed to cool on ice. The precipitate was filtered, re-dissolved in dichloromethane, filtered, and the solution was concentrated *in vacuo* to give the title compound as a white solid (15.36 g, 87%). ^{1}H NMR (400 MHz,

$CDCl_3$) δ: 14.54 (s, 1H), 3.88 (s, 3H), 3.32 (s, 3H), 3.30 (s, 3H), 2.76 (s, 3H). ^{13}C NMR (100 MHz, $CDCl_3$) δ: 169.63, 166.11, 162.55, 151.42, 86.97, 64.55, 27.87, 14.75. HR-MS (FAB): found m/z = 228.09857 (MH^+); calc. for $C_9H_{13}N_3O_4$: 228.09843.

5-(acetyl-*O*-methoxyoxime)-5-bromo-*N*,*N*-dimethylbarbituric acid (4b-Br). To a solution of **4b-H$^+$** (7.27 g, 32 mmol) and triethylamine (4.5 mL, 32 mmol) in dichloromethane (50 mL) at 0 °C was added a solution of bromine (1.65 mL, 32 mmol) in dichloromethane (10 mL). The reaction was stirred for five minutes then extracted with water and brine, dried over magnesium sulfate, and concentrated *in vacuo* to give the title compound as a white solid (9.51 g, 97%). ^1H NMR (400 MHz, $CDCl_3$) δ: 3.87 (s, 3H), 3.35 (s, 6H), 2.06 (s, 3H). ^{13}C NMR (100 MHz, $CDCl_3$) δ: 163.77, 151.70, 150.02, 62.87, 60.13, 30.00, 12.69. HR-MS (FAB): found m/z = 308.00717 (MH^+); calc. for $C_9H_{12}BrN_3O_4$: 308.00690.

5-(acetyl-*O*-methoxyoxime)-5-(*N*-(*N*,*O*-*bis*(*tert*-butoxycarbonyl))-hydroxylamine-*N*,*N*-dimethylbarbituric acid (4b-diBoc). To a solution of *N*,*O*-*bis*(*tert*-butoxycarbonyl)-hydroxylamine (5.83 g, 25 mmol) in dimethylformamide (100 mL) at room temperature was added sodium hydride, 60% (1.1 g, 27.5 mmol), and the reaction stirred for one hour. To this solution was added **4b-Br** (7.65 g, 25 mmol), and the reaction proceeded at room temperature for an additional 20 hours. The reaction was diluted with ether (150 mL) and washed with ammonium chloride (x2), water, and brine. The solvent was removed via rotary evaporation, which gave the title compound as an oil that aerated and solidified *in vacuo*. This material was used without further purification. ^1H NMR (400 MHz, $CDCl_3$) δ: 3.84 (s, 3H), 3.32 (s, 6H), 1.94 (br. m., 3H), 1.52 (s, 9H), 1.46 (br. m., 9H). HR-MS (FAB): found m/z =

459.20898 (MH^+); calc. for $C_{19}H_{30}N_3O_9$: 459.20910.

5-(*N*-hydroxylamine)-5-(acetyl-*O*-methoxyoxime)-*N*,*N*-dimethylbarbituric acid (4a). Methanol (100 mL) at 0 °C was charged with acetyl chloride (25 mL) over 10 minutes then stirred for an additional five minutes. To this acidic solution was added a solution of **4b-diBoc** in methanol (70 mL), and the cloudy reaction was allowed to warm to room temperature in the ice bath over night. The reaction was concentrated *in vacuo*, re-dissolved in dichloromethane, filtered, and the filtrate was concentrated *in vacuo* to give the title compound as a sticky solid. Recrystallization from dichloromethane and hexanes gave white needles (3.98 g, 62% over two steps). ^{1}H NMR (400 MHz, $CDCl_3$) δ: 6.38 (d, 1H, J = 4.0 Hz), 5.32 (d, 1H, J = 4.0 Hz), 3.82 (s, 3H), 3.36 (s, 6H), 1.89 (s, 3H). ^{13}C NMR (100 MHz, $CDCl_3$) δ: 167.10, 152.47, 150.86, 74.93, 62.80, 29.38, 10.93. HR-MS (FAB): found m/z = 259.10454 (MH^+); calc. for $C_9H_{14}N_4O_5$: 259.10424.

4-(acetyl-*O*-methoxyoxime)-*N*-phenyl-3-methyl-pyrazolone (6b-H$^+$). To a suspension of 4-acetyl-*N*-phenyl-3-methyl-pyrazolone (3.69 g, 17.1 mmol) in methanol (50 mL) was added *O*-methoxyhydroxylamine hydrochloride (1.43 g, 17.1 mmol) and sodium bicarbonate (1.44 g, 17.1 mmol). The reaction was heated to reflux for one hour then allowed to cool to room temperature. The reaction was concentrated *in vacuo*, re-dissolved in dichloromethane, filtered, and the filtrate was concentrated *in vacuo* to give the title compound as a red brown oil that solidified upon standing (4.15 g, 99%). ^{1}H NMR (400 MHz, $CDCl_3$) δ: 7.85 (m, 2H), 7.44 (m, 2H), 7.26 (m, 1H), 3.92 (s, 3H), 2.43 (s, 3H), 2.29 (s, 3H). ^{13}C NMR (100 MHz, $CDCl_3$) δ: 170.58, 156.30, 155.54, 154.44, 146.17, 138.22, 128.93, 125.89, 120.67, 120.62,

118.75, 96.46, 62.15, 43.06, 16.94, 15.75, 12.95. HR-MS (FAB): found m/z = 246.12350 (MH^+); calc. for $C_{13}H_{15}N_3O_2$: 246.12425.

4-(acetyl-*O*-methoxyoxime)-4-bromo-*N*-phenyl-3-methyl-pyrazolone (6b-Br). To a biphasic mixture of **6b-H$^+$** (1.078 g, 4.4 mmol) and sodium bicarbonate (0.369 g, 4.4 mmol) in dichloromethane (20 mL) and water (20 mL) at room temperature was added bromine (0.23 mL, 4.4 mmol) at once. The reaction was vigorously stirred for five minutes, transferred to a separatory funnel and shaken until a clear, colorless aqueous layer resulted. The organic layer was separated, dried over magnesium sulfate, filtered, and concentrated *in vacuo* to give the title compound as a brown oil (1.38 g, 97%). ^{1}H NMR (400 MHz, $CDCl_3$) δ: 7.88 (m, 2H), 7.40 (m, 2H), 7.22 (m, 1H), 3.90 (s, 3H), 2.44 (s, 3H), 2.22 (s, 3H). ^{13}C NMR (100 MHz, $CDCl_3$) δ: 167.06, 157.83, 151.27, 137.69, 129.11, 125.78, 119.08, 62.73, 56.61, 15.71, 11.70. HR-MS (FAB): found m/z = 326.03272 (MH^+); calc. for $C_{13}H_{14}BrN_3O_2$: 326.03219.

4-(acetyl-*O*-methoxyoxime)-4-(*N*-(*N*,*O*-*bis*(*tert*-butoxycarbonyl))-hydroxylamine-*N*-phenyl-3-methyl-pyrazolone (6b-diboc). To a solution of *N*,*O*-*bis*(*tert*-butoxycarbonyl)-hydroxylamine (0.992 g, 4.25 mmol) in dimethylformamide (20 mL) at room temperature was added sodium hydride, 60% (0.187 g, 4.68 mmol), and the reaction stirred for one hour. To this solution was added **6b-Br** (1.38 g, 4.25 mmol), and the reaction proceeded at room temperature for 30 minutes. The reaction was diluted with ether (50 mL) and washed with ammonium chloride (x2), water, and brine. The solvent was removed via rotary evaporation, which gave the title compound as an oil that aerated and solidified *in*

vacuo. This material was used without further purification. ^{1}H NMR (400 MHz, $CDCl_3$) δ: 7.89 (m, 2H), 7.37 (m, 2H), 7.16 (m, 1H), 3.85 (s, 3H), 2.24 (br. s., 3H), 2.05 (br. m., 3H), 1.52 (s, 9H), 1.40 (br. m., 9H).

4-(*N*-hydroxylamine)-4-(acetyl-*O*-methoxyoxime)-*N*-phenyl-3-methylpyrazolone (6a). To a solution of **6b-diBoc** from the previous reaction in methanol (50 mL) at 0 °C was added acetyl chloride (3 mL) over three minutes. The reaction was allowed warm to room temperature in the ice bath, and continued to stir overnight. The reaction was concentrated *in vacuo*, re-dissolved in dichloromethane, filtered, and the filtrate was concentrated *in vacuo* to give the title compound as a sticky solid. Recrystallization from dichloromethane and hexanes gave the title compound as white needles (0.412 g, 35% over two steps). ^{1}H NMR (400 MHz, $CDCl_3$) δ: 7.92 (m, 2H), 7.41 (m, 2H), 7.20 (m, 1H), 6.25 (d, 1H, J = 2.5 Hz), 4.68 (d, 1H, J = 2.5 Hz), 3.92 (s, 3H), 2.23 (s, 3H), 1.79 (s, 3H). ^{13}C NMR (100 MHz, $CDCl_3$) δ: 170.23, 159.62, 148.66, 137.85, 129.07, 125.59, 119.03, 78.10, 62.59, 14.43, 11.05. HR-MS (FAB): found m/z = 277.12953 (MH^+); calc. for $C_{13}H_{16}N_4O_3$: 277.13007.

▪ 2.6 References

(1) Paolocci, N.; Saavedra, W. F.; Miranda, K. M.; Martignani, C.; Isoda, T.; Hare, J. M.; Espey, M. G.; Fukuto, J. M.; Feelisch, M.; Wink, D. A.; Kass, D. A. *Proc. Natl. Acad. Sci. U.S.A*. **2001**, *98*, 10463–10468.

(2) Paolocci, N.; Katori, T.; Champion, H. C. St.; John, M. E.; Miranda, K. M.; Fukuto, J. M.; Wink, D. A.; Kass, D. A. *Proc. Natl. Acad. Sci. U.S.A.* **2003**, *100*, 5537–5542.

(3) Paolocci, N.; Jackson, M. I.; Lopez, B. E.; Miranda, K.; Tocchetti, C. G.; Wink, D. A.; Hobbs, A. J.; Fukuto, J. M. *Pharmacol. Ther*. **2007**, *113*, 442–458.

(4) Tocchetti, C. G.; Wang, W.; Froehlich, J. P.; Huke, S.; Aon, M. A.; Wilson, G. M.; Di Benedetto, G.; O'Rourke, B.; Gao, W. D.; Wink, D. A.; Toscano, J. P.; Zaccolo, M.; Bers, D. M.; Valdivia, H. H.; Cheng, H.; Kass, D. A.; Paolocci, N. *Circ. Res*. **2007**, *100*, 96-104.

(5) Froehlich, J. P.; Mahaney, J. E.; Keceli, G.; Pavlos, C. M.; Goldstein, R.; Redwood, A. J.; Sumbilla, C.; Lee, D. I.; Tocchetti, C. G.; Kass, D. A.; Paolocci, N.; Toscano, J. P. *Biochemistry* **2008**, *47*, 13150–13152.

(6) Miranda, K. Coord. *Chem. Rev*. **2005**, *249*, 433–455.

(7) Fukuto, J. M.; Bartberger, M. D.; Dutton, A. S.; Paolocci, N.; Wink, D. A.; Houk, K. N. *Chem. Res. Toxicol*. **2005**, *18*, 790–801.

(8) Irvine, J. C.; Ritchie, R. H.; Favaloro, J. L.; Andrews, K. L.; Widdop, R. E.; Kemp-Harper, B. K. *Trends Pharmacol. Sci*. **2008**, *29*, 601–608.

(9) Fukuto, J. M.; Bianco, C. L.; Chavez, T. A. *Free Radical Biol*. *Med*. **2009**, *47*, 1318–1324.

(10) Flores-Santana, W.; Salmon, D. J.; Donzelli, S.; Switzer, C. H.; Basudhar, D.; Ridnour, L.; Cheng, R.; Glynn, S. A.; Paolocci, N.; Fukuto, J. M.; Miranda, K. M.; Wink, D. A. *Antioxid. Redox Signaling* **2011**, *14*, 1659–1674.

(11) Kemp-Harper, B. K. *Antioxid. Redox Signaling* **2011**, *14*, 1609–1613.

(12) Shafirovich, V.; Lymar, S. V. *Proc. Natl. Acad. Sci. U.S.A*. **2002**, *99*, 7340–7345.

(13) Angeli, A. *Gazz. Chim. Ital*. **1896**, *26*, 17–25.

(14) Piloty, O. *Ber. Dtsch. Chem. Ges*. **1896**, *29*, 1559–1567.

(15) Miranda, K. M.; Nagasawa, H. T.; Toscano, J. P. *Curr. Top. Med. Chem*. **2005**, *5*,

649–664.

(16) DuMond, J. F.; King, S. B. *Antioxid. Redox Signaling* **2011**, *14*, 1637–1648.

(17) Miranda, K. M.; Katori, T.; Torres de Holding, C. L.; Thomas, L.; Ridnour, L. A.; McLendon, W. J.; Cologna, S. M.; Dutton, A. S.; Champion, H. C.; Mancardi, D.; Tocchetti, C. G.; Saavedra, J. E.; Keefer, L. K.; Houk, K. N.; Fukuto, J. M.; Kass, D. A.; Paolocci, N.; Wink, D. A. *J. Med. Chem*. **2005**, *48*, 8220-8228.

(18) Salmon, D. J.; Torres de Holding, C. L.; Thomas, L.; Peterson, K. V.; Goodman, G. P.; Saavedra, J. E.; Srinivasan, A.; Davies, K. M.; Keefer, L. K.; Miranda, K. M. *Inorg. Chem.* **2011**, *50*, 3262–3270.

(19) Sha, X.; Isbell, T. S.; Patel, R. P.; Day, C. S.; King, S. B. *J. Am. Chem. Soc*. **2006**, *128*, 9687–9692.

(20) Shoman, M. E.; DuMond, J. F.; Isbell, T. S.; Crawford, J. H.; Brandon, A.; Honovar, J.; Vitturi, D. A.; White, C. R.; Patel, R. P.; King, S. B. *J. Med. Chem*. **2011**, *54*, 1059–1070.

(21) Corrie, J. E. T.; Kirby, G. W.; Mackinnon, J. W. M. *J. Chem. Soc., Perkin Trans. 1* **1985**, 883–886.

(22) Cohen, A. D.; Zeng, B.-B.; King, S. B.; Toscano, J. P. *J. Am. Chem. Soc*. **2003**, *125*, 1444–1445.

(23) Evans, A. S.; Cohen, A. D.; Gurard-Levin, Z. A.; Kebede, N.; Celius, T. C.; Miceli, A. P.; Toscano, J. P. *Can. J. Chem*. **2011**, *89*, 130–138.

(24) Toscano, J. P.; Brookfield, F. A.; Cohen, A. D.; Courtney, S. M.; Frost, L. M.; Kalish, V. J. U.S. Patent 8,030,356, **2011**.

(25) Nagasawa, H. T.; DeMaster, E. G.; Redfern, B.; Shirota, F. N.; Goon, D. J. W. *J. Med. Chem*. **1990**, *33*, 3120–3122.

(26) Shirota, F. N.; Goon, D. J. W.; DeMaster, E. G.; Nagasawa, H. T. *Biochem. Pharmacol.* **1996**, *52*, 141–147.

(27) DeMaster, E. G.; Redfern, B.; Nagasawa, H. T. *Biochem. Pharmacol*. **1998**, *55*, 2007–2015.

(28) Nagasawa, H. T.; Lee, M. J. C.; Kwon, C. H.; Shirota, F. N.; DeMaster, E. G. *Alcohol* **1992**, *9*, 349–353.

(29) Pihlaja, K.; Seilo, M. *Acta Chem. Scand*. **1969**, *23*, 3003–3010.

(30) Pihlaja, K.; Seilo, M. *Acta Chem. Scand*. **1968**, *22*, 3053–3062.

(31) Doyle, M. P.; Mahapatro, S. N.; Broene, R. D.; Guy, J. K. *J. Am. Chem. Soc*. **1988**, *110*, 593–599.

(32) Wong, P. S. Y.; Hyun, J.; Fukuto, J. M.; Shirota, F. N.; DeMaster, E. G.; Shoeman, D. W.; Nagasawa, H. T. *Biochemistry* **1998**, *37*, 5362–5371.

(33) Krasnov, K. A.; Kartsev, V. G.; Gorovoi, A. S. *Chem. Nat. Compd*. **2000**, *36*, 192–197.

(34) Jursic, B. S.; Neumann, D. M.; Bowdy, K. L.; Stevens, E. D. *J. Heterocycl. Chem*. **2004**, *41*, 233–246 and references therein.

(35) Higashi, Y.; Jitsuiki, D.; Chayama, K.; Yoshizumi, M. *Recent Pat. Cardiovasc. Drug Discovery* **2006**, *1*, 85–93.

(36) Watanabe, T.; Tahara, M.; Todo, S. *Cardiovasc. Ther*. **2008**, *26*, 101–114.

(37) Watanabe, K.; Morinaka, Y.; Iseki, K.; Watanabe, T.; Yuki, S.; Hishi, H. *Redox Report* **2003**, *8*, 151–155.

(38) Melvin, L. S. Jr.; Trost, B. M. *J. Am. Chem. Soc*. **1971**, *94*, 1790–1792.

(39) Raillar, S. P.; Chen, W.; Sullivan, E.; Bajjalieh, W.; Bhandari, A.; Baer, T. A. *J. Comb. Chem*. **2002**, *4*, 470–474.

(40) Jursic, B. S., Neumann, D. M. *Tetrahedron Lett*. **2001**, *42*, 8435–8439.

(41) Nutaitis, C. F.; Schultz, R. A.; Obaza, J.; Smith, F. X. *J. Org. Chem*. **1980**, *45*, 4606–4608.

(42) Patel, J. D.; Shah, P. J. *Asian J. Chem*. **2010**, *22*, 3069–3075.

(43) Staszak, M. A.; Doecke, C. W. *Tetrahedron Lett*. **1993**, *34*, 7043–7044.

▪ 2.7 Supporting Information

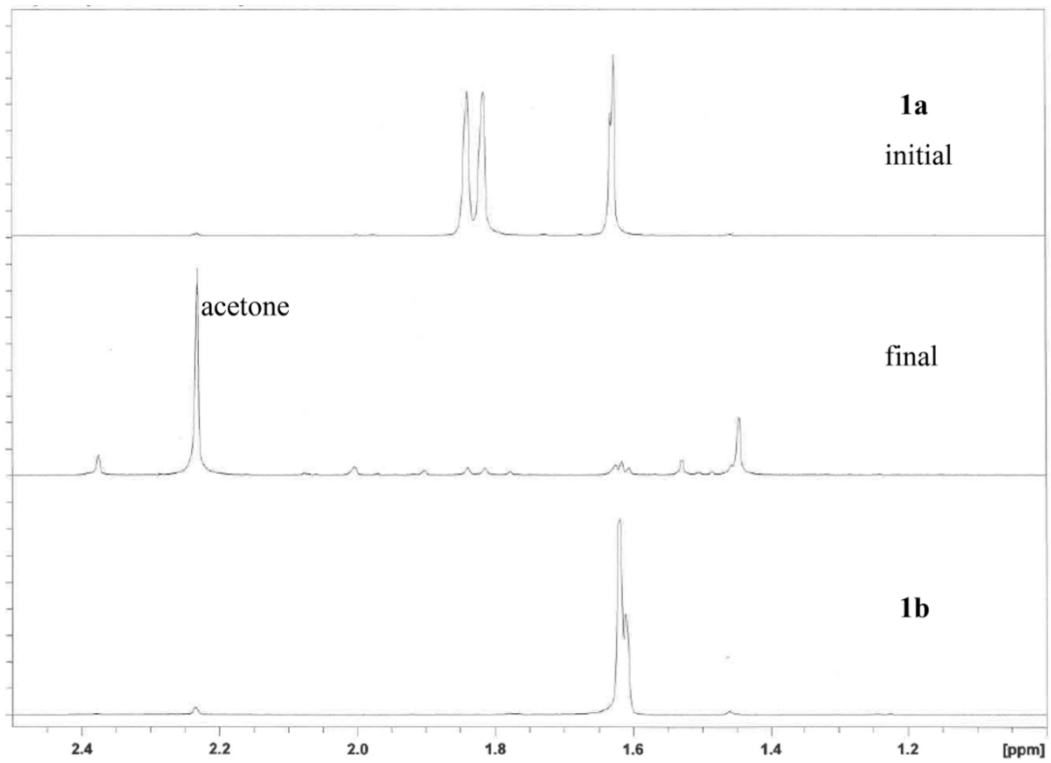

Figure 2-5. ^{1}H NMR spectra of the decomposition of Meldrum's acid donor **1a** in PBS, pH 7.4.

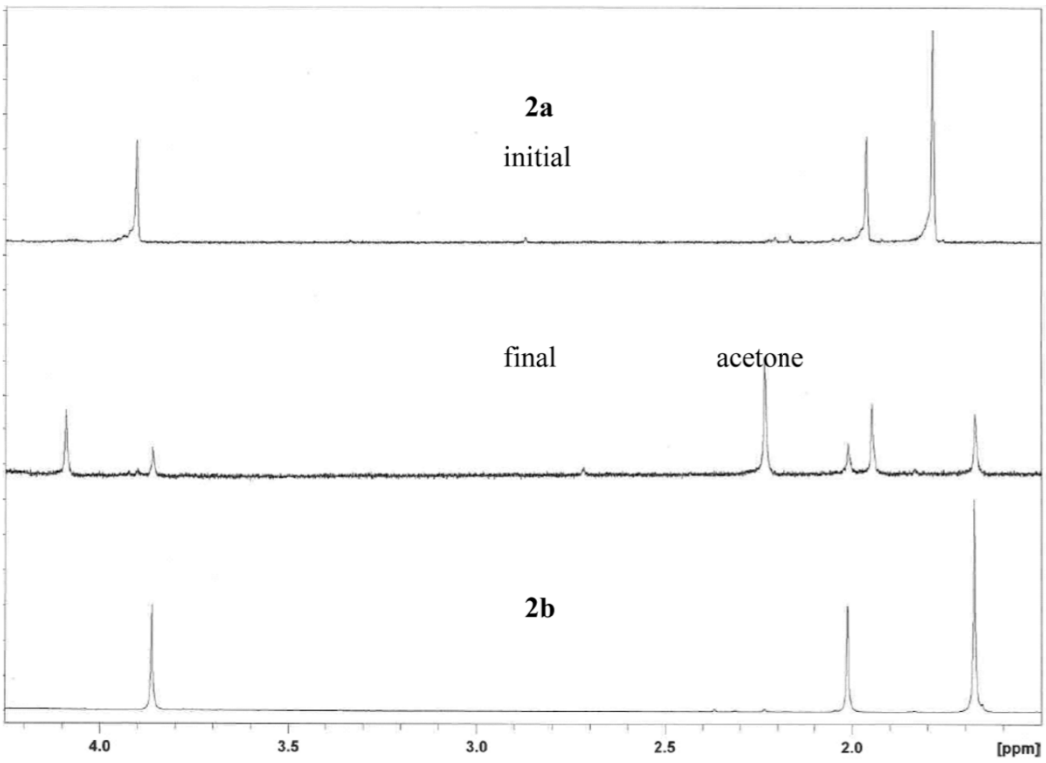

Figure 2-6. ^{1}H NMR spectra of the decomposition of Meldrum's acid donor **2a** in PBS, pH 7.4.

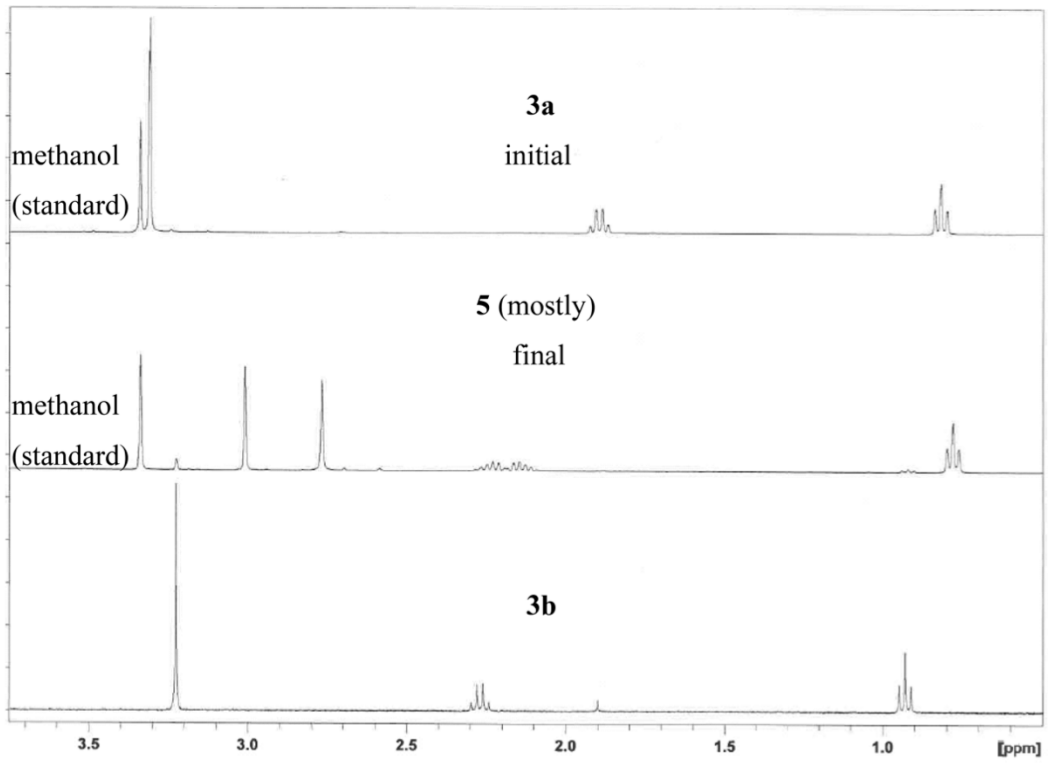

Figure 2-7. ^{1}H NMR spectra of the decomposition of Meldrum's acid donor **3a** in PBS, pH 7.4.

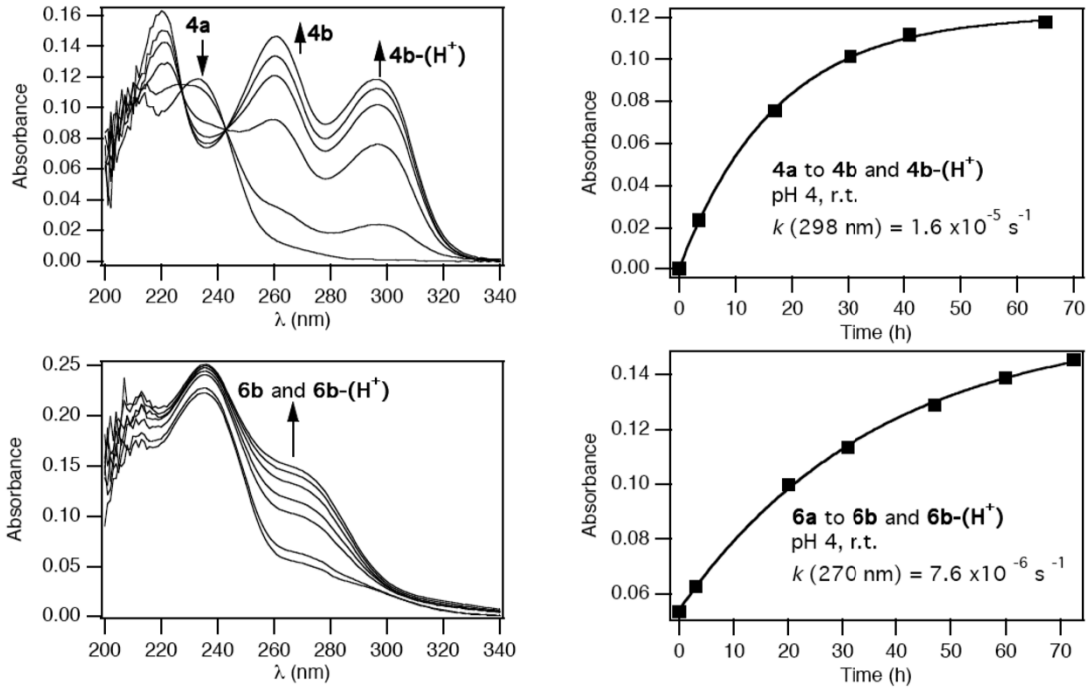

Figure 2-8. UV-vis spectral and kinetic data for the decomposition of barbituric acid donor **4a** and pyrazolone donor **6a** in pH 4 buffer at room temperature.

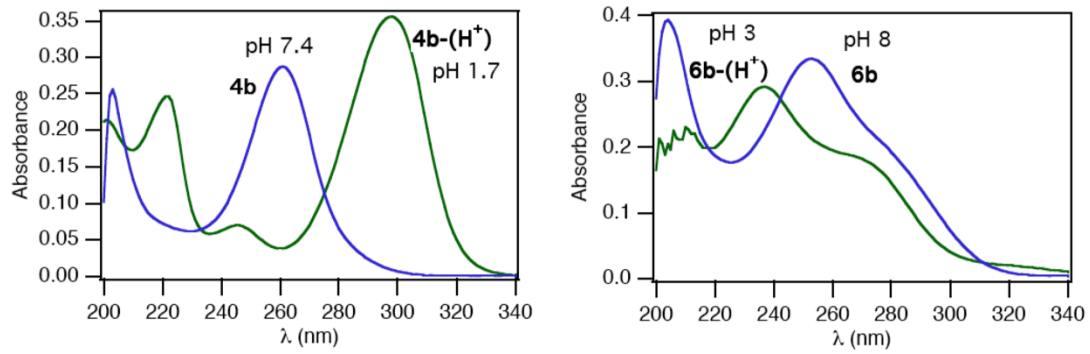

Figure 2-9. UV-vis spectra at low and high pH for byproducts of decomposition from barbituric acid donor **4a** and pyrazolone donor **6a**.

2.7.1 X-Ray Crystallography Data

All reflection intensities were measured at 110(2) K using a KM4/Xcalibur (detector: Sapphire3) with enhance graphite-monochromated Mo *K*α radiation (λ = 0.71073 Å) under the program CrysAlisPro (Version 1.171.35.11 Oxford Diffraction Ltd., 2011). The program CrysAlisPro (Version 1.171.35.11, Oxford Diffraction Ltd., 2011) was used to refine the cell dimensions. Data reduction was done using the program CrysAlisPro (Version 1.171.35.11, Oxford Diffraction Ltd., 2011). The structure was solved with the program SHELXS-97 (Sheldrick, 2008) and was refined on F^2 with SHELXL-97 (Sheldrick, 2008). Analytical numeric absorption corrections based on a multifaceted crystal model were applied using CrysAlisPro (Version 1.171.35.11, Oxford Diffraction Ltd., 2011). The temperature of the data collection was controlled using the system Cryojet (manufactured by Oxford Instruments). The H atoms (except when specified) were placed at calculated positions using the instructions AFIX 23 (only for **3a** and **5**), AFIX 43 (only for **6a**) or AFIX 137 with isotropic displacement parameters having values 1.2 or 1.5 times *U*eq of the attached C atoms. The positions of the H atoms attached to all N (i.e., NH for **2a**, **4a**, **6a** and **5**; NH_2 for **1a** and **3a**) or O (i.e., OH; H_2O only for **1a**) atoms were found from difference Fourier maps. The N–H, O–H and H•••H (only for **1a**) distances were restrained to 0.88 (NH) / 0.99(3) (NH_2), 0.84(3) and 1.33(3) Å (so that the H–O–H bond angle is 104.5°), respectively. All structures are ordered.

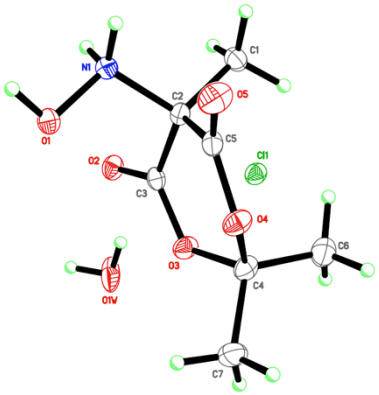

1a, Fw = 243.64, colorless block, 0.34 × 0.22 × 0.10 mm^3, triclinic, *P*-1 (no. 2), a = 6.04443(18), b = 7.6997(2), c = 12.3317(4) Å, α = 74.488(3), β = 85.322(3), γ = 86.211(3)°, V = 550.59(3) Å^3, Z = 2, D_x = 1.470 g cm^{-3}, μ = 0.357 mm^{-1}, abs. corr. range: 0.922–0.969. 4798 Reflections were measured up to a resolution of (sin $\theta/\lambda)_{max}$ = 0.59 Å^{-1}. 1936 Reflections were unique (R_{int} = 0.0180), of which 1680 were observed [$I > 2\sigma(I)$]. 154 Parameters were refined using 6 restraints. $R1/wR2$ [$I > 2\sigma(I)$]: 0.0278/0.0709. $R1/wR2$ [all refl.]: 0.0334/0.0731. S = 1.100. Residual electron density found between −0.26 and 0.32 e Å^{-3}.

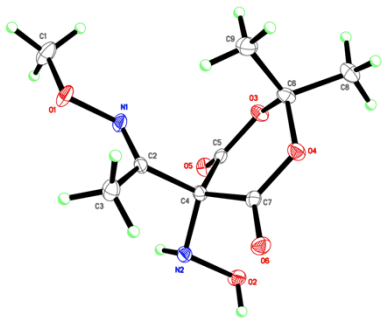

2a, Fw = 246.22, colorless plate, 0.47 × 0.35 × 0.04 mm^3, monoclinic, $P2_1/c$ (no. 14), a = 11.4024(3), b = 12.4341(3), c = 8.0005(3) Å, β = 99.510(3)°, V = 1118.71(6) Å^3, Z = 4, D_x = 1.462 g cm^{-3}, μ = 0.124 mm^{-1}, abs. corr. range: 0.956–0.996. 10603 Reflections were measured up to a resolution of (sin $\theta/\lambda)_{max}$ = 0.65 Å^{-1}. 2575 Reflections were unique (R_{int} = 0.0317), of which 2062 were observed [$I > 2\sigma(I)$]. 164 Parameters were refined with 2 restraints. $R1/wR2$ [$I > 2\sigma(I)$]: 0.0337/0.0795. $R1/wR2$ [all refl.]: 0.0471/0.0849. S = 1.028. Residual electron density found between −0.23 and 0.38 e Å^{-3}.

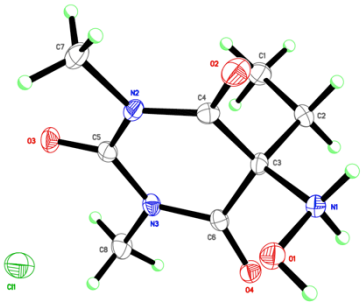

3a, Fw = 251.67, colorless lath, 0.38 × 0.11 × 0.07 mm^3, triclinic, *P*-1 (no. 2), *a* = 7.5765(3), *b* = 7.6395(4), *c* = 11.1394(3) Å, α = 81.909(3), β = 81.289(3), γ = 63.606(4)°, *V* = 568.92(4) Å^3, *Z* = 2, D_x = 1.469 g cm^{-3}, μ = 0.340 mm^{-1}, abs. corr. range: 0.926–0.980. 8665 Reflections were measured up to a resolution of (sin $\theta/\lambda)_{max}$ = 0.62 Å^{-1}. 2291 Reflections were unique (R_{int} = 0.0273), of which 1970 were observed [$I > 2\sigma(I)$]. 160 Parameters were refined with 3 restraints. *R*1/*wR*2 [$I > 2\sigma(I)$]: 0.0295/0.0781. *R*1/*wR*2 [all refl.]: 0.0367/0.0814. S = 1.064. Residual electron density found between −0.25 and 0.31 e Å^{-3}.

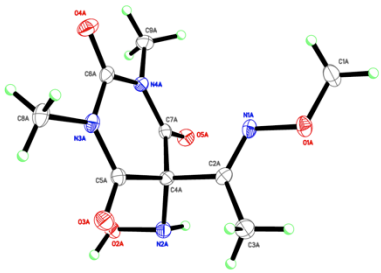

4a, Fw = 258.24, colorless lath, 0.44 × 0.15 × 0.03 mm^3, triclinic, $P\bar{1}$ (no. 2), *a* = 7.7437(3), *b* = 10.5514(4), *c* = 15.0891(6) Å, α = 107.325(3), β = 97.908(3), γ = 90.257(3)°, *V* = 1164.41(8) Å^3, *Z* = 4, D_x = 1.473 g cm^{-3}, μ = 0.121 mm^{-1}, abs. corr. range: 0.957–0.996. 16907 Reflections were measured up to a resolution of (sin $\theta/\lambda)_{max}$ = 0.63 Å^{-1}. 4706 Reflections were unique (R_{int} = 0.0310), of which 3609 were observed [$I > 2\sigma(I)$]. 345 Parameters were refined with 4 restraints. *R*1/*wR*2 [$I > 2\sigma(I)$]: 0.0369/0.0832. *R*1/*wR*2 [all refl.]: 0.0559/0.0895. S = 1.035. Residual electron density found between −0.23 and 0.29 e Å^{-3}.

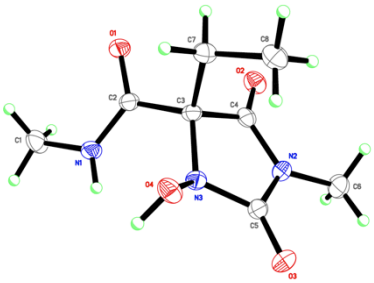

5, Fw = 215.21, colorless small block, 0.21 × 0.13 × 0.10 mm^3, monoclinic, $P2_1/c$ (no. 14), a = 11.1127(4), b = 9.1165(2), c = 10.0702(3) Å, β = 104.117(3)°, V = 989.39(5) Å^3, Z = 4, D_x = 1.445 g cm^{-3}, μ = 0.117 mm^{-1}, abs. corr. range: 0.982–0.991. 5394 Reflections were measured up to a resolution of (sin $\theta/\lambda)_{max}$ = 0.59 Å^{-1}. 1734 Reflections were unique (R_{int} = 0.0305), of which 1390 were observed [$I > 2\sigma(I)$]. 145 Parameters were refined using 2 restraints. $R1/wR2$ [$I > 2\sigma(I)$]: 0.0399/0.1056. $R1/wR2$ [all refl.]: 0.0518/0.1123. S = 1.058. Residual electron density found between −0.26and 0.25 e Å^{-3}.

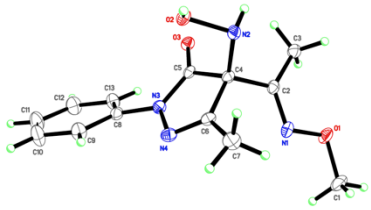

6a, Fw = 276.30, colorless lath, 0.43 × 0.22 × 0.08 mm^3, monoclinic, $P2_1/c$ (no. 14), a = 5.8807(2), b = 26.2720(8), c = 9.1340(3) Å, β = 101.419(4)°, V = 1383.25(8) Å^3, Z = 4, D_x = 1.327 g cm^{-3}, μ = 0.097 mm^{-1}, abs. corr. range: 0.969–0.993. 11490 Reflections were measured up to a resolution of (sin $\theta/\lambda)_{max}$ = 0.63 Å^{-1}. 2803 Reflections were unique (R_{int} =0.0283), of which 2300 were observed [$I > 2\sigma(I)$]. 190 Parameters were refined with 2 restraints. $R1/wR2$ [$I > 2\sigma(I)$]: 0.0376/0.0922. $R1/wR2$ [all refl.]: 0.0484/0.0966. S = 1.038. Residual electron density found between −0.29 and 0.31 e Å^{-3}.

2.7.2 ^{1}H and ^{13}C NMR Spectra

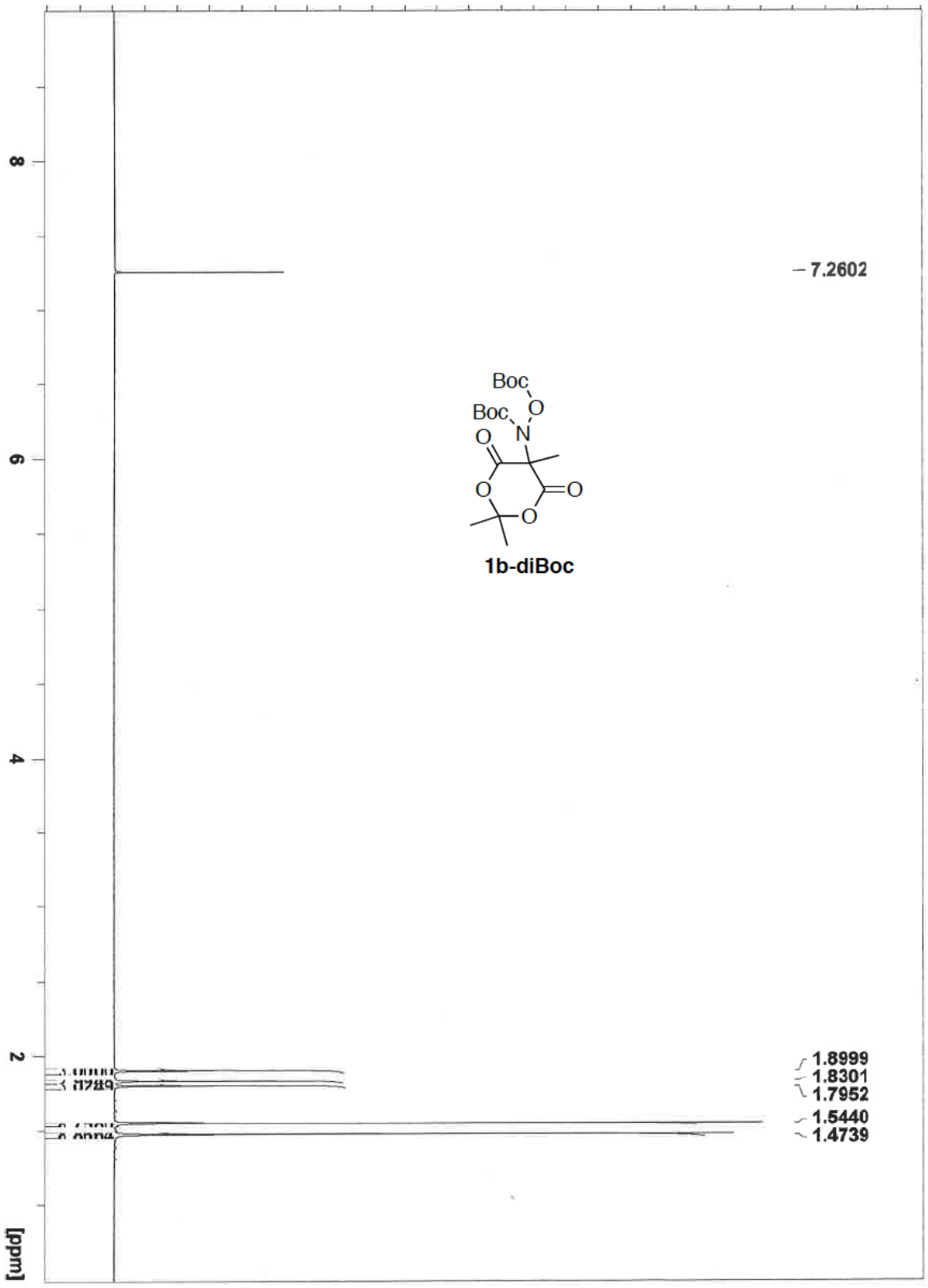

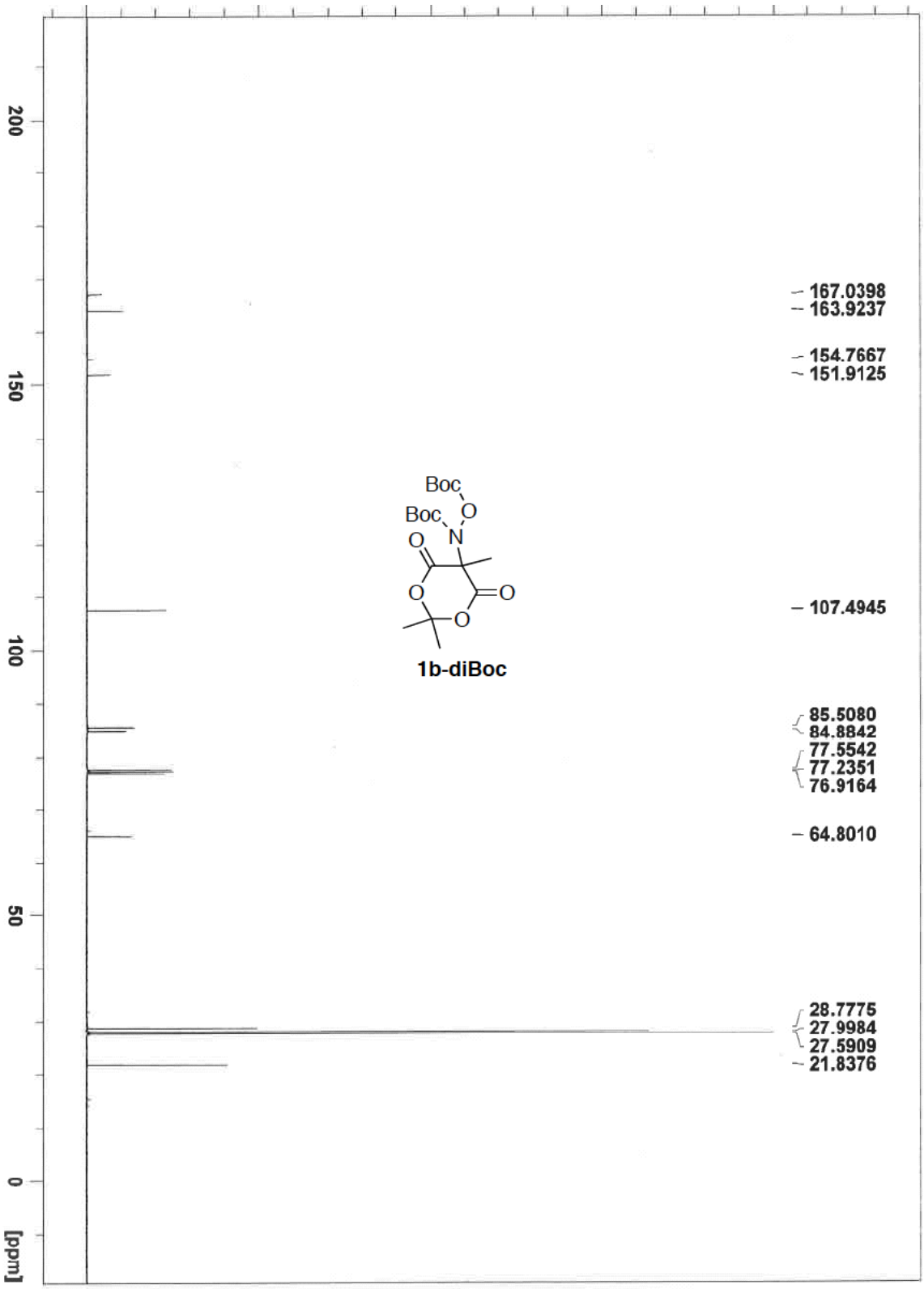
200
150
100
50
0
[ppm]
167.0398
163.9237
154.7667
151.9125
107.4945
85.5080
84.8842
77.5542
77.2351
76.9164
64.8010
28.7775
27.9984
27.5909
21.8376
Boc
Boc
O
N
O
O
O
O
O
1b-diBoc

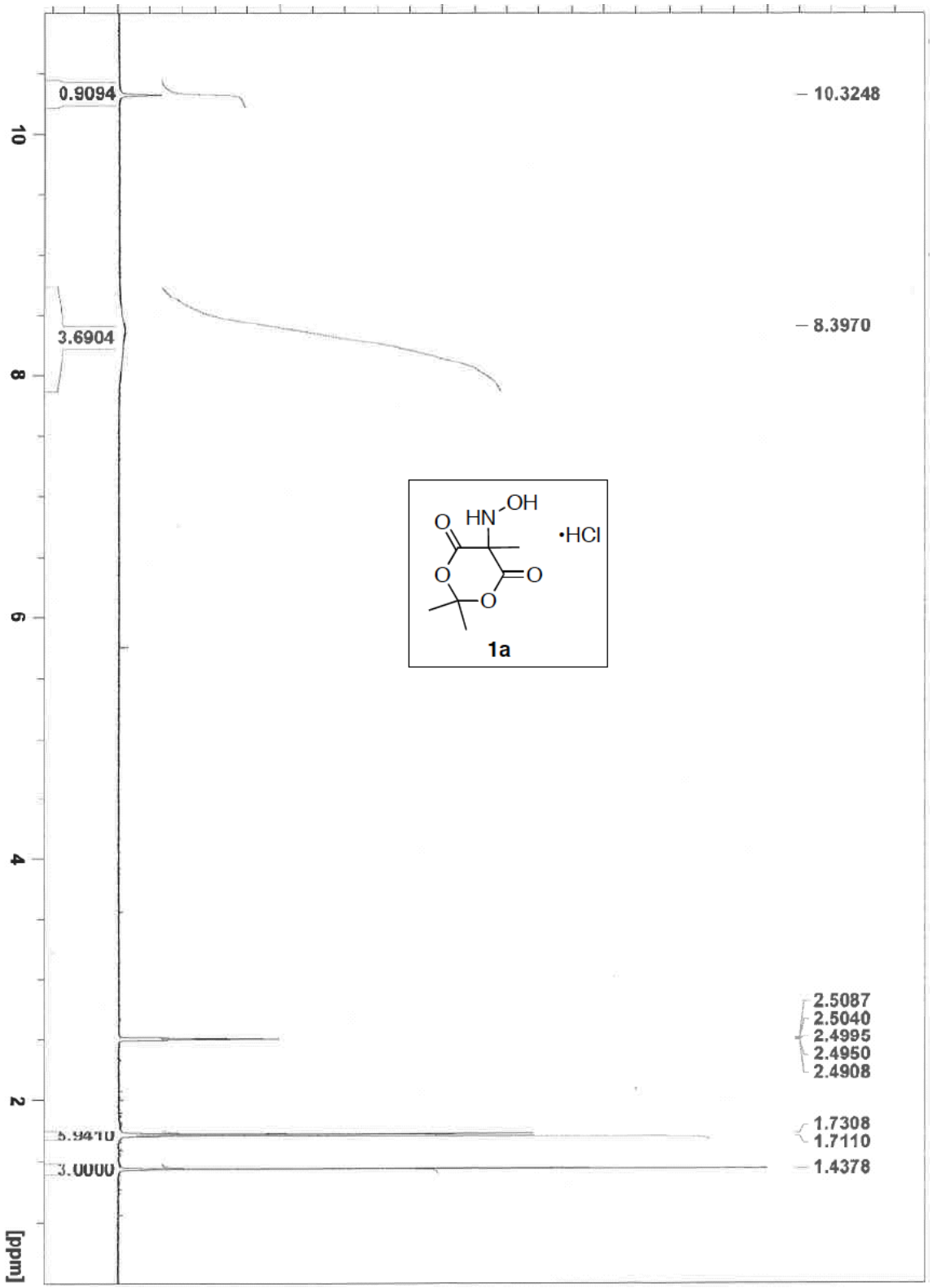
0.9094
3.6904
3.0000
10.3248
8.3970
2.5087
2.5040
2.4995
2.4950
2.4908
1.7308
1.7110
1.4378
HN
OH
•HCl
1a
10
8
6
4
2
[ppm]

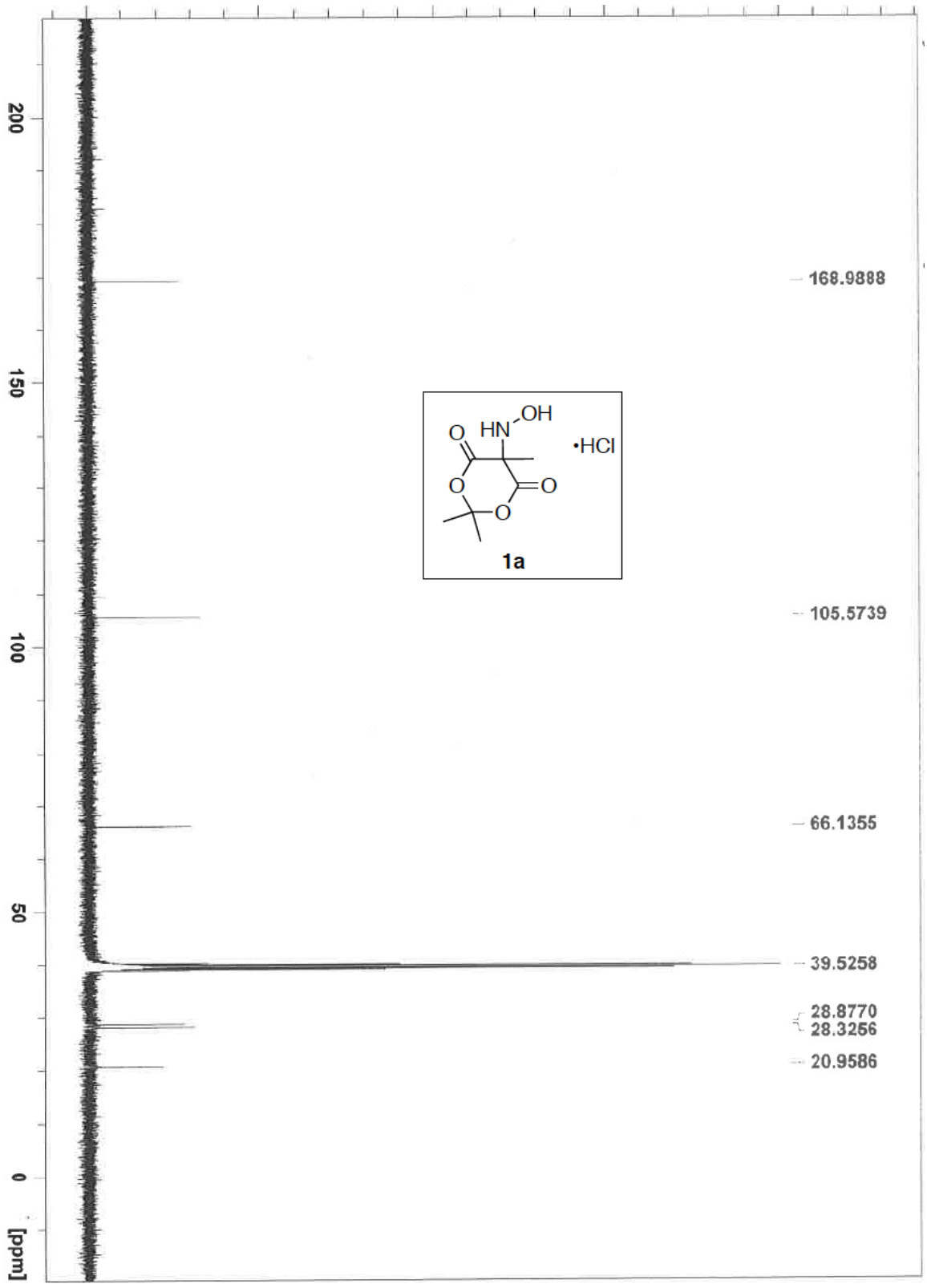
200
150
100
50
0
[ppm]
168.9888
105.5739
66.1355
39.5258
28.8770
28.3256
20.9586
HN
OH
O
O
O
O
•HCl
1a

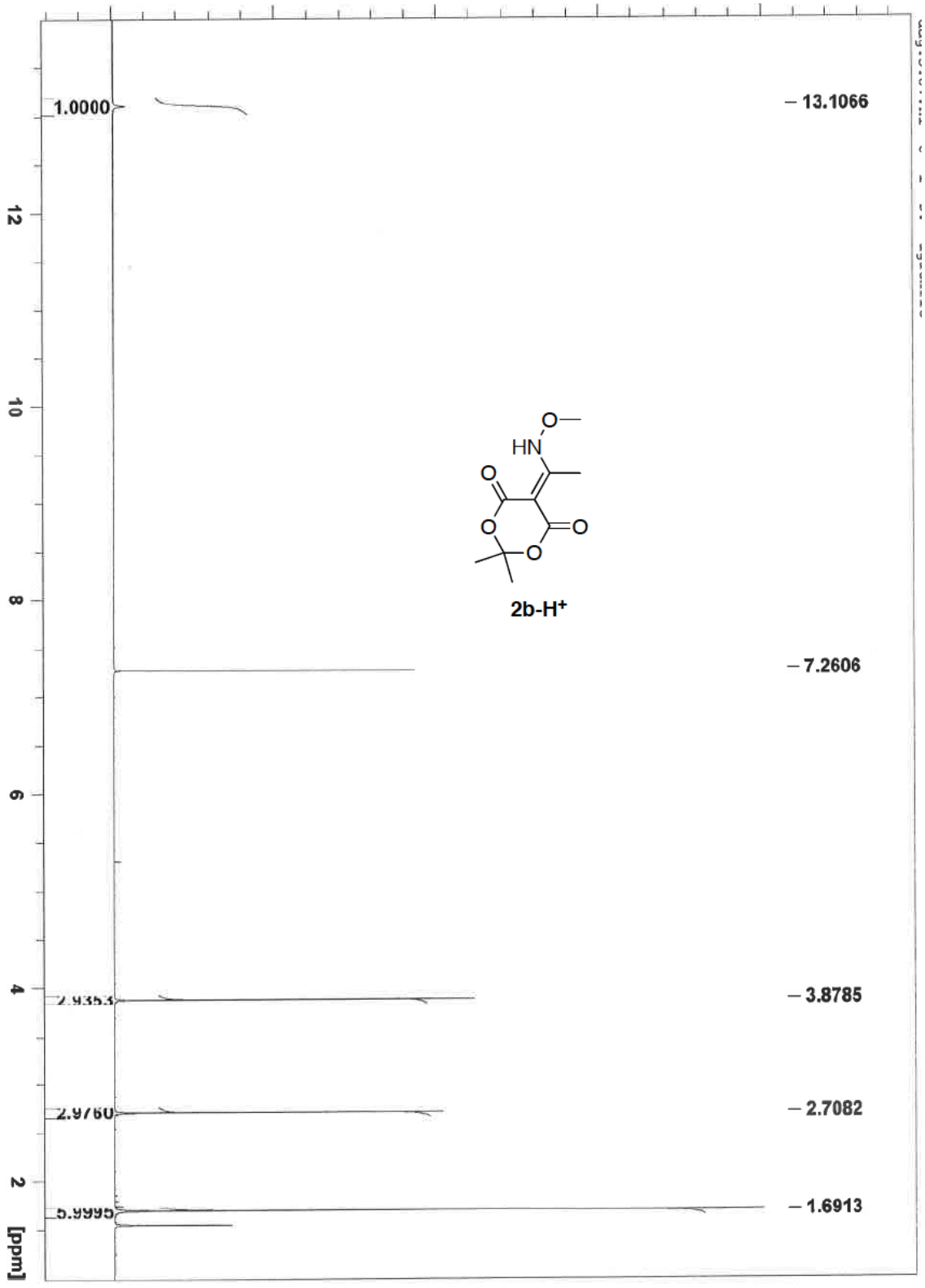
1.0000
13.1066
7.2606
3.8785
2.7082
1.6913
2.9353
2.9760
5.9995
12
10
8
6
4
2
[ppm]
HN
O
O
O
O
O
O
2b-H+

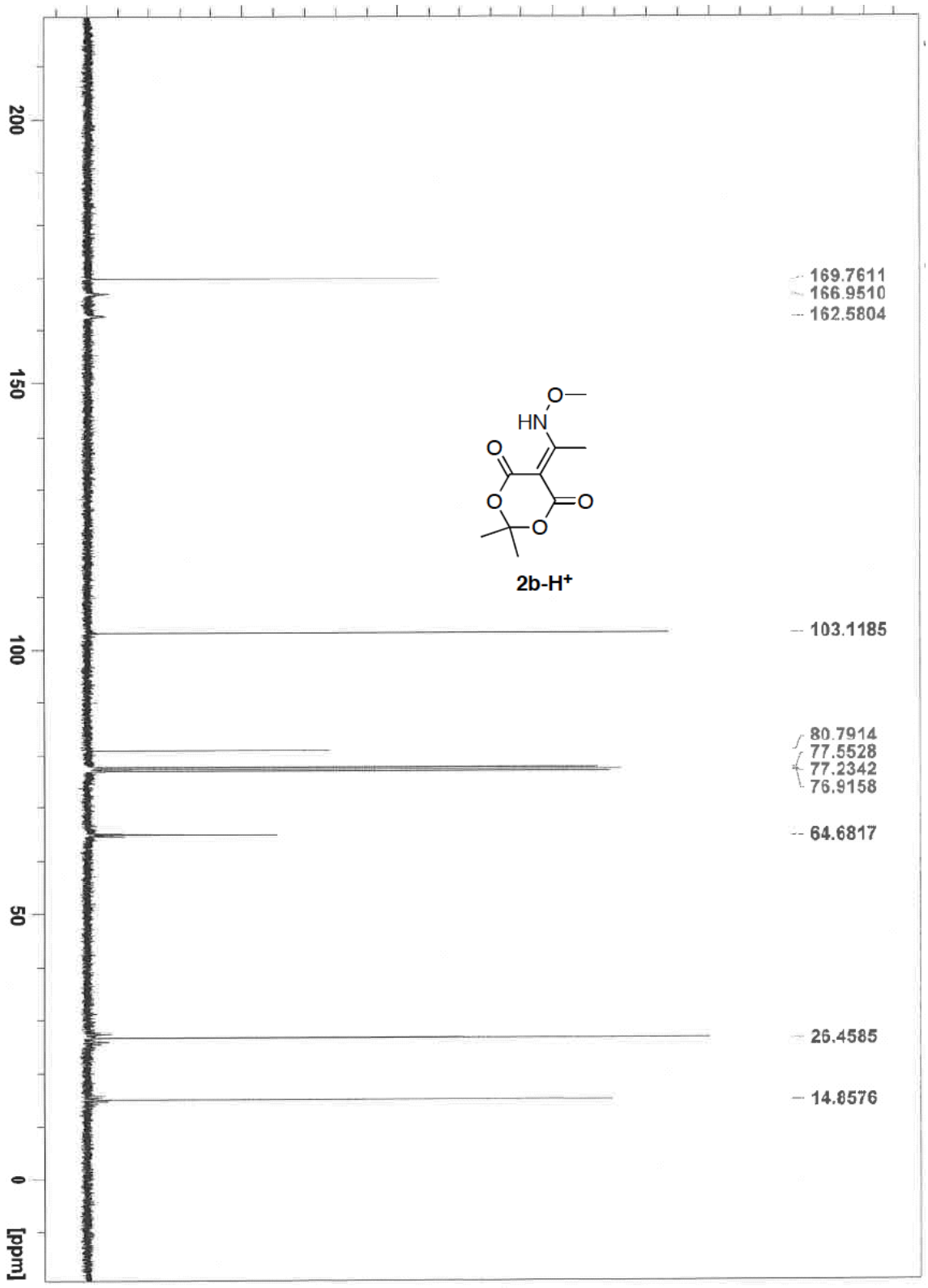
200
150
100
50
0
[ppm]
169.7611
166.9510
162.5804
103.1185
80.7914
77.5528
77.2342
76.9158
64.6817
26.4585
14.8576
HN
O
O
O
O
O
2b-H+

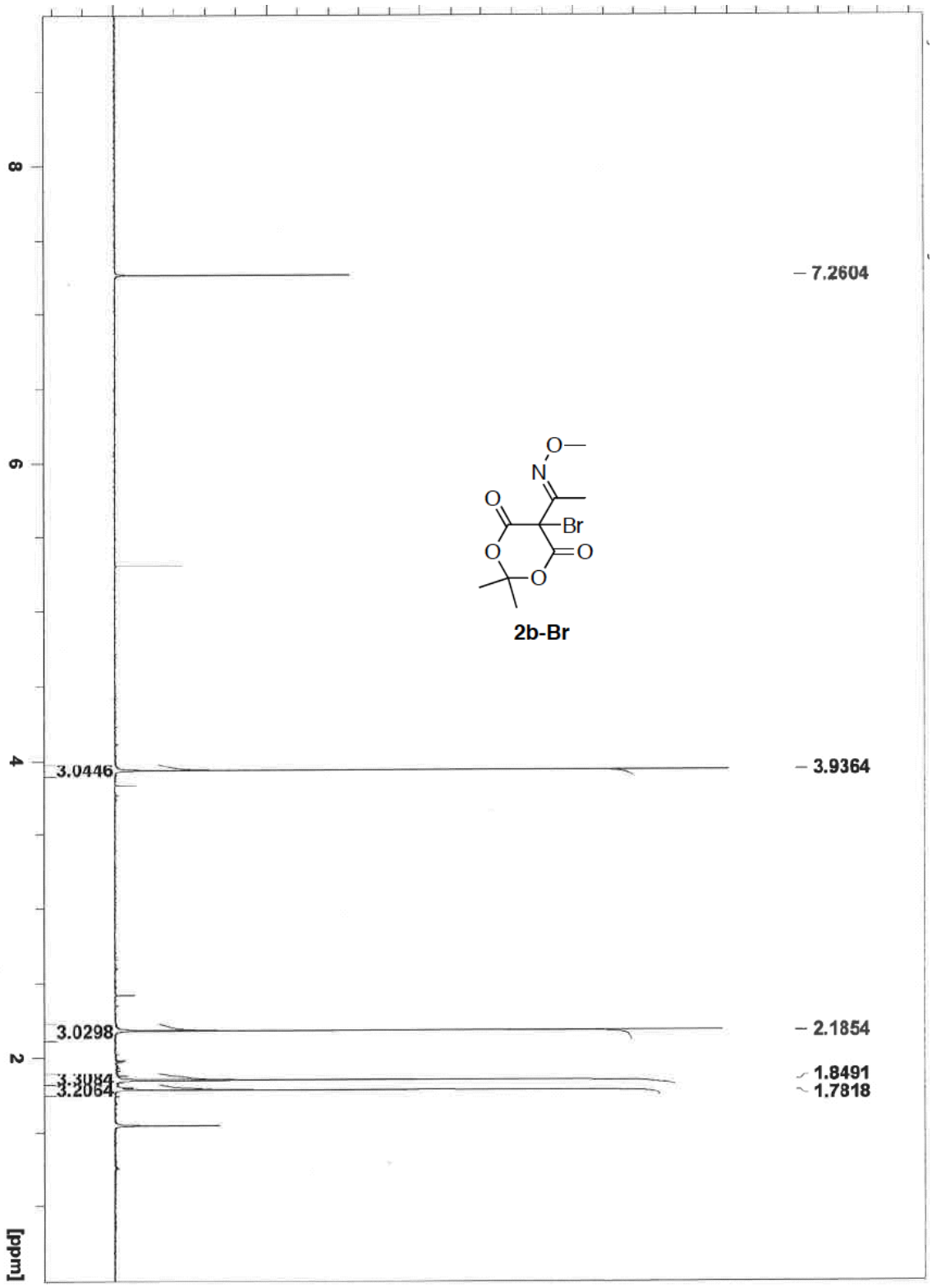
8
6
4
2
[ppm]
7.2604
3.9364
2.1854
1.8491
1.7818
3.0446
3.0298
3.2064
Br
O
N
2b-Br

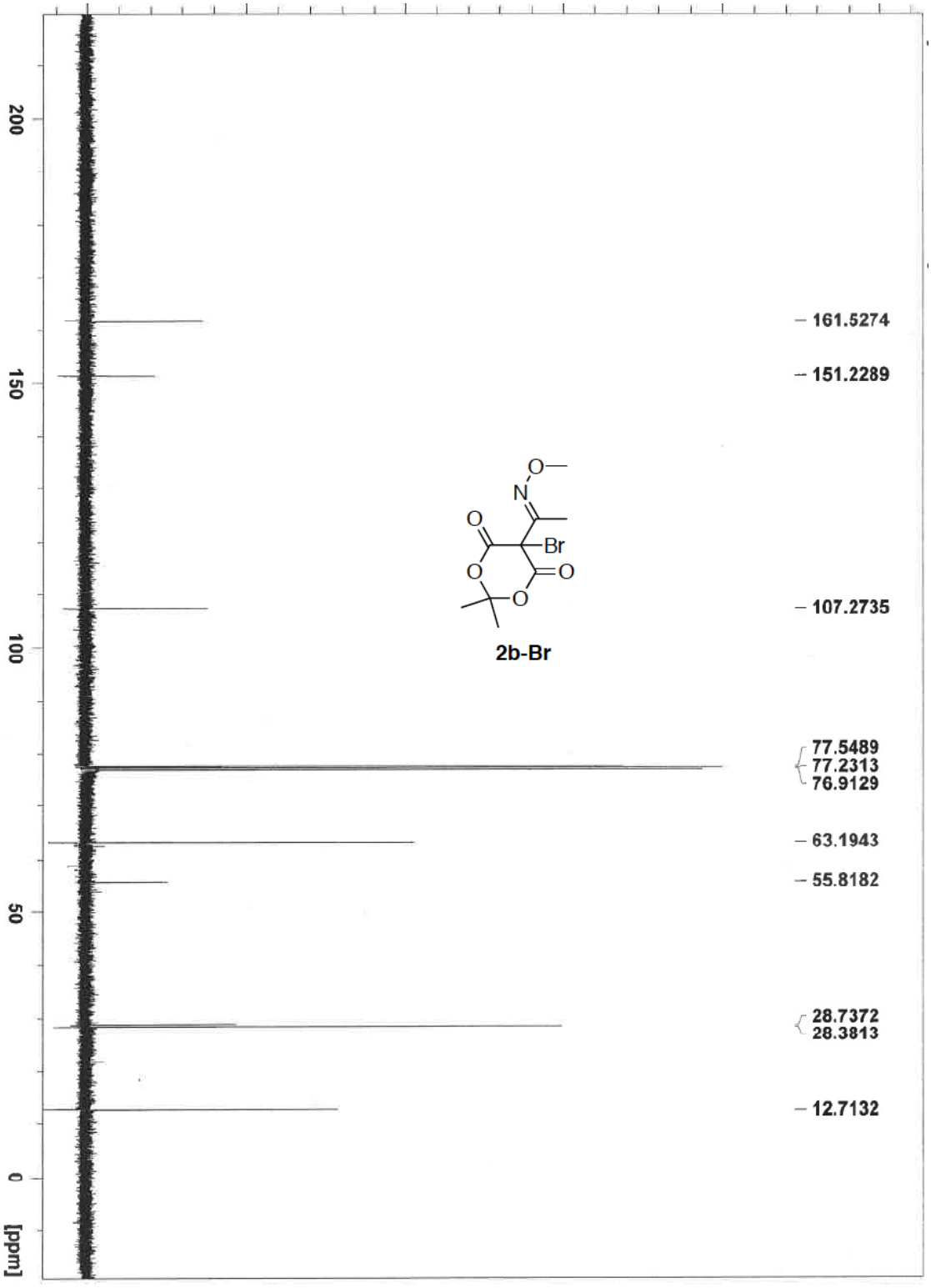
200
150
100
50
0
[ppm]
161.5274
151.2289
107.2735
77.5489
77.2313
76.9129
63.1943
55.8182
28.7372
28.3813
12.7132
O
N
O
Br
O
O
O
O
2b-Br

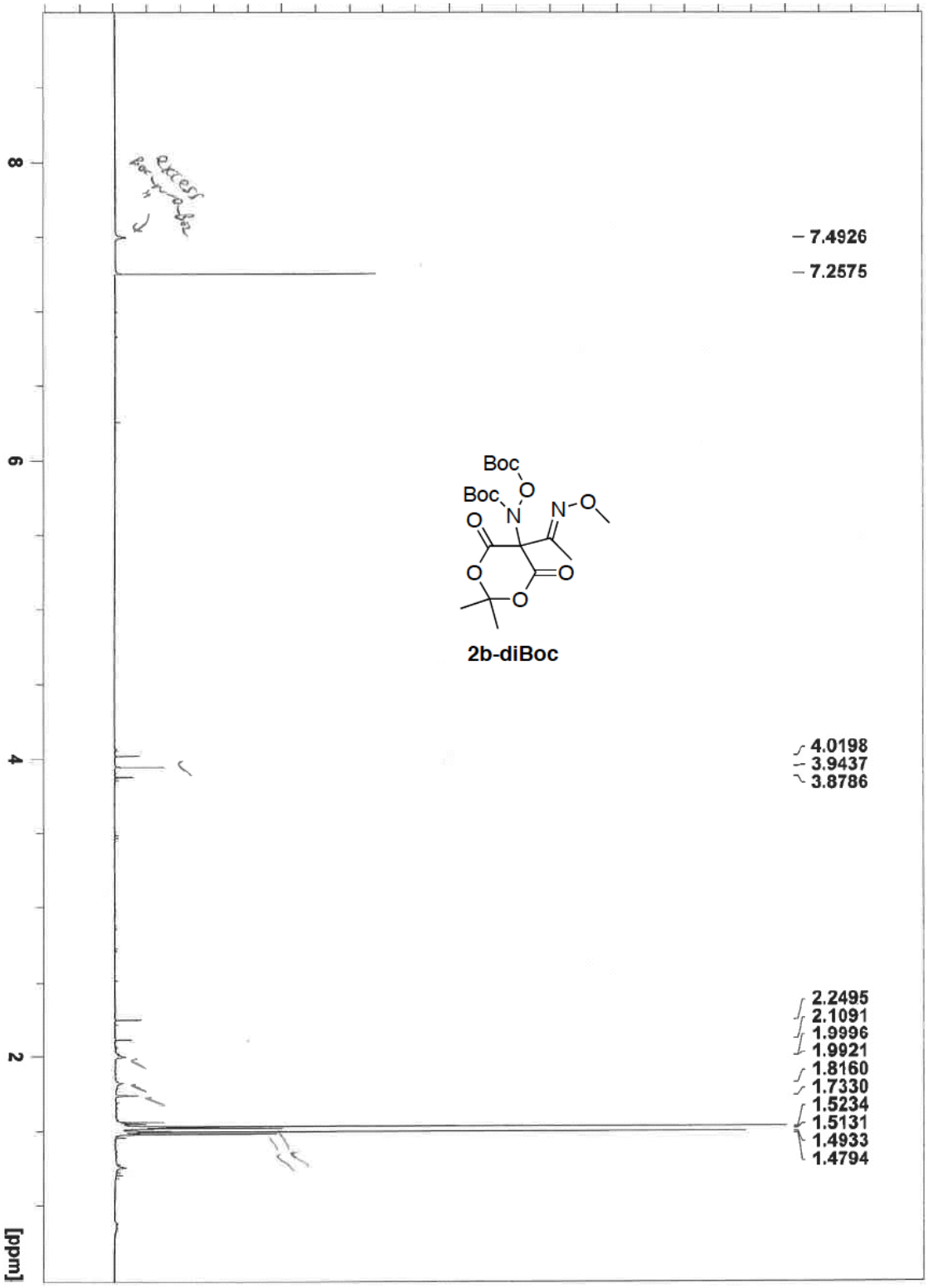
7.4926
7.2575
Boc
Boc
O
N
N
O
O
O
O
O
O
2b-diBoc
4.0198
3.9437
3.8786
2.2495
2.1091
1.9996
1.9921
1.8160
1.7330
1.5234
1.5131
1.4933
1.4794
8
6
4
2
[ppm]

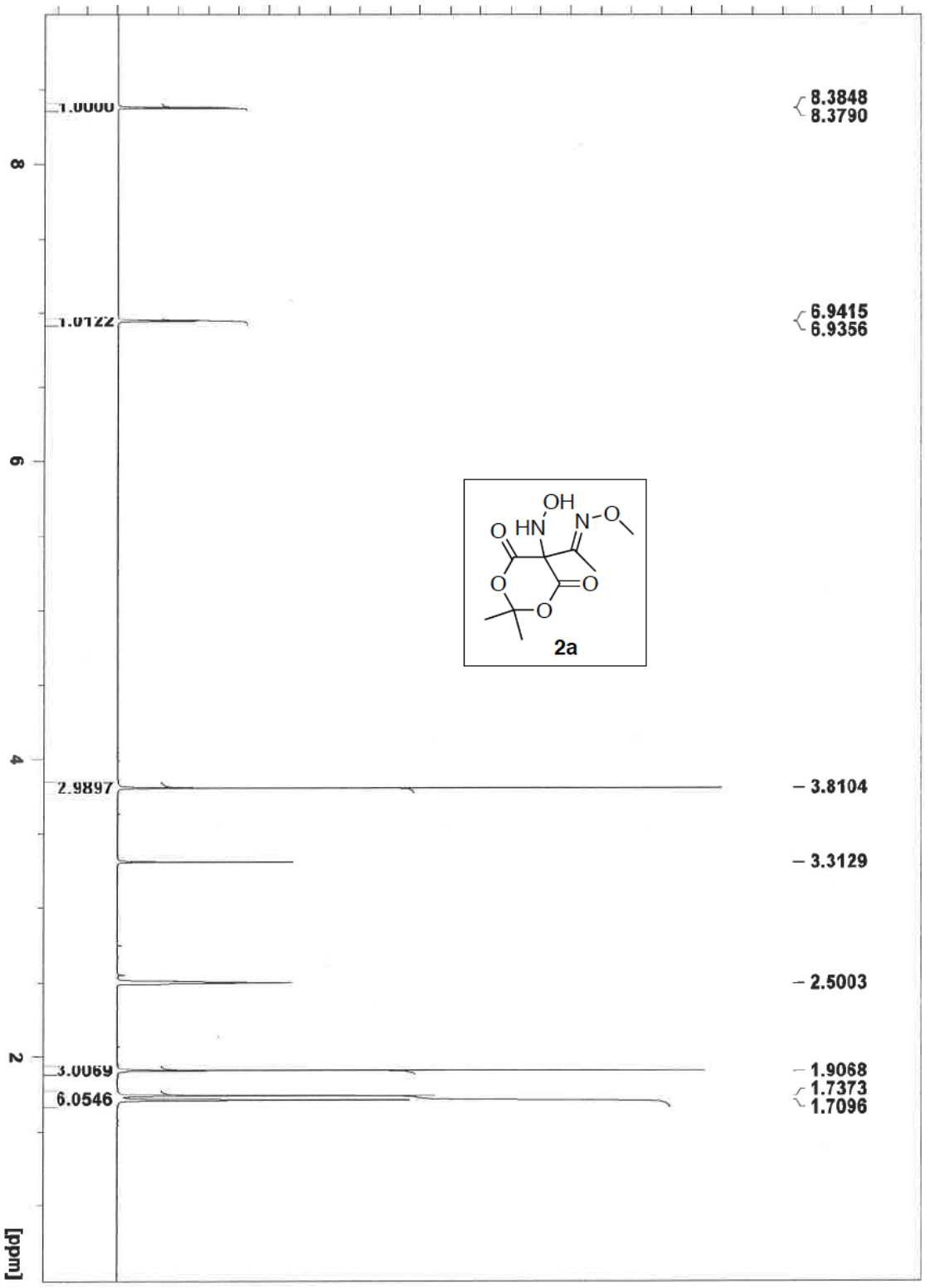
8.3848
8.3790
6.9415
6.9356
3.8104
3.3129
2.5003
1.9068
1.7373
1.7096
2.9897
6.0546
OH
HN
N
O
2a
8
6
4
2
[ppm]

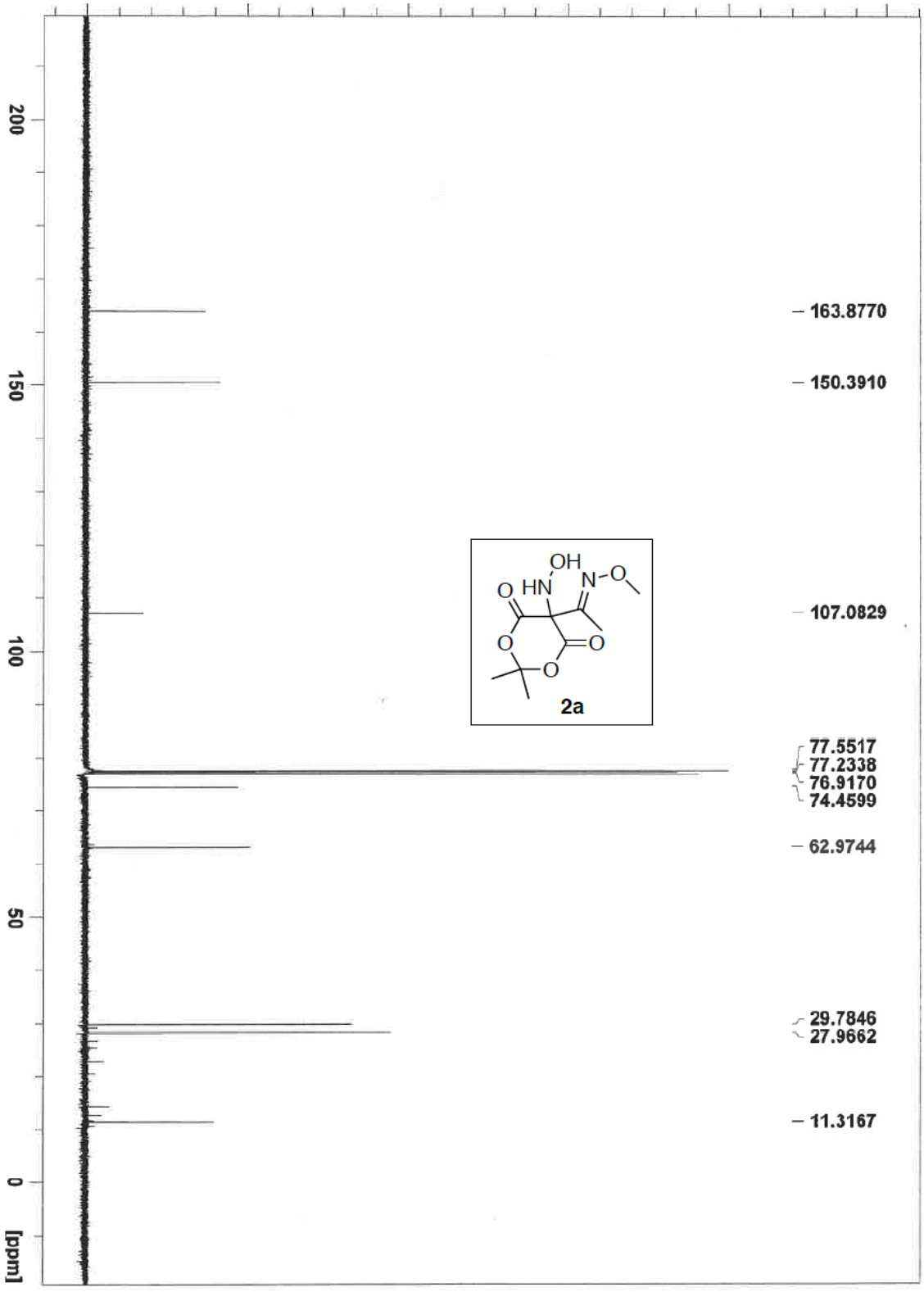
200
150
100
50
0
[ppm]
163.8770
150.3910
107.0829
77.5517
77.2338
76.9170
74.4599
62.9744
29.7846
27.9662
11.3167
OH
HN
N
O
O
O
O
O
2a

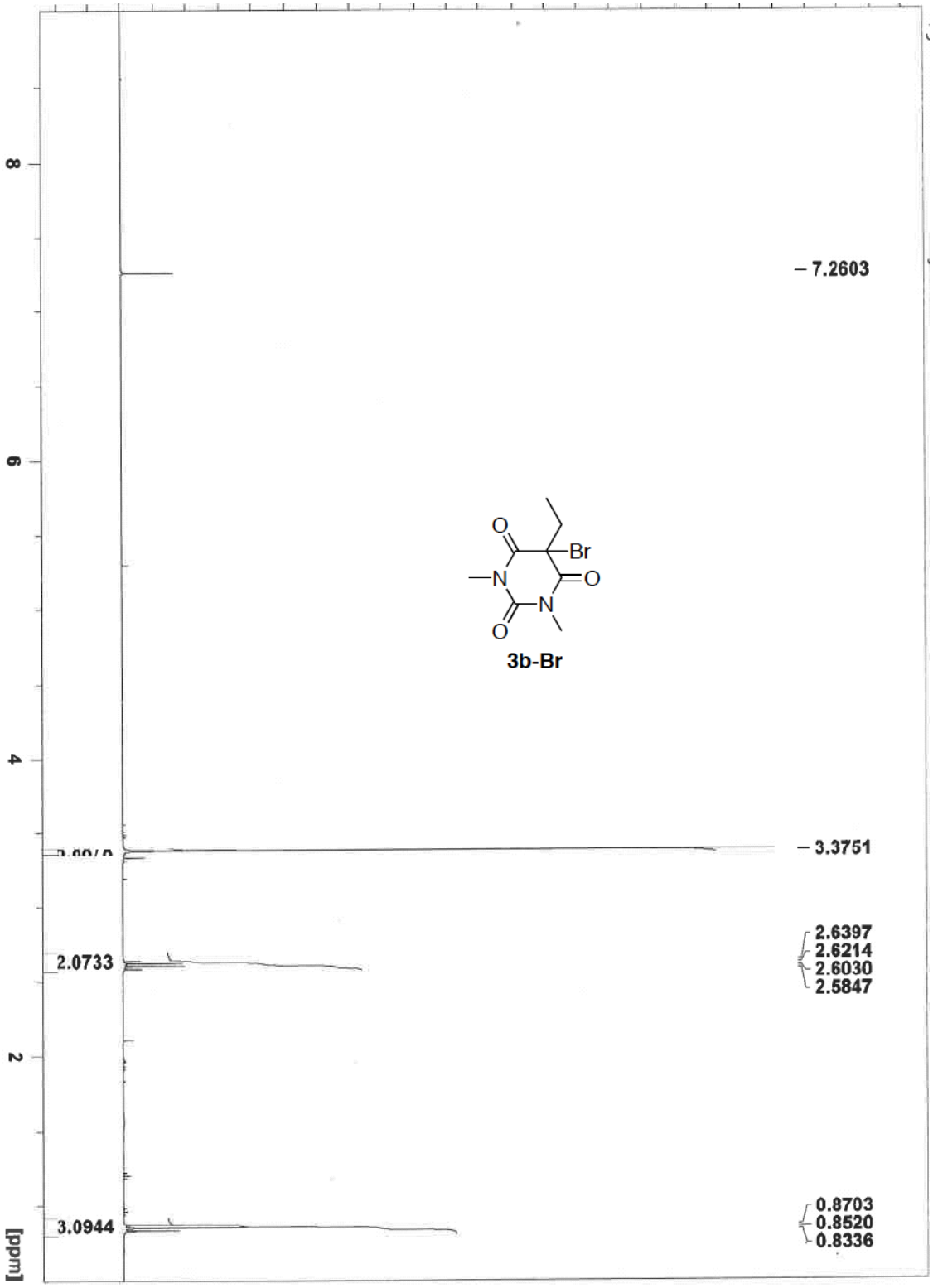
8
6
4
2
[ppm]
7.2603
3.3751
2.6397
2.6214
2.6030
2.5847
2.0733
0.8703
0.8520
0.8336
3.0944
Br
O
N
O
N
O
O

3b-Br

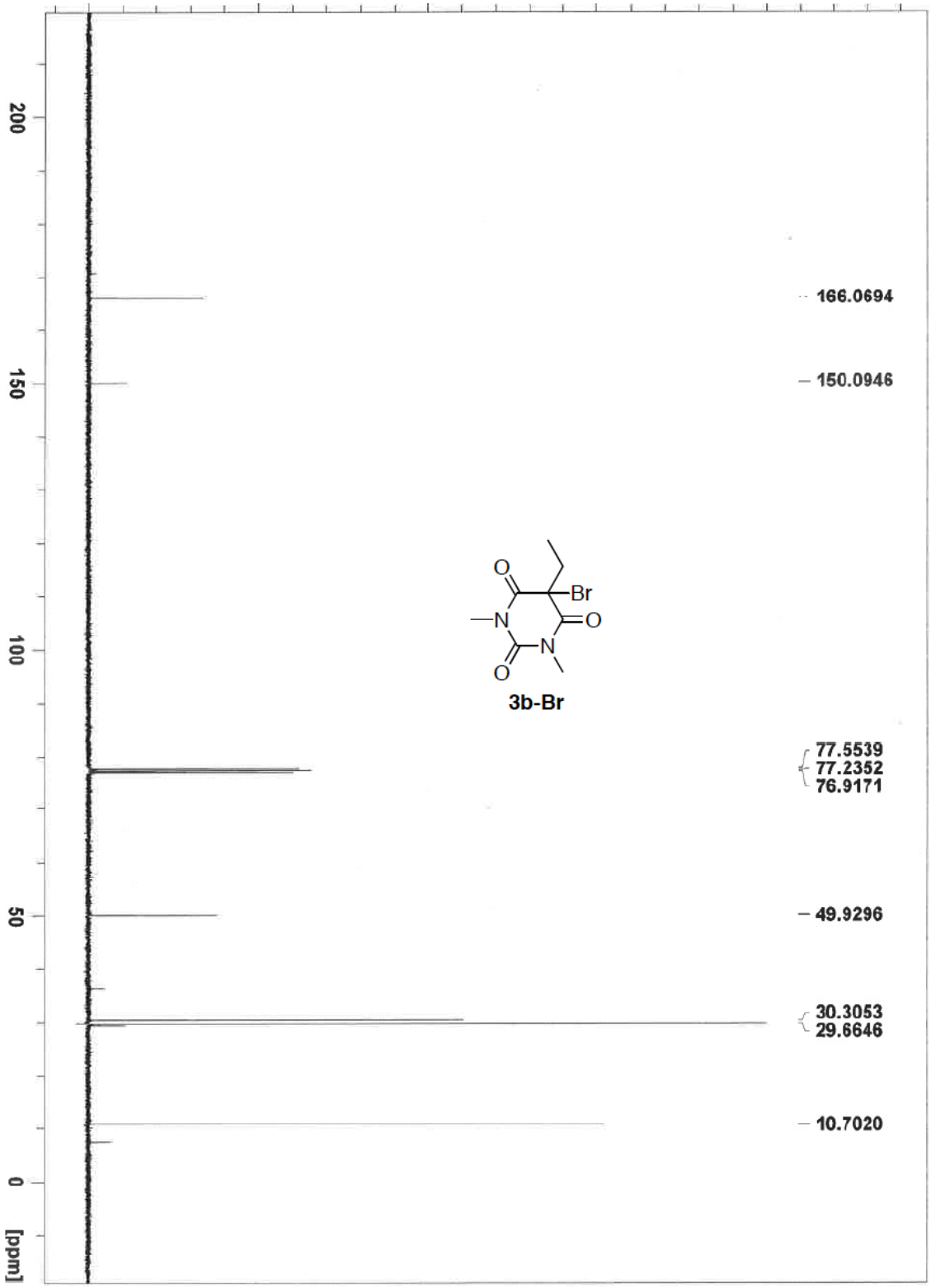
200
150
100
50
0
[ppm]
166.0694
150.0946
77.5539
77.2352
76.9171
49.9296
30.3053
29.6646
10.7020
O
Br
N
O
N
O
3b-Br

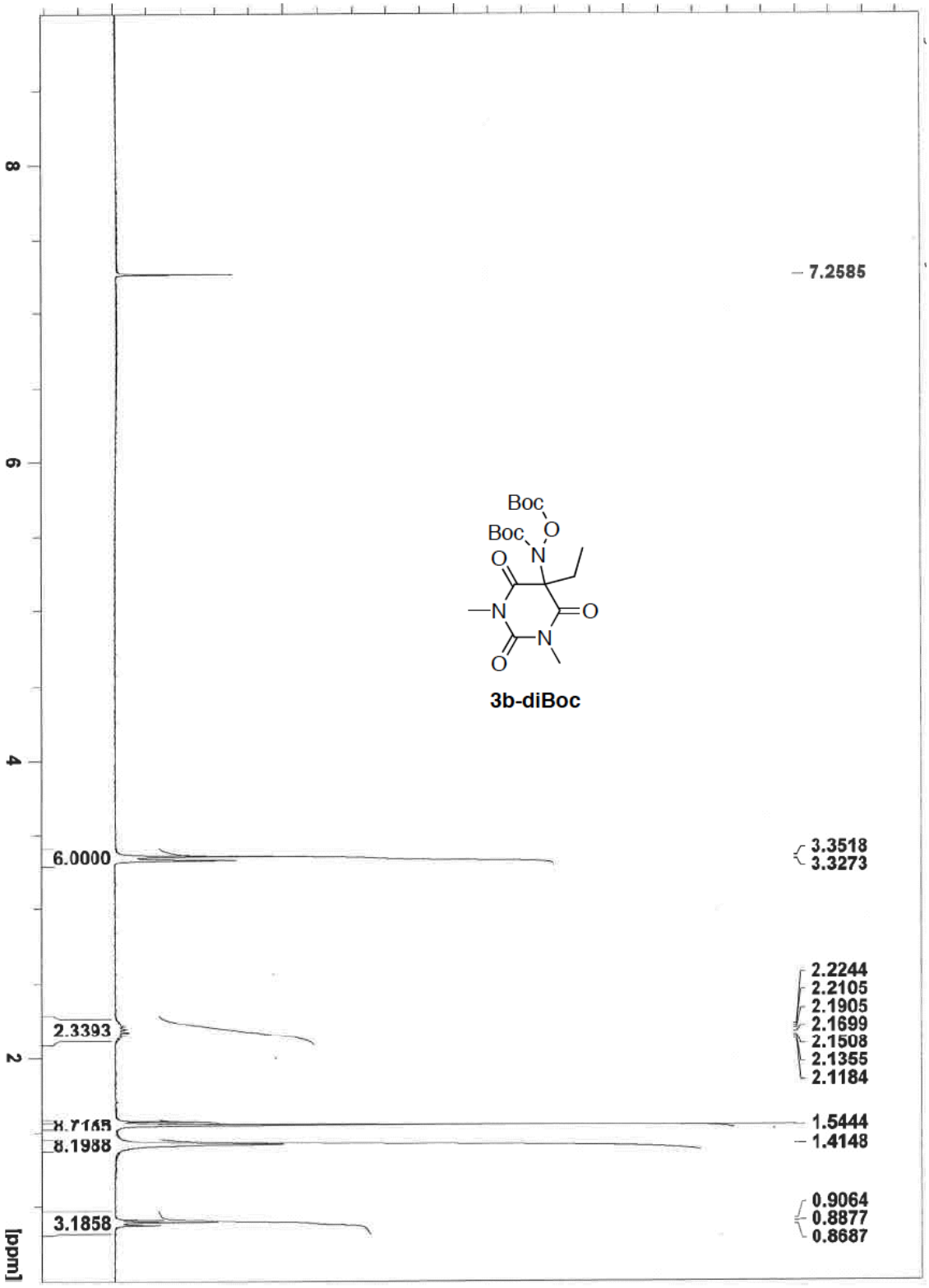
8
6
4
2
[ppm]
7.2585
Boc
Boc
O
N
O
N
O
N
O
O
3b-diBoc
6.0000
2.3393
8.7165
8.1988
3.1858
3.3518
3.3273
2.2244
2.2105
2.1905
2.1699
2.1508
2.1355
2.1184
1.5444
1.4148
0.9064
0.8877
0.8687

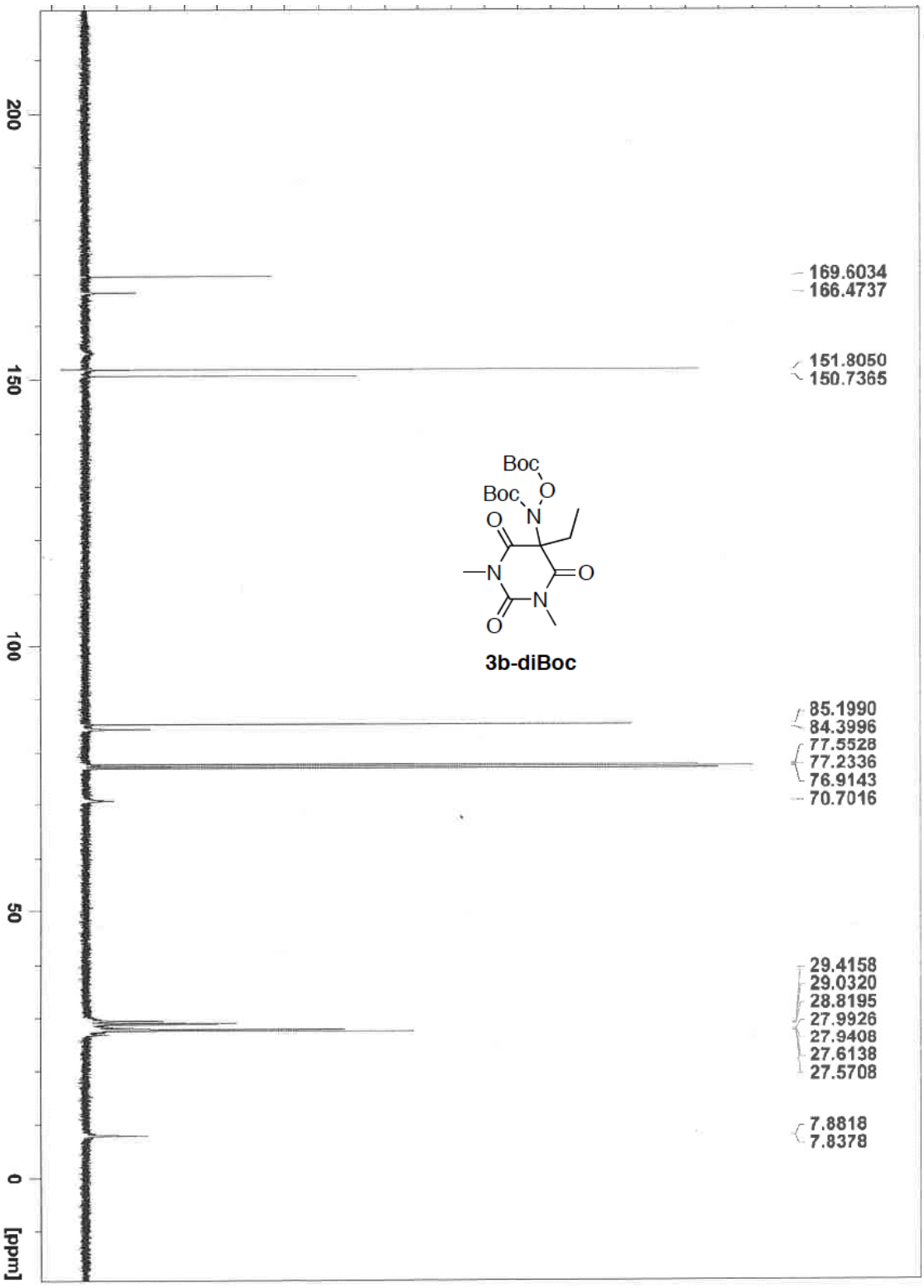
200
150
100
50
0
[ppm]
169.6034
166.4737
151.8050
150.7365
85.1990
84.3996
77.5528
77.2336
76.9143
70.7016
29.4158
29.0320
28.8195
27.9926
27.9408
27.6138
27.5708
7.8818
7.8378
Boc
Boc
O
N
O
N
O
N
O
O
3b-diBoc

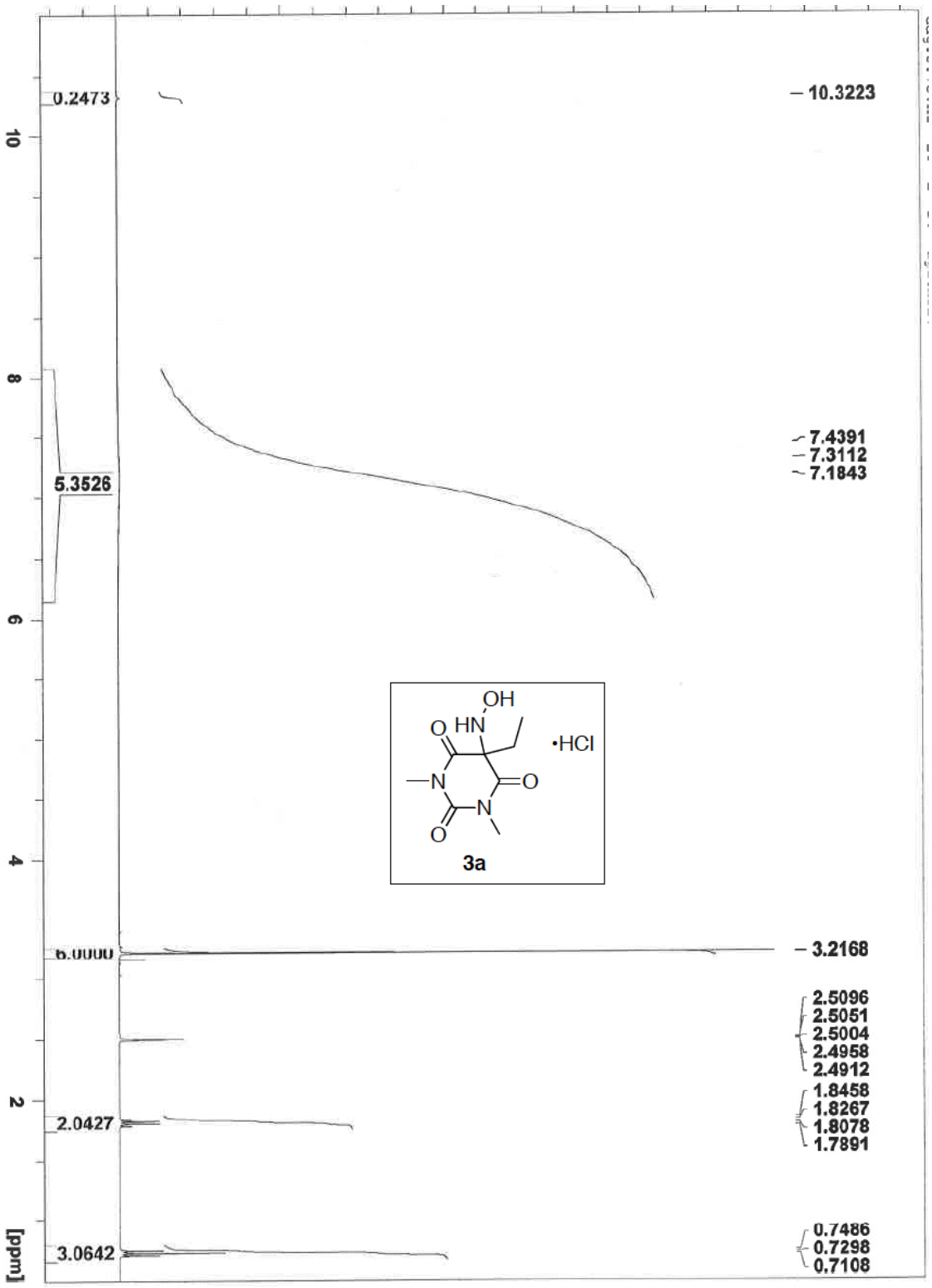
10.3223
0.2473
7.4391
7.3112
7.1843
5.3526
3.2168
6.0000
2.5096
2.5051
2.5004
2.4958
2.4912
1.8458
1.8267
1.8078
1.7891
2.0427
0.7486
0.7298
0.7108
3.0642
[ppm]
OH
HN
O
N
O
•HCl
3a

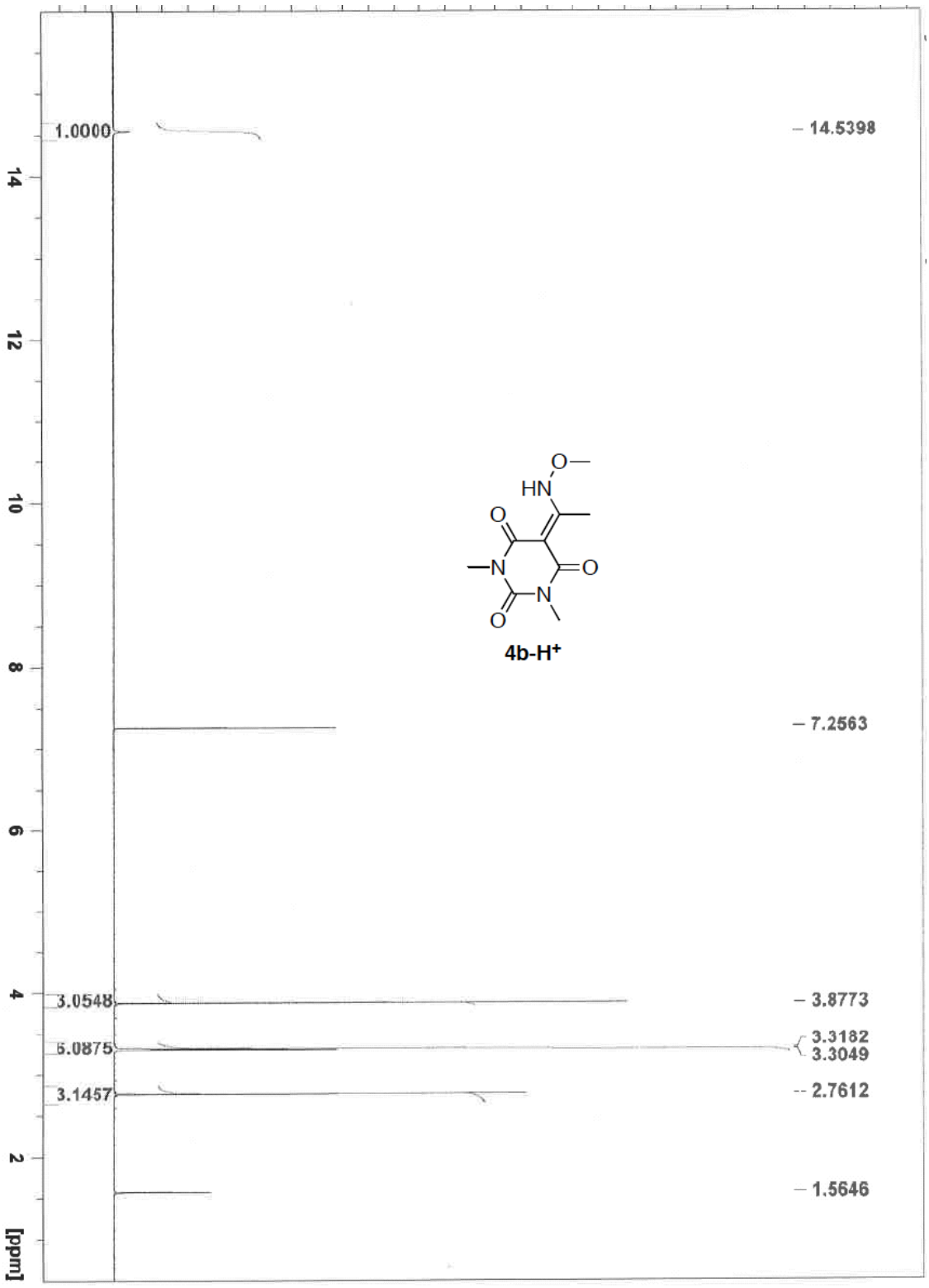
1.0000
14.5398
7.2563
3.0548
3.8773
5.0875
3.3182
3.3049
3.1457
2.7612
1.5646
[ppm]
4b-H+

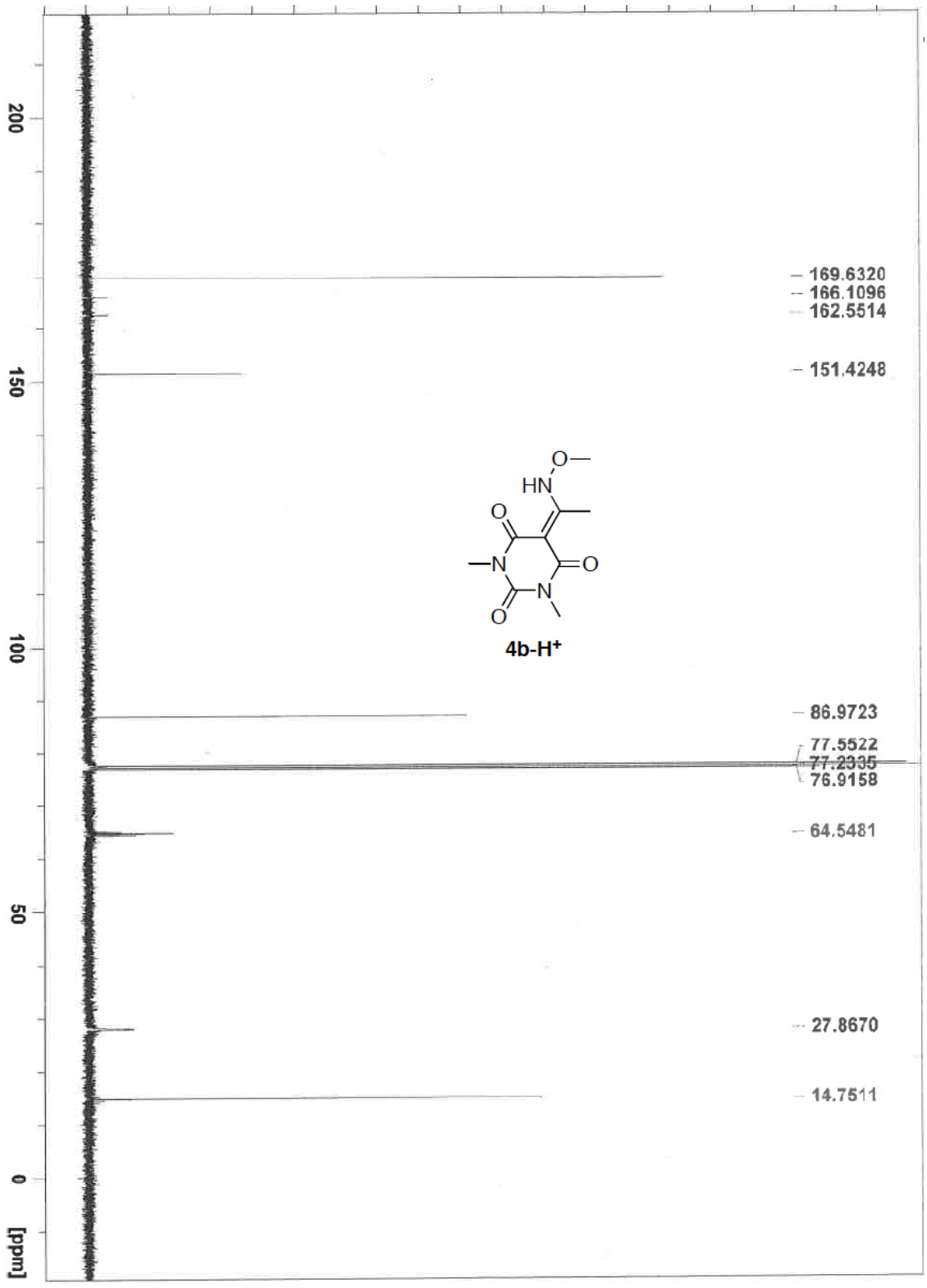
200
150
100
50
0
[ppm]
169.6320
166.1096
162.5514
151.4248
86.9723
77.5522
77.2335
76.9158
64.5481
27.8670
14.7511
HN
O
N
4b-H+

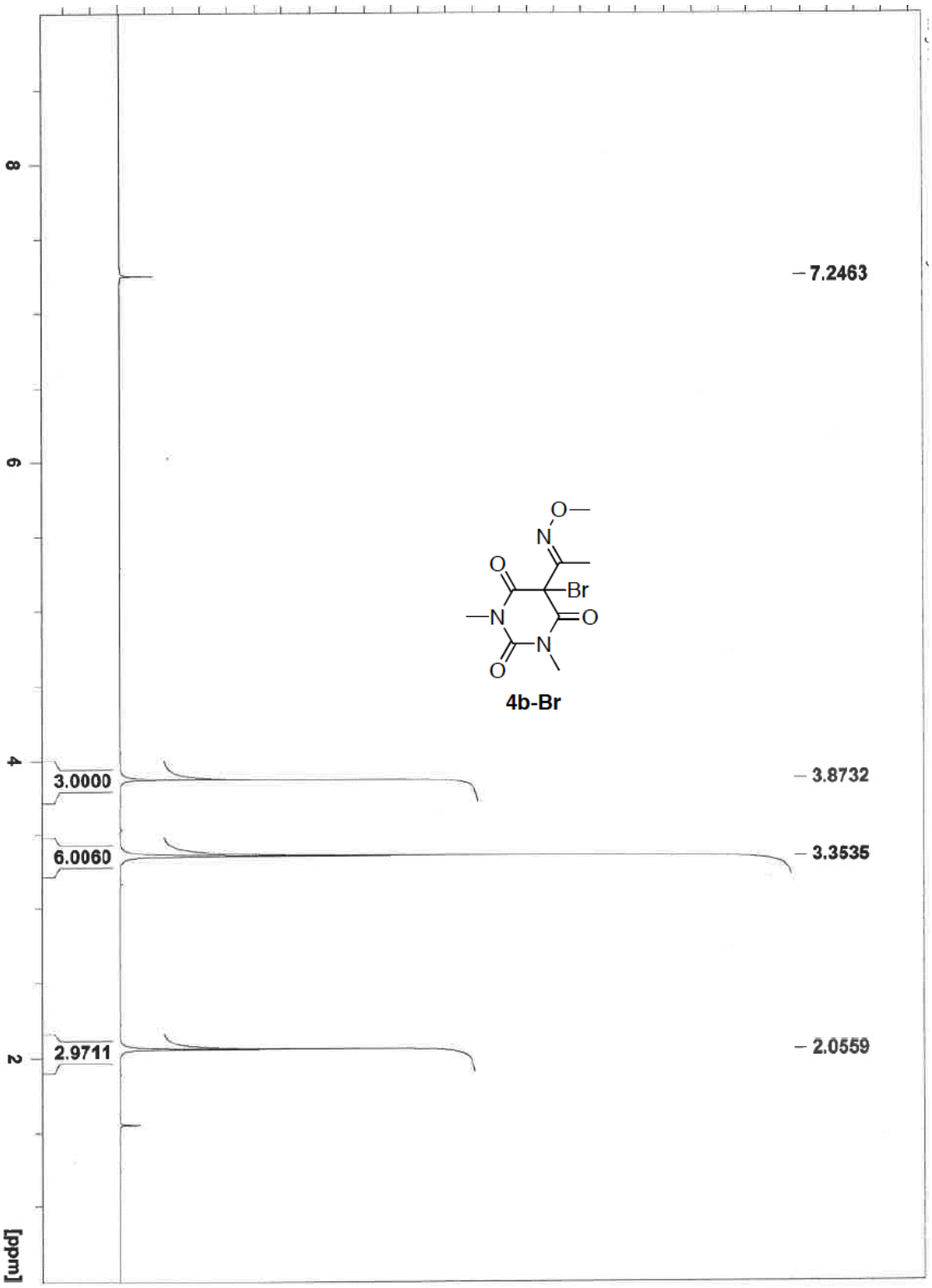
8
6
4
2
[ppm]
7.2463
3.8732
3.3535
2.0559
3.0000
6.0060
2.9711
O
N
O
Br
N
O
N
O
4b-Br

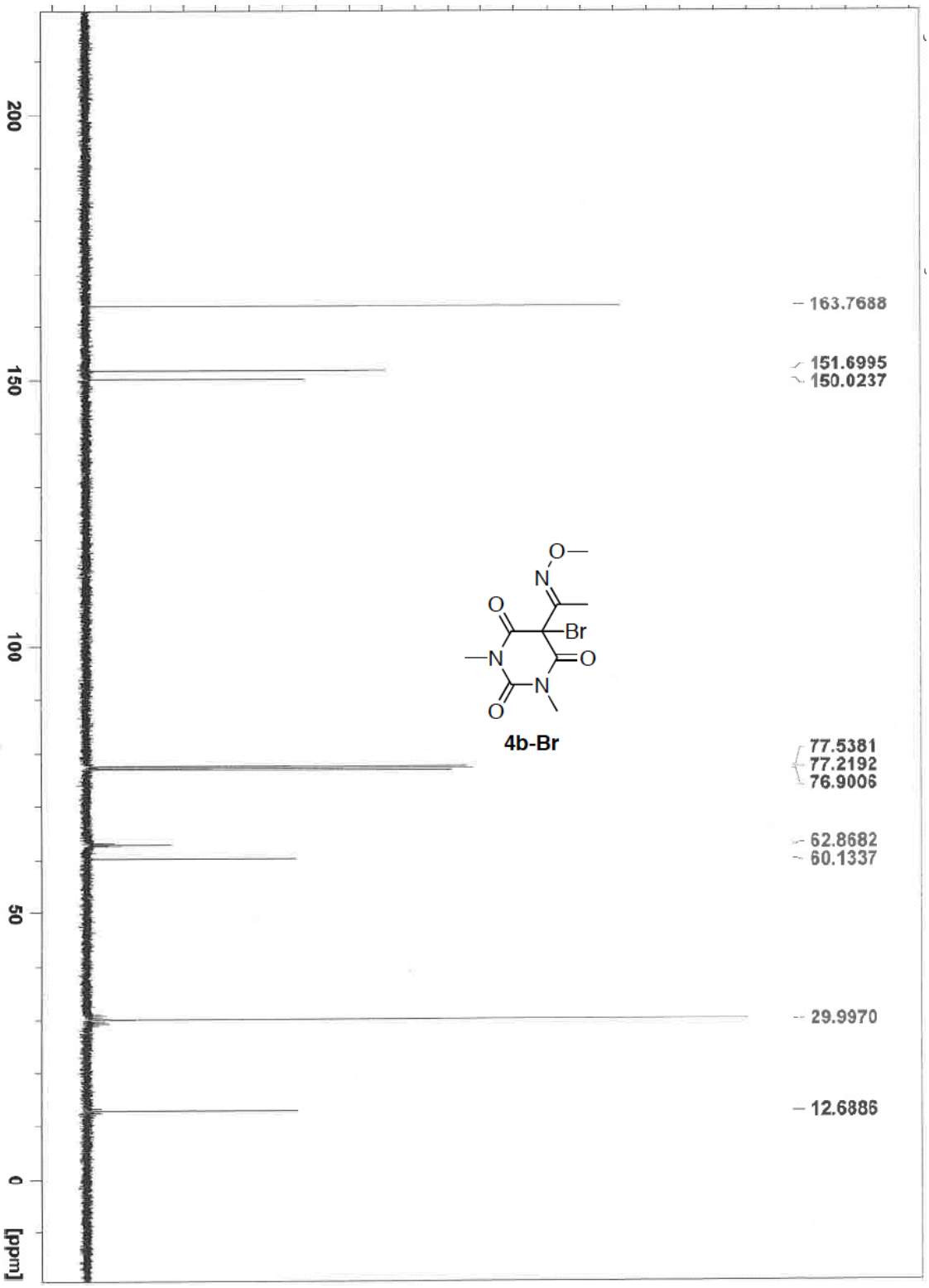
200
150
100
50
0
[ppm]
163.7688
151.6995
150.0237
77.5381
77.2192
76.9006
62.8682
60.1337
29.9970
12.6886
O
N
O
Br
N
O
N
O
4b-Br

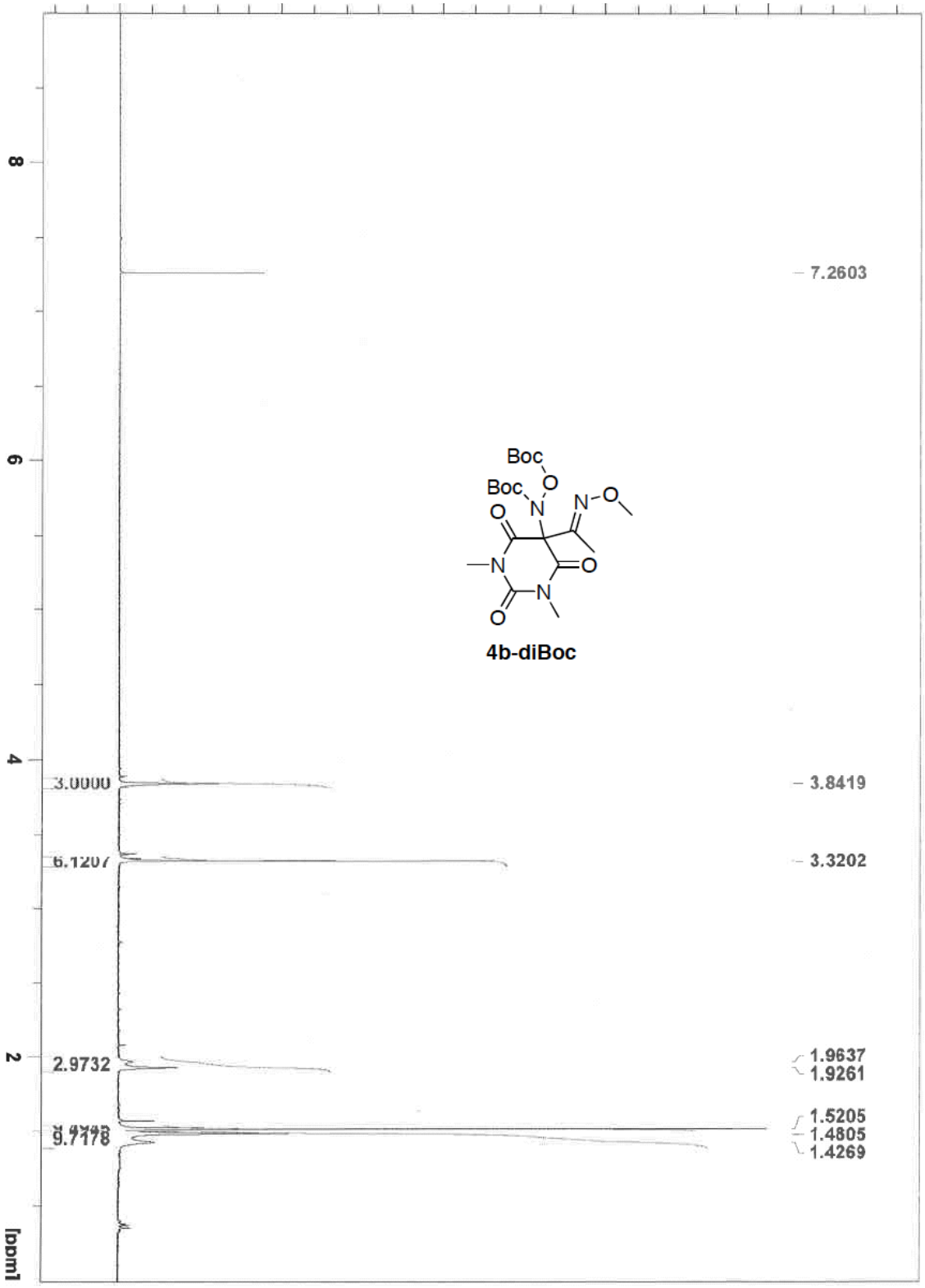
8
6
4
2
[ppm]
7.2603
3.8419
3.3202
1.9637
1.9261
1.5205
1.4805
1.4269
3.0000
2.9732
9.7178
Boc
Boc
O
N
N
O
O
N
O
N
O
4b-diBoc

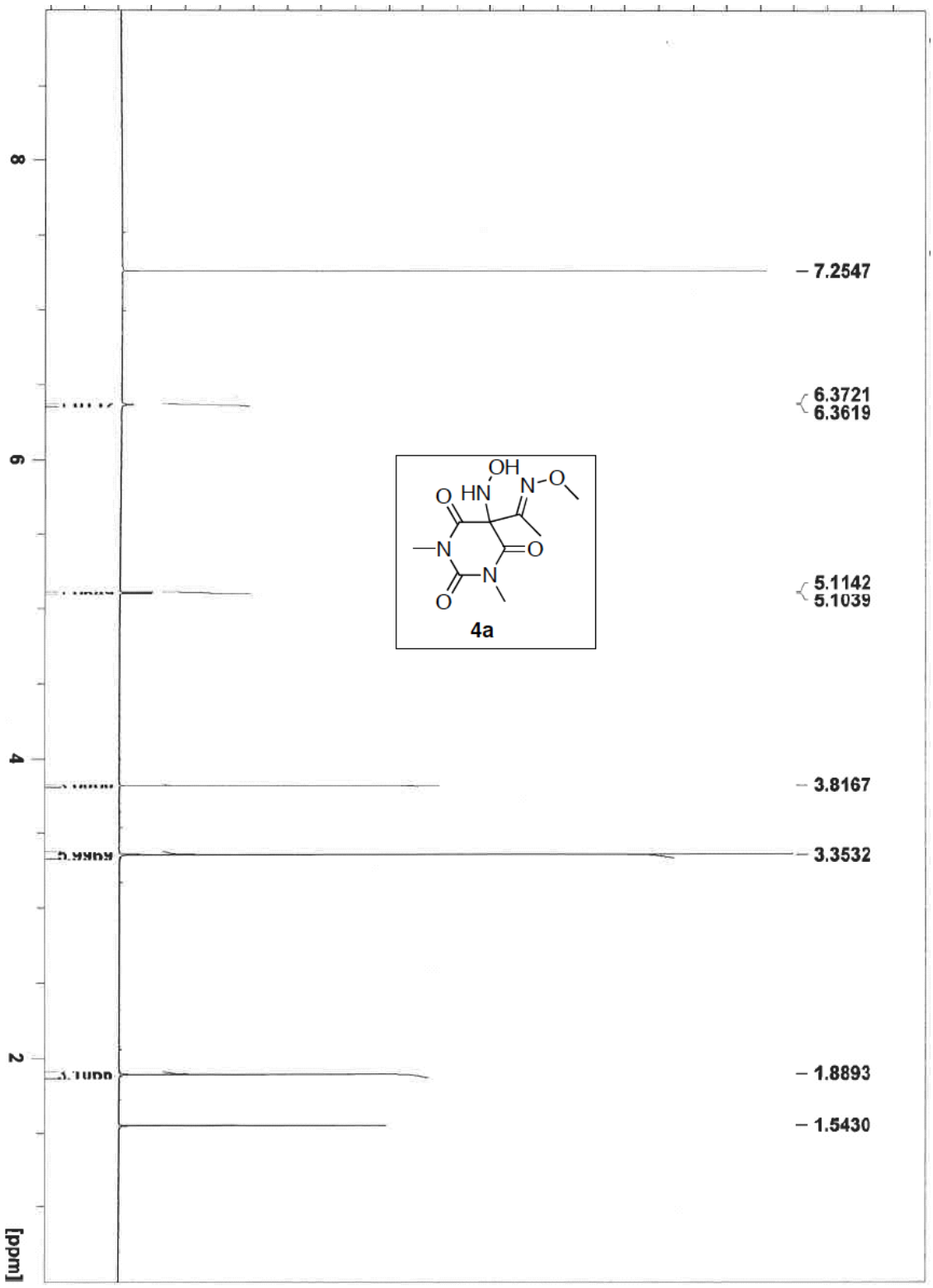
8
6
4
2
[ppm]
7.2547
6.3721
6.3619
5.1142
5.1039
3.8167
3.3532
1.8893
1.5430
OH
HN
O
N
O
N
O
N
O
4a

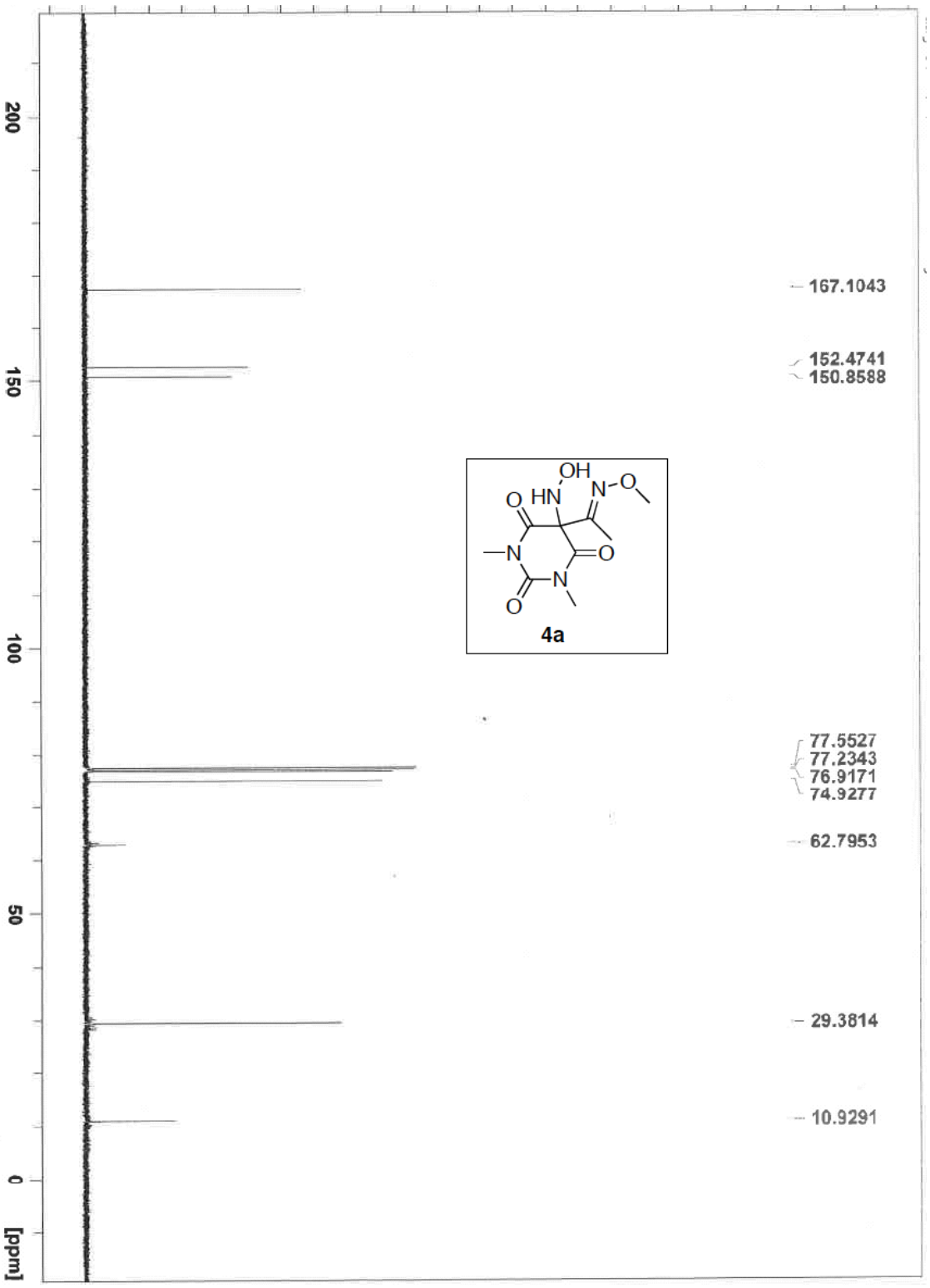
200
150
100
50
0
[ppm]
167.1043
152.4741
150.8588
77.5527
77.2343
76.9171
74.9277
62.7953
29.3814
10.9291
OH
HN
N-O
O
N
O
N
O
4a

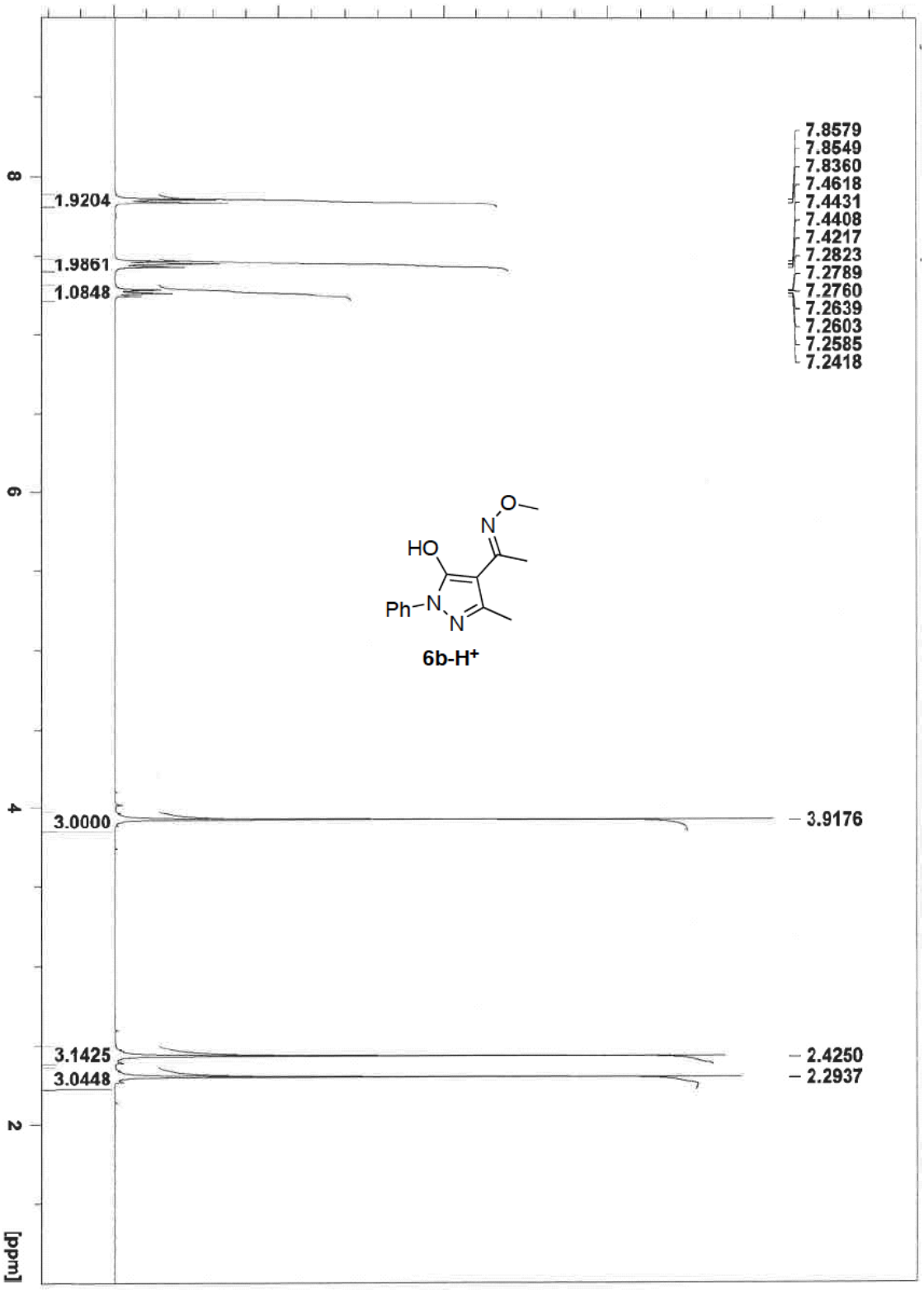
7.8579
7.8549
7.8360
7.4618
7.4431
7.4408
7.4217
7.2823
7.2789
7.2760
7.2639
7.2603
7.2585
7.2418
1.9204
1.9861
1.0848
3.0000
3.9176
3.1425
3.0448
2.4250
2.2937
8
6
4
2
[ppm]
HO
N
O
Ph
N
N

6b-H⁺

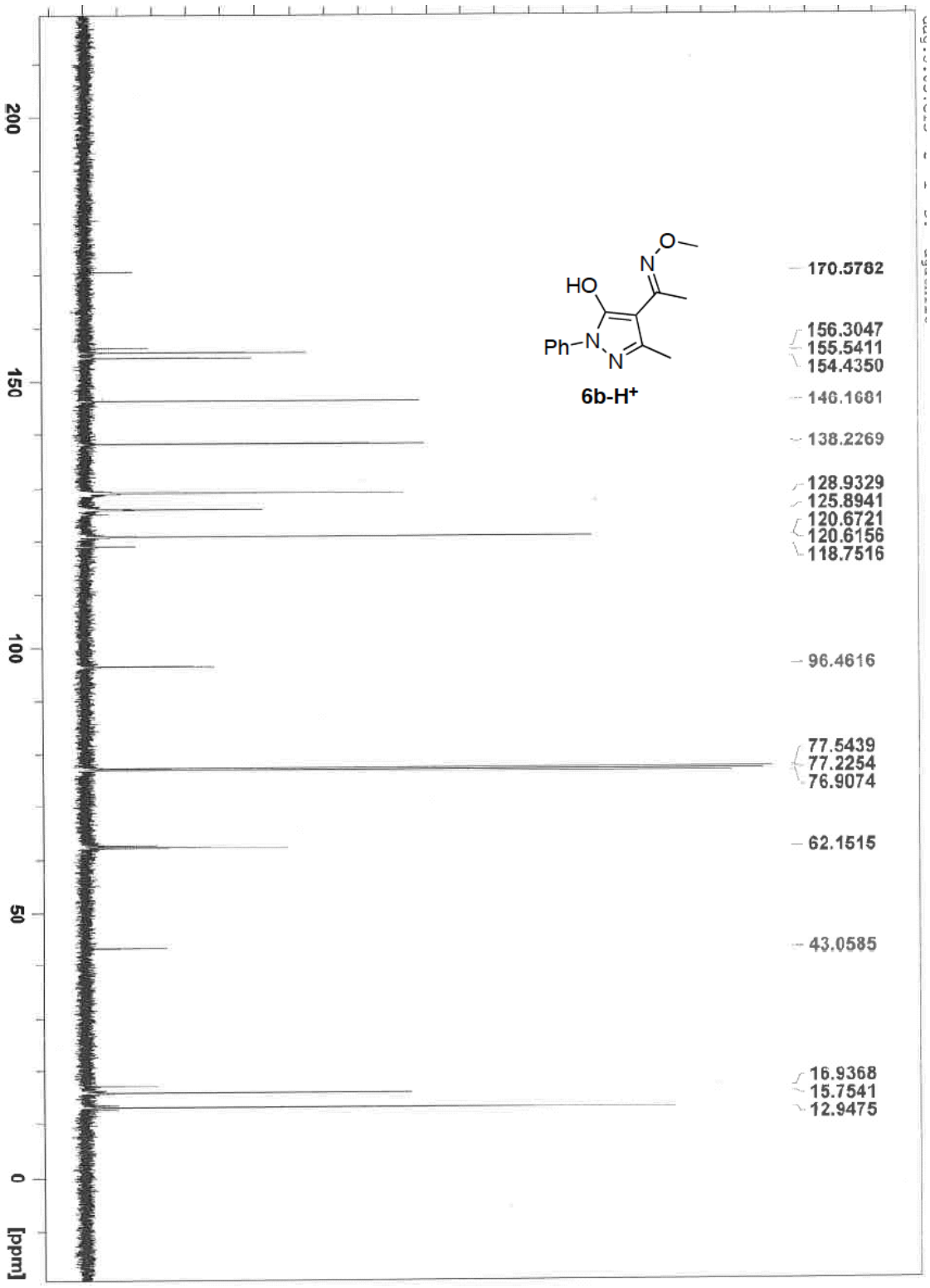
200
150
100
50
0
[ppm]
HO
N
O
Ph
N
N
6b-H+
170.5782
156.3047
155.5411
154.4350
146.1681
138.2269
128.9329
125.8941
120.6721
120.6156
118.7516
96.4616
77.5439
77.2254
76.9074
62.1515
43.0585
16.9368
15.7541
12.9475

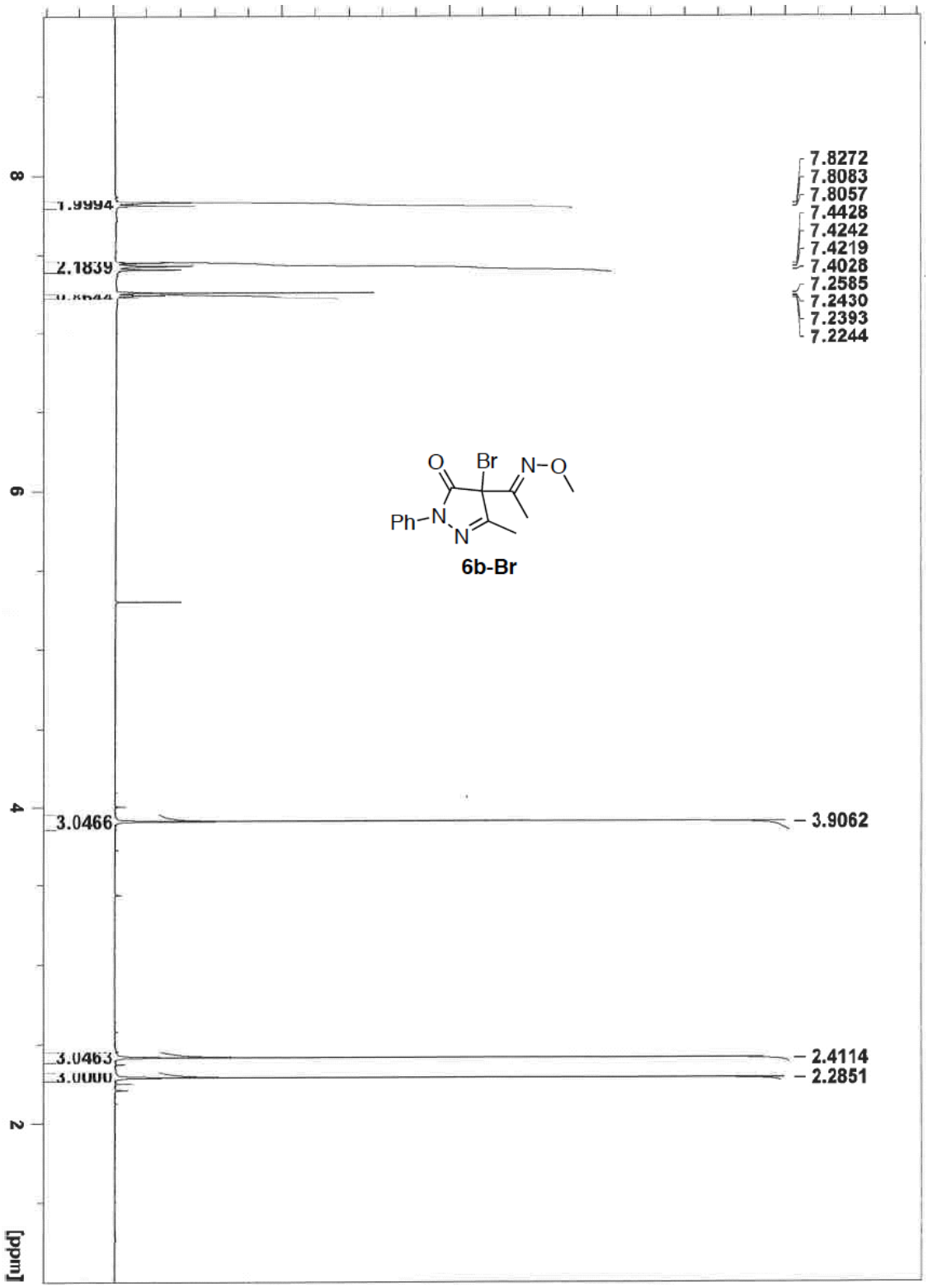
7.8272
7.8083
7.8057
7.4428
7.4242
7.4219
7.4028
7.2585
7.2430
7.2393
7.2244
1.9994
2.1839
3.0466
3.9062
3.0463
2.4114
2.2851
8
6
4
2
[ppm]
O
Br
N–O
Ph–N
N
6b-Br

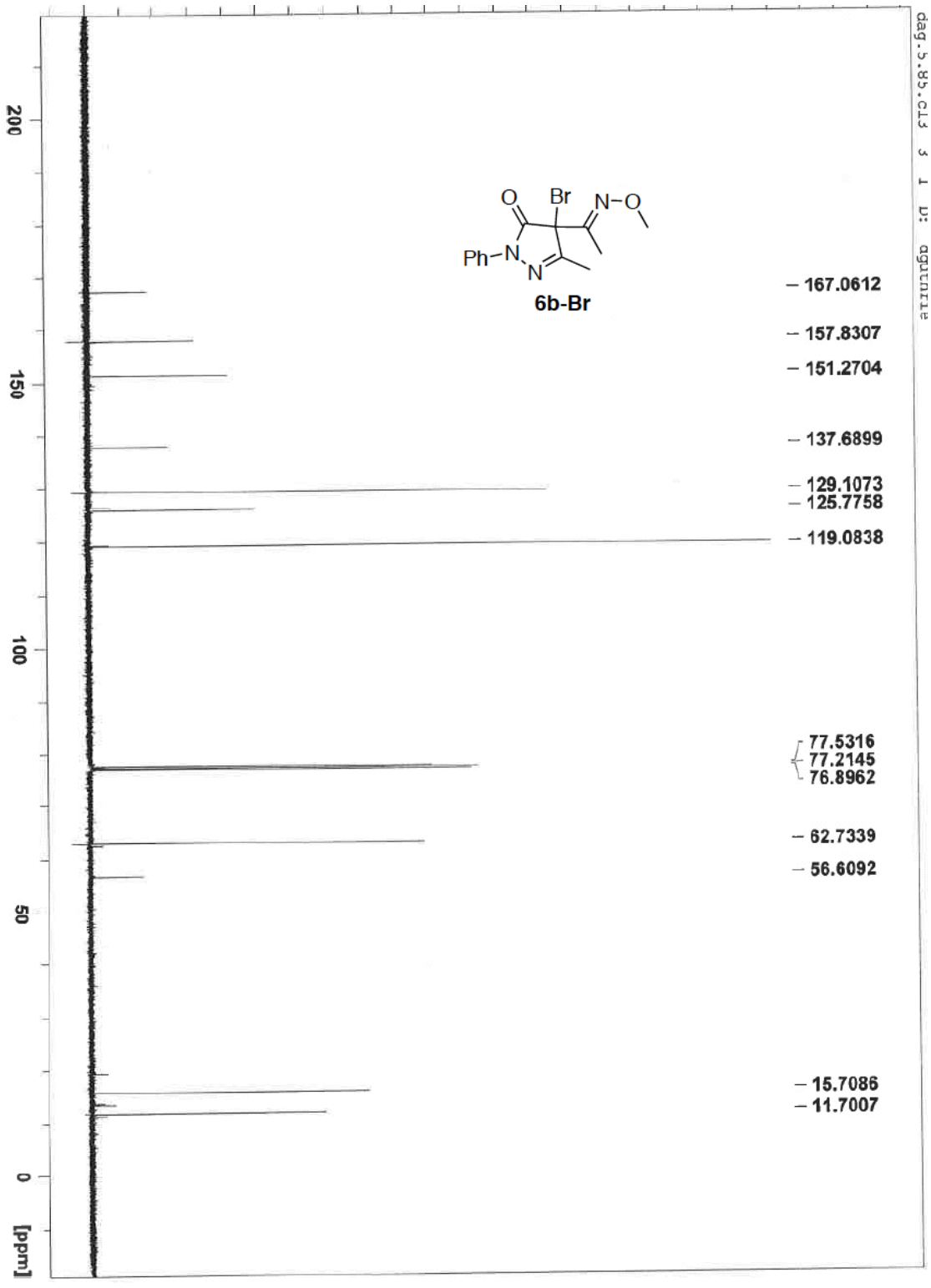
dag-5-85-c13 5 1 1: daturre
200
150
100
50
0
[ppm]
O
Br
N–O
Ph–N
N
6b-Br
167.0612
157.8307
151.2704
137.6899
129.1073
125.7758
119.0838
77.5316
77.2145
76.8962
62.7339
56.6092
15.7086
11.7007

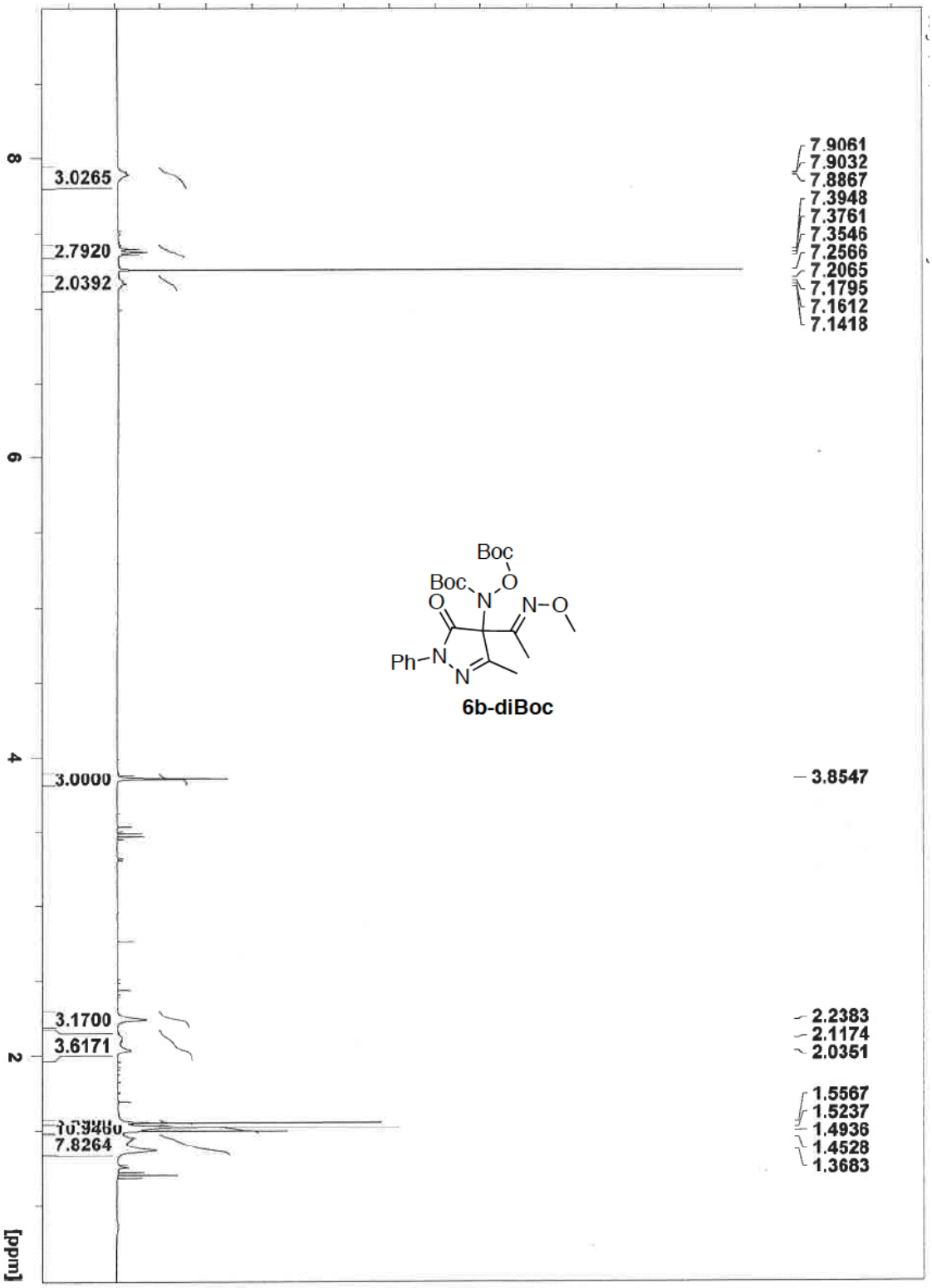
8
6
4
2
[ppm]
3.0265
2.7920
2.0392
3.0000
3.1700
3.6171
7.8264
7.9061
7.9032
7.8867
7.3948
7.3761
7.3546
7.2566
7.2065
7.1795
7.1612
7.1418
3.8547
2.2383
2.1174
2.0351
1.5567
1.5237
1.4936
1.4528
1.3683
Boc
Boc
O
N
O
N
O
Ph
N
N
6b-diBoc

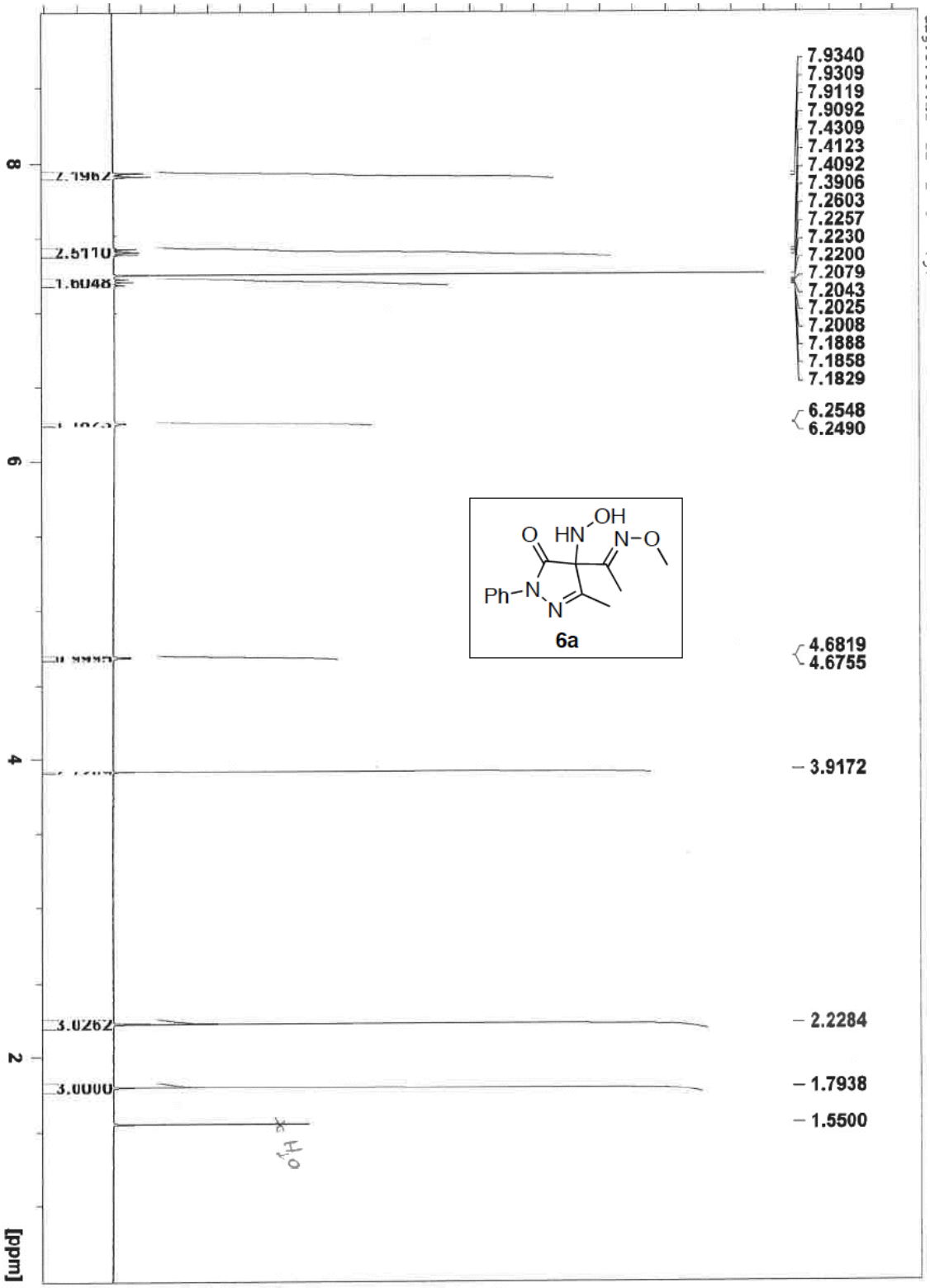
7.9340
7.9309
7.9119
7.9092
7.4309
7.4123
7.4092
7.3906
7.2603
7.2257
7.2230
7.2200
7.2079
7.2043
7.2025
7.2008
7.1888
7.1858
7.1829
6.2548
6.2490
4.6819
4.6755
3.9172
2.2284
1.7938
1.5500
8
6
4
2
[ppm]
O
HN
OH
N–O
Ph–N
N
6a

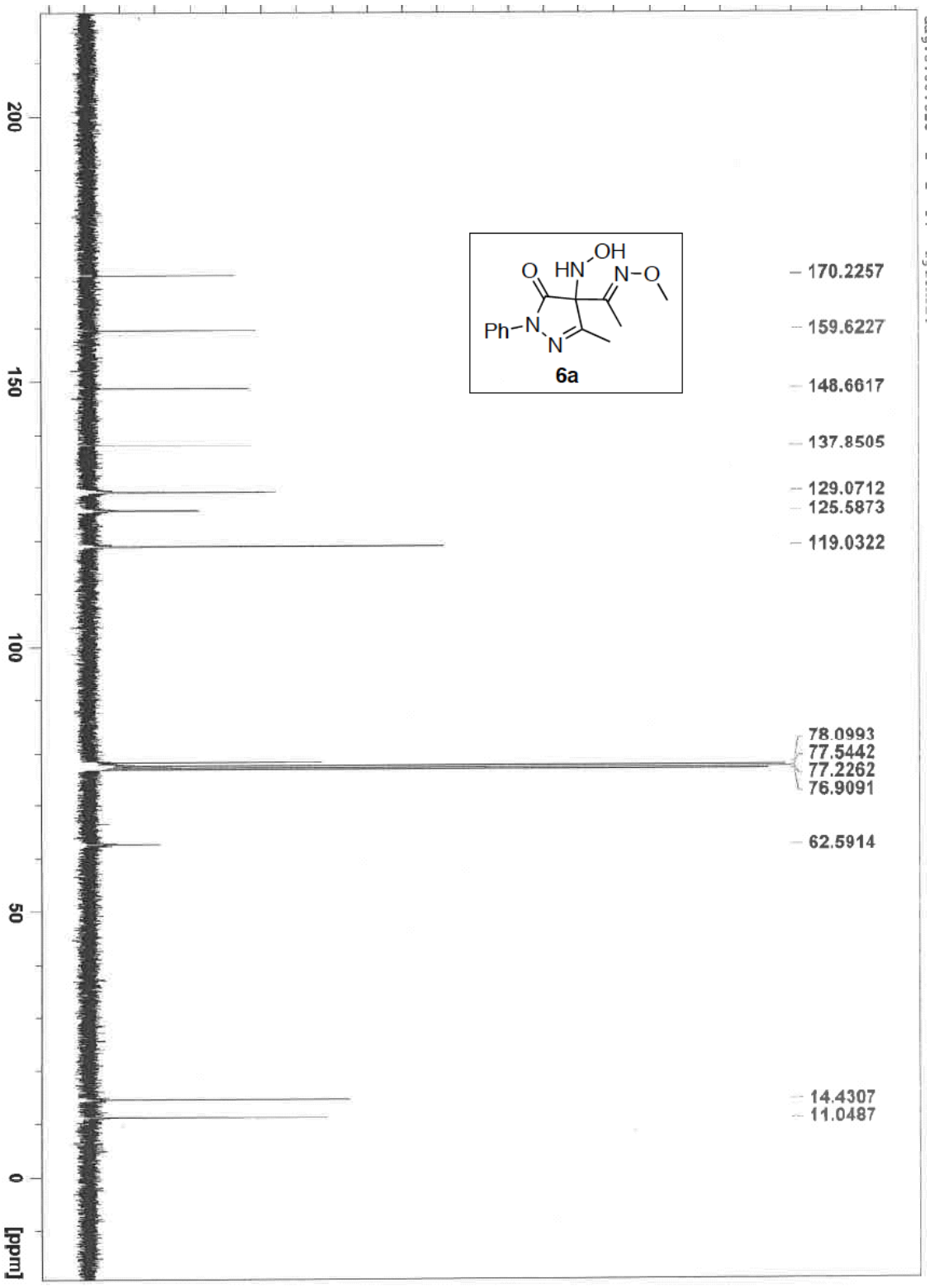
200
150
100
50
0
[ppm]
OH
HN
O
N–O
Ph–N
N
6a
170.2257
159.6227
148.6617
137.8505
129.0712
125.5873
119.0322
78.0993
77.5442
77.2262
76.9091
62.5914
14.4307
11.0487

Chapter 3.

The "Catch-and-Release" of Nitroxyl (HNO) with Pyrazolones

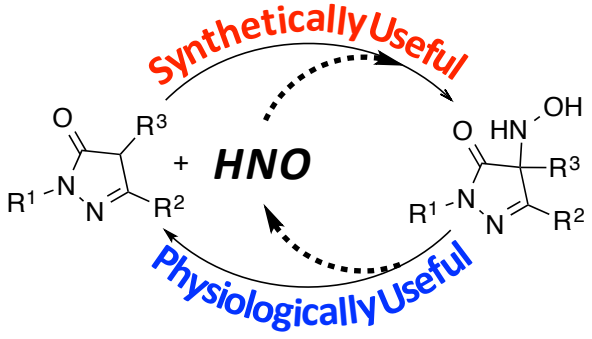

▪ 3.1 Abstract

A first-pass extension of the hydroxylamino-pyrazolone (HAPY) class of nitroxyl (HNO) donors utilizing pyrazolone (PY) leaving groups is described. HNO, a highly reactive "aldehyde mimetic" of significant biological relevance, was used as a reagent along with a variety of PY compounds to synthesize the corresponding HAPY donors in what can be considered an *N*-selective HNO-aldol reaction in up to quantitative yields. The bimolecular rate constant of HNO with PY in pH 7.4 phosphate buffer at 37 °C can reach 8×10^5 $M^{-1}s^{-1}$. The HAPY compounds generate HNO quantitatively (trapped as a phosphine aza-ylide) with half-lives spanning three orders of magnitude under physiologically relevant conditions. DFT calculations confirm the energetically favorable reactions between HNO and the PY enol and enolate, whereas HNO release is expected to occur through the oxyanion of each HAPY compound.

▪ 3.2 Introduction

Heart failure, defined as the inability of the heart to pump enough blood to supply the metabolic demands of the body, affects more than 23 million people worldwide with total annual costs in 2013 of $32 billion in the US alone.[1-3] Nitroxyl (HNO), the one-electron reduced and protonated form of nitric oxide (NO), has been shown to improve both vasorelaxation and myocardial contractility, making it a promising alternative therapeutic in the fight against congestive heart failure.[4-8]

The practical use of HNO as a therapeutic agent is complicated due to its propensity to spontaneously dimerize (k = 8 × 10^6 $M^{-1}s^{-1}$) to hyponitrous acid (HON=NOH), which dehydrates to give nitrous oxide (N_2O).[9] Thus, HNO donors, such as Angeli's salt ($Na_2N_2O_3$), have been utilized to discern the biological activity of HNO.[4-8] Angeli's salt has a relatively short half-life of ca. 2-3 min at pH 7.4, 37 °C,[10] and produces HNO along with an equimolar amount of nitrite, which possesses its own biological activity.[11-12] Unfortunately, Angeli's salt is not ideal from a drug development perspective since derivatives have yet to be successfully realized.

Identifying physiologically useful donor molecules that evolve HNO in a controlled and tunable fashion is an important and ongoing challenge for fundamental research and biomedical applications. Furthermore, sustained release of low concentrations of HNO might be an important step to mimic hypothesized endogenous HNO production.[13] In comparison, the availability of NO donors was invaluable to the elucidation of the biological properties and endogenous

production of NO. Thus, new robust HNO donor platforms amenable to structure activity relationship (SAR) studies designed to optimize both physiochemical and physiological properties are desired.

The most commonly used strategy for prolonging HNO release is through the use of ester prodrugs of otherwise efficient HNO donors. These include acyloxy nitroso compounds,[14-15] esters of primary amine-based diazeniumdiolates such as IPA/NO,[16-19] and precursors to acyl nitroso compounds[20-22] such as *N*,*O*-*bis*-acylated hydroxylamine derivatives.[23] The tunability of this strategy is reliant on the precursor ester hydrolysis rates, which can vary from seconds to hours. However, the overall chemistry of these long-acting HNO donors can be more complicated than is originally anticipated. For example, direct and HNO-mediated reactions of acyloxy nitroso compounds have been demonstrated with thiol-containing proteins,[24-25] dual mechanisms of HNO generation by IPA/NO-AcOM (*i*PrHN-N(O)=NO–CH_2OAc) and IPA/NO-aspirin can occur in the absence of esterase,[18-19] and optimization of HNO production from *N*,*O*-*bis*-acylated hydroxylamine derivatives requires the use of urea-based precursors with arenesulfonyl leaving groups in order to avoid both amide hydrolysis and acyl migration pathways.[23] Additionally, these precursors are all susceptible to esterase-mediated hydrolysis, which complicates drug development since esterase activity not only depends on the substrate, but also shows strong interspecies, interorgan, and interindividual variability.[26]

Previously, we have reported the development of *N*-substituted hydroxylamines as efficient HNO donors based on the general formula (HOHN–X)

where X is a good carbon-based leaving group.[27] The rate and amount of HNO released from these compounds is dependent mainly on the nature of the leaving group X. We identified examples from three independent hydroxylamine-substituted classes shown in Figure 3-1: (1) the hydroxylamino-Meldrum's acid (HAMA) class, (2) the hydroxylamino-barbituric acid (HABA) class, and (3) the hydroxylamino-pyrazolone (HAPY) class.

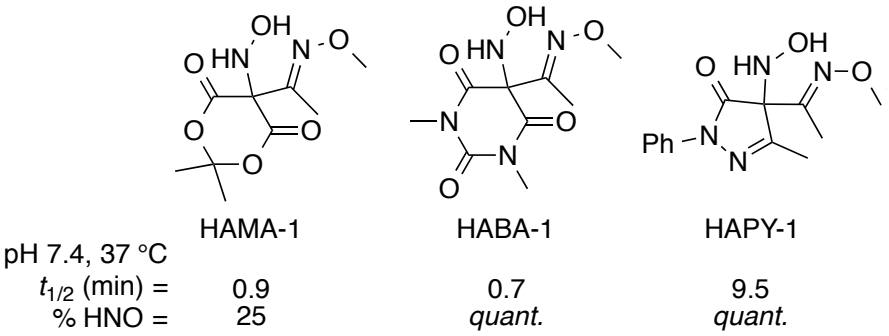

Figure 3-1. Previous examples from the HAMA, HABA, and HAPY classes of HNO donors.

Each example shares in common an *O*-methyloxime moiety attached to the carbon bearing the hydroxylamine group. Simple alkyl group exchanges on the HAMA and HABA scaffolds resulted in negligible HNO production following incubation at pH 7.4, 37 °C due to either competitive hydrolysis or rearrangement mechanisms of their ring core systems, respectively.[27] The hydrolysis pathway remains dominant in HAMA-1 even with *O*-methyloxime substitution. At this point, strategies to curtail these non-HNO producing pathways, such that the HAMA and HABA classes can be expanded, are not obvious, but will be addressed in Chapter 4.

On the other hand, the HAPY class of HNO donors (Scheme 3-1) offers several distinct advantages: (1) the pyrazolone ring is expected to be resistant to hydrolysis

and rearrangement, (2) multiple synthetic handles are available to investigate SAR, and (3) the byproducts are related to edaravone (Radicut),[28-30] a potent antioxidant marketed in Japan to treat acute ischemic stroke, which has been reported to be effective for myocardial ischemia as well.

Scheme 3-1. General HNO Release from HAPY Class

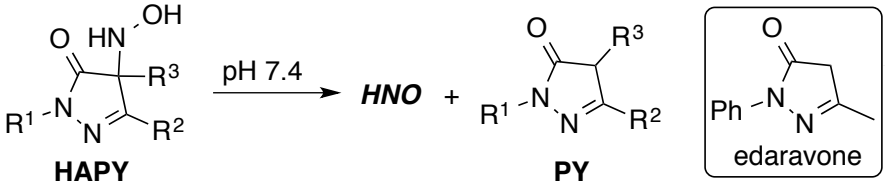

Herein, we are pleased to report a first-pass extension of the HAPY class of HNO donors by varying the groups at the R^1, R^2, and R^3 positions on the pyrazolone ring. In doing so, we have uncovered an unexpected reactivity of HNO with pyrazolones, and have also developed a ^{1}H NMR assay for evaluating half-life and HNO production.

▪ 3.3 Results and Discussion

3.3.1 Early Studies

Due to the deleterious effect simple alkyl groups had on HNO production in the HAMA and HABA classes, we first considered HAPY-2 (R^1 = phenyl, R^2 and R^3 = methyl), which was expected to generate HNO as shown in Scheme 3-1. This precursor was synthesized from the expected organic byproduct of HNO release, PY-2, which was readily prepared through the condensation of ethyl 2-methylacetoacetate and phenylhydrazine. Installation of the hydroxylamine group was accomplished analogously to the previously reported synthesis of HAPY-1 by formation of the corresponding bromide followed by reaction with *N*,*O*-*bis*(*tert*-butoxycarbonyl) hydroxylamine and subsequent acid deprotection (Scheme 3-2, Path A).[27]

Previously, we examined HAPY-1 for HNO production in pH 7.4 phosphate buffered saline at 37 °C by gas chromatographic headspace analysis to quantify the amount of its dimerization product, N_2O, as well as ^{1}H NMR spectroscopy to quantify the amount of the expected organic byproduct PY-1. HNO was confirmed as the source of N_2O for HAPY-1 by quenching with glutathione (GSH), a known efficient trap for HNO.[31-32]

Upon examination of HAPY-2, however, only trace amounts of N_2O were observed following 24 h incubation, and ^{1}H NMR analysis revealed that HAPY-2 was essentially stable. Interestingly, upon 24 h incubation with excess GSH (ca. 5 equivalents), enhanced conversion of HAPY-2 to byproduct PY-2 was observed by

^{1}H NMR spectroscopy; the relative yield of PY-2 was 36%. Importantly, no other products arising from HAPY-2 were observed. Four conclusions can be drawn from these results: (1) the pyrazolone ring *is* stable against hydrolysis and rearrangement, (2) the decomposition rates of HAPY-1 and HAPY-2 differ dramatically, (3) byproduct PY-2 may be an efficient trap for HNO, and (4) an alternative means of monitoring HNO release in an expanded HAPY class is necessary.

3.3.2 Synthesis

Clearly, a large variation in effective half-life is observed when the R^3 position of the pyrazolone ring is interconverted between an *O*-methyloxime group and a methyl group. Moving forward, we probed the R^1 and R^2 positions with simple hydrogen, methyl, and substituted phenyl variations. Accordingly, PY-3 – PY-12 (Table 3-1) were prepared (see Experimental).

Next, we wanted to test the possibility that PY-2 may be an efficient trap for HNO. Therefore, we monitored the reaction of PY-2 and Angeli's salt in 10% D_2O, pH 7.4 phosphate buffer with the metal chelator, diethylenetriaminepentaacetic acid (DTPA), at room temperature by ^{1}H NMR spectroscopy (Figure 3-2). Consistent with our hypothesis, we observe the complete conversion of PY-2 to HAPY-2, which is the first example of what can be considered an *N*-selective HNO-aldol reaction utilizing the smallest nitroso compound, HNO, as the reagent.

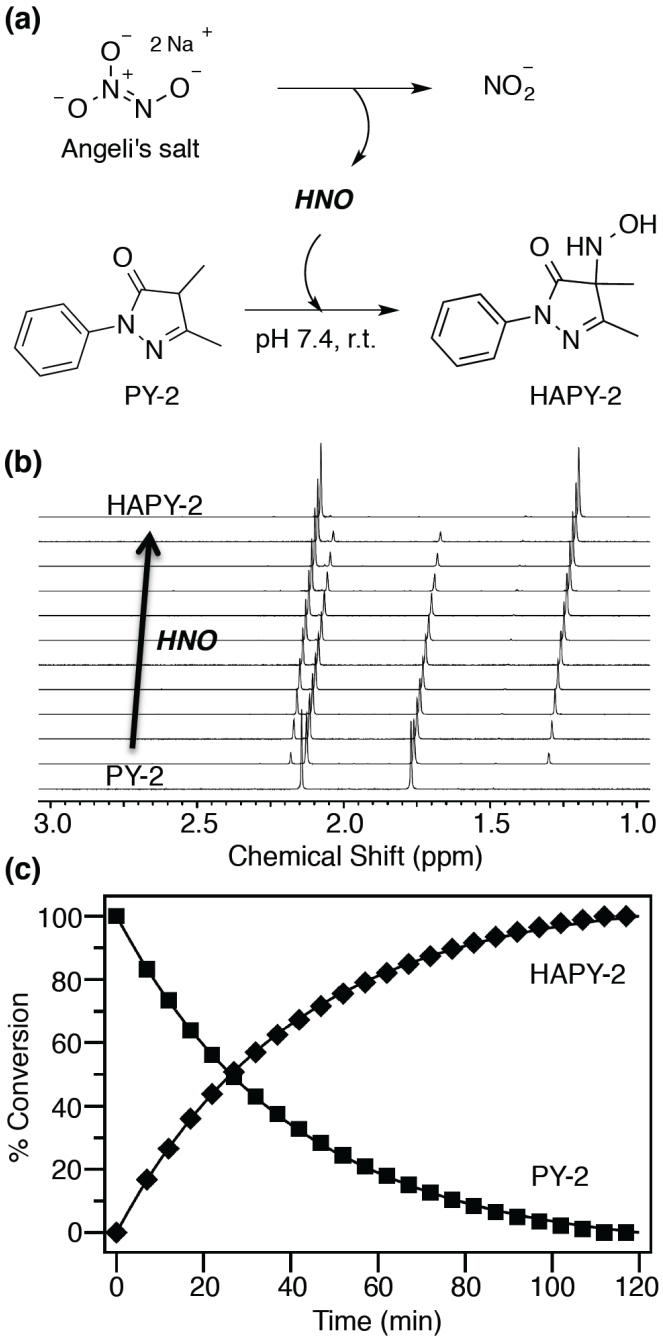

Figure 3-2. (a) The *N*-selective HNO-aldol reaction between PY-2 and Angeli's salt-derived HNO. (b) ^{1}H NMR spectra of the formation of HAPY-2 from PY-2 and Angeli's salt-derived HNO in 10% D_2O, pH 7.4 phosphate buffer (0.25 M) with DTPA (0.2 mM) at room temperature. (c) The kinetics of the reaction using the integrated area of the upfield methyl group of PY-2 relative to the upfield methyl group of HAPY-2. The solid curves are calculated best fits to a single exponential function ($k = 4.0 \times 10^{-4}$ s^{-1} for each fit).

This new reactivity of HNO is not so unexpected given what has been reported in the literature. The chemical similarity between HNO and an aldehyde is greater than between HNO and an oxyacid.[9] In addition, HNO is a potent inhibitor of aldehyde dehydrogenase,[33-34] demonstrating its chemical similarity to acetaldehyde, though HNO is isoelectronic with formaldehyde. Pyrazolones, as well as other reactive enols and enolates, readily form aldol condensation products with aldehydes in aqueous media.[35] Moreover, the nitroso-aldol reaction between carbonyl compounds and nitrosoarene and acyl nitroso compounds to produce enantioselective amines and alcohols following *N–O* bond reduction has been well documented.[36-38]

The reaction of HNO with PY to give HAPY is synthetically attractive, as it is the one-step umpolung strategy (Scheme 3-2, Path B) to the traditional bromination-displacement-deprotection strategy (Scheme 3-2, Path A). As such, we endeavored to find a preparatory procedure for this HNO-aldol reaction and apply it to an expanded HAPY class.

Scheme 3-2. Possible Synthetic Strategies: Traditional (Path A) vs. Umpolung (Path B)

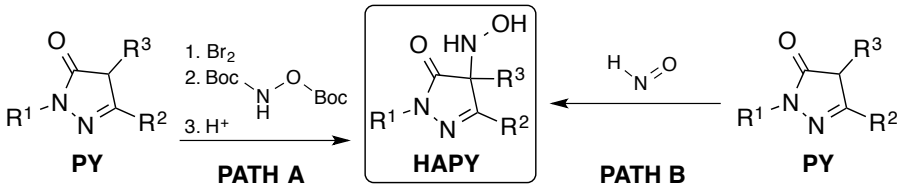

We have been able to develop a general synthetic protocol at room temperature that features the use of Angeli's salt, which has a suitable HNO generation rate for this procedure, and the nitrite byproduct is readily separated

from the HAPY product. To initiate decomposition of Angeli's salt, DTPA was used as a proton source as well as to maintain a buffered solution and preclude HNO reactivity with trace metals. A 50% v/v aqueous ethanol solution allowed both the organic and salt reagents to be readily soluble at typical reaction concentrations (0.1 – 0.4 M) (See Experimental). The use of ethanol also aided in the preliminary drying steps by allowing the mild azeotropic removal of the water. This procedure is applicable for each HAPY example; the isolated synthetic yields are shown in Table 3-1.

Table 3-1. HNO-Aldol Reaction of Pyrazolones

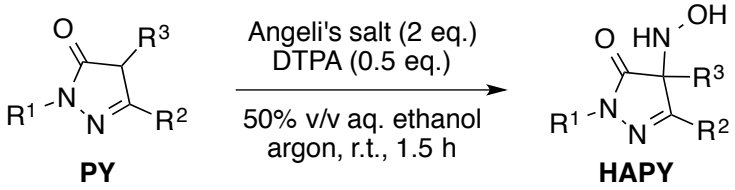

HAPY	R^1	R^2	R^3	% yield
1	Ph	Me	C(=NOMe)Me	74
2	Ph	Me	Me	89
3	Me	Me	C(=NOMe)Me	44
4	Me	Me	Me	76
5	H	Me	C(=NOMe)Me	35
6	H	Me	Me	75
7	4-ClPh	Me	Me	94
8	2-ClPh	Me	Me	96
9	Me	Ph	Me	89
10	Ph	Ph	Me	99
11	Me	4-ClPh	Me	99
12	Me	2-ClPh	Me	87

Surprisingly, even the relatively efficient HNO donor, HAPY-1, can be isolated starting from PY-1 in better yield and in fewer steps when compared to the traditional bromination-displacement-deprotection strategy (1 step, 74% vs. 3

steps, 34% overall). The caveat here is that conversion to HAPY-1, or the other *O*-methyloxime derivatives HAPY-3 and HAPY-5, is not complete, and requires the use of chromatographic separation to isolate. Fortunately, their respective isolated yields correspond well with the conversion yields, and under these reaction conditions, the HAPY products are relatively stable several hours after HNO generation from Angeli's salt has completed. Therefore, we believe the lower yields for these compounds are primarily due to less efficient trapping of HNO rather than the reactivity of the HAPY product. Otherwise, complete conversion was observed in the other HAPY examples, each equipped with a methyl group in the R^3 position, resulting in excellent isolated yields.

3.3.3 Kinetic Evaluation

Given the high conversion yields, particularly for the R^3 = methyl examples, we have quantified this reactivity of HNO with pyrazolones utilizing PY-2 as an example. We employed a competitive trapping experiment using the HNO donor, HABA-1, and *tris*(4,6-dimethyl-3-sulfanatophenyl)phosphine trisodium salt (TXPTS), another efficient and selective trap for HNO at pH 7.4, 37 °C (k_{TXPTS} = 9 × 10^5 $M^{-1}s^{-1}$) following Scheme 3-3.[39-40] HNO reacts with two equivalents of TXPTS to give the diagnostic aza-ylide product as well as the corresponding phosphine oxide, where the rate-limiting step is assumed to be the initial reaction between HNO and the first equivalent of TXPTS.

Scheme 3-3. Competitive HNO Trapping Experiment at pH 7.4, 37 °C

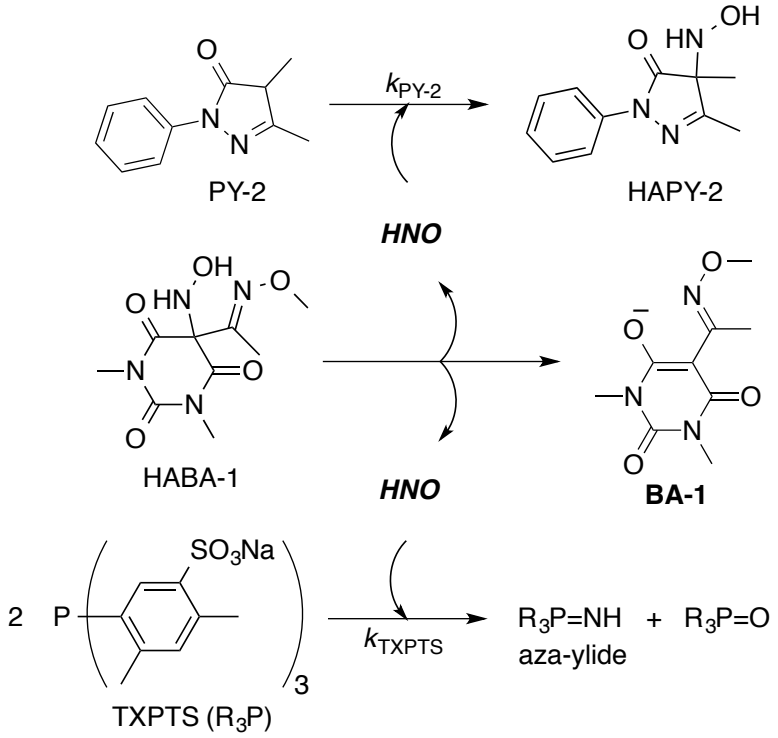

To determine the rate constant for the reaction of PY-2 with HNO (Equation 1), we evaluated the concentration of TXPTS required to achieve equal product distributions of HAPY-2 compared to the aza-ylide product of TXPTS.[40-41] Importantly, all the HNO produced under these conditions must react with either PY-2 or TXPTS in order for Equation 1 to be valid; HNO dimerization cannot occur.

$$k_{\text{PY-2}} = \frac{k_{\text{TXPTS}}[\text{TXPTS}]}{[\text{PY-2}]} \quad (1)$$

Accordingly, due to its diagnostic ^{1}H NMR signals, byproduct BA-1 (Scheme 3-3) served as an internal reference such that all species involved could be quantified, including the aza-ylide product of TXPTS, which had only been characterized by ^{31}P NMR and HPLC previously. The results shown in Figure 3-3 indicate that all HNO is effectively consumed by the traps and that the concentration

of TXPTS required to affect equal product distributions is ca. 8.5 mM, which gives an HNO trapping rate constant for PY-2 of ca. 8×10^5 $M^{-1}s^{-1}$ at pH 7.4, 37 °C, comparable to that of TXPTS.

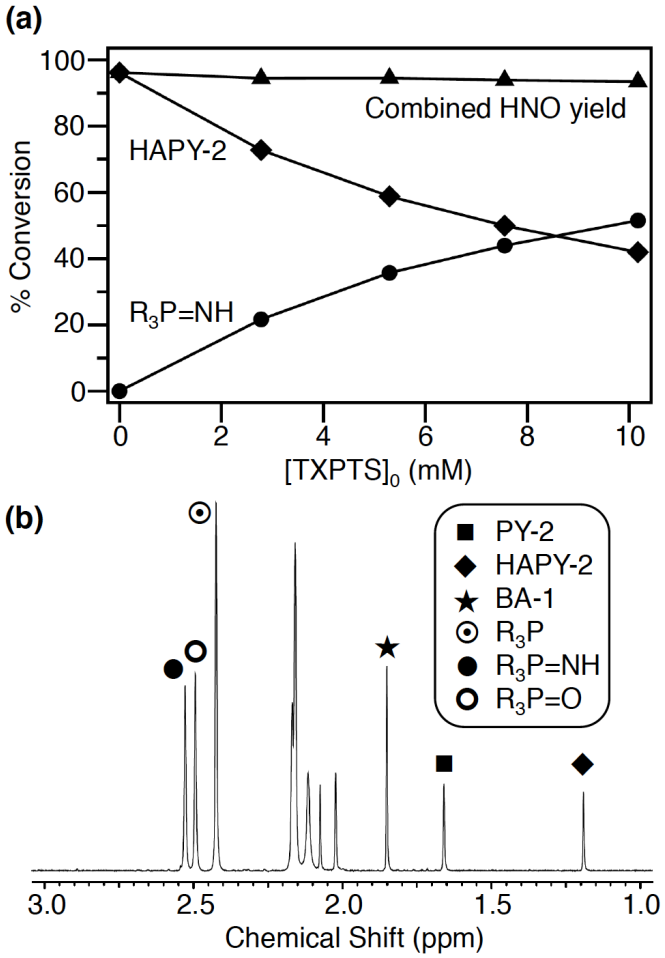

Figure 3-3. Competition for HABA-1-derived HNO at pH 7.4, 37 °C: PY-2 vs. TXPTS. (a) All competition reactions contained HABA-1 (5 mM) and PY-2 (5 mM) in 2.0 mL of 10% D_2O, pH 7.4 phosphate buffer (0.25 M) with DTPA (0.2 mM). Each reaction was incubated under argon for 30 minutes at 37 °C to ensure complete decomposition of HABA-1 before ^1H NMR analysis of the reaction mixture. (b) Representative ^1H NMR spectrum of the reaction mixture, and each designated signal was used in the post-reaction analysis.

These results indicate that PY-2 to HAPY-2 formation is efficient and can be used diagnostically as an alternative means of HNO quantification. Also, the "HNO

transfer reaction" between HABA-1 and PY-2 demonstrates that HNO donors beyond Angeli's salt can be used in the HNO-aldol reaction.

3.3.4 DFT Calculations

We modeled the thermodynamic driving forces for three possible reactions involving HNO with the synthesized pyrazolone examples (Scheme 3-4). All calculations were performed with Spartan '14 at the B3LYP/6-31G* level with an SM8 solvation model for aqueous solvation (Supporting Information).[42] Optimized geometries and vibrational frequencies were calculated for each reactant and product independently. Reaction II was balanced using a hydronium cation and a water molecule on the left and right side of the reaction, respectively. Table 3-2 shows the Gibbs free energy differences for reaction I, II, and III.

Scheme 3-4. Possible Reactions Involving HNO with Pyrazolones

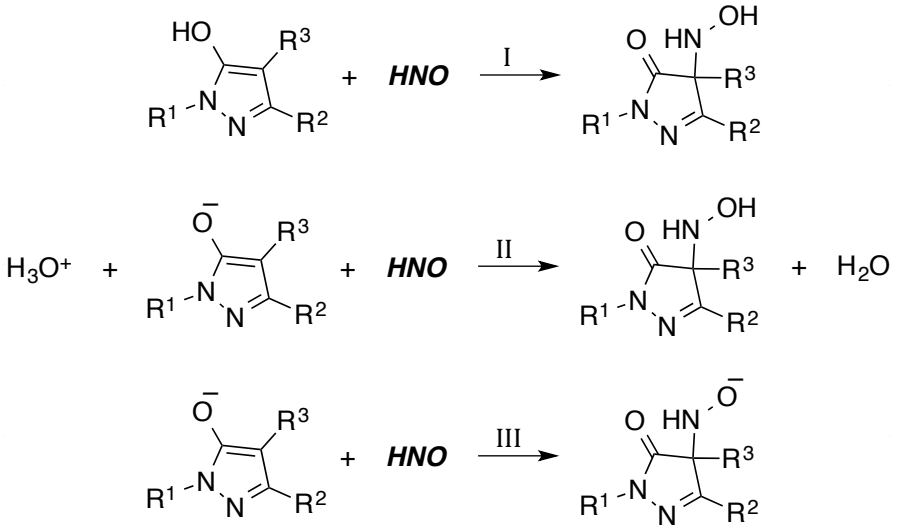

Reaction (I) HNO with neutral PY in the enol tautomer to give neutral HAPY, (II) HNO with the enolate of PY to give neutral HAPY, and (III) HNO with the enolate of PY to give HAPY oxyanion.

Table 4-2. Gibbs Free Energy Differences in Reactions I, II, and III

Entry	R^1	R^2	R^3	ΔG_I° (kcal/mol)	ΔG_{II}° (kcal/mol)	ΔG_{III}° (kcal/mol)
1	Ph	Me	C(=NOMe)Me	-0.7	-27.5	[a]
2	Ph	Me	Me	-13.0	-34.4	13.7
3	Me	Me	C(=NOMe)Me	-0.6	-30.6	[a]
4	Me	Me	Me	-13.1	-38.7	10.2
5	H	Me	C(=NOMe)Me	-0.6	-30.8	[a]
6	H	Me	Me	-12.5	-38.1	10.9
7	4-ClPh	Me	Me	-13.0	-33.5	14.0
8	2-ClPh	Me	Me	-12.2	-36.3	12.0
9	Me	Ph	Me	-10.8	-34.7	13.2
10	Ph	Ph	Me	-11.0	-31.5	[a]
11	Me	4-ClPh	Me	-10.6	-34.3	14.6
12	Me	2-ClPh	Me	-8.0	-32.8	15.8

[a]Ground state structures were not found for these oxyanions since the calculated structures resemble dissociated HNO and the corresponding organic byproduct. Free energies are given for 298.15 K.

Consistent with the experimental results above, these calculations indicate that both reaction I, and particularly, reaction II are thermodynamically favorable for the forward PY to HAPY reaction for all examples. On the other hand, reaction III is thermodynamically unfavorable. In addition, ground state structures were not found for the oxyanions of HAPY-1, HAPY-3, HAPY-5, and HAPY-10 since the calculated structures resemble dissociated HNO and the corresponding PY byproduct. Thus, HNO generation from the expanded HAPY class is expected to be dependent on the pK_a of the HAPY donor, which in turn is likely dependent on the pK_a of the PY bydroduct.

3.3.5 HNO Release from the Expanded HAPY Class

As described above, the reaction of HNO with pyrazolones can be taken advantage of synthetically and potentially used as an alternative means of quantifying HNO production. Yet, the original purpose of this investigation was to

study the HNO production *from* these newly prepared HAPY compounds. With this reversible reactivity in mind, an additional trap for HNO is required to drive the HAPY to PY reaction forward. We had demonstrated this earlier by using GSH, a biologically relevant trap for HNO *in vivo*. However, TXPTS is best suited for these mechanistic studies since it has selective and irreversible reactivity with HNO, and the diagnostic aza-ylide singlet in the ^{1}H NMR spectrum is distinct from the HAPY and PY compounds.

We first examined the effect that increasing [TXPTS] has on the half-life of HAPY-2, as an example. Following a 48 h incubation of HAPY-2 with 0 – 20 equivalents of TXPTS in pH 7.4 phosphate buffer at 37 °C, ^{1}H NMR analysis indicates the incremental consumption of HAPY-2 with TXPTS increasing from 0 to ca. 4 equivalents, whereas the relative percentage of HAPY-2 remains effectively unchanged when TXPTS exceeded ca. 4 equivalents (Figure 3-4). Importantly, these results indicate no bimolecular, direct reaction between TXPTS and HAPY-2 since HAPY-2 consumption is not linear with the change in initial [TXPTS]. Therefore, we believe that the HAPY-2 to PY-2 conversion is the result of the irreversible reaction of the released HNO with TXPTS, thereby minimizing the PY-2 to HAPY-2 back-reaction.

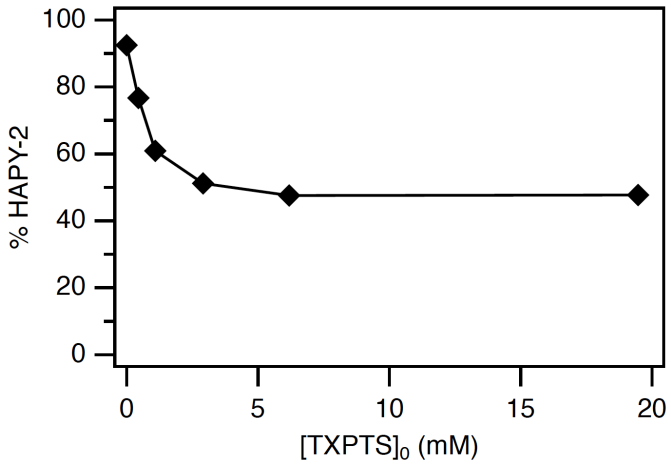

Figure 3-4. Incubation of HAPY-2 at pH 7.4, 37 °C after 48 h as a function of $[TXPTS]_0$. Conditions: HAPY (1 mM) in 10% D_2O, pH 7.4 phosphate buffer (0.25 M) with DTPA (0.2 mM) at 37 °C under argon.

The timecourse for the disappearance of HAPY-2 and appearance of PY-2 and HNO (trapped as the TXPTS aza-ylide) with ca. 6 equivalents of TXPTS as well as representative ^1H NMR spectra at t = 0 h, 240 h, and 480 h are shown in Figure 3-5. With a half-life of 47 h and a quantitative TXPTS aza-ylide yield, HAPY-2 is a very long-lived, yet pure HNO donor.

Fortunately, under these anaerobic assay conditions, the TXPTS aza-ylide product is stable. The TXPTS oxide product slowly increases beyond the expected stoichiometric amount due to oxidation of the excess TXPTS, as maintaining a rigorously anaerobic assay condition for this extended time period is experimentally challenging.

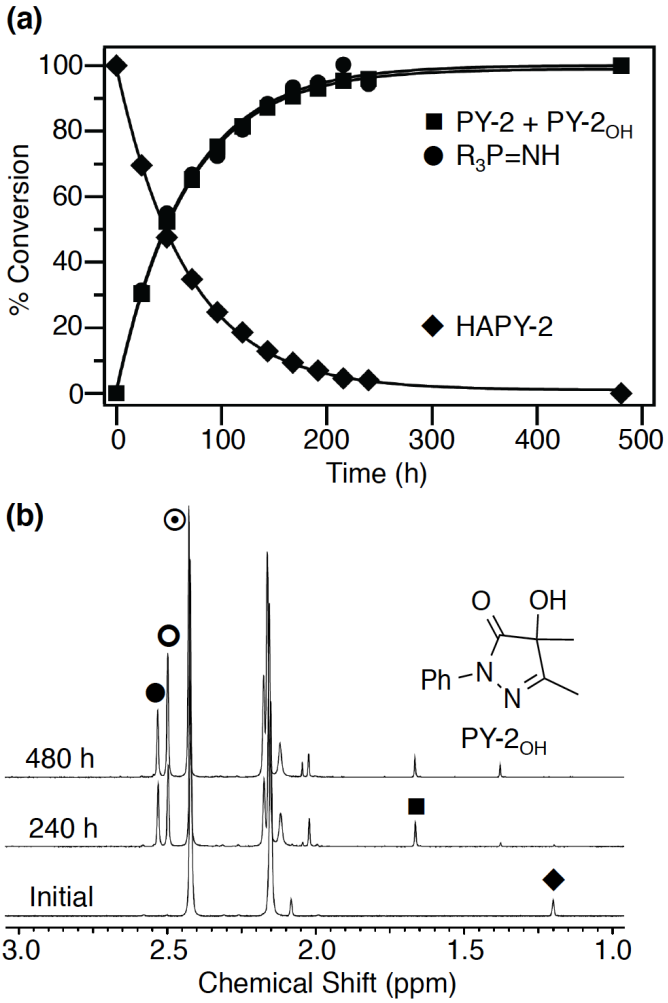

Figure 3-5. (a) Timecourse for the disappearance of HAPY-2 and appearance of PY-2 and TXPTS aza-ylide with added TXPTS (6 equivalents). The solid curves are calculated best fits to a single exponential function (k = 4.1 × 10^{-6} s^{-1} for each fit). (b) ^{1}H NMR spectra at t = 0 h, 240 h, and 480 h; see Experimental for details.

Likewise, an unknown oxidation product forms slowly from the organic byproduct PY-2 (Figure 3-5). Following overnight aerobic incubation of PY-2 in pH 7.4 phosphate buffer at 37 °C in the absence of metal chelator, the oxidized product precipitated from solution, which was briefly reheated in order to affect recrystallization. X-ray crystallography confirmed the identity of the oxidized product as PY-2_{OH}, the corresponding alcohol of PY-2 (Supporting Information).

Recall that PY-2 is a derivative of edaravone, which has beneficial effects attributed to its free radical scavenging ability through a single electron transfer mechanism with reactive oxygen species such as hydroxyl and peroxyl radicals.[43] Therefore, this ^{1}H NMR assay for evaluating half-life and HNO production requires the use of excess TXPTS (> 5 equivalents) under anaerobic conditions in order to reduce complications from the PY to HAPY back-reaction as well as from TXPTS and PY oxidation.

The half-life of HAPY-1 was previously reported to be 9.5 minutes in pH 7.4 phosphate buffer at 37 °C, which was determined by UV-vis analysis in the absence of an additional trap for HNO (such as TXPTS).[27] Following the ^{1}H NMR assay described above, the observed half-life of HAPY-1 was reduced in half to four minutes (Supporting Information), presumably due to minimization of the back-reaction, PY-1 to HAPY-1 (Table 3-3).

Given the large difference in half-lives between HAPY-1 and HAPY-2, we examined additional examples, specifically HAPY-3 – HAPY-12. Since changing the R^3 position clearly has a large effect on half-life, we next explored the perhaps more subtle effects at the R^1 and R^2 positions. With a variety of derivatives in hand, we followed their decomposition according to the ^{1}H NMR protocol used with HAPY-1 and HAPY-2 described above. We also measured the pK_a values of their respective PY byproducts. For solubility reasons, all pK_a measurements were determined in 50% v/v aqueous ethanol by titration. The results are shown in Table 3-3.

Table 3-3. Incubation of HAPY-1 – HAPY-12 in pH 7.4 Phosphate Buffer at 37 °C Under Argon with Added TXPTS

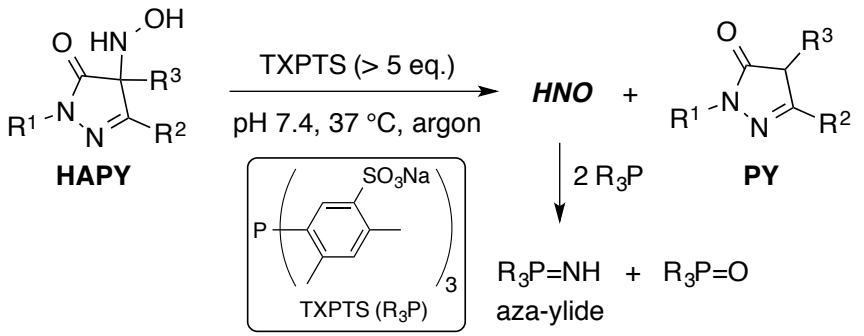

HAPY[a]	R^1	R^2	R^3	$t_{1/2}$ (min)	k (s^{-1})[b]	pK_a of PY[c]
1	Ph	Me	C(=NOMe)Me	4	3.0×10^{-3}	6.8[d]
2	Ph	Me	Me	2793	4.1×10^{-6}	8.8
3	Me	Me	C(=NOMe)Me	11	1.0×10^{-3}	7.4
4	Me	Me	Me	5674	2.0×10^{-6}	9.5
5	H	Me	C(=NOMe)Me	14	8.2×10^{-4}	8.2
6	H	Me	Me	4585	2.5×10^{-6}	10.0
7	4-ClPh	Me	Me	1473	7.8×10^{-6}	8.4
8	2-ClPh	Me	Me	1887	6.1×10^{-6}	8.7
9	Me	Ph	Me	753	1.5×10^{-5}	8.5
10	Ph	Ph	Me	460	2.5×10^{-5}	8.1
11	Me	4-ClPh	Me	799	1.4×10^{-5}	8.0
12	Me	2-ClPh	Me	71	1.6×10^{-4}	8.0

[a]Incubation conditions: HAPY (1 mM) and TXPTS (5 mM) in 10% D_2O, pH 7.4 phosphate buffer (0.25 M) with DTPA (0.2 mM) at 37 °C under argon. HNO yields are quantitative for all examples. [b]The rates are calculated best fits to a single exponential function of the integrated ^{1}H NMR data for HAPY disappearance/PY appearance. [c]Determined by titration in 50% v/v aqueous ethanol. [d]The pK_a of PY-1 was previously determined in water (pK_a of PY-1 = 6.0).[27]

First, we changed the R^1 position from phenyl in HAPY-1 and HAPY-2 to methyl (HAPY-3 and HAPY-4, respectively) and hydrogen (HAPY-5 and HAPY-6, respectively). As the R^1 substituent is changed from phenyl to methyl or hydrogen, we observe a decrease in rate, which seems to correlate well with the pK_a values of the respective PY byproducts. Although the R^3 = *O*-methyloxime derivatives, HAPY-3 and HAPY-5, have half-lives between those of HAPY-1 and HAPY-2, the R^3 = methyl derivatives, HAPY-4 and HAPY-6, have even slower dissociation rates than HAPY-2. Importantly, the HNO yield for all of these precursors remains quantitative, and as

such, HAPY-4 and HAPY-6 are the longest-lived reported pure HNO donors to date with half-lives measuring 95 h and 76 h, respectively.

Next, we explored substitution on the phenyl ring of HAPY-2 with 4-chloro (HAPY-7) and 2-chloro (HAPY-8) groups. These derivatives have slightly faster rates when compared to HAPY-2, but are still over two orders of magnitude slower than HAPY-1.

We then made changes to the R^2 position by first synthesizing HAPY-9, the isomer of HAPY-2. Interestingly, the decomposition rate of HAPY-9 is over three times faster than that of HAPY-2. The impact of R^2 substitution is best illustrated by comparing HAPY-4 with HAPY-9, HAPY-11, and HAPY-12, where the observed rate changes span two orders of magnitude.

All told, by varying groups at the R^1, R^2, and R^3 positions on the pyrazolone ring, the observed rate changes span one, two, and three orders of magnitude, respectively. The distance removed from the carbon bearing the hydroxylamine group is greatest for the R^1 position and shortest for the R^3 position, and inductive effects are expected to follow likewise. However, only the R^3 position allows for additional resonance stabilization in the dissociated PY byproduct, which has the largest impact on the PY byproduct pK_a (e.g., the pK_a difference of PY-1 and PY-2 is two pH units).

As suggested from our calculations, HNO release is governed by the pK_a of the donor, which likely correlates with the pK_a of the byproduct. This trend is reinforced by UV-vis analysis of the decomposition rates of the representative HAPY compounds as a function of pH, where the observed sharp increases reflect rapid PY

formation as a result of HAPY deprotonation (Figure 3-6). Decomposition rates reach the time resolution limit (ca. 0.15 s^{-1}), precluding a complete pK_a analysis for each donor; however, these results indicate that the barrier to dissociation must be very low once deprotonation of the donor occurs. Moreover, with such large approximate pK_a values, HNO evolution at neutral pH suggests a near barrierless dissociation from the deprotonated donor.

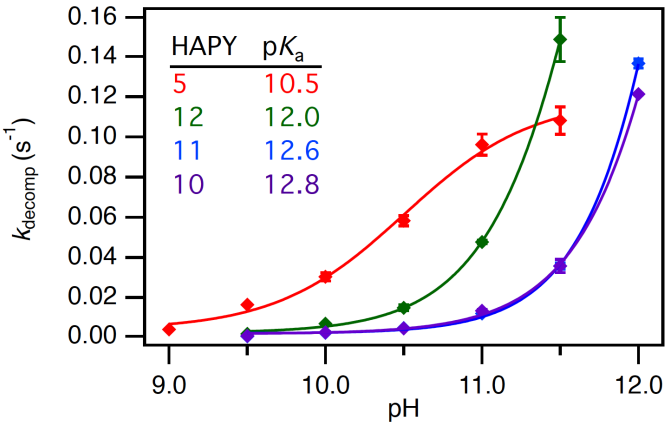

Figure 3-6. Plot of UV-vis determined decomposition rates as a function of pH at 25 °C for HAPY-5 (red), HAPY-10 (purple), HAPY-11 (blue), and HAPY-12 (green). The solid curves are calculated best fits to a sigmoid function (SEM ± 10 %; n ≥ 3).

However, byproduct pK_a alone does not always correlate with donor pK_a. For example, the pK_a values of PY-5, PY-10 – PY-12 are all ca. 8, yet HAPY-5 is more acidic than HAPY-12, which in turn is more acidic than HAPY-10 and HAPY-11 (Figure 3-6). This trend is mirrored in the half-lives of these donors at neutral pH (Table 3-3). The half-lives of HAPY-5, HAPY-10, HAPY-11, and HAPY-12 are 14, 460, 799, and 71 minutes, respectively. The fact that decomposition of HAPY-5 as a function of pH is approaching a limiting rate constant at a pH apparently much lower than that for HAPY-10 – HAPY-12 in this analysis (Figure 3-6) suggests

contribution from deprotonation at the R^1 position proton (N–H) of the pyrazolone ring. This may explain the greater acidity of HAPY-5. In comparison, a pK_a value of 11.5 is estimated for the R^1 position proton of HAPY-6, the R^3 = methyl analog of HAPY-5 (Supporting Information). For the HAPY class as a whole, HNO release following HOHN–PY deprotonation remains the most plausible mechanism in water (Scheme 3-5).

Scheme 3-5. Proposed Mechanism of HNO Release

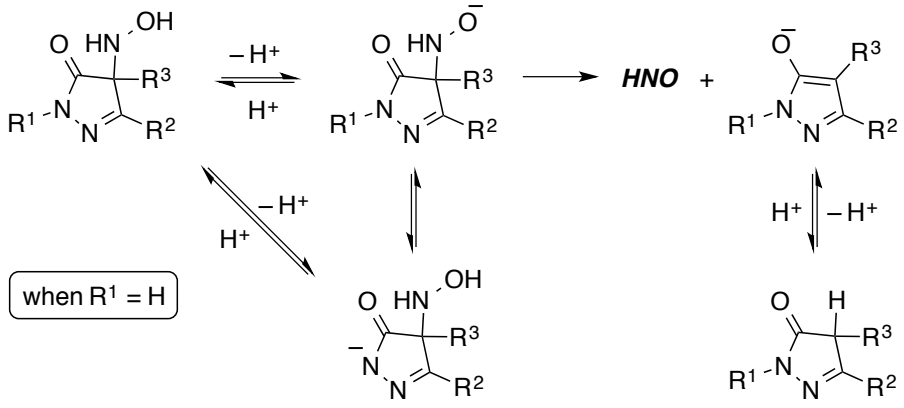

The pK_a values of the PY byproducts are a reflection of the weighted average of the various tautomers that are known to exist in pyrazolones, such as edaravone.[44-46] Presumably, the pK_a value of the carbon formerly bearing the hydroxylamine is the most relevant to predicting SAR for HNO release; however, we can assume from this first-pass study that PY byproducts with pK_a values ≤ ca. 8 in 50% v/v aqueous ethanol are useful targets for further development of the HAPY class.

▪ 3.4 Conclusion

The HAPY class represents a new and robust HNO donor platform capable of producing HNO quantitatively over extended periods of time along with a PY byproduct that is related to edaravone, a potent antioxidant already in clinical use for the treatment of stroke and cardiovascular disease. The HNO release rate is highly tunable by varying the groups at the R^1, R^2, and R^3 positions on the pyrazolone ring, and experimental and computational investigations suggest that the HNO release rate correlates with HAPY and PY pK_a. The catch is a strong affinity that is shared between HNO and the released PY byproduct since the bimolecular rate constant in pH 7.4 phosphate buffer at 37 °C can reach 8×10^5 $M^{-1}s^{-1}$. Given that biological targets for HNO are in excess of HNO *in vivo*, the back-reaction of HNO and PY to give HAPY is expected to be negligible under these conditions, as is the case in the ^1H NMR assay we developed for evaluating half-life and HNO production utilizing the selective, distinctive, and irreversible trap for HNO, TXPTS. Yet, this back-reaction, described herein for the first time as the HNO-aldol reaction with pyrazolones, is an efficient, alternative synthetic strategy to the cumbersome, three-step bromination-displacement-deprotection strategy, thus illustrating a synthetically useful route to HAPY donors. We anticipate utilizing these methodologies for the development of new *N*-substituted hydroxylamines with other suitable carbon-based leaving groups.

▪ 3.5 Experimental

3.5.1 Materials and Methods

All starting materials were of reagent grade and used without further purification. Compounds PY-1 and HAPY-1;[27] PY-2, PY-4, PY-9, and PY-10;[47] PY-6;[48] PY-11 and *N*-methyl-3-(2-chlorophenyl)-pyrazolone;[49] and 4-acetyl-3-methyl-pyrazolone[50] are all known compounds, and were prepared according to literature procedures. Angeli's salt ($Na_2N_2O_3$) was prepared according to King and Nagasawa.[51] *Tris*(4,6-dimethyl-3-sulfanatophenyl)phosphine trisodium salt (TXPTS) was of reagent grade and used without further purification. Synthetic TXPTS aza-ylide was obtained through the amidation of TXPTS using hydroxylamine *O*-sulfonic acid in water.[52] NMR spectra were obtained on a Bruker Avance 400 MHz FT-NMR spectrometer. All chemical shifts are reported in parts per million (ppm) relative to residual $CHCl_3$ (7.26 ppm for ^1H, 77.23 ppm for ^{13}C), residual DMSO (2.50 ppm for ^1H, 39.52 for ^{13}C), or residual MeOH (3.31 ppm for ^1H, 49.15 ppm for ^{13}C). High-resolution mass spectra were obtained on a VG Analytical VG70SE magnetic sector mass spectrometer operating in fast atom bombardment (FAB) mode. Ultraviolet-visible (UV-vis) absorption spectra were obtained using a Hewlett Packard 8453 diode array spectrometer. Buffered solutions (0.1 M) for UV-vis experiments were prepared from $NaPO_3H_2/Na_2PO_3H$ (pH 9.0, 9.5, 10.0, 10.5, 11.0, 11.5, 12.0).

3.5.2 Incubation Procedure of HAPY Donors at pH 7.4, 37 °C with TXPTS

General

All ^{1}H NMR spectra were obtained in pH 7.4 solution containing 0.25 M phosphate buffer, 0.2 mM of the metal chelator diethylenetriaminepentaacetic acid (DTPA), and 10 % D_2O on a Bruker Avance 400 MHz FT-NMR spectrometer using a 1 second presaturation pulse to suppress the water signal. The data were processed with the academic version of ACDLabs NMR processor software: each free induction decay was Fourier transformed, phased, baseline corrected, and integral areas measured for the methyl groups of compounds HAPY-1 – HAPY-12 and PY-1 – PY-2 and the downfield methyl group of TXPTS aza-ylide. The ^{1}H NMR spectrum of the HNO derived TXPTS aza-ylide product matched that of synthetic TXPTS aza-ylide. The HNO yield from compounds HAPY-1 – HAPY-12 was determined from the final TXPTS aza-ylide yield.

NMR Procedure

The NMR procedure used was based on an HPLC protocol developed by S. Bruce King and co-workers.[39-40] To an argon-purged NMR solution (1.00 mL) containing TXPTS (3.3 mg, 5 mM) was added HAPY-1 – HAPY-12 (10 μL of 100 mM in methanol-d_4) to give 1 mM as the initial concentration of HAPY-1 – HAPY-12. The solution was briefly mixed, ca. 0.5 mL was transferred to an argon-purged NMR tube, and an initial ^{1}H NMR spectrum was obtained. The sample was then either (1) externally incubated at 37 °C and ^{1}H NMR spectra were collected at regular time intervals, or (2) internally incubated at 37 °C and ^{1}H NMR spectra were collected

using a canned Bruker pulse sequence, zg2d, modified to include a 1 second presaturation pulse during the relaxation delay.

3.5.3 Experimental Procedures

Scheme 3-6. Synthesis of 4-Acetyl-1,3-dimethyl-pyrazolone (1)

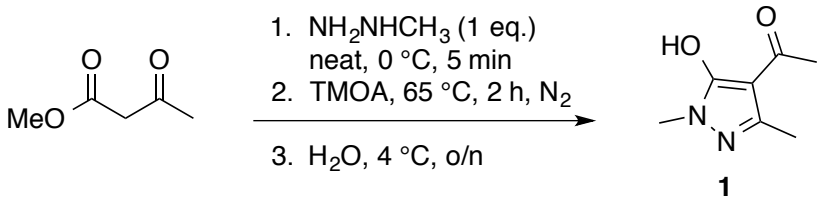

1

4-Acetyl-1,3-dimethyl-pyrazolone (1). To methylacetoacetate (2.32 g, 20 mmol) on ice was added methylhydrazine (1.05 mL, 20 mmol) over two to three minutes with stirring. The reaction was then stirred for five minutes, whereupon 1,3-dimethyl pyrazolone precipitated from solution. The reaction was diluted with ethanol (20 mL) and concentrated *in vacuo* to give dry 1,3-dimethyl pyrazolone as an off-white solid. This was then taken up with trimethylorthoacetate (10 mL) under nitrogen and heated to 65 °C for two hours. The clear, red-orange solution was concentrated *in vacuo*, the solid was dissolved in water (10 mL), and the solution was allowed to stand at 4 °C overnight. Filtration of the resulting precipitate gave the title compound as an orange solid (1.36 g, 44%). ^{1}H NMR (400 MHz, $CDCl_3$) δ: 3.55 (s, 3H), 2.38 (s, 3H), 2.36 (s, 3H). ^{13}C NMR (100 MHz, $CDCl_3$) δ: 195.31, 159.59, 146.84, 103.20, 32.50, 27.45, 15.53. HR-MS (FAB): found *m/z* = 155.08184 (MH^+); calc. for $C_7H_{11}N_2O_2$: 155.08205 (MH^+).

Scheme 3-7. Synthesis of 3-(2-Chlorophenyl)-4-formyl-1-methyl-pyrazolone (2)

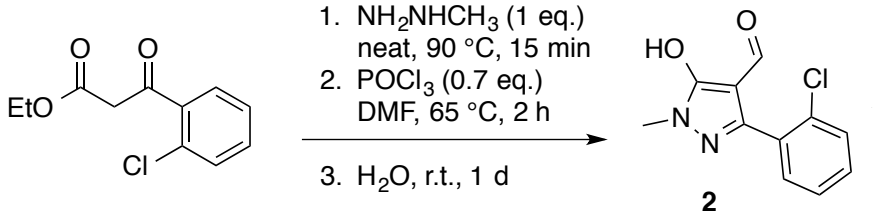

3-(2-Chlorophenyl)-4-formyl-1-methyl-pyrazolone (2). To ethyl (2-chlorobenzoyl)acetate (0.937 g, 4.13 mmol) at room temperature was added methylhydrazine (0.22 mL, 4.1 mmol) over two to three minutes with stirring. The reaction was then heated to 90 °C for 15 min and allowed to cool to room temperature where white solids formed upon standing. This material was recrystallized from hot ethanol and water to give pure *N*-methyl-3-(2-chlorophenyl)-pyrazolone (0.410 g, 48%). To this product dissolved in dimethylformamide (1 mL) was added phosphoryl chloride (0.13 mL, 1.4 mmol), and the reaction was heated to 65 °C with stirring for 2 h followed by addition of water (5 mL). This solution was allowed to stand at room temperature for 1 d, and the resultant yellow precipitate was collected by vacuum filtration to give the title compound (0.370 g, 79%). ^{1}H NMR (400 MHz, DMSO-d_6) δ: 9.51 (s, 1H), 7.44 (m, 4H), 3.60 (s, 3H). ^{13}C NMR (100 MHz, DMSO-d_6) δ: 181.98, 155.60, 132.93, 132.23, 131.72, 130.20, 129.29, 126.88, 104.44, 33.14. HR-MS (FAB): found *m/z* = 237.04354 (MH^+,^{35}Cl), 239.04114 (MH^+,^{37}Cl); calc. for $C_{11}H_{10}ClN_2O_2$: 237.04308 (MH^+,^{35}Cl), 239.04013 (MH^+,^{37}Cl).

Scheme 3-8. Synthesis of 4-(Acetyl-*O*-methoxyoxime)-1,3-dimethyl-pyrazolone (PY-3)

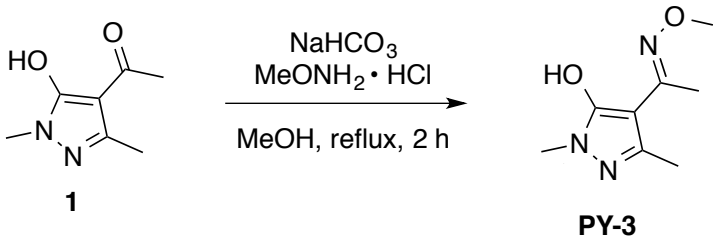

4-(Acetyl-*O*-methoxyoxime)-1,3-methyl-pyrazolone (PY-3). Compound **1** (0.771 g, 5 mmol), *O*-methylhydroxylamine hydrochloride (0.459 g, 5.5 mmol), and sodium bicarbonate (0.462 g, 5.5 mmol) was taken up in methanol (50 mL), and the reaction was refluxed with stirring for 2 h followed by concentration *in vacuo*. The resultant material was taken up in dichloromethane, filtered through cotton, and concentrated *in vacuo* to give the title compound as an off-white solid (0.731 g, 80%). ^{1}H NMR (400 MHz, $CDCl_3$) δ: 3.85 (s, 3H), 3.56 (s, 3H), 2.29 (s, 3H), 2.19 (s, 3H). ^{13}C NMR (100 MHz, $CDCl_3$) δ: 155.18, 153.81, 144.67, 95.21, 62.01, 32.84, 15.63, 13.06. HR-MS (FAB): found *m/z* = 184.10819 (MH^+); calc. for $C_8H_{14}N_3O_2$: 184.10860 (MH^+).

Scheme 3-9. Synthesis of 4-(Acetyl-*O*-methoxyoxime)-3-methyl-pyrazolone (PY-5)

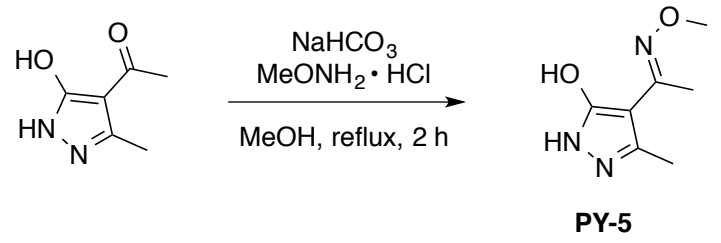

4-(Acetyl-*O*-methoxyoxime)-3-methyl-pyrazolone (PY-5). 4-Acetyl-3-methyl-pyrazolone (2.935 g, 20.9 mmol), *O*-methylhydroxylamine hydrochloride (1.921 g, 23 mmol), and sodium bicarbonate (1.932 g, 23 mmol) was taken up in

methanol (125 mL), and the reaction was refluxed with stirring for 21 h followed by concentration *in vacuo*. The resultant material was taken up in ethyl acetated (2 × 125 mL), filtered through cotton, and concentrated *in vacuo* to give the title compound as a pale yellow solid (2.487 g, 70%). ^{1}H NMR (400 MHz, DMSO-d_6) δ: 3.78 (s, 3H), 2.23 (s, 3H), 2.08 (s, 3H). ^{13}C NMR (100 MHz, DMSO-d_6) δ: 159.86, 151.50, 138.18, 98.49, 60.97, 13.48, 12.24. HR-MS (FAB): found *m/z* = 170.09335 (MH^+); calc. for $C_7H_{12}N_3O_2$: 170.09295 (MH^+).

Scheme 3-10. Synthesis of 4-Methyl-*N*-(4-chlorophenyl)-3-methyl-pyrazolone (PY-7)

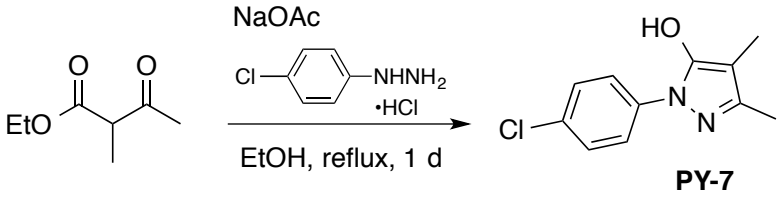

PY-7

4-Methyl-*N*-(4-chlorophenyl)-3-methyl-pyrazolone (PY-7). Ethyl 2-methylacetoacetate (0.71 mL, 5 mmol), 4-chlorophenylhydrazine hydrochloride (0.895 g, 5 mmol), and sodium acetate (0.410 g, 5 mmol) was taken up in ethanol (50 mL), and the reaction was refluxed with stirring for 1 d followed by filtration through cotton and concentration *in vacuo*. The resultant material was recrystallized from hot ethanol and 1N HCl to give the title compound as a white solid (0.867 g, 78%). ^{1}H NMR (400 MHz, DMSO-d_6) δ: 7.75 (d, 2H, J = 8.9 Hz), 7.50 (d, 2H, J = 8.9 Hz), 2.13 (s, 3H), 1.80 (s, 3H). ^{13}C NMR (100 MHz, DMSO-d_6) δ: 157.00, 147.74, 135.68, 129.73, 129.02, 121.95, 99.34, 11.27, 6.58. HR-MS (FAB): found *m/z* = 223.06396 (MH^+,^{35}Cl), 225.06151 (MH^+,^{37}Cl); calc. for $C_{11}H_{12}ClN_2O$: 223.06382 (MH^+,^{35}Cl), 225.06087 (MH^+,^{37}Cl).

Scheme 3-11. Synthesis of 4-Methyl-*N*-(2-chlorophenyl)-3-methyl-pyrazolone (PY-8)

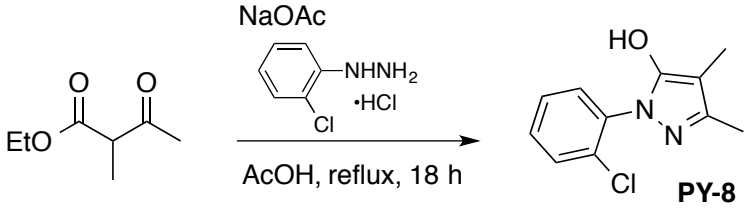

4-Methyl-*N*-(2-chlorophenyl)-3-methyl-pyrazolone (PY-8). Ethyl 2-methylacetoacetate (0.71 mL, 5 mmol), 2-chlorophenylhydrazine hydrochloride (0.895 g, 5 mmol), and sodium acetate (0.410 g, 5 mmol) was taken up in acetic acid (50 mL), and the reaction was refluxed with stirring for 18 h followed by filtration through cotton and concentration *in vacuo*. The resultant material was triturated with diethylether to remove the colored impurities and filtered, then extracted into ethylacetate (2 × 100 mL), washed with water and brine, dried over magnesium sulfate, filtered, and concentrated *in vacuo* to give the title compound as an off-white solid (0.696 g, 63%). ^{1}H NMR (400 MHz, MeOD-d_4) δ: 7.58 (m, 1H), 7.45 (m, 3H), 2.17 (s, 3H), 1.85 (s, 3H). ^{13}C NMR (100 MHz, MeOD-d_4) δ: 164.84, 148.59, 135.09, 134.26, 132.08, 131.66, 131.51, 129.09. HR-MS (FAB): found *m/z* = 223.06348 (MH^+,^{35}Cl), 225.06092 (MH^+,^{37}Cl); calc. for $C_{11}H_{12}ClN_2O$: 223.06382 (MH^+,^{35}Cl), 225.06087 (MH^+,^{37}Cl).

Scheme 3-12. Synthesis of 4-Methyl-*N*-methyl-3-(2-chlorophenyl)-pyrazolone (PY-12)

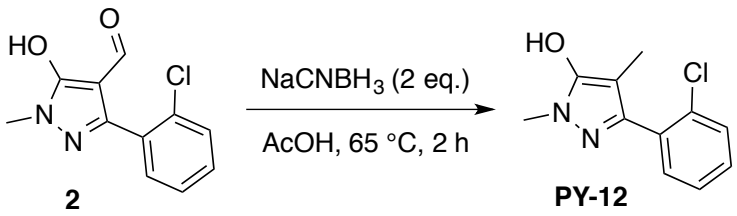

4-Methyl-*N*-methyl-3-(2-chlorophenyl)-pyrazolone (PY-12). To a solution of compound **2** (0.370 g, 1.56 mmol) in acetic acid (20 mL) was added sodium cyanoborohydride (0.211 g, 3.2 mmol), and the reaction was heated to 65 °C and stirred for 2 hours. The reaction was then concentrated *in vacuo*, taken up in 1N HCl, extracted into ethylacetate (2 × 50 mL), washed with brine, dried over magnesium sulfate, filtered, and concentrated *in vacuo*. The resultant viscous oil was triturated with dichloromethane and hexanes and filtered to give the title compound as a white solid (0.070 g, 20%). ^{1}H NMR (400 MHz, DMSO-d_6) δ: 7.51 (d, 1H, J = 6.8 Hz), 7.38 (m, 3H), 3.57 (s, 3H), 1.76 (s, 3H). ^{13}C NMR (100 MHz, DMSO-d_6) δ: 150.47, 145.54, 132.95, 132.69, 132.07, 129.78, 129.44, 126.99, 95.74, 33.23, 7.74. HR-MS (FAB): found m/z = 225.06188 (MH^+,^{37}Cl); calc. for $C_{11}H_{12}ClN_2O$: 225.06087 (MH^+,^{37}Cl).

Scheme 3-13. Synthesis of HAPY Donors via the HNO-Aldol Procedure

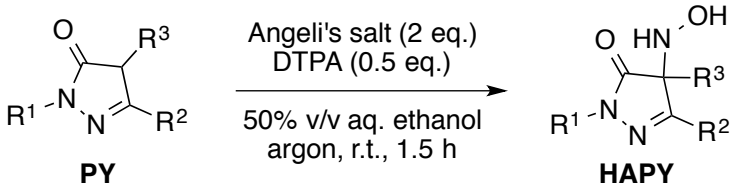

General HNO-aldol procedure:

To the PY substrate (0.20 mmol), Angeli's salt (49 mg, 0.40 mmol), and powdered DTPA (39 mg, 0.10 mmol) under argon at room temperature was added a degassed mixture of 50% v/v aqueous ethanol (1 mL) via syringe. The reaction was allowed to stir for 1.5 hours, diluted with ethanol (>5 mL), and concentrated to dryness *in vacuo* with minimum heat (<30 °C). The material was then taken up in

minimum ethanol, eluted through a short silica plug, and concentrated *in vacuo* to give the desired HAPY product or to allow for further purification if complete conversion was not observed (i.e., the *O*-methyloxime derivatives HAPY-1, HAPY-3, and HAPY-5). The crude reaction mixture was loaded with methanol onto an analytical TLC plate (250 μm thickness) and developed in either 50% v/v ethyl acetate/dichloromethane (HAPY-1) or ethyl acetate (HAPY-3 and HAPY-5). The product band (Rf > 0.5) was scraped off the plate into a flask using a metal spatula. The product is eluted with methanol (10 mL), filtered through cotton, and concentrated *in vacuo* to yield the desired product typically as off-white/white solids. Isolated yields are given in Table 3-1.

Compound Characterization:

4-(*N*-Hydroxylamine)-4-methyl-*N*-phenyl-3-methyl-pyrazolone (HAPY-2). ^{1}H NMR (400 MHz, $CDCl_3$) δ: 7.93 (d, 2H, *J* = 8.8 Hz), 7.40 (dd, 2H, *J* = 7.4 Hz), 7.18 (t, 1H, *J* = 7.4 Hz), 5.70 (b.s., 1H), 4.77 (s, 1H), 2.21 (s, 3H), 1.28 (s, 3H). ^{13}C NMR (100 MHz, $CDCl_3$) δ: 174.06, 162.07, 138.12, 129.05, 125.31, 118.86, 71.23, 16.97, 13.33. HR-MS (FAB): found *m/z* = 220.10932 (MH^+); calc. for $C_{11}H_{14}N_3O_2$: 220.10860 (MH^+).

4-(*N*-Hydroxylamine)-4-(acetyl-*O*-methoxyoxime)-*N*-methyl-3-methyl-pyrazolone (HAPY-3). ^{1}H NMR (400 MHz, $CDCl_3$) δ: 6.12 (s, 1H), 4.67 (s, 1H), 3.90 (s, 3H), 3.33 (s, 3H), 2.12 (s, 3H), 1.74 (s, 3H). ^{13}C NMR (100 MHz, $CDCl_3$) δ: 171.68, 158.97, 76.62, 62.53, 31.77, 14.39, 10.96. HR-MS (FAB): found *m/z* = 215.11454 (MH^+); calc. for $C_8H_{15}N_4O_3$: 215.11442 (MH^+).

4-(*N*-Hydroxylamine)-4-methyl-*N*-methyl-3-methyl-pyrazolone (HAPY-4). ^{1}H NMR (400 MHz, DMSO-d_6) δ: 7.52 (d, 1H, J = 2.8 Hz), 6.25 (d, 1H, J = 2.8 Hz), 3.12 (s, 3H), 1.96 (s, 3H), 1.00 (s, 3H). ^{13}C NMR (100 MHz, DMSO-d_6) δ: 175.34, 161.94, 68.96, 30.73, 15.98, 12.70. HR-MS (FAB): found m/z = 158.09320 (MH^+); calc. for $C_6H_{12}N_3O_2$: 158.09295 (MH^+).

4-(*N*-Hydroxylamine)-4-(acetyl-*O*-methoxyoxime)-3-methyl-pyrazolone (HAPY-5). ^{1}H NMR (400 MHz, DMSO-d_6) δ: 10.96 (s, 1H), 7.76, (d, 1H, J = 2.7 Hz), 6.60 (d, 1H, J = 2.7 Hz), 3.76 (s, 3H), 1.98 (s, 3H), 1.79 (s, 3H). ^{13}C NMR (100 MHz, DMSO-d_6) δ: 173.93, 159.50, 151.82, 74.23, 61.60, 14.85, 10.57. HR-MS (FAB): found m/z = 201.09920 (MH^+); calc. for $C_7H_{13}N_4O_3$: 201.09817 (MH^+).

4-(*N*-Hydroxylamine)-4-methyl-3-methyl-pyrazolone (HAPY-6). ^{1}H NMR (400 MHz, DMSO-d_6) δ: 10.77 (s, 1H), 7.50 (d, 1H, J = 2.9 Hz), 6.16 (d, 1H, J = 2.9 Hz), 1.93 (s, 3H), 0.97 (s, 3H). ^{13}C NMR (100 MHz, DMSO-d_6) δ: 178.26, 161.86, 67.98, 15.96, 13.03. HR-MS (FAB): found m/z = 144.07683 (MH^+); calc. for $C_5H_{10}N_3O_2$: 144.07730 (MH^+).

4-(*N*-Hydroxylamine)-4-methyl-*N*-(4-chlorophenyl)-3-methyl-pyrazolone (HAPY-7). ^{1}H NMR (400 MHz, $CDCl_3$) δ: 7.90 (d, 2H, J = 9.0 Hz), 7.35 (d, 2H, J = 9.0 Hz), 5.66 (d, 1H, J = 2.8 Hz), 4.45 (d, 1H, J = 2.8 Hz), 2.20 (s, 3H), 1.28 (s, 3H). ^{13}C NMR (100 MHz, $CDCl_3$) δ: 173.96, 162.18, 136.77, 130.36, 129.09, 119.92, 71.19, 16.92, 13.31. HR-MS (FAB): found m/z = 254.06968 (MH^+,^{35}Cl), 256.06703 (MH^+,^{37}Cl); calc. for $C_{11}H_{13}ClN_3O_2$: 254.06963 (MH^+,^{35}Cl), 256.06668 (MH^+,^{37}Cl).

4-(*N*-Hydroxylamine)-4-methyl-*N*-(2-chlorophenyl)-3-methyl-pyrazolone (HAPY-8). ^{1}H NMR (400 MHz, DMSO-d_6) δ: 7.73 (d, 1H, J = 2.8 Hz), 7.60

(m, 1H), 7.43 (m, 3H), 6.50 (d, 1H, *J* = 2.8 Hz), 2.07 (s, 3H), 1.17 (s, 3H). ^{13}C NMR (100 MHz, DMSO-d_6) δ: 174.77, 163.32, 134.75, 130.81, 130.12, 129.94, 129.06, 127.96, 69.42, 16.24, 12.90. HR-MS (FAB): found *m/z* = 254.06967 (MH^+,^{35}Cl), 256.06718 (MH^+,^{37}Cl); calc. for $C_{11}H_{13}ClN_3O_2$: 254.06963 (MH^+,^{35}Cl), 256.06668 (MH^+,^{37}Cl).

4-(*N*-Hydroxylamine)-4-methyl-*N*-methyl-3-phenyl-pyrazolone (HAPY-9). ^{1}H NMR (400 MHz, DMSO-d_6) δ: 8.06 (m, 2H), 7.64 (d, 2H, *J* = 2.5 Hz), 7.45 (m, 3H), 6.48 (d, 2H, *J* = 2.5 Hz), 3.29 (s, 3H), 1.21 (s, 3H). ^{13}C NMR (100 MHz, DMSO-d_6) δ: 176.13, 157.36, 130.44, 129.88, 128.60, 126.21, 69.33, 31.20, 17.88. HR-MS (FAB): found *m/z* = 220.10897 (MH^+); calc. for $C_{11}H_{14}N_3O_2$: 220.10860 (MH^+).

4-(*N*-Hydroxylamine)-4-methyl-*N*-phenyl-3-phenyl-pyrazolone (HAPY-10). ^{1}H NMR (400 MHz, $CDCl_3$) δ: 8.21 (m, 2H), 8.05 (m, 2H), 7.45 (m, 5H), 7.24 (m, 1H), 5.95 (d, 1H, *J* = 3.2 Hz), 4.50 (d, 1H, *J* = 3.3 Hz), 1.48 (s, 3H). ^{13}C NMR (100 MHz, $CDCl_3$) δ: 174.98, 157.74, 138.21, 130.97, 130.26, 129.10, 129.09, 126.79, 125.51, 119.01, 71.51, 18.92. HR-MS (FAB): found *m/z* = 282.12461 (MH^+); calc. for $C_{16}H_{16}N_3O_2$: 282.12425 (MH^+).

4-(*N*-Hydroxylamine)-4-methyl-*N*-methyl-3-(4-chlorophenyl)-pyrazolone (HAPY-11). ^{1}H NMR (400 MHz, DMSO-d_6) δ: 8.06 (d, 2H, *J* = 8.7 Hz), 7.66 (d, 1H, *J* = 2.6 Hz), 7.53 (d, 2H, *J* = 8.7 Hz), 6.54 (d, 1H, *J* = 2.6 Hz), 3.29 (s, 3H), 1.19 (s, 3H). ^{13}C NMR (100 MHz, DMSO-d_6) δ: 176.10, 156.36, 134.48, 129.21, 128.72, 127.96, 62.27, 31.24, 17.70. HR-MS (FAB): found *m/z* = 254.06941 (MH^+, ^{35}Cl), 256.06193 (MH^+, ^{37}Cl); calc. for $C_{11}H_{13}ClN_3O_2$: 254.06963 (MH^+, ^{35}Cl), 256.06668 (MH^+, ^{37}Cl).

4-(*N*-Hydroxylamine)-4-methyl-*N*-methyl-3-(2-chlorophenyl)-pyrazolone (HAPY-12). ^{1}H NMR (400 MHz, $CDCl_3$) δ: 7.71 (m, 1H), 7.50 (m, 1H), 7.38 (m, 2H), 5.90 (br, 2H), 3.45 (s, 3H), 1.26 (s, 3H). ^{13}C NMR (100 MHz, $CDCl_3$) δ: 174.87, 158.59, 133.52, 131.13, 131.05, 130.69, 129.29, 127.11, 71.59, 32.00, 16.91. HR-MS (FAB): found *m/z* = 254.06981(MH^+, ^{35}Cl), 256.06755 (MH^+, ^{37}Cl); calc. for $C_{11}H_{13}ClN_3O_2$: 254.06963 (MH^+, ^{35}Cl), 256.06668 (MH^+, ^{37}Cl).

▪ 3.6 References

(1) Go, A. S.; Mozaffarian, D; Roger, V. L.; Benjamin, E. J.; Berry, J. D.; Borden, W. B.; Bravata, D. M.; Dai, S.; Ford, E. S.; Fox, C. S.; Franco, S.; Fullerton, H. J.; Gillespie, C.; Hailpern, S. M.; Heit, J. A.; Howard, V. J.; Huffman, M. D.; Kissela, B. M.; Kittner, S. J.; Lackland, D. T.; Lichtman, J. H.; Lisabeth, L. D.; Magid, D.; Marcus, G. M.; Marelli, A.; Matchar, D. B.; McGuire, D. K.; Mohler, E. R.; Moy, C. S.; Mussolino, M. E.; Nichol, G.; Paynter, N. P.; Schreiner, P. J.; Sorlie, P. D.; Stein, J.; Turan, T. N.; Virani, S. S.; Wong, N. D.; Woo, D.; Turner, M. B. *Circulation,* **2013**, *127*, e6–e245.

(2) McMurray, J. J.; Petrie, M. C.; Murdoch, D. R.; Davie, A. P. *Eur. Heart J.* **1998**, 19 Suppl P: P9–16.

(3) Heidenreich, P. A.; Trogdon, J. G.; Khavjou, O. A.; Butler, J.; Dracup, K.; Ezekowitz, M. D.; Finkelstein, E. A.; Hong, Y.; Johnston, S. C.; Khera, A.; Lloyd-Jones, D. M.; Nelson, S. A.; Nichol, G.; Orenstein, D.; Wilson, P. W. F.; Woo, Y. J. *Circulation* **2011**, *123*, 933–44.

(4) Paolocci, N.; Saavedra, W. F.; Miranda, K. M.; Martignani, C.; Isoda, T.; Hare, J. M.; Espey, M. G.; Fukuto, J. M.; Feelisch, M.; Wink, D. A.; Kass, D. A. *Proc. Natl. Acad. Sci. U.S.A.* **2001**, *98*, 10463–10468.

(5) Paolocci, N.; Katori, T.; Champion, H. C. St.; John, M. E.; Miranda, K. M.; Fukuto, J. M.; Wink, D. A.; Kass, D. A. *Proc. Natl. Acad. Sci. U.S.A.* **2003**, *100*, 5537–5542.

(6) Paolocci, N.; Jackson, M. I.; Lopez, B. E.; Miranda, K.; Tocchetti, C. G.; Wink, D. A.; Hobbs, A. J.; Fukuto, J. M. *Pharmacol. Ther.* **2007**, *113*, 442–458.

(7) Tocchetti, C. G.; Wang, W.; Froehlich, J. P.; Huke, S.; Aon, M. A.; Wilson, G. M.; Di Benedetto, G.; O'Rourke, B.; Gao, W. D.; Wink, D. A.; Toscano, J. P.; Zaccolo, M.; Bers, D. M.; Valdivia, H. H.; Cheng, H.; Kass, D. A.; Paolocci, N. *Circ. Res.* **2007**, *100*, 96–104.

(8) Froehlich, J. P.; Mahaney, J. E.; Keceli, G.; Pavlos, C. M.; Goldstein, R.; Redwood, A. J.; Sumbilla, C.; Lee, D. I.; Tocchetti, C. G.; Kass, D. A.; Paolocci, N.; Toscano, J. P. *Biochemistry* **2008**, *47*, 13150–13152.

(9) Shafirovich, V.; Lymar, S. V. *Proc. Natl. Acad. Sci. U.S.A*. **2002**, *99*, 7340–7345.

(10) Hughes, M. N.; Cammack, R. *Methods Enzymol.* **1998**, *301*, 279–287.

(11) Gladwin, M. T.; Raat, N. J. H.; Shiva, S.; Dezfulian, C.; Hogg, N.; Kim-Shapiro, D. B.; Patel, R. P. *Am. J. Physiol.: Heart Circ. Physiol.* **2006**, *291*, H2026–H2035.

(12) Gladwin, M. T.; Schechter, A. N.; Kim-Shapiro, D. B.; Patel, R. P.; Hogg, N.; Shiva, S.; Cannon, R. O.; Kelm, M.; Wink, D. A.; Espey, M. G.; Oldfield, E. H.; Pluta, R. M.;

Freeman, B. A.; Lancaster, J. R.; Feelisch, M.; Lundberg, J. O. *Nature Chem. Biol.* **2005**, *1*, 308–314.

(13) Choe, C.-U.; Lewerenz, J.; Gerloff, C.; Magnus, T.; Donzelli, S. *Antioxid. Redox Signal.* **2011**, *14*, 1699–1711.

(14) Sha, X.; Isbell, T. S.; Patel, R. P.; Day, C. S.; King, S. B. *J. Am. Chem. Soc.* **2006**, *128*, 9687–9692.

(15) Shoman, M. E.; DuMond, J. F.; Isbell, T. S.; Crawford, J. H.; Brandon, A.; Honovar, J.; Vitturi, D. A.; White, C. R.; Patel, R. P.; King, S. B. *J. Med. Chem*. **2011**, *54*, 1059–1070.

(16) Miranda, K. M.; Katori, T.; Torres de Holding, C. L.; Thomas, L.; Ridnour, L. A.; McLendon, W. J.; Cologna, S. M.; Dutton, A. S.; Champion, H. C.; Mancardi, D.; Tocchetti, C. G.; Saavedra, J. E.; Keefer, L. K.; Houk, K. N.; Fukuto, J. M.; Kass, D. A.; Paolocci, N.; Wink, D. A. *J. Med. Chem.* **2005**, *48*, 8220–8228.

(17) Salmon, D. J.; Torres de Holding, C. L.; Thomas, L.; Peterson, K. V.; Goodman, G. P.; Saavedra, J. E.; Srinivasan, A.; Davies, K. M.; Keefer, L. K.; Miranda, K. M. *Inorg. Chem*. **2011**, *50*, 3262–3270.

(18) Andrei, D.; Salmon, D. J.; Donzelli, S.; Wahab, A.; Klose, J. R.; Citro, M. L.; Saavedra, J. E.; Wink, D. A.; Miranda, K. M.; Keefer, L. K. *J. Am. Chem. Soc.* **2010**, *132*, 16526–16532.

(19) Basudhar, D.; Bharadwaj, G.; Cheng, R. Y.; Jain, S.; Shi, S.; Heinecke, J. L.; Holland, R. J.; Ridnour, L. A.; Caceres, V. M.; Spadari-Bratfisch, R. C.; Paolocci, N.; Velázquez-Martínez, C. A.; Wink, D. A.; Miranda, K. M. *J. Med. Chem*. **2013**, *56*, 7804–7820.

(20) Corrie, J. E. T.; Kirby, G. W.; Mackinnon, J. W. M. *J. Chem. Soc., Perkin Trans.* **1985**, 1, 883–886.

(21) Cohen, A. D.; Zeng, B.-B.; King, S. B.; Toscano, J. P. *J. Am. Chem. Soc.* **2003**, *125*, 1444–1445.

(22) Evans, A. S.; Cohen, A. D.; Gurard-Levin, Z. A.; Kebede, N.; Celius, T. C.; Miceli, A. P.; Toscano, J. P. *Can. J. Chem.* **2011**, *89*, 130–138.

(23) Sutton, A. D.; Williamson, M.; Weismiller, H.; Toscano, J. P. *Org. Lett*. **2012**, *14*, 472–475.

(24) Mitroka, S.; Shoman, M. E.; DuMond, J. F.; Bellavia, L.; Aly, O. M.; Abdel-Aziz, M.; Kim-Shapiro, D. B.; King, S. B. *J. Med. Chem*. **2013**, *56*, 6583–6592.

(25) Shoman, M. E.; DuMond, J. F.; Isbell, T. S.; Crawford, J. H.; Brandon, A.; Honovar, J.; Vitturi, D. A.; White, C. R.; Patel, R. P.; King, S. B. *J. Med. Chem*. **2011**, *54*, 1059–1070.

(26) Bodor, N.; Buchwald, P. *Retrometabolic Drug Design and Targeting*. Hoboken: John Wiley & Sons, **2012**.

(27) Guthrie, D. A.; Kim, N. Y.; Siegler, M. A.; Moore, C. D.; Toscano, J. P. *J. Am. Chem. Soc.* **2012**, *134*, 1962–1965.

(28) Higashi, Y.; Jitsuiki, D.; Chayama, K.; Yoshizumi, M. *Recent Pat. Cardiovasc. Drug Discovery* **2006**, *1*, 85–93.

(29) Watanabe, T.; Tahara, M.; Todo, S. *Cardiovasc. Ther*. **2008**, *26*, 101–114.

(30) Watanabe, K.; Morinaka, Y.; Iseki, K.; Watanabe, T.; Yuki, S.; Hishi, H. *Redox Report* **2003**, *8*, 151–155.

(31) Doyle, M. P.; Mahapatro, S. N.; Broene, R. D.; Guy, J. K. *J. Am. Chem. Soc.* **1988**, *110*, 593–599.

(32) Wong, P. S. Y.; Hyun, J.; Fukuto, J. M.; Shirota, F. N.; DeMaster, E. G.; Shoeman, D. W.; Nagasawa, H. T. *Biochemistry* **1998**, *37*, 5362–5371.

(33) Nagasawa, H. T.; DeMaster, E. G.; Redfern, B.; Shirota, F. N.; Goon, D. J. W. *J. Med. Chem.* **1990**, *33*, 3120–3122.

(34) DeMaster, E. G.; Redfern, B.; Nagasawa, H. T. *Biochem. Pharmacol*. **1998**, *55*, 2007–2015.

(35) Deb, M. L.; Bhuyan, P. J. *Tetrahedron Lett*. **2005**, *46*, 6453–6456.

(36) Sandoval, D.; Frazier, C. P.; Bugarin, A.; Read de Alaniz, J. *J. Am. Chem. Soc*. **2012**, *134*, 18948**–**18951.

(37) Baidya, M.; Griffin, K. A.; Yamamoto, H. *J. Am. Chem. Soc*. **2012**, *134*, 18566**–**18569.

(38) Palmer, L. I.; Frazier, C. P.; Read de Alaniz, J. *Synthesis* **2014**, *46*, 269–280.

(39) Reisz, J. A.; Klorig, E. B.; Wright, M. W.; King, S. B. *Org. Lett.* **2009**, *11*, 2719–2721.

(40) Reisz, J. A.; Zink, C. N.; King, S. B. *J. Am. Chem. Soc.* **2011**, *133*, 11675–11685.

(41) Miranda, K. M.; Paolocci, N.; Katori, T.; Thomas, D. D.; Ford, E.; Bartberger, M. D.; Espey, M. G.; Kass, D. A.; Feelisch, M.; Fukuto, J. M.; Wink, D. A. *Proc. Natl. Acad. Sci. U.S.A.* **2003**, *100*, 9196–9201.

(42) Shao Y.; Molnar, L. F.; Jung, Y.; Kussmann, J.; Ochsenfeld, C.; Brown, S. T.; Gilbert, A. T. B.; Slipchenko, L. V.; Levchenko, S. V.; O'Neill, D. P.; DiStasio Jr., R. A.; Lochan, R. C.; Wang, T.; Beran, G. J. O.; Besley, N. A.; Herbert, J. M.; Lin, C. Y.; Van Voorhis, T.; Chien, S. H.; Sodt, A.; Steele, R. P.; Rassolov, V. A.; Maslen, P. E.; Korambath, P. P.; Adamson, R. D.; Austin, B.; Baker, J.; Byrd, E. F. C.; Dachsel, H.; Doerksen, R. J.; Dreuw, A.; Dunietz, B. D.; Dutoi, A. D.; Furlani, T. R.; Gwaltney, S. R.; Heyden, A.; Hirata, S.; Hsu, C-P.; Kedziora, G.; Khalliulin, R. Z.; Klunzinger, P.; Lee, A. M.; Lee, M. S.; Liang, W. Z.; Lotan, I.; Nair, N.; Peters, B.; Proynov, E. I.; Pieniazek, P. A.; Rhee, Y. M.; Ritchie, J.; Rosta, E.; Sherrill, C. D.; Simmonett, A. C.; Subotnik, J. E.; Woodcock III, H. L.; Zhang, W.; Bell, A. T.; Chakraborty, A. K.; Chipman, D. M.; Keil, F. J.; Warshel, A.; Hehre, W. J.; Schaefer, H. F.; Kong, J.; Krylov, A. I.; Gill, P. M. W.; Head-Gordon, M. *Phys. Chem. Chem. Phys.* **2006**, *8*, 3172–3191.

(43) Pérez-González, A.; Galano, A. *J. Phys. Chem. B* **2012**, *116*, 1180–1188.

(44) Ono, S.; Okazaki, K.; Sakurai, M.; Inoue, Y. *J. Phys. Chem. A* **1997**, *101*, 3769–3775.

(45) Lin, M.; Katsumura, Y.; Hata, K.; Muroya, Y.; Nakagawa, K. *J. Photochem. Photobiol. B: Biol.* **2007**, *89*, 36–43.

(46) Pérez-González, A.; Galano, A. *J. Phys. Chem. B* **2011**, *115*, 1306–1314.

(47) Katrizky, A. R.; Barczynski, P.; Ostercamp, D. L. *J. Chem. Soc., Perkin Trans. 2* **1987**, 969–975.

(48) Kosower, E. M.; Pazhenchevsky, B. *J. Am. Chem. Soc.* **1980**, *102*, 4983–4993.

(49) Li, M.; Liu, C.-L.; Yang, J.-C.; Zhang, J.-B.; Li, Z.-N.; Zhang, H; Li, Z.-M. *J. Agric. Food Chem.* **2010**, *58*, 2664–2667.

(50) Janin, Y. L.; Huel, C.; Flad, G.; Thirot, S. *Eur. J. Org. Chem.* **2002**, 1763–1769.

(51) King, S. B.; Nagasawa, H. T. *Methods Enzymol.* **1999**, *301*, 211–220.

(52) Armstrong, A.; Jones, L. H.; Knight, J. D.; Kelsey, R. D. *Org. Lett*. **2005**, *7*, 713–716.

▪ 3.7 Supporting Information

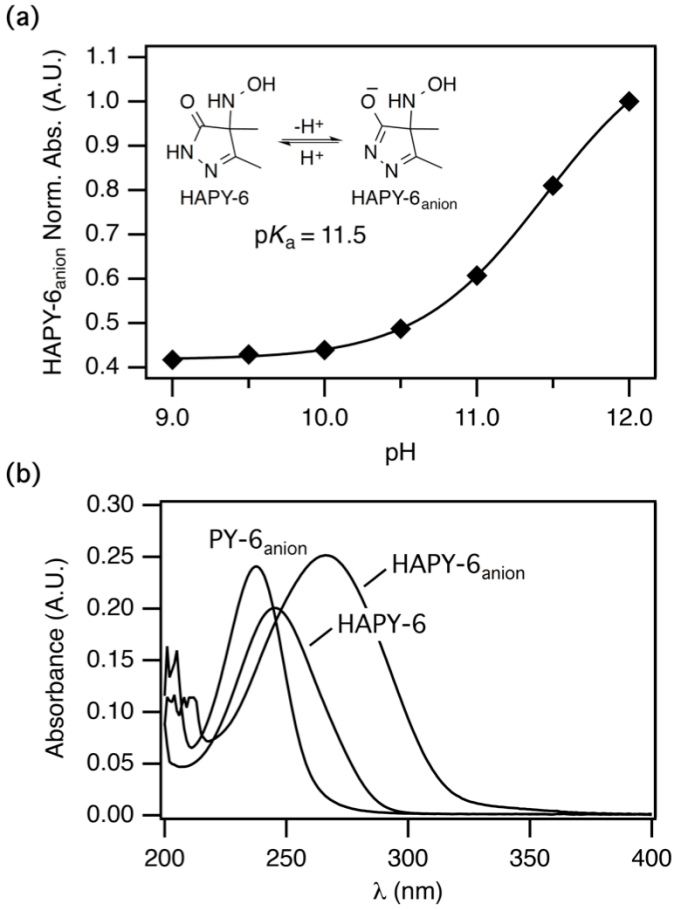

Figure 3-7. (a) Plot of the concentration of HAPY-6_{anion} (λ_{max} = 266 nm) as a function of pH. The solid curve is a calculated best fit to a sigmoid function. (b) Initial UV-vis spectra of HAPY-6 in pH 9.0 and pH 12.0 compared with the expected byproduct of HNO release, PY-6_{anion}, at pH 12.0.

3.7.1 X-Ray Crystallography Data

All reflection intensities were measured at 110(2) K using a KM4/Xcalibur (detector: Sapphire3) with enhance graphite-monochromated Mo *K*α radiation (λ = 0.71073 Å) under the program CrysAlisPro (Version 1.171.36.20, Agilent Technologies, 2012). The program CrysAlisPro (Version 1.171.36.20, Agilent Technologies, 2012) was used to refine the cell dimensions. Data reduction was

done using the program CrysAlisPro (Version 1.171.36.20, Agilent Technologies, 2012). The structure was solved with the program SHELXS-97 (Sheldrick, 2008) and was refined on F^2 with SHELXL-97 (Sheldrick, 2008). Analytical numeric absorption corrections based on a multifaceted crystal model were applied using CrysAlisPro (Version 1.171.36.20, Agilent Technologies, 2012). The temperature of the data collection was controlled using the system Cryojet (manufactured by Oxford Instruments). The H atoms were placed at calculated positions using the instructions AFIX 43, AFIX 137 or AFIX 147 with isotropic displacement parameters having values 1.2 or 1.5 times *U*eq of the attached C or O atoms.

The structure is ordered.

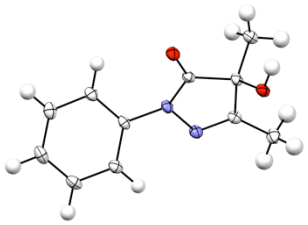

PY-2$_{OH}$: Fw = 204.23, colorless irregular block, 0.55 × 0.38 × 0.19 mm^3, monoclinic, *P*-1 (no. 2), a = 6.9967(3), b = 8.5345(5), c = 9.7334(6) Å, α = 110.752(5), β = 94.833(4), γ = 106.902(5)°, V = 508.51(5) Å^3, Z = 2, D_x = 1.334 g cm^{-3}, μ = 0.094 mm^{-1}, abs. corr. range: 0.966–0.987. 6277 Reflections were measured up to a resolution of $(\sin\theta/\lambda)_{max}$ = 0.65 Å^{-1}. 2332 Reflections were unique (R_{int} = 0.0210), of which 2063 were observed [$I > 2\sigma(I)$]. 139 Parameters were refined. $R1/wR2$ [$I > 2\sigma(I)$]: 0.0350/0.0976. $R1/wR2$ [all refl.]: 0.0399/0.1011. S = 1.059. Residual electron density found between –0.23 and 0.35 e Å^{-3}.

3.7.2 Density Functional Theory (DFT) Calculations

All calculations were performed at the B3LYP/6-31G* level with an SM8 solvation model for aqueous solvation using Spartan '14 modeling software.[42] Optimized geometries and vibrational frequencies were calculated for each reactant and product independently, and free energies are given for 298.15 K.

Table 3-4. B3LYP/6-31G* Optimized Geometries, Energies, and Entropy Corrections for Nitroxyl (HNO)

B3LYP/6-31G* Energy (E): -130.470851 hartrees
Entropy Correction (Hv-TSv): -19.0649 kJ/mol
G° = E + "entropy correction": -81876.18923 kcal/mol

Atom	Atomic Number	Cartesian Coordinates (Angstroms) X	Y	Z
N	7	0.5680553	0.1586597	0.0000000
O	8	-0.6301148	-0.0406719	0.0000000
H	1	1.0645314	-0.7852429	0.0000000

Table 3-5. B3LYP/6-31G* Calculated IR Frequencies (cm^{-1}, uncorrected) and Intensities for Nitroxyl (HNO)

	cm^{-1}	Intensity		cm^{-1}	Intensity		cm^{-1}	Intensity
1	1565	20.87	**2**	1652	93.41	**3**	2940	62.00

Table 3-6. B3LYP/6-31G* Optimized Geometries, Energies, and Entropy Corrections for Water (H_2O)

B3LYP/6-31G* Energy (E): -76.423559 hartrees
Entropy Correction (Hv-TSv): 6.5320 kJ/mol
G° = E + "entropy correction": -47954.9099 kcal/mol

Atom	Atomic Number	Cartesian Coordinates (Angstroms) X	Y	Z
H	1	0.0000000	-0.2976214	-0.7243625
O	8	0.0000000	-0.3250377	0.2494010
H	1	0.0000000	0.6226591	0.4749616

Table 3-7. B3LYP/6-31G* Calculated IR Frequencies (cm^{-1}, uncorrected) and Intensities for Water (H_2O)

	cm^{-1}	Intensity		cm^{-1}	Intensity		cm^{-1}	Intensity
1	1677	110.10	**2**	3688	21.14	**3**	3778	84.71

Table 3-8. B3LYP/6-31G* Optimized Geometries, Energies, and Entropy Corrections for Hydronium (H_3O^+)

B3LYP/6-31G* Energy (E): -76.853354 hartrees
Entropy Correction (Hv-TSv): 41.0536 kJ/mol
G° = E + "entropy correction": -48216.35927 kcal/mol

Atom	Atomic Number	Cartesian Coordinates (Angstroms) X	Y	Z
H	1	0.2212214	0.0000000	-0.8952325
O	8	0.2542327	0.0000000	0.0897557
H	1	-0.2377271	-0.7945454	0.4027384
H	1	-0.2377271	0.7945454	0.4027384

Table 3-9. B3LYP/6-31G* Calculated IR Frequencies (cm^{-1}, uncorrected) and Intensities for Hydronium (H_3O^+)

	cm^{-1}	Intensity		cm^{-1}	Intensity		cm^{-1}	Intensity
1	1082	495.92	**3**	1694	132.51	**5**	3621	519.14
2	1683	131.89	**4**	3555	83.48	**6**	3622	519.02

Table 3-10. B3LYP/6-31G* Optimized Geometries, Energies, and Entropy Corrections for enol of PY-1

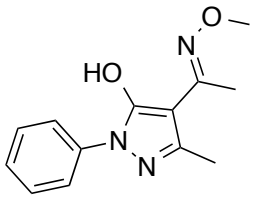

PY-1

B3LYP/6-31G* Energy (E): -819.063789 hartrees
Entropy Correction (Hv-TSv): 593.6595 kJ/mol
G° = E + "entropy correction": -513828.0111 kcal/mol

Atom	Atomic Number	Cartesian Coordinates (Angstroms) X	Y	Z
C	6	1.0871638	-0.4580564	0.2122397
C	6	-0.0636156	0.2755546	-0.0876464
N	7	-1.1482101	-0.4837613	0.2241276
N	7	-0.7475821	-1.7157646	0.7148325
C	6	0.5806836	-1.6993132	0.7099278
C	6	1.3126104	-2.9080556	1.2006235
H	1	1.9323130	-2.6797126	2.0741340
H	1	1.9717968	-3.3227835	0.4309135
H	1	0.5890499	-3.6760667	1.4846787
C	6	2.4410749	0.0480357	0.0104945
N	7	2.5039287	1.2348280	-0.5146796
O	8	3.8104584	1.7210969	-0.6941023
C	6	3.6374492	-0.7727021	0.3990201
H	1	4.5650719	-0.2400914	0.1964479
H	1	3.6434253	-1.7177815	-0.1531426
H	1	3.5956342	-1.0217433	1.4641223
C	6	3.7449648	3.0130085	-1.3045828
H	1	3.2688472	2.9607942	-2.2896587
H	1	4.7830032	3.3328302	-1.4136398
H	1	3.2046990	3.7234865	-0.6695527
O	8	-0.1628993	1.5078744	-0.6098399
H	1	0.7865376	1.7928542	-0.7450680
C	6	-2.5354003	-0.1957249	0.0850639
C	6	-5.2742824	0.3115746	-0.1690959
C	6	-2.9980489	1.1246046	0.0307135
C	6	-3.4414918	-1.2614098	0.0208271
C	6	-4.8042339	-1.0012895	-0.1022510
C	6	-4.3651147	1.3669795	-0.1027382
H	1	-2.2996952	1.9484376	0.0892735
H	1	-3.0668937	-2.2758815	0.0749875
H	1	-5.4989478	-1.8341673	-0.1505906
H	1	-4.7155919	2.3935833	-0.1456589
H	1	-6.3367040	0.5087628	-0.2701802

Table 3-11. B3LYP/6-31G* Calculated IR Frequencies (cm^{-1}, uncorrected) and Intensities for enol of PY-1

	cm^{-1}	Intensity		cm^{-1}	Intensity		cm^{-1}	Intensity
1	30	0.23	**32**	715	99.26	**63**	1459	334.71
2	33	0.78	**33**	766	83.34	**64**	1482	57.86
3	50	3.92	**34**	775	54.26	**65**	1492	78.87
4	69	1.14	**35**	845	0.25	**66**	1496	1.72

5	82	2.22	**36**	854	0.32	**67**	1505	14.90
6	85	2.01	**37**	914	233.21	**68**	1508	8.52
7	126	1.83	**38**	927	5.11	**69**	1509	12.68
8	158	1.36	**39**	972	0.83	**70**	1523	59.98
9	173	2.92	**40**	995	0.48	**71**	1529	76.94
10	212	0.23	**41**	1006	2.40	**72**	1534	45.07
11	237	0.70	**42**	1019	1.70	**73**	1540	12.52
12	248	2.69	**43**	1037	43.44	**74**	1549	93.18
13	274	1.78	**44**	1054	87.82	**75**	1607	876.46
14	286	2.45	**45**	1063	0.28	**76**	1648	17.62
15	302	14.68	**46**	1066	344.97	**77**	1655	171.60
16	335	13.68	**47**	1071	2.23	**78**	1661	38.61
17	352	0.43	**48**	1088	54.45	**79**	3056	111.82
18	362	0.55	**49**	1099	24.04	**80**	3072	20.93
19	404	1.41	**50**	1118	19.85	**81**	3084	13.14
20	419	0.32	**51**	1148	12.09	**82**	3125	49.49
21	449	28.26	**52**	1180	2.37	**83**	3131	6.70
22	463	26.41	**53**	1190	0.50	**84**	3142	8.76
23	520	6.32	**54**	1212	1.90	**85**	3156	22.11
24	542	0.48	**55**	1219	25.21	**86**	3174	106.77
25	600	28.71	**56**	1256	68.74	**87**	3181	875.98
26	629	0.26	**57**	1349	26.91	**88**	3199	2.69
27	649	10.92	**58**	1369	2.81	**89**	3209	0.52
28	654	5.85	**59**	1373	61.52	**90**	3218	26.42
29	691	21.40	**60**	1383	94.09	**91**	3231	32.17
30	706	2.31	**61**	1421	51.21	**92**	3252	2.80
31	707	7.75	**62**	1435	32.60	**93**	3266	1.35

Table 3-12. B3LYP/6-31G* Optimized Geometries, Energies, and Entropy Corrections for PY-1$_{anion}$

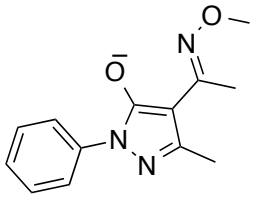

PY-1$_{anion}$

B3LYP/6-31G* Energy (E): -818.591456 hartrees
Entropy Correction (Hv-TSv): 559.3385 kJ/mol
G° = E + "entropy correction": -513539.8209 kcal/mol

Atom	Atomic Number	Cartesian Coordinates (Angstroms) X	Y	Z
C	6	1.0413380	-0.2404651	0.1380892
C	6	-0.1393269	0.5512025	-0.0433794
N	7	-1.2031753	-0.3616604	0.1555978
N	7	-0.7423973	-1.6493189	0.4107325
C	6	0.5804145	-1.5633352	0.4110811
C	6	1.3533720	-2.8284664	0.6314983
H	1	1.8279155	-2.8606546	1.6192000
H	1	2.1450933	-2.9530380	-0.1149146
H	1	0.6680419	-3.6782628	0.5627761
C	6	2.4109696	0.2377362	0.0342045
N	7	2.6442558	1.2715884	-0.7230983
O	8	4.0326232	1.6367288	-0.6574269
C	6	3.5140608	-0.4387426	0.8151040
H	1	4.1293426	0.3161667	1.3138306
H	1	4.1845123	-0.9989005	0.1525964
H	1	3.1111067	-1.1172289	1.5650840
C	6	4.2251706	2.8049231	-1.4488498
H	1	3.9592333	2.6273889	-2.4980535
H	1	5.2903696	3.0381429	-1.3733572
H	1	3.6333255	3.6482203	-1.0724254
O	8	-0.2985039	1.7791404	-0.2879009
C	6	-2.5956807	-0.1415550	0.0980185
C	6	-5.3919047	0.2245714	-0.0080896
C	6	-3.1396548	1.1328132	-0.1469884
C	6	-3.4710198	-1.2265906	0.2913158
C	6	-4.8496350	-1.0384031	0.2375801
C	6	-4.5237357	1.3000102	-0.1978091
H	1	-2.4646084	1.9642392	-0.2941583
H	1	-3.0460758	-2.2042262	0.4795761
H	1	-5.5007576	-1.8945240	0.3899734
H	1	-4.9178014	2.2943697	-0.3894650
H	1	-6.4668676	0.3681305	-0.0503423

Table 3-13. B3LYP/6-31G* Calculated IR Frequencies (cm^{-1}, uncorrected) and Intensities for PY-1_{anion}

	cm^{-1}	Intensity		cm^{-1}	Intensity		cm^{-1}	Intensity
1	16	0.41	**31**	747	49.39	**61**	1435	45.87
2	42	1.25	**32**	762	52.34	**62**	1479	88.57
3	44	8.71	**33**	763	84.99	**63**	1487	347.36
4	81	2.24	**34**	846	220.92	**64**	1494	49.81
5	89	7.82	**35**	854	140.00	**65**	1498	21.13

6	111	0.16	**36**	855	45.51	**66**	1499	5.44
7	150	2.17	**37**	907	5.49	**67**	1506	49.78
8	156	0.78	**38**	964	0.10	**68**	1515	134.02
9	169	4.19	**39**	978	0.88	**69**	1523	21.26
10	206	1.55	**40**	1006	25.59	**70**	1537	21.00
11	228	3.13	**41**	1014	6.61	**71**	1537	278.51
12	249	0.84	**42**	1036	50.25	**72**	1559	269.75
13	270	5.26	**43**	1049	112.26	**73**	1571	551.34
14	291	2.57	**44**	1055	15.23	**74**	1623	240.69
15	298	2.09	**45**	1061	84.22	**75**	1637	122.45
16	346	12.59	**46**	1067	0.73	**76**	1658	230.26
17	353	1.76	**47**	1081	238.40	**77**	3040	156.75
18	370	6.93	**48**	1092	21.54	**78**	3063	50.34
19	396	4.24	**49**	1100	43.28	**79**	3075	22.64
20	419	0.01	**50**	1158	1.49	**80**	3098	76.41
21	451	68.25	**51**	1179	0.93	**81**	3120	16.40
22	464	13.16	**52**	1180	2.02	**82**	3129	18.28
23	522	5.69	**53**	1191	0.41	**83**	3147	32.85
24	558	0.62	**54**	1201	0.84	**84**	3159	27.77
25	609	36.70	**55**	1223	12.04	**85**	3199	19.26
26	632	1.05	**56**	1335	423.32	**86**	202	16.66
27	647	7.53	**57**	1352	71.90	**87**	3209	29.67
28	667	32.08	**58**	1365	59.44	**88**	3235	30.56
29	703	4.24	**59**	1391	138.73	**89**	3251	5.06
30	704	11.36	**60**	1414	9.06	**90**	3256	9.48

Table 3-14. B3LYP/6-31G* Optimized Geometries, Energies, and Entropy Corrections for HAPY-1

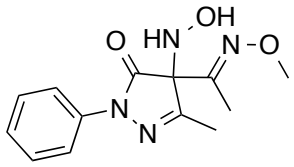

HAPY-1

B3LYP/6-31G* Energy (E): -949.560389 hartrees
Entropy Correction (Hv-TSv): 639.1283 kJ/mol
G° = E + "entropy correction": -595704.9348 kcal/mol

Atom	Atomic Number	Cartesian Coordinates (Angstroms) X	Y	Z
C	6	1.0639329	-0.0863496	0.4900204
C	6	-0.2392076	0.7109256	0.2736413

N	7	-1.2404253	-0.2293610	0.1490905
N	7	-0.7506639	-1.5483685	0.2299369
C	6	0.5209355	-1.5114092	0.4200677
O	8	-0.3589544	1.9333473	0.2324030
C	6	1.3359479	-2.7451277	0.5770011
H	1	1.7683876	-2.7917979	1.5840137
H	1	2.1685015	-2.7567514	-0.1336008
H	1	0.7108883	-3.6271654	0.4251715
C	6	2.0958626	0.1818373	-0.6093115
N	7	3.3141312	0.1232105	-0.2156869
O	8	4.2371190	0.3445380	-1.2472646
C	6	1.6242359	0.4283042	-2.0123874
H	1	1.2858321	1.4653858	-2.1222327
H	1	0.7735617	-0.2173345	-2.2551072
H	1	2.4243849	0.2463049	-2.7301620
C	6	5.5643100	0.2263813	-0.7175134
H	1	5.7389419	0.9668077	0.0692271
H	1	6.2277979	0.4173109	-1.5629176
H	1	5.7437491	-0.7793896	-0.3247562
N	7	1.5187321	0.1270728	1.8763323
H	1	2.3929038	-0.3973713	1.9719817
O	8	1.9613500	1.4968668	2.0340057
H	1	1.2989067	1.8555898	2.6498427
C	6	-2.6365865	-0.0439986	-0.0478155
C	6	-5.3947609	0.2622861	-0.4422363
C	6	-3.4713716	-1.1700753	-0.0934802
C	6	-3.1848728	1.2387020	-0.1990033
C	6	-4.5585847	1.3773801	-0.3947854
C	6	-4.8407360	-1.0092505	-0.2902648
H	1	-3.0403236	-2.1554003	0.0223837
H	1	-2.5422649	2.1065112	-0.1623943
H	1	-4.9715993	2.3748902	-0.5109604
H	1	-5.4749934	-1.8896793	-0.3241846
H	1	-6.4623387	0.3830062	-0.5957517

Table 3-15. B3LYP/6-31G* Calculated IR Frequencies (cm^{-1}, uncorrected) and Intensities for HAPY-1

	cm^{-1}	Intensity		cm^{-1}	Intensity		cm^{-1}	Intensity
1	27	0.23	**35**	709	15.43	**69**	1393	275.98
2	29	0.37	**36**	749	25.63	**70**	1429	20.77
3	34	0.40	**37**	766	13.64	**71**	1442	15.30
4	83	4.24	**38**	775	59.53	**72**	1488	3.66
5	88	4.16	**39**	834	80.46	**73**	1490	11.15

6	95	2.98	**40**	860	0.02	**74**	1495	18.68
7	109	2.42	**41**	891	91.08	**75**	1504	7.09
8	123	0.37	**42**	908	113.44	**76**	1505	2.57
9	126	7.16	**43**	931	5.83	**77**	1509	7.76
10	137	1.17	**44**	951	79.45	**78**	1516	11.63
11	158	4.16	**45**	978	0.00	**79**	1517	14.42
12	169	7.50	**46**	1001	1.01	**80**	1534	38.13
13	186	4.20	**47**	1009	4.86	**81**	1541	198.09
14	197	3.72	**48**	1017	0.20	**82**	1642	0.81
15	231	8.91	**49**	1020	6.12	**83**	1659	104.74
16	253	31.42	**50**	1034	12.07	**84**	1691	124.21
17	279	3.44	**51**	1045	41.44	**85**	1702	457.96
18	289	41.99	**52**	1056	361.95	**86**	1779	18.21
19	307	48.89	**53**	1061	46.18	**87**	3064	101.91
20	326	25.70	**54**	1080	12.44	**88**	3070	6.45
21	339	19.59	**55**	1081	20.59	**89**	3075	3.88
22	366	9.12	**56**	1097	13.18	**90**	3129	5.09
23	385	9.64	**57**	1130	4.00	**91**	3138	47.03
24	420	0.60	**58**	1163	98.37	**92**	3143	8.77
25	425	20.81	**59**	1189	2.09	**93**	3175	6.88
26	452	3.79	**60**	1190	0.09	**94**	3179	20.46
27	494	19.92	**61**	1212	5.43	**95**	3185	6.93
28	516	2.46	**62**	1215	16.49	**96**	3207	2.75
29	530	5.16	**63**	1243	18.56	**97**	3215	28.22
30	593	27.90	**64**	1283	28.14	**98**	3230	33.61
31	621	8.78	**65**	1299	236.05	**99**	3263	0.46
32	631	0.54	**66**	1353	28.85	**100**	3270	3.48
33	660	50.43	**67**	1366	36.55	**101**	3442	39.54
34	697	2.26	**68**	1377	62.28	**102**	3714	97.56

Table 3-16. B3LYP/6-31G* Optimized Geometries, Energies, and Entropy Corrections for HAPY-1$_{anion}$

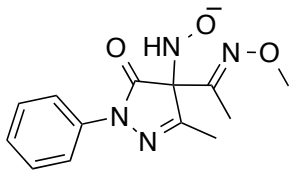

HAPY-1$_{anion}$

B3LYP/6-31G* Energy (E): -949.073224 hartrees
Entropy Correction (Hv-TSv): 595.3271 kJ/mol
G° = E + "entropy correction": Not a ground state structure; HNO is dissociated

Atom	Atomic Number	Cartesian Coordinates (Angstroms) X	Y	Z
C	6	1.0214091	-0.1571378	-0.2418336
C	6	-0.2097519	0.5647410	-0.4462345
N	7	-1.2183146	-0.3865459	-0.1867631
N	7	-0.6879684	-1.6253974	0.1469285
C	6	0.6238100	-1.4894948	0.1117294
O	8	-0.4362384	1.7591017	-0.7750128
C	6	1.4758425	-2.6769185	0.4213738
H	1	2.1330056	-2.4844335	1.2761106
H	1	2.1332761	-2.9251359	-0.4184093
H	1	0.8314792	-3.5318636	0.6460040
C	6	2.3647372	0.3459400	-0.4758830
N	7	3.3632689	-0.4588540	-0.2535859
O	8	4.6030172	0.1877153	-0.5318817
C	6	2.5837684	1.7607122	-0.9593730
H	1	3.1822046	2.3181304	-0.2300227
H	1	1.6352280	2.2700151	-1.1163234
H	1	3.1668447	1.7475798	-1.8865645
C	6	5.6609478	-0.7353628	-0.2727489
H	1	5.6645765	-1.0541235	0.7760335
H	1	6.5820887	-0.1917828	-0.4961351
H	1	5.5870078	-1.6189226	-0.9173902
N	7	0.7492864	1.0344728	2.2311922
H	1	1.7762160	0.7853203	2.1133852
O	8	0.6256630	2.2511769	2.1080485
C	6	-2.6226410	-0.2321559	-0.2014021
C	6	-5.4320806	0.0015406	-0.2150673
C	6	-3.2344019	0.9737642	-0.5864039
C	6	-3.4341817	-1.3171117	0.1757170
C	6	-4.8212249	-1.1945907	0.1659633
C	6	-4.6257346	1.0766866	-0.5881506
H	1	-2.6097311	1.8082664	-0.8715913
H	1	-2.9561548	-2.2418577	0.4721800
H	1	-5.4242128	-2.0478765	0.4628041
H	1	-5.0748328	2.0190565	-0.8893220
H	1	-6.5134279	0.0942735	-0.2205125

Table 3-17. B3LYP/6-31G* Calculated IR Frequencies (cm^{-1}, uncorrected) and Intensities for HAPY-1_{anion}

	cm^{-1}	Intensity		cm^{-1}	Intensity		cm^{-1}	Intensity
1	2	0.28	**34**	665	110.32	**67**	1441	77.83
2	18	0.14	**35**	692	4.94	**68**	1471	500.43

3	34	3.08	**36**	704	11.11	**69**	1480	27.72
4	46	7.93	**37**	737	37.43	**70**	1489	12.46
5	62	2.92	**38**	764	53.30	**71**	1498	52.46
6	79	10.99	**39**	770	42.84	**72**	1501	2.64
7	88	1.27	**40**	851	225.74	**73**	1505	503.18
8	91	8.15	**41**	854	1.58	**74**	1511	29.70
9	106	2.31	**42**	890	186.90	**75**	1520	255.51
10	130	3.80	**43**	910	5.25	**76**	1534	18.80
11	144	1.71	**44**	965	0.13	**77**	1537	55.56
12	162	4.62	**45**	978	0.78	**78**	1540	149.85
13	170	2.28	**46**	1014	7.64	**79**	1561	52.05
14	212	3.66	**47**	1019	22.97	**80**	1572	116.86
15	218	2.64	**48**	1038	96.23	**81**	1602	670.36
16	241	4.12	**49**	1053	252.10	**82**	1621	262.52
17	254	23.24	**50**	1058	75.10	**83**	1638	79.99
18	262	5.54	**51**	1073	2.85	**84**	1659	231.84
19	294	17.73	**52**	1075	9.68	**85**	2933	43.62
20	319	4.22	**53**	1088	55.89	**86**	3048	158.56
21	340	17.66	**54**	1096	28.48	**87**	3067	44.30
22	350	1.87	**55**	1102	118.89	**88**	3068	29.35
23	380	13.09	**56**	1158	7.64	**89**	3112	68.62
24	393	0.62	**57**	1178	3.03	**90**	3117	16.26
25	419	0.06	**58**	1180	0.54	**91**	3124	16.04
26	434	7.78	**59**	1200	10.02	**92**	3149	36.44
27	476	74.97	**60**	1203	1.42	**93**	3165	28.99
28	496	61.84	**61**	1232	24.38	**94**	3195	5.78
29	523	5.61	**62**	1338	453.64	**95**	3202	10.07
30	564	2.33	**63**	1349	7.93	**96**	3210	31.36
31	611	32.08	**64**	1364	18.14	**97**	3229	35.15
32	633	0.48	**65**	1378	261.74	**98**	3252	3.86
33	658	15.88	**66**	1431	21.43	**99**	3261	7.67

Table 3-18. B3LYP/6-31G* Optimized Geometries, Energies, and Entropy Corrections for enol of PY-2

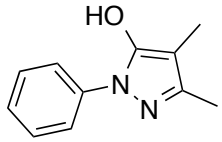

PY-2

B3LYP/6-31G* Energy (E): -611.117576 hartrees
Entropy Correction (Hv-TSv): 457.2947 kJ/mol
G° = E + "entropy correction": -383372.4829 kcal/mol

Atom	Atomic Number	Cartesian Coordinates (Angstroms) X	Y	Z
C	6	2.1225504	0.1528301	0.3568273
C	6	0.9272259	0.8410004	0.2653613
N	7	-0.0788429	-0.0606165	0.0263349
N	7	0.4364668	-1.3386332	-0.0555839
C	6	1.7466909	-1.1991077	0.1424989
C	6	3.4884350	0.7182159	0.6082297
H	1	3.4500363	1.6063280	1.2504923
H	1	4.0050531	1.0023207	-0.3174947
H	1	4.1226819	-0.0110011	1.1225173
C	6	2.6425378	-2.3959032	0.1351472
H	1	3.1765132	-2.5027597	1.0870542
H	1	3.4016929	-2.3230346	-0.6525512
H	1	2.0582706	-3.3042645	-0.0333340
C	6	-1.4674844	0.1566178	-0.1843021
C	6	-4.2109983	0.5168441	-0.6164062
C	6	-2.1929693	-0.7877473	-0.9227621
C	6	-2.1188945	1.2770635	0.3470062
C	6	-3.4838143	1.4522461	0.1190631
C	6	-3.5578803	-0.6054159	-1.1298831
H	1	-1.6763431	-1.6545416	-1.3157656
H	1	-1.5668890	2.0010319	0.9305245
H	1	-3.9788428	2.3253991	0.5329286
H	1	-4.1093133	-1.3449140	-1.7024438
H	1	-5.2736902	0.6581987	-0.7859690
O	8	0.6465056	2.1668639	0.3607940
H	1	1.4913022	2.6529789	0.4317162

Table 3-19. B3LYP/6-31G* Calculated IR Frequencies (cm^{-1}, uncorrected) and Intensities for enol of PY-2

	cm^{-1}	Intensity		cm^{-1}	Intensity		cm^{-1}	Intensity
1	31	2.99	**25**	774	48.41	**49**	1448	7.62
2	57	1.17	**26**	822	2.26	**50**	1484	138.98
3	66	4.86	**27**	850	0.42	**51**	1492	43.05
4	106	0.15	**28**	923	5.48	**52**	1508	9.26
5	125	1.89	**29**	969	0.61	**53**	1509	27.00
6	164	6.73	**30**	977	50.59	**54**	1519	12.54
7	222	54.07	**31**	992	0.63	**55**	1525	14.09
8	227	6.17	**32**	1017	7.02	**56**	1537	108.07
9	235	55.78	**33**	1026	81.51	**57**	1551	217.77
10	279	2.51	**34**	1057	5.24	**58**	1633	212.09
11	294	27.52	**35**	1064	3.91	**59**	1649	66.34

12	339	3.13	**36**	1080	2.04	**60**	1661	69.69
13	350	10.32	**37**	1099	54.28	**61**	3047	61.73
14	399	2.51	**38**	1112	1.56	**62**	3059	40.58
15	420	1.40	**39**	1121	127.06	**63**	3099	29.99
16	516	5.34	**40**	1187	18.57	**64**	3110	16.14
17	566	21.78	**41**	1190	1.09	**65**	3125	24.91
18	608	7.51	**42**	1211	0.28	**66**	3150	20.63
19	630	0.35	**43**	1243	110.23	**67**	3206	0.24
20	654	2.15	**44**	1328	64.54	**68**	3216	25.58
21	666	14.36	**45**	1357	41.53	**69**	3227	35.93
22	688	5.30	**46**	1369	4.24	**70**	3247	5.10
23	706	20.88	**47**	1416	272.46	**71**	3267	1.21
24	742	58.88	**48**	1438	112.34	**72**	3676	240.49

Table 3-20. B3LYP/6-31G* Optimized Geometries, Energies, and Entropy Corrections for PY-2$_{anion}$

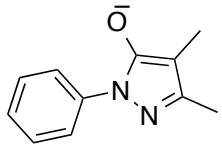

PY-2$_{anion}$

B3LYP/6-31G* Energy (E): -610.654618 hartrees
Entropy Correction (Hv-TSv): 425.1610 kJ/mol
G° = E + "entropy correction": -383089.6528 kcal/mol

Atom	Atomic Number	Cartesian Coordinates (Angstroms) X	Y	Z
C	6	2.1728663	0.2358654	0.4538906
C	6	0.9766007	0.9853925	0.4540959
N	7	-0.0160307	0.0653284	0.0160514
N	7	0.5257457	-1.1924461	-0.2442987
C	6	1.8262128	-1.0607008	0.0253448
C	6	3.5141416	0.7728354	0.8451327
H	1	3.4086559	1.8176222	1.1592336
H	1	4.2437135	0.7506808	0.0225115
H	1	3.9680800	0.2218178	1.6811854
C	6	2.7375860	-2.2346342	-0.1434214
H	1	3.2487202	-2.4834294	0.7952988
H	1	3.5189254	-2.0318774	-0.8868652
H	1	2.1684599	-3.1100880	-0.4703671
C	6	-1.3964928	0.2640981	-0.1755972
C	6	-4.1726379	0.6021774	-0.5730418

C	6	-2.1866133	-0.7896022	-0.6738015
C	6	-2.0179069	1.4921154	0.1209485
C	6	-3.3896071	1.6466861	-0.0800147
C	6	-3.5547742	-0.6153203	-0.8668224
H	1	-1.7033019	-1.7320225	-0.8986633
H	1	-1.4052122	2.2981611	0.5014999
H	1	-3.8426442	2.6053594	0.1579587
H	1	-4.1384651	-1.4462559	-1.2532664
H	1	-5.2391649	0.7340099	-0.7258435
O	8	0.7531433	2.2042270	0.7588514

Table 3-21. B3LYP/6-31G* Calculated IR Frequencies (cm^{-1}, uncorrected) and Intensities for PY-2_{anion}

	cm^{-1}	Intensity		cm^{-1}	Intensity		cm^{-1}	Intensity
1	42	0.04	**24**	762	69.07	**47**	1424	33.45
2	48	0.47	**25**	828	1.38	**48**	1476	137.25
3	61	6.87	**26**	856	0.04	**49**	1495	88.25
4	141	5.39	**27**	905	5.85	**50**	1505	4.79
5	145	3.99	**28**	963	0.14	**51**	1509	106.04
6	163	1.30	**29**	968	72.37	**52**	1521	8.56
7	212	9.57	**30**	976	1.07	**53**	1525	39.49
8	216	1.35	**31**	1013	10.61	**54**	1535	340.57
9	269	0.06	**32**	1020	98.48	**55**	1543	393.07
10	297	20.60	**33**	1056	1.27	**56**	1607	333.43
11	336	4.18	**34**	1056	2.17	**57**	1635	83.29
12	362	3.07	**35**	1076	1.12	**58**	1657	267.98
13	388	2.93	**36**	1091	5.44	**59**	3021	156.26
14	422	0.05	**37**	1105	64.24	**60**	3050	71.70
15	524	5.75	**38**	1139	110.61	**61**	3057	60.54
16	573	37.07	**39**	1150	43.25	**62**	3099	24.45
17	629	6.69	**40**	1176	0.86	**63**	3106	35.50
18	632	7.94	**41**	1200	1.07	**64**	3140	30.38
19	647	3.24	**42**	1315	75.29	**65**	3192	21.49
20	662	20.67	**43**	1341	378.03	**66**	3205	24.77
21	706	10.18	**44**	1355	122.44	**67**	3227	27.64
22	730	11.63	**45**	1365	64.77	**68**	3248	7.99
23	761	67.05	**46**	1418	10.45	**69**	3249	8.00

Table 3-22. B3LYP/6-31G* Optimized Geometries, Energies, and Entropy Corrections for HAPY-2

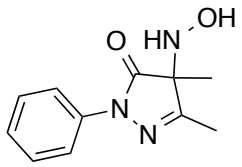

HAPY-2

B3LYP/6-31G* Energy (E): -741.635611 hartrees
Entropy Correction (Hv-TSv): 507.8082 kJ/mol
G° = E + "entropy correction": -465261.6516 kcal/mol

Atom	Atomic Number	Cartesian Coordinates (Angstroms) X	Y	Z
C	6	2.0161767	0.0452028	0.1943700
C	6	0.6729899	0.7849498	0.1911063
N	7	-0.2972683	-0.1858562	0.0513906
N	7	0.2601273	-1.4768462	-0.0789356
C	6	1.5434213	-1.3790149	-0.0262766
O	8	0.4988254	2.0000667	0.2987924
C	6	2.7343876	0.2189836	1.5410064
H	1	2.9570282	1.2751040	1.7036802
H	1	3.6724088	-0.3444284	1.5401906
H	1	2.1150097	-0.1438793	2.3674034
N	7	2.7905458	0.4681273	-0.9952550
H	1	3.6122847	-0.1423931	-1.0423555
O	8	3.3883890	1.7651380	-0.7487484
H	1	2.8534671	2.3531064	-1.3080297
C	6	2.4244736	-2.5709806	-0.1539292
H	1	3.0900016	-2.6605798	0.7117954
H	1	3.0579115	-2.4923223	-1.0461661
H	1	1.8207289	-3.4769776	-0.2369940
C	6	-1.7113854	-0.0595583	0.0042242
C	6	-4.5080376	0.1334114	-0.0871999
C	6	-2.4943611	-1.2146547	-0.1376554
C	6	-2.3323787	1.1953480	0.1009018
C	6	-3.7236885	1.2778737	0.0542909
C	6	-3.8824875	-1.1101880	-0.1826809
H	1	-2.0089846	-2.1784822	-0.2111539
H	1	-1.7302199	2.0859052	0.2106387
H	1	-4.1915778	2.2548293	0.1302724
H	1	-4.4751223	-2.0131073	-0.2936607
H	1	-5.5900248	0.2099211	-0.1230802

Table 3-23. B3LYP/6-31G* Calculated IR Frequencies (cm^{-1}, uncorrected) and Intensities for HAPY-2

	cm^{-1}	Intensity		cm^{-1}	Intensity		cm^{-1}	Intensity
1	18	0.17	**28**	758	25.04	**55**	1398	268.05
2	39	2.57	**29**	775	60.34	**56**	1419	8.51
3	89	0.38	**30**	824	32.55	**57**	1441	26.00
4	95	9.50	**31**	860	0.02	**58**	1491	17.41
5	143	10.46	**32**	892	34.42	**59**	1495	11.49
6	152	3.46	**33**	898	15.39	**60**	1502	10.55
7	169	1.41	**34**	928	6.00	**61**	1504	0.80
8	202	21.89	**35**	956	47.06	**62**	1517	7.66
9	233	25.21	**36**	977	0.00	**63**	1524	5.68
10	238	15.14	**37**	998	0.89	**64**	1540	215.38
11	248	43.33	**38**	1016	0.21	**65**	1641	0.33
12	265	4.85	**39**	1020	27.06	**66**	1658	121.68
13	286	35.88	**40**	1028	28.75	**67**	1686	174.60
14	306	24.70	**41**	1050	10.16	**68**	1695	424.49
15	337	13.63	**42**	1060	4.50	**69**	3063	8.25
16	368	3.77	**43**	1090	30.76	**70**	3075	16.09
17	385	3.69	**44**	1116	19.44	**71**	3121	5.21
18	418	0.01	**45**	1138	25.14	**72**	3145	20.17
19	459	1.94	**46**	1156	65.38	**73**	3169	19.09
20	527	5.97	**47**	1169	66.32	**74**	3169	1.40
21	578	35.11	**48**	1189	0.04	**75**	3207	2.87
22	614	19.29	**49**	1210	5.24	**76**	3216	27.71
23	621	9.02	**50**	1263	93.76	**77**	3229	33.64
24	631	0.62	**51**	1325	228.24	**78**	3263	0.65
25	666	20.84	**52**	1352	15.19	**79**	3270	3.28
26	708	16.91	**53**	1364	23.42	**80**	3431	18.00
27	739	14.60	**54**	1369	33.68	**81**	3727	110.14

Table 3-24. B3LYP/6-31G* Optimized Geometries, Energies, and Entropy Corrections for HAPY-2_{anion}

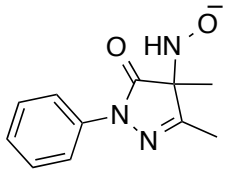

HAPY-2_{anion}

B3LYP/6-31G* Energy (E): -741.128834 hartrees
Entropy Correction (Hv-TSv): 472.3790 kJ/mol
G° = E + "entropy correction": -464952.1122 kcal/mol

Atom	Atomic Number	Cartesian Coordinates (Angstroms) X	Y	Z
C	6	-0.5851225	-1.8410150	-0.6197223
C	6	-0.8742383	-0.3633975	-0.7956171
N	7	-0.0355121	0.2992146	0.0807645
N	7	0.8736889	-0.5848576	0.6978832
C	6	0.6139977	-1.7798839	0.2827816
C	6	1.4055153	-2.9445603	0.7616526
H	1	0.7606522	-3.6549387	1.2943702
H	1	2.1977787	-2.6084607	1.4347797
H	1	1.8546016	-3.4835739	-0.0800410
O	8	-1.6892290	0.1603122	-1.5601201
C	6	-0.4185344	-2.5795818	-1.9387354
H	1	-1.4179523	-2.6942216	-2.3698320
H	1	0.0044723	-3.5747330	-1.7660285
H	1	0.2303553	-2.0469064	-2.6421870
N	7	-1.7607184	-2.4126529	0.2493755
H	1	-1.3790081	-3.3699158	0.4147602
O	8	-2.9309768	-2.5559829	-0.5124102
C	6	0.1052156	1.6892137	0.3313896
C	6	0.4211168	4.4293966	0.8661404
C	6	1.2038182	2.1439144	1.0774891
C	6	-0.8398397	2.6136198	-0.1418705
C	6	-0.6703675	3.9716346	0.1278788
C	6	1.3532210	3.5043547	1.3385028
H	1	1.9226777	1.4233990	1.4454247
H	1	-1.6856117	2.2636904	-0.7167978
H	1	-1.4113673	4.6712110	-0.2479444
H	1	2.2098924	3.8363245	1.9172339
H	1	0.5414747	5.4883966	1.0708794

Table 3-25. B3LYP/6-31G* Calculated IR Frequencies (cm^{-1}, uncorrected) and Intensities for HAPY-2_{anion}

	cm^{-1}	Intensity		cm^{-1}	Intensity		cm^{-1}	Intensity
1	34	4.68	**27**	752	34.30	**53**	1388	205.26
2	45	8.86	**28**	768	49.72	**54**	1408	6.93
3	95	11.20	**29**	794	25.81	**55**	1432	18.95
4	118	11.21	**30**	846	22.36	**56**	1456	24.31
5	144	5.80	**31**	855	0.08	**57**	1492	12.67
6	157	11.89	**32**	915	47.36	**58**	1497	26.33
7	180	23.17	**33**	921	5.15	**59**	1502	1.47
8	191	1.97	**34**	968	100.47	**60**	1507	4.60
9	219	1.17	**35**	970	0.27	**61**	1532	7.26

10	261	8.70	**36**	985	1.32	**62**	1540	225.31
11	265	3.52	**37**	1017	1.00	**63**	1639	10.47
12	273	9.77	**38**	1025	27.45	**64**	1656	128.86
13	311	11.84	**39**	1039	11.73	**65**	1672	142.86
14	324	12.54	**40**	1049	3.48	**66**	1690	466.97
15	367	2.25	**41**	1060	4.30	**67**	3058	47.77
16	385	1.95	**42**	1090	22.56	**68**	3062	12.81
17	417	46.28	**43**	1109	5.04	**69**	3089	129.42
18	421	4.82	**44**	1133	18.48	**70**	3121	8.91
19	522	26.70	**45**	1160	147.86	**71**	3130	9.18
20	540	102.86	**46**	1174	11.14	**72**	3139	33.78
21	579	33.33	**47**	1184	0.08	**73**	3167	11.43
22	615	18.89	**48**	1210	3.48	**74**	3208	4.48
23	632	0.35	**49**	1284	110.65	**75**	3216	26.52
24	662	74.89	**50**	1338	353.54	**76**	3232	30.45
25	670	26.11	**51**	1353	1.71	**77**	3260	1.00
26	705	15.59	**52**	1366	4.99	**78**	3260	4.41

Table 3-26. B3LYP/6-31G* Optimized Geometries, Energies, and Entropy Corrections for enol of PY-3

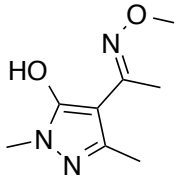

PY-3

B3LYP/6-31G* Energy (E): -627.325837 hartrees
Entropy Correction (Hv-TSv): 461.1102 kJ/mol
G° = E + "entropy correction": -393542.4007 kcal/mol

Atom	Atomic Number	Cartesian Coordinates (Angstroms) X	Y	Z
C	6	-0.2117165	-0.3782990	0.2462173
C	6	-1.3804963	0.2784643	-0.1632792
N	7	-2.4375791	-0.4139166	0.2985989
N	7	-2.0337805	-1.5237325	1.0072797
C	6	-0.7012002	-1.5037328	0.9784114
C	6	0.0466954	-2.5962676	1.6767293
H	1	0.7457341	-2.2019945	2.4212847
H	1	0.6253607	-3.2080483	0.9755823
H	1	-0.6661328	-3.2496960	2.1865172
C	6	1.1294478	0.0974972	-0.0699223
N	7	1.1680806	1.1917473	-0.7706509

O	8	2.4705308	1.6458672	-1.0568078
C	6	2.3462076	-0.6450003	0.4049565
H	1	3.2526653	-0.2477427	-0.0491260
H	1	2.2610682	-1.7085304	0.1669553
H	1	2.4375174	-0.5628602	1.4939823
C	6	2.3821808	2.8257731	-1.8589235
H	1	1.8818318	2.6209890	-2.8118639
H	1	3.4150725	3.1273586	-2.0432778
H	1	1.8534343	3.6256731	-1.3289804
O	8	-1.5297495	1.4058440	-0.8864367
H	1	-0.5966072	1.6984320	-1.0758074
C	6	-3.8491973	-0.1271563	0.1019346
H	1	-4.3561877	-0.0896454	1.0681966
H	1	-4.3132448	-0.8993898	-0.5165407
H	1	-3.9399353	0.8383663	-0.3950294

Table 3-27. B3LYP/6-31G* Calculated IR Frequencies (cm^{-1}, uncorrected) and Intensities for enol of PY-3

	cm^{-1}	Intensity		cm^{-1}	Intensity		cm^{-1}	Intensity
1	22	0.10	**25**	717	8.59	**49**	1503	63.32
2	34	1.49	**26**	761	61.57	**50**	1506	7.25
3	75	5.05	**27**	893	9.55	**51**	1509	3.93
4	89	1.13	**28**	912	227.67	**52**	1511	15.30
5	115	2.52	**29**	1015	13.69	**53**	1515	29.04
6	122	0.22	**30**	1017	25.68	**54**	1523	20.72
7	156	5.66	**31**	1061	84.39	**55**	1529	26.72
8	170	3.88	**32**	1068	145.82	**56**	1533	32.97
9	214	0.26	**33**	1072	37.34	**57**	1554	172.19
10	225	3.12	**34**	1075	165.19	**58**	1632	461.76
11	245	0.97	**35**	1117	29.60	**59**	1649	152.86
12	265	12.90	**36**	1168	80.26	**60**	3054	113.30
13	311	18.64	**37**	1174	11.28	**61**	3068	26.96
14	331	4.08	**38**	1177	3.10	**62**	3081	9.36
15	351	0.30	**39**	1220	12.35	**63**	3094	68.74
16	376	2.06	**40**	1267	30.10	**64**	3122	52.39
17	391	1.78	**41**	1363	12.40	**65**	3126	13.34
18	452	40.97	**42**	1391	52.96	**66**	3144	7.21
19	543	1.05	**43**	1423	47.18	**67**	3151	25.58
20	593	32.78	**44**	1433	58.16	**68**	3165	15.66
21	598	0.28	**45**	1447	257.45	**69**	3173	25.43
22	642	21.72	**46**	1472	66.74	**70**	3195	12.92
23	665	12.34	**47**	1481	17.45	**71**	3203	3.38
24	679	74.44	**48**	1491	54.63	**72**	3264	754.22

Table 3-28. B3LYP/6-31G* Optimized Geometries, Energies, and Entropy Corrections for PY-3$_{anion}$

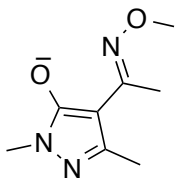

PY-3$_{anion}$

B3LYP/6-31G* Energy (E): -626.848205 hartrees
Entropy Correction (Hv-TSv): 426.5004 kJ/mol
G° = E + "entropy correction": -393250.9542 kcal/mol

Atom	Atomic Number	Cartesian Coordinates (Angstroms) X	Y	Z
C	6	-0.3346942	-0.2609653	0.0973249
C	6	-1.5699444	0.1997584	-0.4797535
N	7	-2.5424000	-0.5428637	0.1781073
N	7	-2.0303789	-1.3968058	1.1365803
C	6	-0.7117221	-1.2344043	1.0734404
C	6	0.1376431	-2.0141835	2.0315224
H	1	0.8874638	-1.3801724	2.5172620
H	1	0.6761595	-2.8363911	1.5443308
H	1	-0.5049207	-2.4499974	2.8026253
C	6	0.9983652	0.2001395	-0.2479022
N	7	1.1321513	1.4161998	-0.6979328
O	8	2.5035344	1.6685108	-1.0551299
C	6	2.1841575	-0.7288520	-0.1209954
H	1	2.7803008	-0.6888713	-1.0378414
H	1	1.8672733	-1.7566830	0.0508188
H	1	2.8492221	-0.4202722	0.6944233
C	6	2.5906919	2.9872791	-1.5840300
H	1	1.9744194	3.1015521	-2.4843166
H	1	3.6442279	3.1332571	-1.8364705
H	1	2.2808203	3.7375897	-0.8463813
O	8	-1.8386159	1.0385592	-1.3949349
C	6	-3.9689709	-0.4637713	-0.0374820
H	1	-4.1381616	0.2646574	-0.8321890
H	1	-4.4902361	-0.1389822	0.8701586
H	1	-4.3763856	-1.4342876	-0.3412344

Table 3-29. B3LYP/6-31G* Calculated IR Frequencies (cm^{-1}, uncorrected) and Intensities for PY-3_{anion}

	cm^{-1}	Intensity		cm^{-1}	Intensity		cm^{-1}	Intensity
1	38	2.89	**24**	755	74.88	**47**	1494	21.72
2	70	9.18	**25**	765	29.76	**48**	1497	6.24
3	83	4.77	**26**	842	326.98	**49**	1508	3.22
4	96	1.68	**27**	910	4.07	**50**	1510	108.99
5	96	2.43	**28**	1001	20.77	**51**	1518	7.97
6	129	0.43	**29**	1018	33.93	**52**	1519	19.51
7	135	3.21	**30**	1051	20.32	**53**	1532	279.28
8	157	0.17	**31**	1053	12.51	**54**	1537	44.50
9	205	1.34	**32**	1065	263.30	**55**	1547	348.01
10	209	2.43	**33**	1072	7.02	**56**	1556	285.76
11	260	15.34	**34**	1089	91.99	**57**	1617	309.46
12	275	2.81	**35**	1166	15.03	**58**	3039	159.48
13	300	9.96	**36**	1175	1.76	**59**	3056	101.19
14	329	4.23	**37**	1176	2.12	**60**	3060	111.76
15	343	5.81	**38**	1214	4.04	**61**	3073	18.82
16	375	8.10	**39**	1266	50.70	**62**	3098	78.98
17	395	4.97	**40**	1378	76.21	**63**	3110	23.50
18	450	59.72	**41**	1399	78.77	**64**	3115	44.53
19	555	2.46	**42**	1414	11.11	**65**	3125	18.00
20	597	43.61	**43**	1433	12.25	**66**	3141	36.08
21	611	13.11	**44**	1453	40.44	**67**	3158	28.58
22	650	7.22	**45**	1474	65.64	**68**	3174	7.86
23	687	0.44	**46**	1483	350.71	**69**	3193	20.20

Table 3-30. B3LYP/6-31G* Optimized Geometries, Energies, and Entropy Corrections for HAPY-3

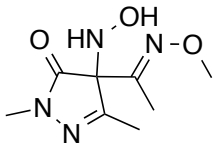

HAPY-3

B3LYP/6-31G* Energy (E): -757.822294 hartrees
Entropy Correction (Hv-TSv): 506.6847 kJ/mol
G° = E + "entropy correction": -475419.2093 kcal/mol

Atom	Atomic Number	Cartesian Coordinates (Angstroms) X	Y	Z
C	6	-0.4111603	0.1041208	0.4470887
C	6	-1.5883892	0.9838121	-0.0358315
N	7	-2.5584909	0.1104262	-0.4213701
N	7	-2.1847825	-1.2360739	-0.3080871
C	6	-0.9897666	-1.2873857	0.1708483
O	8	-1.6580260	2.2153714	-0.0611850
C	6	-0.2925146	-2.5708186	0.4495690
H	1	-0.1118135	-2.6856895	1.5256516
H	1	0.6829038	-2.6071418	-0.0469285
H	1	-0.9049513	-3.4088517	0.1105242
C	6	0.8685781	0.3549938	-0.3493739
N	7	1.9506335	0.2648761	0.3321381
O	8	3.1025254	0.4809399	-0.4401179
C	6	0.7683663	0.6308088	-1.8213250
H	1	0.5529442	1.6921151	-1.9932739
H	1	-0.0489088	0.0559450	-2.2683874
H	1	1.7005015	0.3804069	-2.3289710
C	6	4.2587311	0.3077303	0.3892907
H	1	4.2579340	1.0236861	1.2171601
H	1	5.1114274	0.4964859	-0.2655344
H	1	4.3116646	-0.7120693	0.7833482
N	7	-0.3059603	0.2309312	1.9120659
H	1	0.4950551	-0.3408744	2.1928522
O	8	0.1331940	1.5685075	2.2559190
H	1	-0.6539719	1.9339646	2.6961316
C	6	-3.8753482	0.4365458	-0.9385315
H	1	-3.9564017	1.5227103	-0.9778217
H	1	-4.6524413	0.0331807	-0.2843899
H	1	-4.0015319	0.0213463	-1.9414587

Table 3-31. B3LYP/6-31G* Calculated IR Frequencies (cm^{-1}, uncorrected) and Intensities for HAPY-3

	cm^{-1}	Intensity		cm^{-1}	Intensity		cm^{-1}	Intensity
1	32	0.43	**28**	690	3.91	**55**	1484	5.55
2	55	1.01	**29**	755	35.08	**56**	1493	10.18
3	75	2.16	**30**	763	8.43	**57**	1497	21.20
4	89	4.99	**31**	860	87.93	**58**	1501	2.85
5	94	1.66	**32**	896	147.81	**59**	1505	7.99
6	96	2.61	**33**	930	68.32	**60**	1514	18.18
7	109	0.98	**34**	961	27.47	**61**	1514	16.64
8	131	3.03	**35**	1006	7.31	**62**	1516	1.66

9	147	7.03	**36**	1025	17.00	**63**	1532	28.44
10	162	4.20	**37**	1031	62.72	**64**	1541	14.90
11	165	4.78	**38**	1045	24.87	**65**	1676	140.74
12	171	2.10	**39**	1056	324.32	**66**	1687	492.57
13	207	7.90	**40**	1067	59.43	**67**	1771	20.29
14	246	10.64	**41**	1082	14.25	**68**	3064	3.51
15	267	35.38	**42**	1094	14.86	**69**	3064	108.06
16	299	10.54	**43**	1177	2.90	**70**	3072	5.21
17	311	5.07	**44**	1181	2.21	**71**	3089	60.87
18	325	2.02	**45**	1211	15.68	**72**	3122	6.79
19	345	106.84	**46**	1227	33.61	**73**	3131	8.66
20	361	8.81	**47**	1253	101.70	**74**	3137	48.09
21	394	6.47	**48**	1286	8.41	**75**	3159	16.07
22	421	26.24	**49**	1306	78.29	**76**	3169	8.34
23	496	28.87	**50**	1381	65.60	**77**	3178	23.83
24	510	5.90	**51**	1424	86.86	**78**	3179	2.32
25	576	20.50	**52**	1427	54.09	**79**	3198	2.37
26	598	36.28	**53**	1444	37.42	**80**	3444	39.50
27	628	10.21	**54**	1472	19.27	**81**	3712	95.73

Table 3-32. B3LYP/6-31G* Optimized Geometries, Energies, and Entropy Corrections for HAPY-3$_{anion}$

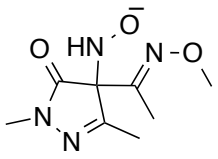

HAPY-3$_{anion}$

B3LYP/6-31G* Energy (E): -757.331535 hartrees
Entropy Correction (Hv-TSv): 464.0413 kJ/mol
G° = E + "entropy correction": Not a ground state structure; HNO is dissociated

Atom	Atomic Number	Cartesian Coordinates (Angstroms) X	Y	Z
C	6	0.0872656	0.0684498	0.3658208
C	6	1.2979246	0.8315112	0.6024001
N	7	2.2709033	-0.1340585	0.8091683
N	7	1.7938754	-1.4257887	0.6464609
C	6	0.4940703	-1.3033009	0.4319634
O	8	1.5440824	2.0742055	0.6299941
C	6	-0.3294275	-2.5357479	0.2448249
H	1	-0.8626694	-2.5103062	-0.7120475

H	1	-1.0951830	-2.6341128	1.0212262
H	1	0.3249818	-3.4125133	0.2697758
C	6	-1.2538124	0.6009183	0.2050941
N	7	-2.2474037	-0.2369475	0.2378647
O	8	-3.4847387	0.4384561	0.0169207
C	6	-1.4615905	2.0784945	-0.0155002
H	1	-1.8421149	2.2501671	-1.0297131
H	1	-0.5288079	2.6242506	0.1236331
H	1	-2.2265246	2.4587568	0.6691172
C	6	-4.5355779	-0.5268662	0.0480426
H	1	-4.4116873	-1.2760519	-0.7425309
H	1	-5.4553654	0.0384819	-0.1200850
H	1	-4.5839222	-1.0334565	1.0190078
N	7	0.9485974	0.2827475	-2.1685213
H	1	1.2896092	1.2103046	-1.7895147
O	8	1.9250200	-0.4569775	-2.3279562
C	6	3.6978831	0.1061294	0.7552683
H	1	3.8761549	1.1392343	1.0567862
H	1	4.0857019	-0.0473567	-0.2594004
H	1	4.2126989	-0.5720706	1.4397845

Table 3-33. B3LYP/6-31G* Calculated IR Frequencies (cm^{-1}, uncorrected) and Intensities for HAPY-3_{anion}

	cm^{-1}	Intensity		cm^{-1}	Intensity		cm^{-1}	Intensity
1	29	0.25	**27**	616	73.08	**53**	1490	576.63
2	38	0.42	**28**	665	36.57	**54**	1492	24.13
3	52	0.35	**29**	682	15.63	**55**	1499	3.12
4	70	3.26	**30**	755	20.87	**56**	1502	22.45
5	86	7.65	**31**	766	15.27	**57**	1516	37.33
6	93	12.20	**32**	870	353.72	**58**	1525	107.40
7	111	14.29	**33**	945	30.05	**59**	1534	36.54
8	121	4.40	**34**	1007	15.24	**60**	1535	21.37
9	126	14.51	**35**	1023	16.04	**61**	1539	14.14
10	152	7.67	**36**	1053	238.06	**62**	1560	92.75
11	155	1.58	**37**	1055	137.41	**63**	1571	528.20
12	164	1.70	**38**	1069	4.81	**64**	1581	98.10
13	207	0.17	**39**	1074	3.10	**65**	1627	185.42
14	227	1.71	**40**	1101	102.31	**66**	2976	35.41
15	246	38.60	**41**	1153	6.63	**67**	3046	159.94
16	251	15.09	**42**	1172	3.49	**68**	3057	117.23
17	269	16.85	**43**	1185	53.54	**69**	3063	38.81
18	310	6.36	**44**	1219	4.99	**70**	3065	22.68
19	331	30.82	**45**	1267	29.93	**71**	3109	69.76

20	357	6.31	**46**	1351	74.95	**72**	3120	18.55
21	383	1.90	**47**	1397	89.78	**73**	3121	22.07
22	396	0.51	**48**	1424	26.41	**74**	3137	39.41
23	450	27.37	**49**	1438	28.86	**75**	3143	37.69
24	561	2.89	**50**	1452	62.57	**76**	3165	28.54
25	581	79.57	**51**	1461	603.10	**77**	3181	3.45
26	600	26.89	**52**	1474	52.39	**78**	3185	8.56

Table 3-34. B3LYP/6-31G* Optimized Geometries, Energies, and Entropy Corrections for enol of PY-4

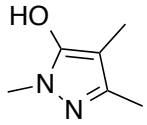

PY-4

B3LYP/6-31G* Energy (E): -419.379039 hartrees
Entropy Correction (Hv-TSv): 326.8122 kJ/mol
G° = E + "entropy correction": -263086.0114 kcal/mol

Atom	Atomic Number	Cartesian Coordinates (Angstroms) X	Y	Z
C	6	0.7239106	0.3076125	0.1668687
C	6	-0.4797297	0.9893448	0.0611517
N	7	-1.4518539	0.1006997	-0.2659170
N	7	-0.9444521	-1.1698650	-0.3642765
C	6	0.3630098	-1.0341897	-0.1147889
C	6	2.0774420	0.8678795	0.4864347
H	1	2.0064582	1.7868117	1.0807486
H	1	2.6628199	1.1043045	-0.4117460
H	1	2.6669962	0.1594699	1.0786204
C	6	1.2681189	-2.2242216	-0.1518605
H	1	1.7798839	-2.3719851	0.8071372
H	1	2.0468256	-2.1164824	-0.9165081
H	1	0.6943423	-3.1281054	-0.3739173
O	8	-0.8208944	2.2996057	0.2353313
N	7	-0.0007461	2.8220369	0.3208369
C	6	-2.8777055	0.3539588	-0.3810899
H	1	-3.0322903	1.3816949	-0.7114779
H	1	-3.3901363	0.2037703	0.5747163
H	1	-3.2919992	-0.3323399	-1.1202638

Table 3-35. B3LYP/6-31G* Calculated IR Frequencies (cm^{-1}, uncorrected) and Intensities for enol of PY-4

	cm^{-1}	Intensity		cm^{-1}	Intensity		cm^{-1}	Intensity
1	30	0.12	**18**	857	10.77	**35**	1510	32.30
2	66	0.39	**19**	1004	62.18	**36**	1516	8.48
3	115	0.75	**20**	1015	5.22	**37**	1524	1.77
4	119	15.42	**21**	1063	4.76	**38**	1529	15.73
5	168	13.50	**22**	1076	6.54	**39**	1535	23.22
6	203	105.04	**23**	1087	10.50	**40**	1567	122.04
7	229	4.67	**24**	1121	195.15	**41**	1632	156.41
8	272	10.59	**25**	1193	14.57	**42**	3044	62.38
9	284	20.48	**26**	1225	62.64	**43**	3052	44.96
10	291	10.71	**27**	1285	28.68	**44**	3082	74.81
11	371	0.39	**28**	1311	75.92	**45**	3096	36.96
12	556	12.39	**29**	1415	98.14	**46**	3104	17.12
13	569	12.08	**30**	1429	121.29	**47**	3116	32.00
14	603	5.57	**31**	1449	4.10	**48**	3145	24.36
15	650	1.56	**32**	1472	36.42	**49**	3162	15.88
16	693	4.09	**33**	1500	33.51	**50**	3198	5.90
17	730	35.49	**34**	1509	32.28	**51**	3692	220.42

Table 3-36. B3LYP/6-31G* Optimized Geometries, Energies, and Entropy Corrections for PY-4_{anion}

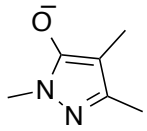

PY-4_{anion}

B3LYP/6-31G* Energy (E): -418.909769 hartrees
Entropy Correction (Hv-TSv): 295.4126 kJ/mol
G° = E + "entropy correction": -262799.0449 kcal/mol

Atom	Atomic Number	Cartesian Coordinates (Angstroms) X	Y	Z
C	6	0.6948843	0.4201498	0.3085493
C	6	-0.5340356	1.1247330	0.3729937
N	7	-1.4609388	0.2467705	-0.1885770
N	7	-0.9021361	-0.9531029	-0.5911495
C	6	0.3964831	-0.8238997	-0.2842223
C	6	2.0146416	0.9412946	0.7857945

H	1	2.7450431	1.0826949	-0.0254231
H	1	2.4948658	0.2822624	1.5236082
H	1	1.8706660	1.9177436	1.2637127
C	6	1.3446436	-1.9423536	-0.5820399
H	1	1.8475834	-2.3007844	0.3257564
H	1	2.1345081	-1.6316254	-1.2786021
H	1	0.8043331	-2.7826340	-1.0294037
O	8	-0.8380649	2.2909054	0.8184417
C	6	-2.8782399	0.4783549	-0.3305169
H	1	-3.1917360	0.3955491	-1.3775224
H	1	-3.0777956	1.4898056	0.0286376
H	1	-3.4647051	-0.2358636	0.2599628

Table 3-37. B3LYP/6-31G* Calculated IR Frequencies (cm^{-1}, uncorrected) and Intensities for PY-4_{anion}

	cm^{-1}	Intensity		cm^{-1}	Intensity		cm^{-1}	Intensity
1	58	2.80	**17**	884	7.23	**33**	1509	185.01
2	74	0.12	**18**	994	39.45	**34**	1521	20.79
3	119	0.48	**19**	1016	12.97	**35**	1521	5.53
4	129	10.05	**20**	1055	29.31	**36**	1523	24.16
5	165	0.91	**21**	1060	3.22	**37**	1538	141.29
6	203	10.83	**22**	1080	1.17	**38**	1556	131.94
7	257	0.42	**23**	1155	86.10	**39**	1585	315.63
8	260	16.92	**24**	1191	1.87	**40**	3013	158.50
9	296	9.46	**25**	1259	72.87	**41**	3044	97.53
10	367	4.57	**26**	1308	79.07	**42**	3047	72.14
11	569	39.99	**27**	1388	96.05	**43**	3053	130.48
12	592	12.01	**28**	1419	2.92	**44**	3089	31.87
13	612	5.33	**29**	1429	24.21	**45**	3098	42.31
14	650	0.93	**30**	1458	77.28	**46**	3104	53.41
15	738	10.41	**31**	1480	209.44	**47**	3134	34.36
16	761	33.18	**32**	1505	4.77	**48**	3167	10.07

Table 3-38. B3LYP/6-31G* Optimized Geometries, Energies, and Entropy Corrections for HAPY-4

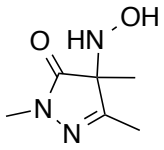

HAPY-4

B3LYP/6-31G* Energy (E): -549.89706 hartrees
Entropy Correction (Hv-TSv): 376.6585 kJ/mol
G° = E + "entropy correction": -344975.3307 kcal/mol

Atom	Atomic Number	Cartesian Coordinates (Angstroms) X	Y	Z
C	6	0.6674974	-0.0312016	0.2081174
C	6	-0.5732141	0.8736346	0.1660289
N	7	-1.6275977	0.0417863	-0.0540181
N	7	-1.2521411	-1.3016038	-0.2243723
C	6	0.0305132	-1.3773154	-0.1035355
O	8	-0.6244446	2.1023471	0.3060451
C	6	1.3235318	-0.0041299	1.5958698
H	1	1.6603111	1.0093295	1.8223900
H	1	2.1868379	-0.6764463	1.6180184
H	1	0.6187408	-0.3236712	2.3701152
N	7	1.5557045	0.3364823	-0.9185137
H	1	2.3018885	-0.3652952	-0.9494583
O	8	2.2909875	1.5422003	-0.5842923
H	1	1.8345244	2.2194901	-1.1112639
C	6	0.7597784	-2.6674931	-0.2355038
H	1	1.3401742	-2.8860519	0.6681470
H	1	1.4646004	-2.6380902	-1.0757288
H	1	0.0514905	-3.4807230	-0.4081954
C	6	-3.0238089	0.4081661	-0.1969990
H	1	-3.6343621	-0.1292852	0.5327235
H	1	-3.3819217	0.1733043	-1.2030979
H	1	-3.1037844	1.4811849	-0.0224786

Table 3-39. B3LYP/6-31G* Calculated IR Frequencies (cm^{-1}, uncorrected) and Intensities for HAPY-4

	cm^{-1}	Intensity		cm^{-1}	Intensity		cm^{-1}	Intensity
1	62	5.71	**21**	760	22.89	**41**	1492	18.15
2	88	11.70	**22**	847	43.49	**42**	1495	13.76

3	97	15.63	**23**	891	19.29	**43**	1509	9.81
4	130	5.37	**24**	939	25.60	**44**	1513	11.24
5	139	12.94	**25**	965	31.05	**45**	1521	1.88
6	168	0.28	**26**	1024	47.74	**46**	1532	8.00
7	206	69.21	**27**	1033	3.95	**47**	1543	18.21
8	214	24.00	**28**	1052	29.65	**48**	1669	210.81
9	248	4.68	**29**	1067	70.06	**49**	1677	448.01
10	256	6.15	**30**	1138	3.80	**50**	3062	10.19
11	270	26.74	**31**	1158	29.01	**51**	3075	17.46
12	311	14.92	**32**	1179	2.57	**52**	3087	61.46
13	328	13.61	**33**	1248	113.47	**53**	3119	7.11
14	357	4.13	**34**	1259	24.02	**54**	3144	21.22
15	409	11.21	**35**	1335	51.97	**55**	3156	18.41
16	575	20.86	**36**	1372	51.17	**56**	3165	13.26
17	585	40.67	**37**	1423	31.30	**57**	3166	10.87
18	610	6.67	**38**	1427	80.26	**58**	3196	3.16
19	622	3.76	**39**	1447	60.59	**59**	3433	19.99
20	742	14.36	**40**	1473	18.53	**60**	3722	104.49

Table 3-40. B3LYP/6-31G* Optimized Geometries, Energies, and Entropy Corrections for HAPY-4$_{anion}$

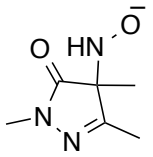

HAPY-4$_{anion}$

B3LYP/6-31G* Energy (E): -549.389029 hartrees
Entropy Correction (Hv-TSv): 341.0871 kJ/mol
G° = E + "entropy correction": -344665.0384 kcal/mol

Atom	Atomic Number	Cartesian Coordinates (Angstroms) X	Y	Z
C	6	-0.5432454	-0.5334428	-0.1322298
C	6	-0.9702601	0.9245379	-0.0008716
N	7	0.1330444	1.5965676	0.4273200
N	7	1.2815950	0.7911809	0.4877507
C	6	0.9364003	-0.4052621	0.1425796
C	6	1.9247615	-1.5166368	0.1202060
H	1	1.6515057	-2.2897245	0.8499816
H	1	2.9192178	-1.1352786	0.3647358
H	1	1.9565019	-1.9975274	-0.8639804
O	8	-2.0764501	1.4342318	-0.2325479

C	6	-0.9161180	-1.1262694	-1.4855654
H	1	-1.9989014	-1.2813192	-1.4884047
H	1	-0.4254366	-2.0958613	-1.6238354
H	1	-0.6334576	-0.4761163	-2.3209763
N	7	-1.1508515	-1.3030395	1.0646519
H	1	-0.6697767	-2.2196969	0.9409594
O	8	-2.5348735	-1.5291215	0.8861759
C	6	0.2612520	3.0212057	0.6709507
H	1	0.6104355	3.2039516	1.6910040
H	1	-0.7237901	3.4685721	0.5351626
H	1	0.9684468	3.4690483	-0.0330666

Table 3-41. B3LYP/6-31G* Calculated IR Frequencies (cm^{-1}, uncorrected) and Intensities for HAPY-4_{anion}

	cm^{-1}	Intensity		cm^{-1}	Intensity		cm^{-1}	Intensity
1	64	11.66	**20**	752	18.12	**39**	1471	44.92
2	79	0.35	**21**	803	29.37	**40**	1493	10.98
3	113	14.69	**22**	862	11.13	**41**	1496	22.44
4	123	8.82	**23**	943	87.51	**42**	1500	3.16
5	144	7.52	**24**	968	36.52	**43**	1512	9.09
6	169	17.18	**25**	1022	13.81	**44**	1529	4.51
7	177	1.22	**26**	1036	18.10	**45**	1540	15.22
8	247	10.61	**27**	1049	7.19	**46**	1661	308.37
9	253	5.87	**28**	1066	36.65	**47**	1674	385.58
10	268	18.82	**29**	1117	22.19	**48**	3057	13.43
11	296	5.49	**30**	1164	24.59	**49**	3059	46.02
12	312	10.33	**31**	1169	8.31	**50**	3082	81.05
13	357	2.93	**32**	1248	87.60	**51**	3103	106.21
14	403	14.07	**33**	1270	17.28	**52**	3115	12.91
15	559	80.55	**34**	1344	73.82	**53**	3130	23.45
16	580	23.97	**35**	1405	14.88	**54**	3136	29.82
17	587	25.07	**36**	1419	116.74	**55**	3150	21.38
18	608	2.36	**37**	1432	7.13	**56**	3164	12.21
19	686	74.56	**38**	1451	15.32	**57**	3191	4.53

Table 3-42. B3LYP/6-31G* Optimized Geometries, Energies, and Entropy Corrections for enol of PY-5

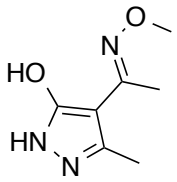

PY-5

B3LYP/6-31G* Energy (E): -588.01246 hartrees
Entropy Correction (Hv-TSv): 391.2127 kJ/mol
G° = E + "entropy correction": -368889.6087 kcal/mol

Atom	Atomic Number	Cartesian Coordinates (Angstroms) X	Y	Z
C	6	-0.7796140	-0.3777535	0.2542232
C	6	-1.9453394	0.2748677	-0.1660934
N	7	-2.9923681	-0.4228846	0.3037214
N	7	-2.6007109	-1.5228842	1.0285410
C	6	-1.2689904	-1.4983019	0.9991359
C	6	-0.5179078	-2.5821689	1.7071310
H	1	0.1771001	-2.1794777	2.4508123
H	1	0.0651319	-3.1963464	1.0118701
H	1	-1.2293269	-3.2349895	2.2194956
C	6	0.5625838	0.0947998	-0.0654699
N	7	0.6005916	1.1785570	-0.7819402
O	8	1.9024583	1.6315985	-1.0718533
C	6	1.7789790	-0.6378384	0.4248813
H	1	2.6880788	-0.2318612	-0.0157719
H	1	1.7070153	-1.7017436	0.1834914
H	1	1.8532190	-0.5578960	1.5152806
C	6	1.8123587	2.8012924	-1.8889049
H	1	1.3134307	2.5834523	-2.8397091
H	1	2.8447020	3.1032234	-2.0761727
H	1	1.2811750	3.6065311	-1.3696061
H	1	-3.9754845	-0.2111343	0.1749576
O	8	-2.1036530	1.3941550	-0.8999366
H	1	-1.1734291	1.6868031	-1.0980833

Table 3-43. B3LYP/6-31G* Calculated IR Frequencies (cm^{-1}, uncorrected) and Intensities for enol of PY-5

	cm^{-1}	Intensity		cm^{-1}	Intensity		cm^{-1}	Intensity
1	33	1.51	**22**	725	5.67	**43**	1492	35.93
2	73	3.95	**23**	755	36.43	**44**	1500	21.15
3	107	0.52	**24**	785	16.05	**45**	1507	7.11
4	123	2.06	**25**	909	216.01	**46**	1508	1.77
5	131	0.92	**26**	1002	24.90	**47**	1523	50.13
6	171	3.39	**27**	1005	63.80	**48**	1525	54.39
7	215	0.07	**28**	1060	163.27	**49**	1533	37.65
8	223	0.04	**29**	1066	223.66	**50**	1550	131.23
9	249	0.79	**30**	1073	1.80	**51**	1615	435.28
10	296	21.67	**31**	1086	19.87	**52**	1651	167.08
11	328	7.62	**32**	1108	23.57	**53**	3054	113.57
12	349	0.89	**33**	1143	17.99	**54**	3068	23.25
13	359	4.65	**34**	1179	2.41	**55**	3080	9.26
14	408	3.20	**35**	1220	9.79	**56**	3122	52.40
15	446	41.41	**36**	1255	97.67	**57**	3126	13.45
16	469	116.89	**37**	1332	8.36	**58**	3143	7.08
17	543	0.05	**38**	1408	16.76	**59**	3151	25.27
18	562	6.51	**39**	1422	69.35	**60**	3173	24.30
19	598	29.48	**40**	1443	303.53	**61**	3196	12.22
20	651	87.10	**41**	1444	38.59	**62**	3283	690.65
21	685	20.61	**42**	1484	22.88	**63**	3602	262.74

Table 3-44. B3LYP/6-31G* Optimized Geometries, Energies, and Entropy Corrections for PY-5_{anion}

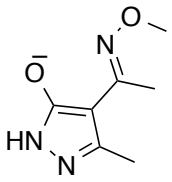

PY-5_{anion}

B3LYP/6-31G* Energy (E): -587.534096 hartrees
Entropy Correction (Hv-TSv): 355.5968 kJ/mol
G° = E + "entropy correction": -368597.9434 kcal/mol

Atom	Atomic Number	Cartesian Coordinates (Angstroms) X	Y	Z
C	6	-0.9483545	-0.3252580	0.0668253
C	6	-2.1846271	0.1432293	-0.5021595
N	7	-3.1384302	-0.6311003	0.1334290
N	7	-2.6370704	-1.4981195	1.0830477
C	6	-1.3204277	-1.3236420	1.0236699
C	6	-0.4654010	-2.1160239	1.9658167
H	1	0.2809817	-1.4861849	2.4619818
H	1	0.0770980	-2.9264504	1.4635803
H	1	-1.1049322	-2.5689024	2.7294542
C	6	0.3836614	0.1477886	-0.2655238
N	7	0.5156371	1.3758495	-0.6825143
O	8	1.8876679	1.6383713	-1.0335552
C	6	1.5703995	-0.7831263	-0.1645514
H	1	2.1621629	-0.7238259	-1.0832846
H	1	1.2539988	-1.8141342	-0.0125523
H	1	2.2395566	-0.4913326	0.6536921
C	6	1.9763834	2.9738319	-1.5184447
H	1	1.3645221	3.1178585	-2.4176107
H	1	3.0310281	3.1285861	-1.7611115
H	1	1.6628257	3.6998679	-0.7582788
H	1	-4.1403707	-0.5409830	0.0115610
O	8	-2.4663093	1.0037002	-1.3934711

Table 3-45. B3LYP/6-31G* Calculated IR Frequencies (cm^{-1}, uncorrected) and Intensities for PY-5_{anion}

	cm^{-1}	Intensity		cm^{-1}	Intensity		cm^{-1}	Intensity
1	41	3.17	**21**	737	21.79	**41**	1483	257.20
2	86	7.80	**22**	773	25.41	**42**	1492	5.80
3	99	0.09	**23**	806	32.93	**43**	1498	6.04
4	103	4.21	**24**	847	323.79	**44**	1509	28.56
5	133	0.56	**25**	993	110.63	**45**	1510	61.13
6	148	8.07	**26**	1005	3.48	**46**	1519	20.35
7	182	3.67	**27**	1052	38.09	**47**	1539	36.47
8	203	0.51	**28**	1055	157.99	**48**	1547	504.23
9	239	25.51	**29**	1071	0.92	**49**	1552	392.07
10	274	3.42	**30**	1082	60.04	**50**	1618	333.90
11	287	2.61	**31**	1100	114.19	**51**	3039	159.00
12	329	7.24	**32**	1117	0.90	**52**	3056	49.27
13	363	13.12	**33**	1186	2.00	**53**	3073	19.85
14	406	12.73	**34**	1209	7.52	**54**	3098	79.21
15	433	63.34	**35**	1246	4.95	**55**	3109	22.57

16	455	74.50	**36**	1353	24.10	**56**	3125	18.20
17	552	2.95	**37**	1396	97.12	**57**	3141	35.87
18	590	24.77	**38**	1416	5.53	**58**	3157	28.06
19	622	13.95	**39**	1437	42.64	**59**	3194	20.16
20	669	19.37	**40**	1478	171.09	**60**	3598	91.18

Table 3-46. B3LYP/6-31G* Optimized Geometries, Energies, and Entropy Corrections for HAPY-5

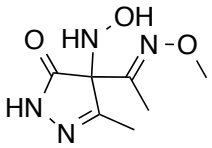

HAPY-5

B3LYP/6-31G* Energy (E): -718.508674 hartrees
Entropy Correction (Hv-TSv): 436.148 kJ/mol
G° = E + "entropy correction": -450766.4176 kcal/mol

Atom	Atomic Number	Cartesian Coordinates (Angstroms) X	Y	Z
C	6	-0.5488549	-0.0087294	0.2966453
C	6	-1.7267288	0.8757830	-0.1846993
N	7	-2.6779534	-0.0082044	-0.5827926
N	7	-2.3182464	-1.3525688	-0.4735570
C	6	-1.1275857	-1.4021806	0.0163923
O	8	-1.8059484	2.1045011	-0.2029808
C	6	-0.4319475	-2.6849130	0.3024980
H	1	-0.2620499	-2.7999768	1.3802743
H	1	0.5480581	-2.7214621	-0.1847925
H	1	-1.0404730	-3.5235534	-0.0422009
C	6	0.7253335	0.2418650	-0.5083225
N	7	1.8124673	0.1579845	0.1660064
O	8	2.9570116	0.3746046	-0.6178078
C	6	0.6149579	0.5107946	-1.9809948
H	1	0.4563406	1.5811067	-2.1591741
H	1	-0.2388798	-0.0218305	-2.4111505
H	1	1.5247947	0.2074508	-2.5007872
C	6	4.1211686	0.2044737	0.2004180
H	1	4.1264605	0.9203995	1.0283668
H	1	4.9672743	0.3954420	-0.4623339
H	1	4.1810197	-0.8151659	0.5942052
N	7	-0.4365070	0.1165113	1.7602777

H	1	0.3653749	-0.4557015	2.0371990
O	8	0.0025082	1.4545650	2.1033947
H	1	-0.7771808	1.8117802	2.5632944
H	1	-3.5892628	0.2264404	-0.9620430

Table 3-47. B3LYP/6-31G* Calculated IR Frequencies (cm^{-1}, uncorrected) and Intensities for HAPY-5

	cm^{-1}	Intensity		cm^{-1}	Intensity		cm^{-1}	Intensity
1	22	0.40	**25**	644	10.62	**49**	1440	3.70
2	69	0.50	**26**	751	16.51	**50**	1482	7.26
3	84	6.70	**27**	763	29.93	**51**	1494	10.68
4	94	2.24	**28**	771	28.47	**52**	1498	17.91
5	107	1.65	**29**	875	73.80	**53**	1503	1.40
6	117	1.96	**30**	898	127.44	**54**	1504	9.41
7	146	5.84	**31**	929	99.14	**55**	1514	8.33
8	156	1.31	**32**	997	15.51	**56**	1515	17.12
9	161	1.45	**33**	1012	4.43	**57**	1532	28.05
10	169	2.81	**34**	1029	20.34	**58**	1683	40.40
11	195	0.05	**35**	1047	32.07	**59**	1699	661.42
12	251	15.62	**36**	1056	367.58	**60**	1768	19.84
13	277	10.47	**37**	1079	17.17	**61**	3063	82.20
14	309	6.08	**38**	1082	28.89	**62**	3064	26.50
15	319	16.94	**39**	1103	30.23	**63**	3069	2.86
16	342	62.99	**40**	1178	2.53	**64**	3121	7.41
17	353	63.09	**41**	1195	72.07	**65**	3130	8.65
18	407	6.58	**42**	1210	11.83	**66**	3136	48.34
19	415	7.01	**43**	1284	18.18	**67**	3168	8.49
20	468	83.46	**44**	1297	70.56	**68**	3175	9.05
21	512	12.01	**45**	1306	46.84	**69**	3177	17.27
22	518	95.25	**46**	1380	50.74	**70**	3445	38.86
23	584	23.42	**47**	1401	82.80	**71**	3596	211.53
24	600	33.21	**48**	1427	22.04	**72**	3712	96.51

Table 3-48. B3LYP/6-31G* Optimized Geometries, Energies, and Entropy Corrections for HAPY-5$_{anion}$

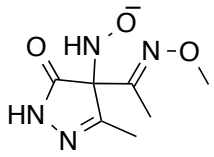

HAPY-5$_{anion}$

B3LYP/6-31G* Energy (E): -718.017094 hartrees
Entropy Correction (Hv-TSv): 390.2085 kJ/mol
G° = E + "entropy correction": Not a ground state structure; HNO is dissociated

Atom	Atomic Number	Cartesian Coordinates (Angstroms) X	Y	Z
C	6	-0.8897996	-0.0602097	-0.3755040
C	6	-2.1403720	0.4651086	-0.8926977
N	7	-3.0637703	-0.4846269	-0.5049160
N	7	-2.5341821	-1.5414715	0.2082488
C	6	-1.2334508	-1.2994091	0.2584175
O	8	-2.4449829	1.5052057	-1.5492058
C	6	-0.3454993	-2.2635734	0.9760941
H	1	0.2079265	-1.7668265	1.7814772
H	1	0.4048671	-2.6974744	0.3078198
H	1	-0.9566355	-3.0641779	1.4038529
C	6	0.4293010	0.5143274	-0.5686257
N	7	1.4619714	-0.2287839	-0.3027021
O	8	2.6739920	0.5051555	-0.4851190
C	6	0.5677570	1.9433334	-1.0322508
H	1	0.9590270	2.5572568	-0.2119993
H	1	-0.3948145	2.3366768	-1.3580932
H	1	1.2964940	2.0101347	-1.8460412
C	6	3.7715652	-0.3612935	-0.2023398
H	1	3.7404422	-0.7198888	0.8332440
H	1	4.6678317	0.2444917	-0.3563794
H	1	3.7865801	-1.2227483	-0.8803739
N	7	-1.5177289	1.3686555	1.8136065
H	1	-2.0739699	1.9453067	1.1192516
O	8	-2.3087944	0.7394192	2.5201555
H	1	-4.0637551	-0.4245880	-0.6559201

Table 3-49. B3LYP/6-31G* Calculated IR Frequencies (cm^{-1}, uncorrected) and Intensities for HAPY-5_{anion}

	cm^{-1}	Intensity		cm^{-1}	Intensity		cm^{-1}	Intensity
1	-43	9.32	**24**	592	60.63	**47**	1477	44.06
2	-23	5.04	**25**	612	46.13	**48**	1492	422.03
3	37	0.02	**26**	673	43.84	**49**	1494	326.15
4	69	7.21	**27**	751	4.92	**50**	1499	9.72
5	82	6.97	**28**	758	26.54	**51**	1505	9.83
6	85	9.82	**29**	798	48.47	**52**	1521	122.49
7	102	5.76	**30**	873	321.76	**53**	1532	26.68
8	116	2.85	**31**	994	75.95	**54**	1534	28.44
9	140	13.05	**32**	1020	7.15	**55**	1559	137.63
10	147	6.69	**33**	1055	315.63	**56**	1570	66.82
11	191	13.72	**34**	1070	5.24	**57**	1579	581.46
12	221	26.61	**35**	1077	3.01	**58**	1630	193.38
13	226	33.74	**36**	1092	85.53	**59**	2955	46.71
14	251	14.40	**37**	1115	3.85	**60**	3046	154.17
15	271	24.63	**38**	1117	51.06	**61**	3063	41.50
16	301	2.37	**39**	1174	2.32	**62**	3066	24.39
17	319	7.10	**40**	1206	4.41	**63**	3108	70.93
18	358	23.17	**41**	1256	28.29	**64**	3121	23.51
19	400	4.16	**42**	1340	54.49	**65**	3123	21.35
20	443	57.34	**43**	1391	78.61	**66**	3144	35.69
21	457	38.81	**44**	1422	34.21	**67**	3163	28.67
22	499	46.78	**45**	1442	65.03	**68**	3179	2.18
23	561	6.17	**46**	1468	506.54	**69**	3604	125.20

Table 3-50. B3LYP/6-31G* Optimized Geometries, Energies, and Entropy Corrections for enol of PY-6

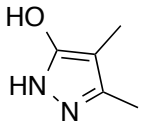

PY-6

B3LYP/6-31G* Energy (E): -380.066128 hartrees
Entropy Correction (Hv-TSv): 257.5155 kJ/mol
G° = E + "entropy correction": -238433.3682 kcal/mol

Atom	Atomic Number	Cartesian Coordinates (Angstroms) X	Y	Z
C	6	-0.0012941	-0.6332998	0.0008509
C	6	-1.1319720	0.1690625	-0.0008776

N	7	-0.7232614	1.4601851	-0.0007344
N	7	0.6407509	1.5700133	-0.0000300
C	6	1.0674297	0.3027823	-0.0021440
H	1	-1.3124565	2.2840479	-0.0019890
C	6	2.5304030	-0.0053629	-0.0012923
H	1	2.8175404	-0.5974393	0.8763593
H	1	3.1115569	0.9207396	0.0081250
H	1	2.8216184	-0.5834513	-0.8865503
C	6	0.0730538	-2.1305192	0.0015701
H	1	-0.8785170	-2.5844753	0.3018988
H	1	0.8270675	-2.4916253	0.7101548
H	1	0.3309510	-2.5403349	-0.9833823
O	8	-2.4716296	-0.0968927	0.0107040
H	1	-2.5928740	-1.0596865	-0.0935414

Table 3-51. B3LYP/6-31G* Calculated IR Frequencies (cm^{-1}, uncorrected) and Intensities for enol of PY-6

	cm^{-1}	Intensity		cm^{-1}	Intensity		cm^{-1}	Intensity
1	107	0.54	**15**	770	5.10	**29**	1508	7.09
2	149	3.63	**16**	961	28.59	**30**	1514	17.49
3	172	20.86	**17**	1006	63.24	**31**	1525	4.11
4	195	120.92	**18**	1065	1.53	**32**	1530	3.01
5	233	2.14	**19**	1085	2.57	**33**	1554	192.56
6	276	23.17	**20**	1109	147.03	**34**	1633	158.23
7	289	6.36	**21**	1145	18.46	**35**	3046	55.26
8	332	28.88	**22**	1156	98.10	**36**	3055	38.10
9	429	66.66	**23**	1222	40.20	**37**	3099	39.21
10	506	25.80	**24**	1363	93.42	**38**	3105	14.06
11	568	15.16	**25**	1415	117.86	**39**	3115	37.48
12	672	9.45	**26**	1440	34.55	**40**	3145	24.02
13	697	5.55	**27**	1453	3.72	**41**	3610	244.42
14	708	26.22	**28**	1499	20.40	**42**	3693	201.57

Table 3-52. B3LYP/6-31G* Optimized Geometries, Energies, and Entropy Corrections for PY-6$_{anion}$

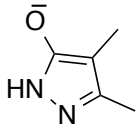

PY-6$_{anion}$

B3LYP/6-31G* Energy (E): -379.595625 hartrees
Entropy Correction (Hv-TSv): 223.0236 kJ/mol
G° = E + "entropy correction": -238146.3671 kcal/mol

Atom	Atomic Number	Cartesian Coordinates (Angstroms) X	Y	Z
C	6	-0.5055753	-0.2929715	0.0094368
C	6	-1.6958443	0.4786730	0.0310258
N	7	-1.2333856	1.7879491	0.0146000
N	7	0.1432923	1.9066690	-0.0096111
C	6	0.5606684	0.6332797	-0.0140311
H	1	-1.8115821	2.6192789	0.0377488
C	6	2.0259655	0.3327436	-0.0418937
H	1	2.3369844	-0.2536002	0.8327180
H	1	2.5998043	1.2649098	-0.0509318
H	1	2.3047904	-0.2504693	-0.9293832
C	6	-0.4480373	-1.7892726	0.0139251
H	1	-1.4671978	-2.1918933	0.0546738
H	1	0.0993244	-2.1976523	0.8763337
H	1	0.0316277	-2.2078543	-0.8834214
O	8	-2.9408349	0.1602103	0.0588103

Table 3-53. B3LYP/6-31G* Calculated IR Frequencies (cm^{-1}, uncorrected) and Intensities for PY-6$_{anion}$

	cm^{-1}	Intensity		cm^{-1}	Intensity		cm^{-1}	Intensity
1	22	1.49	**14**	792	9.27	**27**	1506	4.77
2	98	14.75	**15**	930	27.34	**28**	1510	158.45
3	116	19.85	**16**	988	99.94	**29**	1521	5.87
4	154	0.59	**17**	1059	0.02	**30**	1522	34.16
5	213	29.17	**18**	1079	1.07	**31**	1538	344.05
6	256	5.18	**19**	1100	39.91	**32**	1589	342.40
7	282	0.88	**20**	1151	22.90	**33**	3016	138.65
8	431	63.46	**21**	1182	59.35	**34**	3044	67.14
9	540	20.70	**22**	1285	36.81	**35**	3048	68.66

10	584	39.29	**23**	1382	52.25	**36**	3090	31.54
11	670	15.41	**24**	1414	41.68	**37**	3099	42.34
12	712	4.09	**25**	1424	13.72	**38**	3134	33.88
13	750	4.88	**26**	1483	201.85	**39**	3598	78.35

Table 3-54. B3LYP/6-31G* Optimized Geometries, Energies, and Entropy Corrections for HAPY-6

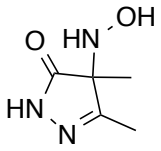

HAPY-6

B3LYP/6-31G* Energy (E): -510.583141 hartrees
Entropy Correction (Hv-TSv): 307.2283 kJ/mol
G° = E + "entropy correction": -320322.0869 kcal/mol

Atom	Atomic Number	Cartesian Coordinates (Angstroms) X	Y	Z
C	6	-0.1231117	-0.2841939	-0.2004076
C	6	-0.5695334	1.1804075	-0.0493404
N	7	0.5740192	1.8688917	0.2043141
N	7	1.7211724	1.0733400	0.3064389
C	6	1.3639491	-0.1497289	0.1014574
H	1	0.6520336	2.8642383	0.3828779
C	6	2.3389161	-1.2732784	0.1361728
H	1	2.0866292	-1.9919373	0.9259469
H	1	3.3438520	-0.8908740	0.3276289
H	1	2.3410928	-1.8205552	-0.8132553
O	8	-1.7099599	1.6472889	-0.1405069
C	6	-0.3857942	-0.7933624	-1.6248209
H	1	-1.4567545	-0.7631111	-1.8342776
H	1	-0.0357026	-1.8250926	-1.7289102
H	1	0.1360561	-0.1775020	-2.3641289
N	7	-0.7478580	-1.0779252	0.8818552
H	1	-0.3211791	-2.0090747	0.8535154
O	8	-2.1281272	-1.3655358	0.5397668
H	1	-2.6192221	-0.7693255	1.1298996

Table 3-55. B3LYP/6-31G* Calculated IR Frequencies (cm^{-1}, uncorrected) and Intensities for HAPY-6

	cm^{-1}	Intensity		cm^{-1}	Intensity		cm^{-1}	Intensity
1	72	1.11	**18**	762	20.41	**35**	1445	3.26
2	107	11.46	**19**	772	25.94	**36**	1494	15.81
3	146	4.39	**20**	848	43.93	**37**	1496	12.60
4	167	0.16	**21**	889	27.51	**38**	1505	8.08
5	211	11.25	**22**	951	45.77	**39**	1517	6.96
6	222	3.03	**23**	995	11.99	**40**	1528	6.63
7	248	10.05	**24**	1033	46.22	**41**	1678	33.73
8	259	69.69	**25**	1055	14.43	**42**	1687	694.59
9	297	16.35	**26**	1092	48.60	**43**	3062	9.32
10	328	46.33	**27**	1130	9.10	**44**	3075	15.38
11	345	8.86	**28**	1160	39.22	**45**	3117	7.78
12	425	5.85	**29**	1216	114.02	**46**	3145	20.50
13	496	146.70	**30**	1308	10.75	**47**	3164	22.65
14	561	31.22	**31**	1333	52.49	**48**	3164	2.31
15	582	27.74	**32**	1371	47.68	**49**	3432	19.67
16	629	12.17	**33**	1402	74.86	**50**	3596	180.30
17	719	2.54	**34**	1433	11.92	**51**	3723	106.80

Table 3-56. B3LYP/6-31G* Optimized Geometries, Energies, and Entropy Corrections for HAPY-6_{anion}

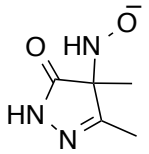

HAPY-6_{anion}

B3LYP/6-31G* Energy (E): -510.074697 hartrees
Entropy Correction (Hv-TSv): 271.0122 kJ/mol
G° = E + "entropy correction": -320011.6896 kcal/mol

Atom	Atomic Number	Cartesian Coordinates (Angstroms) X	Y	Z
C	6	-0.4927162	0.0571893	-0.0258868
C	6	-0.9209071	1.5173689	0.0957674
N	7	0.1644597	2.1619140	0.5993900
N	7	1.3110047	1.3644929	0.6975040
C	6	0.9744477	0.1744040	0.3220017
H	1	0.2596872	3.1648622	0.7270012
C	6	1.9563979	-0.9428053	0.3309540

H	1	1.6436007	-1.7258667	1.0337293
H	1	2.9395489	-0.5716188	0.6304642
H	1	2.0349519	-1.4081767	-0.6580721
O	8	-2.0035828	2.0417263	-0.1941132
C	6	-0.8021749	-0.5218591	-1.4011459
H	1	-1.8841000	-0.6740782	-1.4558142
H	1	-0.3070144	-1.4910060	-1.5266485
H	1	-0.4799470	0.1354452	-2.2163044
N	7	-1.1669328	-0.7167229	1.1328865
H	1	-0.6860714	-1.6357450	1.0274271
O	8	-2.5406521	-0.9295239	0.8808598

Table 3-57. B3LYP/6-31G* Calculated IR Frequencies (cm^{-1}, uncorrected) and Intensities for HAPY-6_{anion}

	cm^{-1}	Intensity		cm^{-1}	Intensity		cm^{-1}	Intensity
1	76	8.82	**17**	719	7.34	**33**	1431	19.99
2	125	12.45	**18**	780	27.70	**34**	1455	5.73
3	145	6.77	**19**	809	53.11	**35**	1495	14.89
4	172	4.57	**20**	865	13.04	**36**	1496	17.26
5	185	25.56	**21**	952	87.88	**37**	1505	3.94
6	221	7.30	**22**	994	23.53	**38**	1531	6.69
7	262	4.31	**23**	1038	16.96	**39**	1670	88.81
8	292	9.81	**24**	1051	2.60	**40**	1682	667.30
9	297	13.96	**25**	1089	39.43	**41**	3058	18.37
10	327	11.68	**26**	1112	4.41	**42**	3059	36.26
11	411	4.12	**27**	1166	39.26	**43**	3101	108.12
12	466	141.37	**28**	1218	98.16	**44**	3115	13.73
13	552	40.23	**29**	1316	21.79	**45**	3130	24.43
14	572	63.13	**30**	1342	60.57	**46**	3135	27.95
15	584	17.67	**31**	1391	35.34	**47**	3164	12.86
16	686	62.14	**32**	1408	9.04	**48**	3582	164.09

Table 3-58. B3LYP/6-31G* Optimized Geometries, Energies, and Entropy Corrections for enol of PY-7

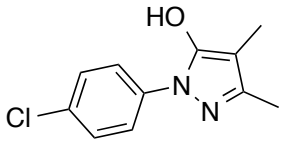

PY-7

B3LYP/6-31G* Energy (E): -1070.713457 hartrees
Entropy Correction (Hv-TSv): 428.275 kJ/mol
G° = E + "entropy correction": -671779.9705 kcal/mol

Atom	Atomic Number	Cartesian Coordinates (Angstroms) X	Y	Z
C	6	2.1469309	0.1991542	0.3509865
C	6	0.9368068	0.8625249	0.2877277
N	7	-0.0503943	-0.0546695	0.0203817
N	7	0.4953009	-1.3172743	-0.1063928
C	6	1.8016649	-1.1536564	0.0909005
C	6	3.5008279	0.7844591	0.6203555
H	1	4.0244202	1.0753723	-0.2990946
H	1	4.1407686	0.0675226	1.1452472
H	1	3.4403161	1.6738718	1.2589193
C	6	2.7273231	-2.3259204	0.0367473
H	1	3.2532179	-2.4651693	0.9890382
H	1	3.4927047	-2.1930456	-0.7366409
H	1	2.1694585	-3.2398206	-0.1827363
C	6	-1.4435647	0.1275925	-0.1706938
C	6	-4.1867605	0.4048679	-0.5628041
C	6	-2.1664704	-0.8699977	-0.8394864
C	6	-2.1117259	1.2622779	0.3084588
C	6	-3.4836204	1.4032004	0.1042086
C	6	-3.5375350	-0.7349192	-1.0326464
H	1	-1.6449124	-1.7487209	-1.1959934
H	1	-1.5713562	2.0334560	0.8389297
H	1	-3.9991341	2.2823034	0.4738905
H	1	-4.0937156	-1.5083043	-1.5501446
Cl	17	-5.9270524	0.5801524	-0.8146434
O	8	0.6272398	2.1765554	0.4300985
H	1	1.4592615	2.6781875	0.5353866

Table 3-59. B3LYP/6-31G* Calculated IR Frequencies (cm^{-1}, uncorrected) and Intensities for enol of PY-7

	cm^{-1}	Intensity		cm^{-1}	Intensity		cm^{-1}	Intensity
1	31	2.54	**25**	708	6.82	**49**	1440	85.08
2	44	0.95	**26**	712	24.19	**50**	1449	19.47
3	58	0.91	**27**	747	29.68	**51**	1454	81.98
4	98	1.17	**28**	827	5.20	**52**	1498	82.49
5	128	0.86	**29**	833	5.96	**53**	1500	28.60
6	137	1.59	**30**	845	52.12	**54**	1509	13.56
7	171	8.02	**31**	960	2.21	**55**	1518	42.80
8	224	18.57	**32**	971	0.90	**56**	1528	65.32
9	233	66.59	**33**	977	85.97	**57**	1536	124.34
10	254	7.88	**34**	1025	35.37	**58**	1546	360.14
11	260	12.47	**35**	1029	85.17	**59**	1630	98.68
12	286	40.50	**36**	1063	3.70	**60**	1643	191.78

13	318	3.92	**37**	1081	2.01	**61**	1651	14.55
14	332	5.01	**38**	1095	85.71	**62**	3049	60.60
15	371	1.71	**39**	1104	45.85	**63**	3060	38.99
16	409	0.82	**40**	1121	107.44	**64**	3101	29.35
17	423	0.73	**41**	1140	7.31	**65**	3111	14.96
18	489	72.68	**42**	1188	30.69	**66**	3123	25.41
19	518	10.88	**43**	1211	0.17	**67**	3151	19.93
20	568	26.19	**44**	1246	108.70	**68**	3237	3.78
21	609	3.66	**45**	1328	39.76	**69**	3238	2.91
22	642	0.23	**46**	1337	23.93	**70**	3258	0.51
23	654	1.34	**47**	1355	50.24	**71**	3277	1.90
24	688	4.67	**48**	1416	314.96	**72**	3678	254.39

Table 3-60. B3LYP/6-31G* Optimized Geometries, Energies, and Entropy Corrections for PY-7$_{anion}$

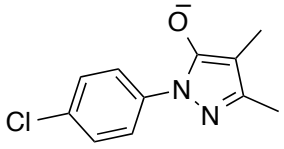

PY-7$_{anion}$

B3LYP/6-31G* Energy (E): -1070.252293 hartrees
Entropy Correction (Hv-TSv): 396.8443 kJ/mol
G° = E + "entropy correction": -671498.0981 kcal/mol

Atom	Atomic Number	Cartesian Coordinates (Angstroms)		
		X	Y	Z
C	6	2.1946860	0.2838020	0.4359125
C	6	0.9825510	1.0062959	0.4480322
N	7	0.0078511	0.0632125	0.0148065
N	7	0.5754042	-1.1816594	-0.2547642
C	6	1.8742019	-1.0192859	0.0053024
C	6	3.5277727	0.8483567	0.8167531
H	1	4.2564484	0.8221205	-0.0063419
H	1	3.9915539	0.3201282	1.6622015
H	1	3.4063037	1.8967990	1.1122662
C	6	2.8130204	-2.1694426	-0.1750890
H	1	3.3358874	-2.4094906	0.7593047
H	1	3.5842002	-1.9424254	-0.9219920
H	1	2.2645479	-3.0574721	-0.5031799
C	6	-1.3744179	0.2299787	-0.1593881
C	6	-4.1424053	0.4993190	-0.5187974
C	6	-2.1464147	-0.8418914	-0.6470979
C	6	-2.0220140	1.4430469	0.1430328

C	6	-3.3980138	1.5727298	-0.0368584
C	6	-3.5197750	-0.7087685	-0.8255335
H	1	-1.6473002	-1.7738842	-0.8790494
H	1	-1.4270581	2.2658989	0.5154843
H	1	-3.8838491	2.5130149	0.2016573
H	1	-4.0999910	-1.5441342	-1.2022381
Cl	17	-5.8818819	0.6661331	-0.7405949
O	8	0.7286919	2.2176179	0.7561712

Table 3-61. B3LYP/6-31G* Calculated IR Frequencies (cm^{-1}, uncorrected) and Intensities for PY-7_{anion}

	cm^{-1}	Intensity		cm^{-1}	Intensity		cm^{-1}	Intensity
1	41	0.54	**24**	710	23.03	**47**	1422	11.69
2	49	1.63	**25**	730	10.57	**48**	1431	40.20
3	66	0.11	**26**	763	57.25	**49**	1455	47.97
4	111	3.71	**27**	835	8.70	**50**	1486	184.58
5	119	6.79	**28**	840	18.12	**51**	1505	5.52
6	144	0.17	**29**	842	45.76	**52**	1514	120.43
7	174	0.03	**30**	956	0.24	**53**	1522	7.56
8	220	1.68	**31**	968	0.14	**54**	1530	431.26
9	254	0.81	**32**	975	99.84	**55**	1531	171.27
10	257	8.06	**33**	1020	3.33	**56**	1544	365.46
11	266	15.14	**34**	1023	104.94	**57**	1606	282.14
12	319	2.69	**35**	1057	0.42	**58**	1626	149.89
13	348	8.36	**36**	1079	1.14	**59**	1647	183.01
14	378	2.59	**37**	1098	87.53	**60**	3022	156.52
15	396	1.07	**38**	1104	17.32	**61**	3052	69.31
16	425	0.03	**39**	1114	12.82	**62**	3057	59.30
17	491	78.12	**40**	1148	47.73	**63**	3101	23.41
18	519	9.45	**41**	1156	103.79	**64**	3106	35.12
19	578	44.08	**42**	1197	2.27	**65**	3141	29.75
20	634	9.78	**43**	1313	41.86	**66**	3228	6.16
21	647	2.77	**44**	1328	0.84	**67**	3233	5.06
22	649	9.64	**45**	1350	153.51	**68**	3252	12.51
23	702	0.23	**46**	1355	440.78	**69**	3256	1.49

Table 3-62. B3LYP/6-31G* Optimized Geometries, Energies, and Entropy Corrections for HAPY-7

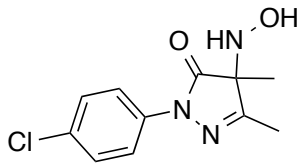

HAPY-7

B3LYP/6-31G* Energy (E): -1201.231562 hartrees
Entropy Correction (Hv-TSv): 478.7001 kJ/mol
G° = E + "entropy correction": -753669.2042 kcal/mol

Atom	Atomic Number	Cartesian Coordinates (Angstroms) X	Y	Z
C	6	2.7769855	0.0734007	0.1852081
C	6	1.4174387	0.7828539	0.1953124
N	7	0.4689417	-0.2113990	0.0624142
N	7	1.0536506	-1.4896300	-0.0742113
C	6	2.3346470	-1.3616343	-0.0324991
O	8	1.2121547	1.9921314	0.3057915
C	6	3.5044012	0.2621569	1.5248401
H	1	3.7092888	1.3223552	1.6840992
H	1	4.4524696	-0.2841381	1.5162414
H	1	2.8995808	-0.1108878	2.3574634
N	7	3.5282170	0.5148003	-1.0122642
H	1	4.3631615	-0.0765175	-1.0707819
O	8	4.0963516	1.8254844	-0.7707427
H	1	3.5520284	2.3983802	-1.3368225
C	6	3.2418540	-2.5326761	-0.1684802
H	1	3.9102694	-2.6124444	0.6960293
H	1	3.8723010	-2.4337670	-1.0607405
H	1	2.6587625	-3.4515686	-0.2561509
C	6	-0.9442866	-0.1175298	0.0281684
C	6	-3.7270813	0.0081553	-0.0380896
C	6	-1.7025138	-1.2892183	-0.1103153
C	6	-1.5958534	1.1209709	0.1336159
C	6	-2.9877866	1.1794142	0.1002418
C	6	-3.0923446	-1.2266853	-0.1439568
H	1	-1.1994714	-2.2431280	-0.1915062
H	1	-1.0184684	2.0279878	0.2410289
H	1	-3.4897170	2.1370264	0.1818724
H	1	-3.6744346	-2.1346503	-0.2522999
Cl	17	-5.4913476	0.0886939	-0.0812267

Table 3-63. B3LYP/6-31G* Calculated IR Frequencies (cm^{-1}, uncorrected) and Intensities for HAPY-7

	cm^{-1}	Intensity		cm^{-1}	Intensity		cm^{-1}	Intensity
1	24	0.06	**28**	712	0.47	**55**	1370	51.55
2	33	1.22	**29**	713	10.33	**56**	1397	305.58
3	70	0.64	**30**	741	12.63	**57**	1421	8.23
4	88	4.50	**31**	758	31.31	**58**	1442	18.42
5	128	8.58	**32**	826	52.25	**59**	1460	7.11
6	140	0.91	**33**	839	0.67	**60**	1491	16.29
7	145	6.68	**34**	848	58.45	**61**	1495	14.48
8	183	0.43	**35**	892	31.86	**62**	1507	9.18
9	224	48.43	**36**	898	30.75	**63**	1519	8.42
10	228	1.64	**37**	956	53.65	**64**	1526	4.34
11	240	1.80	**38**	970	0.39	**65**	1535	402.65
12	252	3.31	**39**	976	0.41	**66**	1629	2.18
13	259	20.78	**40**	1020	29.03	**67**	1648	49.64
14	268	64.38	**41**	1023	24.15	**68**	1687	138.66
15	317	7.66	**42**	1031	37.95	**69**	1697	448.28
16	319	6.15	**43**	1052	11.19	**70**	3065	7.36
17	334	30.59	**44**	1098	68.25	**71**	3075	15.78
18	386	16.19	**45**	1102	33.11	**72**	3122	4.77
19	399	1.59	**46**	1126	24.48	**73**	3146	19.61
20	421	0.16	**47**	1150	8.45	**74**	3169	17.51
21	432	14.95	**48**	1157	75.82	**75**	3170	2.61
22	508	50.15	**49**	1170	64.03	**76**	3236	3.56
23	524	10.99	**50**	1209	6.92	**77**	3242	2.95
24	580	31.40	**51**	1267	84.17	**78**	3269	0.46
25	615	18.67	**52**	1324	226.29	**79**	3274	4.62
26	622	7.06	**53**	1334	5.44	**80**	3432	18.60
27	645	0.64	**54**	1349	7.92	**81**	3726	108.20

Table 3-64. B3LYP/6-31G* Optimized Geometries, Energies, and Entropy Corrections for HAPY-7_{anion}

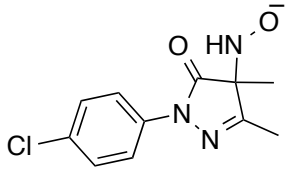

HAPY-7_{anion}

B3LYP/6-31G* Energy (E): -1200.725219 hartrees
Entropy Correction (Hv-TSv): 441.7324 kJ/mol
G° = E + "entropy correction": -753360.3049 kcal/mol

Atom	Atomic Number	Cartesian Coordinates (Angstroms) X	Y	Z
C	6	2.0163014	0.3394052	0.1477668
C	6	0.6710296	1.0231604	0.2777659
N	7	-0.2755822	0.0687389	-0.0484915
N	7	0.3082644	-1.2030962	-0.2302067
C	6	1.5843375	-1.0811307	-0.0725480
O	8	0.4435130	2.1920972	0.6009742
C	6	2.9477287	0.6039421	1.3194044
H	1	3.3166921	1.6289950	1.2145568
H	1	3.8014922	-0.0807744	1.2859500
H	1	2.4511379	0.4869038	2.2887888
N	7	2.6154928	0.8316134	-1.2263691
H	1	3.4409156	0.1926845	-1.2678103
O	8	3.1067641	2.1390282	-1.1240479
C	6	2.4846453	-2.2579280	-0.2037196
H	1	3.0726231	-2.4040749	0.7094484
H	1	3.1949953	-2.1076477	-1.0262410
H	1	1.8975772	-3.1581045	-0.3997391
C	6	-1.6860478	0.1696036	-0.1135305
C	6	-4.4703474	0.3065651	-0.2621748
C	6	-2.4438544	-0.9883174	-0.3493711
C	6	-2.3427577	1.4009380	0.0444668
C	6	-3.7332190	1.4643111	-0.0293988
C	6	-3.8319092	-0.9204205	-0.4238685
H	1	-1.9348690	-1.9345875	-0.4746130
H	1	-1.7650800	2.2954191	0.2293589
H	1	-4.2338987	2.4182615	0.0949025
H	1	-4.4087715	-1.8199666	-0.6067134
Cl	17	-6.2271733	0.3943814	-0.3545402

Table 3-65. B3LYP/6-31G* Calculated IR Frequencies (cm^{-1}, uncorrected) and Intensities for HAPY-7_{anion}

	cm^{-1}	Intensity		cm^{-1}	Intensity		cm^{-1}	Intensity
1	20	2.70	**27**	660	64.97	**53**	1349	1.12
2	36	7.77	**28**	707	0.26	**54**	1387	221.71
3	72	12.90	**29**	713	12.31	**55**	1413	6.64
4	103	7.14	**30**	754	22.15	**56**	1427	21.76
5	124	1.95	**31**	793	18.23	**57**	1449	14.48
6	131	11.12	**32**	836	1.12	**58**	1461	15.25
7	149	10.19	**33**	845	64.70	**59**	1491	13.27
8	174	0.88	**34**	847	33.94	**60**	1494	24.01
9	176	25.32	**35**	914	73.55	**61**	1507	5.55

10	228	2.32	**36**	964	0.31	**62**	1532	54.46
11	238	12.24	**37**	972	39.78	**63**	1533	384.50
12	255	1.34	**38**	973	70.51	**64**	1626	7.69
13	263	14.14	**39**	1023	5.02	**65**	1646	66.18
14	306	6.26	**40**	1027	53.14	**66**	1671	141.39
15	318	1.89	**41**	1041	11.55	**67**	1690	463.20
16	325	17.49	**42**	1049	2.09	**68**	3058	45.74
17	375	16.01	**43**	1098	43.31	**69**	3062	11.02
18	396	4.03	**44**	1104	46.34	**70**	3081	136.99
19	400	26.96	**45**	1114	2.42	**71**	3120	8.90
20	422	0.30	**46**	1145	12.63	**72**	3128	9.51
21	486	183.93	**47**	1159	144.32	**73**	3139	31.79
22	520	18.23	**48**	1174	13.14	**74**	3168	11.42
23	537	51.60	**49**	1206	5.90	**75**	3236	4.08
24	579	34.57	**50**	1284	96.96	**76**	3244	2.51
25	618	14.70	**51**	1329	70.85	**77**	3267	0.65
26	645	0.71	**52**	1341	316.91	**78**	3268	3.03

Table 3-66. B3LYP/6-31G* Optimized Geometries, Energies, and Entropy Corrections for enol of PY-8

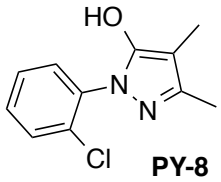

PY-8

B3LYP/6-31G* Energy (E): -1070.706172 hartrees
Entropy Correction (Hv-TSv): 427.4027 kJ/mol
G° = E + "entropy correction": -671775.6076 kcal/mol

Atom	Atomic Number	Cartesian Coordinates (Angstroms) X	Y	Z
C	6	2.0102059	-0.4648007	0.5621577
C	6	0.8635377	0.2502545	0.8563888
N	7	-0.1056050	-0.1063171	-0.0393297
N	7	0.3793226	-1.0244047	-0.9509619
C	6	1.6409416	-1.2352406	-0.5732994
C	6	3.3339922	-0.4244936	1.2646933
H	1	4.1199995	0.0222200	0.6435480
H	1	3.6713936	-1.4286113	1.5469951
H	1	3.2847875	0.1613801	2.1895681
C	6	2.5036537	-2.1992028	-1.3219940
H	1	2.8642192	-3.0042009	-0.6702461
H	1	3.3887390	-1.7037016	-1.7388054

H	1	1.9430103	-2.6501610	-2.1450038
C	6	-1.4109972	0.4355684	-0.1823846
C	6	-3.9687940	1.5256670	-0.5372636
C	6	-2.3996267	0.2732937	0.7990635
C	6	-1.7338488	1.1308744	-1.3531600
C	6	-3.0043379	1.6684441	-1.5357814
C	6	-3.6685348	0.8271255	0.6305761
H	1	-0.9667111	1.2356262	-2.1123342
H	1	-3.2346011	2.2052625	-2.4498877
H	1	-4.4128526	0.6935593	1.4073530
H	1	-4.9590208	1.9504075	-0.6647259
Cl	17	-2.0854466	-0.6722956	2.2503228
O	8	0.5754934	1.1934759	1.7887655
H	1	1.3710803	1.3402708	2.3357458

Table 3-67. B3LYP/6-31G* Calculated IR Frequencies (cm^{-1}, uncorrected) and Intensities for enol of PY-8

	cm^{-1}	Intensity		cm^{-1}	Intensity		cm^{-1}	Intensity
1	33	1.56	**25**	702	28.48	**49**	1435	58.60
2	53	10.05	**26**	727	15.42	**50**	1458	3.26
3	62	0.43	**27**	748	48.96	**51**	1479	50.69
4	81	2.65	**28**	776	45.14	**52**	1500	21.68
5	143	2.66	**29**	831	3.91	**53**	1503	2.91
6	158	1.75	**30**	878	1.11	**54**	1511	14.49
7	160	1.75	**31**	955	2.38	**55**	1515	50.77
8	195	77.30	**32**	980	33.42	**56**	1522	42.11
9	203	44.37	**33**	989	0.02	**57**	1533	87.81
10	230	5.37	**34**	1025	67.61	**58**	1543	178.45
11	253	2.27	**35**	1050	91.76	**59**	1630	9.50
12	280	5.61	**36**	1062	1.53	**60**	1638	231.04
13	299	11.39	**37**	1067	10.90	**61**	1648	4.59
14	322	5.88	**38**	1085	0.50	**62**	3050	58.68
15	376	2.72	**39**	1105	88.77	**63**	3057	41.89
16	425	17.39	**40**	1128	31.28	**64**	3103	38.19
17	457	1.77	**41**	1155	10.96	**65**	3108	9.74
18	479	11.22	**42**	1192	2.07	**66**	3116	39.14
19	525	2.43	**43**	1194	21.12	**67**	3148	21.28
20	570	19.59	**44**	1244	118.32	**68**	3222	0.23
21	607	6.05	**45**	1291	23.08	**69**	3230	8.15
22	651	10.33	**46**	1326	18.02	**70**	3239	8.46
23	660	9.53	**47**	1348	17.11	**71**	3245	8.15
24	692	2.66	**48**	1416	181.44	**72**	3690	218.80

Table 3-68. B3LYP/6-31G* Optimized Geometries, Energies, and Entropy Corrections for PY-8$_{anion}$

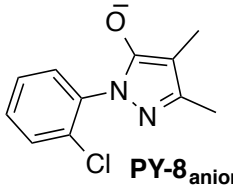

PY-8$_{anion}$

B3LYP/6-31G* Energy (E): -1070.23931 hartrees
Entropy Correction (Hv-TSv): 396.2348 kJ/mol
G° = E + "entropy correction": -671490.0968 kcal/mol

Atom	Atomic Number	Cartesian Coordinates (Angstroms)		
		X	Y	Z
C	6	2.0488394	-0.4547807	0.6732204
C	6	0.8850112	0.2325763	1.0919322
N	7	-0.1051665	-0.1773655	0.1626278
N	7	0.4155817	-0.9969108	-0.8432390
C	6	1.6949486	-1.1614089	-0.4941640
C	6	3.3789927	-0.3759652	1.3555536
H	1	4.1609339	0.0787658	0.7290756
H	1	3.7604503	-1.3598536	1.6650657
H	1	3.2878349	0.2398132	2.2582559
C	6	2.5777630	-2.0380294	-1.3259581
H	1	2.9783519	-2.8769486	-0.7425796
H	1	3.4400100	-1.4833596	-1.7176142
H	1	2.0150523	-2.4448066	-2.1716801
C	6	-1.3729743	0.4104668	-0.0279127
C	6	-3.8806924	1.6273616	-0.4793853
C	6	-2.3800156	0.3869379	0.9508520
C	6	-1.6760306	1.0259198	-1.2538388
C	6	-2.9114976	1.6212338	-1.4846631
C	6	-3.6132640	1.0059542	0.7379666
H	1	-0.9044936	1.0166202	-2.0159943
H	1	-3.1082025	2.0901976	-2.4434522
H	1	-4.3594092	0.9720800	1.5241633
H	1	-4.8439575	2.1000091	-0.6407624
Cl	17	-2.1629646	-0.5002093	2.4600389
O	8	0.6748985	1.0617018	2.0324920

Table 3-69. B3LYP/6-31G* Calculated IR Frequencies (cm^{-1}, uncorrected) and Intensities for PY-8_{anion}

	cm^{-1}	Intensity		cm^{-1}	Intensity		cm^{-1}	Intensity
1	42	5.88	**24**	725	28.55	**47**	1418	4.51
2	52	1.53	**25**	738	6.64	**48**	1435	32.61
3	84	6.30	**26**	757	49.08	**49**	1475	21.02
4	84	1.72	**27**	777	63.54	**50**	1485	181.03
5	148	0.62	**28**	845	4.83	**51**	1506	34.36
6	156	4.15	**29**	867	1.99	**52**	1508	185.60
7	164	3.46	**30**	938	2.44	**53**	1522	20.69
8	193	1.66	**31**	962	0.14	**54**	1524	125.77
9	225	3.93	**32**	977	49.40	**55**	1532	23.99
10	249	9.04	**33**	1019	60.89	**56**	1547	287.80
11	276	10.69	**34**	1048	104.71	**57**	1605	385.20
12	292	2.54	**35**	1057	1.00	**58**	1624	44.59
13	328	0.79	**36**	1069	3.17	**59**	1646	91.07
14	378	15.86	**37**	1079	1.38	**60**	3016	160.71
15	424	17.04	**38**	1115	22.08	**61**	3049	72.08
16	456	4.16	**39**	1128	31.23	**62**	3050	67.77
17	477	6.66	**40**	1158	30.16	**63**	3097	27.67
18	537	1.32	**41**	1160	57.61	**64**	3102	38.30
19	583	34.24	**42**	1183	0.22	**65**	3139	30.81
20	626	10.27	**43**	1284	27.21	**66**	3219	5.10
21	651	7.88	**44**	1319	5.77	**67**	3232	5.07
22	653	22.24	**45**	1338	28.59	**68**	3236	13.96
23	704	19.67	**46**	1360	260.49	**69**	3249	9.33

Table 3-70. B3LYP/6-31G* Optimized Geometries, Energies, and Entropy Corrections for HAPY-8

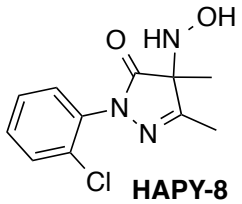

HAPY-8

B3LYP/6-31G* Energy (E): -1201.222966 hartrees
Entropy Correction (Hv-TSv): 477.8088 kJ/mol
G° = E + "entropy correction": -753664.0231 kcal/mol

Atom	Atomic Number	Cartesian Coordinates (Angstroms) X	Y	Z
C	6	2.2817321	-0.0177457	0.2688175
C	6	1.0272969	0.8396164	0.4837288
N	7	-0.0175173	0.0889766	0.0003750
N	7	0.3972948	-1.1364559	-0.5714507
C	6	1.6791582	-1.2113101	-0.4553921
O	8	0.9481848	1.9609140	0.9870888
C	6	2.9099090	-0.4133844	1.6133213
H	1	3.2373575	0.4831657	2.1428553
H	1	3.7757557	-1.0620810	1.4486435
H	1	2.1905218	-0.9516564	2.2386700
N	7	3.1771564	0.7022694	-0.6645613
H	1	3.9335794	0.0583216	-0.9165962
O	8	3.8893644	1.7413134	0.0532837
H	1	3.4344628	2.5490270	-0.2392482
C	6	2.4424833	-2.3813923	-0.9682229
H	1	3.0255412	-2.8490391	-0.1671004
H	1	3.1482463	-2.0796454	-1.7517812
H	1	1.7567019	-3.1206404	-1.3875296
C	6	-1.3846274	0.4664273	-0.0590371
C	6	-4.0718109	1.2421372	-0.2090304
C	6	-2.3756730	-0.2535516	0.6237485
C	6	-1.7604804	1.5871168	-0.8065502
C	6	-3.0942273	1.9800705	-0.8767881
C	6	-3.7148700	0.1227208	0.5415044
H	1	-0.9896113	2.1404116	-1.3314190
H	1	-3.3670089	2.8525395	-1.4606602
H	1	-4.4629190	-0.4546876	1.0725257
H	1	-5.1149983	1.5348998	-0.2661351
Cl	17	-1.9472110	-1.6342617	1.6261022

Table 3-71. B3LYP/6-31G* Calculated IR Frequencies (cm^{-1}, uncorrected) and Intensities for HAPY-8

	cm^{-1}	Intensity		cm^{-1}	Intensity		cm^{-1}	Intensity
1	24	1.40	**28**	708	31.62	**55**	1372	38.87
2	39	4.70	**29**	724	7.40	**56**	1408	169.47
3	63	0.06	**30**	745	29.75	**57**	1421	8.41
4	73	2.94	**31**	759	12.81	**58**	1443	8.99
5	113	9.93	**32**	776	55.50	**59**	1483	20.65
6	126	0.41	**33**	831	39.27	**60**	1488	22.04
7	154	6.40	**34**	874	3.43	**61**	1495	8.18
8	161	3.77	**35**	892	21.56	**62**	1511	9.25

9	198	0.74	**36**	904	27.12	**63**	1517	12.44
10	223	4.58	**37**	952	14.33	**64**	1527	42.97
11	229	26.30	**38**	956	39.48	**65**	1530	90.28
12	245	16.24	**39**	990	0.20	**66**	1631	8.34
13	256	52.21	**40**	1024	36.95	**67**	1646	25.04
14	283	2.93	**41**	1030	19.93	**68**	1675	68.78
15	287	11.26	**42**	1052	57.78	**69**	1697	440.03
16	318	37.46	**43**	1055	43.89	**70**	3065	9.35
17	344	27.38	**44**	1070	11.31	**71**	3075	16.52
18	351	8.64	**45**	1106	41.17	**72**	3121	6.60
19	405	14.31	**46**	1132	26.33	**73**	3144	19.96
20	460	2.85	**47**	1153	33.09	**74**	3166	12.90
21	463	5.31	**48**	1157	28.06	**75**	3168	8.29
22	491	12.20	**49**	1187	59.09	**76**	3222	0.30
23	539	8.66	**50**	1194	5.22	**77**	3230	8.64
24	579	32.79	**51**	1266	37.45	**78**	3239	9.21
25	613	14.87	**52**	1299	2.17	**79**	3245	6.28
26	624	6.84	**53**	1326	114.70	**80**	3433	18.29
27	656	21.89	**54**	1341	3.46	**81**	3721	109.56

Table 3-72. B3LYP/6-31G* Optimized Geometries, Energies, and Entropy Corrections for HAPY-8$_{anion}$

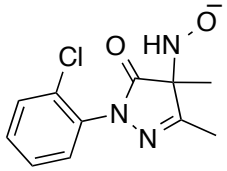

HAPY-8$_{anion}$

B3LYP/6-31G* Energy (E): -1200.71576 hartrees
Entropy Correction (Hv-TSv): 441.9393 kJ/mol
G° = E + "entropy correction": -753354.3198 kcal/mol

Atom	Atomic Number	Cartesian Coordinates (Angstroms) X	Y	Z
C	6	1.9840536	-0.0650869	0.2881352
C	6	0.7259482	0.7356831	0.5833366
N	7	-0.2968389	0.0623918	-0.0418269
N	7	0.1214935	-1.1533489	-0.6245823
C	6	1.3906675	-1.2627719	-0.4109039
O	8	0.5976840	1.7712501	1.2421687
C	6	2.8105354	-0.3559995	1.5333240
H	1	3.3214159	0.5733963	1.8032577

H	1	3.5631840	-1.1209815	1.3161559
H	1	2.2000641	-0.7036349	2.3738781
N	7	2.7687141	0.7423455	-0.7893335
H	1	3.4987068	0.0378942	-1.0307676
O	8	3.4280650	1.8479496	-0.2182222
C	6	2.1454816	-2.4460290	-0.9052102
H	1	2.6399054	-2.9693711	-0.0790047
H	1	2.9281333	-2.1422900	-1.6114255
H	1	1.4642719	-3.1380090	-1.4064551
C	6	-1.6611018	0.4493766	-0.1131967
C	6	-4.3398360	1.2587538	-0.3043321
C	6	-2.6841014	-0.3150891	0.4674749
C	6	-2.0037113	1.6336447	-0.7764955
C	6	-3.3313368	2.0427185	-0.8661520
C	6	-4.0179606	0.0779681	0.3624964
H	1	-1.2045136	2.2184096	-1.2190578
H	1	-3.5725907	2.9644478	-1.3848655
H	1	-4.7879755	-0.5370791	0.8138943
H	1	-5.3782075	1.5643815	-0.3793295
Cl	17	-2.3101503	-1.7709206	1.3770394

Table 3-73. B3LYP/6-31G* Calculated IR Frequencies (cm^{-1}, uncorrected) and Intensities for HAPY-8_{anion}

	cm^{-1}	Intensity		cm^{-1}	Intensity		cm^{-1}	Intensity
1	12	7.91	**27**	673	60.24	**53**	1341	71.96
2	41	7.61	**28**	706	31.19	**54**	1398	137.72
3	70	10.73	**29**	723	1.59	**55**	1405	6.93
4	77	0.38	**30**	752	45.95	**56**	1428	14.34
5	130	16.54	**31**	769	51.50	**57**	1454	12.49
6	151	5.98	**32**	798	23.06	**58**	1477	19.15
7	162	6.04	**33**	851	29.97	**59**	1491	11.04
8	172	10.19	**34**	870	1.47	**60**	1495	23.05
9	192	13.06	**35**	914	56.87	**61**	1506	4.25
10	198	6.77	**36**	949	3.05	**62**	1527	139.31
11	239	4.20	**37**	961	78.64	**63**	1533	5.86
12	260	1.85	**38**	978	0.12	**64**	1628	9.56
13	269	2.89	**39**	1024	18.65	**65**	1643	31.55
14	285	7.60	**40**	1040	22.92	**66**	1664	119.52
15	306	6.00	**41**	1051	4.97	**67**	1688	408.66
16	333	12.67	**42**	1055	78.58	**68**	3058	39.31
17	349	11.50	**43**	1069	15.42	**69**	3060	22.44
18	402	7.51	**44**	1109	19.52	**70**	3100	120.02
19	442	24.33	**45**	1118	26.98	**71**	3117	13.39

20	460	4.71	**46**	1149	32.06	**72**	3130	12.27
21	486	7.53	**47**	1164	57.36	**73**	3139	34.33
22	534	17.23	**48**	1187	14.04	**74**	3163	11.16
23	554	78.09	**49**	1191	28.01	**75**	3216	7.50
24	581	39.70	**50**	1277	26.70	**76**	3228	6.54
25	614	12.72	**51**	1301	3.26	**77**	3239	11.18
26	653	32.07	**52**	1335	92.87	**78**	3247	4.88

Table 3-74. B3LYP/6-31G* Optimized Geometries, Energies, and Entropy Corrections for enol of PY-9

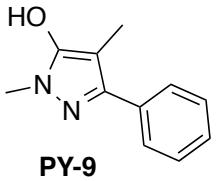

PY-9

B3LYP/6-31G* Energy (E): -611.119386 hartrees
Entropy Correction (Hv-TSv): 460.2285 kJ/mol
G° = E + "entropy correction": -383372.9175 kcal/mol

Atom	Atomic Number	Cartesian Coordinates (Angstroms) X	Y	Z
C	6	1.2279980	-0.5972430	0.4991380
C	6	2.4013577	0.1075204	0.2694476
N	7	2.1039122	1.2267176	-0.4360540
N	7	0.7658943	1.3160387	-0.6797098
C	6	0.2371656	0.2116743	-0.1255479
C	6	3.0174180	2.2813104	-0.8472432
H	1	2.6416284	2.7180891	-1.7726173
H	1	4.0051926	1.8525931	-1.0188724
H	1	3.0916560	3.0615029	-0.0835099
C	6	1.1030536	-1.8674621	1.2876683
H	1	1.1123806	-2.7673902	0.6595223
H	1	0.1767964	-1.8845898	1.8704190
H	1	1.9266650	-1.9656083	2.0053586
C	6	-1.2186751	-0.0085336	-0.2003982
C	6	-4.0079908	-0.3934044	-0.3544722
C	6	-1.7694665	-1.3008983	-0.2096477
C	6	-2.0956528	1.0882743	-0.2786995
C	6	-3.4724796	0.8973322	-0.3570598
C	6	-3.1498683	-1.4904623	-0.2825808
H	1	-4.1299724	1.7600045	-0.4136283
H	1	-3.5517949	-2.4992946	-0.2905957

H	1	-5.0823659	-0.5399752	-0.4100304
H	1	-1.1151326	-2.1651687	-0.1852482
H	1	-1.6785141	2.0898479	-0.2747765
O	8	3.6960940	-0.1133755	0.6334065
H	1	3.7647008	-1.0174995	0.9957315

Table 3-75. B3LYP/6-31G* Calculated IR Frequencies (cm^{-1}, uncorrected) and Intensities for enol of PY-9

	cm^{-1}	Intensity		cm^{-1}	Intensity		cm^{-1}	Intensity
1	47	0.88	**25**	791	21.17	**49**	1471	20.84
2	79	2.01	**26**	822	19.14	**50**	1480	38.19
3	81	3.96	**27**	861	0.65	**51**	1493	54.14
4	110	1.86	**28**	930	5.04	**52**	1511	36.13
5	133	12.86	**29**	969	0.76	**53**	1518	2.64
6	171	0.03	**30**	994	0.41	**54**	1528	24.11
7	197	95.33	**31**	1016	17.31	**55**	1530	9.66
8	224	36.49	**32**	1017	1.38	**56**	1557	11.27
9	254	1.91	**33**	1039	125.37	**57**	1566	156.26
10	271	10.77	**34**	1065	22.36	**58**	1611	122.58
11	295	5.48	**35**	1072	5.55	**59**	1640	13.01
12	327	8.54	**36**	1080	6.02	**60**	1665	10.27
13	331	4.50	**37**	1112	3.05	**61**	3046	57.58
14	391	0.88	**38**	1151	150.03	**62**	3088	77.89
15	419	0.08	**39**	1186	32.76	**63**	3097	35.82
16	513	4.33	**40**	1189	0.02	**64**	3124	24.91
17	576	12.15	**41**	1212	0.15	**65**	3168	13.03
18	614	6.99	**42**	1263	37.10	**66**	3201	3.39
19	633	0.17	**43**	1281	20.68	**67**	3202	4.58
20	660	0.54	**44**	1308	59.11	**68**	3209	11.43
21	672	19.80	**45**	1338	30.54	**69**	3221	38.19
22	712	19.17	**46**	1366	3.17	**70**	3227	41.21
23	719	33.13	**47**	1409	242.41	**71**	3234	13.79
24	747	27.00	**48**	1452	2.57	**72**	3686	233.62

Table 3-76. B3LYP/6-31G* Optimized Geometries, Energies, and Entropy Corrections for PY-9$_{anion}$

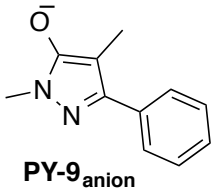

PY-9$_{anion}$

B3LYP/6-31G* Energy (E): -610.65229 hartrees
Entropy Correction (Hv-TSv): 427.8126 kJ/mol
G° = E + "entropy correction": -383087.5582 kcal/mol

Atom	Atomic Number	Cartesian Coordinates (Angstroms)		
		X	Y	Z
C	6	1.3873872	-0.6600497	0.4897516
C	6	2.6076012	0.0428783	0.3189587
N	7	2.2356149	1.2318268	-0.3061037
N	7	0.8880471	1.3234881	-0.5463574
C	6	0.3798171	0.1753032	-0.0567854
C	6	3.1283292	2.2806060	-0.7441372
H	1	3.1363312	2.3695207	-1.8367973
H	1	4.1297505	2.0210210	-0.3964293
H	1	2.8324021	3.2463104	-0.3212992
C	6	1.3116520	-1.9830485	1.1889925
H	1	1.1618477	-2.8371274	0.5105789
H	1	0.5066699	-2.0259792	1.9339693
H	1	2.2604707	-2.1597804	1.7102829
C	6	-1.0762991	-0.0387740	-0.1342891
C	6	-3.8784665	-0.4051650	-0.3002595
C	6	-1.6504389	-1.3191218	-0.0362381
C	6	-1.9455505	1.0541851	-0.3237955
C	6	-3.3230140	0.8732176	-0.4083032
C	6	-3.0324851	-1.4983433	-0.1151773
H	1	-3.9646119	1.7380241	-0.5528181
H	1	-3.4423410	-2.5012523	-0.0365185
H	1	-4.9535061	-0.5446702	-0.3605654
H	1	-1.0055811	-2.1815766	0.0867416
H	1	-1.5096619	2.0447466	-0.4012644
O	8	3.8160354	-0.2462400	0.6378631

Table 3-77. B3LYP/6-31G* Calculated IR Frequencies (cm^{-1}, uncorrected) and Intensities for PY-9_{anion}

	cm^{-1}	Intensity		cm^{-1}	Intensity		cm^{-1}	Intensity
1	1	1.15	**24**	786	19.28	**47**	1450	183.48
2	76	0.82	**25**	846	9.80	**48**	1462	7.39
3	92	3.36	**26**	858	0.38	**49**	1480	1.45
4	110	0.58	**27**	922	4.26	**50**	1500	92.30
5	126	1.88	**28**	961	0.77	**51**	1511	351.61
6	142	7.47	**29**	981	0.42	**52**	1522	5.39
7	200	0.46	**30**	1003	16.69	**53**	1530	26.04
8	254	0.57	**31**	1015	3.27	**54**	1544	1.76
9	274	10.12	**32**	1032	29.67	**55**	1558	34.52
10	284	10.15	**33**	1045	38.75	**56**	1570	609.40
11	330	21.56	**34**	1062	6.26	**57**	1633	1.82
12	343	2.74	**35**	1063	9.58	**58**	1660	28.89
13	379	6.84	**36**	1107	8.28	**59**	3008	142.59
14	419	0.11	**37**	1181	0.15	**60**	3048	49.14
15	514	1.44	**38**	1188	2.26	**61**	3059	167.43
16	575	29.13	**39**	1206	8.54	**62**	3095	49.50
17	632	0.25	**40**	1220	59.81	**63**	3117	44.87
18	641	5.76	**41**	1279	79.65	**64**	3176	8.26
19	673	26.18	**42**	1293	67.68	**65**	3200	6.32
20	684	6.66	**43**	1334	12.97	**66**	3208	11.91
21	708	28.16	**44**	1364	0.31	**67**	3220	32.72
22	741	30.66	**45**	1388	74.48	**68**	3227	47.41
23	770	34.57	**46**	1426	47.60	**69**	3236	19.36

Table 3-78. B3LYP/6-31G* Optimized Geometries, Energies, and Entropy Corrections for HAPY-9

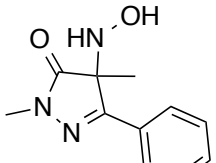

HAPY-9

B3LYP/6-31G* Energy (E): -741.63449 hartrees
Entropy Correction (Hv-TSv): 512.2117 kJ/mol
G° = E + "entropy correction": -465259.8957 kcal/mol

Atom	Atomic Number	Cartesian Coordinates (Angstroms) X	Y	Z
C	6	1.0125600	-0.6692558	0.2153561
C	6	2.2888911	0.1852619	0.1244898
N	7	1.8650175	1.4731938	-0.0042953
N	7	0.4813263	1.5965305	-0.0566489
C	6	-0.0506499	0.4161510	0.0453318
O	8	3.4623994	-0.2001839	0.1589396
C	6	2.6909867	2.6592805	-0.1446975
H	1	2.5273393	3.1264055	-1.1192492
H	1	3.7319206	2.3478749	-0.0583799
H	1	2.4552136	3.3790341	0.6425725
C	6	0.9685895	-1.3720509	1.5822995
H	1	1.8616314	-1.9893731	1.6969529
H	1	0.0870029	-2.0093915	1.6773197
H	1	0.9429793	-0.6355219	2.3916157
N	7	1.0024272	-1.5491405	-0.9795268
H	1	0.0837359	-1.9931988	-1.0413619
O	8	1.8786507	-2.6809718	-0.7545329
H	1	2.6695788	-2.4413727	-1.2667492
C	6	-1.5097912	0.2501149	0.0075625
C	6	-4.3131036	-0.0041323	-0.0819019
C	6	-2.1250484	-1.0059323	0.1494981
C	6	-2.3317816	1.3800373	-0.1813970
C	6	-3.7137825	1.2521718	-0.2237262
C	6	-3.5137396	-1.1300527	0.1029770
H	1	-4.3281243	2.1353549	-0.3693306
H	1	-3.9660717	-2.1102211	0.2153978
H	1	-5.3937440	-0.1003443	-0.1163385
H	1	-1.5285805	-1.8968204	0.3074828
H	1	-1.8661609	2.3525189	-0.2936337

Table 3-79. B3LYP/6-31G* Calculated IR Frequencies (cm^{-1}, uncorrected) and Intensities for HAPY-9

	cm^{-1}	Intensity		cm^{-1}	Intensity		cm^{-1}	Intensity
1	29	0.39	**28**	760	20.04	**55**	1430	20.23
2	62	3.14	**29**	789	18.32	**56**	1438	140.57
3	79	1.65	**30**	815	31.56	**57**	1472	11.39
4	100	0.67	**31**	861	0.64	**58**	1490	7.37
5	105	0.20	**32**	884	34.06	**59**	1511	8.02
6	143	0.81	**33**	940	36.34	**60**	1515	12.53
7	157	2.20	**34**	942	5.86	**61**	1517	8.48
8	183	0.44	**35**	968	37.31	**62**	1526	10.90

9	223	1.18	**36**	980	0.71	**63**	1539	43.71
10	255	2.56	**37**	1006	0.88	**64**	1545	1.46
11	266	6.62	**38**	1017	5.32	**65**	1603	48.55
12	279	3.37	**39**	1025	65.12	**66**	1640	3.62
13	310	11.46	**40**	1033	11.63	**67**	1662	1.22
14	320	3.11	**41**	1062	4.10	**68**	1681	795.96
15	340	9.81	**42**	1064	135.20	**69**	3085	16.47
16	354	7.95	**43**	1119	5.91	**70**	3090	70.78
17	416	0.28	**44**	1130	10.54	**71**	3157	18.45
18	422	23.86	**45**	1176	2.86	**72**	3161	15.35
19	448	147.96	**46**	1194	4.76	**73**	3178	19.31
20	498	3.47	**47**	1195	20.31	**74**	3198	2.19
21	614	54.69	**48**	1218	4.14	**75**	3208	1.03
22	629	2.34	**49**	1247	59.82	**76**	3216	13.54
23	653	18.67	**50**	1263	116.76	**77**	3227	38.36
24	665	49.07	**51**	1336	71.94	**78**	3237	30.74
25	674	16.46	**52**	1357	77.75	**79**	3240	9.05
26	707	40.21	**53**	1371	7.72	**80**	3467	32.15
27	745	27.03	**54**	1383	90.70	**81**	3722	110.52

Table 3-80. B3LYP/6-31G* Optimized Geometries, Energies, and Entropy Corrections for HAPY-9$_{anion}$

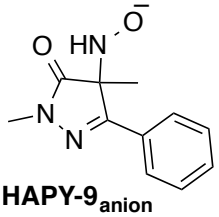

HAPY-9$_{anion}$

B3LYP/6-31G* Energy (E): -741.126974 hartrees
Entropy Correction (Hv-TSv): 474.0132 kJ/mol
G° = E + "entropy correction": -464950.5545 kcal/mol

Atom	Atomic Number	Cartesian Coordinates (Angstroms) X	Y	Z
C	6	1.2764962	-0.7474886	0.1782950
C	6	2.5265486	0.1224540	0.1656210
N	7	2.1171916	1.3534442	-0.2534907
N	7	0.7397602	1.4532432	-0.3931339
C	6	0.2169947	0.2958418	-0.1071504
O	8	3.6894455	-0.1837435	0.4594785
C	6	2.9359409	2.5369040	-0.4460429
H	1	2.8715108	2.8824925	-1.4814572
H	1	3.9658407	2.2641707	-0.2148596

H	1	2.6069866	3.3381188	0.2207626
C	6	1.1497547	-1.5371552	1.4763380
H	1	1.8133722	-2.4036164	1.3724180
H	1	0.1265930	-1.8819308	1.6430550
H	1	1.4525048	-0.9490498	2.3494737
N	7	1.4101965	-1.6521582	-1.0980736
H	1	0.4570413	-2.0649519	-1.1307571
O	8	2.3126587	-2.7060934	-0.8801456
C	6	-1.2432139	0.1325789	-0.1335099
C	6	-4.0521725	-0.1135134	-0.1959353
C	6	-1.8589997	-1.1309869	-0.0905173
C	6	-2.0694527	1.2729757	-0.2037348
C	6	-3.4533379	1.1496905	-0.2367667
C	6	-3.2485835	-1.2504401	-0.1242023
H	1	-4.0672163	2.0436126	-0.2894513
H	1	-3.6955463	-2.2394061	-0.0941441
H	1	-5.1332434	-0.2088874	-0.2178957
H	1	-1.2474177	-2.0258434	-0.0452331
H	1	-1.5996532	2.2497380	-0.2289403

Table 3-81. B3LYP/6-31G* Calculated IR Frequencies (cm^{-1}, uncorrected) and Intensities for HAPY-9_{anion}

	cm^{-1}	Intensity		cm^{-1}	Intensity		cm^{-1}	Intensity
1	47	4.15	**27**	755	30.53	**53**	1406	38.11
2	74	7.31	**28**	779	41.54	**54**	1421	35.94
3	81	4.74	**29**	802	26.73	**55**	1450	60.70
4	95	5.86	**30**	839	17.72	**56**	1470	29.72
5	107	6.44	**31**	860	0.01	**57**	1486	5.84
6	130	8.06	**32**	938	3.62	**58**	1508	2.33
7	152	7.60	**33**	955	108.59	**59**	1514	9.40
8	179	15.28	**34**	974	87.76	**60**	1535	2.40
9	214	4.73	**35**	975	27.71	**61**	1539	38.46
10	252	6.49	**36**	989	1.56	**62**	1544	7.73
11	263	6.51	**37**	1016	1.41	**63**	1592	67.38
12	277	4.43	**38**	1030	54.48	**64**	1637	3.13
13	303	11.82	**39**	1035	7.56	**65**	1660	7.84
14	320	21.60	**40**	1061	49.67	**66**	1674	755.80
15	350	1.39	**41**	1063	9.44	**67**	3051	56.49
16	354	13.33	**42**	1111	30.58	**68**	3086	94.21
17	407	22.28	**43**	1116	4.88	**69**	3119	9.41
18	418	0.14	**44**	1170	2.05	**70**	3152	79.69
19	495	31.91	**45**	1187	0.09	**71**	3156	18.29
20	551	169.96	**46**	1204	19.59	**72**	3158	44.21

21	606	53.37	**47**	1216	0.40	**73**	3195	3.30
22	630	2.32	**48**	1257	90.64	**74**	3203	8.21
23	649	15.82	**49**	1268	72.49	**75**	3212	0.20
24	663	33.94	**50**	1336	41.51	**76**	3219	36.89
25	706	25.65	**51**	1362	105.34	**77**	3231	33.54
26	710	54.56	**52**	1370	37.73	**78**	3239	15.47

Table 3-82. B3LYP/6-31G* Optimized Geometries, Energies, and Entropy Corrections for enol of PY-10

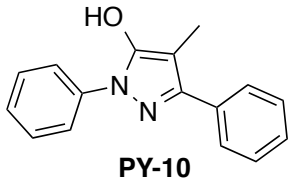

PY-10

B3LYP/6-31G* Energy (E): -802.857405 hartrees
Entropy Correction (Hv-TSv): 591.8378 kJ/mol
G° = E + "entropy correction": -503658.7947 kcal/mol

Atom	Atomic Number	Cartesian Coordinates (Angstroms) X	Y	Z
C	6	0.6190253	-1.5419797	-0.4078239
C	6	-0.7627205	-1.5676442	-0.3403067
N	7	-1.2101896	-0.3088748	-0.0367705
N	7	-0.1536048	0.5523998	0.1129437
C	6	0.9405550	-0.1864878	-0.1083434
C	6	1.5006064	-2.6963825	-0.7842054
H	1	0.9598387	-3.4141770	-1.4124238
H	1	1.8810409	-3.2458470	0.0859163
H	1	2.3647230	-2.3610609	-1.3655826
C	6	2.2664195	0.4566920	-0.0613719
C	6	4.7831802	1.7181873	0.0323677
C	6	3.4134765	-0.2538861	0.3290590
C	6	2.4035742	1.8152623	-0.3970127
C	6	3.6478726	2.4379771	-0.3494189
C	6	4.6598900	0.3714472	0.3733615
H	1	3.7322454	3.4871297	-0.6172362
H	1	5.5328870	-0.1954986	0.6823726
H	1	3.3283444	-1.2938586	0.6241404
H	1	1.5213391	2.3701210	-0.6986160
H	1	5.7530943	2.2050815	0.0642763
C	6	-2.5372962	0.1459544	0.2047603
C	6	-5.1230323	1.0886885	0.7023162
C	6	-2.7344581	1.2177707	1.0838086

C	6	-3.6313975	-0.4472634	-0.4355218
C	6	-4.9182968	0.0237368	-0.1744576
C	6	-4.0244075	1.6852435	1.3241675
H	1	-1.8744415	1.6717303	1.5608996
H	1	-3.4790075	-1.2640530	-1.1284014
H	1	-5.7619109	-0.4436996	-0.6728570
H	1	-4.1673822	2.5163474	2.0078957
H	1	-6.1265651	1.4526225	0.8979332
O	8	-1.6503479	-2.5780193	-0.5216694
H	1	-1.1530541	-3.4176595	-0.5741992

Table 3-83. B3LYP/6-31G* Calculated IR Frequencies (cm^{-1}, uncorrected) and Intensities for enol of PY-10

	cm^{-1}	Intensity		cm^{-1}	Intensity		cm^{-1}	Intensity
1	33	0.21	**32**	775	46.75	**63**	1366	6.51
2	37	1.16	**33**	785	2.99	**64**	1370	5.28
3	64	7.57	**34**	794	30.19	**65**	1413	405.59
4	71	0.70	**35**	853	0.55	**66**	1450	1.55
5	91	0.44	**36**	861	0.82	**67**	1482	41.49
6	145	2.02	**37**	927	5.59	**68**	1486	76.62
7	156	0.37	**38**	933	4.54	**69**	1495	64.93
8	186	2.61	**39**	969	1.18	**70**	1512	18.32
9	241	89.46	**40**	971	0.54	**71**	1520	3.40
10	249	34.21	**41**	981	83.63	**72**	1532	101.95
11	261	1.79	**42**	994	0.32	**73**	1551	213.65
12	272	4.47	**43**	996	0.29	**74**	1560	7.10
13	304	21.66	**44**	1017	1.11	**75**	1611	224.36
14	311	1.79	**45**	1019	0.06	**76**	1641	18.21
15	343	4.61	**46**	1032	49.91	**77**	1651	32.05
16	397	11.68	**47**	1057	11.15	**78**	1660	80.33
17	418	0.03	**48**	1066	9.39	**79**	1665	2.02
18	420	1.18	**49**	1073	0.86	**80**	3048	55.86
19	431	1.74	**50**	1102	94.39	**81**	3099	31.57
20	500	5.30	**51**	1112	3.01	**82**	3129	20.36
21	530	5.37	**52**	1115	20.28	**83**	3202	3.89
22	627	24.00	**53**	1146	67.51	**84**	3209	1.06
23	629	3.79	**54**	1190	0.98	**85**	3209	9.29
24	633	1.09	**55**	1192	0.08	**86**	3218	22.75
25	648	6.75	**56**	1211	13.44	**87**	3220	31.39
26	664	2.78	**57**	1212	1.78	**88**	3227	44.42
27	684	10.88	**58**	1224	95.98	**89**	3230	36.73
28	706	23.97	**59**	1266	36.12	**90**	3235	14.81
29	712	36.75	**60**	1322	42.29	**91**	3246	4.83
30	721	13.62	**61**	1338	40.01	**92**	3263	1.62

31	749	54.81	**62**	1358	42.80	**93**	3678	247.95

Table 3-84. B3LYP/6-31G* Optimized Geometries, Energies, and Entropy Corrections for PY-10$_{anion}$

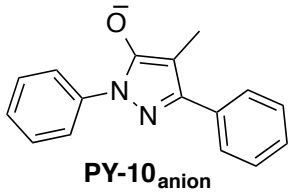

PY-10$_{anion}$

B3LYP/6-31G* Energy (E): -802.396021 hartrees
Entropy Correction (Hv-TSv): 559.9689 kJ/mol
G° = E + "entropy correction": -503376.889 kcal/mol

Atom	Atomic Number	Cartesian Coordinates (Angstroms) X	Y	Z
C	6	0.5877823	-1.6487395	-0.5006172
C	6	-0.8220144	-1.7396280	-0.4572379
N	7	-1.2498622	-0.4490629	-0.0484478
N	7	-0.1831551	0.4068535	0.1546939
C	6	0.9086299	-0.3221948	-0.1225465
C	6	1.4466011	-2.7899562	-0.9539548
H	1	0.8112985	-3.5315763	-1.4526901
H	1	1.9573597	-3.3145024	-0.1321617
H	1	2.2231495	-2.4776978	-1.6633283
C	6	2.2291824	0.3272171	-0.0217897
C	6	4.7393409	1.6118817	0.1782162
C	6	3.4130714	-0.4144293	0.1366930
C	6	2.3341554	1.7307083	-0.0720907
C	6	3.5701037	2.3630683	0.0288553
C	6	4.6521531	0.2210286	0.2327917
H	1	3.6185338	3.4474429	-0.0162790
H	1	5.5484665	-0.3797918	0.3568734
H	1	3.3588974	-1.4950530	0.2021845
H	1	1.4237230	2.3078141	-0.1948343
H	1	5.7032688	2.1060004	0.2516160
C	6	-2.5586502	0.0282472	0.1754316
C	6	-5.1533108	1.0400719	0.6278965
C	6	-2.7455969	1.3419436	0.6438939
C	6	-3.6893078	-0.7742876	-0.0635151
C	6	-4.9668576	-0.2626744	0.1644642
C	6	-4.0294093	1.8344226	0.8645367
H	1	-1.8710045	1.9536050	0.8256370
H	1	-3.5379165	-1.7834009	-0.4216525

H	1	-5.8227922	-0.9035756	-0.0287253
H	1	-4.1445891	2.8521298	1.2269159
H	1	-6.1517268	1.4282331	0.8020086
O	8	-1.5995240	-2.7140975	-0.7228374

Table 3-85. B3LYP/6-31G* Calculated IR Frequencies (cm^{-1}, uncorrected) and Intensities for PY-10_{anion}

	cm^{-1}	Intensity		cm^{-1}	Intensity		cm^{-1}	Intensity
1	23	0.02	**31**	767	78.68	**61**	1358	85.32
2	30	1.13	**32**	787	25.05	**62**	1364	25.98
3	56	3.46	**33**	807	0.83	**63**	1366	33.17
4	80	3.31	**34**	855	0.02	**64**	1431	68.17
5	90	2.46	**35**	859	0.65	**65**	1461	127.51
6	165	2.61	**36**	907	4.90	**66**	1482	6.70
7	182	2.19	**37**	927	3.99	**67**	1496	77.64
8	192	0.87	**38**	962	0.13	**68**	1515	18.17
9	241	0.42	**39**	965	2.04	**69**	1518	379.82
10	264	5.04	**40**	977	54.29	**70**	1534	36.86
11	265	1.94	**41**	978	12.57	**71**	1536	364.43
12	287	1.61	**42**	983	1.00	**72**	1560	47.56
13	325	26.81	**43**	1014	9.71	**73**	1592	582.92
14	361	2.42	**44**	1016	0.34	**74**	1634	14.54
15	395	10.61	**45**	1027	70.91	**75**	1639	40.39
16	416	4.75	**46**	1056	3.08	**76**	1656	287.35
17	419	0.42	**47**	1063	5.42	**77**	1662	5.37
18	420	0.86	**48**	1073	1.64	**78**	3016	146.13
19	508	4.23	**49**	1095	12.10	**79**	3069	46.62
20	531	3.06	**50**	1106	38.44	**80**	3105	41.48
21	629	19.03	**51**	1112	37.47	**81**	3202	14.01
22	633	0.16	**52**	1162	39.01	**82**	3203	0.48
23	635	16.90	**53**	1179	0.98	**83**	3208	32.52
24	671	13.25	**54**	1184	0.10	**84**	3210	13.70
25	682	11.48	**55**	1198	21.34	**85**	3222	31.88
26	689	19.35	**56**	1208	3.84	**86**	3228	42.54
27	704	10.82	**57**	1228	108.56	**87**	3230	32.71
28	709	25.68	**58**	1312	7.95	**88**	3237	20.69
29	734	30.88	**59**	1336	70.24	**89**	3250	5.94
30	761	51.57	**60**	1339	384.45	**90**	3251	11.55

Table 3-86. B3LYP/6-31G* Optimized Geometries, Energies, and Entropy Corrections for HAPY-10

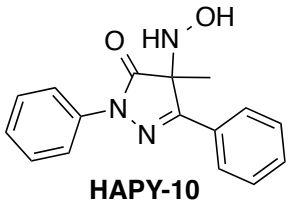

HAPY-10

B3LYP/6-31G* Energy (E): -933.372296 hartrees
Entropy Correction (Hv-TSv): 642.0662 kJ/mol
G° = E + "entropy correction": -585546.0586 kcal/mol

Atom	Atomic Number	Cartesian Coordinates (Angstroms) X	Y	Z
C	6	0.6850904	-1.4545779	-0.2182886
C	6	-0.8513867	-1.4496239	-0.1897632
N	7	-1.2322829	-0.1256317	-0.1167440
N	7	-0.1319754	0.7339636	-0.0702362
C	6	0.9628826	0.0406611	-0.1070471
O	8	-1.5872908	-2.4352332	-0.2214676
C	6	1.1636317	-2.0868864	-1.5354078
H	1	0.7536342	-3.0951320	-1.6183335
H	1	2.2527805	-2.1473983	-1.5798884
H	1	0.8204587	-1.4957583	-2.3903047
N	7	1.1245847	-2.1166907	1.0346444
H	1	2.1285027	-1.9586819	1.1440246
O	8	1.0462816	-3.5529657	0.8786509
H	1	0.2487414	-3.7790549	1.3868325
C	6	2.2684791	0.7128273	-0.0503085
C	6	4.7395962	2.0551694	0.0855368
C	6	3.4796683	0.0026086	-0.1220755
C	6	2.3217714	2.1146356	0.0918799
C	6	3.5417087	2.7744032	0.1564857
C	6	4.7028734	0.6695156	-0.0531301
H	1	3.5605634	3.8543372	0.2654562
H	1	5.6249166	0.1001397	-0.1112976
H	1	3.4826797	-1.0742238	-0.2419299
H	1	1.3941304	2.6718797	0.1519862
H	1	5.6912117	2.5746515	0.1384401
C	6	-2.5355596	0.4408332	-0.0386223
C	6	-5.0806281	1.6034625	0.1264071
C	6	-2.6679045	1.8290255	0.1069274
C	6	-3.6806154	-0.3670378	-0.1039676
C	6	-4.9411877	0.2236066	-0.0203399
C	6	-3.9361121	2.3990698	0.1882407

H	1	-1.7800972	2.4447934	0.1559613
H	1	-3.5787873	-1.4369623	-0.2152150
H	1	-5.8199457	-0.4121162	-0.0713553
H	1	-4.0236929	3.4752117	0.3022628
H	1	-6.0666718	2.0520643	0.1911934

Table 3-87. B3LYP/6-31G* Calculated IR Frequencies (cm^{-1}, uncorrected) and Intensities for HAPY-10

	cm^{-1}	Intensity		cm^{-1}	Intensity		cm^{-1}	Intensity
1	18	0.15	**35**	760	20.39	**69**	1356	10.14
2	34	1.10	**36**	775	60.41	**70**	1365	32.57
3	49	1.51	**37**	790	14.26	**71**	1370	2.08
4	68	1.22	**38**	803	31.92	**72**	1375	98.29
5	78	0.35	**39**	858	0.20	**73**	1412	195.60
6	99	4.89	**40**	859	0.49	**74**	1430	15.55
7	120	0.25	**41**	884	46.68	**75**	1492	7.80
8	165	4.60	**42**	901	26.37	**76**	1504	4.37
9	187	10.66	**43**	929	5.12	**77**	1507	16.11
10	215	12.99	**44**	943	3.40	**78**	1513	3.99
11	232	2.28	**45**	952	42.81	**79**	1525	18.14
12	253	45.76	**46**	976	0.04	**80**	1541	203.93
13	260	10.32	**47**	980	0.52	**81**	1546	21.97
14	264	0.32	**48**	999	0.76	**82**	1612	48.12
15	277	37.31	**49**	1007	0.75	**83**	1639	2.64
16	303	52.80	**50**	1015	3.39	**84**	1649	19.73
17	329	9.01	**51**	1017	24.37	**85**	1658	105.97
18	346	21.08	**52**	1018	10.46	**86**	1663	2.26
19	373	0.49	**53**	1023	48.25	**87**	1700	678.40
20	411	6.84	**54**	1060	5.25	**88**	3084	14.02
21	415	0.03	**55**	1063	4.99	**89**	3157	17.73
22	419	0.07	**56**	1101	53.68	**90**	3177	17.63
23	495	2.25	**57**	1113	34.32	**91**	3208	2.99
24	501	15.13	**58**	1119	2.52	**92**	3208	1.33
25	531	3.25	**59**	1141	28.12	**93**	3216	26.99
26	631	2.62	**60**	1170	162.37	**94**	3217	10.55
27	631	1.05	**61**	1190	0.54	**95**	3227	36.18
28	638	37.52	**62**	1196	0.03	**96**	3230	34.23
29	674	24.42	**63**	1198	67.28	**97**	3236	31.94
30	675	11.16	**64**	1212	4.62	**98**	3239	8.30
31	681	61.98	**65**	1219	1.50	**99**	3263	0.96
32	705	35.67	**66**	1254	81.02	**100**	3272	3.90
33	708	17.94	**67**	1323	250.44	**101**	3467	31.71
34	741	23.21	**68**	1349	62.33	**102**	3721	111.77

Table 3-88. B3LYP/6-31G* Optimized Geometries, Energies, and Entropy Corrections for HAPY-10$_{anion}$

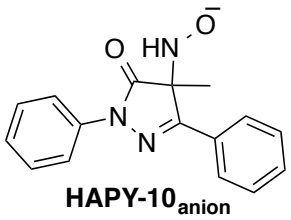

HAPY-10$_{anion}$

B3LYP/6-31G* Energy (E): -932.875214 hartrees
Entropy Correction (Hv-TSv): 598.8653 kJ/mol
G° = E + "entropy correction": Not a ground state structure; HNO is dissociated

Atom	Atomic Number	Cartesian Coordinates (Angstroms) X	Y	Z
C	6	0.6208385	-1.2860540	0.6656423
C	6	-0.8112153	-1.3671016	0.6841239
N	7	-1.2444588	-0.0938899	0.2585264
N	7	-0.1771051	0.7648798	0.0290382
C	6	0.9193137	0.0612257	0.2928946
O	8	-1.5620971	-2.3170827	1.0284011
N	7	0.6796230	-2.1687163	-1.6363697
H	1	1.1648782	-1.2484115	-1.8398544
O	8	1.5486646	-3.0650790	-1.6038462
C	6	-2.5582049	0.3835152	0.0503369
C	6	-5.1541459	1.3879612	-0.3792844
C	6	-3.6778669	-0.4515827	0.2084836
C	6	-2.7524241	1.7240395	-0.3259289
C	6	-4.0391680	2.2132490	-0.5371203
C	6	-4.9584101	0.0578721	-0.0067834
H	1	-3.5230971	-1.4813578	0.4989275
H	1	-1.8843208	2.3586941	-0.4496016
H	1	-4.1637464	3.2522055	-0.8286242
H	1	-5.8084707	-0.6065086	0.1208261
H	1	-6.1549597	1.7735803	-0.5451710
C	6	1.4940225	-2.3292042	1.2652167
H	1	2.3282155	-1.8969897	1.8276544
H	1	1.9223784	-2.9959827	0.4916114
H	1	0.9073198	-2.9630433	1.9403888
C	6	2.2425797	0.6976480	0.1675166
C	6	4.7643040	1.9264876	-0.0846158
C	6	2.3955678	2.0779643	0.3881807
C	6	3.3758414	-0.0546104	-0.1893711
C	6	4.6238540	0.5571211	-0.3127798
C	6	3.6426168	2.6846743	0.2625202

H	1	1.5199800	2.6572093	0.6622742
H	1	3.2684785	-1.1150869	-0.3976961
H	1	5.4839347	-0.0429939	-0.5949038
H	1	3.7383065	3.7514281	0.4426956
H	1	5.7371308	2.3994048	-0.1775215

Table 3-89. B3LYP/6-31G* Calculated IR Frequencies (cm^{-1}, uncorrected) and Intensities for HAPY-10_{anion}

	cm^{-1}	Intensity		cm^{-1}	Intensity		cm^{-1}	Intensity
1	24	0.20	**34**	714	24.95	**67**	1359	663.49
2	37	2.61	**35**	740	68.67	**68**	1366	359.05
3	40	4.61	**36**	764	54.79	**69**	1372	10.15
4	59	0.68	**37**	772	104.57	**70**	1379	472.29
5	68	2.60	**38**	786	25.83	**71**	1454	146.69
6	91	4.47	**39**	808	2.19	**72**	1473	22.88
7	116	7.08	**40**	856	0.05	**73**	1487	20.82
8	140	36.06	**41**	867	1.00	**74**	1499	7.83
9	159	5.47	**42**	912	4.68	**75**	1510	32.03
10	168	7.33	**43**	939	5.26	**76**	1527	172.23
11	209	5.17	**44**	966	0.04	**77**	1536	16.13
12	225	1.57	**45**	971	101.83	**78**	1539	306.12
13	244	6.36	**46**	976	7.07	**79**	1550	97.27
14	262	4.18	**47**	981	1.02	**80**	1560	19.45
15	268	7.48	**48**	994	5.65	**81**	1604	697.37
16	287	99.77	**49**	1015	6.73	**82**	1636	5.62
17	324	18.20	**50**	1016	0.35	**83**	1640	56.14
18	332	2.43	**51**	1032	78.78	**84**	1658	250.28
19	379	2.93	**52**	1058	3.62	**85**	1663	8.35
20	394	8.37	**53**	1065	14.28	**86**	2937	117.92
21	420	0.25	**54**	1079	105.37	**87**	2951	70.12
22	420	0.26	**55**	1096	15.59	**88**	3077	54.72
23	445	2.59	**56**	1110	29.61	**89**	3126	30.43
24	509	5.55	**57**	1120	53.45	**90**	3198	4.91
25	528	5.55	**58**	1152	33.70	**91**	3203	8.56
26	631	6.30	**59**	1181	0.25	**92**	3206	0.82
27	631	0.21	**60**	1185	0.52	**93**	3210	31.51
28	637	29.34	**61**	1203	8.34	**94**	3214	20.24
29	666	44.84	**62**	1215	0.47	**95**	3222	45.41
30	679	34.67	**63**	1233	105.36	**96**	3228	35.64
31	684	26.18	**64**	1325	165.56	**97**	3231	30.28
32	697	7.33	**65**	1339	34.94	**98**	3253	3.93
33	705	11.43	**66**	1344	178.07	**99**	3258	8.56

Table 3-90. B3LYP/6-31G* Optimized Geometries, Energies, and Entropy Corrections for enol of PY-11

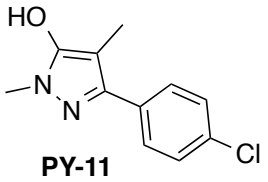

PY-11

B3LYP/6-31G* Energy (E): -1070.715916 hartrees
Entropy Correction (Hv-TSv): 430.195 kJ/mol
G° = E + "entropy correction": -671781.0547 kcal/mol

Atom	Atomic Number	Cartesian Coordinates (Angstroms) X	Y	Z
C	6	1.2518005	-0.5980621	0.5122775
C	6	2.4249337	0.1091910	0.2888789
N	7	2.1298133	1.2256819	-0.4223208
N	7	0.7950345	1.3109130	-0.6762665
C	6	0.2645184	0.2071882	-0.1224044
C	6	3.0448283	2.2802394	-0.8311217
H	1	2.6728788	2.7153555	-1.7587098
H	1	4.0334008	1.8514617	-0.9975443
H	1	3.1152361	3.0612414	-0.0679351
C	6	1.1243018	-1.8658631	1.3041563
H	1	1.1179793	-2.7666788	0.6773598
H	1	0.2065188	-1.8733620	1.9004758
H	1	1.9560881	-1.9707971	2.0110970
C	6	-1.1898147	-0.0102012	-0.2084521
C	6	-3.9619952	-0.3771073	-0.3807061
C	6	-1.7523254	-1.2966452	-0.1777530
C	6	-2.0587659	1.0877278	-0.3387105
C	6	-3.4361190	0.9134118	-0.4270946
C	6	-3.1317532	-1.4872732	-0.2593203
H	1	-4.0953446	1.7688897	-0.5225919
H	1	-3.5524999	-2.4864577	-0.2368829
H	1	-1.1117487	-2.1683842	-0.1125449
H	1	-1.6395924	2.0874155	-0.3676247
Cl	17	-5.7125828	-0.6030888	-0.4773068
O	8	3.7175608	-0.1062282	0.6623692
H	1	3.7876485	-1.0085682	1.0286761

Table 3-91. B3LYP/6-31G* Calculated IR Frequencies (cm^{-1}, uncorrected) and Intensities for enol of PY-11

	cm^{-1}	Intensity		cm^{-1}	Intensity		cm^{-1}	Intensity
1	41	1.01	**25**	715	9.45	**49**	1448	46.20
2	54	0.62	**26**	743	12.97	**50**	1454	23.81
3	78	1.60	**27**	749	44.35	**51**	1472	29.57
4	87	0.88	**28**	823	12.10	**52**	1480	98.96
5	133	11.68	**29**	837	6.80	**53**	1510	34.40
6	150	9.99	**30**	851	42.41	**54**	1518	2.61
7	174	1.03	**31**	955	1.68	**55**	1527	29.72
8	201	116.27	**32**	975	0.34	**56**	1530	14.29
9	227	1.99	**33**	1016	25.42	**57**	1550	51.29
10	238	9.56	**34**	1024	106.41	**58**	1565	154.50
11	275	8.15	**35**	1046	93.02	**59**	1605	95.89
12	283	5.76	**36**	1073	7.58	**60**	1631	43.34
13	296	10.72	**37**	1080	6.90	**61**	1651	1.59
14	319	2.78	**38**	1097	91.83	**62**	3046	54.73
15	359	1.13	**39**	1139	7.00	**63**	3089	77.45
16	409	1.67	**40**	1150	137.82	**64**	3098	35.21
17	422	0.16	**41**	1185	31.01	**65**	3124	25.08
18	481	61.39	**42**	1209	0.09	**66**	3168	12.52
19	519	10.82	**43**	1264	44.87	**67**	3202	4.21
20	578	3.72	**44**	1281	18.84	**68**	3226	4.77
21	612	4.57	**45**	1308	55.33	**69**	3231	3.34
22	644	1.23	**46**	1331	15.20	**70**	3240	10.53
23	661	0.51	**47**	1337	17.37	**71**	3245	5.00
24	706	2.80	**48**	1402	203.52	**72**	3687	230.58

Table 3-92. B3LYP/6-31G* Optimized Geometries, Energies, and Entropy Corrections for PY-11_{anion}

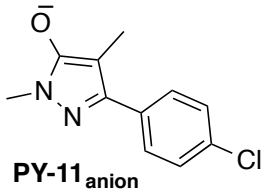

PY-11_{anion}

B3LYP/6-31G* Energy (E): -1070.249995 hartrees
Entropy Correction (Hv-TSv): 400.0009 kJ/mol
G° = E + "entropy correction": -671495.9016 kcal/mol

Atom	Atomic Number	Cartesian Coordinates (Angstroms) X	Y	Z
C	6	1.4250965	-0.6924571	0.4543984
C	6	2.6377142	0.0309382	0.3114764
N	7	2.2488660	1.2493368	-0.2427793
N	7	0.9009310	1.3453544	-0.4538949
C	6	0.4038333	0.1659918	-0.0304670
C	6	3.1195936	2.3547442	-0.5736850
H	1	3.0771841	2.5854211	-1.6439065
H	1	4.1352147	2.0593725	-0.3052537
H	1	2.8412982	3.2551339	-0.0152845
C	6	1.3870493	-2.0765982	1.0287998
H	1	1.0197794	-2.8348430	0.3224716
H	1	0.7681769	-2.1570887	1.9333641
H	1	2.4079439	-2.3635767	1.3073333
C	6	-1.0509396	-0.0421594	-0.1247114
C	6	-3.8398327	-0.3695892	-0.3197644
C	6	-1.6754536	-1.2409101	0.2635885
C	6	-1.8787253	0.9869129	-0.6192540
C	6	-3.2564871	0.8332999	-0.7189639
C	6	-3.0576782	-1.4097020	0.1703812
H	1	-3.8721947	1.6399439	-1.1017165
H	1	-3.5162460	-2.3430436	0.4784494
H	1	-1.0788006	-2.0590494	0.6460662
H	1	-1.4123823	1.9169838	-0.9243198
Cl	17	-5.5872521	-0.5684468	-0.4350212
O	8	3.8533111	-0.2659694	0.5926930

Table 3-93. B3LYP/6-31G* Calculated IR Frequencies (cm^{-1}, uncorrected) and Intensities for PY-11_{anion}

	cm^{-1}	Intensity		cm^{-1}	Intensity		cm^{-1}	Intensity
1	20	0.17	**24**	721	0.37	**47**	1423	79.97
2	53	0.16	**25**	748	24.25	**48**	1438	17.32
3	57	1.08	**26**	776	35.56	**49**	1455	42.29
4	108	0.20	**27**	835	4.52	**50**	1461	81.02
5	122	12.91	**28**	848	17.85	**51**	1504	534.06
6	139	0.05	**29**	850	34.38	**52**	1517	5.80
7	235	0.56	**30**	951	0.02	**53**	1525	20.50
8	238	0.38	**31**	976	0.14	**54**	1530	3.65
9	250	0.74	**32**	1014	60.33	**55**	1541	16.93
10	255	12.33	**33**	1025	13.09	**56**	1554	54.52
11	290	7.64	**34**	1044	36.80	**57**	1568	679.71
12	306	14.51	**35**	1053	30.99	**58**	1622	4.27

13	314	0.57	**36**	1072	0.38	**59**	1649	4.75
14	381	5.06	**37**	1102	66.37	**60**	3021	132.30
15	385	4.72	**38**	1138	16.65	**61**	3060	49.26
16	421	0.08	**39**	1171	1.49	**62**	3061	167.52
17	487	89.03	**40**	1207	8.22	**63**	3100	46.68
18	520	4.91	**41**	1220	45.96	**64**	3117	41.89
19	580	18.84	**42**	1282	105.10	**65**	3176	7.67
20	639	3.48	**43**	1293	55.23	**66**	3225	3.37
21	654	4.14	**44**	1331	4.96	**67**	3231	4.32
22	677	2.80	**45**	1336	8.76	**68**	3239	11.57
23	720	14.72	**46**	1388	73.42	**69**	3258	7.60

Table 3-94. B3LYP/6-31G* Optimized Geometries, Energies, and Entropy Corrections for HAPY-11

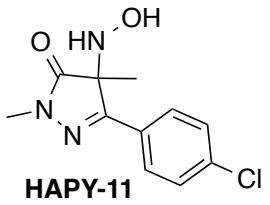

HAPY-11

B3LYP/6-31G* Energy (E): -1201.230331 hartrees
Entropy Correction (Hv-TSv): 480.9956 kJ/mol
G° = E + "entropy correction": -753667.8831 kcal/mol

Atom	Atomic Number	Cartesian Coordinates (Angstroms) X	Y	Z
C	6	1.7456823	-0.6788200	0.2144890
C	6	3.0286965	0.1651453	0.1129251
N	7	2.6149644	1.4577745	-0.0133936
N	7	1.2340914	1.5920486	-0.0521997
C	6	0.6923159	0.4168513	0.0551792
O	8	4.1984846	-0.2298326	0.1391310
C	6	3.4487285	2.6384016	-0.1566082
H	1	3.2792916	3.1105660	-1.1275954
H	1	4.4880555	2.3191341	-0.0811883
H	1	3.2254139	3.3563943	0.6357755
C	6	1.7097332	-1.3847856	1.5798629
H	1	2.6020638	-2.0046604	1.6856240
H	1	0.8281522	-2.0215208	1.6798203
H	1	1.6922063	-0.6511661	2.3919213
N	7	1.7149915	-1.5560907	-0.9819664
H	1	0.7932286	-1.9960883	-1.0315031
O	8	2.5889624	-2.6917181	-0.7707863

H	1	3.3697030	-2.4596622	-1.3015316
C	6	-0.7688461	0.2716010	0.0303977
C	6	-3.5592270	0.0693836	-0.0284572
C	6	-1.4066537	-0.9696437	0.1937991
C	6	-1.5735207	1.4121454	-0.1663263
C	6	-2.9573688	1.3185353	-0.1951346
C	6	-2.7966755	-1.0775060	0.1638517
H	1	-3.5663170	2.2022616	-0.3467142
H	1	-3.2762776	-2.0409970	0.2923746
H	1	-0.8308444	-1.8724597	0.3580895
H	1	-1.0965560	2.3764063	-0.2967558
Cl	17	-5.3209297	-0.0516556	-0.0637007

Table 3-95. B3LYP/6-31G* Calculated IR Frequencies (cm^{-1}, uncorrected) and Intensities for HAPY-11

	cm^{-1}	Intensity		cm^{-1}	Intensity		cm^{-1}	Intensity
1	22	0.71	**28**	712	5.66	**55**	1367	68.06
2	54	1.08	**29**	729	11.70	**56**	1432	87.50
3	69	2.03	**30**	745	27.42	**57**	1436	85.10
4	84	3.70	**31**	763	27.43	**58**	1448	14.18
5	92	0.78	**32**	817	37.51	**59**	1472	10.30
6	113	6.46	**33**	836	10.96	**60**	1509	5.86
7	133	2.25	**34**	853	35.56	**61**	1514	12.71
8	154	2.92	**35**	884	39.30	**62**	1517	18.92
9	208	3.30	**36**	940	44.65	**63**	1528	7.14
10	222	3.08	**37**	960	1.17	**64**	1538	10.75
11	234	39.38	**38**	969	44.45	**65**	1539	81.29
12	240	1.80	**39**	988	0.18	**66**	1596	29.48
13	280	74.87	**40**	1020	79.49	**67**	1629	17.16
14	289	1.09	**41**	1035	75.53	**68**	1649	45.56
15	294	8.06	**42**	1039	42.26	**69**	1684	816.60
16	319	10.97	**43**	1068	116.69	**70**	3088	74.78
17	350	45.62	**44**	1097	104.65	**71**	3092	12.86
18	357	2.90	**45**	1130	9.05	**72**	3160	15.38
19	376	2.67	**46**	1150	9.57	**73**	3161	15.70
20	420	0.19	**47**	1175	2.66	**74**	3199	2.06
21	427	23.05	**48**	1195	18.11	**75**	3205	21.30
22	481	62.22	**49**	1220	3.29	**76**	3235	5.68
23	513	9.20	**50**	1249	59.32	**77**	3237	0.08
24	620	56.91	**51**	1264	133.16	**78**	3249	10.65
25	637	4.31	**52**	1330	35.96	**79**	3250	2.16
26	662	27.79	**53**	1341	30.73	**80**	3464	30.44
27	669	11.35	**54**	1355	98.71	**81**	3721	113.44

Table 3-96. B3LYP/6-31G* Optimized Geometries, Energies, and Entropy Corrections for HAPY-11$_{anion}$

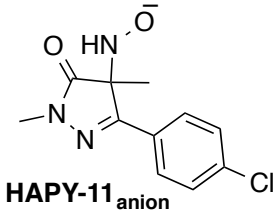

HAPY-11$_{anion}$

B3LYP/6-31G* Energy (E): -1200.723566 hartrees
Entropy Correction (Hv-TSv): 449.1237 kJ/mol
G° = E + "entropy correction": -753357.501 kcal/mol

Atom	Atomic Number	Cartesian Coordinates (Angstroms) X	Y	Z
C	6	1.2948369	-0.6741042	0.4013380
C	6	2.5510678	0.1403525	0.1227574
N	7	2.1487305	1.1913447	-0.6484319
N	7	0.7733111	1.2562336	-0.8046996
C	6	0.2425771	0.2445727	-0.1800840
O	8	3.7118643	-0.0733711	0.4930840
C	6	2.9751961	2.2545045	-1.1928803
H	1	2.6779548	3.2200050	-0.7751465
H	1	2.8808814	2.2895291	-2.2814557
H	1	4.0086214	2.0384710	-0.9212023
C	6	1.1790899	-1.0345834	1.8782796
H	1	1.8821904	-1.8565906	2.0512189
H	1	0.1717026	-1.3667804	2.1384257
H	1	1.4333279	-0.1928264	2.5316034
N	7	1.4074698	-1.9193954	-0.5465835
H	1	0.4525575	-2.3157270	-0.4393963
O	8	2.3118557	-2.8649306	-0.0392392
C	6	-1.2184887	0.0976314	-0.1607725
C	6	-4.0133177	-0.1134340	-0.1642467
C	6	-2.0281232	1.1635366	-0.6040221
C	6	-1.8560979	-1.0735617	0.2835377
C	6	-3.2461754	-1.1848821	0.2821598
C	6	-3.4131302	1.0653329	-0.6101957
H	1	-3.7213462	-2.0972228	0.6242933
H	1	-4.0219523	1.8944206	-0.9523826
H	1	-1.5475368	2.0737028	-0.9437378
H	1	-1.2677857	-1.9191182	0.6216110
Cl	17	-5.7692809	-0.2431095	-0.1638320

Table 3-97. B3LYP/6-31G* Calculated IR Frequencies (cm^{-1}, uncorrected) and Intensities for HAPY-11_{anion}

	cm^{-1}	Intensity		cm^{-1}	Intensity		cm^{-1}	Intensity
1	45	5.78	**27**	704	33.21	**53**	1365	123.57
2	59	0.92	**28**	715	12.76	**54**	1415	21.07
3	76	14.51	**29**	734	8.13	**55**	1421	46.59
4	86	5.27	**30**	759	33.68	**56**	1446	21.10
5	113	2.11	**31**	801	68.36	**57**	1459	72.74
6	122	9.83	**32**	839	15.43	**58**	1509	2.40
7	159	1.68	**33**	843	14.23	**59**	1522	12.15
8	173	17.87	**34**	852	30.98	**60**	1534	3.90
9	180	7.24	**35**	959	131.63	**61**	1537	23.06
10	225	2.97	**36**	970	21.04	**62**	1538	58.38
11	243	4.35	**37**	978	1.00	**63**	1585	44.72
12	251	8.41	**38**	991	83.05	**64**	1625	27.91
13	286	16.22	**39**	1021	51.66	**65**	1647	18.21
14	300	9.12	**40**	1037	37.13	**66**	1650	284.15
15	324	1.00	**41**	1047	7.50	**67**	1685	540.97
16	359	8.61	**42**	1096	85.24	**68**	3061	51.84
17	377	5.79	**43**	1101	113.06	**69**	3098	94.98
18	408	27.73	**44**	1126	89.27	**70**	3122	9.14
19	424	0.63	**45**	1144	14.20	**71**	3150	103.01
20	459	43.71	**46**	1184	4.45	**72**	3169	18.03
21	501	30.53	**47**	1205	17.36	**73**	3190	31.64
22	509	55.21	**48**	1216	1.26	**74**	3205	3.06
23	553	164.16	**49**	1258	49.23	**75**	3221	10.21
24	617	36.64	**50**	1299	105.40	**76**	3235	0.52
25	638	9.18	**51**	1335	3.18	**77**	3241	7.54
26	663	18.91	**52**	1340	14.60	**78**	3248	4.14

Table 3-98. B3LYP/6-31G* Optimized Geometries, Energies, and Entropy Corrections for enol of PY-12

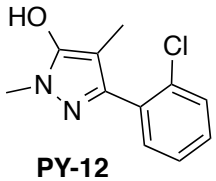

PY-12

B3LYP/6-31G* Energy (E): -1070.710534 hartrees
Entropy Correction (Hv-TSv): 430.0694 kJ/mol
G° = E + "entropy correction": -671777.7074 kcal/mol

Atom	Atomic Number	Cartesian Coordinates (Angstroms) X	Y	Z
C	6	1.2687381	-0.6845066	0.1740961
C	6	2.4040455	0.1142365	0.2069352
N	7	2.0374216	1.3981192	-0.0316850
N	7	0.6897942	1.5029493	-0.2132336
C	6	0.2332420	0.2450688	-0.1018371
C	6	2.8908524	2.5753940	-0.0612848
H	1	2.6800865	3.1568968	-0.9607480
H	1	3.9305955	2.2500359	-0.0733531
H	1	2.7173946	3.2012915	0.8183437
C	6	1.2095492	-2.1597120	0.4349228
H	1	1.4419363	-2.7571421	-0.4549806
H	1	0.2124100	-2.4588550	0.7716120
H	1	1.9108717	-2.4509551	1.2268217
C	6	-1.2251275	0.0071254	-0.1759793
C	6	-4.0272737	-0.3746367	-0.1991932
C	6	-2.0733285	0.7245014	0.6876360
C	6	-1.8384950	-0.8897698	-1.0655857
C	6	-3.2187280	-1.0910967	-1.0791011
C	6	-3.4529592	0.5436595	0.6804692
H	1	-3.6487194	-1.7942695	-1.7833899
H	1	-4.0752217	1.1123322	1.3638434
H	1	-5.1009555	-0.5327519	-0.2098827
H	1	-1.6148840	1.4298166	1.3725620
Cl	17	-0.8825452	-1.7625516	-2.2715532
O	8	3.7150271	-0.1678176	0.4452569
H	1	3.8162730	-1.1373627	0.4993081

Table 3-99. B3LYP/6-31G* Calculated IR Frequencies (cm^{-1}, uncorrected) and Intensities for enol of PY-12

	cm^{-1}	Intensity		cm^{-1}	Intensity		cm^{-1}	Intensity
1	43	1.76	**25**	724	8.88	**49**	1448	2.08
2	44	0.19	**26**	746	23.37	**50**	1465	13.12
3	72	2.89	**27**	752	12.51	**51**	1477	23.21
4	90	2.02	**28**	778	45.69	**52**	1482	132.11
5	132	5.38	**29**	825	23.41	**53**	1510	27.72
6	136	13.90	**30**	883	0.47	**54**	1517	11.95
7	163	1.16	**31**	957	2.39	**55**	1521	5.71
8	182	15.13	**32**	988	0.06	**56**	1527	35.01
9	215	104.55	**33**	1014	13.45	**57**	1547	4.34
10	228	2.29	**34**	1030	60.36	**58**	1572	155.87
11	259	8.57	**35**	1054	125.21	**59**	1611	85.55

12	292	14.03	**36**	1072	6.55	**60**	1623	51.88
13	298	4.58	**37**	1078	5.33	**61**	1654	4.04
14	314	4.46	**38**	1088	77.05	**62**	3049	52.48
15	357	2.83	**39**	1149	14.18	**63**	3093	72.20
16	421	17.71	**40**	1161	120.35	**64**	3100	30.00
17	453	5.87	**41**	1185	6.57	**65**	3130	20.38
18	473	10.76	**42**	1192	0.23	**66**	3165	17.12
19	522	2.36	**43**	1256	27.32	**67**	3205	2.94
20	576	9.99	**44**	1288	30.38	**68**	3214	0.37
21	615	5.83	**45**	1294	12.45	**69**	3223	11.67
22	654	18.62	**46**	1308	85.09	**70**	3234	20.78
23	662	3.25	**47**	1333	2.74	**71**	3241	9.03
24	707	25.78	**48**	1408	214.27	**72**	3690	242.69

Table 3-100. B3LYP/6-31G* Optimized Geometries, Energies, and Entropy Corrections for PY-12$_{anion}$

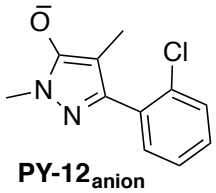

PY-12$_{anion}$

B3LYP/6-31G* Energy (E): -1070.242766 hartrees
Entropy Correction (Hv-TSv): 399.4654 kJ/mol
G° = E + "entropy correction": -671491.4933 kcal/mol

Atom	Atomic Number	Cartesian Coordinates (Angstroms) X	Y	Z
C	6	1.4297665	-0.7280154	0.1634182
C	6	2.6149212	0.0488761	0.2374611
N	7	2.1806109	1.3596018	0.0499032
N	7	0.8227485	1.4658153	-0.1409676
C	6	0.3855910	0.1931895	-0.0742168
C	6	3.0180163	2.5356561	-0.0124193
H	1	2.9909902	2.9942252	-1.0077092
H	1	4.0387684	2.2204458	0.2115265
H	1	2.6975543	3.2836594	0.7204662
C	6	1.3895340	-2.2063190	0.3924421
H	1	1.5828029	-2.7953073	-0.5159923
H	1	0.4166419	-2.5331395	0.7781964
H	1	2.1559981	-2.4936633	1.1240491
C	6	-1.0719389	-0.0432802	-0.1509590
C	6	-3.8863172	-0.4072599	-0.1659528
C	6	-1.9236168	0.7043382	0.6875471

C	6	-1.6971193	-0.9591548	-1.0139833
C	6	-3.0795610	-1.1527327	-1.0224326
C	6	-3.3043341	0.5343600	0.6842625
H	1	-3.5093976	-1.8735835	-1.7088584
H	1	-3.9199002	1.1300703	1.3508681
H	1	-4.9608276	-0.5598796	-0.1726420
H	1	-1.4543899	1.4257288	1.3481327
Cl	17	-0.7550505	-1.8676836	-2.2077211
O	8	3.8385088	-0.2759476	0.4455808

Table 3-101. B3LYP/6-31G* Calculated IR Frequencies (cm^{-1}, uncorrected) and Intensities for PY-12$_{anion}$

	cm^{-1}	Intensity		cm^{-1}	Intensity		cm^{-1}	Intensity
1	34	0.98	**24**	736	2.04	**47**	1436	61.72
2	55	0.74	**25**	749	27.75	**48**	1449	113.42
3	72	0.46	**26**	769	10.05	**49**	1461	9.73
4	92	0.92	**27**	776	67.65	**50**	1471	17.52
5	124	0.08	**28**	852	10.10	**51**	1503	419.71
6	133	12.14	**29**	878	0.93	**52**	1512	15.06
7	163	1.23	**30**	947	2.75	**53**	1522	7.30
8	178	0.69	**31**	975	0.21	**54**	1524	24.77
9	226	0.83	**32**	1010	12.77	**55**	1551	159.30
10	254	2.59	**33**	1031	26.05	**56**	1564	269.46
11	287	9.44	**34**	1050	101.13	**57**	1590	177.55
12	303	11.69	**35**	1056	26.17	**58**	1616	9.37
13	317	11.82	**36**	1074	2.95	**59**	1650	4.57
14	352	2.44	**37**	1089	42.89	**60**	3022	134.55
15	419	18.92	**38**	1145	8.52	**61**	3066	62.38
16	455	17.71	**39**	1186	0.22	**62**	3069	138.62
17	471	11.45	**40**	1220	55.00	**63**	3105	46.12
18	528	0.72	**41**	1230	8.34	**64**	3143	49.99
19	581	28.23	**42**	1273	86.46	**65**	3181	15.45
20	635	2.09	**43**	1284	3.70	**66**	3213	2.54
21	655	20.92	**44**	1306	56.17	**67**	3223	13.37
22	691	4.95	**45**	1331	2.35	**68**	3234	22.73
23	712	32.68	**46**	1394	75.57	**69**	3243	9.36

Table 3-102. B3LYP/6-31G* Optimized Geometries, Energies, and Entropy Corrections for HAPY-12

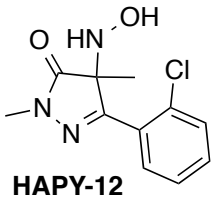

HAPY-12

B3LYP/6-31G* Energy (E): -1201.220982 hartrees
Entropy Correction (Hv-TSv): 481.3899 kJ/mol
G° = E + "entropy correction": -753661.9222 kcal/mol

Atom	Atomic Number	Cartesian Coordinates (Angstroms)		
		X	Y	Z
C	6	1.2191291	-0.8757850	0.0806324
C	6	2.5003867	-0.0413677	0.2509508
N	7	2.0972747	1.1632027	0.7498347
N	7	0.7147166	1.2685746	0.8905761
C	6	0.1790996	0.1531967	0.5204658
O	8	3.6624157	-0.3781222	0.0053310
C	6	2.9339191	2.3069961	1.0667669
H	1	2.6840903	3.1536684	0.4223967
H	1	3.9698295	2.0122475	0.8992419
H	1	2.7982690	2.5981430	2.1109020
C	6	1.2911929	-2.1395399	0.9487114
H	1	2.1717872	-2.7187327	0.6637892
H	1	0.4040342	-2.7601559	0.7983481
H	1	1.3693946	-1.8852040	2.0106885
N	7	1.0128659	-1.1158829	-1.3672839
H	1	0.0789286	-1.5225818	-1.4733599
O	8	1.8748288	-2.1956326	-1.8046529
H	1	2.5431161	-1.7301722	-2.3356671
C	6	-1.2899593	-0.0257394	0.4982282
C	6	-4.0845419	-0.4156443	0.5093985
C	6	-1.8855061	-1.0343100	1.2782063
C	6	-2.1444001	0.7795207	-0.2791539
C	6	-3.5250510	0.5898983	-0.2769111
C	6	-3.2637844	-1.2287637	1.2895626
H	1	-4.1498393	1.2265665	-0.8927613
H	1	-3.6923379	-2.0088390	1.9095908
H	1	-5.1603033	-0.5580134	0.5067946
H	1	-1.2516414	-1.6521557	1.9031232
Cl	17	-1.5053065	2.0530868	-1.3293838

Table 3-103. B3LYP/6-31G* Calculated IR Frequencies (cm^{-1}, uncorrected) and Intensities for HAPY-12

	cm^{-1}	Intensity		cm^{-1}	Intensity		cm^{-1}	Intensity
1	25	0.48	**28**	704	46.11	**55**	1370	68.11
2	55	0.84	**29**	739	22.31	**56**	1426	12.59
3	72	3.93	**30**	745	19.10	**57**	1432	134.85
4	86	1.01	**31**	759	34.30	**58**	1469	6.97
5	93	0.77	**32**	776	51.07	**59**	1473	43.71
6	116	6.40	**33**	820	23.69	**60**	1508	5.85
7	139	1.32	**34**	884	19.71	**61**	1513	12.67
8	154	0.29	**35**	888	17.28	**62**	1520	14.44
9	180	13.14	**36**	936	42.18	**63**	1527	9.70
10	233	66.64	**37**	964	5.40	**64**	1532	18.53
11	247	24.96	**38**	967	25.94	**65**	1542	27.71
12	258	5.82	**39**	997	0.16	**66**	1619	4.12
13	269	18.32	**40**	1023	60.47	**67**	1643	17.46
14	281	7.98	**41**	1034	57.59	**68**	1650	18.67
15	294	5.30	**42**	1054	76.73	**69**	1687	658.97
16	316	19.37	**43**	1062	89.02	**70**	3078	15.61
17	336	3.31	**44**	1090	14.36	**71**	3090	62.15
18	354	17.69	**45**	1127	8.45	**72**	3152	15.92
19	411	17.74	**46**	1162	6.34	**73**	3162	15.84
20	412	7.39	**47**	1178	2.14	**74**	3168	15.31
21	455	10.88	**48**	1200	3.15	**75**	3198	2.12
22	464	12.86	**49**	1205	8.80	**76**	3219	2.05
23	515	1.60	**50**	1250	99.47	**77**	3232	13.69
24	612	43.58	**51**	1257	50.85	**78**	3243	8.51
25	636	8.31	**52**	1304	6.33	**79**	3256	5.41
26	653	21.57	**53**	1318	25.10	**80**	3435	23.83
27	690	3.09	**54**	1347	55.81	**81**	3719	108.69

Table 3-104. B3LYP/6-31G* Optimized Geometries, Energies, and Entropy Corrections for HAPY-12$_{anion}$

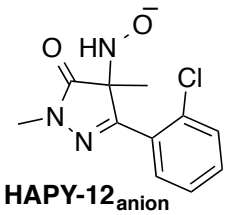

HAPY-12$_{anion}$

B3LYP/6-31G* Energy (E): -1200.713193 hartrees
Entropy Correction (Hv-TSv): 445.1987 kJ/mol
G° = E + "entropy correction": -753351.93 kcal/mol

Atom	Atomic Number	Cartesian Coordinates (Angstroms) X	Y	Z
C	6	1.2678813	-0.6989743	-0.2354491
C	6	2.5292334	0.0969556	0.0547601
N	7	2.1175863	1.3808600	0.2674859
N	7	0.7324748	1.5103648	0.3040883
C	6	0.2183360	0.3409755	0.0831598
O	8	3.7025328	-0.2962609	0.0947223
C	6	2.9447879	2.5293061	0.5919196
H	1	2.7925998	3.3268526	-0.1400153
H	1	3.9843059	2.2016374	0.5655375
H	1	2.7017690	2.9065684	1.5888003
C	6	1.2394100	-2.0391026	0.4799732
H	1	1.9850129	-2.6691929	-0.0157334
H	1	0.2622363	-2.5181390	0.3723935
H	1	1.4765982	-1.9560601	1.5464223
N	7	1.2244901	-0.8711379	-1.8056417
H	1	0.2585456	-1.2601583	-1.8911308
O	8	2.1197043	-1.8624342	-2.2267148
C	6	-1.2488857	0.1630544	0.0443132
C	6	-4.0508320	-0.2145894	0.0956645
C	6	-1.8516645	-0.7734254	0.9067195
C	6	-2.1060999	0.9079187	-0.7885184
C	6	-3.4879794	0.7222490	-0.7685295
C	6	-3.2298558	-0.9636736	0.9376613
H	1	-4.1093499	1.3122248	-1.4324461
H	1	-3.6560395	-1.6896661	1.6218398
H	1	-5.1270949	-0.3526332	0.1063234
H	1	-1.2121141	-1.3347802	1.5779229
Cl	17	-1.4775890	2.1012609	-1.9355283

Table 3-105. B3LYP/6-31G* Calculated IR Frequencies (cm^{-1}, uncorrected) and Intensities for HAPY-12$_{anion}$

	cm^{-1}	Intensity		cm^{-1}	Intensity		cm^{-1}	Intensity
1	28	3.36	**27**	700	17.42	**53**	1353	88.59
2	49	6.93	**28**	704	63.01	**54**	1403	20.11
3	69	7.36	**29**	743	21.64	**55**	1425	51.66
4	74	2.40	**30**	754	36.49	**56**	1455	69.44
5	86	11.16	**31**	773	56.16	**57**	1466	40.04
6	119	13.00	**32**	791	25.81	**58**	1504	2.19
7	142	13.15	**33**	836	7.01	**59**	1508	8.68
8	148	1.23	**34**	884	0.20	**60**	1518	20.09
9	178	0.45	**35**	958	5.36	**61**	1524	3.17
10	196	26.46	**36**	961	121.91	**62**	1529	19.66
11	246	2.74	**37**	984	40.74	**63**	1586	56.26
12	251	6.92	**38**	989	41.89	**64**	1613	15.15
13	277	2.66	**39**	1028	76.77	**65**	1624	46.87
14	300	21.30	**40**	1044	11.10	**66**	1647	7.71
15	312	2.98	**41**	1055	49.67	**67**	1674	666.74
16	343	0.69	**42**	1077	44.26	**68**	3055	49.35
17	370	48.33	**43**	1086	27.25	**69**	3063	129.14
18	406	20.66	**44**	1120	30.48	**70**	3088	83.27
19	435	5.01	**45**	1151	6.68	**71**	3124	6.92
20	452	8.11	**46**	1171	2.36	**72**	3144	32.70
21	468	4.29	**47**	1190	1.12	**73**	3156	19.19
22	514	46.17	**48**	1217	13.27	**74**	3199	3.48
23	535	153.02	**49**	1264	93.62	**75**	3222	0.43
24	606	51.78	**50**	1280	28.01	**76**	3233	8.45
25	643	26.57	**51**	1295	10.08	**77**	3243	10.71
26	652	16.14	**52**	1319	12.08	**78**	3247	9.89

3.7.3 ^{1}H and ^{13}C NMR Spectra

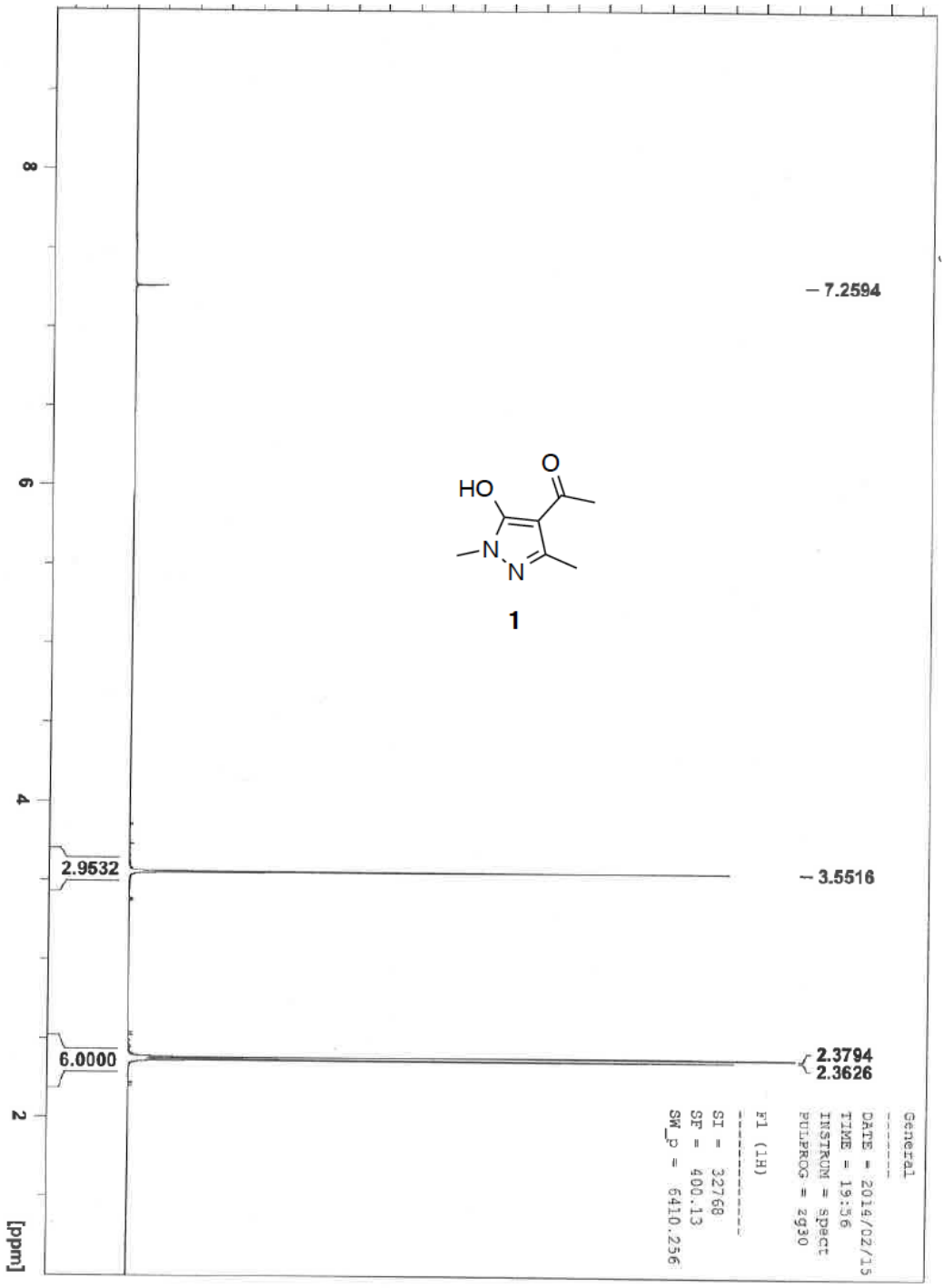

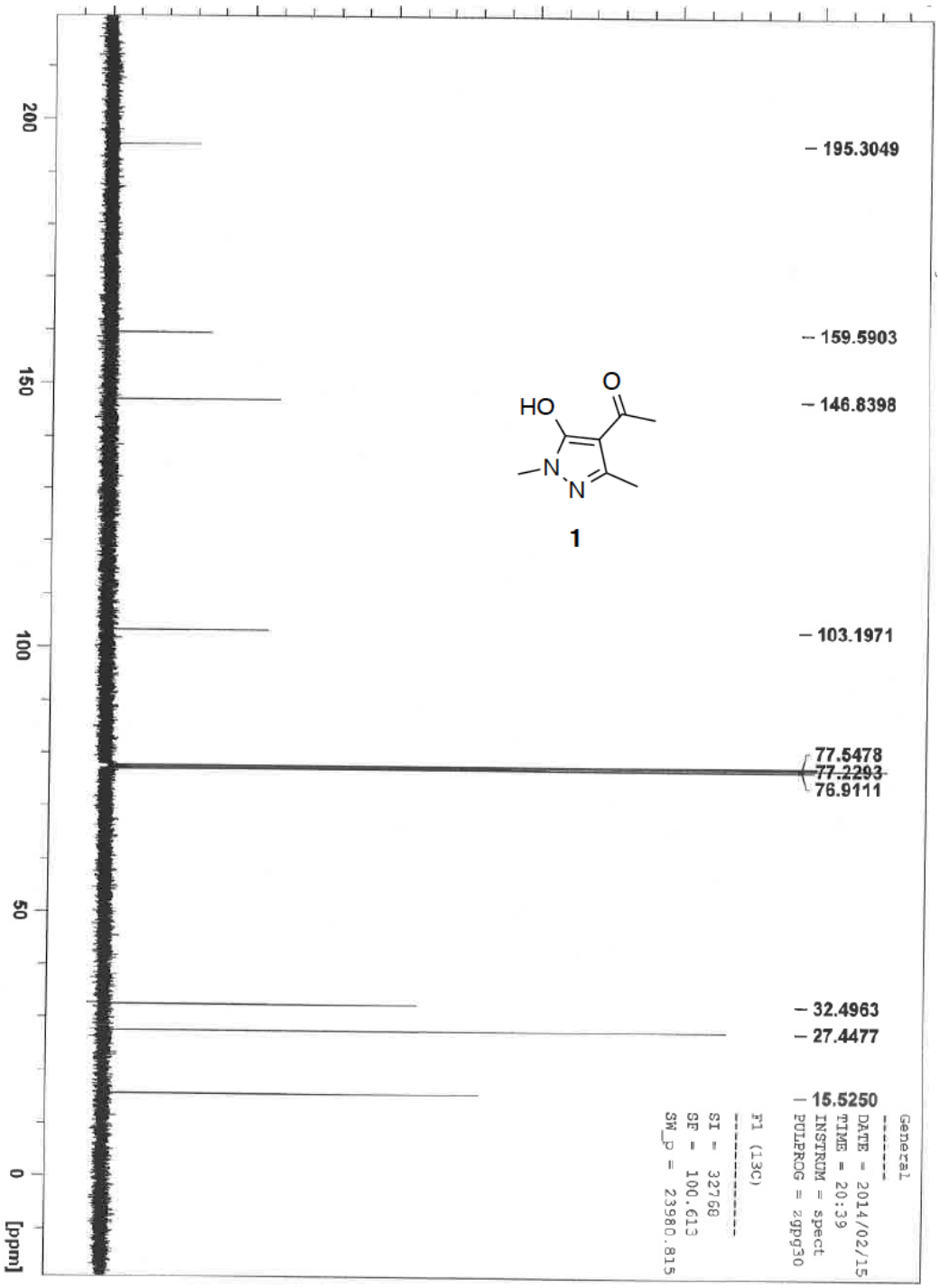
195.3049
159.5903
146.8398
103.1971
77.5478
77.2293
76.9111
32.4963
27.4477
15.5250
HO
O
N
N
1
200
150
100
50
0
[ppm]
General
DATE = 2014/02/15
TIME = 20:39
INSTRUM = spect
PULPROG = zgpg30
F1 (13C)
SI = 32768
SF = 100.613
SW_p = 23980.815

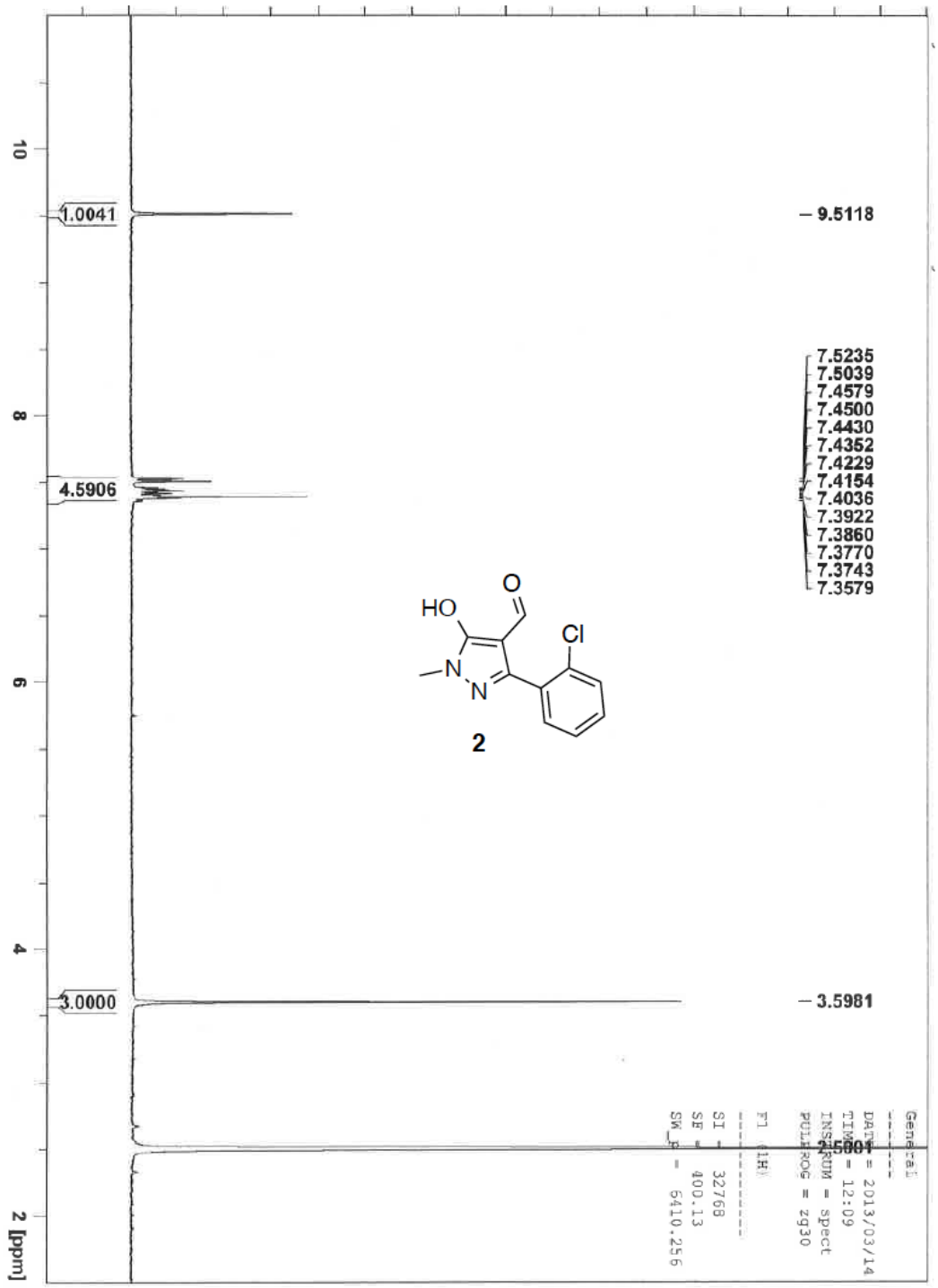
1.0041
4.5906
3.0000
9.5118
7.5235
7.5039
7.4579
7.4500
7.4430
7.4352
7.4229
7.4154
7.4036
7.3922
7.3860
7.3770
7.3743
7.3579
3.5981
2.5001
HO
O
Cl
N
N
2
10
8
6
4
2 [ppm]

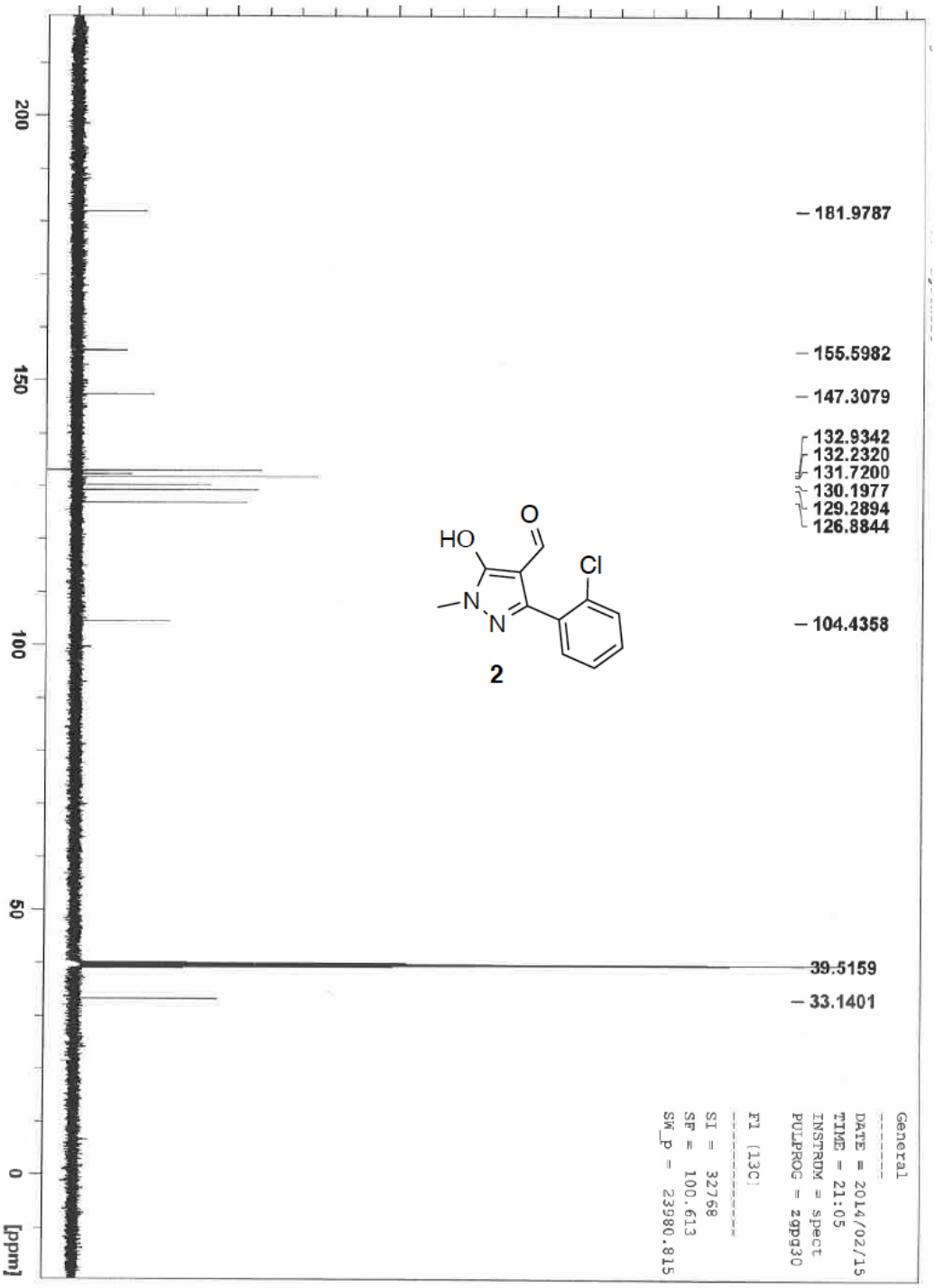
181.9787
155.5982
147.3079
132.9342
132.2320
131.7200
130.1977
129.2894
126.8844
104.4358
39.5159
33.1401
HO
O
Cl
N
N
2
200
150
100
50
0
[ppm]
General
DATE = 2014/02/15
TIME = 21:05
INSTRUM = spect
PULPROG = zgpg30
F1 [13C]
SI = 32768
SF = 100.613
SW_p = 23980.815

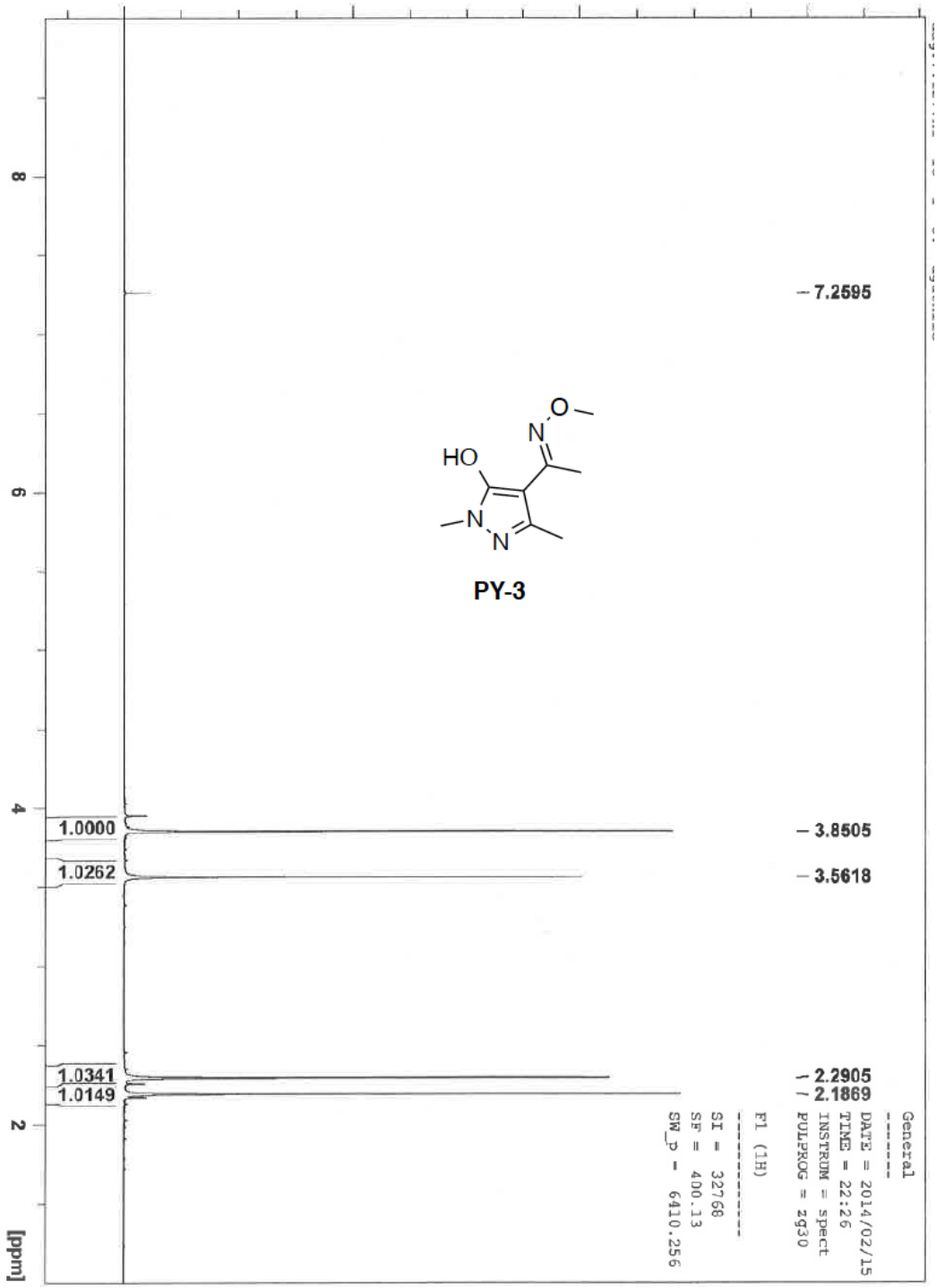
7.2595
3.8505
3.5618
2.2905
2.1869
1.0000
1.0262
1.0341
1.0149
8
6
4
2
[ppm]
General
DATE = 2014/02/15
TIME = 22:26
INSTRUM = spect
PULPROG = zg30
F1 (1H)
SI = 32768
SF = 400.13
SW_p = 6410.256
HO
N
O
N
N

PY-3

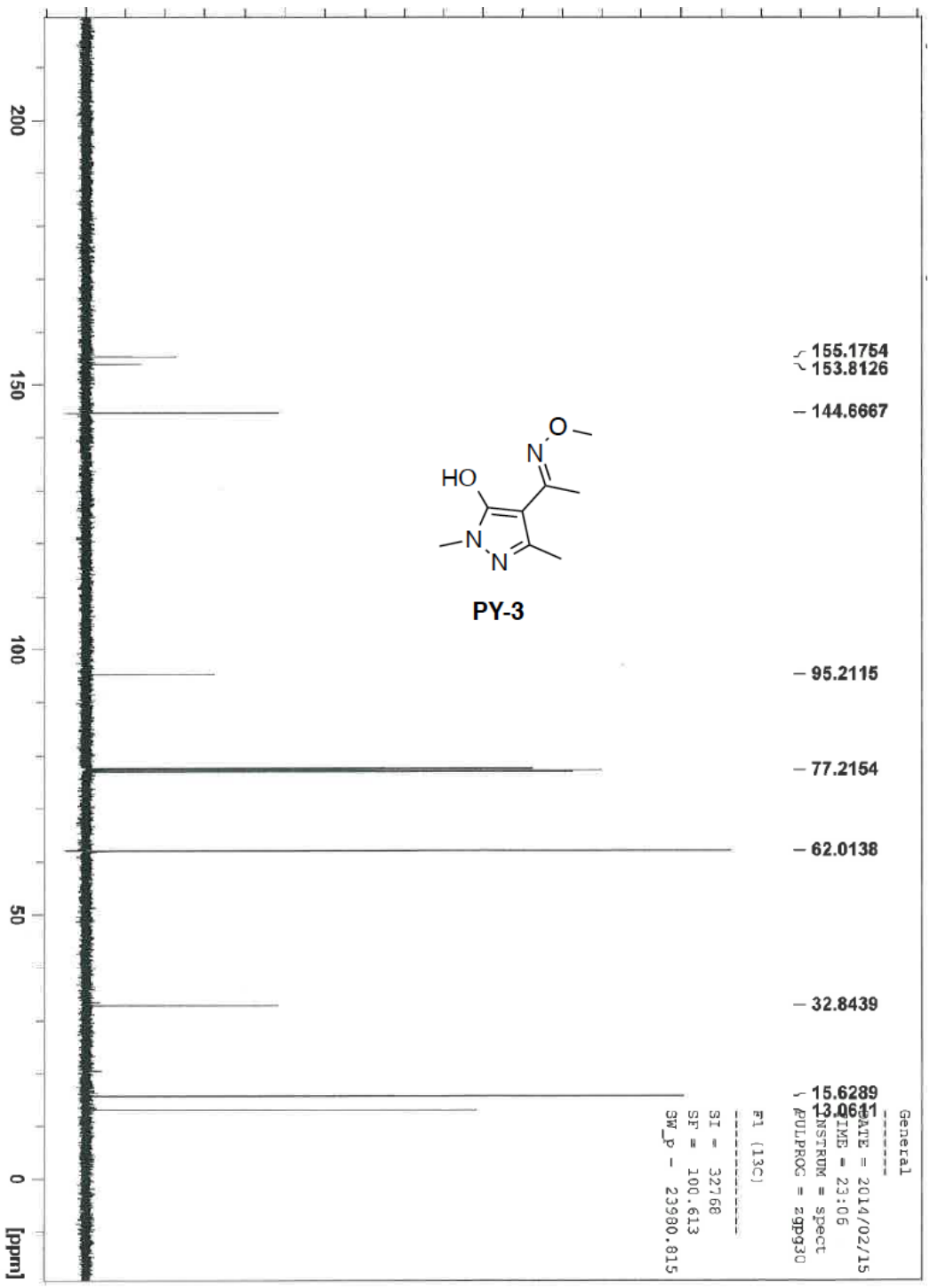
155.1754
153.8126
144.6667
95.2115
77.2154
62.0138
32.8439
15.6289
13.0611
HO
N
O
N
N
PY-3
200
150
100
50
0
[ppm]
General
DATE = 2014/02/15
TIME = 23:06
INSTRUM = spect
PULPROG = zgpg30
F1 (13C)
SI = 32768
SF = 100.613
SW_p = 23980.015

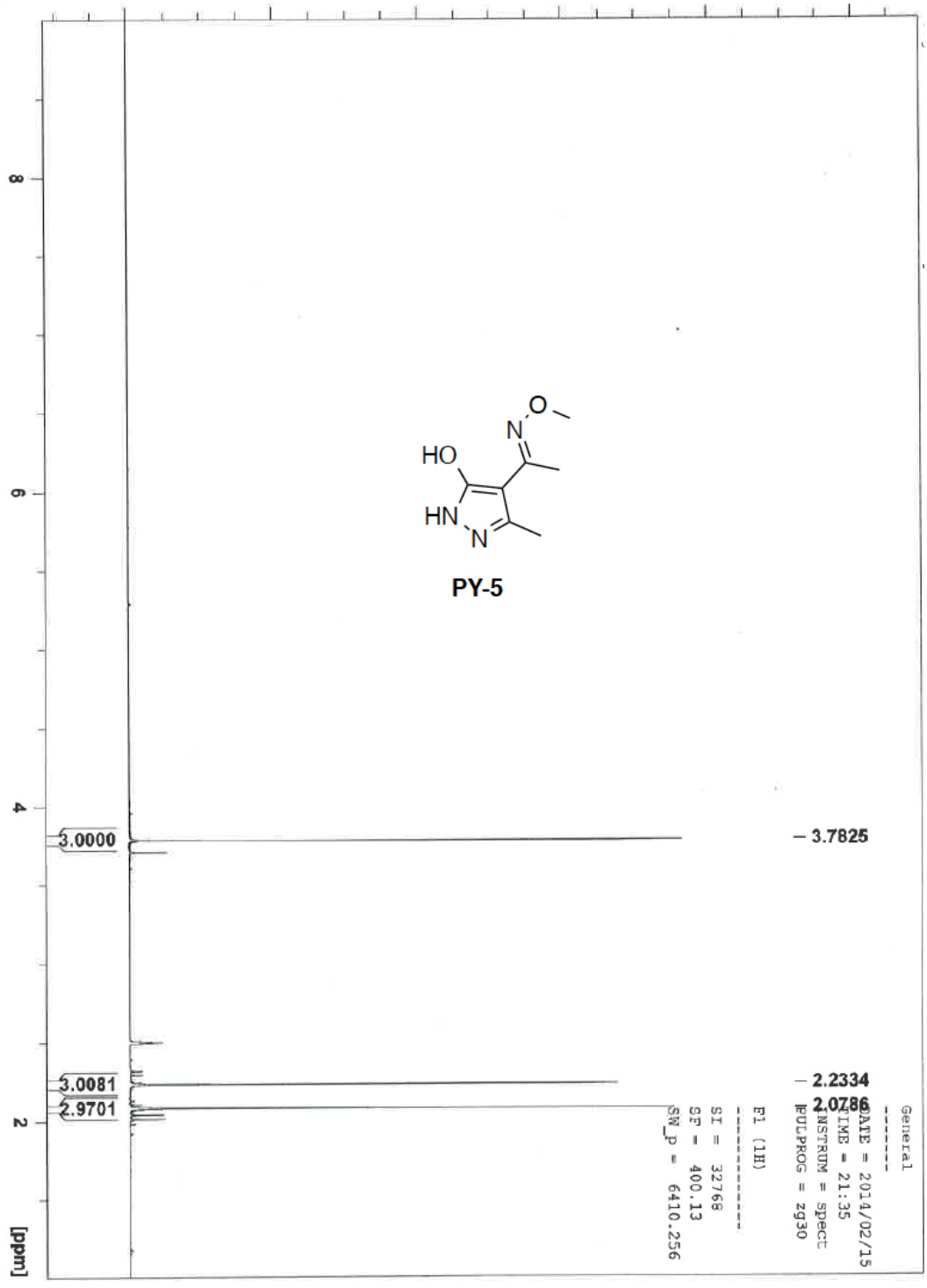
HO
N
O
HN
N
PY-5
3.0000
3.0081
2.9701
3.7825
2.2334
2.0786
[ppm]
8
6
4
2
General
DATE = 2014/02/15
TIME = 21:35
INSTRUM = spect
PULPROG = zg30
F1 (1H)
SI = 32768
SF = 400.13
SW_p = 6410.256

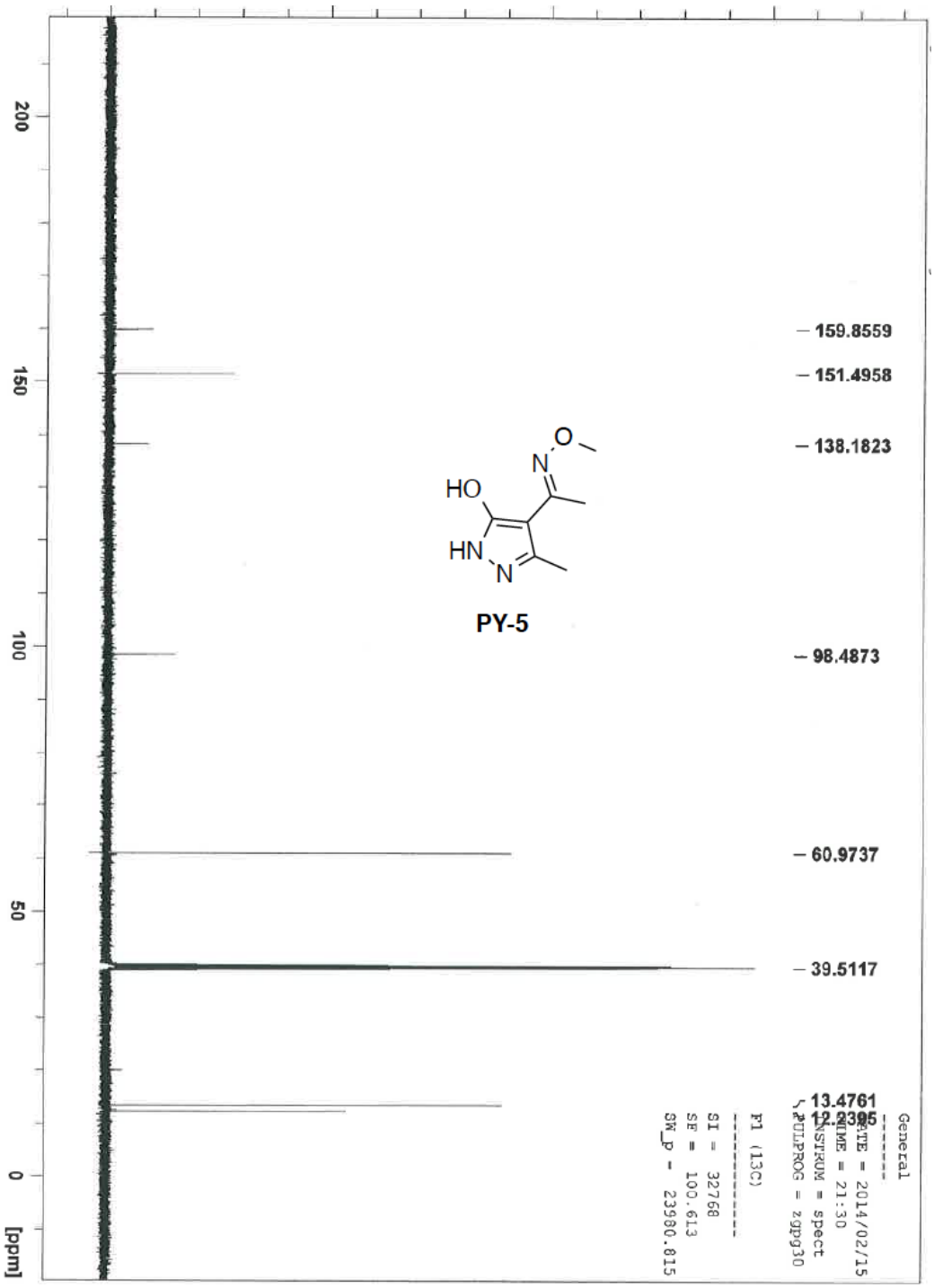
200
150
100
50
0
[ppm]
159.8559
151.4958
138.1823
98.4873
60.9737
39.5117
13.4761
12.2395
HO
HN
N
N
O
PY-5
General
F1 (13C)
SI = 32768
SF = 100.613
SW_p = 23980.815
PULPROG = zgpg30
INSTRUM = spect
TIME = 21:30
DATE = 2014/02/15

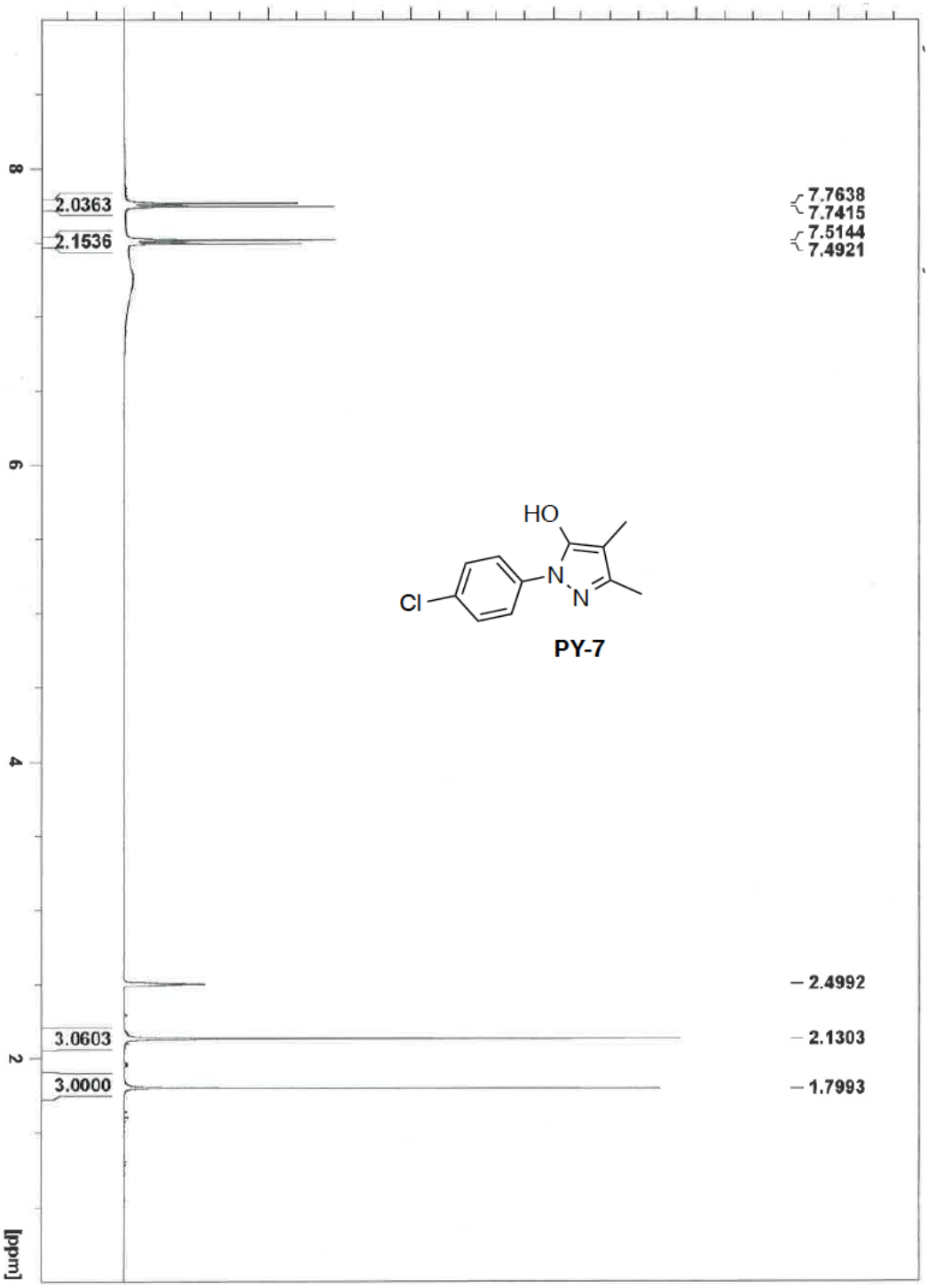
8
6
4
2
[ppm]
2.0363
2.1536
3.0603
3.0000
7.7638
7.7415
7.5144
7.4921
2.4992
2.1303
1.7993
HO
N
N
Cl
PY-7

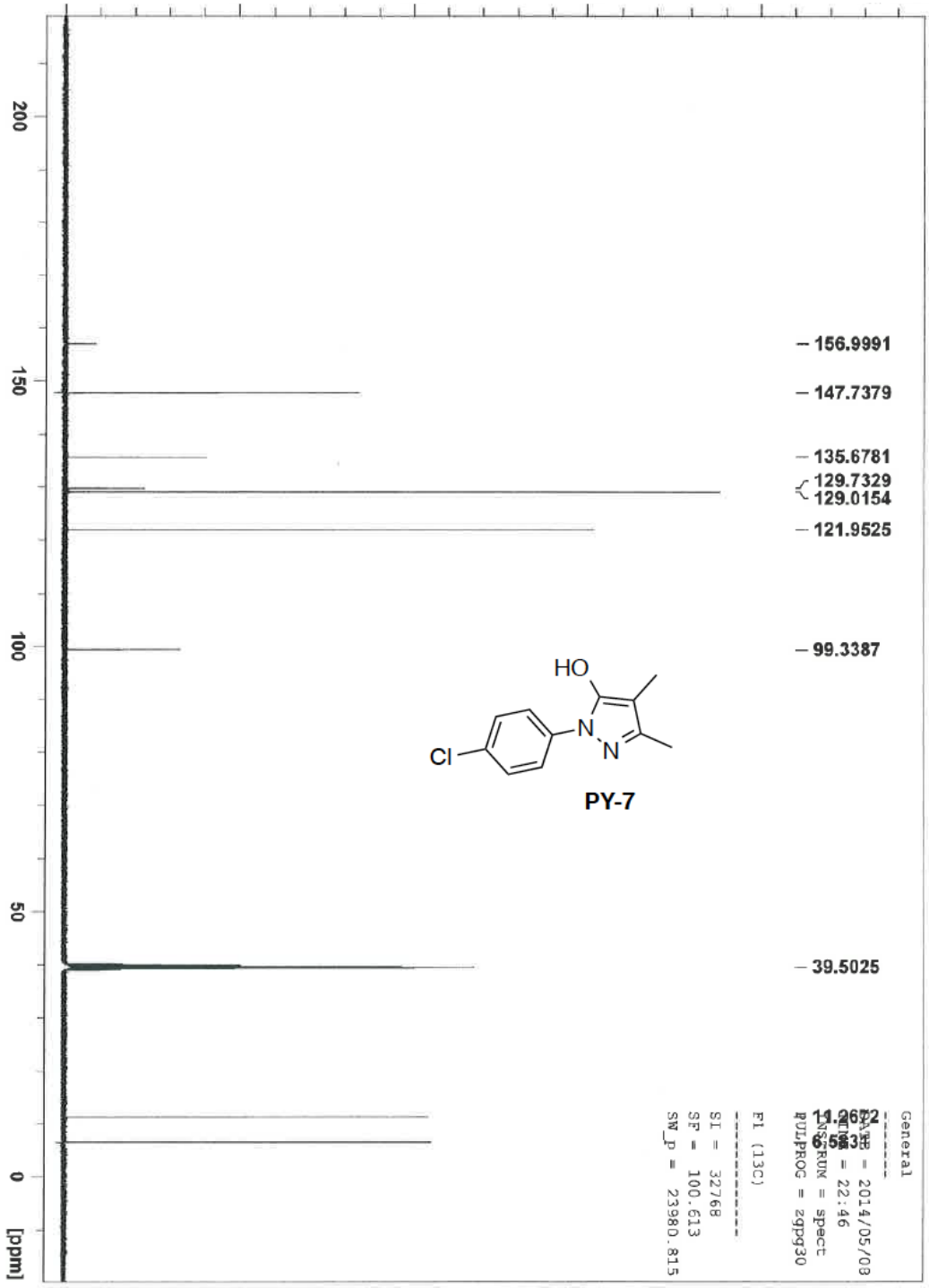
156.9991
147.7379
135.6781
129.7329
129.0154
121.9525
99.3387
39.5025
11.2672
6.5833
HO
N
N
Cl
PY-7
200
150
100
50
0
[ppm]
General
PULPROG = zgpg30
F1 (13C)
SI = 32768
SF = 100.613
SW_p = 23980.815

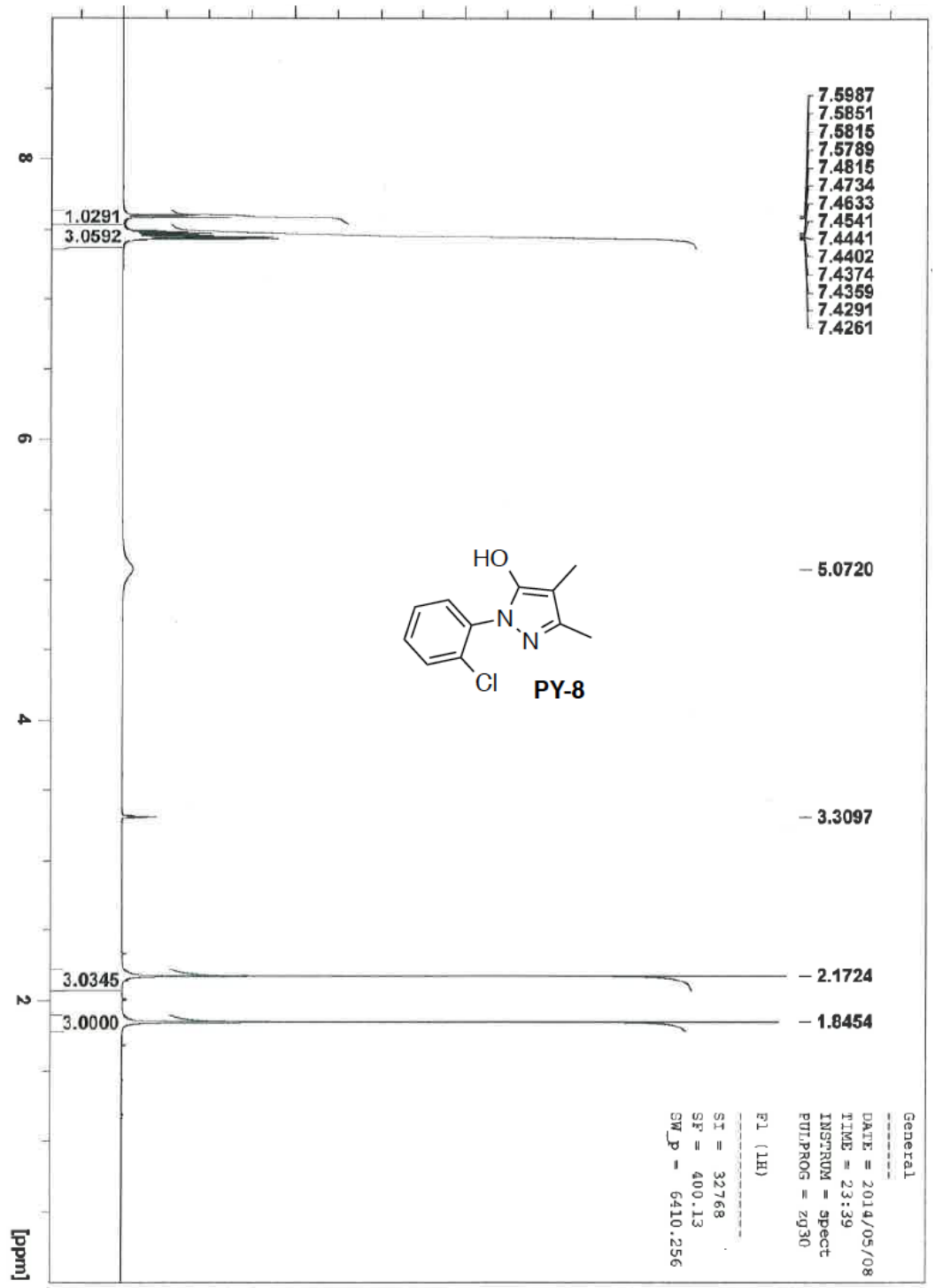
7.5987
7.5851
7.5815
7.5789
7.4815
7.4734
7.4633
7.4541
7.4441
7.4402
7.4374
7.4359
7.4291
7.4261
1.0291
3.0592
5.0720
3.3097
3.0345
3.0000
2.1724
1.8454
HO
N
N
Cl
PY-8
[ppm]
General
DATE = 2014/05/08
TIME = 23:39
INSTRUM = spect
PULPROG = zg30
F1 (1H)
SI = 32768
SF = 400.13
SW_p = 6410.256

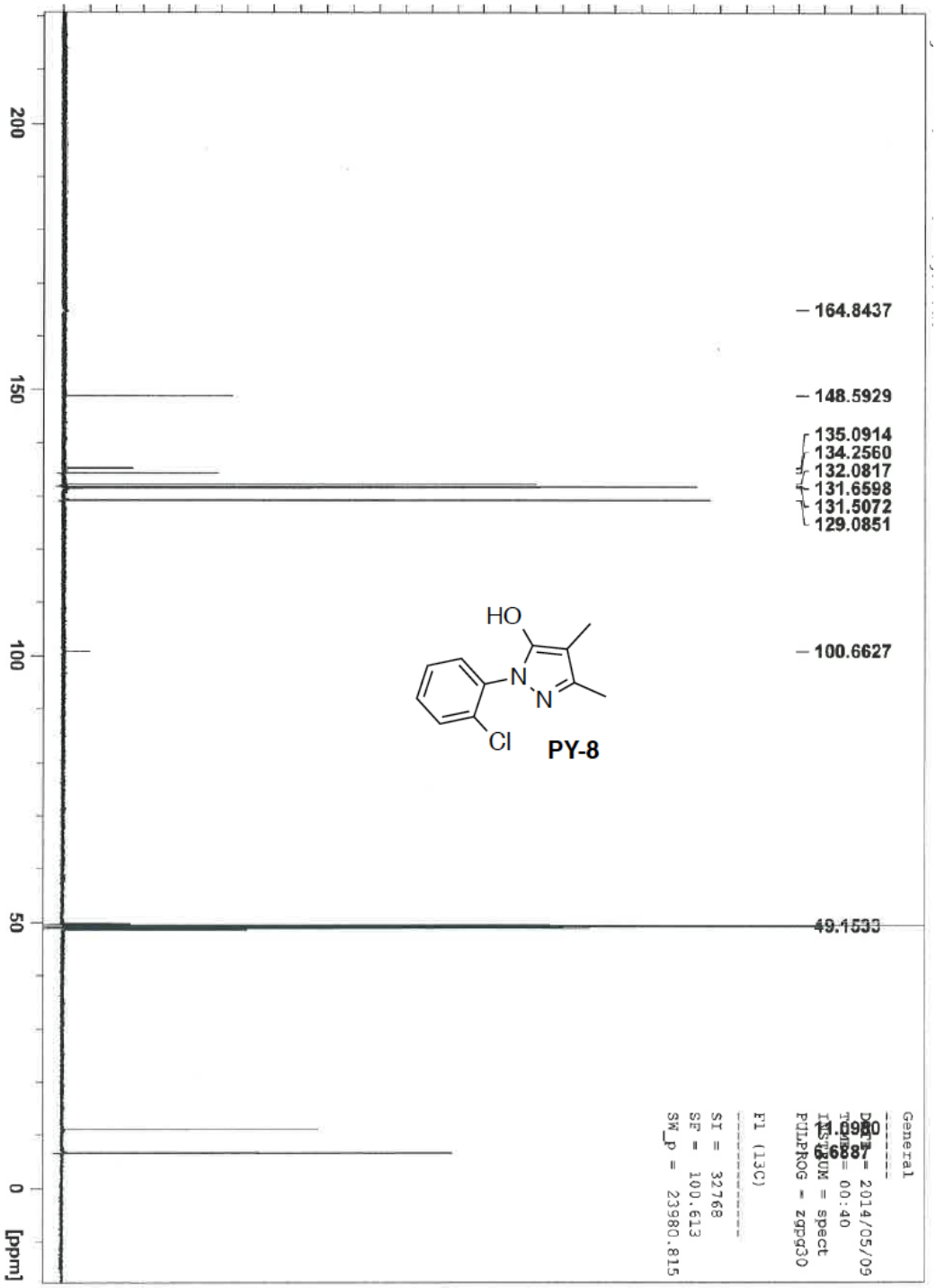
200
150
100
50
0
[ppm]
164.8437
148.5929
135.0914
134.2560
132.0817
131.6598
131.5072
129.0851
100.6627
49.1533
HO
N
N
Cl
PY-8
General
PULPROG = zgpg30
F1 (13C)
SI = 32768
SF = 100.613
SW_p = 23980.815

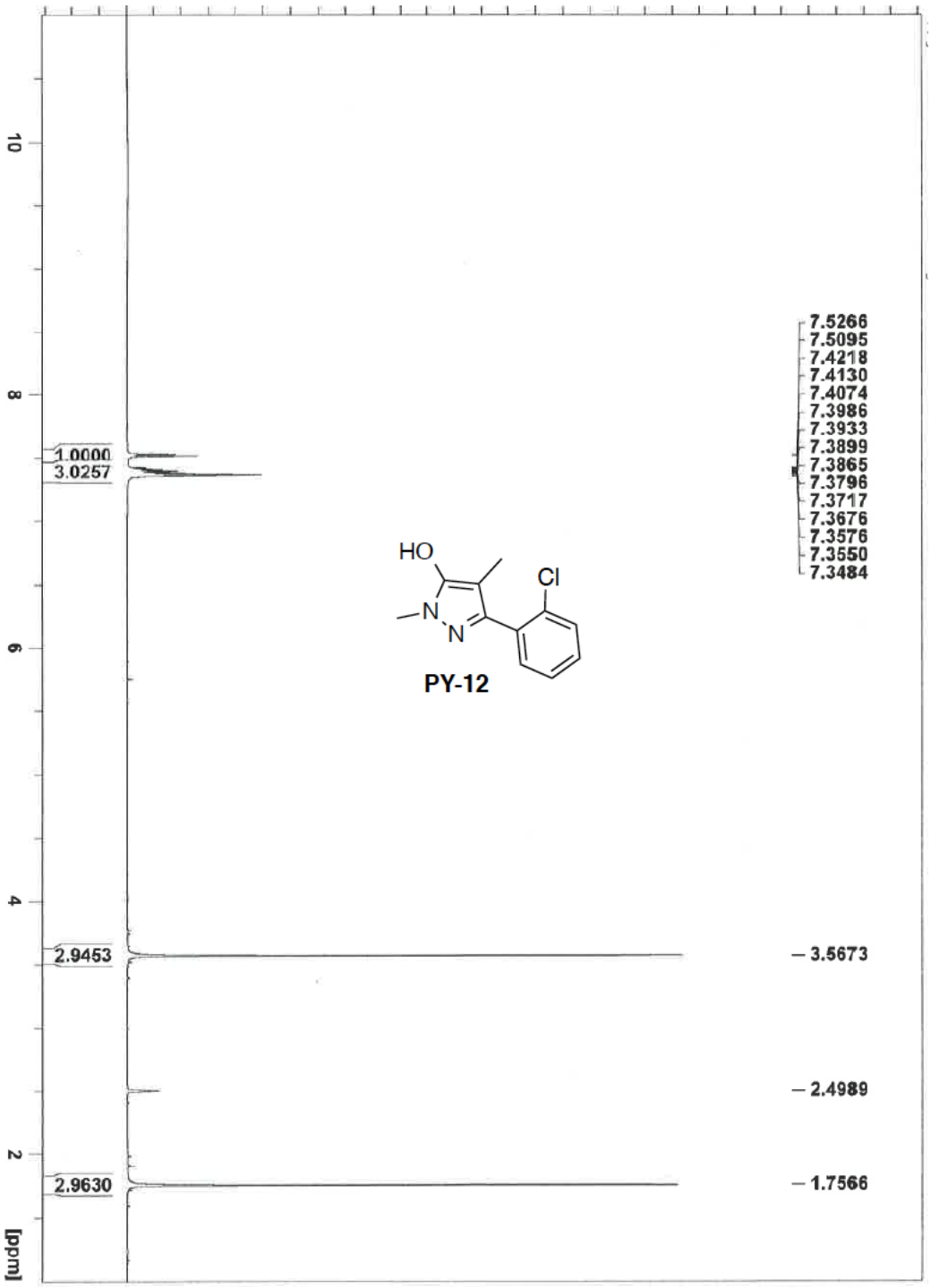
10
8
6
4
2
[ppm]
1.0000
3.0257
2.9453
2.9630
7.5266
7.5095
7.4218
7.4130
7.4074
7.3986
7.3933
7.3899
7.3865
7.3796
7.3717
7.3676
7.3576
7.3550
7.3484
3.5673
2.4989
1.7566
HO
Cl
N
N
PY-12

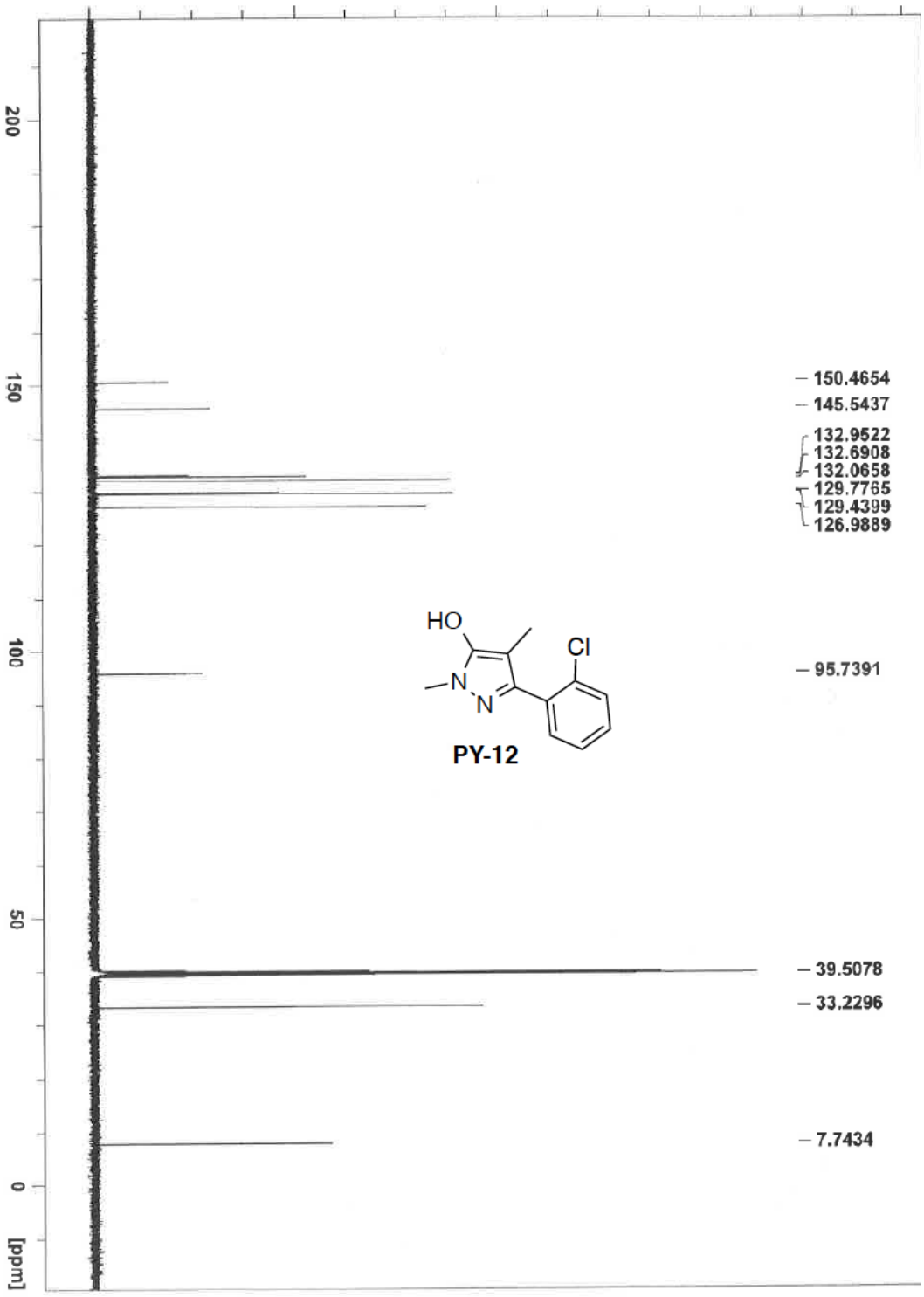
200
150
100
50
0
[ppm]
150.4654
145.5437
132.9522
132.6908
132.0658
129.7765
129.4399
126.9889
95.7391
39.5078
33.2296
7.7434
HO
Cl
N
N
PY-12

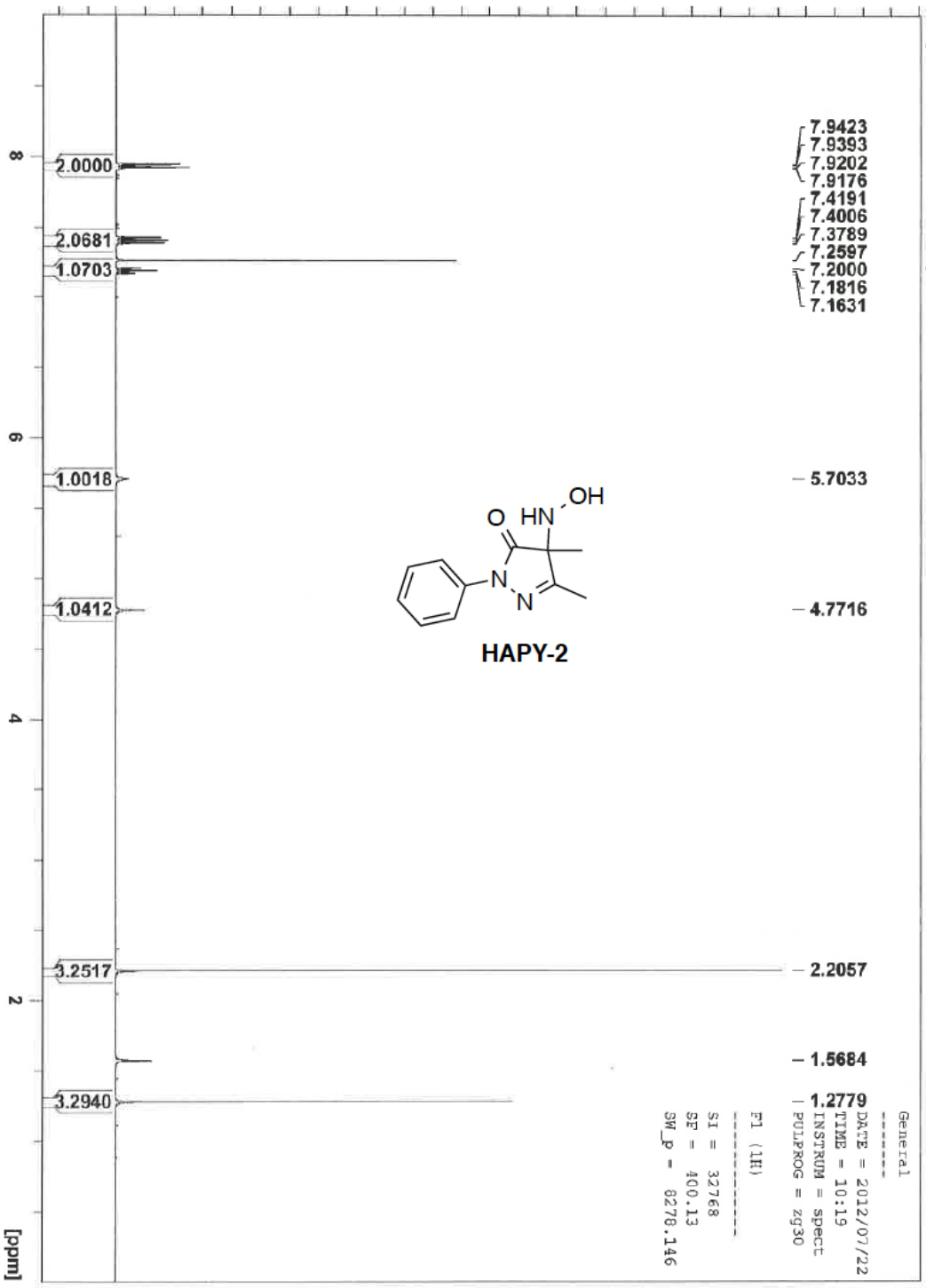
7.9423
7.9393
7.9202
7.9176
7.4191
7.4006
7.3789
7.2597
7.2000
7.1816
7.1631
2.0000
2.0681
1.0703
1.0018
1.0412
3.2517
3.2940
5.7033
4.7716
2.2057
1.5684
1.2779
O HN OH
N N
HAPY-2
[ppm]
8
6
4
2
General
DATE = 2012/07/22
TIME = 10:19
INSTRUM = spect
PULPROG = zg30
F1 (1H)
SI = 32768
SF = 400.13
SW_p = 8278.146

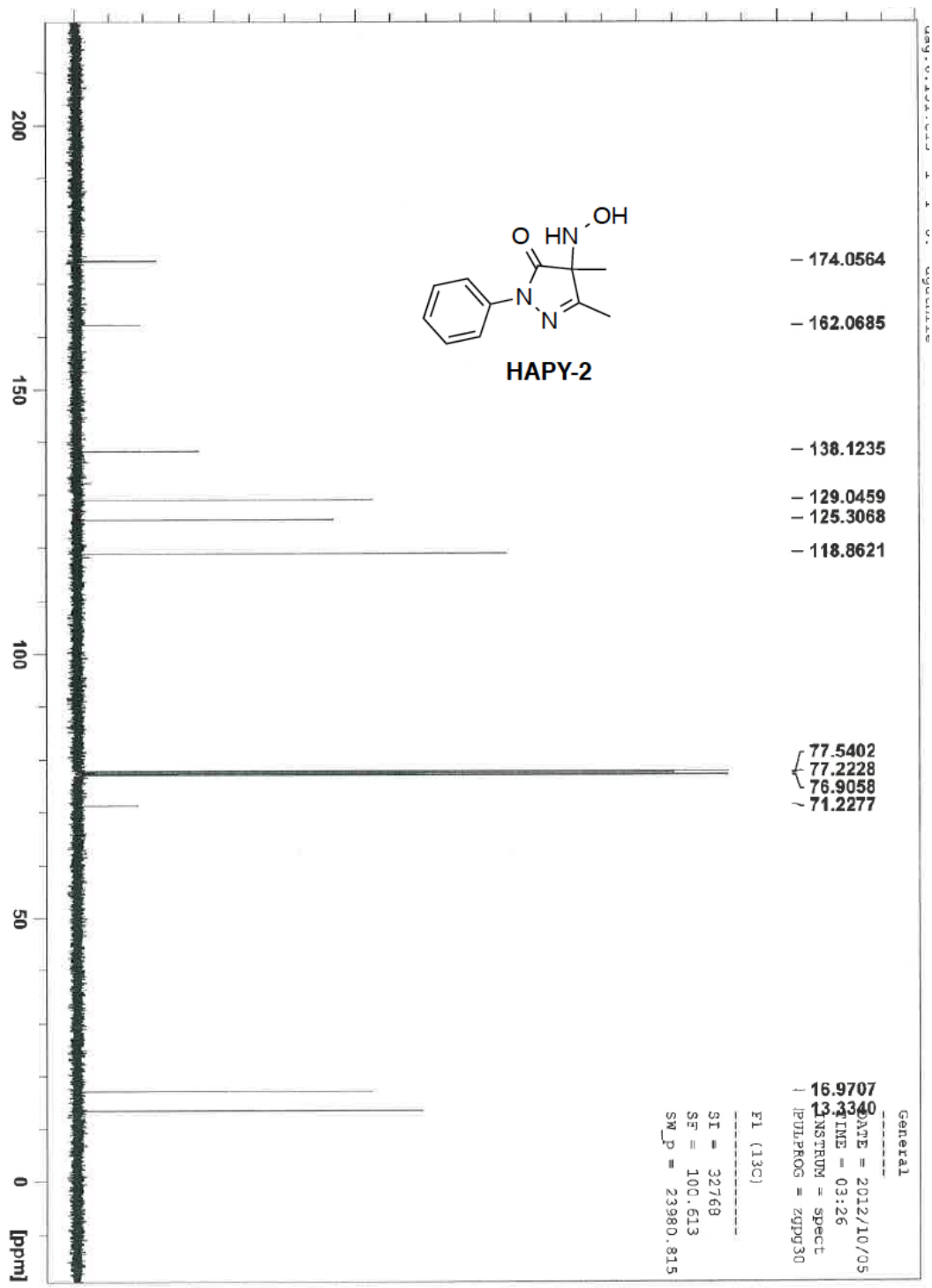
HAPY-2
174.0564
162.0685
138.1235
129.0459
125.3068
118.8621
77.5402
77.2228
76.9058
71.2277
16.9707
13.3340
200
150
100
50
0
[ppm]
General
DATE = 2012/10/05
TIME = 03:26
INSTRUM = spect
PULPROG = zgpg30
F1 (13C)
SI = 32768
SF = 100.613
SW_p = 23980.815

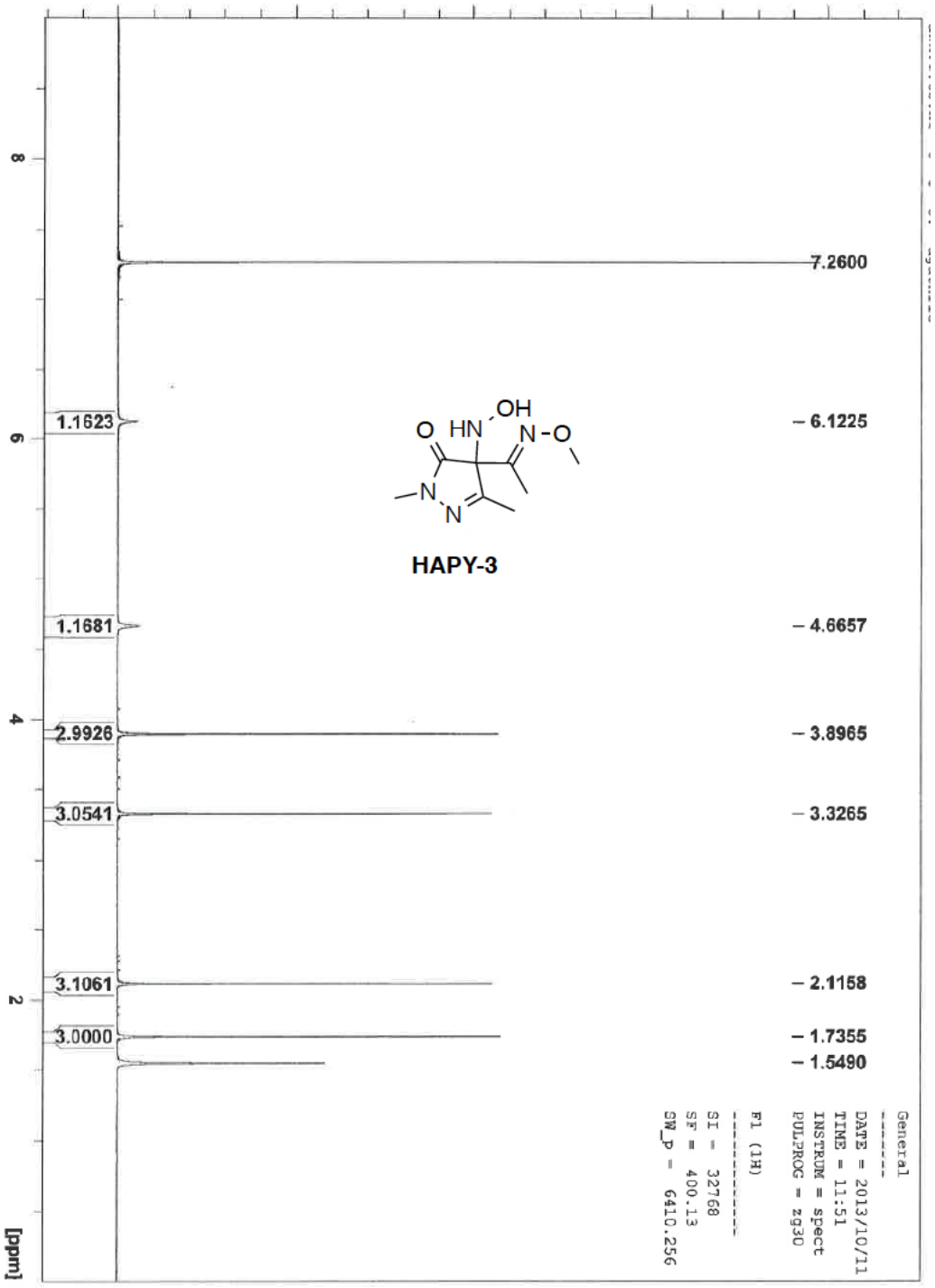
7.2600
6.1225
4.6657
3.8965
3.3265
2.1158
1.7355
1.5490
1.1623
1.1681
2.9926
3.0541
3.1061
3.0000
HAPY-3
[ppm]
General
DATE = 2013/10/11
TIME = 11:51
INSTRUM = spect
PULPROG = zg30
F1 (1H)
SI = 32768
SF = 400.13
SW_p = 6410.256

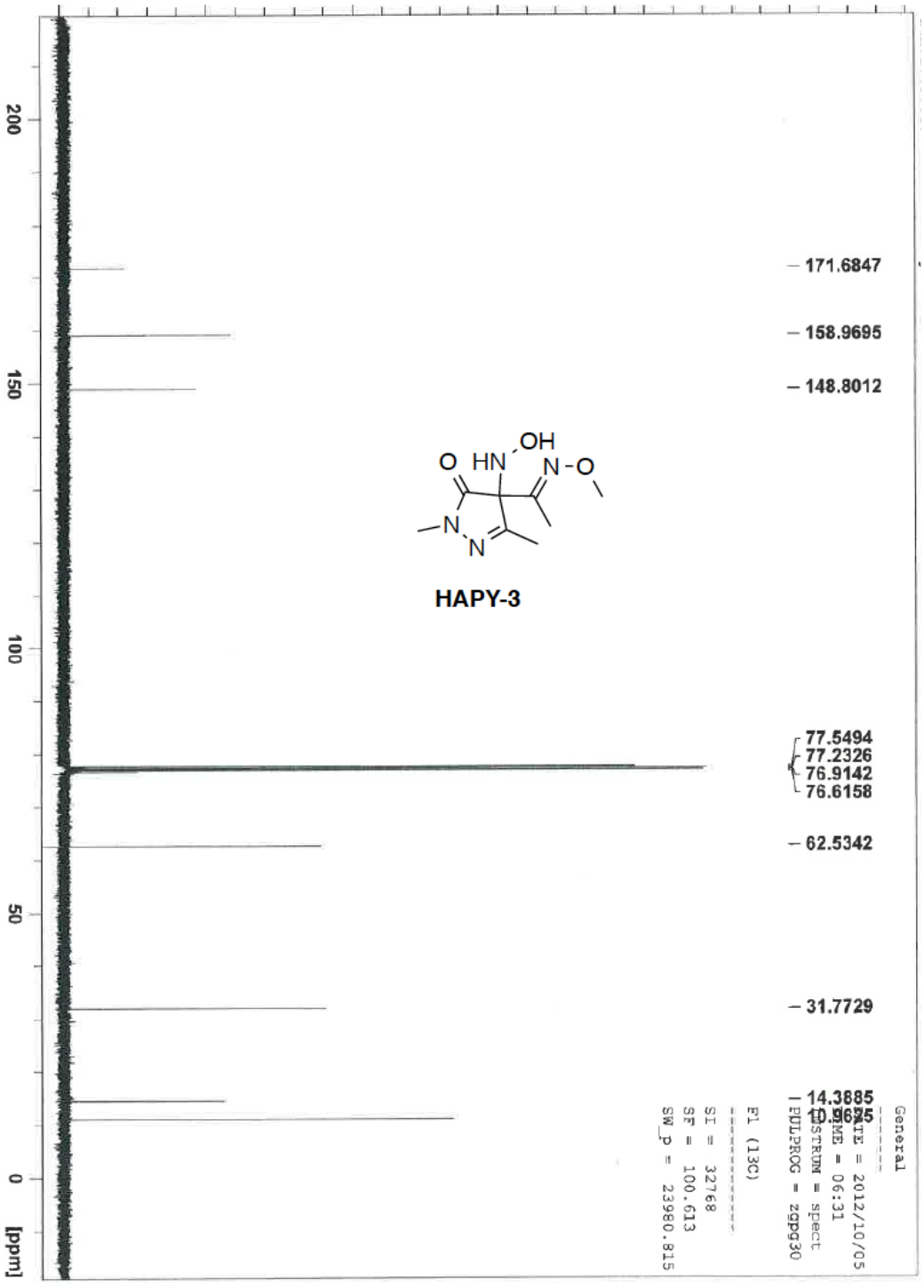
200
150
100
50
0
[ppm]
171.6847
158.9695
148.8012
77.5494
77.2326
76.9142
76.6158
62.5342
31.7729
14.3885
10.9625
O
HN
OH
N-O
N
N
HAPY-3
General
DATE = 2012/10/05
TIME = 06:31
INSTRUM = spect
PULPROG = zgpg30
F1 (13C)
SI = 32768
SF = 100.613
SW_p = 23960.815

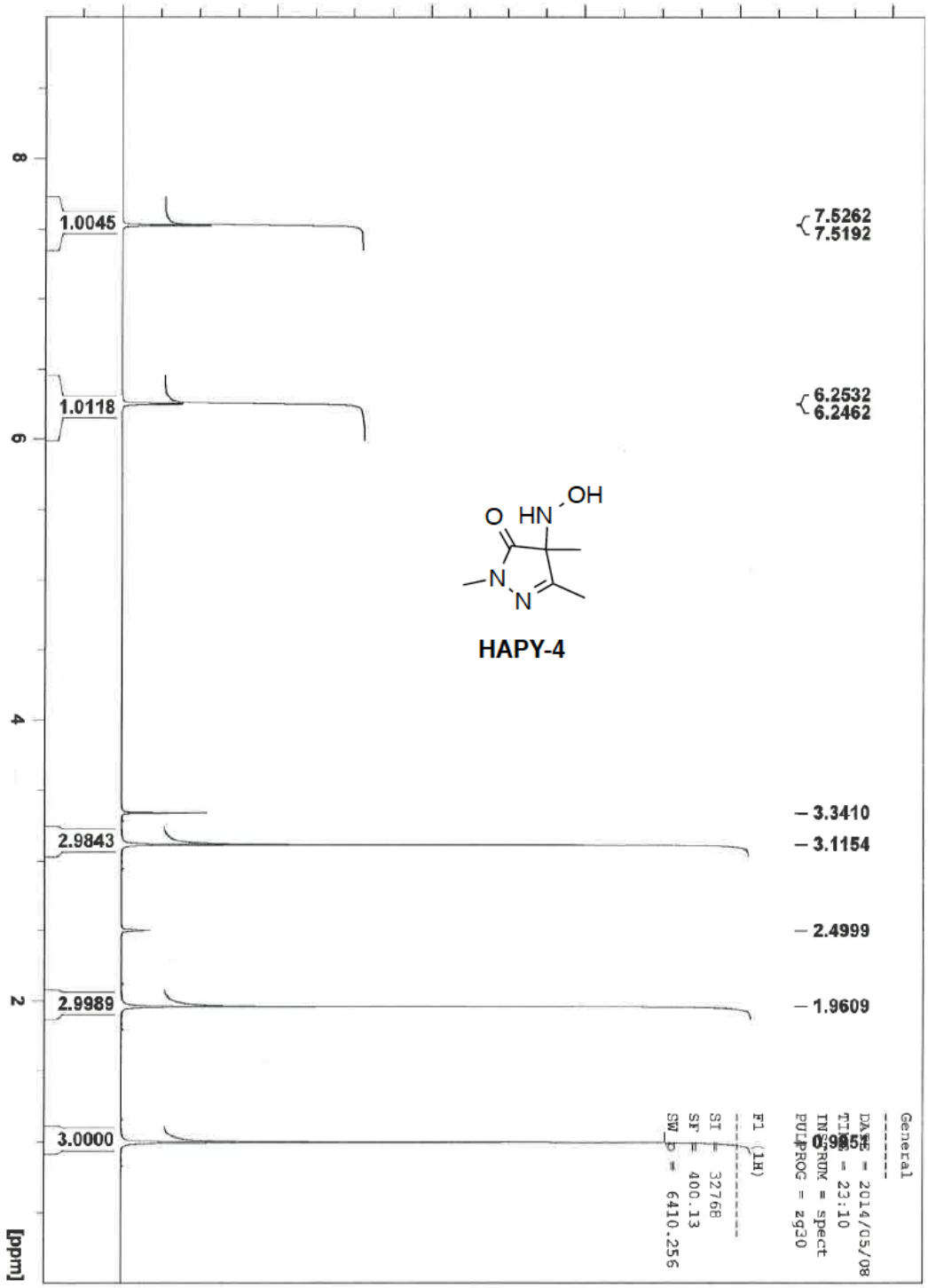
7.5262
7.5192
6.2532
6.2462
3.3410
3.1154
2.4999
1.9609
1.0045
1.0118
2.9843
2.9989
3.0000
O HN OH
N
N
HAPY-4
[ppm]
8
6
4
2
General
DATE = 2014/05/08
INSTRUM = spect
PULPROG = zg30
F1 (1H)
SI = 32768
SF = 400.13
SW_p = 6410.256

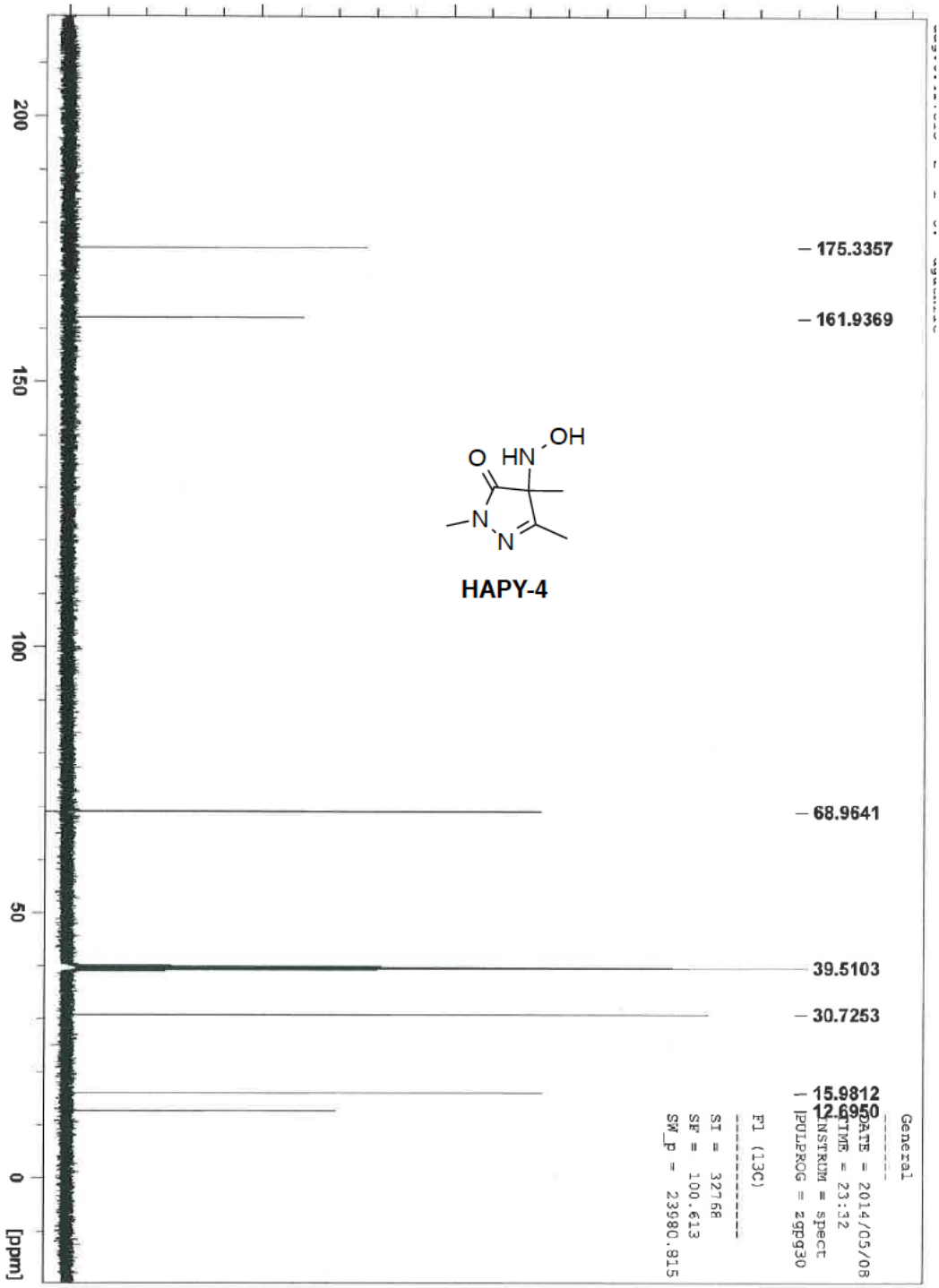
200
150
100
50
0
[ppm]
175.3357
161.9369
68.9641
39.5103
30.7253
15.9812
12.6950
OH
O HN
N
N
HAPY-4
General
DATE = 2014/05/08
TIME = 23:32
INSTRUM = spect
PULPROG = zgpg30
F1 (13C)
SI = 32768
SF = 100.613
SW_p = 23980.815

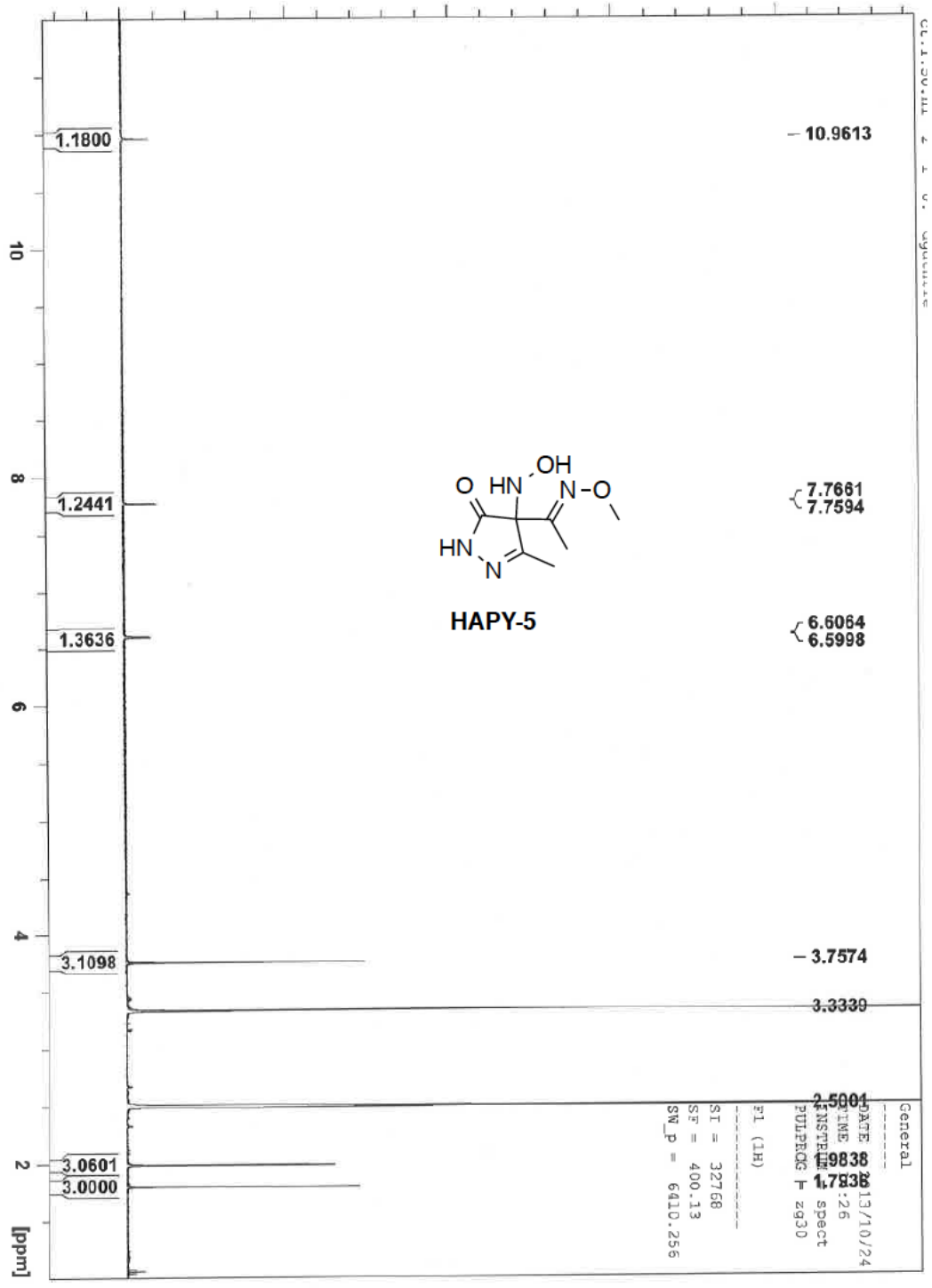
1.1800
1.2441
1.3636
3.1098
3.0601
3.0000
10.9613
7.7661
7.7594
6.6064
6.5998
3.7574
3.3339
2.5001
1.9838
1.7838
HAPY-5
[ppm]
General
DATE 2013/10/24
TIME 11:26
EXPSTD spect
PULPROG zg30
F1 (1H)
SI = 32768
SF = 400.13
SW_p = 6410.256

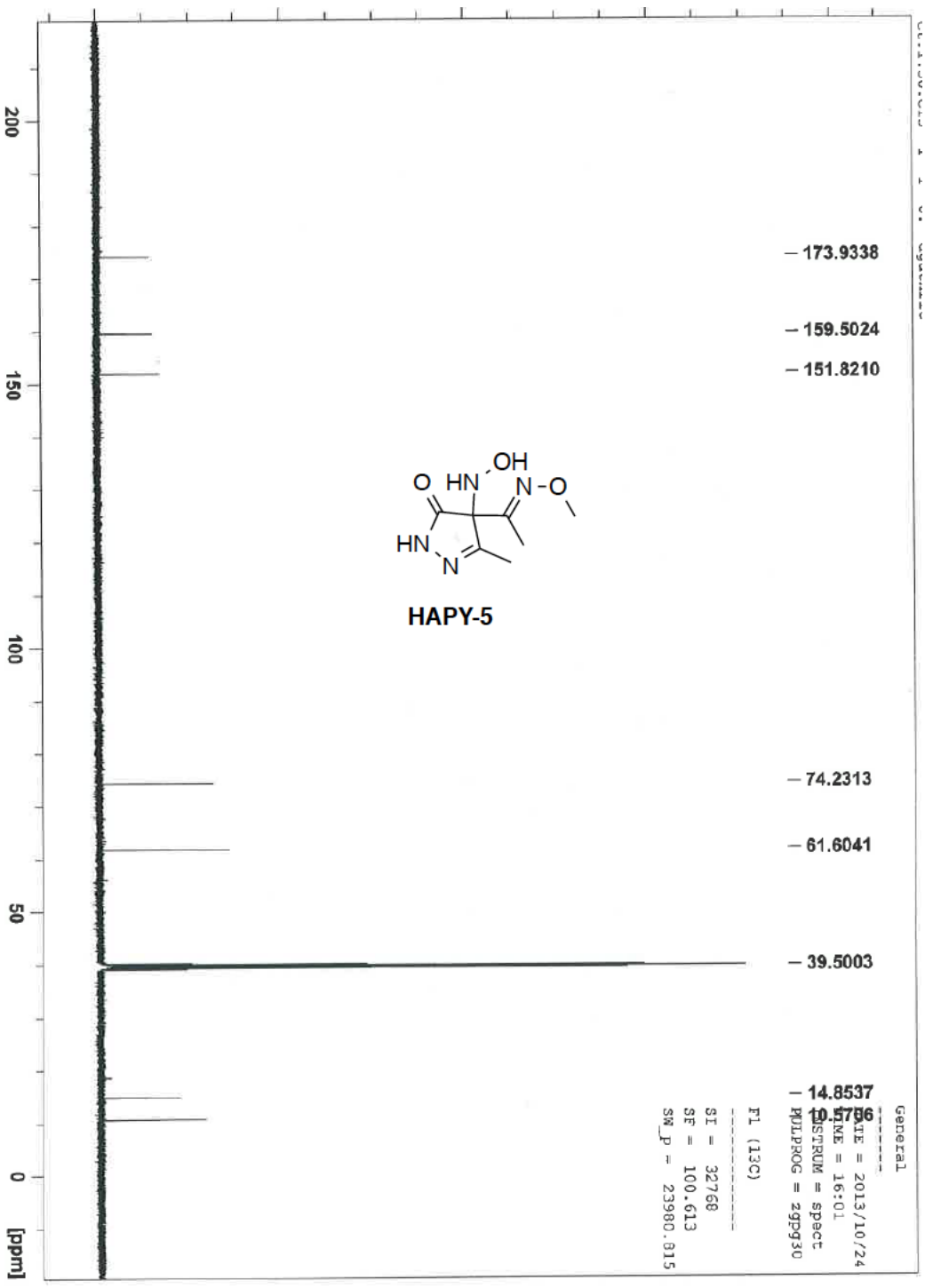
200
150
100
50
0
[ppm]
173.9338
159.5024
151.8210
74.2313
61.6041
39.5003
14.8537
10.5796
HN
OH
O
HN
N
O
N
HAPY-5
General
DATE = 2013/10/24
TIME = 16:01
INSTRUM = spect
PULPROG = zgpg30
F1 (13C)
SI = 32768
SF = 100.613
SW_p = 23980.815

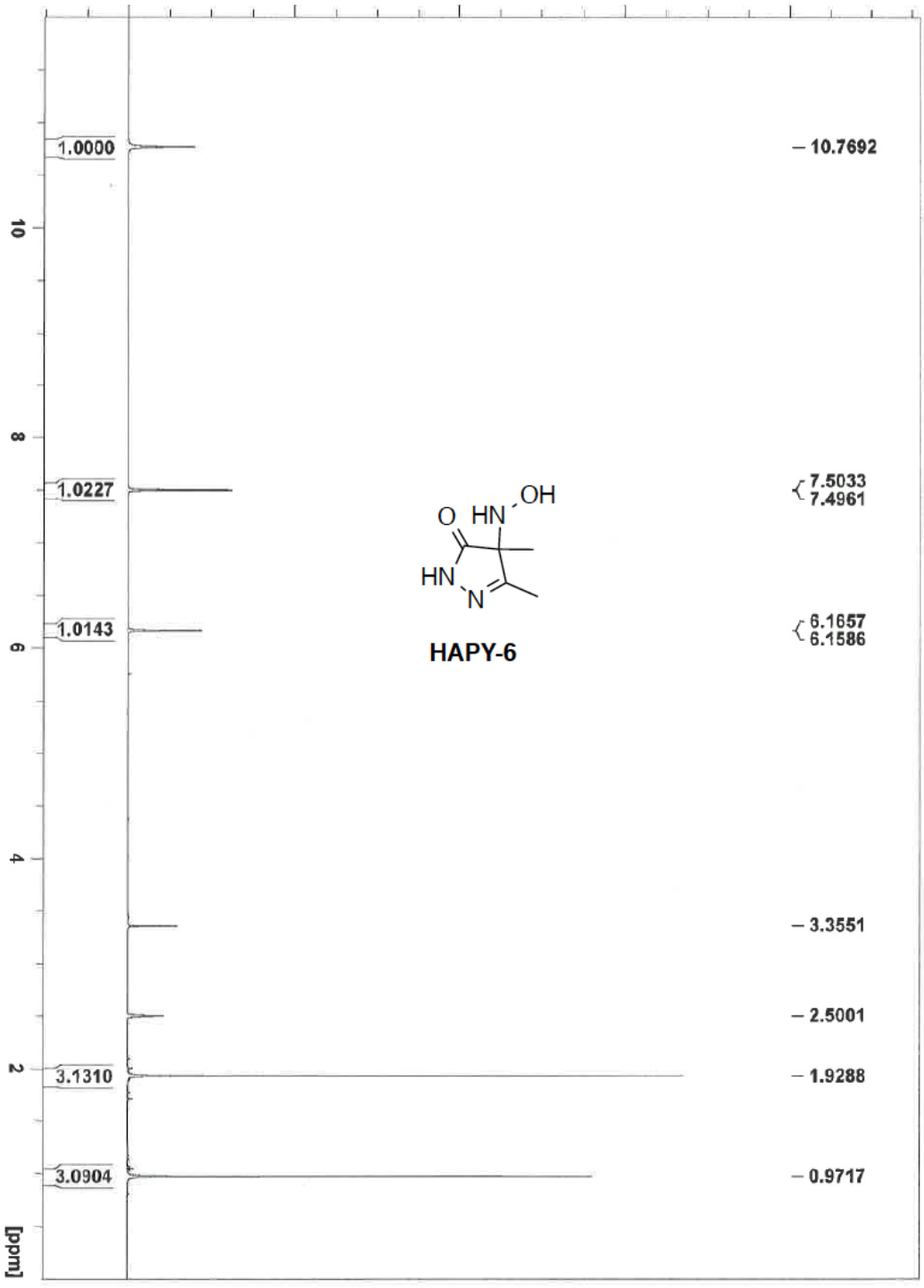
1.0000
1.0227
1.0143
3.1310
3.0904
10.7692
7.5033
7.4961
6.1657
6.1586
3.3551
2.5001
1.9288
0.9717
HAPY-6
[ppm]

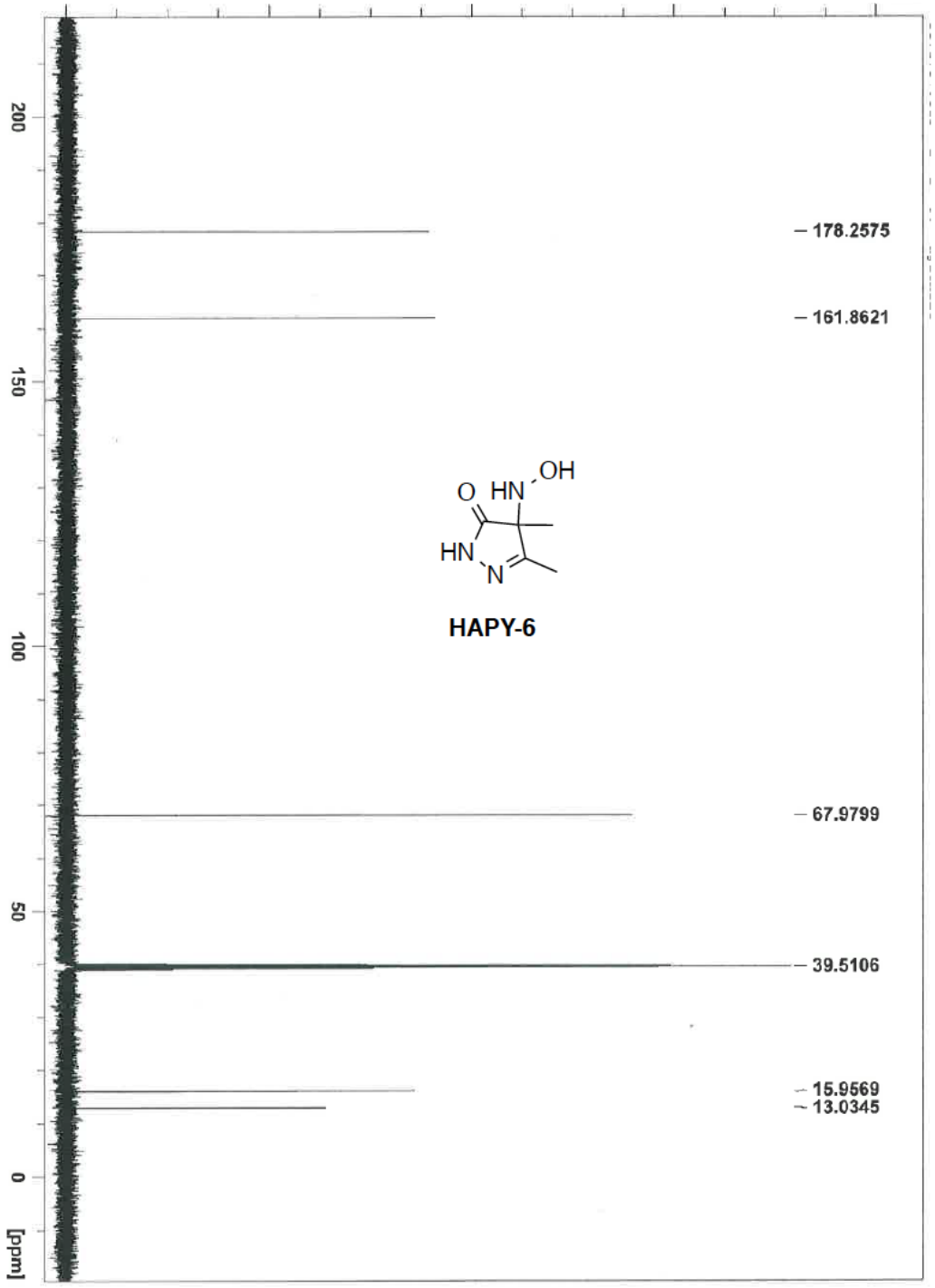
200
150
100
50
0
[ppm]
178.2575
161.8621
67.9799
39.5106
15.9569
13.0345
O
HN
OH
HN
N
HAPY-6

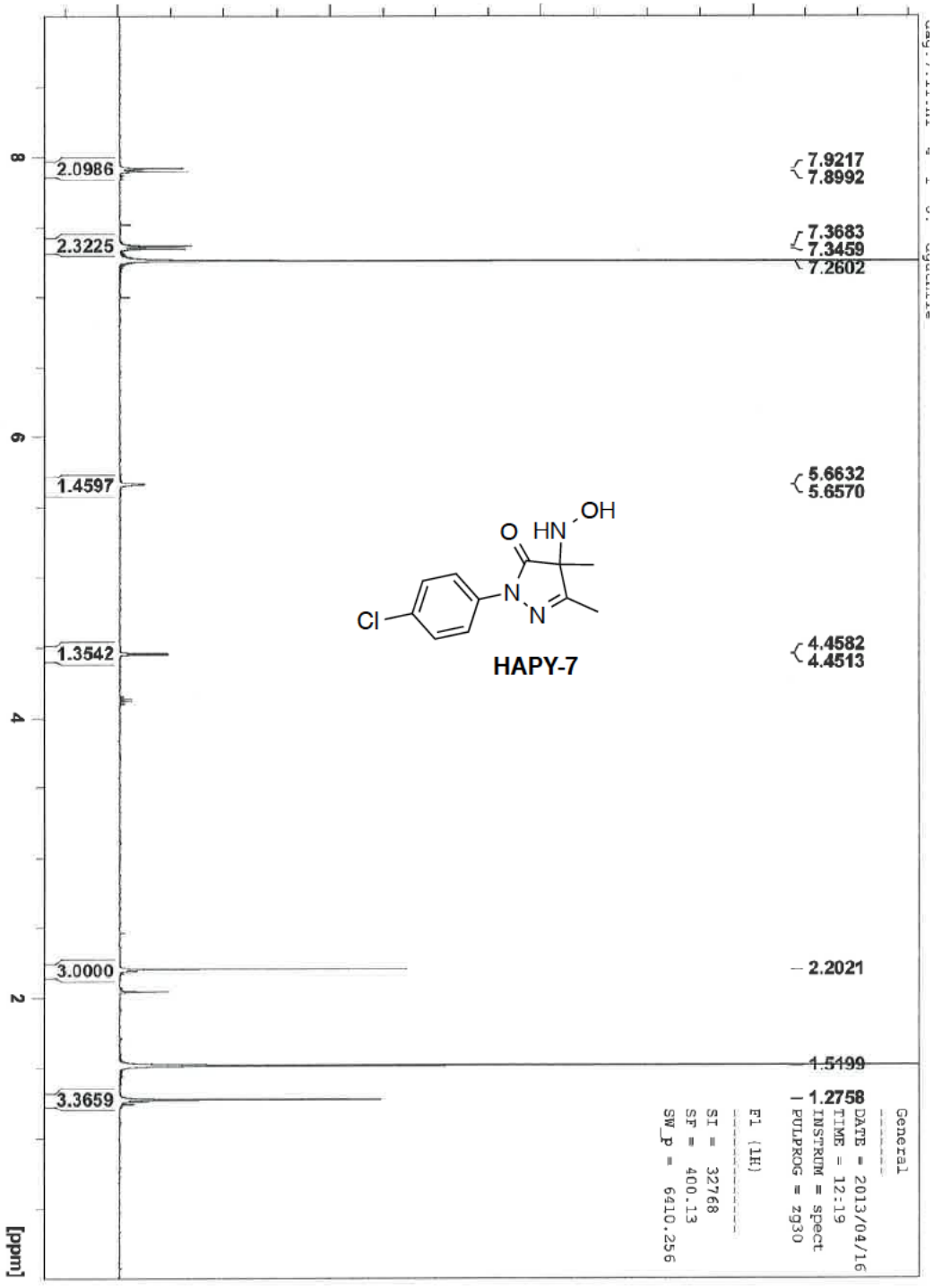
8
6
4
2
[ppm]
2.0986
2.3225
1.4597
1.3542
3.0000
3.3659
7.9217
7.8992
7.3683
7.3459
7.2602
5.6632
5.6570
4.4582
4.4513
2.2021
1.5199
1.2758
O
HN
OH
N
N
Cl
HAPY-7
General
DATE = 2013/04/16
TIME = 12:19
INSTRUM = spect
PULPROG = zg30
F1 (1H)
SI = 32768
SF = 400.13
SW_p = 6410.256

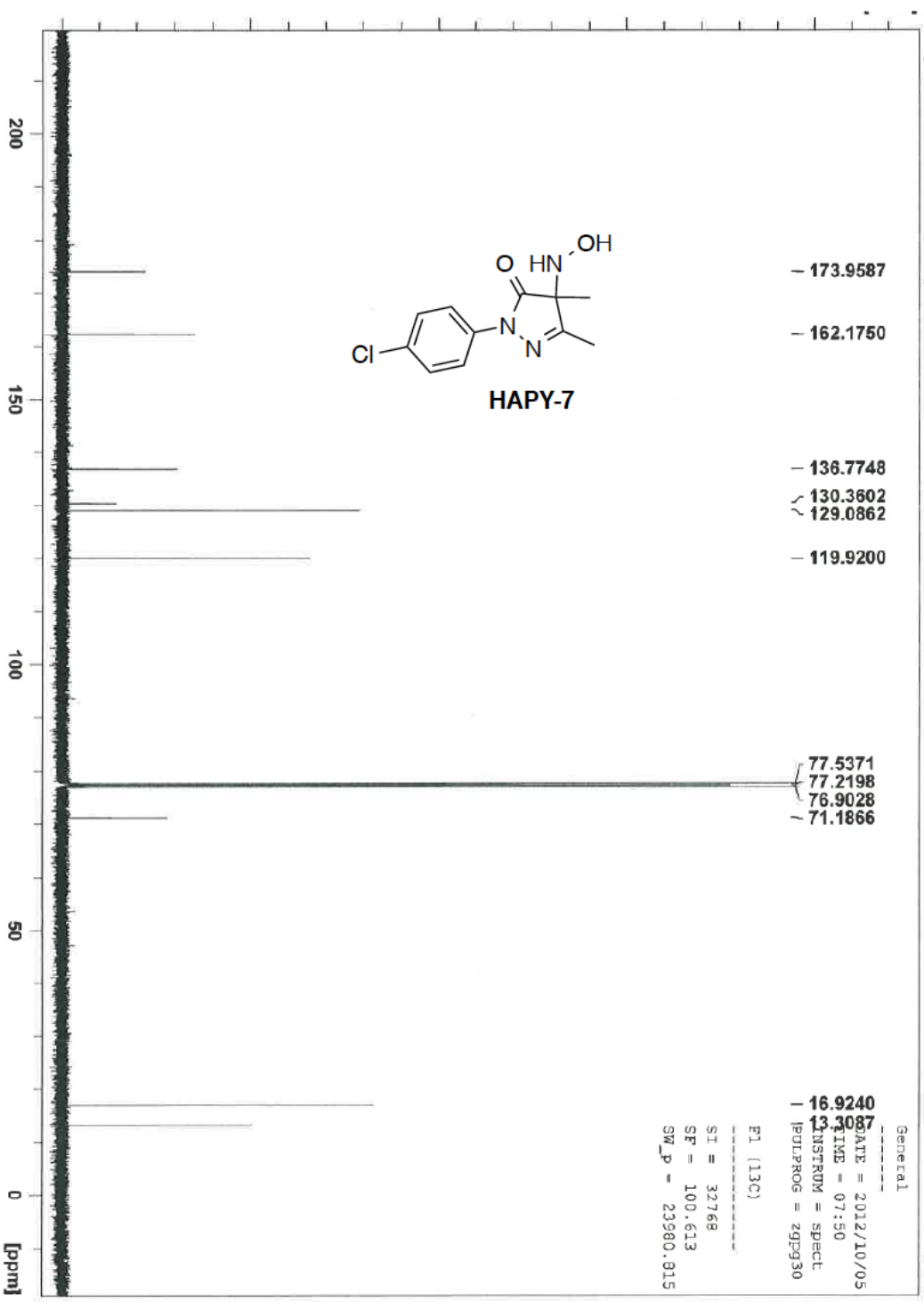
HAPY-7
173.9587
162.1750
136.7748
130.3602
129.0862
119.9200
77.5371
77.2198
76.9028
71.1866
16.9240
13.3087
200
150
100
50
0
[ppm]
General
DATE = 2012/10/05
TIME = 07:50
INSTRUM = spect
PULPROG = zgpg30
F1 (13C)
SI = 32768
SF = 100.613
SW_p = 23980.815

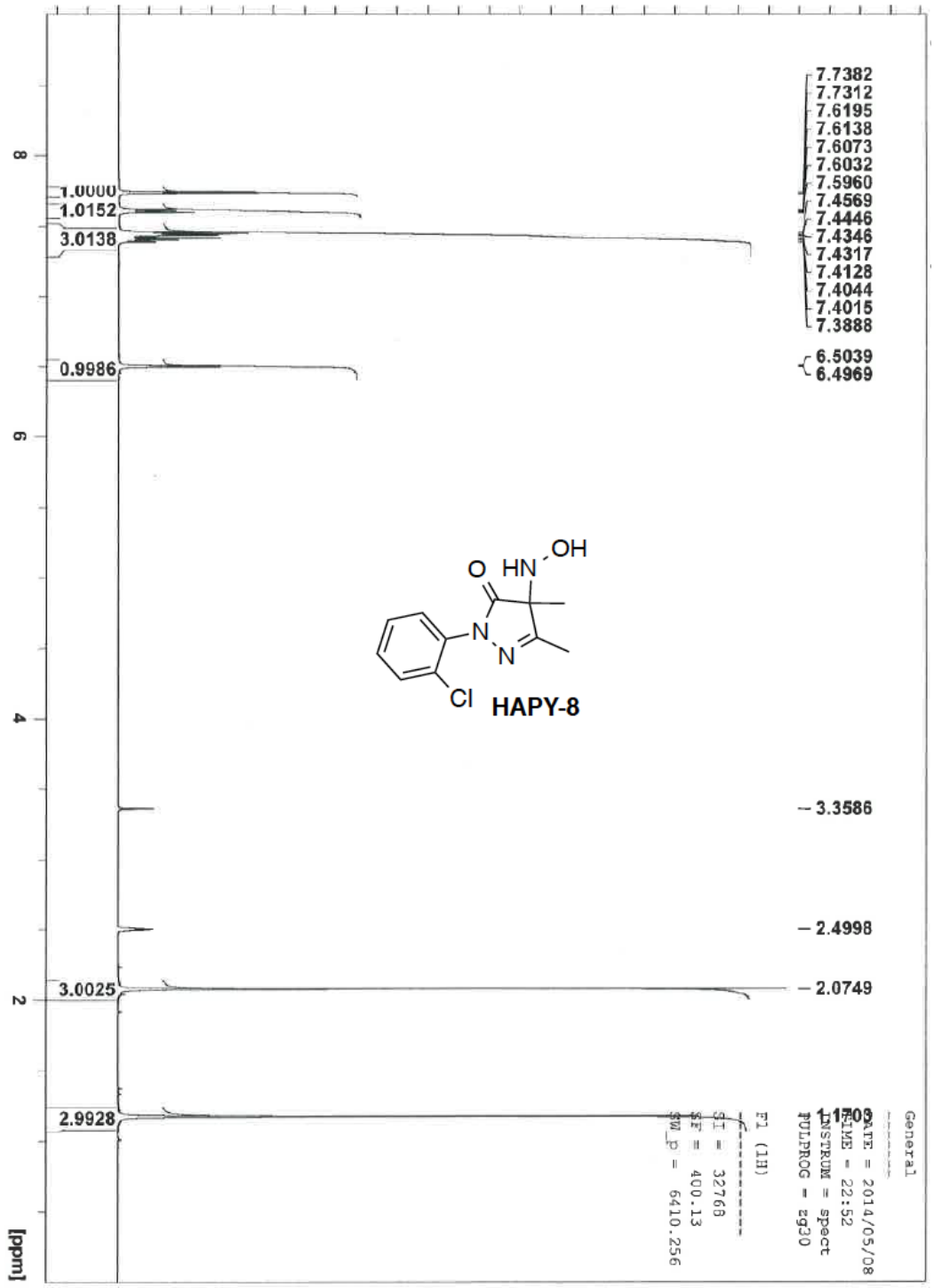
7.7382
7.7312
7.6195
7.6138
7.6073
7.6032
7.5960
7.4569
7.4446
7.4346
7.4317
7.4128
7.4044
7.4015
7.3888
6.5039
6.4969
1.0000
1.0152
3.0138
0.9986
3.0025
2.9928
3.3586
2.4998
2.0749
1.1703
OH
HN
O
N
N
Cl
HAPY-8
[ppm]
8
6
4
2
General
DATE = 2014/05/08
TIME = 22:52
INSTRUM = spect
PULPROG = zg30
F1 (1H)
SI = 32768
SF = 400.13
SW_p = 6410.256

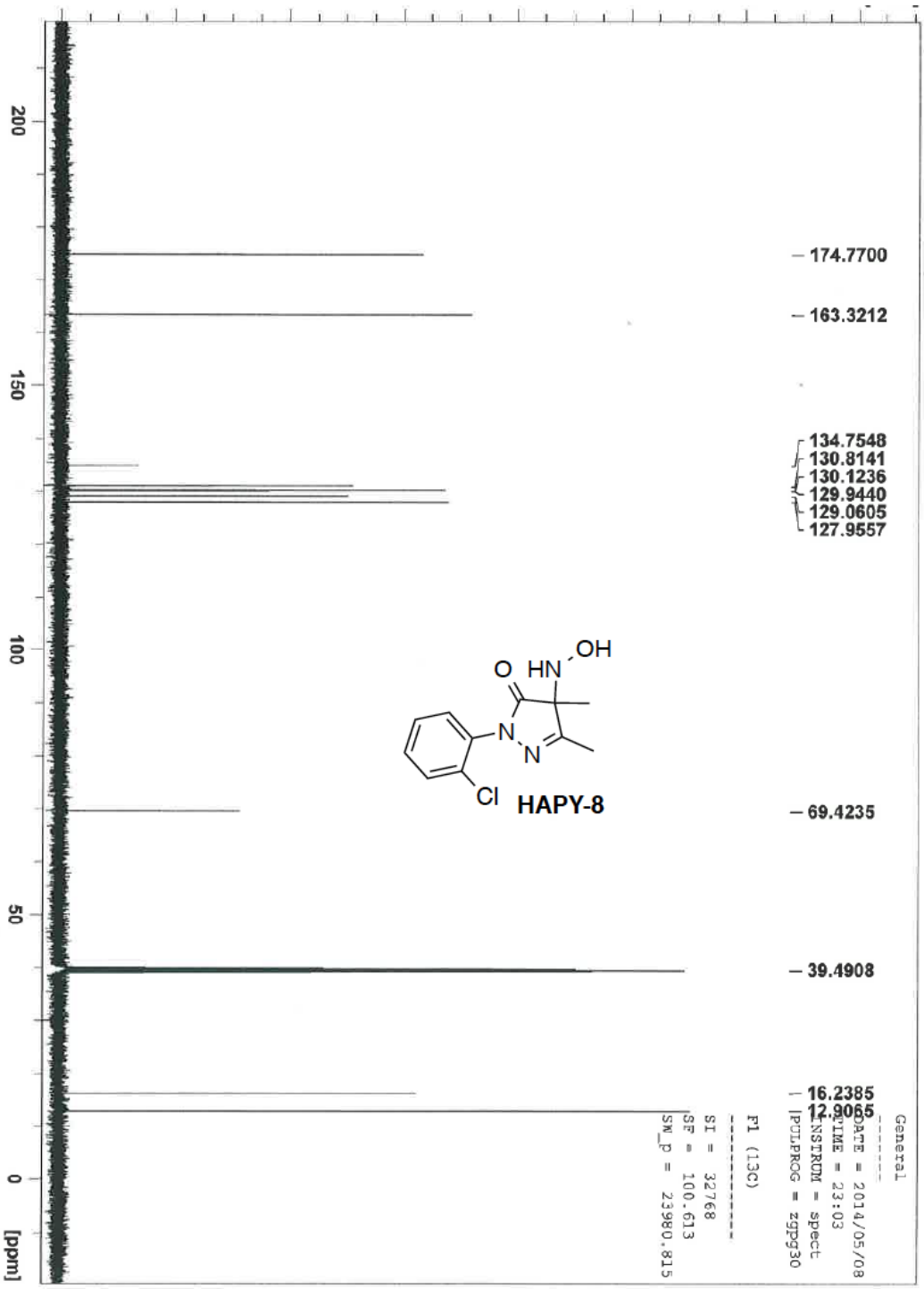
200
150
100
50
0
[ppm]
174.7700
163.3212
134.7548
130.8141
130.1236
129.9440
129.0605
127.9557
69.4235
39.4908
16.2385
12.9065
O
HN
OH
N
N
Cl
HAPY-8
General
DATE = 2014/05/08
TIME = 23:03
INSTRUM = spect
PULPROG = zgpg30
F1 (13C)
SI = 32768
SF = 100.613
SW_p = 23980.815

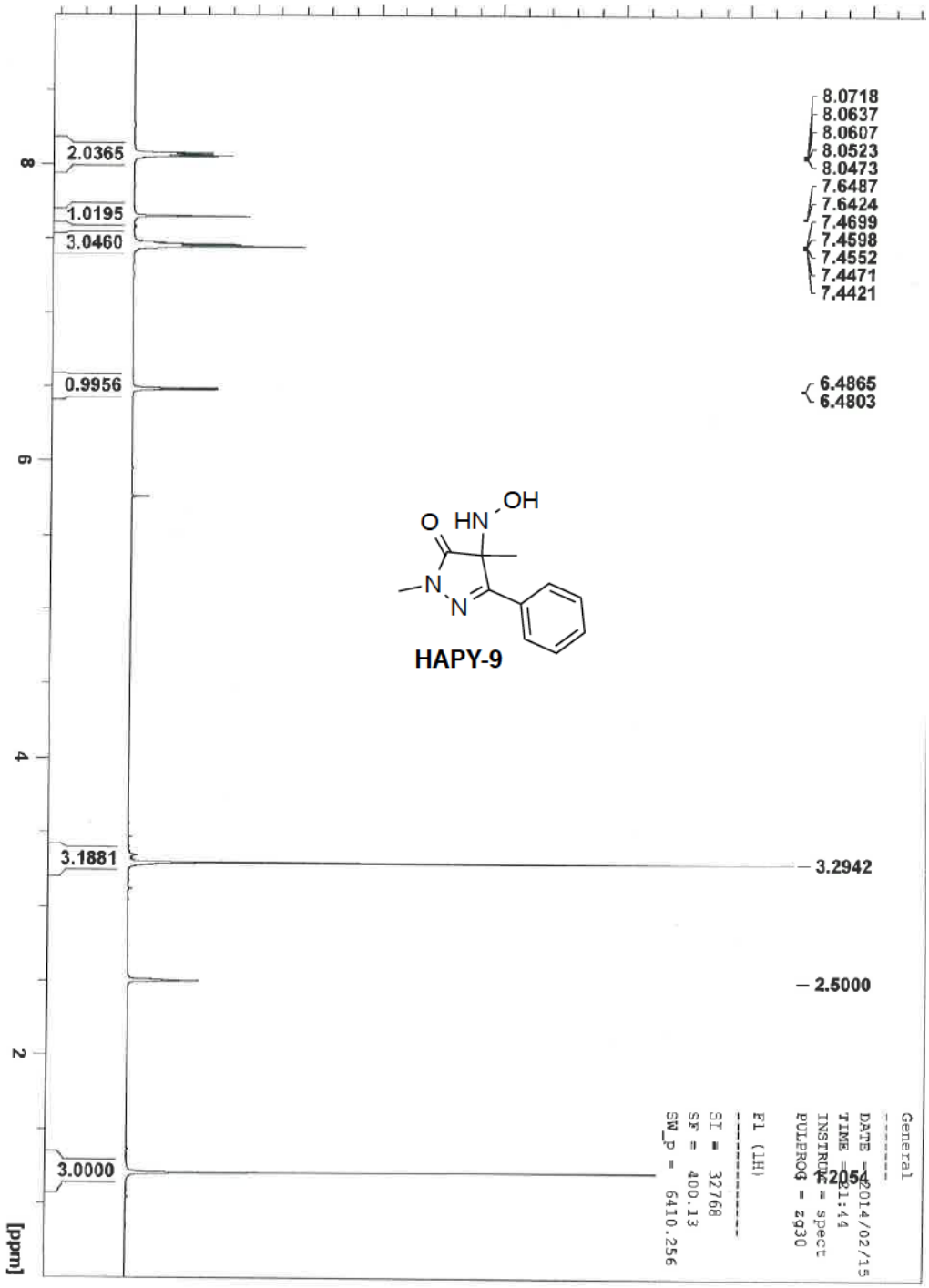
8.0718
8.0637
8.0607
8.0523
8.0473
7.6487
7.6424
7.4699
7.4598
7.4552
7.4471
7.4421
6.4865
6.4803
3.2942
2.5000
2.2054
2.0365
1.0195
3.0460
0.9956
3.1881
3.0000
O HN OH
N N
HAPY-9
[ppm]
General
DATE = 2014/02/15
TIME = 21:44
INSTRUM = spect
PULPROG = zg30
FL (LH)
SI = 32768
SF = 400.13
SW_p = 6410.256

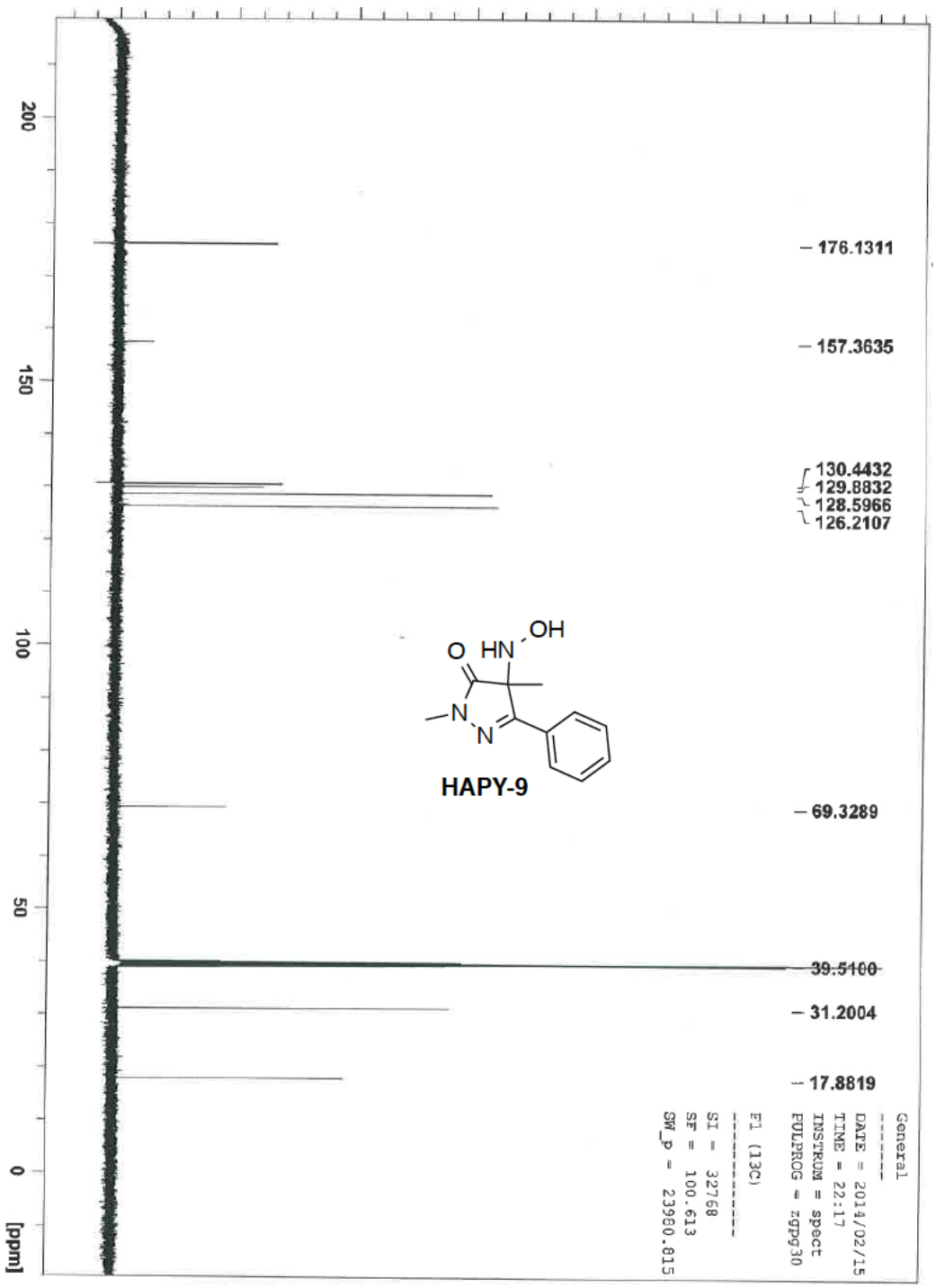
176.1311
157.3635
130.4432
129.8832
128.5966
126.2107
69.3289
39.5100
31.2004
17.8819
HAPY-9
200
150
100
50
0
[ppm]
General
DATE = 2014/02/15
TIME = 22:17
INSTRUM = spect
PULPROG = zgpg30
F1 (13C)
SI = 32768
SF = 100.613
SW_p = 23980.815

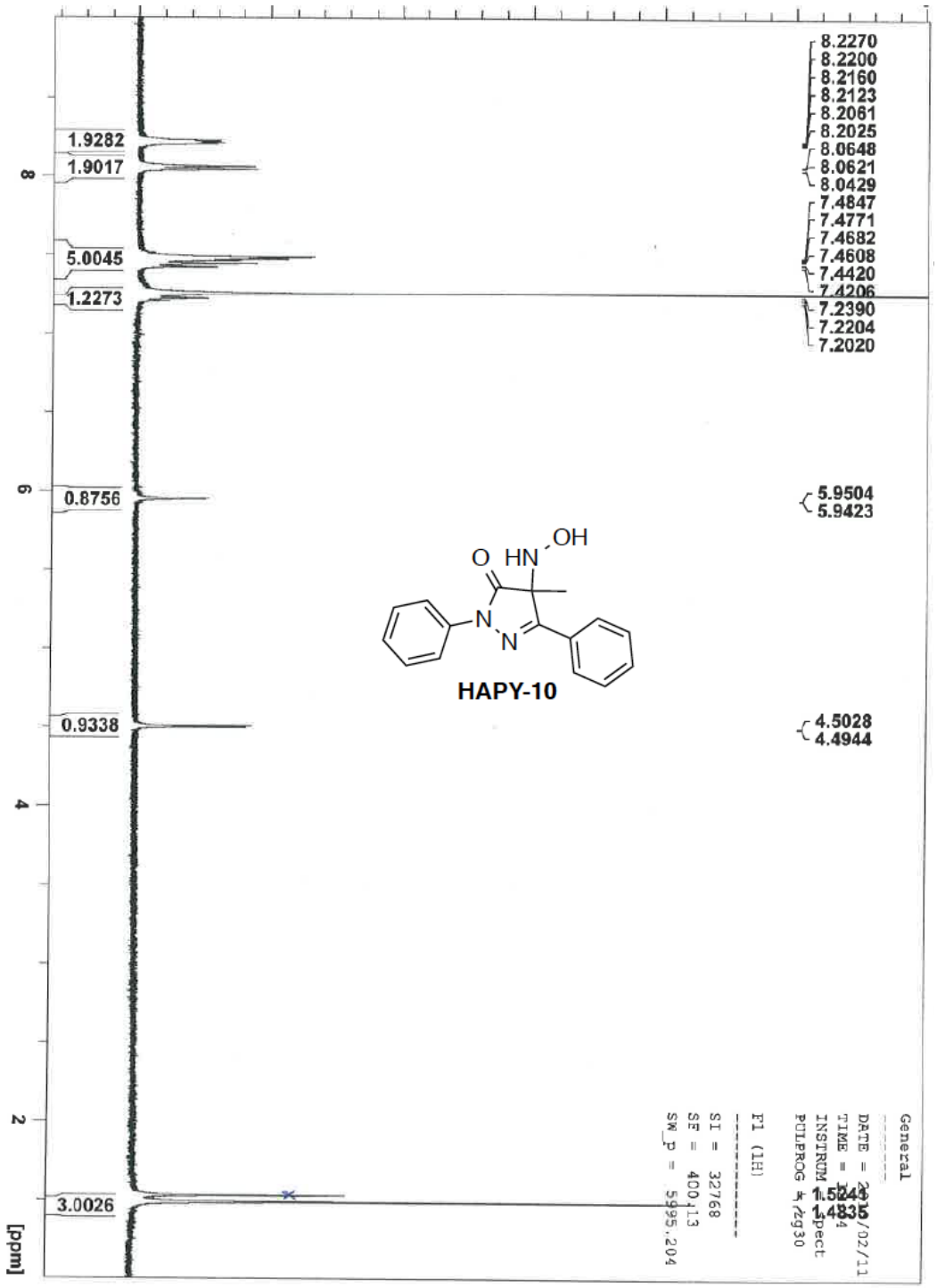
8.2270
8.2200
8.2160
8.2123
8.2061
8.2025
8.0648
8.0621
8.0429
7.4847
7.4771
7.4682
7.4608
7.4420
7.4206
7.2390
7.2204
7.2020
5.9504
5.9423
4.5028
4.4944
1.9282
1.9017
5.0045
1.2273
0.8756
0.9338
3.0026
1.5243
1.4835
O HN OH
N
N
HAPY-10
General
DATE = 2015/02/11
TIME = 13:04
INSTRUM spect
PULPROG zg30
F1 (1H)
SI = 32768
SF = 400.13
SW_p = 5995.204
8
6
4
2
[ppm]

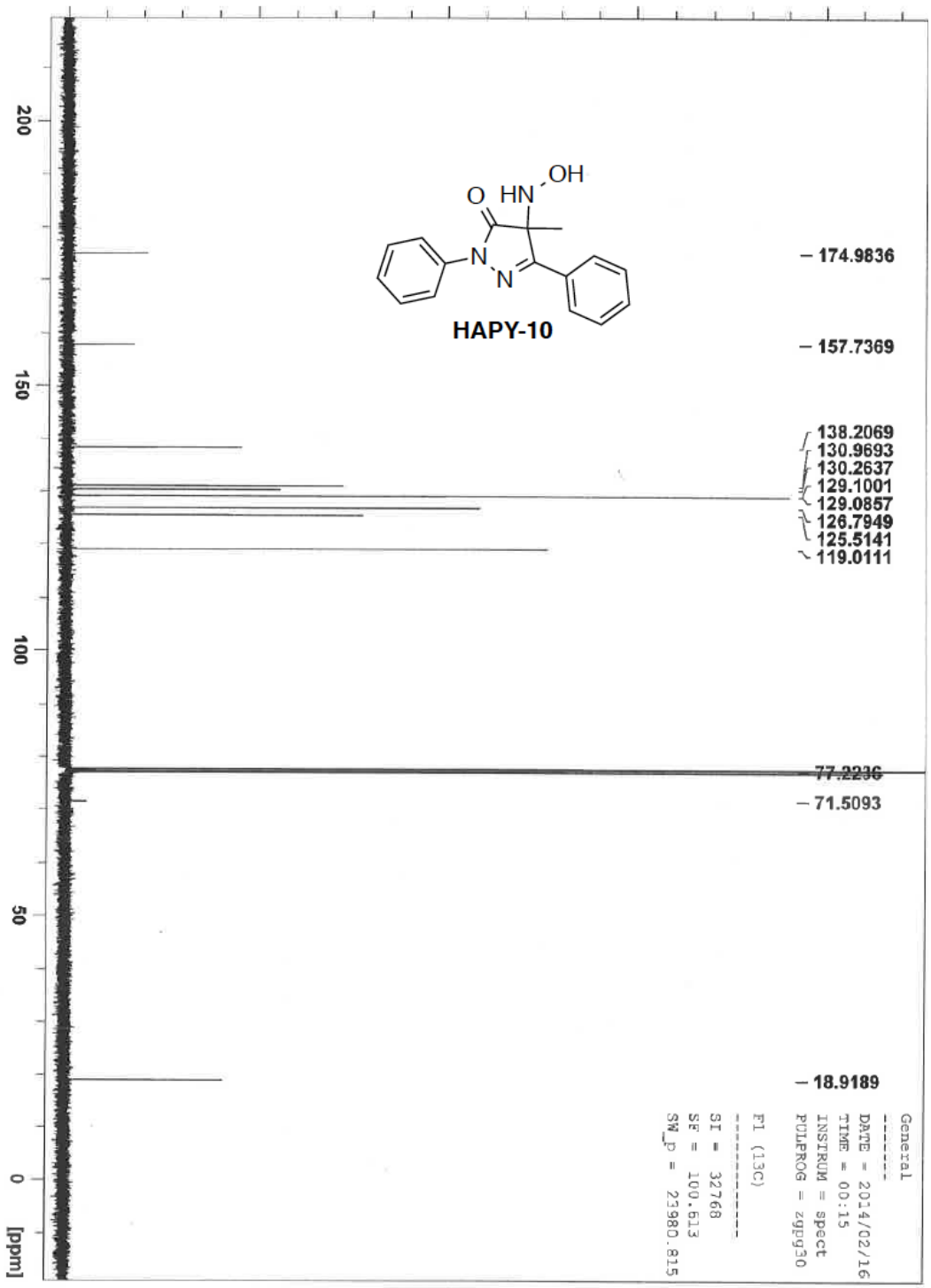
HAPY-10
O
HN
OH
N
N
174.9836
157.7369
138.2069
130.9693
130.2637
129.1001
129.0857
126.7949
125.5141
119.0111
77.2236
71.5093
18.9189
200
150
100
50
0
[ppm]
General
DATE = 2014/02/16
TIME = 00:15
INSTRUM = spect
PULPROG = zgpg30
F1 (13C)
SI = 32768
SF = 100.613
SW_p = 23980.815

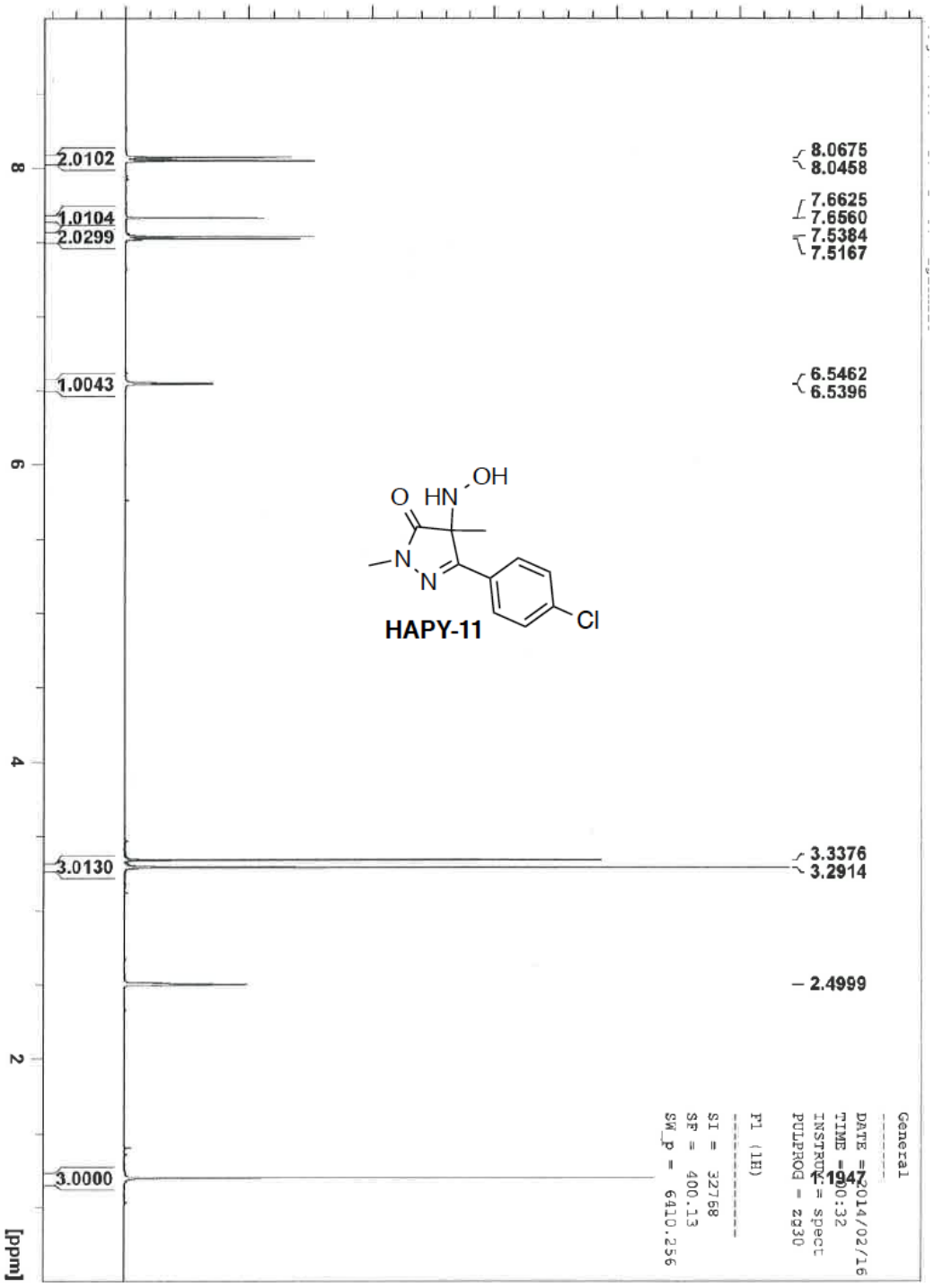
8.0675
8.0458
7.6625
7.6560
7.5384
7.5167
6.5462
6.5396
3.3376
3.2914
2.4999
2.0102
1.0104
2.0299
1.0043
3.0130
3.0000
HAPY-11
Cl
OH
HN
O
N
N
[ppm]
8
6
4
2
General
DATE = 2014/02/16
TIME = 20:32
INSTRUM = spect
PULPROG = zg30
F1 (1H)
SI = 32768
SF = 400.13
SW_p = 6410.256
1947

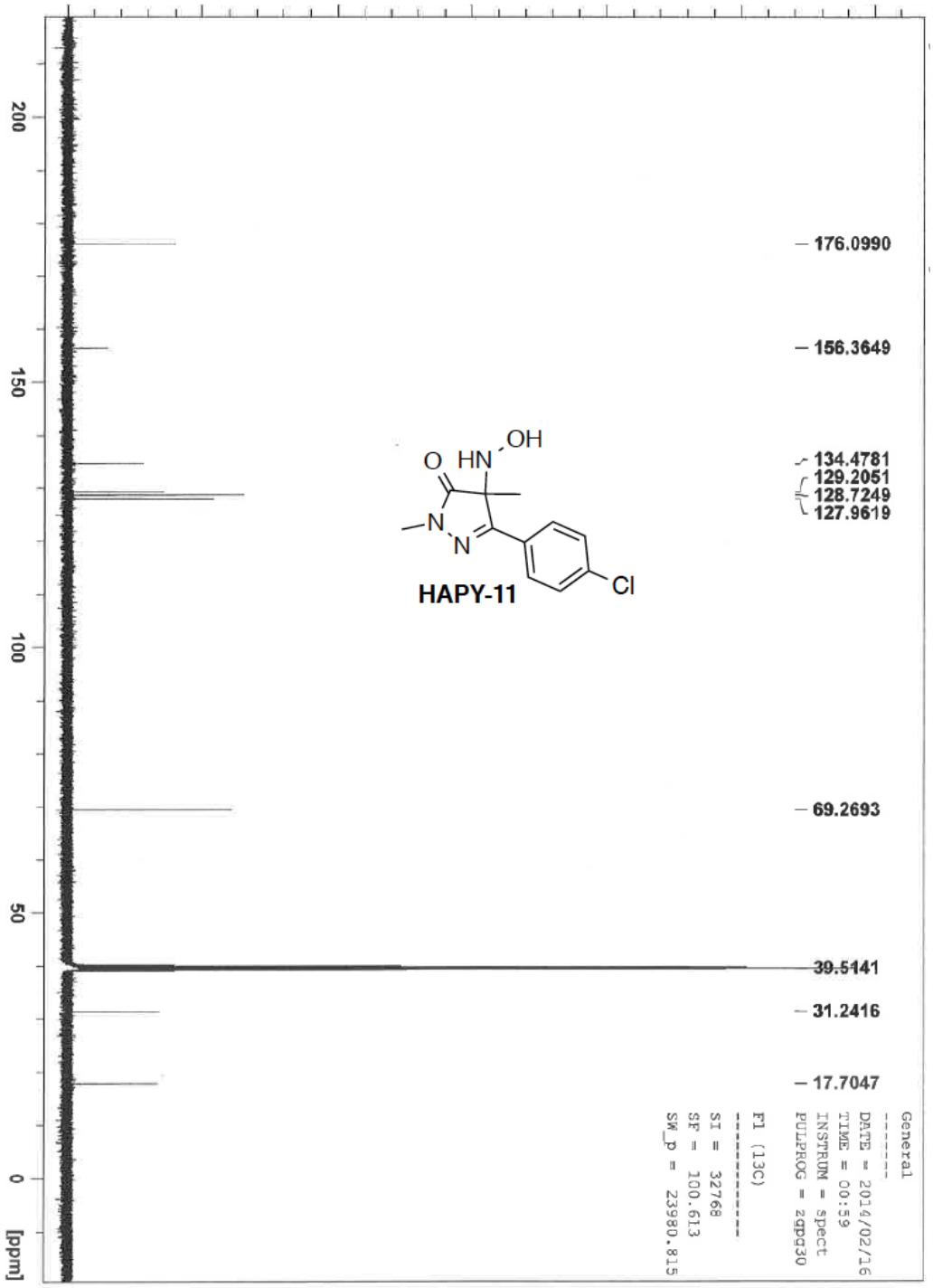
176.0990
156.3649
134.4781
129.2051
128.7249
127.9619
69.2693
39.5141
31.2416
17.7047
HAPY-11
O
HN
OH
N
N
Cl
200
150
100
50
0
[ppm]
General
DATE = 2014/02/16
TIME = 00:59
INSTRUM = spect
PULPROG = zgpg30
F1 (13C)
SI = 32768
SF = 100.613
SW_p = 23980.815

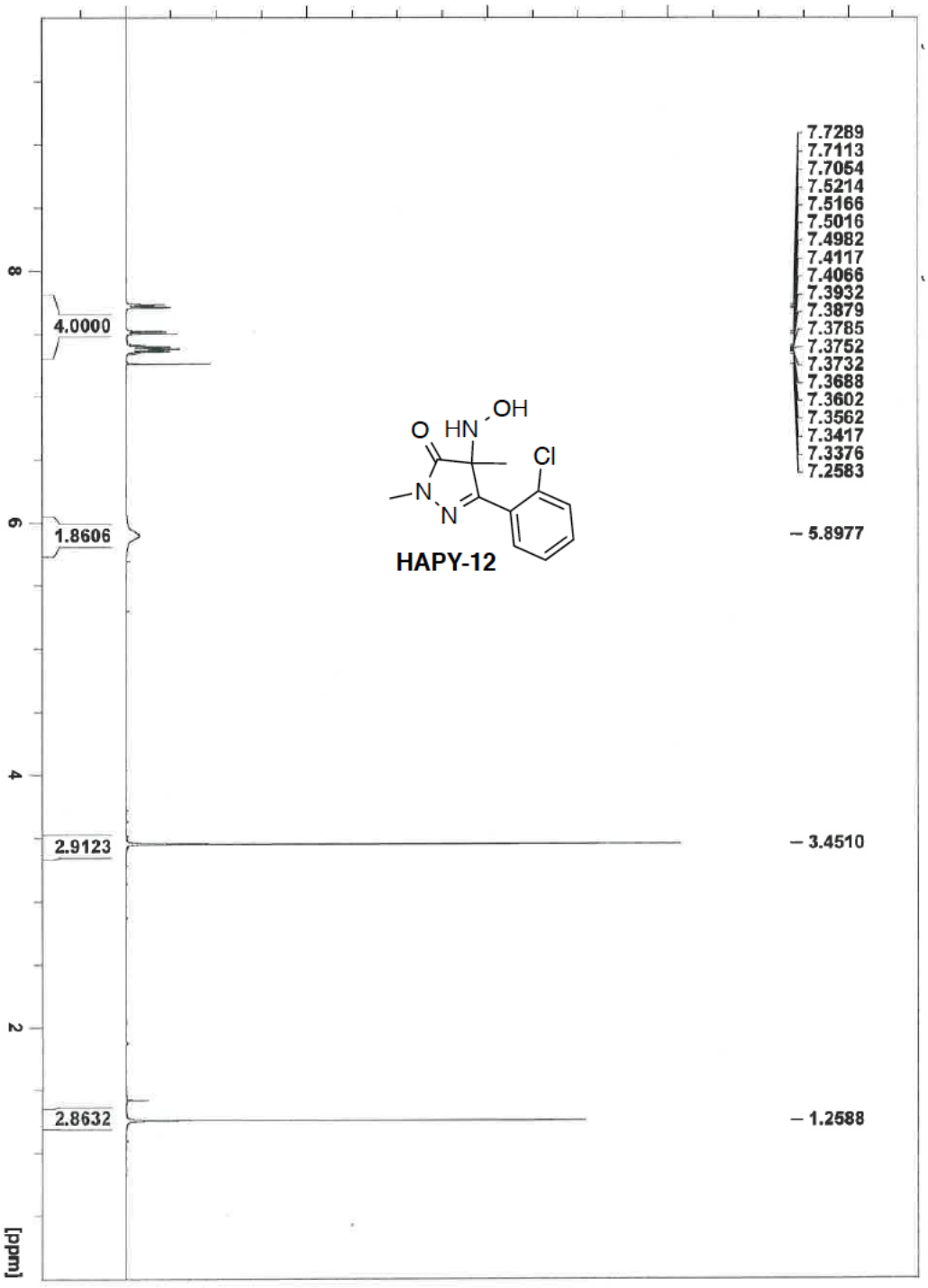
7.7289
7.7113
7.7054
7.5214
7.5166
7.5016
7.4982
7.4117
7.4066
7.3932
7.3879
7.3785
7.3752
7.3732
7.3688
7.3602
7.3562
7.3417
7.3376
7.2583
4.0000
1.8606
2.9123
2.8632
5.8977
3.4510
1.2588
OH
O HN
Cl
N
N
HAPY-12
8
6
4
2
[ppm]

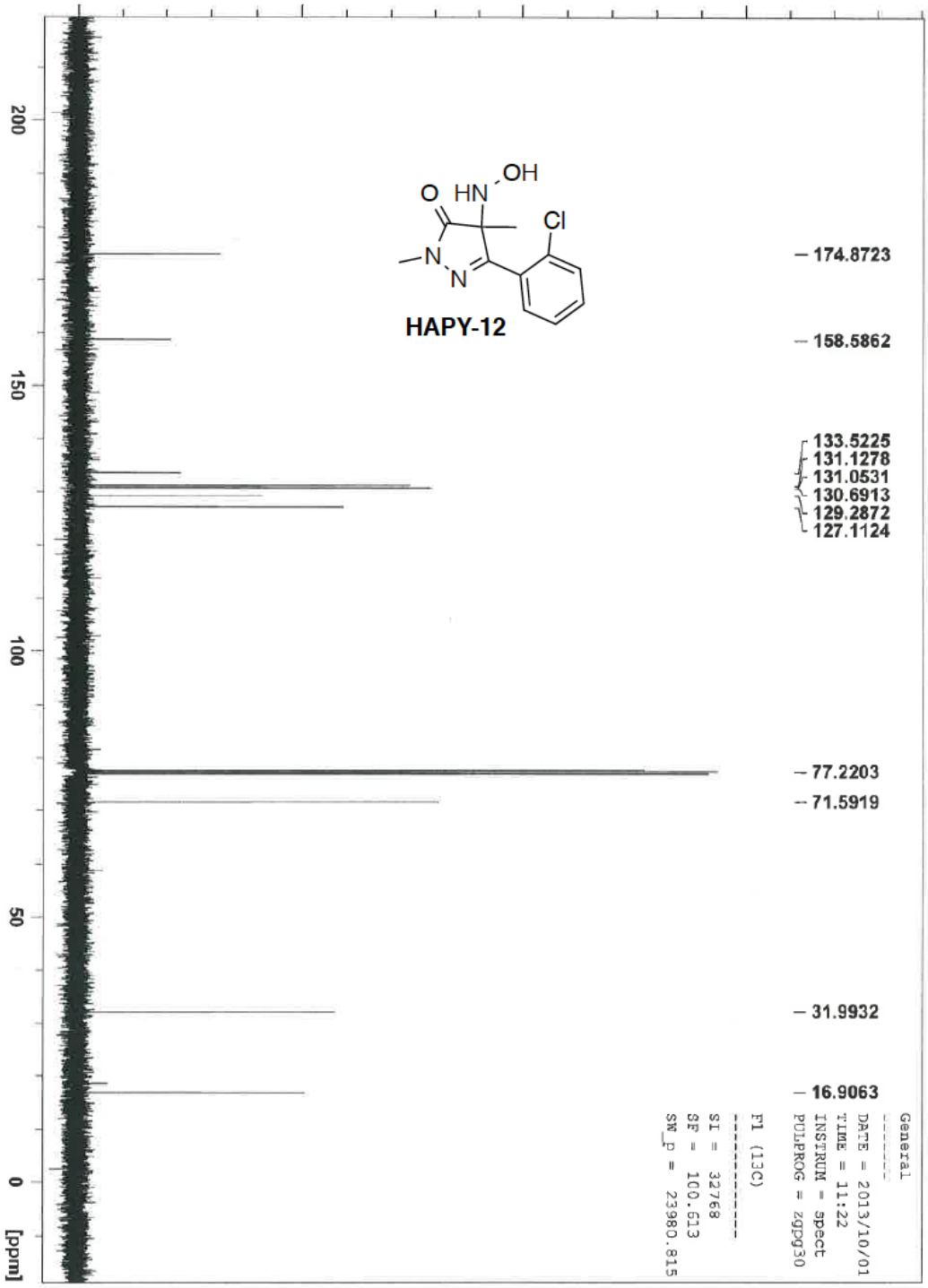
HAPY-12
O
HN
OH
Cl
N
N
174.8723
158.5862
133.5225
131.1278
131.0531
130.6913
129.2872
127.1124
77.2203
71.5919
31.9932
16.9063
200
150
100
50
0
[ppm]
General
DATE = 2013/10/01
TIME = 11:22
INSTRUM = spect
PULPROG = zgpg30
F1 (13C)
SI = 32768
SF = 100.613
SW_p = 23980.815

Chapter 4.

Curtailing the Hydroxylaminobarbituric Acid – Hydantoin Rearrangement to Favor Nitroxyl (HNO) Generation

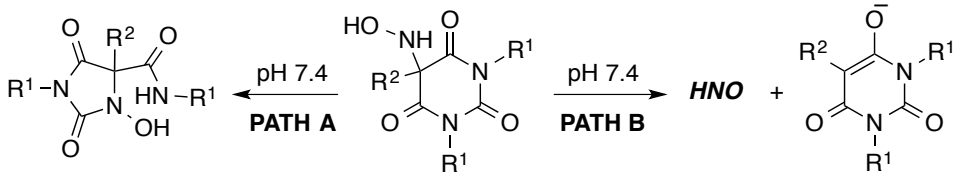

▪ 4.1 Abstract

Novel derivatives of the hydroxylamino-barbituric acid (HABA) class of nitroxyl (HNO) donors utilizing alkyl barbiturate leaving groups as unexpected HNO donors have been synthesized. We previously reported the only example in the HABA class of HNO donors that has an alkyl group in the R^2 position. However, this particular example (R^2 = ethyl) produced negligible amounts of HNO due to a competitive rearrangement mechanism. Herein, we identify new strategies to circumvent this non-HNO producing mechanism that allow the use of alkyl substituents in the R^2 position. The timecourse and stoichiometry for the *in vitro* conversion of these compounds to HNO (trapped as a phosphine aza-ylide) and the corresponding alkyl barbiturate byproduct were determined by proton NMR spectroscopy under physiologically relevant conditions (pH 7.4, 37 °C). HNO has been shown to have positive cardiovascular effects in *in vitro* and *in vivo* models of failing hearts.

▪ 4.2 Introduction

Heart failure, defined as the inability of the heart to pump enough blood to supply the metabolic demands of the body, affects more than 23 million people worldwide with total annual costs in 2013 of $32 billion in the US alone.[1-3] Nitroxyl (HNO) therapy has recently been identified as a potential, alternative treatment for congestive heart failure presumably due its ability to undergo a reversible direct reaction with thiolates in selected target proteins causing increases in both relaxation and contractility parameters in cardiovascular tissue.[4] Furthermore, HNO treatment could also expand to alcoholism, vascular dysfunction, and cancer.[5-8]

Limiting these efforts has been the lack of viable HNO donor platforms amenable to structure activity relationship studies designed to optimize physiochemical and physiological properties. A balance between reactivity and stability is inherent for HNO donors, which are required to be stable enough to store and handle, yet reactive enough to evolve HNO, a very reactive gas, under mild conditions (i.e., pH 7.4, 37 °C). As such, HNO evolution from molecular architectures with high reactive potentials is often in competition with alternative, undesired decomposition pathways. Thus, most all HNO donors reported to date have been restricted to examples with fast HNO release profiles.

Previously, we reported a new class of HNO donors based on the general strategy shown in Scheme 4-1 for *N*-substituted hydroxylamines where X is a good leaving group.[9] Piloty's acid and its derivatives, with sulfinate leaving groups, are classic examples of this strategy.[10-11]

Scheme 4-1. General Strategy for HNO Release

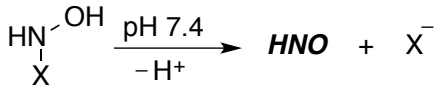

Piloty's acid itself is quite stable at pH 7.4 ($t_{1/2}$ > 1 h), and under physiological conditions is oxidized, presumably to the corresponding nitroxide, and becomes an NO donor.[12] In order to favor deprotonation and HNO formation, vs. oxidation, electron-withdrawing groups were attached to the phenyl ring such that the pK_a of the *N*-hydroxysulfonamide precursor was decreased along with an increased stability of the sulfinate leaving group.[10]

We have also utilized this strategy with good carbon-based leaving groups (e.g., barbiturate) such that HNO is released along with a stable carbanion at neutral pH (Scheme 4-2).[9] Like the Piloty's acid class, the hydroxylamino-barbituric acid (HABA) class also suffers from an alternative decomposition pathway, albeit by way of an intramolecular rearrangement mechanism rather than oxidation. For example, HABA-2 rearranges almost completely to the corresponding hydantoin, **1**, with a half-life at pH 7.4, 37 °C of 62 minutes (Scheme 4-2). The only reported example of a pure HNO donor in this class is HABA-1, which has a short half-life at pH 7.4, 37 °C of 0.7 minutes.[9] By exchanging the ethyl group in the R^2 position with an *O*-methyloxime, thus creating a more stable carbanion leaving group, HNO production was expedited, and the non-HNO producing rearrangement pathway was avoided.

Scheme 4-2. Previous Examples of the HABA Class of Potential HNO Donors

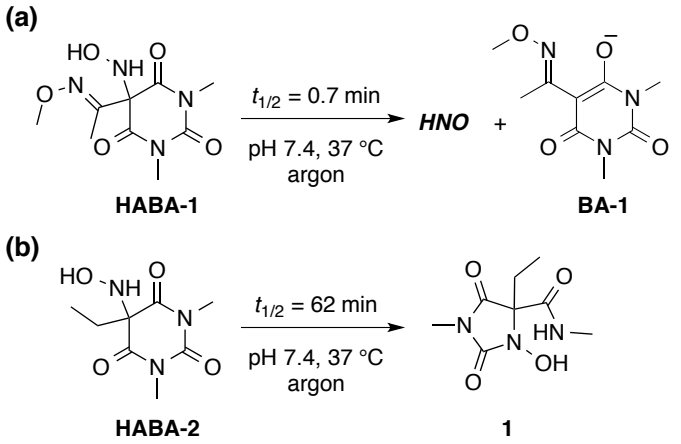

Accessing longer-lived HNO donors with half-lives on the order of minutes to hours, particularly within the same donor class, is expected to have a broad impact on optimizing HNO release rate for the treatment of any number of potential diseases, including congestive heart failure, alcoholism, vascular dysfunction, and cancer. Furthermore, sustained release of low concentrations of HNO might be an important step to mimic hypothesized endogenous HNO generation.[13] To expand the HABA class of HNO donors, we need to (1) understand what favors the rearrangement pathway and (2) create solutions that minimize or eliminate the possibility of rearrangement.

Herein, we are pleased to report two independent strategies that protect against rearrangement to favor HNO generation: (1) exchange the ethyl group in the R^2 position with benzyl and (2) exchange the *N*-Me groups of the barbituric acid ring with *N*-H groups. In both instances, we demonstrate that the non-HNO producing rearrangement pathway becomes kinetically unfavorable, thereby allowing quantitative HNO production under physiologically relevant conditions. Moreover, the benzyl-HABA scaffold is amenable to substitutions on the phenyl ring

enabling further optimization of physiochemical and pharmacological properties. We have also prepared such substituted benzyl-HABA compounds with electron-withdrawing and electron-donating groups. Taken together, we have successfully extended the HABA class of pure HNO donors with half-lives on the order of approximately 19–107 minutes under physiologically relevant conditions.

▪ 4.3 Results and Discussion

4.3.1 Synthesis

In order to protect against the hydantoin rearrangement (Scheme 4-2b), the electrophilicity of the *C*-2 carbon of the barbituric acid ring and/or the nucleophilicity of the hydroxylamine nitrogen must be tempered. We first considered exchanging the ethyl group in the R^2 position with substituted benzyl groups to give HABA-3, HABA-4, and HABA-5 (Table 4-1). We also considered HABA-6, the 1,3-unsubstituted derivative of HABA-2. These new compounds can be prepared from the corresponding byproducts of HNO release, BA-3 – BA-6, which are all known compounds and can be readily prepared (see Experimental).

Taking advantage of the chemical similarity between HNO and an aldehyde, we have recently developed an HNO-aldol procedure as an efficient synthetic procedure for the expansion of the hydroxylamino-pyrazolone (HAPY) class of HNO donors, as discussed in Chapter 3. Likewise, we wanted to apply this procedure to the expansion of the HABA class. Fortunately, HABA-3 – HABA-6 can all be prepared in excellent yields as shown in Table 4-1. Moreover, this HNO-aldol procedure is scalable, as, for example, HABA-3 can be readily prepared on the gram scale under identical concentration and reaction time as the 50 mg scale without loss in isolated yield or product purity.

Table 4-1. HNO-Aldol Reaction of Barbituric Acids

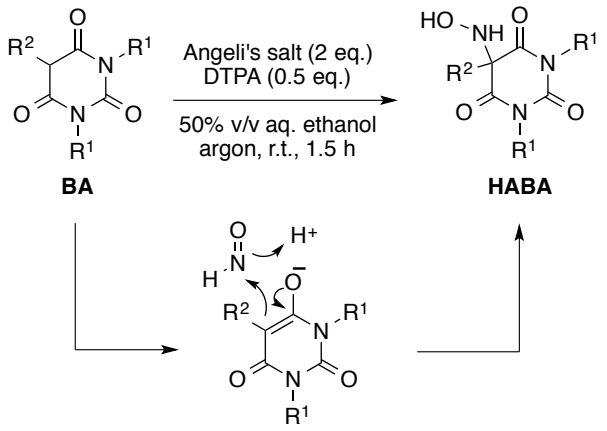

HABA	R^1	R^2	% yield
3	Me	Bn	99
4	Me	4-OMeBn	99
5	Me	4-ClBn	99
6	H	Et	76

4.3.2 HNO Release from the Expanded HABA Class

The dimerization of HNO and subsequent dehydration gives nitrous oxide (N_2O).[14] Traditionally, HNO production from a potential HNO donor can be assessed by the amount of N_2O formed following donor decomposition. This assay is performed using gas chromatographic headspace analysis at pH 7.4, 37 °C with a metal chelator, such as diethylenetriaminepentaacetic acid (DTPA), under inert atmosphere to preclude reactivity of HNO with oxygen and trace metals. Unfortunately, this assay is not applicable to the measurement of HNO production from the extended HABA class series, since the byproduct of HNO release, BA, has a strong affinity for HNO, as highlighted in the syntheses of these precursors. Thus, an alternative method for evaluating HNO production must be utilized.

As discussed in Chapter 3, we have developed a ^{1}H NMR method utilizing the selective, distinctive, and irreversible trap for HNO, *tris*(4,6-dimethyl-3-sulfanatophenyl)phosphine trisodium salt (TXPTS), for the extended HAPY class of HNO donors. Moreover, this assay can be used to monitor the timecourse and stoichiometry of the HNO donor, the released byproduct, as well as HNO itself. The reaction scheme for the conversion of HABA-3 – HABA-6 to BA-3 – BA-6 and HNO (trapped as one molecule of an aza-ylide and one molecule of a phosphine oxide) is shown in Table 4-2. Importantly, no other organic products arising from compounds HABA-3 – HABA-6 are observed. Interestingly, when HABA-2 is incubated in the presence of TXPTS, HNO release becomes comparable with rearrangement; the yield of the expected byproduct, BA-2, and the HNO-derived TXPTS aza-ylide is 59% relative to the corresponding hydantoin, compound **1**.

Table 4-2. Incubation of HABA-3 – HABA-6 in pH 7.4 Phosphate Buffer at 37 °C Under Argon with Added TXPTS

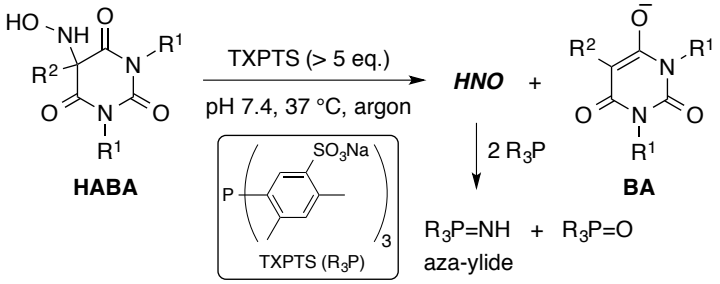

HABA[a]	R^1	R^2	$t_{1/2}$ (min)	k (s^{-1})[b]	% HNO[c]	pK_a of BA[d]
3	Me	Bn	38	3.1×10^{-4}	99	4.2
4	Me	4-OMeBn	79	1.5×10^{-4}	96	4.3
5	Me	4-ClBn	19	6.0×10^{-4}	92	3.7
6	H	Et	107	1.1×10^{-4}	97	4.1

[a]Incubation conditions: HABA (1 mM) and TXPTS (5 mM) in 10% D_2O, pH 7.4 phosphate buffer (0.25 M) with DTPA (0.2 mM) at 37 °C under argon. [b]The rates are calculated best fits to a single exponential function of the integrated ^{1}H NMR data for HABA disappearance/BA appearance. [c]HNO yields were determined from the final TXPTS aza-ylide yield. [d]Determined by titration in 50% v/v aqueous ethanol.

As an example, the complete decomposition of HABA-3 to give BA-3 and HNO-derived TXPTS aza-ylide under physiologically relevant conditions following the ^{1}H NMR assay described above is shown in Figure 4-1a, and the decompositions of HABA-3 – HABA-6 are shown in Figure 4-1b. The acidity of the benzyl barbituric acid byproduct, BA-3, is comparable to benzoic acid. Like benzoic acid, the substituents on benzyl barbituric acid affect the acidity; that is, their acidities are increased by electron-withdrawing groups and decreased by electron-donating groups. This substituent effect has been demonstrated to obey Hammett's equation on a series of 5-substituted-benzyl-1,3-unsubtituted-barbituric acid derivatives.[15]

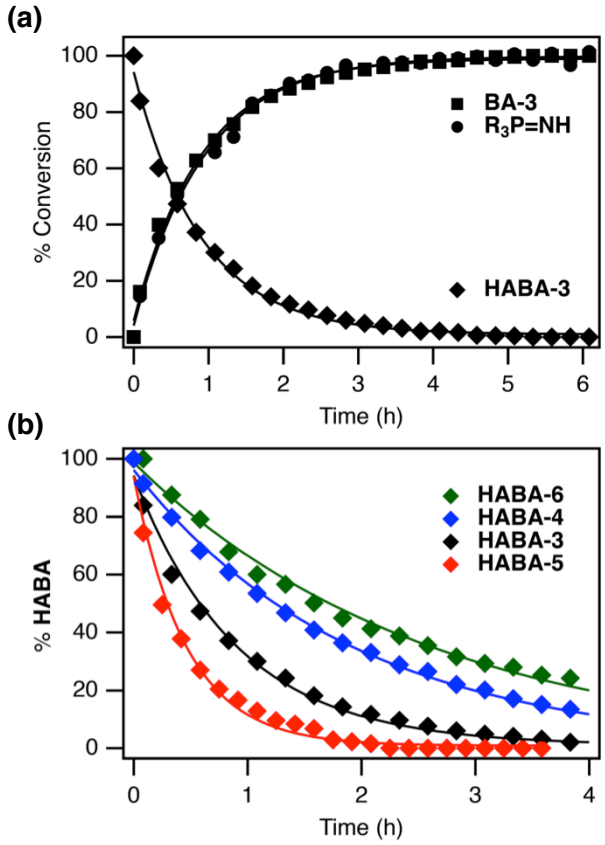

Figure 4-1. (a) Timecourse for the disappearance of HABA-3 and appearance of BA-3 and TXPTS aza-ylide with added TXPTS. The solid curves are calculated best fits to a single exponential function of the integrated ^{1}H NMR data (k = 3.1 × 10^{-4} s^{-1} for each fit). (b) Disappearance of HABA-3 (black), HABA-4 (blue), HABA-5 (red), and HABA-6 (green) under conditions outlined in Table 2.

As such, the rate of decomposition of HABA-3, HABA-4, and HABA-5 correlate with the pK_a values of their respective BA byproducts. As the stability of the resultant carbanion increases, so too does the rate of HNO evolution. The pK_a of the resultant byproducts, BA-3 – BA-5, also affects the pK_a of the corresponding HABA donors as well (Figure 4-2a), where the sharp increases in observed rate reflect rapid BA formation as a result of HABA deprotonation.

In a similar fashion to the previously studied HAPY class, the decomposition rates reach the time resolution limit (ca. 0.15 s^{-1}), precluding a complete pK_a analysis for each donor. Just as before, we believe these results indicate that the barrier to HNO dissociation must be low once deprotonation of the donor occurs. Yet, the longest-lived HNO donor in this series is HABA-6, which does not follow same trend. As stated above and shown in Figure 4-2b, the ring nitrogen proton is mildly acidic. With a measured pK_a of ca. 7.4, the pK_a of HABA-6 as a whole is more acidic than the other HABA compounds. The relatively slower decomposition of HABA-6 is presumably due to slow tautomerization of the HOHN–BA-6 proton to the ring nitrogen anion, since the difference in acidity of these two positions are expected to be ca. 3-4 pK_a units, based on the pK_a values of the other HABA compounds. Figure 4-3c shows the initial spectra of HABA-6 in a variety of phosphate buffers from pH 5.0 to pH 9.5. As the pH of the buffer increases, a new starting absorbance at 242 nm is observed, which is consistent with other mono-anion 5,5-disubstituted barbituric acids. For example, the λ_{max} of the mono-anion of 5,5-diethylbarbituric acid, barbital, is 238 nm.[16] Also, we are confident the expected byproduct of HNO release, BA-6_{anion}, is not observed in the initial spectra of HABA-6

in any of the buffers, and therefore, does not contribute to the absorbance of HABA-6_{anion} in this UV-vis spectral analysis.

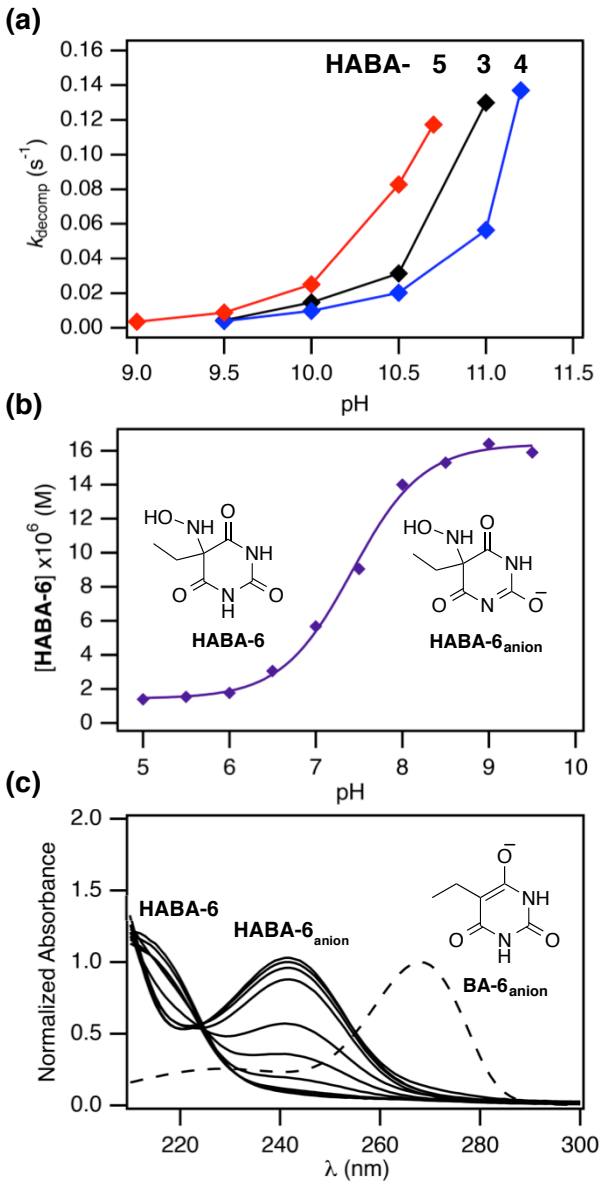

Figure 4-2. (a) Plot of UV-vis determined decomposition rates as a function of pH at 25 °C for HABA-3 (black), HABA-4 (blue), and HABA-5 (red). (b) Plot of the concentration of HABA-6_{anion} (purple, λ_{max} = 242 nm) as a function of pH. The solid curve is a calculated best fit to a sigmoid function (pK_a = 7.4). (c) Initial UV-vis spectra of HABA-6 from pH 5.0 to 9.5 compared with the expected byproduct of HNO release, BA-6_{anion}, at pH 9.5.

4.3.3 Rearrangement Studies

The aminobarbituric acid–hydantoin rearrangement is a ring contraction of 5-aminobarbituric acids and has been previously studied as a novel method of producing hydantoins, which are important medicinal compounds.[17,18] When the R^1 position is unsubstituted, the rearrangement follows a deprotonation–elimination–addition mechanism (Scheme 4-3a). However, 1,3-disubstituion prevents the formation of an isocyanate intermediate, and a mechanism involving a carbamate intermediate becomes operative (Scheme 4-3b). These reactions are performed under forcing conditions (i.e., up to 4 equivalents of NaOEt and 120 °C in ethanol for 5 h).

Scheme 4-3. Decomposition of Amino- and Hydroxylamino-Barbituric Acids

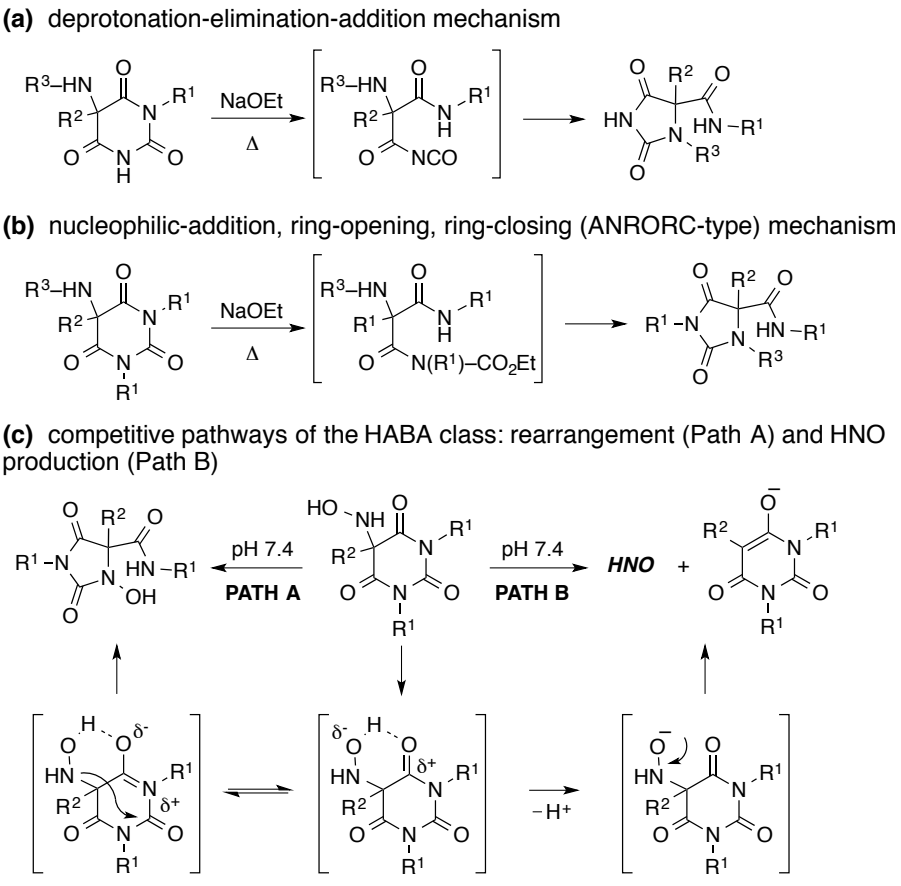

In the same time, period but under much milder conditions (pH 7.4, 37 °C, 5 h), the rearrangement of HABA-2 is complete, and the measured half-life is 62 minutes (Scheme 4-3c, Path A; Figure 4-3). However, if the HOHN–BA-2 hydrogen is replaced with a methyl group (compound **2**, Figure 4-3) then only approximately 4% of the corresponding rearranged hydantoin product is observed after 5 hours at pH 7.4, 37 °C (Figure 4-3). Thus, the relatively facile rearrangement of HABA-2 is due in part to the ability of the free HOHN–BA-2 hydrogen to activate the barbituric acid ring during the rearrangement, which likely follows a direct nucleophilic addition of the hydroxylamine nitrogen prior to ring contraction rather than formation of a carbamic acid intermediate, since no other product or intermediate is observed throughout the rearrangement process for either HABA-2 or compound **2**. On the other hand, this activation is also expected to facilitate HOHN–BA deprotonation and HNO production (Scheme 4-3c, Path B).

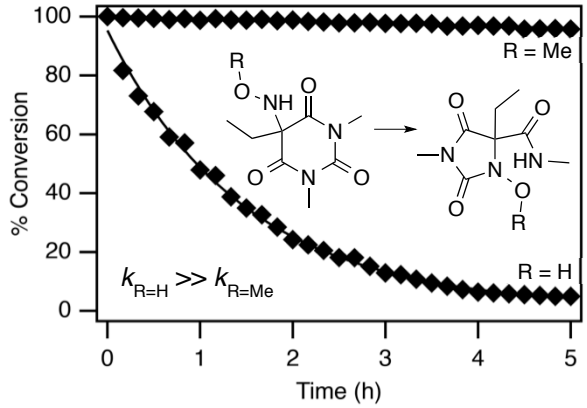

Figure 4-3. Hydantoin formation from HABA-2 (R = H) vs. compound **2** (R = Me).

Because the barbiturate ring of HABA-6 is approximately 50% anionic in pH 7.4 buffer, the electrophilicity of the *C*-2 carbon is substantially reduced, and attack by the hydroxylamine nitrogen becomes exceedingly less likely. Ring opening to the

corresponding isocyanate intermediate is also evidently not possible, since no rearranged product is observed during the decomposition of HABA-6. Even under conditions to disfavor HNO release (i.e., no TXPTS and under argon), the rearranged hydantoin product was not observed even after two days of incubation at pH 7.4 and 37 °C. As with the aminobarbituric acid–hydantoin rearrangement of 1,3-unsubstituted derivatives, the isocyanate intermediate likely requires more forcing conditions for formation.

Similarly, when the benzyl derivative, HABA-3, is incubated under conditions to disfavor HNO release, again in the absence of TXPTS and under argon, the relative rate of rearrangement is substantially slower when compared to HABA-2. After one day of incubation at pH 7.4 and 37 °C, the relative ratio of HABA-3:BA-3:hydantoin is 48:26:36. Given the high rate of HNO release in the presence of a good trap for HNO, such as TXPTS, relative to the rate of rearrangement, the possibility of rearrangement in the substituted-benzyl derivatives is expected to be negligible *in vivo*, where biological targets for HNO are in excess of HNO.

An explanation as to why rearrangement in HABA-3 is so much slower when compared to HABA-2 is not yet fully understood, since the ability of the free HOHN–BA-3 hydrogen to activate the barbituric acid ring during the rearrangement is also possible with HABA-3. Therefore, we employed computational investigations to study the differences between HABA-2 and HABA-3.

A potential explanation for the differences may be due to the ground state structures of each donor. The lowest energy conformation of HABA-3, both determined computationally and in the crystal structure, is in a intramolecular π-

stacking motif, where there is a filled-empty interaction of the HOMO of the phenyl ring with the LUMO of the barbituric acid ring (Figure 4-4a). Specifically, the dihedral angles of the benzyl group relative to the hydroxylamine in the lowest energy calculated structure and in the crystal structure are 177° and 170°, respectively, thus positioning the two rings in an overlapping conformation (Supporting Information). Even though the two rings are not parallel with respect to one another, there is evidently sufficient interaction to allow HABA-3 to exist primarily in this π-stacking conformation.

In order for nucleophilic attack of the hydroxylamine nitrogen to occur, this π-stacking interaction must be disrupted in order to form a tetrahedral intermediate (Figure 4-4b), which may explain the kinetic unfavorability to rearrangement, as rearrangement to the corresponding hydantoin is thermodynamically favorable for both HABA-2 and HABA-3. Although the calculated tetrahedral intermediates from HABA-2 and HABA-3 are ground state structures, presumably they are relatively similar in energy to the expected transition state of each reaction. Assuming this is true, the activation barrier to the tetrahedral intermediate (Figure 4-3b, step 1), is approximately one kcal/mol higher in energy for HABA-3 relative to HABA-2, and the corresponding rate of hydantoin formation is then expected to be one order of magnitude slower. In other words, if HABA-2 rearrangement occurs with a half-life of approximately one hour, a half-life of approximately 10 hours is expected for the rearrangement of HABA-3, which is relatively consistent given the observed propensity to rearrangement for these two compounds. Although, other factors such as steric effects or hydroxylamine nucleophilicity may also be relevant.

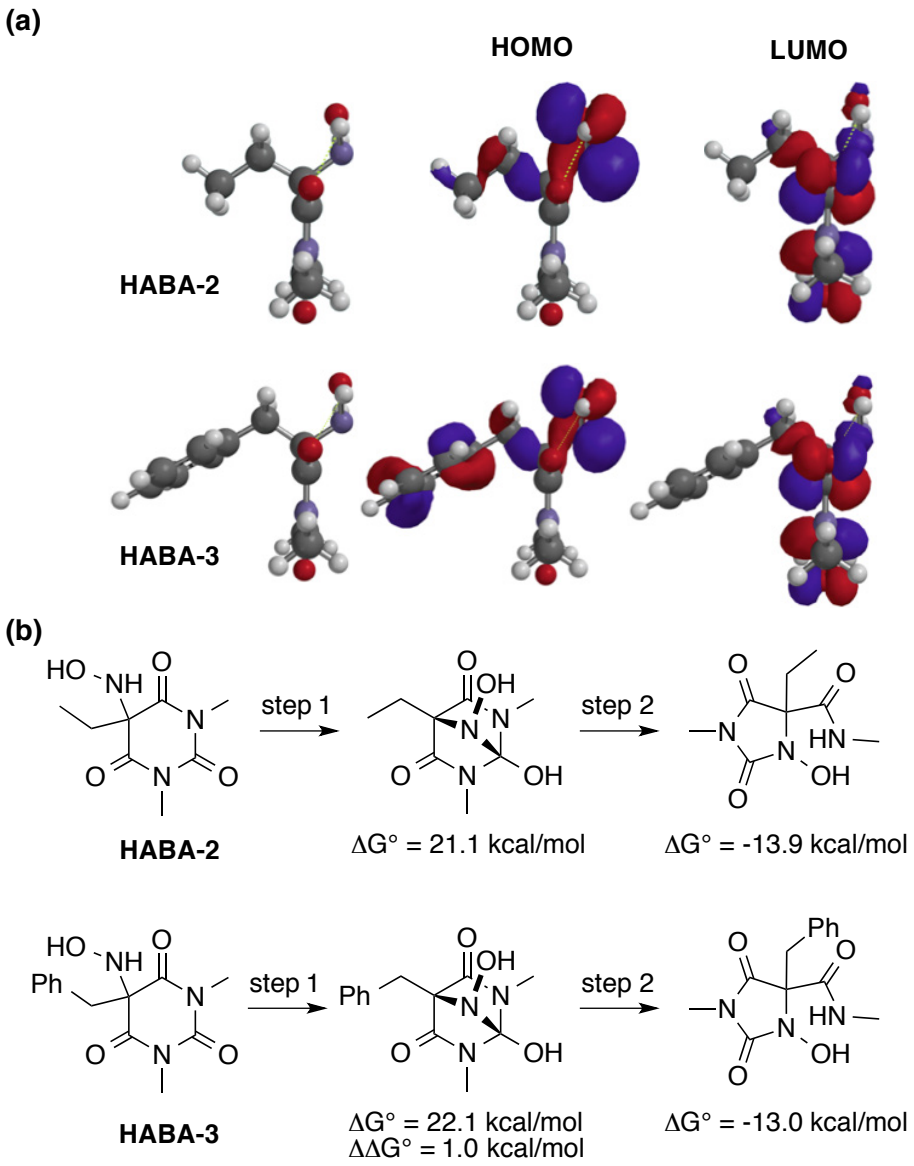

Figure 4-4. All calculations were performed with Spartan '14 at the B3LYP/6-31G* level with an SM8 solvation model for aqueous solvation (Supporting Information).[19] Optimized geometries and vibrational frequencies were calculated for each reactant and product independently, and free energies are given for 298.15 K. (a) The calculated structures of HABA-2 and HABA-3 and their respective HOMO and LUMO orbital densities. (b) The stepwise scheme and energetics of the rearrangement of HABA-2 and HABA-3 involving a tetrahedral intermediate.

4.3.4 Barbiturates as HNO Donors

As shown in Table 4-2, the half-lives of HABA-3 – HABA-6 are on the order of an hour, making these compounds useful in a biological setting for comparing long-lived HNO donors with short-lived HNO donors, such as Angeli's salt. Ideally, the byproduct of HNO release would be innocuous and readily cleared from the body. Otherwise, the synergistic, or antagonistic, relationship between HNO and the released byproduct must be taken into account when studying the pharmacology of these HNO donors. For example, nitrite, the byproduct of HNO release from Angeli's salt, possesses its own biological activity,[20-21] as does the pyrazolone byproducts from the HAPY class of HNO donors, which are derivatives of edaravone, a potent antioxidant already in clinical use for the treatment of stroke and cardiovascular disease.[22-24]

Barbiturates have clinical applications as sedatives, hypnotics, anesthetics, and antiseizure drugs. Active barbiturates must be weak acids, meaning that at least one of the barbituric acid ring nitrogens, whose pK_a values range from 7.1 to 8.1, is unsubstituted. Also, active barbiturates must have a lipid/water partition coefficient between certain limits in order to cross the blood-brain barrier. Thus, the substitution patterns are important for the biological activity described above. The active substitution patterns are 5,5-disubstituted and 1,5,5-trisubstituted barbituric acids.[25] Currently, there are several barbiturates used clinically, including phenobarbital, a core medicine in the World Health Organization list of essential medicines.[26] All other substitution patterns are considered to be inactive. These include 5-monosubstituted, 1,3,5-trisubstituted, and 1,3,5,5-

tetrasubstutituted barbituric acids. Therefore, the released byproducts of HNO release in the extended HABA class of HNO donors, BA-3 – BA-6, are all expected to have minimal or negligible pharmacological effects.

For the HABA class as a whole, HNO release following HOHN–BA deprotonation remains the most plausible mechanism in water (Scheme 4-4), as was the case for the previously studied HAPY class of HNO donors.

Scheme 4-4. Mechanism of HNO Release in pH 7.4 Phosphate Buffer at 37 °C

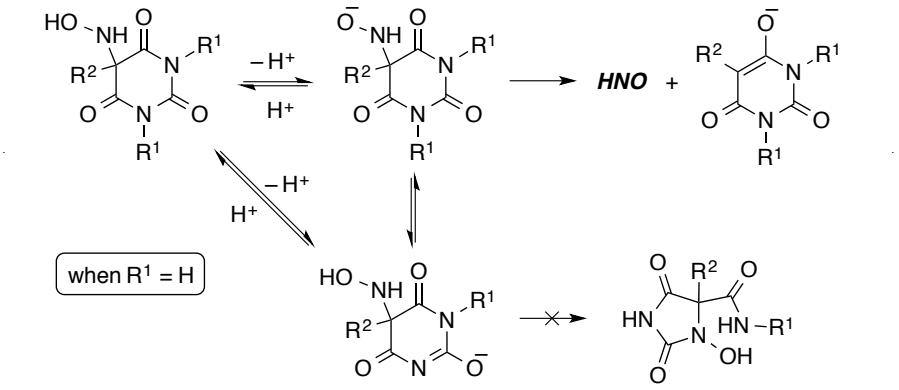

▪ 4.4 Conclusion

Compounds HABA-3 – HABA-6 are quantitatively converted to BA-3 – BA-6 and HNO, trapped as a TXPTS aza-ylide, with a half-life range of approximately 19 – 107 minutes in pH 7.4 phosphate buffer at 37°C. The alternative, undesired rearrangement mechanism that can occur with the HABA class of compounds has been shown to be kinetically unfavorable for this expanded HABA series under physiologically relevant conditions, including the *O*-methylated model compound **2**, which may suggest future pro-drug strategies. Another potentially practical benefit enjoyed by the HABA class is that these donors are achiral, removing the need for any study into the differences in physiological effects between enantiomers. Taken together with the HAPY class of HNO donors discussed in Chapter 3, whose half-life range span minutes to days, the effects that long-lived, pure HNO donors have on the treatments of any number of potential diseases may now be evaluated.

▪ 4.5 Experimental

4.5.1 Methods and Materials

All starting materials were of reagent grade and used without further purification. Compounds BA-3 – BA-6,[27-28] *N*-(*tert*-butoxycarbonyl)-*O*-methyl-hydroxylamine,[29] and 5-bromo-5-ethyl-*N*,*N*-dimethyl-barbituric acid[9] are all known compounds, and were prepared according to literature procedures. Angeli's salt ($Na_2N_2O_3$) was prepared according to King and Nagasawa.[30] *Tris*(4,6-dimethyl-3-sulfanatophenyl)phosphine trisodium salt (TXPTS) was of reagent grade and used without further purification. Synthetic TXPTS aza-ylide was obtained through the amidation of TXPTS using hydroxylamine *O*-sulfonic acid in water.[31] NMR spectra were obtained on a Bruker Avance 400 MHz FT-NMR spectrometer. All chemical shifts are reported in parts per million (ppm) relative to residual $CHCl_3$ (7.26 ppm for ^1H, 77.23 ppm for ^{13}C) or residual DMSO (2.50 ppm for ^1H, 39.52 for ^{13}C). High-resolution mass spectra were obtained on a VG Analytical VG70SE magnetic sector mass spectrometer operating in fast atom bombardment (FAB) mode. Ultraviolet-visible (UV-vis) absorption spectra were obtained using a Hewlett Packard 8453 diode array spectrometer. Buffered solutions (0.1 M) for UV-vis experiments were prepared from $NaPO_3H_2/Na_2PO_3H$ (pH 5.0, 5.5, 6.0, 6.5, 7.0, 7.5, 8.0, 8.5, 9.0, 9.5, 10.0, 10.5, 10.7, 11.0, 11.2).

4.5.2 Incubation Procedure of HABA Donors at pH 7.4, 37 °C with TXPTS

General

All ^{1}H NMR spectra were obtained in pH 7.4 solution containing 0.25 M phosphate buffer, 0.2 mM of the metal chelator diethylenetriaminepentaacetic acid (DTPA), and 10 % D_2O on a Bruker Avance 400 MHz FT-NMR spectrometer using a 1 second presaturation pulse to suppress the water signal. The data were processed with the academic version of ACDLabs NMR processor software: each free induction decay was Fourier transformed, phased, baseline corrected, and integral areas measured for the *N*-methyl groups of compounds HABA-3 – HABA-5 and BA-3 – BA-5, the (-$CH_2\underline{CH_3}$) groups of HABA-6 and BA-6, and the downfield methyl group of TXPTS aza-ylide. The ^{1}H NMR spectrum of the HNO derived TXPTS aza-ylide product matched that of synthetic TXPTS aza-ylide. The HNO yield from compounds HABA-3 – HABA-6 was determined from the final TXPTS aza-ylide yield.

NMR Procedure

The NMR procedure used was based on an HPLC protocol developed by S. Bruce King and co-workers.[32-33] To an argon-purged NMR solution (1.00 mL) containing TXPTS (3.3 mg, 5 mM) was added HABA-3 – HABA-6 (10 μL of 100 mM in methanol-d_4) to give 1 mM as the initial concentration of HABA-3 – HABA-6. The solution was briefly mixed, ca. 0.5 mL was transferred to an argon-purged NMR tube, and the sample was then internally incubated at 37 °C and ^{1}H NMR spectra were collected using a canned Bruker pulse sequence, zg2d, modified to include a 1 second presaturation pulse during the relaxation delay.

4.5.3 Experimental Procedures

Scheme 4-5. Synthesis of HABA Donors via the HNO-Aldol Procedure

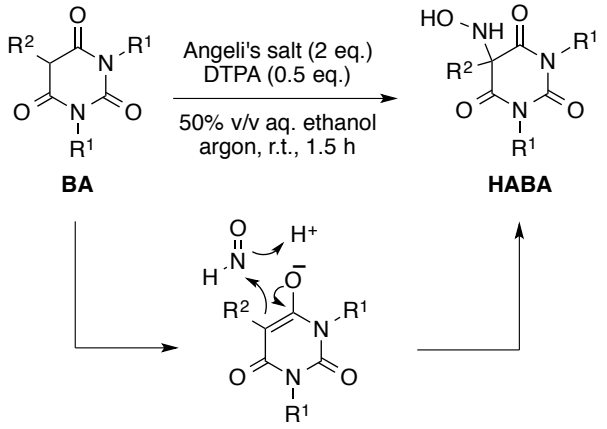

5-(*N*-hydroxylamino)-5-benzyl-*N,N*-dimethylbarbituric acid (HABA-3). To 5-benzyl-*N,N*-dimethylbarbituric acid (BA-3) (1.231 g, 5 mmol), Angeli's salt (1.22 g, 10 mmol), and powdered DTPA (0.983 g, 2.5 mmol) under nitrogen at room temperature was cannulated a degassed mixture of 50% aqueous ethanol (25 mL). The reaction was allowed to vigorously stir for 10 minutes in order to dissolve all solids followed by normal stirring under a gentle stream of nitrogen for an additional 1.5 hours. At which time, precipitation of a white solid was observed. The reaction was then diluted with ethanol (200 mL) and concentrated to dryness *in vacuo* with minimum heat (<30 °C). The resultant material was then taken up in dichloromethane (3 × 20 mL), filtered through cotton, and concentrated *in vacuo* to give the title compound as a white solid (1.385 g, 99%). ^{1}H NMR (400 MHz, $CDCl_3$) δ: 7.26 (m, 3H), 6.96 (m, 2H), 6.28 (d, 1H, *J* = 3.2 Hz), 4.98 (d, 1H, *J* = 3.4 Hz, 1H), 3.13 (s, 6H), 3.08 (s, 2H). ^{13}C NMR (100 MHz, $CDCl_3$) δ: 170.01, 150.02, 131.75, 129.19,

128.95, 128.71, 73.64, 42.89, 28.78. HR-MS (FAB): found *m/z* = 278.11411 (MH^+); calc. for $C_{13}H_{16}N_3O_4$: 278.11408.

5-(*N*-hydroxylamino)-5-(4-methoxybenzyl)-*N,N*-dimethylbarbituric acid (HABA-4). To 5-(4-methoxybenzyl)-*N,N*-dimethylbarbituric acid (BA-4) (55 mg, 0.2 mmol), Angeli's salt (49 mg, 0.4 mmol), and powdered DTPA (39 mg, 0.1 mmol) under argon at room temperature was added a degassed mixture of 50% aqueous ethanol (1 mL). The reaction was allowed to stir for 1.5 hours, diluted with ethanol (>5 mL), and concentrated to dryness *in vacuo* with minimum heat (<30 °C). The material was then taken up in dichloromethane, filtered through cotton, and concentrated *in vacuo* to give the title compound as a white solid (61 mg, 99%). ^1H NMR (400 MHz, $CDCl_3$) δ: 6.88 (d, 2H, *J* = 8.6 Hz), 6.76 (d, 2H, *J* = 8.7 Hz), 6.25 (br. s, 1H), 5.09 (br. s, 1H), 3.76 (s, 3H), 3.15 (s, 6H), 3.03 (s, 2H). ^{13}C NMR (100 MHz, $CDCl_3$) δ: 159.73, 150.11, 130.32, 123.47, 114.27, 73.70, 55.43, 42.08, 28.82. HR-MS (FAB): found *m/z* = 308.12476 (MH^+); calc. for $C_{14}H_{18}N_3O_5$: 308.12465.

5-(*N*-hydroxylamino)-5-(4-chlorobenzyl)-*N,N*-dimethylbarbituric acid (HABA-5). To 5-(4-chlorobenzyl)-*N,N*-dimethylbarbituric acid (BA-5) (56 mg, 0.2 mmol), Angeli's salt (49 mg, 0.4 mmol), and powdered DTPA (39 mg, 0.1 mmol) under argon at room temperature was added a degassed mixture of 50% aqueous ethanol (1 mL). The reaction was allowed to stir for 1.5 hours, diluted with ethanol (>5 mL), and concentrated to dryness *in vacuo* with minimum heat (<30 °C). The material was then taken up in dichloromethane, filtered through cotton, and concentrated *in vacuo* to give the title compound as a white solid (61 mg, 99%). ^1H NMR (400 MHz, $CDCl_3$) δ: 7.24 (d, 2H, *J* = 8.5 Hz), 6.91(d, 2H, *J* = 8.5 Hz), 6.23 (d, 1H, *J*

= 3.3 Hz), 4.98 (d, 1H, *J* = 3.3 Hz), 3.17 (s, 6H), 3.06 (s, 2H). ^{13}C NMR (100 MHz, $CDCl_3$) δ: 169.96, 149.93, 134.71, 130.60, 130.31, 129.19, 73.14, 41.74, 28.88. HR-MS (FAB): found *m/z* = 312.07483 (MH^+, ^{35}Cl), 314.07293 (MH^+, ^{37}Cl); calc. for $C_{13}H_{15}ClN_3O_4$: 312.07511 (MH^+, ^{35}Cl), 314.07246 (MH^+, ^{37}Cl).

5-(*N*-hydroxylamino)-5-ethyl-barbituric acid (HABA-6). To 5-ethyl-barbituric acid (BA-6) (0.781 g, 5 mmol), Angeli's salt (1.22 g, 10 mmol), and powdered DTPA (0.983 g, 2.5 mmol) under nitrogen at room temperature was cannulated a degassed mixture of 50% aqueous ethanol (25 mL). The reaction was allowed to vigorously stir for 10 minutes in order to dissolve all solids followed by normal stirring under a gentle stream of nitrogen for an additional 1.5 hours. The reaction was then diluted with ethanol (200 mL), filtered through cotton, and the clear filtrate was concentrated to dryness *in vacuo* with minimum heat (<30 °C). The resultant material was then triturated with diethylether and filtered to give the title compound as a light yellow solid (0.707 g, 76%). ^{1}H NMR (400 MHz, DMSO-d_6) δ: 11.50 (br. s, 2H), 7.95 (s, 1H), 6.23 (s, 1H), 1.66 (q, 2H, *J* = 7.5 Hz), 0.73 (t, 3H, *J* = 7.5 Hz). ^{13}C NMR (100 MHz, DMSO-d_6) δ: 172.07, 149.96, 70.88, 26.92, 7.79. HR-MS (FAB): found *m/z* = 188.06752 (MH^+); calc. for $C_6H_{10}N_3O_4$: 188.06713 (MH^+).

Scheme 4-6. Synthesis of the Model Compound, 2

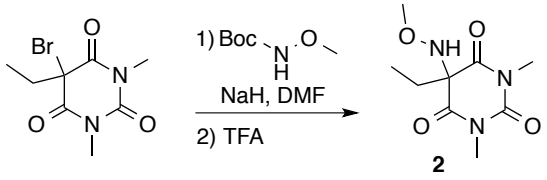

2

5-(*N*-(*O*-methyl)-hydroxylamino)-5-ethyl-*N,N*-dimethylbarbituric acid (2). To a solution of *N*-(*tert*-butoxycarbonyl)-*O*-methyl-hydroxylamine (0.294 g, 2 mmol) in dimethylformamide (25 mL) at room temperature was added sodium hydride, 60% (0.088 g, 2.2 mmol), and the reaction stirred for one hour under nitrogen. To this solution was added 5-bromo-5-ethyl-*N*,*N*-dimethyl-barbituric acid (0.526 g, 2 mmol), and the reaction proceeded at room temperature for an additional 24 hours. The reaction was then diluted with ether (50 mL) and washed with ammonium chloride (× 2), water, brine, dried over magnesium sulfate, filtered, and concentrated *in vacuo* to give crude 5-(*N*-(*N*-(*tert*-butoxycarbonyl)-*O*-methyl)-hydroxylamino)-5-ethyl-*N*,*N*-dimethylbarbituric acid (ca. 50% pure by ^{1}H NMR, contaminated by an unknown product), which was used without further purification. This material was then taken up in dichloromethane (10 mL) and trifluoroacetic acid (10 mL) and allowed to stir at room temperature for one hour followed by concentration *in vacuo* to give a mixture of the title compound along with unchanged contaminant. The mixture was dissolved in diethylether, diluted with hexanes, and concentrated via rotary evaporation out of the water bath in order to effect precipitation of the unknown product as an off-white solid (0.125 g). The filtrate was concentrated *in vacuo* to give the title compound (ca. 90% pure by ^{1}H NMR) as a light yellow oil (0.065 mg, 14%). ^{1}H NMR (400 MHz, $CDCl_3$) δ: 5.93

(br. s., 1H), 3.49 (s, 3H), 3.38 (s, 3H), 1.87 (q, 2H), 0.82 (t, 3H). ^{13}C NMR (100 MHz, $CDCl_3$) δ: 170.27, 150.91, 71.42, 62.94, 29.72, 29.03, 7.92. HR-MS (FAB): found *m/z* = 230.11431 (MH^+); calc. for $C_9H_{16}N_3O_4$: 230.11408.

▪ 4.6 References

(1) Go, A. S.; Mozaffarian, D; Roger, V. L.; Benjamin, E. J.; Berry, J. D.; Borden, W. B.; Bravata, D. M.; Dai, S.; Ford, E. S.; Fox, C. S.; Franco, S.; Fullerton, H. J.; Gillespie, C.; Hailpern, S. M.; Heit, J. A.; Howard, V. J.; Huffman, M. D.; Kissela, B. M.; Kittner, S. J.; Lackland, D. T.; Lichtman, J. H.; Lisabeth, L. D.; Magid, D.; Marcus, G. M.; Marelli, A.; Matchar, D. B.; McGuire, D. K.; Mohler, E. R.; Moy, C. S.; Mussolino, M. E.; Nichol, G.; Paynter, N. P.; Schreiner, P. J.; Sorlie, P. D.; Stein, J.; Turan, T. N.; Virani, S. S.; Wong, N. D.; Woo, D.; Turner, M. B. *Circulation* **2013**, *127*, e6–e245.

(2) McMurray, J. J.; Petrie, M. C.; Murdoch, D. R.; Davie, A. P. *Eur. Heart J.* **1998**, 19 Suppl P: P9-16.

(3) Heidenreich, P. A.; Trogdon, J. G.; Khavjou, O. A.; Butler, J.; Dracup, K.; Ezekowitz, M. D.; Finkelstein, E. A.; Hong, Y.; Johnston, S. C.; Khera, A.; Lloyd-Jones, D. M.; Nelson, S. A.; Nichol, G.; Orenstein, D.; Wilson, P. W. F.; Woo, J. *Circulation* **2011**, *123*, 933–44.

(4) Tocchetti, C. G.; Stanley, B. A.; Murray, C. I.; Sivakumaran, V.; Donzelli, S.; Mancardi, D.; Pagliaro, P.; Gao, W. D.; van Eyk, J.; Kass, D. A.; Wink, D. A.; Paolocci, N. *Antioxid. Redox Signal.* **2011**, *14*, 1687–1698.

(5) Flores-Santana, W.; Salmon, D. J.; Donzelli, S.; Switzer, C. H.; Basudhar, D.; Ridnour, L.; Cheng, R.; Glynn, S. A.; Paolocci, N.; Fukuto, J. M.; Miranda, K. M.; Wink, D. A. *Antioxid. Redox Signal*. **2011**, *14*, 1659–1674.

(6) Paolocci, N.; Katori, T.; Champion, H. C.; St John, M. E.; Miranda, K. M.; Fukuto, J. M.; Wink, D. A.; Kass, D. A. *Proc. Natl. Acad. Sci. U. S. A*. **2003**, *100*, 5537–5542.

(7) Paolocci, N.; Saavedra, W. F.; Miranda, K. M.; Martignani, C.; Isoda, T.; Hare, J. M.; Espey, M. G.; Fukuto, J. M.; Feelisch, M.; Wink, D. A.; Kass, D. A. *Proc. Natl. Acad. Sci. U. S. A.* **2001**, *98*, 10463–10468.

(8) Kemp-Harper, B. K. *Antioxid. Redox Signal*. **2011**, *14*, 1609–1613.

(9) Guthrie, D. A.; Kim, N. Y.; Siegler, M. A.; Moore, C. D.; Toscano, J. P. *J. Am. Chem. Soc.* **2012**, *134*, 1962–1965.

(10) Toscano, J. P.; Brookfield, F. A.; Cohen, A. D.; Courtney, S. M.; Frost, L. M.; Kalish, V. J. "*N*-Hydroxysulfonamide Derivatives as Physiologically Useful Nitroxyl Donors" U.S. Patent 8,030,356, **2011**.

(11) Bonner, F.T.; Ko, Y. *Inorg. Chem*. **1992**, *31*, 2514–2519.

(12) Zamora, R.; Grzesiok, A.; Weber, H.; Feelisch, M. *Biochem. J.* **1995**, *312*, 333–339.

(13) Choe, C.-U.; Lewerenz, J; Gerloff, C.; Magnus, T.; Donzelli, S. *Antioxid. Redox Signal.* **2011**, *14*, 1699–1711.

(14) Shafirovich, V.; Lymar, S. V. *Proc. Natl. Acad. Sci. U.S.A*. **2002**, *99*, 7340–7345.

(15) Tate, J. V.; Tinnerman II, W. N.; Jurevics, V.; Jeskey, H.; Biehl, E. R. *J. Heterocyclic Chem.* **1986**, *23*, 9–11.

(16) Garrett, E. R.; Bojarski, J. T.; Yakatan, G. J. *J. Pharm. Sci.* **1971**, *60*, 1145–1154.

(17) Gütschow, M.; Hecker, T.; Eger, K. *Synthesis* **1999**, 410–414.

(18) Meusel, M.; Ambrożak, A.; Hecker, T.; Gütschow, M. *J. Org. Chem.* **2002**, *68*, 4684–4692.

(19) Shao Y.; Molnar, L. F.; Jung, Y.; Kussmann, J.; Ochsenfeld, C.; Brown, S. T.; Gilbert, A. T. B.; Slipchenko, L. V.; Levchenko, S. V.; O'Neill, D. P.; DiStasio Jr., R. A.; Lochan, R. C.; Wang, T.; Beran, G. J. O.; Besley, N. A.; Herbert, J. M.; Lin, C. Y.; Van Voorhis, T.; Chien, S. H.; Sodt, A.; Steele, R. P.; Rassolov, V. A.; Maslen, P. E.; Korambath, P. P.; Adamson, R. D.; Austin, B.; Baker, J.; Byrd, E. F. C.; Dachsel, H.; Doerksen, R. J.; Dreuw, A.; Dunietz, B. D.; Dutoi, A. D.; Furlani, T. R.; Gwaltney, S. R.; Heyden, A.; Hirata, S.; Hsu, C-P.; Kedziora, G.; Khalliulin, R. Z.; Klunzinger, P.; Lee, A. M.; Lee, M. S.; Liang, W. Z.; Lotan, I.; Nair, N.; Peters, B.; Proynov, E. I.; Pieniazek, P. A.; Rhee, Y. M.; Ritchie, J.; Rosta, E.; Sherrill, C. D.; Simmonett, A. C.; Subotnik, J. E.; Woodcock III, H. L.; Zhang, W.; Bell, A. T.; Chakraborty, A. K.; Chipman, D. M.; Keil, F. J.; Warshel, A.; Hehre, W. J.; Schaefer, H. F.; Kong, J.; Krylov, A. I.; Gill, P. M. W.; Head-Gordon, M. *Phys. Chem. Chem. Phys.* **2006**, *8*, 3172–3191.

(20) Gladwin, M. T.; Raat, N. J. H.; Shiva, S.; Dezfulian, C.; Hogg, N.; Kim-Shapiro, D. B.; Patel, R. P. *Am. J. Physiol.: Heart Circ. Physiol.* **2006**, *291*, H2026–H2035.

(21) Gladwin, M. T.; Schechter, A. N.; Kim-Shapiro, D. B.; Patel, R. P.; Hogg, N.; Shiva, S.; Cannon, R. O.; Kelm, M.; Wink, D. A.; Espey, M. G.; Oldfield, E. H.; Pluta, R. M.; Freeman, B. A.; Lancaster, J. R.; Feelisch, M.; Lundberg, J. O. *Nature Chem. Biol.* **2005**, *1*, 308–314.

(22) Higashi, Y.; Jitsuiki, D.; Chayama, K.; Yoshizumi, M. *Recent Pat. Cardiovasc. Drug Discovery* **2006**, *1*, 85–93.

(23) Watanabe, T.; Tahara, M.; Todo, S. *Cardiovasc. Ther*. **2008**, *26*, 101–114.

(24) Watanabe, K.; Morinaka, Y.; Iseki, K.; Watanabe, T.; Yuki, S.; Hishi, H. *Redox Report* **2003**, *8*, 151–155.

(25) Williams, D. A.; Lemke, T. L. *Foye's Principles of Medicinal Chemistry*. 5th ed. Baltimore: Lippincott Williams & Wilkins, **2002**.

(26) 18th WHO Model List of Essential Medicines (April 2013).

(27) Jursic, B. S.; Stevens, E. D. *Tetrahedron Lett*. **2003**, *44*, 2203–2210.

(28) Lofberg, C.; Grigg, R.; Keep, A.; Derrick, A.; Sridharan, V.; Kilner, C. *Chem. Commun.* **2006**, 5000–5002.

(29) Kawase, M.; Kitamura, T.; Kikugawa, Y. *J. Org. Chem.* **1989**, *54*, 3394–3403.

(30) King, S. B.; Nagasawa, H. T. *Methods Enzymol.* **1999**, *301*, 211–220.

(31) Armstrong, A.; Jones, L. H.; Knight, J. D.; Kelsey, R. D. *Org. Lett*. **2005**, *7*, 713–716.

(32) Reisz, J. A.; Klorig, E. B.; Wright, M. W.; King, S. B. *Org. Lett.* **2009**, *11*, 2719–2721.

(33) Reisz, J. A.; Zink, C. N.; King, S. B. *J. Am. Chem. Soc.* **2011**, *133*, 11675–11685.

▪ 4.7 Supporting Information

4.7.1 X-Ray Crystallography Data

All reflection intensities were measured at 110(2) K using a SuperNova diffractometer (equipped with Atlas detector) with Cu *K*α radiation (λ = 1.54178 Å) under the program CrysAlisPro (Version 1.171.36.32 Agilent Technologies, 2013). The program CrysAlisPro (Version 1.171.36.32 Agilent Technologies, 2013) was used to refine the cell dimensions. Data reduction was done using the program CrysAlisPro (Version 1.171.36.32 Agilent Technologies, 2013). The structure was solved with the program SHELXS-2013 (Sheldrick, 2013) and was refined on F^2 with SHELXL-2013 (Sheldrick, 2013). Analytical numeric absorption corrections based on a multifaceted crystal model were applied using CrysAlisPro (Version 1.171.36.32 Agilent Technologies, 2013). The temperature of the data collection was controlled using the system Cryojet (manufactured by Oxford Instruments). The H atoms were placed at calculated positions (unless otherwise specified) using the instructions AFIX 23, AFIX 43 or AFIX 137 with isotropic displacement parameters having values 1.2 or 1.5 times *U*eq of the attached C atoms. The H atoms attached to N3X and O4X (X = A, B and C) were found from difference Fourier map, and their coordinates were refined freely (but the N–H and O–H distances were restrained to be within acceptable ranges using the DFIX instructions).

The structure is ordered. Some unresolved electron density – *i.e.*, most likely a very disordered solvent DCM molecule (with at least 3 different orientations) – has been taken out in the final refinement (SQUEEZE details are provided in the CIF file).

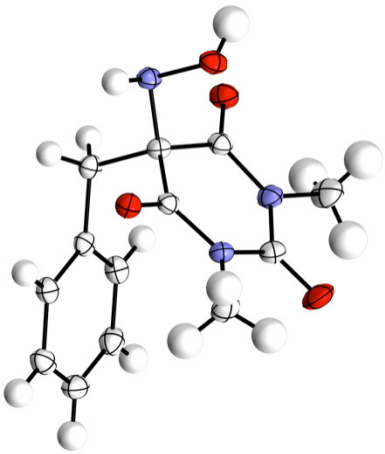

HABA-3: Fw = 277.28, thick colorless plate, 0.58 × 0.48 × 0.14 mm^3, monoclinic, $P2_1/c$ (no. 14), a = 15.08539(16), b = 22.7205(2), c = 12.63479(12) Å, β = 95.2052(9)°, V = 4312.69(7) Å^3, Z = 12, D_x = 1.281 g cm^{-3}, μ = 0.811 mm^{-1}, abs. corr. range: 0.751–0.907. 25707 Reflections were measured up to a resolution of (sin $\theta/\lambda)_{max}$ = 0.62 Å^{-1}. 8452 Reflections were unique (R_{int} = 0.0326), of which 7495 were observed [$I > 2\sigma(I)$]. 574 Parameters were refined using 6 restraints. $R1/wR2$ [$I > 2\sigma(I)$]: 0.0452/0.1284. $R1/wR2$ [all refl.]: 0.0503/0.1333. S = 1.057. Residual electron density found between −0.31 and 0.47 e Å^{-3}.

4.7.2 Density Functional Theory (DFT) Calculations

All calculations were performed at the B3LYP/6-31G* level with an SM8 solvation model for aqueous solvation using Spartan '14 modeling software.[19] Optimized geometries and vibrational frequencies were calculated for each reactant and product independently, and free energies are given for 298.15 K.

Table 4-3. B3LYP/6-31G* Optimized Geometries, Energies, and Entropy Corrections for HABA-2

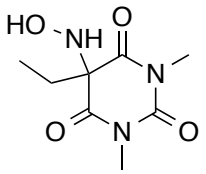

HABA-2

B3LYP/6-31G* Energy (E): -777.830211 hartrees
Entropy Correction (Hv-TSv): 489.3164 kJ/mol
G° = E + "entropy correction": -487978.5084 kcal/mol

Atom	Atomic Number	Cartesian Coordinates (Angstroms) X	Y	Z
C	6	-0.6049300	0.8417058	0.4349930
N	7	-0.0984525	-0.6657865	-1.4894891
N	7	-0.0411970	-1.5727172	0.7351163
C	6	0.1705384	-1.7435236	-0.6359966
C	6	-0.4511740	-0.3916519	1.3217852
C	6	-0.5300454	0.5720091	-1.0633262
N	7	-2.0156861	1.2836506	0.6784233
H	1	-2.1106114	1.3518565	1.6937114
O	8	-2.1938759	2.6639788	0.2659752
H	1	-2.1722711	2.5762678	-0.7061935
O	8	0.5512101	-2.8167159	-1.0835504
O	8	-0.6847358	-0.3065386	2.5248496
O	8	-0.8530035	1.4529791	-1.8634389
C	6	0.1816692	-2.7670242	1.5764488
H	1	-0.5153830	-3.5554505	1.2907173
H	1	0.0157055	-2.4761208	2.6098956
H	1	1.2014042	-3.1256746	1.4385383
C	6	0.0517574	-0.9318365	-2.9351619
H	1	-0.7102807	-1.6381381	-3.2679932

H	1	1.0370686	-1.3562363	-3.1223527
H	1	-0.0647327	0.0132877	-3.4581450
C	6	0.4667668	1.8918398	0.8439986
H	1	0.3340905	2.0597033	1.9176854
H	1	0.2013473	2.8189427	0.3329428
C	6	1.9204494	1.5154621	0.5441506
H	1	2.5824359	2.3141660	0.8927911
H	1	2.1014350	1.3949339	-0.5292235
H	1	2.2305006	0.5966313	1.0528481

Table 4-4. B3LYP/6-31G* Calculated IR Frequencies (cm^{-1}, uncorrected) and Intensities for HABA-2

	cm^{-1}	Intensity		cm^{-1}	Intensity		cm^{-1}	Intensity
1	29	0.65	**27**	735	34.66	**53**	1474	60.94
2	56	0.37	**28**	752	5.71	**54**	1490	234.93
3	67	1.78	**29**	777	10.85	**55**	1515	26.84
4	72	1.98	**30**	816	1.57	**56**	1525	22.36
5	97	0.20	**31**	844	38.74	**57**	1526	4.54
6	120	3.92	**32**	933	20.68	**58**	1531	10.88
7	141	40.35	**33**	951	26.65	**59**	1536	10.55
8	151	5.20	**34**	989	17.69	**60**	1539	6.86
9	187	2.47	**35**	992	44.26	**61**	1542	54.27
10	210	3.78	**36**	1008	13.12	**62**	1557	8.11
11	241	1.43	**37**	1066	99.45	**63**	1652	1129.43
12	269	0.50	**38**	1088	32.89	**64**	1666	535.19
13	297	34.45	**39**	1104	99.22	**65**	1745	23.16
14	311	23.94	**40**	1111	108.14	**66**	3068	27.21
15	328	50.45	**41**	1186	2.05	**67**	3089	17.01
16	348	81.88	**42**	1186	2.74	**68**	3119	21.76
17	368	69.15	**43**	1203	13.43	**69**	3120	24.13
18	385	66.61	**44**	1226	74.95	**70**	3127	21.10
19	397	29.74	**45**	1267	78.27	**71**	3136	38.99
20	405	52.68	**46**	1314	48.77	**72**	3154	28.57
21	436	15.01	**47**	1324	277.89	**73**	3196	6.85
22	467	2.63	**48**	1356	275.72	**74**	3198	7.04
23	493	52.41	**49**	1380	352.25	**75**	3236	0.63
24	595	14.90	**50**	1410	119.42	**76**	3237	0.57
25	672	0.58	**51**	1421	476.02	**77**	3470	38.93
26	728	13.05	**52**	1445	9.57	**78**	3654	150.67

Table 4-5. B3LYP/6-31G* Optimized Geometries, Energies, and Entropy Corrections for Tetrahedral Intermediate from HABA-2

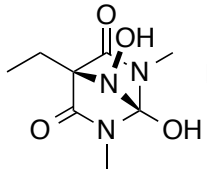

Tetrahedral Intermediate from HABA-2

B3LYP/6-31G* Energy (E): -777.794907 hartrees
Entropy Correction (Hv-TSv): 484.8890 kJ/mol
G° = E + "entropy correction": -487957.413 kcal/mol

Atom	Atomic Number	Cartesian Coordinates (Angstroms) X	Y	Z
C	6	0.6826550	-0.7093715	-0.2520754
N	7	-0.6638236	1.1747810	-0.4012703
N	7	-1.5222246	-0.9329473	0.3774277
C	6	-0.8979778	0.3314648	0.8103178
C	6	-0.6000347	-1.5750505	-0.3777609
C	6	0.3612552	0.5797245	-1.0763558
N	7	0.4494646	-0.2058469	1.1430580
O	8	1.3206431	0.9286983	1.3526051
H	1	1.5560453	0.8394727	2.2944745
O	8	-0.7329593	-2.6064246	-1.0367486
O	8	0.9084712	0.9658204	-2.1078447
C	6	-2.9579868	-1.1824439	0.4010370
H	1	-3.3405700	-1.0059545	1.4074358
H	1	-3.1218680	-2.2265420	0.1345554
H	1	-3.4901284	-0.5499528	-0.3179059
C	6	-0.9678759	2.6021024	-0.4649829
H	1	-0.5853145	3.1176106	0.4195906
H	1	-2.0433129	2.7739396	-0.5618622
H	1	-0.4799754	3.0020120	-1.3549919
O	8	-1.5022385	0.9617342	1.8580946
H	1	-2.3028962	1.4311970	1.5506580
C	6	1.9648948	-1.4526110	-0.5714643
H	1	1.8531246	-1.8182832	-1.5982688
H	1	1.9956406	-2.3446943	0.0631897
C	6	3.2749579	-0.6676887	-0.4427477
H	1	4.1086776	-1.2996592	-0.7657019
H	1	3.4665574	-0.3591720	0.5873357
H	1	3.2667994	0.2280852	-1.0697986

Table 4-6. B3LYP/6-31G* Calculated IR Frequencies (cm^{-1}, uncorrected) and Intensities for Tetrahedral Intermediate from HABA-2

	cm^{-1}	Intensity		cm^{-1}	Intensity		cm^{-1}	Intensity
1	64	2.65	**27**	709	5.40	**53**	1448	30.37
2	83	5.37	**28**	771	16.37	**54**	1454	447.21
3	91	2.24	**29**	788	5.14	**55**	1479	112.57
4	101	4.52	**30**	810	12.27	**56**	1487	29.10
5	129	3.12	**31**	871	3.18	**57**	1505	9.17
6	139	12.35	**32**	900	65.50	**58**	1526	14.83
7	144	3.40	**33**	933	45.67	**59**	1531	5.13
8	173	1.41	**34**	953	105.28	**60**	1533	20.08
9	209	5.63	**35**	970	106.74	**61**	1544	6.05
10	237	82.42	**36**	993	100.40	**62**	1546	6.21
11	250	55.86	**37**	1019	43.75	**63**	1555	28.57
12	261	111.24	**38**	1034	92.91	**64**	1699	340.80
13	266	61.52	**39**	1067	88.55	**65**	1728	806.93
14	278	80.49	**40**	1146	5.65	**66**	3072	26.67
15	288	30.52	**41**	1162	141.79	**67**	3076	43.67
16	296	10.30	**42**	1175	26.44	**68**	3078	29.60
17	320	18.51	**43**	1189	319.40	**69**	3090	44.75
18	348	1.49	**44**	1200	14.20	**70**	3107	10.33
19	390	13.23	**45**	1239	107.36	**71**	3138	45.73
20	471	16.79	**46**	1257	87.70	**72**	3159	43.03
21	473	17.12	**47**	1307	66.72	**73**	3163	11.90
22	519	31.52	**48**	1326	74.74	**74**	3163	11.65
23	564	3.96	**49**	1335	32.30	**75**	3182	5.49
24	596	18.75	**50**	1375	153.75	**76**	3197	2.74
25	615	3.54	**51**	1381	164.44	**77**	3673	204.94
26	650	7.39	**52**	1410	2.93	**78**	3702	182.78

Table 4-7. B3LYP/6-31G* Optimized Geometries, Energies, and Entropy Corrections for Hydantoin from HABA-2 (compound 1)

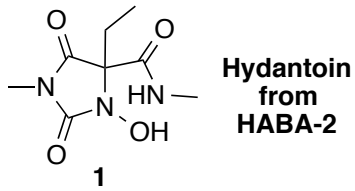

Hydantoin from HABA-2

1

B3LYP/6-31G* Energy (E): -777.851209 hartrees
Entropy Correction (Hv-TSv): 486.2711 kJ/mol
G° = E + "entropy correction": -487992.4127 kcal/mol

Atom	Atomic Number	Cartesian Coordinates (Angstroms) X	Y	Z
C	6	-0.0923132	-0.2368749	0.4267483
C	6	0.7843110	0.8332527	-0.2507468
N	7	1.8410586	0.1750048	-0.8351464
C	6	1.8269383	-1.2004694	-0.5413791
N	7	0.8327013	-1.3788250	0.3949683
O	8	0.3357460	-2.6632163	0.6304976
H	1	-0.3725122	-2.7324241	-0.0604980
C	6	-1.3065838	-0.5242424	-0.5075757
O	8	-1.4574763	-1.6577741	-1.0169122
O	8	2.5912806	-2.0404216	-0.9992780
O	8	0.5681921	2.0364942	-0.2901556
N	7	-2.1552555	0.4825832	-0.7081676
H	1	-1.8902035	1.4052629	-0.3761125
C	6	-3.3356421	0.3682620	-1.5636172
H	1	-3.0568503	0.3221934	-2.6202480
H	1	-3.9650164	1.2410281	-1.3943085
H	1	-3.8929627	-0.5345995	-1.3094252
C	6	2.8994572	0.8381860	-1.5957025
H	1	2.4473976	1.5424362	-2.2944613
H	1	3.4533294	0.0740824	-2.1390680
H	1	3.5740892	1.3774046	-0.9268999
C	6	-0.5420573	0.1456049	1.8509254
H	1	-1.1951835	-0.6549214	2.2144060
H	1	-1.1521484	1.0495159	1.7766900
C	6	0.6015516	0.3833344	2.8369923
H	1	1.2520981	1.2036314	2.5140236
H	1	1.2150905	-0.5121467	2.9708426
H	1	0.1909640	0.6576385	3.8136085

Table 4-8. B3LYP/6-31G* Calculated IR Frequencies (cm^{-1}, uncorrected) and Intensities for Hydantoin from HABA-2 (compound 1)

	cm^{-1}	Intensity		cm^{-1}	Intensity		cm^{-1}	Intensity
1	16	1.27	**27**	707	7.98	**53**	1487	100.04
2	36	7.25	**28**	759	39.31	**54**	1498	18.07
3	61	1.41	**29**	771	25.07	**55**	1500	122.82
4	80	0.62	**30**	809	28.13	**56**	1519	46.42
5	102	2.70	**31**	823	1.68	**57**	1527	7.51
6	115	1.59	**32**	905	17.46	**58**	1536	15.56
7	132	1.69	**33**	941	20.89	**59**	1537	4.44
8	150	20.66	**34**	984	12.40	**60**	1537	9.58
9	158	20.86	**35**	1011	100.88	**61**	1542	30.10

10	182	2.91	**36**	1051	22.41	**62**	1575	237.76
11	190	1.32	**37**	1068	171.69	**63**	1656	184.52
12	230	10.32	**38**	1097	18.81	**64**	1690	1459.61
13	260	21.20	**39**	1122	19.29	**65**	1775	117.23
14	277	2.15	**40**	1173	23.94	**66**	3065	26.55
15	280	10.20	**41**	1187	22.62	**67**	3084	19.65
16	314	21.96	**42**	1202	3.70	**68**	3091	39.64
17	325	18.49	**43**	1214	5.93	**69**	3105	28.43
18	377	39.20	**44**	1240	27.51	**70**	3125	18.66
19	397	29.81	**45**	1282	44.35	**71**	3136	27.92
20	415	28.10	**46**	1294	86.48	**72**	3148	40.55
21	534	28.25	**47**	1303	73.90	**73**	3163	22.09
22	553	37.40	**48**	1343	10.76	**74**	3185	7.68
23	576	123.64	**49**	1379	47.55	**75**	3206	7.96
24	605	5.26	**50**	1415	327.95	**76**	3213	0.99
25	668	184.68	**51**	1440	4.07	**77**	3352	402.65
26	676	49.41	**52**	1469	470.84	**78**	3565	170.69

Table 4-9. B3LYP/6-31G* Optimized Geometries, Energies, and Entropy Corrections for HABA-3

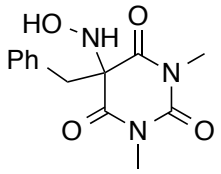

HABA-3

B3LYP/6-31G* Energy (E): -969.569250 hartrees
Entropy Correction (Hv-TSv): 622.8451 kJ/mol
G° = E + "entropy correction": -608264.5669 kcal/mol

Atom	Atomic Number	Cartesian Coordinates (Angstroms) X	Y	Z
C	6	-1.4148263	0.6247761	0.3800361
N	7	-0.9742004	-0.8976144	-1.5490269
N	7	-0.9003589	-1.8012850	0.6754580
C	6	-0.7295250	-1.9832829	-0.6996249
C	6	-1.2474823	-0.6057805	1.2692675
C	6	-1.3285577	0.3620266	-1.1193586
N	7	-2.8343955	1.0379468	0.6104583
H	1	-2.9449738	1.1009460	1.6248198
O	8	-3.0387488	2.4135406	0.2004997
H	1	-3.0194143	2.3335491	-0.7722264

O	8	-0.4006397	-3.0704827	-1.1529572
O	8	-1.4300681	-0.5039606	2.4796402
O	8	-1.5980966	1.2649146	-1.9139484
C	6	-0.6804412	-2.9958690	1.5167346
H	1	-1.3739723	-3.7840064	1.2234202
H	1	-0.8540530	-2.7061992	2.5491599
H	1	0.3414716	-3.3521675	1.3870168
C	6	-0.8433367	-1.1686104	-2.9954580
H	1	-1.5799466	-1.9122462	-3.3010751
H	1	0.1559919	-1.5490832	-3.2046696
H	1	-1.0137365	-0.2333456	-3.5208156
C	6	-0.3746770	1.7091848	0.8070813
H	1	-0.5473907	1.8830182	1.8729592
H	1	-0.6517544	2.6195928	0.2740368
C	6	1.0803261	1.3671886	0.5622397
C	6	3.7940664	0.7600796	0.1172980
C	6	1.8516439	0.7527184	1.5596992
C	6	1.6959238	1.6808662	-0.6590690
C	6	3.0395190	1.3773883	-0.8816871
C	6	3.1959216	0.4500528	1.3397052
H	1	1.3938920	0.5171470	2.5169891
H	1	1.1164719	2.1706635	-1.4374423
H	1	3.4979254	1.6317544	-1.8327907
H	1	3.7768082	-0.0220165	2.1265470
H	1	4.8406339	0.5285958	-0.0529168

Table 4-10. B3LYP/6-31G* Calculated IR Frequencies (cm^{-1}, uncorrected) and Intensities for HABA-3

	cm^{-1}	Intensity		cm^{-1}	Intensity		cm^{-1}	Intensity
1	32	0.17	**34**	742	26.24	**67**	1381	341.81
2	38	0.21	**35**	752	8.51	**68**	1411	103.28
3	65	0.05	**36**	773	31.94	**69**	1423	525.50
4	74	1.05	**37**	781	10.88	**70**	1473	66.36
5	76	2.67	**38**	843	4.81	**71**	1489	254.49
6	87	5.07	**39**	871	0.16	**72**	1501	0.78
7	104	1.08	**40**	878	24.21	**73**	1517	26.69
8	118	35.16	**41**	898	5.00	**74**	1524	15.13
9	127	35.46	**42**	938	10.22	**75**	1524	15.99
10	165	0.42	**43**	959	28.05	**76**	1533	3.58
11	173	6.08	**44**	973	10.30	**77**	1539	63.64
12	205	5.64	**45**	978	0.14	**78**	1547	8.50
13	237	6.20	**46**	992	42.25	**79**	1556	6.31

14	282	13.06	**47**	1002	0.59	**80**	1643	3.59
15	286	66.98	**48**	1018	0.36	**81**	1656	1171.51
16	315	3.80	**49**	1034	5.67	**82**	1665	12.83
17	325	93.67	**50**	1058	162.92	**83**	1670	515.39
18	345	53.46	**51**	1062	2.07	**84**	1749	18.50
19	374	44.43	**52**	1102	125.30	**85**	3101	15.60
20	390	29.88	**53**	1115	17.44	**86**	3120	20.66
21	394	33.30	**54**	1151	74.71	**87**	3121	22.21
22	402	37.38	**55**	1184	1.36	**88**	3162	4.54
23	424	0.29	**56**	1185	1.09	**89**	3193	12.72
24	433	15.05	**57**	1190	2.33	**90**	3195	8.17
25	466	9.86	**58**	1192	0.21	**91**	3197	6.44
26	482	37.22	**59**	1219	2.08	**92**	3198	7.75
27	497	32.19	**60**	1231	0.93	**93**	3208	5.14
28	579	14.09	**61**	1267	82.96	**94**	3214	56.13
29	624	8.15	**62**	1276	50.88	**95**	3228	28.99
30	635	0.05	**63**	1325	328.24	**96**	3237	0.60
31	674	1.94	**64**	1347	169.28	**97**	3240	0.67
32	720	40.70	**65**	1362	9.25	**98**	3468	47.65
33	733	20.18	**66**	1376	39.93	**99**	3659	152.10

Table 4-11. B3LYP/6-31G* Optimized Geometries, Energies, and Entropy Corrections for Tetrahedral Intermediate from HABA-3

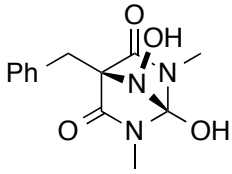

Tetrahedral Intermediate from HABA-3

B3LYP/6-31G* Energy (E): -969.531043 hartrees
Entropy Correction (Hv-TSv): 615.0554 kJ/mol
G° = E + "entropy correction": -608242.4535 kcal/mol

Atom	Atomic Number	Cartesian Coordinates (Angstroms) X	Y	Z
C	6	-0.3427742	-0.6164885	-0.3472655
N	7	-1.7098888	1.2484088	-0.4628308
N	7	-2.5194092	-0.8675358	0.3495542
C	6	-1.9000724	0.4072400	0.7611990
C	6	-1.6134196	-1.5022917	-0.4302133
C	6	-0.7007258	0.6632307	-1.1671376
N	7	-0.5369928	-0.1034517	1.0540916
O	8	0.3025911	1.0576321	1.2294310

H	1	0.8389397	0.8135918	2.0047001
O	8	-1.7479128	-2.5451185	-1.0706060
O	8	-0.1928524	1.0461800	-2.2193422
C	6	-3.9477418	-1.1457395	0.4320903
H	1	-4.2915614	-0.9846525	1.4549900
H	1	-4.1010789	-2.1909282	0.1636579
H	1	-4.5221183	-0.5188935	-0.2586696
C	6	-2.0657555	2.6618687	-0.5447626
H	1	-1.6893930	3.2049308	0.3257873
H	1	-3.1480604	2.7936395	-0.6284639
H	1	-1.6053830	3.0644986	-1.4481676
O	8	-2.4899514	1.0345895	1.8187620
H	1	-3.3097450	1.4811969	1.5277412
C	6	0.9421954	-1.3535595	-0.6990596
H	1	0.9205801	-1.4986221	-1.7841385
H	1	0.8723837	-2.3519431	-0.2567094
C	6	2.2524503	-0.7088992	-0.2856689
C	6	4.7095564	0.4285637	0.4870530
C	6	2.8800902	0.2517499	-1.0902291
C	6	2.8813536	-1.0972351	0.9050960
C	6	4.0975251	-0.5320941	1.2932827
C	6	4.0970928	0.8154471	-0.7066315
H	1	2.4016941	0.5617658	-2.0143798
H	1	2.4138765	-1.8543627	1.5299078
H	1	4.5692095	-0.8497822	2.2185716
H	1	4.5686040	1.5570705	-1.3451162
H	1	5.6581530	0.8675996	0.7812166

Table 4-12. B3LYP/6-31G* Calculated IR Frequencies (cm^{-1}, uncorrected) and Intensities for Tetrahedral Intermediate from HABA-3

	cm^{-1}	Intensity		cm^{-1}	Intensity		cm^{-1}	Intensity
1	8	63.69	**34**	717	42.19	**67**	1370	15.46
2	40	35.48	**35**	764	17.19	**68**	1380	225.16
3	47	2.55	**36**	774	6.30	**69**	1388	51.26
4	63	7.74	**37**	813	11.63	**70**	1393	4.27
5	95	4.33	**38**	837	9.18	**71**	1457	470.23
6	113	90.94	**39**	865	1.40	**72**	1477	73.15
7	131	17.03	**40**	867	9.61	**73**	1483	81.82
8	140	5.78	**41**	884	6.53	**74**	1498	4.72
9	149	3.52	**42**	909	80.82	**75**	1504	13.58
10	163	11.11	**43**	931	11.70	**76**	1530	10.40
11	180	3.85	**44**	952	167.83	**77**	1536	19.00
12	193	5.47	**45**	972	2.08	**78**	1545	10.32

13	226	14.61	**46**	996	16.29	**79**	1549	2.80
14	240	210.91	**47**	1000	43.89	**80**	1556	36.50
15	254	53.40	**48**	1001	48.16	**81**	1643	2.05
16	271	5.24	**49**	1019	1.30	**82**	1664	9.22
17	279	25.88	**50**	1033	156.96	**83**	1702	368.50
18	293	4.54	**51**	1043	99.55	**84**	1731	793.40
19	334	9.37	**52**	1060	5.67	**85**	3079	34.01
20	345	5.39	**53**	1070	17.42	**86**	3081	24.46
21	387	9.59	**54**	1116	2.69	**87**	3084	46.12
22	421	0.24	**55**	1171	195.95	**88**	3123	10.30
23	462	2.97	**56**	1186	283.47	**89**	3160	12.81
24	469	28.52	**57**	1188	0.44	**90**	3164	11.12
25	480	13.70	**58**	1203	8.82	**91**	3180	5.15
26	519	31.19	**59**	1213	0.66	**92**	3192	13.83
27	567	6.40	**60**	1227	2.40	**93**	3196	0.02
28	604	1.12	**61**	1238	100.30	**94**	3197	2.56
29	609	17.00	**62**	1257	86.71	**95**	3207	19.04
30	616	19.31	**63**	1266	15.83	**96**	3213	58.40
31	635	0.47	**64**	1307	65.44	**97**	3224	25.75
32	659	15.78	**65**	1329	116.28	**98**	3671	205.04
33	708	9.66	**66**	1362	2.23	**99**	3716	175.84

Table 4-13. B3LYP/6-31G* Optimized Geometries, Energies, and Entropy Corrections for Hydantoin from HABA-3

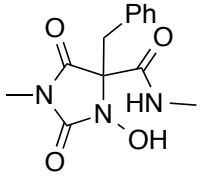

Hydantoin from HABA-3

B3LYP/6-31G* Energy (E): -969.588678 hartrees
Entropy Correction (Hv-TSv): 619.5569 kJ/mol
G° = E + "entropy correction": -608277.5441 kcal/mol

Atom	Atomic Number	Cartesian Coordinates (Angstroms) X	Y	Z
C	6	-0.5728124	-0.3925610	-0.4654126
C	6	0.2945958	0.6820689	-1.1469397
N	7	1.3679730	0.0344917	-1.7078855
C	6	1.3654973	-1.3424930	-1.4099210
N	7	0.3469391	-1.5300012	-0.5088406
O	8	-0.1266742	-2.8134577	-0.2400513

H	1	-0.8621108	-2.8967473	-0.9005879
C	6	-1.8064300	-0.6810948	-1.3729762
O	8	-1.9987581	-1.8314813	-1.8254712
O	8	2.1553679	-2.1716769	-1.8439265
O	8	0.0528999	1.8793996	-1.2096308
N	7	-2.6249465	0.3435873	-1.6058148
H	1	-2.3248596	1.2694655	-1.3132675
C	6	-3.8219207	0.2313936	-2.4381963
H	1	-3.5622865	0.1484151	-3.4975699
H	1	-4.4299129	1.1221482	-2.2847258
H	1	-4.3932668	-0.6513532	-2.1478209
C	6	2.4311829	0.7056765	-2.4540935
H	1	1.9822381	1.4067382	-3.1579184
H	1	2.9976145	-0.0539708	-2.9906609
H	1	3.0930613	1.2487810	-1.7758284
C	6	-1.0136280	-0.0126943	0.9727521
H	1	-1.6605203	-0.8191389	1.3319161
H	1	-1.6291923	0.8870064	0.9018293
C	6	0.1231389	0.2201962	1.9448935
C	6	2.2141150	0.6602418	3.7717818
C	6	0.6519409	-0.8393271	2.6941818
C	6	0.6572268	1.5036175	2.1249357
C	6	1.6960648	1.7228613	3.0302783
C	6	1.6888791	-0.6220647	3.6010237
H	1	0.2510178	-1.8401618	2.5588985
H	1	0.2575762	2.3329778	1.5487777
H	1	2.0959008	2.7241574	3.1602023
H	1	2.0850418	-1.4543736	4.1753436
H	1	3.0190469	0.8293737	4.4807252

Table 4-14. B3LYP/6-31G* Calculated IR Frequencies (cm^{-1}, uncorrected) and Intensities for Hydantoin from HABA-3

	cm^{-1}	Intensity		cm^{-1}	Intensity		cm^{-1}	Intensity
1	19	0.52	**34**	718	54.88	**67**	1377	0.87
2	39	0.80	**35**	752	51.71	**68**	1417	339.55
3	48	4.83	**36**	774	8.12	**69**	1473	429.52
4	56	3.03	**37**	779	8.28	**70**	1490	53.91
5	68	1.86	**38**	814	18.29	**71**	1493	59.95
6	95	0.46	**39**	846	7.21	**72**	1502	40.70
7	110	0.69	**40**	862	0.65	**73**	1504	179.90
8	115	0.25	**41**	887	1.82	**74**	1522	50.21
9	121	2.33	**42**	921	0.50	**75**	1532	14.94
10	157	21.16	**43**	950	11.10	**76**	1535	5.85

11	167	12.38	**44**	970	1.53	**77**	1541	37.64
12	178	3.24	**45**	987	62.39	**78**	1547	7.41
13	197	1.93	**46**	998	1.03	**79**	1579	271.93
14	218	4.27	**47**	1019	0.48	**80**	1644	3.31
15	256	18.11	**48**	1029	26.79	**81**	1659	166.19
16	284	1.55	**49**	1057	114.57	**82**	1667	4.81
17	289	33.67	**50**	1062	27.19	**83**	1694	1502.79
18	312	8.04	**51**	1073	100.26	**84**	1778	117.22
19	339	5.40	**52**	1104	20.43	**85**	3090	41.44
20	378	44.02	**53**	1127	20.17	**86**	3093	18.01
21	389	33.71	**54**	1181	22.68	**87**	3105	28.23
22	405	30.65	**55**	1192	0.01	**88**	3150	4.98
23	418	0.04	**56**	1201	4.92	**89**	3163	21.21
24	469	2.44	**57**	1215	4.90	**90**	3185	7.81
25	542	53.45	**58**	1218	1.15	**91**	3192	8.54
26	554	29.97	**59**	1229	6.48	**92**	3200	0.66
27	586	8.59	**60**	1237	3.03	**93**	3206	7.97
28	608	102.76	**61**	1252	36.47	**94**	3208	26.56
29	628	31.45	**62**	1295	86.37	**95**	3214	0.85
30	635	0.45	**63**	1297	126.92	**96**	3215	53.71
31	665	200.27	**64**	1322	10.98	**97**	3224	24.22
32	680	20.46	**65**	1361	13.82	**98**	3359	416.87
33	714	16.30	**66**	1367	2.44	**99**	3557	185.92

4.7.3 ^{1}H and ^{13}C NMR Spectra

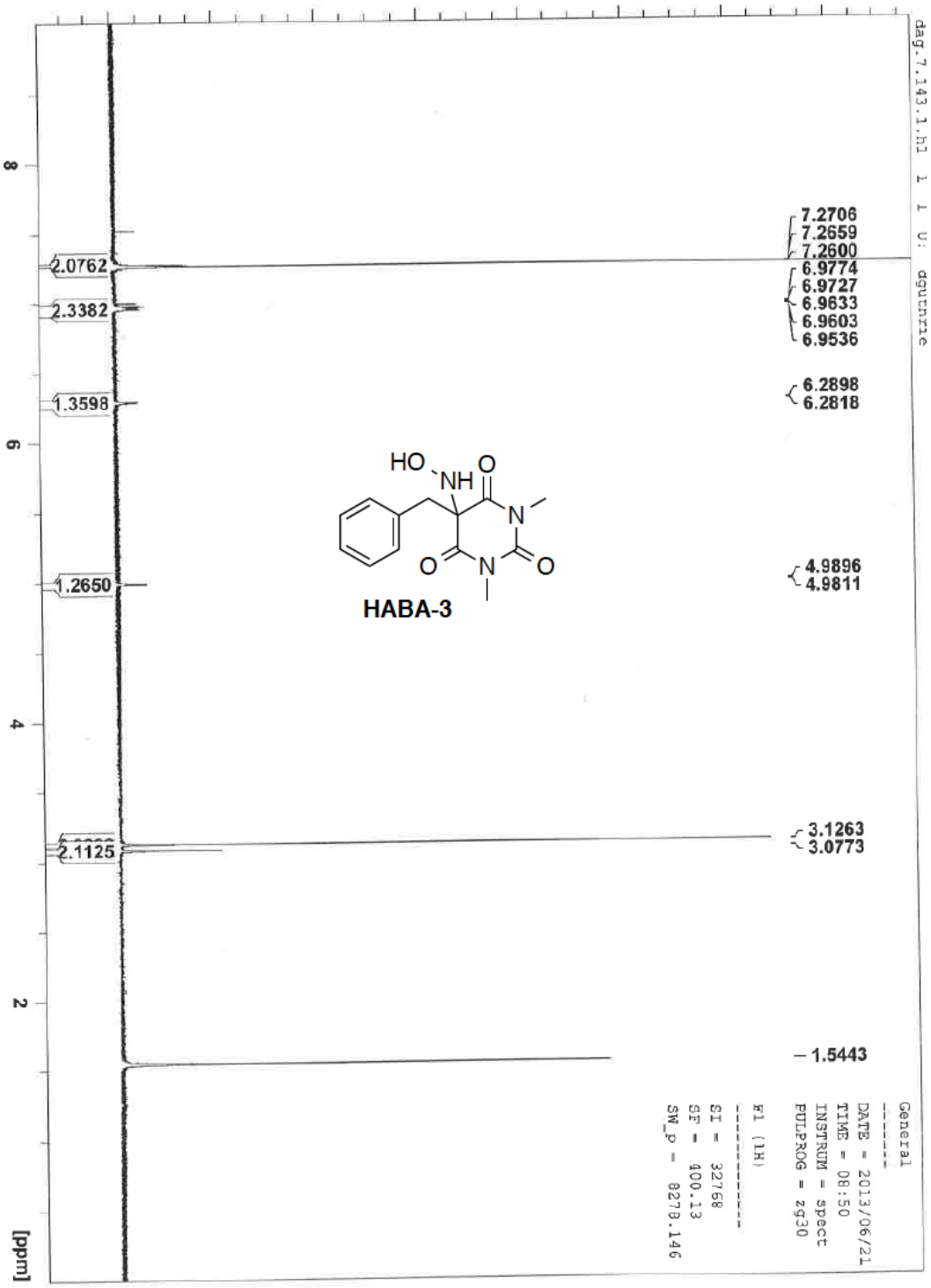

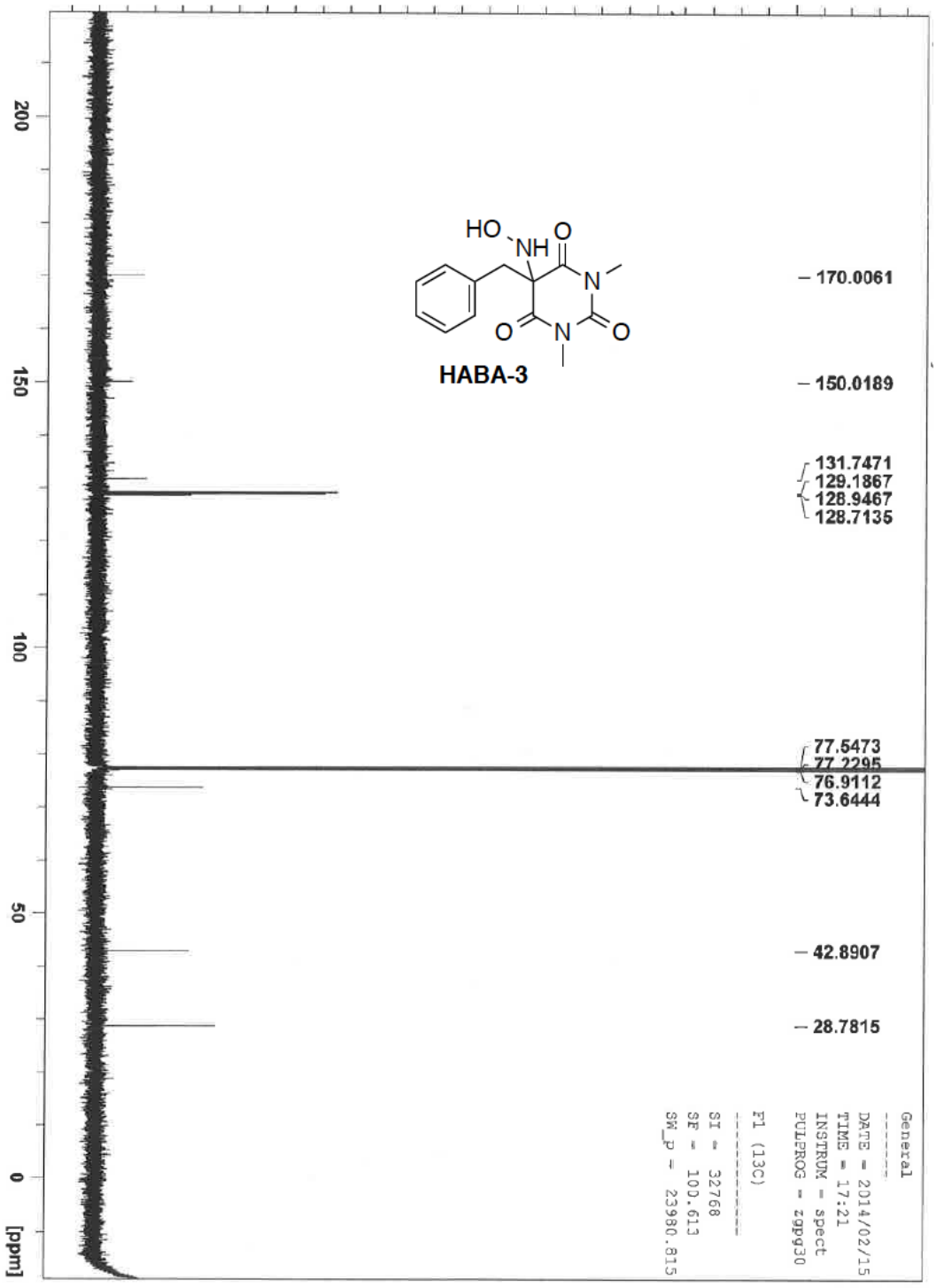
HO
NH
O
N
O
N
O
HABA-3
170.0061
150.0189
131.7471
129.1867
128.9467
128.7135
77.5473
77.2295
76.9112
73.6444
42.8907
28.7815
200
150
100
50
0
[ppm]
General
DATE = 2014/02/15
TIME = 17:21
INSTRUM = spect
PULPROG = zgpg30
F1 (13C)
SI = 32768
SF = 100.613
SW_p = 23980.815

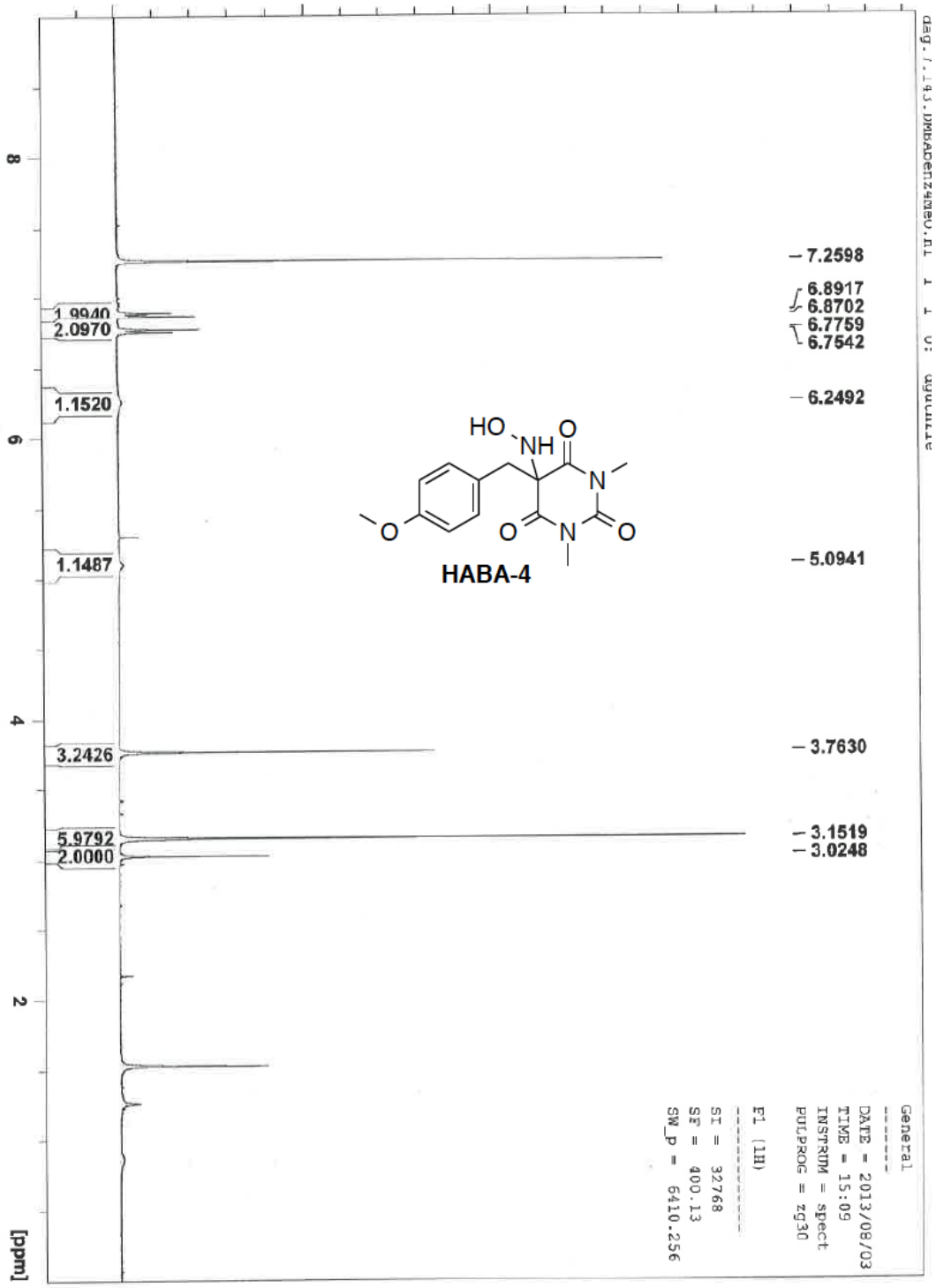
HABA-4
7.2598
6.8917
6.8702
6.7759
6.7542
6.2492
5.0941
3.7630
3.1519
3.0248
1.9940
2.0970
1.1520
1.1487
3.2426
5.9792
2.0000
[ppm]

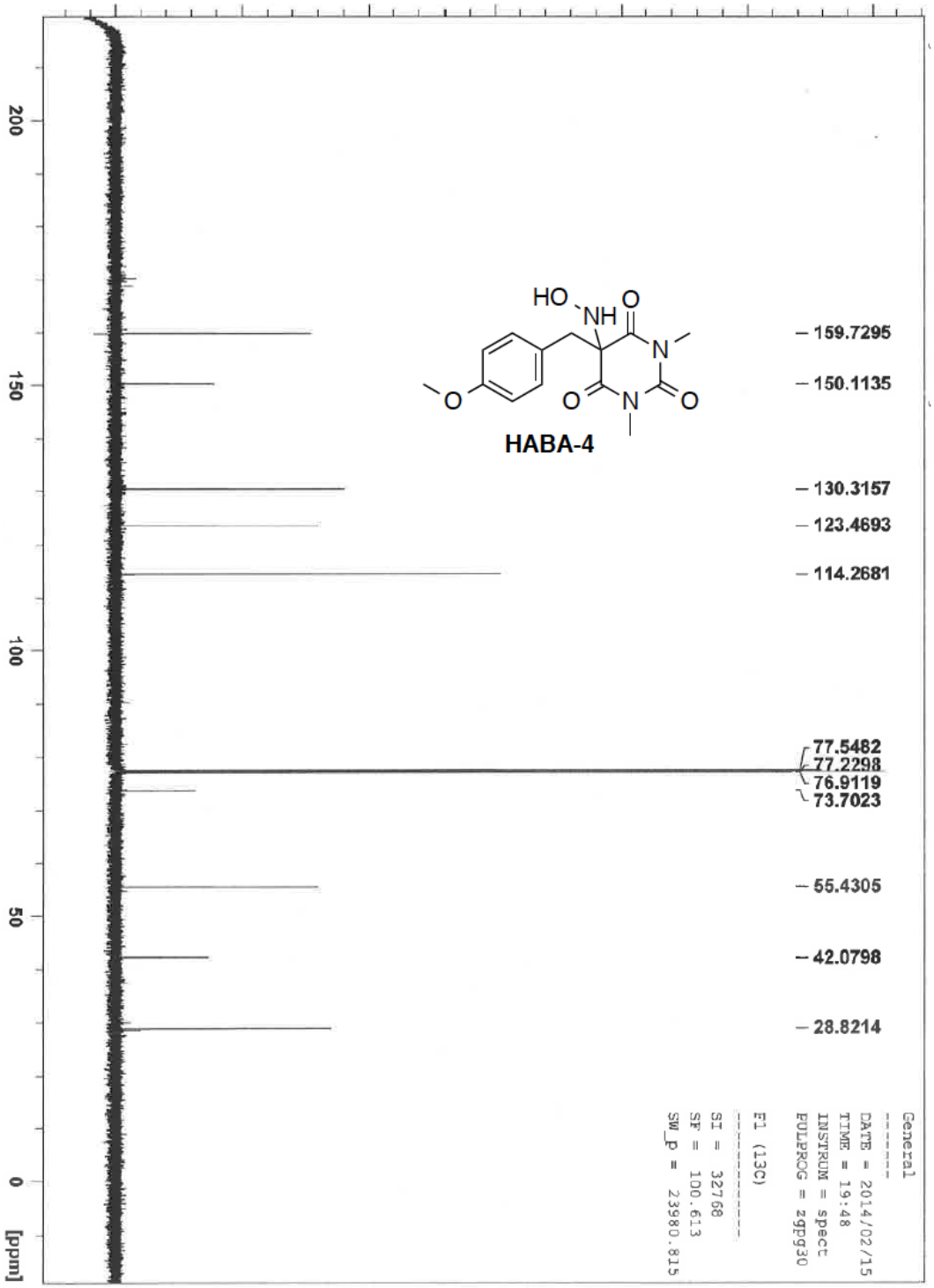
HO
NH
O
N
O
O
N
O
HABA-4
159.7295
150.1135
130.3157
123.4693
114.2681
77.5482
77.2298
76.9119
73.7023
55.4305
42.0798
28.8214
200
150
100
50
0
[ppm]
General
DATE = 2014/02/15
TIME = 19:48
INSTRUM = spect
PULPROG = zgpg30
F1 (13C)
SI = 32768
SF = 100.613
SW_p = 23980.815

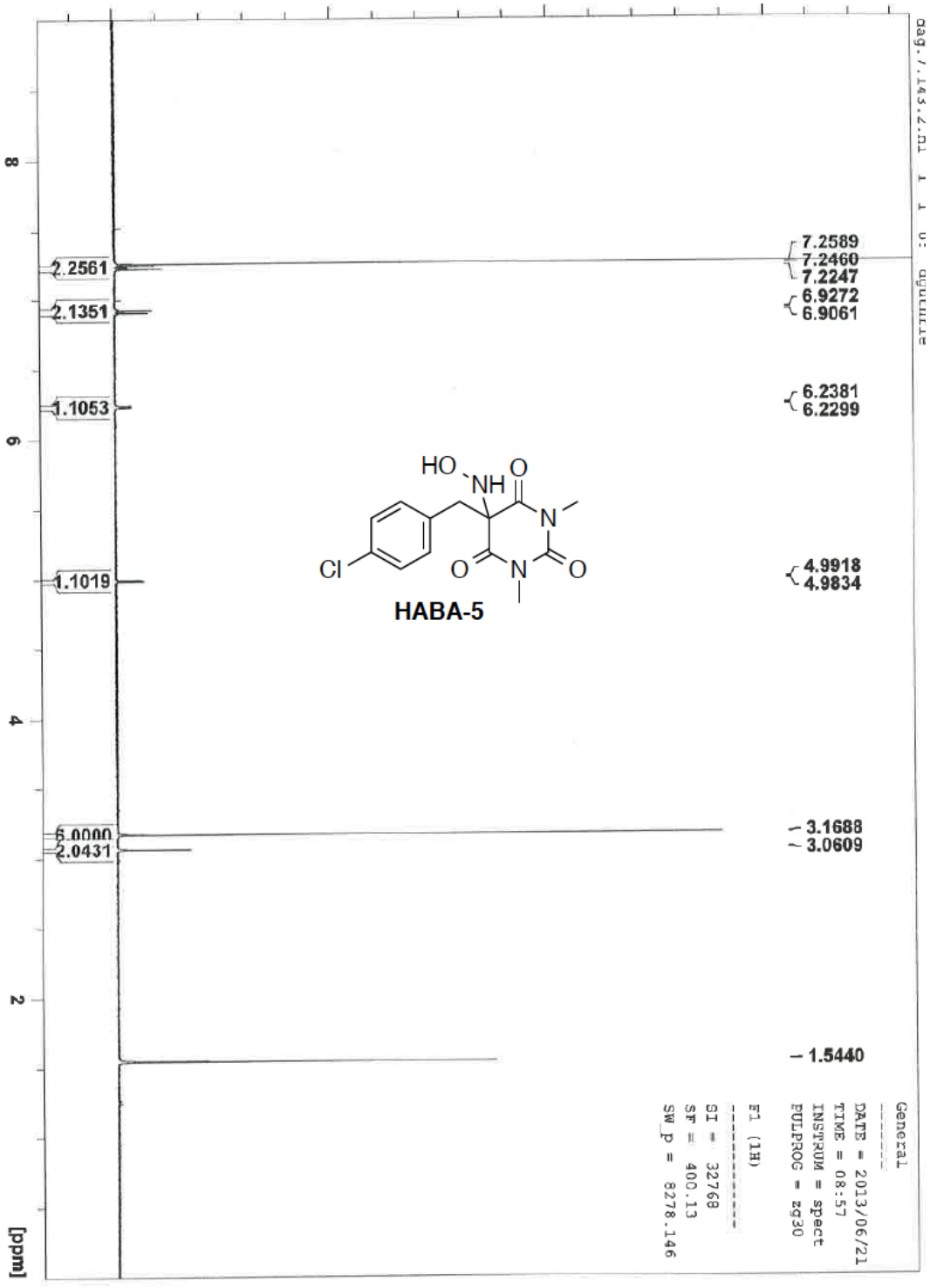
HO
NH
O
N
Cl
O
N
O
HABA-5
7.2589
7.2460
7.2247
6.9272
6.9061
6.2381
6.2299
4.9918
4.9834
3.1688
3.0609
1.5440
2.2561
2.1351
1.1053
1.1019
6.0000
2.0431
8
6
4
2
[ppm]

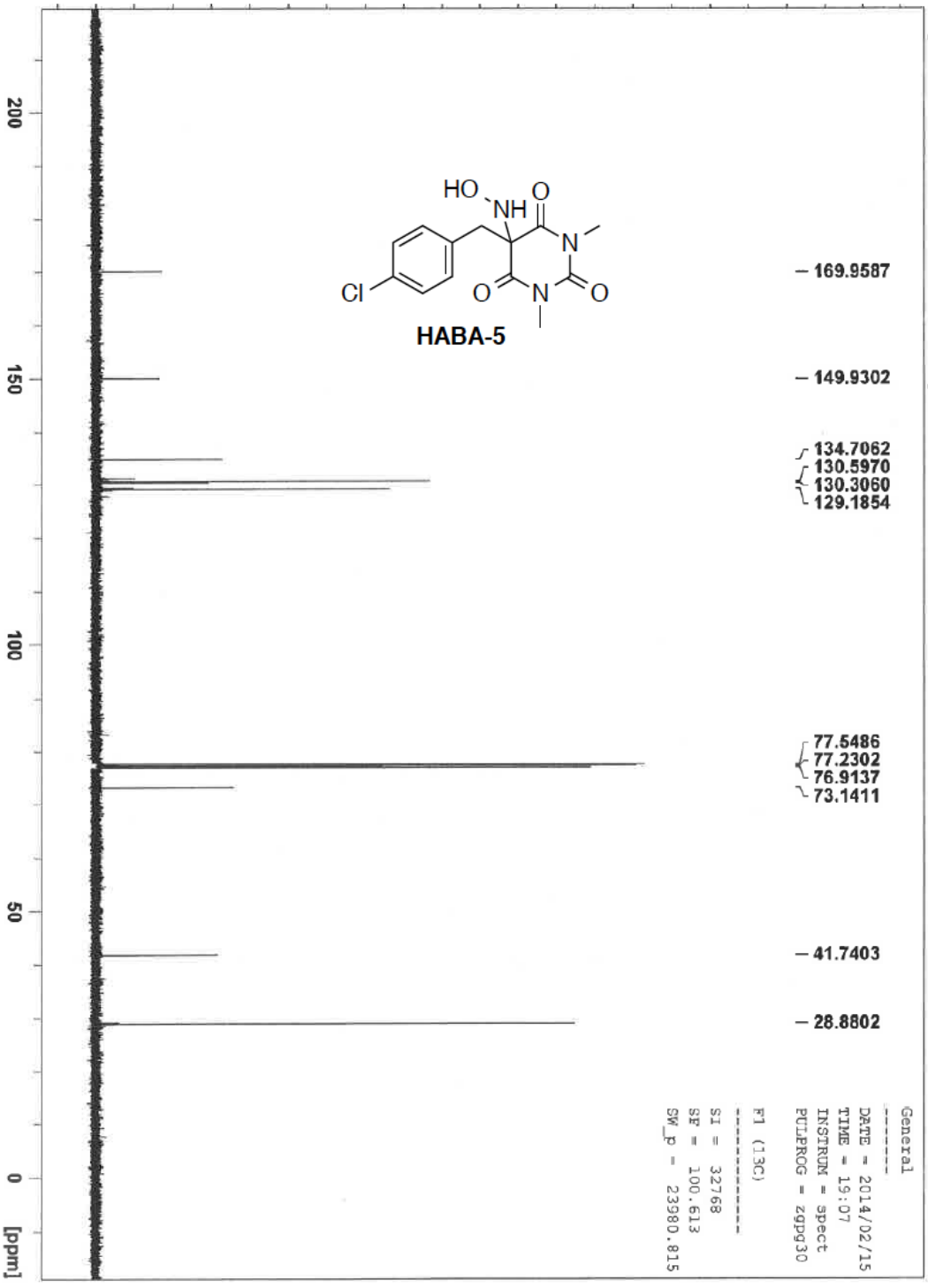
HO
NH
O
N
Cl
O
N
O
HABA-5
169.9587
149.9302
134.7062
130.5970
130.3060
129.1854
77.5486
77.2302
76.9137
73.1411
41.7403
28.8802
200
150
100
50
0
[ppm]
General
DATE = 2014/02/15
TIME = 19:07
INSTRUM = spect
PULPROG = zgpg30
F1 (13C)
SI = 32768
SF = 100.613
SW_p = 23980.815

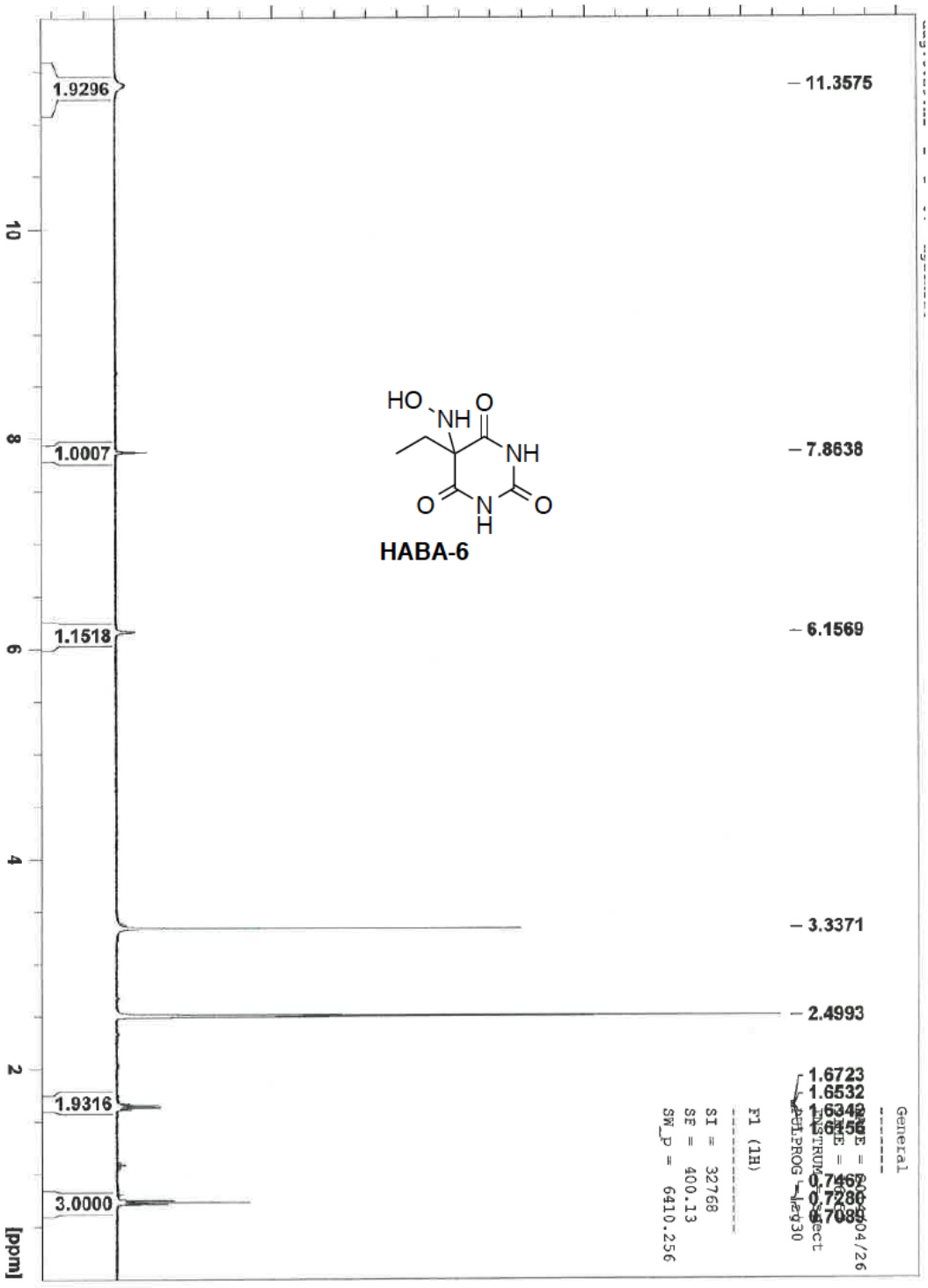
HABA-6
11.3575
7.8638
6.1569
3.3371
2.4993
1.6723
1.6532
1.9296
1.0007
1.1518
1.9316
3.0000
[ppm]

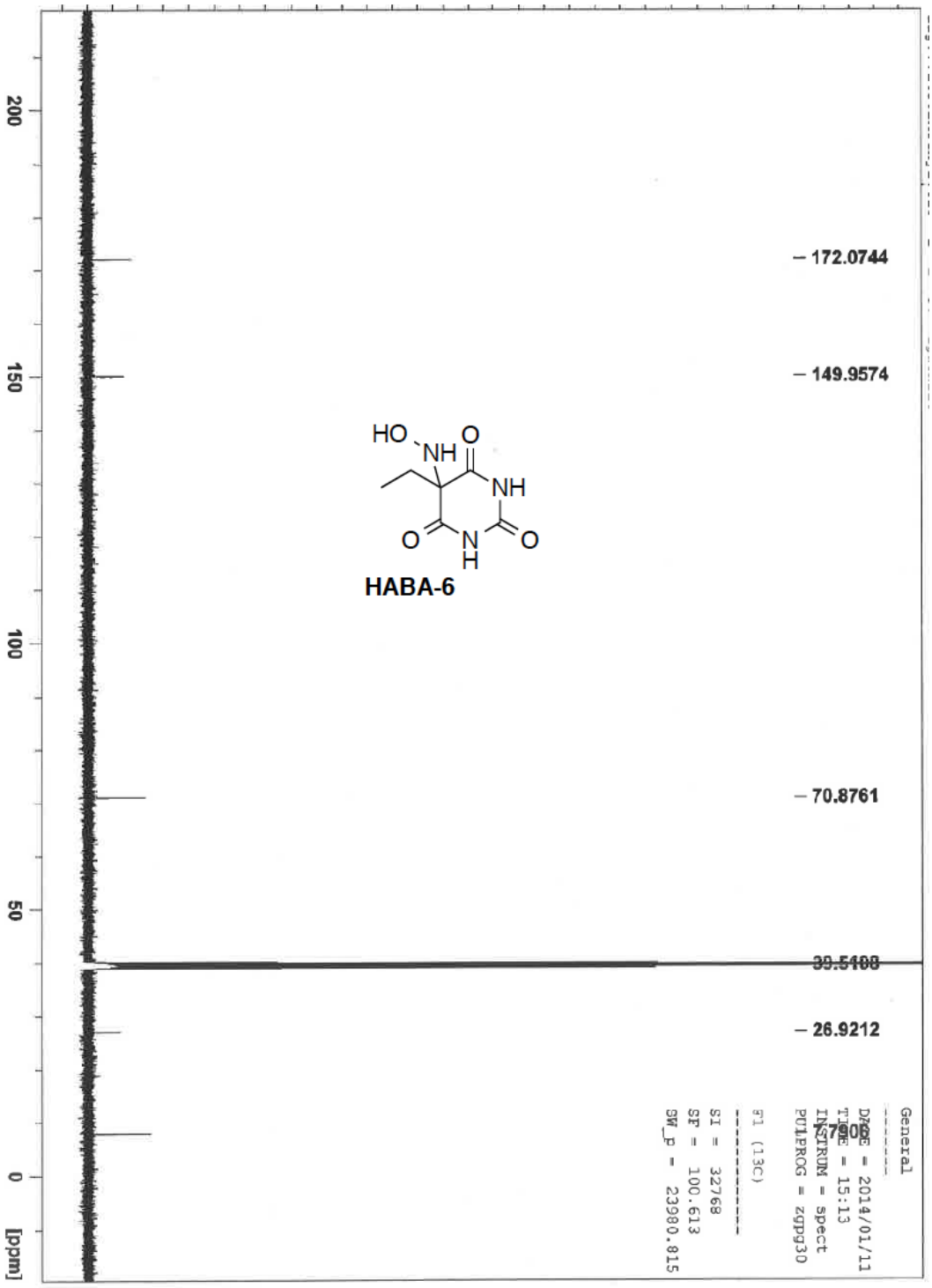
200
150
100
50
0
[ppm]
172.0744
149.9574
70.8761
39.5108
26.9212
HO
NH
O
NH
O
N
H
O
HABA-6
General
DATE = 2014/01/11
TIME = 15:13
INSTRUM = spect
PULPROG = zgpg30
F1 (13C)
SI = 32768
SF = 100.613
SW_p = 23980.815

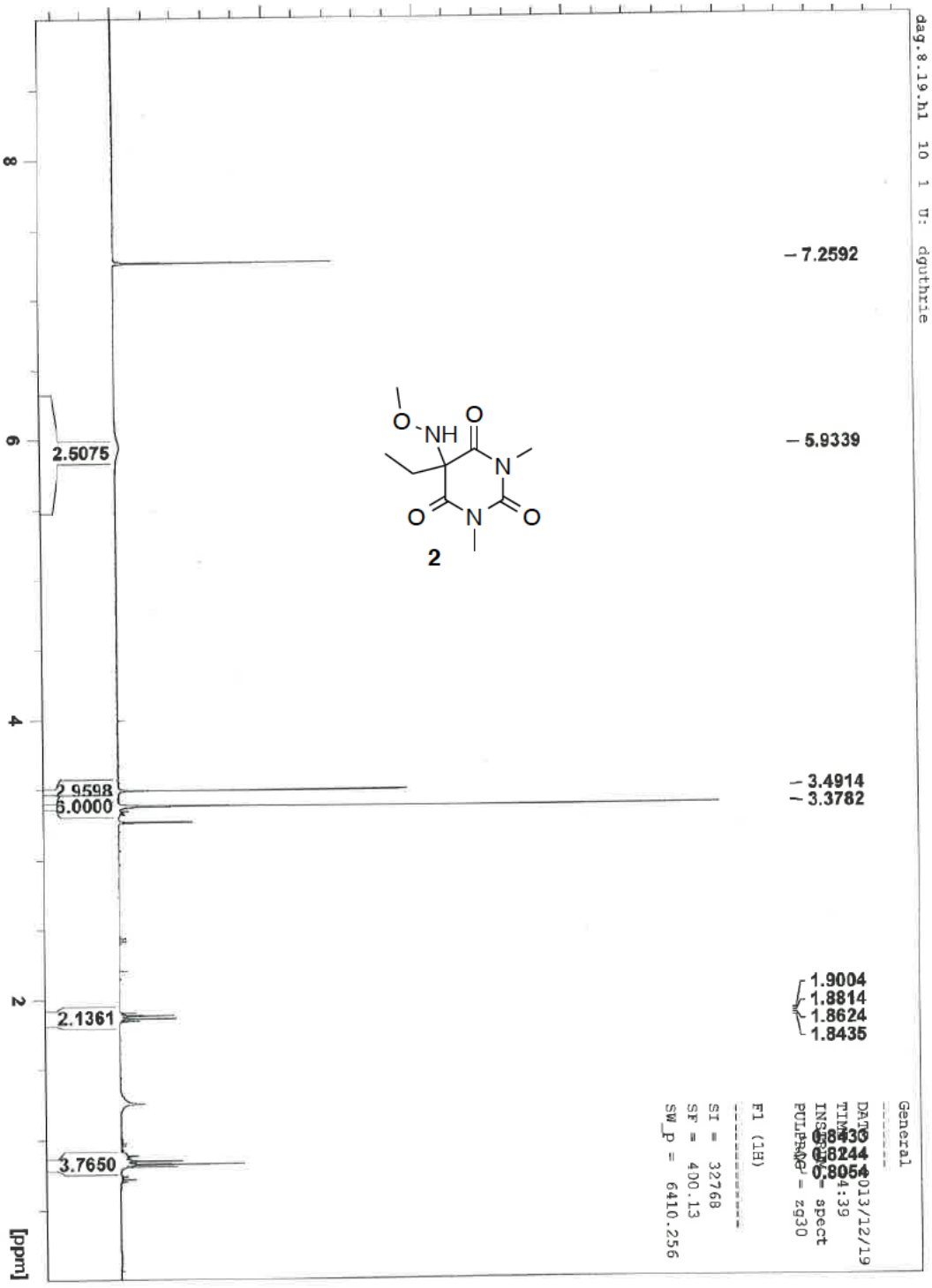
dag.8.19.h1 10 1 U: dguthrie
7.2592
5.9339
3.4914
3.3782
1.9004
1.8814
1.8624
1.8435
2.5075
2.9598
6.0000
2.1361
3.7650
O
NH
N
O
N
O
2
8
6
4
2
[ppm]
General
DAT
TIM
INS
PUL
F1 (1H)
SI = 32768
SF = 400.13
SW_p = 6410.256

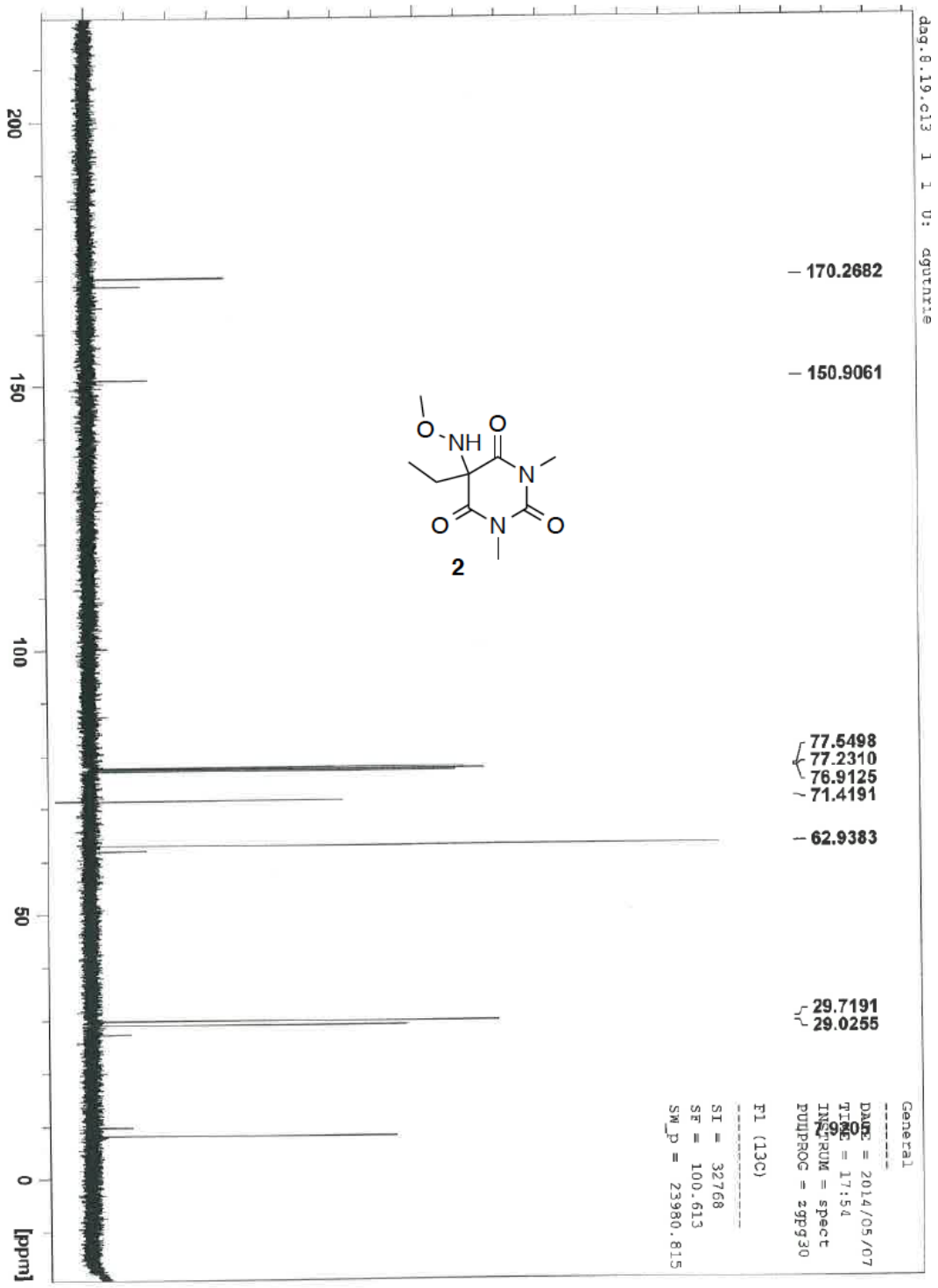
dag.8.19.c13 1 1 U: dgutnrie
200
150
100
50
0
[ppm]
170.2682
150.9061
77.5498
77.2310
76.9125
71.4191
62.9383
29.7191
29.0255
7.9206
O
NH
O
N
O
N
O
2
General
DATE = 2014/05/07
TIME = 17:54
INSTRUM = spect
PULPROG = zgpg30
F1 (13C)
SI = 32768
SF = 100.613
SW_p = 23980.815

Chapter 5.

The HNO-Aldol Screening Assay Using ^{1}H NMR Spectroscopy

The hydroxylamino-X (HAX) general class of nitroxyl (HNO) donors, where X is based on Meldrum's acid (HAMA), barbituric acid (HABA), or pyrazolone (HAPY), is capable of releasing HNO quantitatively under nonenzymatic, physiological conditions, with the rate and amount of HNO released being dependent mainly on the nature of the carbon-based leaving group. As shown in Figure 5-1, the rate of HNO release can be varied over four orders of magnitude and is dependent on the pK_a of the carbon-based acid byproduct, X–H, which can be varied over six pH units. The most physiologically useful donors in terms of HNO release rate have byproducts with pK_a values ≤ ca. 8 in 50% v/v aq. ethanol (i.e., ca. ≤ 7 in water).

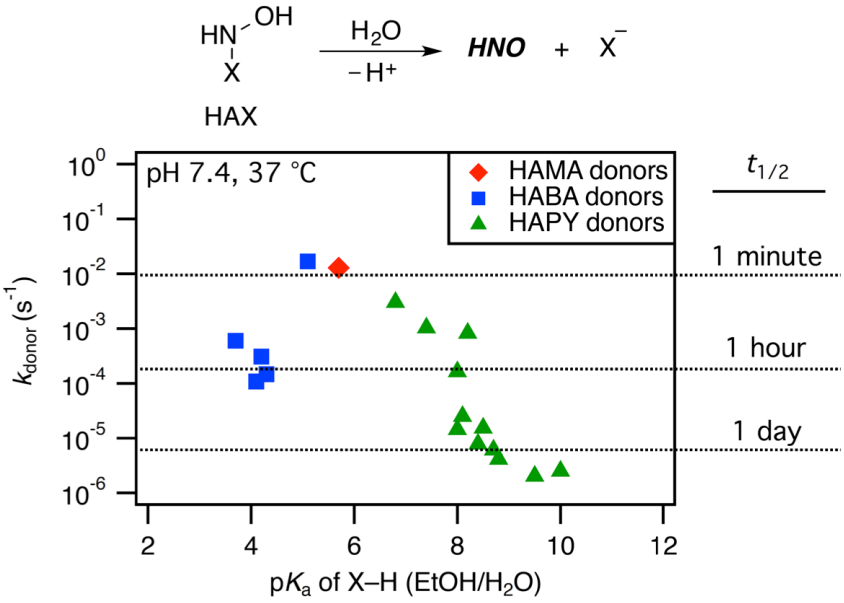

Figure 5-1. Decomposition rates for the HAX general class of HNO donors as a function pK_a of X–H, the byproduct of HNO release. Each pK_a value was determined by titration

in 50% v/v aqueous ethanol. Each rate is the calculated best fit to a single exponential. The decomposition reaction was carried out in the presence of added TXPTS to minimize contribution of the back reaction, save for the HAMA and HABA examples, which have half-lives around one minute, where there is negligible back reaction (see Table 5-1). See Chapters 2, 3, and 4, as well as Table 5-1, for compound structures.

Moving forward, we will continue to broaden the scope of the HAX general class by applying what we have learned about the inherent reactivity of HNO with the carbon-based byproduct of release, X–H/X^-. That is, often what makes a good leaving group so too makes a good nucleophile, particularly with the nitroso functionality of HNO.

The HNO-aldol screening assay using ^{1}H NMR spectroscopy was developed to identify potential HNO donors, as well as potential HNO traps for detection purposes. This assay predicts the success of the preparatory HNO-aldol procedure, as well as which functional groups to avoid since some scaffolds are prone to hydroxylamine-assisted hydrolysis and rearrangement mechanisms. As there exists a large library of potential HNO donors that fall into the HAX general class, efficiently screening out the possibilities are important as well. All of this information can be obtained quickly and effectively without the need to synthesize and isolate the potential HNO donor itself. Multiple experiments may be performed in parallel.

HNO-aldol screening assay procedure: Dissolve 1 mg of byproduct (X–H) in 1.2 mL of 10% D_2O, pH 7.4 phosphate buffer (0.25 M) with DTPA (0.2 mM). Transfer 0.6 mL to an NMR tube and take an initial ^{1}H NMR spectrum using a 1 second presaturation pulse to suppress the water signal. To the remaining 0.6 mL of

solution, add 1 mg of Angeli's salt, transfer to a second NMR tube, and let stand at room temperature under air for ca. 30 minutes, then take another ^{1}H NMR spectrum. Signs of a new product, or products, will be evident if HNO trapping is occurring. If a new product does form, then externally incubate the sample at 37 °C and continue to check the reaction progress by ^{1}H NMR at regular time intervals. Keeping the sample under air allows for the dissolved oxygen to serve as an alternative trap for HNO such that the reaction may be reversible, albeit this reverse reaction will be much slower than if a better trap (e.g., TXPTS) were added following the completion of Angeli's salt decomposition (ca. 2 h). By not adding TXPTS, potential alternative decomposition mechanisms may be observed; it is important to be made aware of these pathways. Any new, undesired products that form may be compared to the byproduct standard solution used for the initial spectrum in order to identify decomposition pathways independent of HNO trapping.

HNO-aldol screening assay observations: The observations may be divided into five categories: (A) complete trapping of HNO and reversible reaction, (B) incomplete trapping of HNO and reversible reaction, (C) complete trapping of HNO and irreversible reaction, (D) incomplete trapping of HNO and irreversible reaction, and (E) no reaction with HNO. Potential HNO donors fall into categories A and B, and the HNO-aldol preparatory procedure will be most successful with category A compounds. The most successful traps for HNO detection will fall into category C, particularly if the reaction is clean and the new product is distinctive; but category A compounds may also serve as traps for HNO detection if it is later observed that the reverse reaction is very slow in the presence of TXPTS. Compounds prone to

alternative, non-HNO decomposition mechanisms fall into categories C and D, and the source of the instability in each scaffold should assessed as to whether or not this may be curtailed to favor HNO generation. The compounds that fall into category E will require synthesis and isolation of the corresponding HAX compound in order to assess its fate.

This assay has already proven its usefulness. Upon its inception, the assay was pivotal to the understanding of the decomposition mechanism for the HAPY class of HNO donors discussed in Chapter 3. Moreover, as the ethyl-based HABA compound, discussed in Chapters 2 and 3, was known to rearrange to the corresponding hydantoin product, it was expected that all alkyl-based HABA compounds would favor rearrangement. Thus, were it not for the efficiency of this assay, the benzyl-HABA compounds, discussed in Chapter 4, would not have been pursued. Shown in Scheme 5-1 is the assay itself utilizing Angeli's salt as the initial HNO donor, and in Table 5-1 are the current results of this assay, where most of the successes are described in Chapters 2, 3, and 4.

Scheme 5-1. The HNO-Aldol Screening Assay Using ^{1}H NMR Spectroscopy

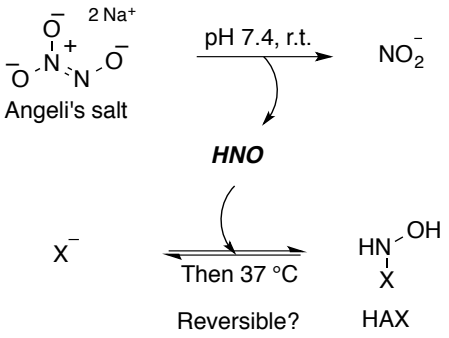

Categories:
(A) Complete trapping of HNO / Reversible
(B) Incomplete trapping of HNO / Reversible
(C) Complete trapping of HNO / Irreversible
(D) Incomplete trapping of HNO / Irreversible
(E) No reaction with HNO

Table 5-1. The HNO-Aldol Screening Assay Using ^{1}H NMR Spectroscopy: Results

Entry	Starting Material (X–H)	Desired Product (HAX)	Category	Notes
1	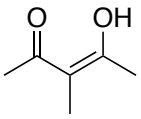	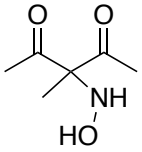	C	Multiple product formation
2	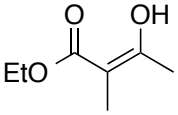	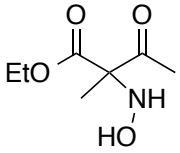	D	Only get loss of EtOH over time
3	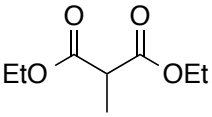	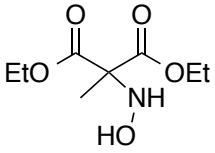	E	Non-enolizable proton
4	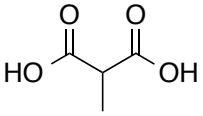	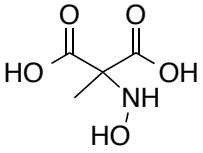	E	Non-enolizable proton
5	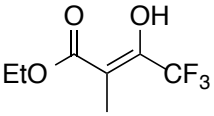	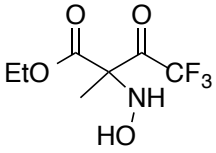	C	Only get loss of EtOH over time
6	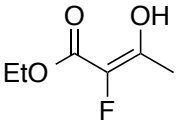	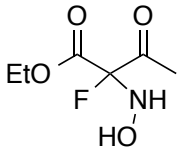	D	Only get loss of EtOH over time
7	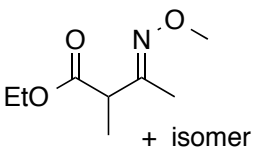	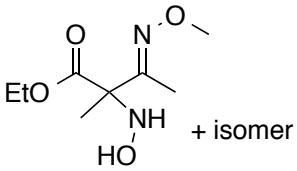	E	Non-enolizable proton
8	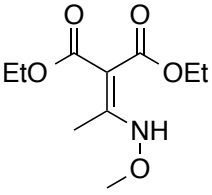	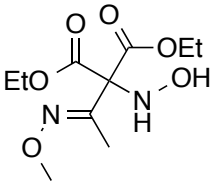	D	Only get loss of EtOH over time
9	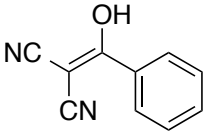	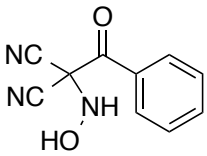	E	No reaction

10	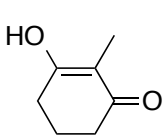	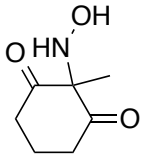	C	First product converted to new unknown product(s)
11	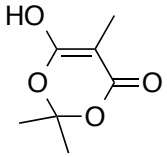	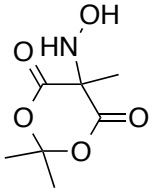	C	Only get loss of acetone over time; See Chapter 2
12	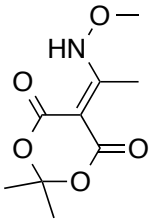	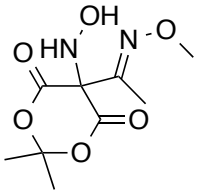	E	No reaction; See Chapter 2
13	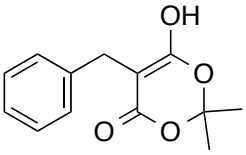	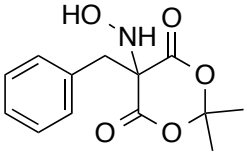	C	Only get loss of acetone over time
14	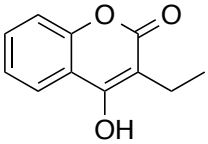	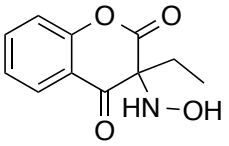	C	First product converted to new unknown product(s)
15	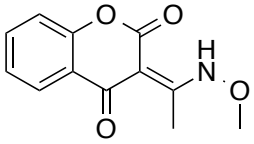	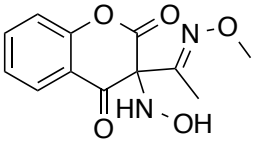	E	No reaction
16	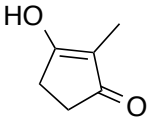	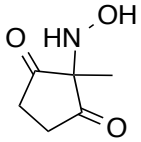	B	ca. 10% trapping
17	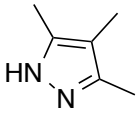	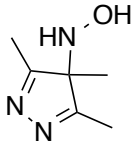	E	No reaction
18	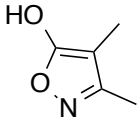	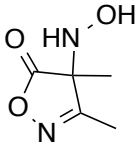	E	No reaction
19	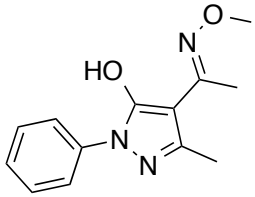	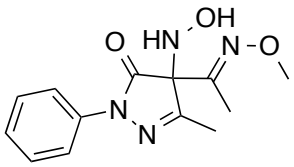	B	See Chapter 3

20	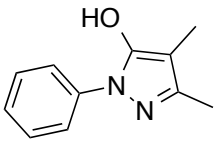	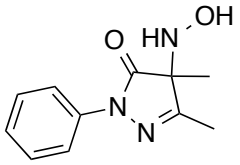	A	See Chapter 3
21	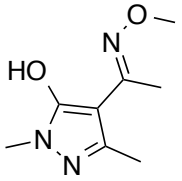	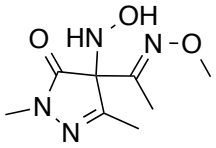	B	See Chapter 3
22	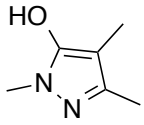	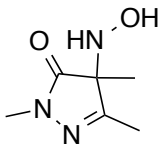	A	See Chapter 3
23	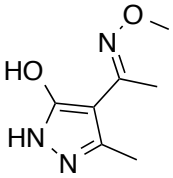	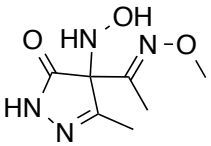	B	See Chapter 3
24	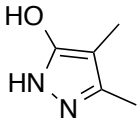	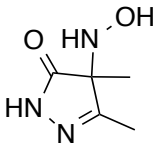	A	See Chapter 3
25	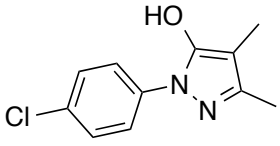	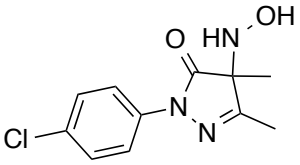	A	See Chapter 3
26	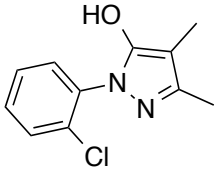	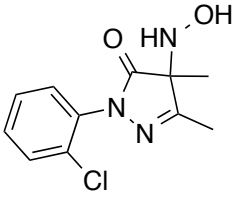	A	See Chapter 3
27	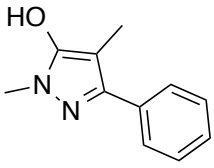	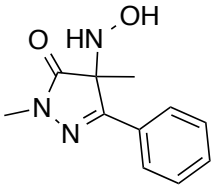	A	See Chapter 3
28	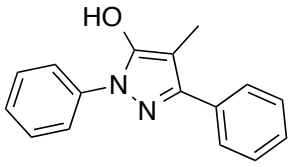	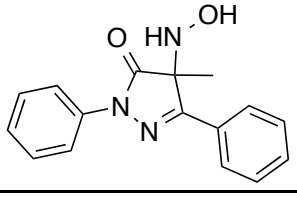	A	See Chapter 3

29	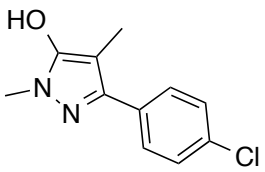	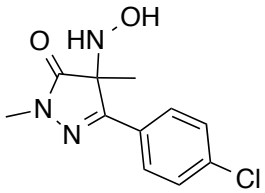	A	See Chapter 3
30	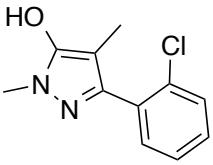	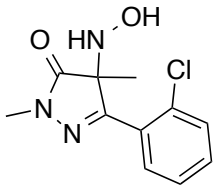	A	See Chapter 3
31	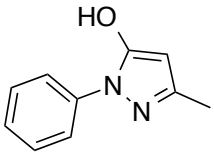	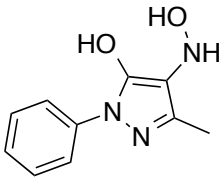	C	Rxn. turned pink/red. Two new Me groups (1:1). Dehydration product likely
32	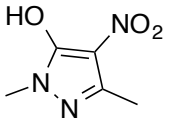	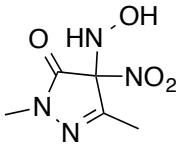	E	No reaction
33	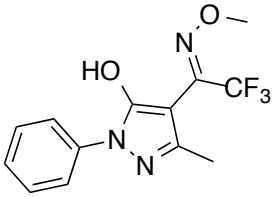	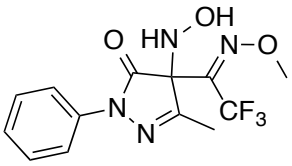	E	No reaction
34	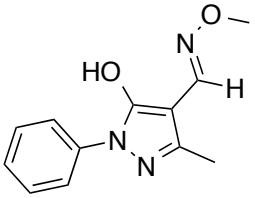	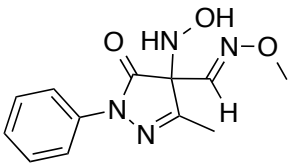	E	No reaction
35	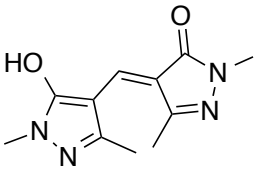	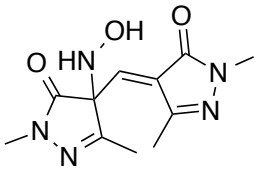	E	No reaction
36	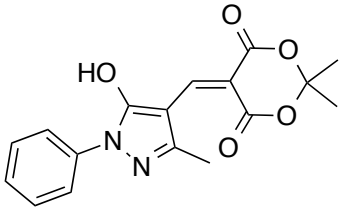	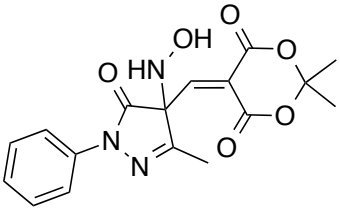	E	No reaction

37	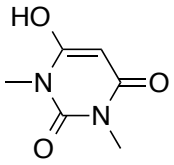	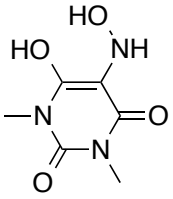	D	ca. 50% trapping + minor products; rxn. turned purple; oxime/nitroso product likely
38	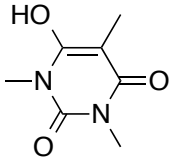	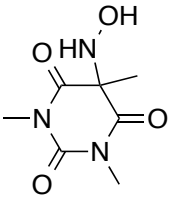	C	Get hydantoin formation
39	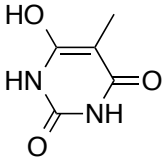	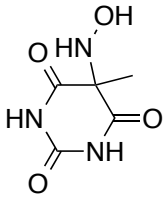	A	Preparatory HNO-aldol TBD
40	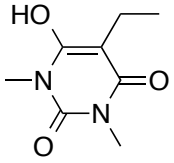	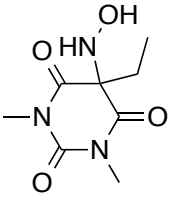	C	See Chapters 2&4
41	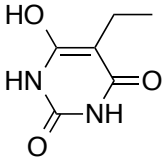	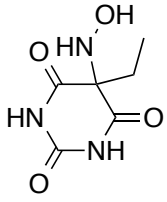	A	See Chapter 4
42	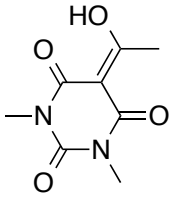	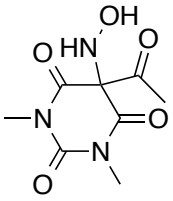	E	No reaction
43	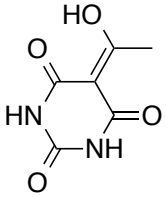	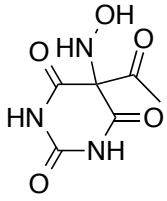	E	No reaction
44	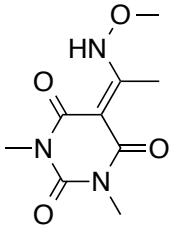	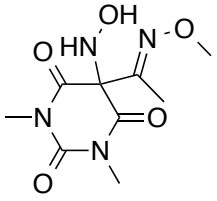	E	No reaction

45	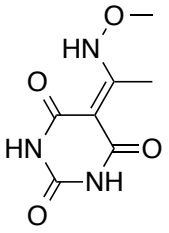	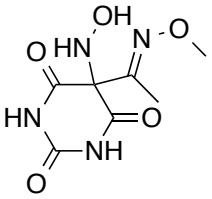	E	No reaction
46	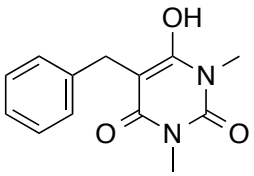	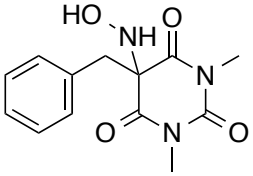	A	See Chapter 4
47	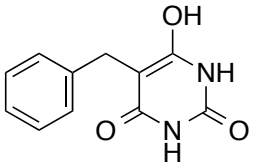	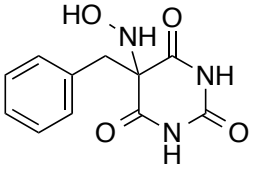	A	Preparatory HNO-aldol TBD
48	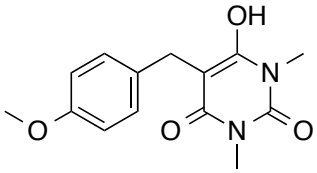	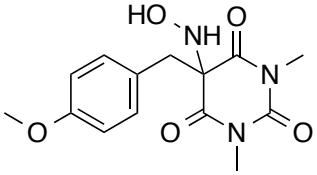	A	See Chapter 4
49	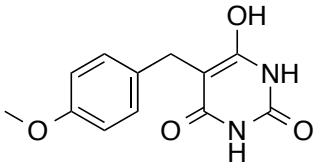	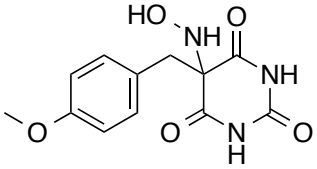	A	Preparatory HNO-aldol TBD
50	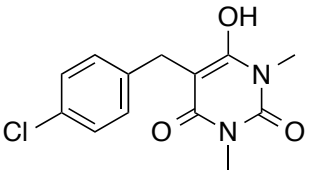	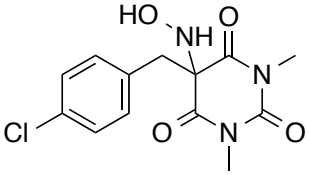	A	See Chapter 4
51	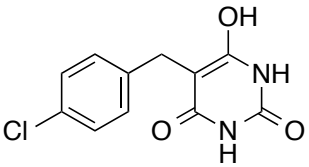	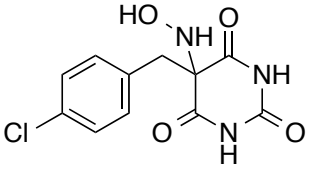	A	Preparatory HNO-aldol TBD
52	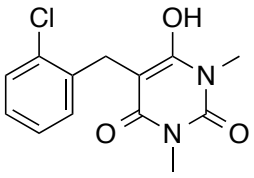	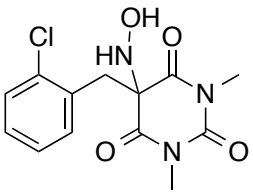	A	Preparatory HNO-aldol TBD
53	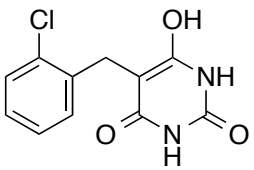	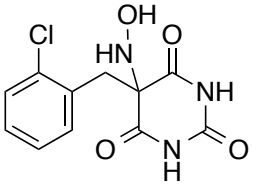	A	Preparatory HNO-aldol TBD

54	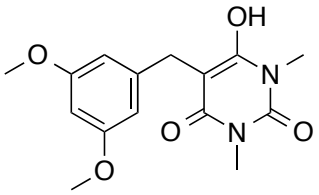	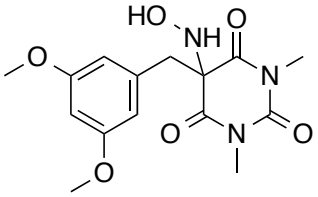	A	Preparatory HNO-aldol TBD
55	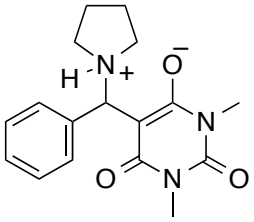	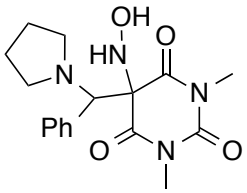	D	ca. 10% trapping; likely hydantoin formation
56	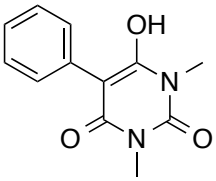	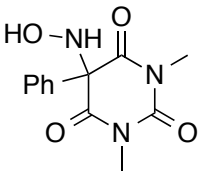	B,D	ca. 60% trapping; final hydantoin yield is 51%
57	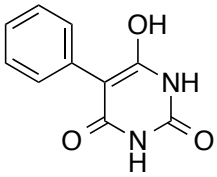	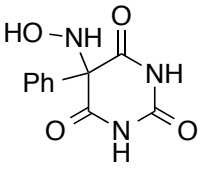	B	ca. 10% trapping
58	$K^{13}CN$	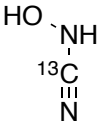	D	pH 10.0 using Piloty's Acid (^{13}C NMR); three new carbons as potential products (130.63, 129.10, 123.33)

Curriculum Vita

Daryl Austin Guthrie was born in Richmond, VA on April 14, 1982. His interests in chemistry began when he was 16 years old as he was responsible for the analysis of swimming pool water, teaching the public about water chemistry, and the retail sale of chemicals at Pla-Mor Pools where he worked throughout high school and college.

In 2005, Daryl graduated from Randolph-Macon College with an ACS-certified Bachelor of Science degree in Chemistry. He did his undergraduate research in the laboratory of Professor John D. Thoburn where his senior thesis was on the development of chiropticenes, a miniaturized binary storage device.

In the fall of 2005, Daryl matriculated in the Chemistry Department at Johns Hopkins University. After a brief stint in the laboratory of Professor John D. Tovar, Daryl joined the laboratory of Professor John P. Toscano where his PhD thesis was on the development of new, physiologically useful nitroxyl (HNO) donors. In May of 2014, Daryl received his Doctorate of Philosophy in Chemistry.

During his tenure at Johns Hopkins University, Daryl received the Martin and Mary Kilpatrick Fellowship, as well as a Faculty of 1000 prime recommendation regarding a new finding, technical advance on the chemical biology of HNO. Daryl has authored two patent applications, licensed multiple pre-clinical heart failure drug candidates to Cardioxyl Pharmaceuticals, and supervised five undergraduate researchers resulting in three publications and three honors theses to date.